

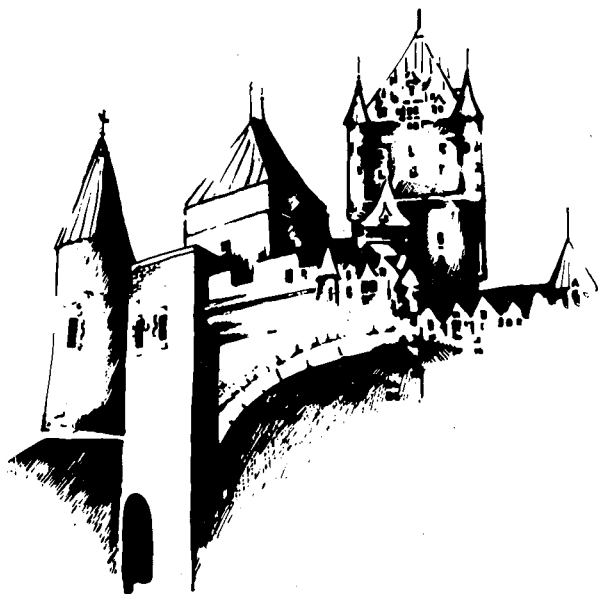
**National Academies of Science and Engineering
National Research Council
of the
United States of America**

**UNITED STATES NATIONAL COMMITTEE
International Union of Radio Science**



**National Radio Science Meeting
Bioelectromagnetics Symposium
June 18 - 22, 1979**

**Sponsored by USNC/URSI
held jointly with
International Symposium of
Antennas and Propagation Society
Institute of Electrical and Electronics Engineers
University of Washington
Seattle, Washington
U.S.A.**



Next year
Visit historic Quebec
Attend the 1980
**INTERNATIONAL IEEE/AP-S
SYMPOSIUM**
and
**NORTH AMERICAN
RADIO SCIENCE MEETING**
at
UNIVERSITÉ LAVAL, QUÉBEC
June 2-6, 1980

For information write to

J.A. Cummins
Département de Génie Électrique
Université Laval
Sainte-Foy Québec, Canada G1K 7P4

United States National Committee
INTERNATIONAL UNION OF RADIO SCIENCE

PROGRAM AND ABSTRACTS



1979 Spring Meeting
June 18-22

Held Jointly with
ANTENNAS AND PROPAGATION SOCIETY
INSTITUTE OF ELECTRICAL AND ELECTRONICS ENGINEERS

Seattle, Washington

NOTE:

Programs and Abstracts of the USNC/URSI Meetings are available from:

USNC/URSI
National Academy of Sciences
2101 Constitution Avenue, N.W.
Washington, D.C. 20418

The full papers are not published in any collected format; requests for them should be addressed to the authors who may have them published on their own initiative. Please note that these meetings are national and they are not organized by international URSI, nor are the programs available from the international Secretariat.

U.S. National Committee
for the
International Union of Radio Science

MEMBERSHIP

Officers

Chairman	*Dr. C. Gordon Little
Vice-Chairman	*Mr. George H. Hagn
Secretary	*Prof. Thomas B. A. Senior

Members Representing Societies, Groups and Institutes

American Geophysical Union	Dr. Christopher T. Russell
Institute of Electrical & Electronic Engineering	Dr. Ernst Weber
IEEE Antennas & Propagation Society	Mr. Robert C. Hansen
IEEE Circuits & Systems Society	Dr. Mohammed S. Ghausi
IEEE Communications Society	Mr. Amos E. Joel
IEEE Electromagnetic Compatibility Society	(Vacant)
IEEE Information Theory Group	Dr. Aaron D. Wyner
IEEE Microwave Theory & Techniques Society	Dr. Kenneth J. Button
IEEE Quantum Electronics Application Society	Dr. Robert A. Bartolini
Optical Society of America	Dr. Steven F. Clifford

Members-at-Large

Professor Leonard S. Taylor
Dr. Donald E. Barrick
Professor Arthur W. Guy

Liaison Representatives from Government Agencies

National Telecommunications & Information Administration	Mr. Samuel E. Probst
National Science Foundation	Dr. Wilfred K. Klemperer
Department of Commerce	(Vacant)
National Aeronautics & Space Administration	Dr. Erwin R. Schmerling
Federal Communications Commission	(Vacant)
Department of Defense	Mr. Emil Paroulek

Liaison Representatives from Government Agencies (Cont'd)

Department of the Army	Mr. Allan W. Anderson
Department of the Navy	Dr. Leo Young
Department of the Air Force	Dr. Allen C. Schell

Voting *Ex-Officio* Members

- a. Chairmen of the USNC-URSI Commissions
- | | |
|--------------|---------------------------|
| Commission A | Dr. Ramon C. Baird |
| Commission B | Prof. George A. Deschamps |
| Commission C | Prof. Mischa Schwartz |
| Commission D | Dr. Kenneth J. Button |
| Commission E | Dr. Arthur D. Spaulding |
| Commission F | Dr. Robert K. Crane |
| Commission G | Dr. Jules Aarons |
| Commission H | Dr. Robert W. Fredricks |
| Commission J | Dr. Alan T. Moffet |
- b. Foreign Secretary of the U.S.
National Academy of Sciences Dr. Thomas F. Malone
- c. Chairman, Office of Physical
Sciences - NRC Dr. Ralph O. Simmons

Non-Voting *Ex-Officio* Members

- a. Immediate Past Chairman of
USNC-URSI *Dr. John V. Evans
- b. Officers of URSI resident in the United States
(including Honorary Presidents)
- | | |
|--------------------|--------------------------|
| Vice President | *Prof. William E. Gordon |
| Honorary President | *Prof. Henry G. Booker |
- c. Chairman & Vice Chairman of
Commissions of URSI resident
in the United States
- | | |
|--------------------------|-----------------------------|
| Chairman of Commission B | Prof. Leopold B. Felsen |
| Chairman of Commission C | Prof. Jack K. Wolf |
| Chairman of Commission E | Mr. George H. Hagn |
| Chairman of Commission F | Prof. Alan T. Waterman, Jr. |
| Chairman of Commission H | Prof. Frederick W. Crawford |

Honorary Members

Dr. Harold H. Beverage
Prof. Arthur H. Waynick

* Members of USNC-URSI Executive Committee

DESCRIPTION OF
INTERNATIONAL UNION OF RADIO SCIENCE

The International Union of Radio Science is one of 18 world scientific unions organized under the International Council of Scientific Unions (ICSU). It is commonly designated as URSI (from its French name, Union Radio Scientifique Internationale). Its aims are (1) to promote the scientific study of radio communications, (2) to aid and organize radio research requiring co-operation on an international scale and to encourage the discussion and publications of the results, (3) to facilitate agreement upon common methods of measurement and the standardization of measuring instruments, and (4) to stimulate and to coordinate studies of the scientific aspects of telecommunications using electromagnetic waves, guided and unguided. The International Union itself is an organizational framework to aid in promoting these objectives. The actual technical work is largely done by the National Committees in the various countries.

The officers of the International Union are:

President:	Prof. W. N. Christiansen (Australia)
Past President:	M. J. Voge (France)
Vice-Presidents:	Prof. W. E. Gordon (USA) Dr. A. P. Mitra (India) Prof. A. Smolinski (Poland) Prof. F. L. Stumpers (Netherlands)
Secretary General:	Prof. P. Hontoy (Belgium)
Honorary Presidents:	H. G. Booker (USA) B. Decaux (France) W. Dieminger (West Germany) J. A. Ratcliffe (UK) R. L. Smith-Rose (UK)

The Secretary's office and the headquarters of the organization are located at Rue de Nieuwenhove, 81, B-1180 Brussels, Belgium. The Union is supported by contributions (dues) from 36 member countries. Additional funds for symposia and other scientific activities of the Union are provided by ICSU from contributions received for this purpose from UNESCO.

The International Union, as of the XVIII General Assembly held in Lima, Peru, August 1975, has nine bodies called Commissions for centralizing studies in the principal technical fields. The names of the Commissions and the chairmen and vice-chairmen follow.

- A. Electromagnetic Metrology
 Chairman: Prof. S. Okamura (Japan)
 Vice-Chairman: Prof. V. Koss (West Germany)
- B. Fields and Waves
 Chairman: Prof. L. B. Felsen (USA)
 Vice-Chairman: Prof. H. G. Unger (West Germany)
- C. Signals and Systems
 Chairman: Prof. V. Zima (Czechoslovakia)
 Vice-Chairman: Dr. J. K. Wolf (USA)
- D. Physical Electronics
 Chairman: Prof. G. W. Farnell (Canada)
 Vice-Chairman: Dr. J. LeMézec (France)
- E. Electromagnetic Noise and Interference
 Chairman: Mr. G. Hagn (USA)
 Vice-Chairman: Prof. S. Lundquist (Sweden)
- F. Wave Phenomena in Non-ionized Media
 Chairman: Prof. A. T. Waterman (USA)
 Vice-Chairman: Dr. D. Gjessing (Norway)
- G. Ionospheric Radio and Propagation
 Chairman: Dr. B. Hultqvist (Sweden)
 Vice-Chairman: Dr. P. Bauer (France)
- H. Waves in Plasmas
 Chairman: Prof. F. W. Crawford (USA)
 Vice-Chairman: Dr. M. Petit (France)
- J. Radio Astronomy
 Chairman: Prof. H. Tanaka (Japan)
 Vice-Chairman: Dr. V. Radhakrishnan (India)

Every three years, the International Union holds a meeting called the General Assembly. The next General Assembly, the XX will be held in Washington, D.C., USA in August 1981. The Secretariat prepares and distributes the Proceedings of these General Assemblies. The International Union arranges international symposia on specific subjects pertaining to the work of one Commission or to several Commissions. The International Union also cooperates with other Unions in international symposia on subjects of joint interest.

Radio is unique among the fields of scientific work in having a specific adaptability to large-scale international research programs, for many of the phenomena that must be studied are worldwide in extent and yet are in a measure subject to control by experimenters. Exploration of space and the extension of scientific observations to the space environment is dependent

on radio for its communication link and at the same time expands the scope of radio research. One of its branches, radio astronomy, involves cosmos-wide phenomena. URSI has in all this a distinct field of usefulness in furnishing a meeting ground for the numerous workers in the manifold aspects of radio research; its meetings and committee activities furnish valuable means of promoting research through exchange of ideas.

STEERING COMMITTEE

Irene C. Peden, Chairperson
 James Lambert, Vice Chairperson
 James Yee, Treasurer

Technical Program

Akira Ishimaru Thomas Senior
 Arthur Guy

Arrangements

Thomas Blakney Rubens Sigelmann

Registration

Douglas Connell

Publications

Mervin Vincent Hudson Burke

Programs

Eliza Wojtaszek

Advisers

C.-K. Chou Walter Curtis
 Thomas Dalby Vernon Westburg
 Donald Reynolds Myron Swarm
 James Meditch

Publicity

Ronald Trainer

Technical Program Committee

T. B. A. Senior &
 A. Ishimaru, Chairmen
 R. C. Baird
 R. K. Crane
 G. A. Deschamps
 E. J. Fremouw
 H. Kobayashi
 D. Ilic
 R. D. Martin
 J. M. Morris
 A. D. Spaulding

Bioelectromagnetics Symposium

A. W. Guy

Non-Linear Electromagnetics
 Symposium

P. L. E. Uslenghi



Dr. Hendricus Bremmer

The U.S. National Committee of URSI, together with the Antennas and Propagation Society of IEEE wish to honor the 75th birthday of Dr. Hendricus Bremmer, and welcome his presence at the 1979 combined meeting of these societies in Seattle, Washington.

It is hardly necessary to list the many scientific and technical achievements of this man. Dr. Bremmer is recognized throughout the world for his contributions, which he has shared with the scientific community through well over 100 publications spanning a period of nearly 50 years. As one of the world's foremost authorities on electromagnetic wave propagation, Dr. Bremmer has made significant contributions in practically every branch of this field. It is characteristic of this man that he did not terminate his career in 1965 upon retirement from 30 years of service at the Phillips Research Laboratories, Eindhoven, but continued as a scientist and educator for another decade at Eindhoven Institute of Technology. During this latter period he has been a prolific contributor to the technical literature, particularly in the field of wave propagation in stochastic media.

Dr. Bremmer, we salute you on your 75th birthday and wish you many more prosperous years in which to continue your work, and to savour the reward of observing the continued development by other scientists of the many lines of investigation which you pioneered.

1979 MEETING
CONDENSED PROGRAM

		ROOM
SUNDAY, JUNE 17		
8:00 p.m.	ASNI C95.4 Meeting	Condon Rm. (Univ. Tower)
MONDAY, JUNE 18		
8:30-12:00 a.m.		
AP-S 1	Array Synthesis	KANE 130
B 1	High Frequency Scattering	KANE 120
F 1	Scattering by Turbulence	KANE 110
C/E	(Combined Session) Telecommunication Systems in Non- Gaussian Environments	HUB 106B
8:30-10:00 a.m.		
BEMS 1	Opening Session	HUB Aud.
10:20-11:50 a.m.		
BEMS 2	Thermoregulation	HUB Aud.
1:30- 5:00 p.m.		
AP-S 2(a)	Reflector Antennas: Analysis and Synthesis	KANE 130
AP-S 2(b)	Part I: Microstrip Antenna (Theoretical) Part II: Microstrip Antenna (Experimental)	KANE 210 KANE 220 KANE 120
AP-S 2(c)	Numerical Techniques	KANE 120
B 2	Waves in Random Media I	KANE 120
AP-S/F-2	(Combined Session) John W. Wright Memorial Session on Radio Oceanography	KANE 110
C 1	High Time-Bandwidth Product Signals: Theory and Applications	HUB 106B
G 1	Diagnostics, Effects, and Modifications of the Ionosphere	HUB 309A
1:30- 3:00 p.m.		
BEMS 3	Nervous System	HUB Aud.
3:20- 4:50 p.m.		
BEMS 4	Physiology	HUB Aud.
5:00 p.m.		
	Commission B Business Meeting	KANE 120
	Commission G Business Meeting	HUB 309A

ROOM

MONDAY, JUNE 18 (Cont.)

5:30 p.m.

Bioelectromagnetics Society Board Meeting

Pres. Rm.
(Univ. Tower)

6:30 p.m.

Wave Propagation Standards Committee Meeting

HUB 106B

8:00 p.m.

H. Bremmer: Walker-Ames Lecture on Wave Propagation

KANE 120

TUESDAY, JUNE 19

8:30-12:00 a.m.

AP-S 3 Adaptive Techniques and Synthetic Aperture Radar

KANE 130

B 3 Antennas (Arrays)

KANE 120

F 3 Propagation Within the Earth

KANE 110

C 2 New Satellite Systems for the 80's and Beyond

HUB 106B

G 2 Transmission and In-Situ Measurements of Natural and Enhanced Ionospheric Irregularities

HUB 309A

8:30-10:00 a.m.

BEMS 5 Theoretical/Experimental Dosimetry (I)

HUB Aud.

9:00 a.m.

CCIR US Study Group Meeting

KANE
Walker-Ames

10:20-11:50 a.m.

BEMS 6 Theoretical/Experimental Dosimetry (II)

HUB Aud.

12:00-12:30 p.m.

AP-S "Meet your Ad Com" Meeting

KANE 130

1:30- 4:50 p.m.

BEMS A Poster Session on Medical Applications

HUB 108
West Lounge

1:30- 5:00 p.m.

AP-S 4(a) Inverse Problems

KANE 130

AP-S 4(b) Reflector Antennas and Feeds

KANE 210

AP-S 4(c) Part I: Guided Waves

Part II: Atmospheric Propagation

KANE 220

B 4(a) Field Penetration and Scattering

KANE 120

B 4(b) Waves in Random Media II

HUB Aud.

ROOM

TUESDAY, JUNE 19 (Cont.)

1:30- 5:00 p.m.

AP/B	A	Poster Session on Antennas	KANE Walker-Ames
F	4	Scattering from Rough Surfaces	KANE 110
E		Characterization and Measurement of Noise	HUB 106B
G	3	Polarization Effect and Large-Scale Structures of the Ionosphere	HUB 309A

5:30- 6:30 p.m.

Boarding for Salmon Bake on Blake Island

WEDNESDAY, June 20

9:00-11:30 a.m.

Plenary Session KANE 130

12:00 noon

Conference Luncheon HUB
Ballroom

2:30 p.m.

Antenna Standards Committee Meeting EEB 420

2:00- 5:30 p.m.

AP-S	5(a)	Lens and Horn Antennas	KANE 130
AP-S	5(b)	Part I: Microstrip Antennas (Theoretical)	
		Part II: Electrically-Small Antennas	KANE 210
AP-S	5(c)	Scattering and Electromagnetic Theory	KANE 220
BREMMER		Bremmer Commemorative Anniversary Session	KANE 120
AP/B	B	Poster Session on Wave Phenomena	KANE Walker-Ames
F	5	Earth-Space Propagation	KANE 110
H		Observed and Predicted Phenomena in Laboratory and Natural Plasmas	HUB 106B
BEMS	7	Blood Brain Barrier	HUB Aud.

5:00 p.m.

		Bioelectromagnetics Society Membership Meeting	HUB Aud.
		AP-S Local Chapter Chairman's Meeting	Pres. Rm. (Univ. Tower)

5:30 p.m.

		Commission C Business Meeting	HUB 309A
		Commission F Business Meeting	KANE 110
		Commission H Business Meeting	HUB 106B
		AP-S Ad Com Meeting	Condon Rm. (Univ. Tower)

THURSDAY, JUNE 21

ROOM

8:30-12:00 a.m.

AP-S	6	Space Antenna Systems and Measurements	KANE 130
B	5	Transients	KANE 120
F	6	Part I: Propagation Above Surface: Modes and Rays	
		Part II: Scattering by Snow and Ice	KANE 110
A	1	Measurements of Electromagnetic Parameters and Materials	HUB 309A

8:45-11:50 a.m.

NL	1	Nonlinear Electromagnetics I	HUB 106B
----	---	------------------------------	----------

8:30-10:15 a.m.

BEMS	8	Dielectric Properties: Physical Measurements	HUB Aud.
------	---	---	----------

10:35-11:50 a.m.

BEMS	9	Special Topics	HUB Aud.
------	---	----------------	----------

12:00 noon

URSI International Working Group
Meeting on "Measurements Related
to Interaction of Electromagnetic
Fields with Biological Systems"

Regents Rm.
(Univ. Tower)

1:30- 4:50 p.m.

BEMS	B	Poster Session on Cellular Effects: Raman Spectra and Millimeter Waves	HUB 108 West Lounge
------	---	---	------------------------

1:30-5:00 p.m.

AP-S	7(a)	Environmental Effects on Electro- magnetic Propagation	KANE 130
AP-S	7(b)	Part I: High Frequency Diffraction Part II: Near Field Calculations and Measurements	KANE 210
AP-S	7(c)	Part I: Transients Part II: Composite Dielectrics/Radomes	KANE 220
B	6	Antennas II	KANE 120
AP/B	C	Poster Session on Scattering	KANE Walker-Ames
F	7	Radiooceanography	KANE 110
NL	2	(Co-sponsored by B and BEMS) Nonlinear Electromagnetics II	HUB 106B
A	2	Measurements of Radar Cross Sections, Antenna Properties, and Electro- magnetic Emissions	HUB 309A

5:30 p.m.

Commission A Business Meeting

Pres. Rm.
(Univ. Tower)

		ROOM	
FRIDAY, JUNE 22			
8:30-12:00 a.m.			
AP-S	8	Array Analysis/Design	KANE 130
B	7	Guided Waves	KANE 120
F	8	Propagation Modeling	KANE 110
NL	3	Nonlinear Electromagnetics III	HUB 106B
8:30-10:00 a.m.			
BEMS	10	Round-Table: Cellular Effects, Raman Spectra and Millimeter Waves	HUB Aud.
10:20-11:50 a.m.			
BEMS	11	Medical Applications	HUB Aud.
1:30- 3:00 p.m.			
BEMS	12	Reproduction, Growth, and Development (I)	HUB Aud.
3:20- 5:05 p.m.			
BEMS	13	Reproduction, Growth, and Development (II)	HUB Aud.

TABLE OF CONTENTS

URSI	pages 1 - 323
BIO-BEMS	pages 324 - 503
(Author Index	pages 504 - 515)

PLENARY SESSION
JOINT USNC/URSI - AP-S - BEMS
WEDNESDAY AM 9:00-11:30
KANE HALL 130

Chairman: A. Ishimaru
University of Washington
Seattle, WA

Opening Remarks: I. C. Peden, Steering Committee Chairperson
University of Washington
Seattle, WA

Welcome: G. M. Beckmann, Provost
University of Washington
Seattle, WA

I. J. Stampalia
Director of Engineering Technology
Boeing Aerospace Company
Seattle, WA

	<u>Page</u>
1. Rays and Modes in Guided Propagation L. B. Felsen, Polytechnic Institute of New York, Farmingdale, NY	2
2. The Interferometer Array in Radio Astronomy G. W. Swenson, Jr., University of Illinois at Urbana-Champaign, Urbana, IL	3
3. Historical Overview and State-of-Art on the Quantification of EM Bio-Effects A. W. Guy, University of Washington, Seattle, WA	4
4. Satelliteborne Synthetic Aperture Radar K. Tomiyasu, General Electric Co., Philadelphia, PA	5
5. The Activities of the Antenna Society of the Chinese Electronics Institute Mao Yu-Kuan, Northwest Telecommunication Engineering Institute, Xian, Shanxi, People's Republic of China	6

BREMMER SESSION
WEDNESDAY P.M. 2:00 - 5:30
KANE HALL 120

BREMMER BIRTHDAY CELEBRATION

Chairman: J. R. Wait
ERL/NOAA
Boulder, CO

	<u>Page</u>
1. Ground Wave Theory Via Normal Modes - An Historical Perspective J. R. Wait, ERL/NOAA, Boulder, CO	8
2. Propagation Along Concave Surfaces L. G. Felsen, Polytechnic Institute of New York, Farmingdale, NY	9
3. Speckle Interferometry for a Partially-Coherent Source R. L. Fante, Rome Air Development Center, Hanscom AFB, MA	10
4. A. Wigner-Distribution Matrix for a Stochastic Medium H. Bremmer, Emeritus Professor, Technical University, Eindhoven, The Netherlands	11
5. Waves in Random Media: Limiting Irradiance Distribution D. A. de Wolf, RCA Laboratories, Princeton, NJ	12
6. Forward Scatter Theory and Diffusion Theory for Waves in Random Media A. Ishimaru, University of Washington, Seattle, WA	13

SESSION A-1
THURSDAY AM 8:30-12:00
HUB 309-A

MEASUREMENTS OF ELECTROMAGNETIC PARAMETERS AND MATERIALS

Chairman: D. G. Dudley
University of Arizona
Tucson, AZ

	<u>Page</u>
1. A Coaxial Line Technique for One-Sided Nondestructive Material Measurements F. E. Gardiol, J. C. E. Besson, J. R. Mosig, Ecole Polytechnique Federale, Lausanne, Switzerland	15
2. TM Cylindrical Cavity Measurement of Dielectric Constant and Loss Tangent D. G. Dudley, University of Arizona, Tucson, AZ, J. A. Fuller, Georgia Institute of Technology, Atlanta, GA and R. G. Semelberger, Science Applications, Inc., Tucson, AZ	16
3. Electromagnetic Interaction Between a Conducting Cylinder and a Solenoid in Relative Motion J. R. Wait and D. A. Hill, U.S. Department of Commerce, Boulder, CO	17
4. Copper Conductivity at Millimeter Wave Frequencies L. W. Hinderks, Corporate Computer Systems Inc., Aberdeen, NJ and A. Maione, Bell Laboratories, Holmdel, NJ	18
5. Applications of the Infrared Detection of Surface Currents R. W. Burton and C. V. Stewart, U.S. Air Force Academy, CO	19
6. Analysis of the Quantum Limited DC Squid Magnetometer and Voltage Amplifier C. D. Tesche, LuTech, Inc., Berkeley, CA	20

SESSION A-2
THURSDAY PM 1:30-5:00
HUB 309A

MEASUREMENTS OF RADAR CROSS SECTIONS, ANTENNA PROPERTIES, AND
ELECTROMAGNETIC EMISSIONS

Chairman: C. F. Stubenrauch
National Bureau of Standards
Boulder, CO

	<u>Page</u>
1. Performance of Broad-Band Radar Scattering Measurement System Using Amplitude and Phase Post Processing Techniques E. K. Walton, The Ohio State University ElectroScience Laboratory, Columbus, OH	22
2. Broad Band Scattering Signatures of Cone-Like Objects E. K. Walton and J. D. Young, The Ohio State University ElectroScience Laboratory, Columbus, OH	23
3. Use of Orbiting Wire for Calibration of Circularly Polarized Radar Returns H. Inada, M.I.T. Lincoln Laboratory, Lexington, MA	24
4. Far-Field Estimation from Near-Field Measurements Taken Along a Straight Line Segment M. T. Martins da Silva, SP, Brazil and A. R. Panicali, University of Sao Paulo, SP, Brazil	25
5. The Use of King-Type Current Probes for Broadband Transient Measurements L. W. Pearson, Y. M. Lee, University of Kentucky, Lexington, KY	26

SESSION B-1
MONDAY AM 8:30-12:00
KANE HALL 120

HIGH FREQUENCY SCATTERING

Chairman: Y. Rahmat-Samii
Jet Propulsion Laboratory
Pasadena, CA

	<u>Page</u>
1. Application of the Uniform GTD to the Diffraction by Aperture in a Thick Screen R. Tiberio, University of Florence, Florence, ITALY and R. G. Kouyoumjian, The Ohio State University, Columbus, OH	28
2. High Frequency Electromagnetic Fields on Perfectly Conducting Concave Surfaces E. Topuz and L. B. Felsen, Polytechnic Institute of New York, Farmingdale, NY	29
3. Scattering by Resistive Strips T. B. A. Senior, The University of Michigan, Ann Arbor, MI	30
4. Ray-Optical Theory of Coupling between and Radiation from Adjacent Parallel Plate Waveguides P. F. Driessen and E. V. Jull, University of British Columbia, Vancouver, B. C., Canada	31
5. Edge Currents on Rectangular Plates V. V. Liepa, The University of Michigan, Ann Arbor, MI	32
6. Scattering from a Corner Formed by Two Line Elements K. M. Mitzner and S. A. Sloan, Northrop Corporation, Hawthorne, CA	33
7. Radiation from Sources on Smooth Convex Surfaces with Edges - a Spectral Domain Approach S. Safavi-Naini and R. Mittra, University of Illinois, Urbana, IL	34
8. Evanescent Wave Tracking in a Slab Waveguide with Transverse and Longitudinal Refractive Index Variation G. Jacobsen and L. B. Felsen, Polytechnic Institute of New York, Farmingdale, NY	35
9. On the Asymptotic Theory of Inhomogeneous Wave Tracking and its Relevance to the Inverse Scattering of Gaussian Beams P. Einziger, The Technion-Israel Institute of Technology and S. Raz, The Technion-Israel Institute of Technology, Currently on Sabbatical Leave at the University of Houston, Houston, TX	36
10. GTD Analysis of the Near-Field Patterns of Pyramidal Horns J. S. Narasimhan and K. Sudhakar Rao, Indian Institute of Technology, Madras, INDIA	37

SESSION B-2
MONDAY PM 1:30-5:00
KANE HALL 120

WAVES IN RANDOM MEDIA I

Chairman: D. deWolf
RCA David Sarnoff Lab
Princeton, NJ

	<u>Page</u>
1. Depolarization and Scattering of Electromagnetic Waves by Irregular Boundaries for Arbitrary Incident and Scatter Angles --Full Wave Solutions E. Bahar and G. G. Rajan, University of Nebraska, Lincoln, NB	39
2. Scattering and Absorption Spectra for Platelike Hydrometeors H. Weil and C. M. Chu, University of Michigan, Ann Arbor, MI	40
3. Near-Forward Multiple Scattering by a Random Slab of Large Particles E. A. Marouf, Stanford University, Stanford, CA and University of Alexandria, Alexandria, Egypt	41
4. Effects of Anisotropic Irregularities on Phase Scintillations R. Woo and J. W. Armstrong, Jet Propulsion Lab, Pasadena, CA	42
5. High-Altitude Turbulence Measurements for Optical Propagation Predictions C. A. Levis and J. P. Serafin, Ohio State University, Columbus, OH	43
6. Detection Effects on Higher Order Statistics of Light Fluctuations Due to Atmospheric Turbulence A. Consortini and L. Ronchi, Istituto di Ricerca sulle Onde Elettromagnetiche of CNR, Firenze, Italy	44
7. Resolution Through the Atmosphere of Optical Adaptive Systems A. Consortini, F. Pasqualetti and L. Ronchi, Istituto di Ricerca sulle Onde Elettromagnetiche of CNR, Firenze, Italy	45
8. Backscattered Pulse Shape Due to Small-Angle Multiple Scattering from a Slab of Random Medium K. J. Painter and A. Ishimaru, University of Washington, Seattle, WA	46

SESSION B-3
TUESDAY AM 8:30-12:00
KANE HALL 120

ANTENNAS I (ARRAYS)

Chairman: K. G. Balmain
University of Toronto
Toronto, Canada

	<u>Page</u>
1. Linear Array Synthesis Using Prony's Method E. K. Miller and G. J. Burke, University of California, Livermore, CA	48
2. An Array Thinning Technique D. Y. Ho and B. D. Steinberg, University of Pennsylvania, Philadelphia, PA	49
3. On the Current Distribution on Printed Parasitic Thin Wire Arrays I. E. Rana and N. G. Alexopoulos, University of California Los Angeles, CA	50
4. Analysis of a Phased Array of Dipoles Printed on Periodic Dielectric Slabs Over a Ground Plane R. S. Chu, Hughes Aircraft Company, Fullerton, CA, and S. S. Wang, The Aerospace Corporation, El Segundo, CA	51
5. Periodic-Structure-Ray Approach to Analysis of Arrays on Concave Surfaces H. Ahn, B. Tomasic and A. Hessel, Polytechnic Institute of New York, Farmingdale, NY	52
6. Currents on a Yagi Structure of Inclined Dipoles W. K. Kahn, Naval Research Laboratory, Washington, D.C.	53
7. Resonance Phenomena on Yagi Arrays J. M. Tranquilla, University of New Brunswick, Fredericton, Canada and K. G. Balmain, University of Toronto, Canada	54
8. Analysis of the Loop-Coupled Log-Periodic Dipole Array J. M. Tranquilla, University of New Brunswick, Fredericton, Canada and K. G. Balmain, University of Toronto, Canada	55
9. The Influence of a Borehole on the Mutual Impedance of an Array of Coplanar Loops R. G. Olsen and N. A. Sanford, Washington State University Pullman, WA	56
10. An Analysis of the Mutual Coupling Between Antennas on a Smooth Convex Surface P. H. Pathak and N. N. Wang, The Ohio State University, Columbus, OH	57

SESSION B-4 (a)
TUESDAY PM 1:30-5:00
KANE HALL 120

FIELD PENETRATION AND SCATTERING

Chairman: R. F. Harrington
Syracuse University
Syracuse, NY

	<u>Page</u>
1. Field Penetration Through Small Apertures: The First-Order Correction J. Van Bladel, Rijksuniversiteit Gent, Gent, Belgium	59
2. Diffraction by a Narrow Slit in an Impedance Plane R. A. Hurd, National Research Council of Canada, Ottawa, Canada	60
3. Penetration and Scattering of EM Fields by Advanced Composite Bodies of Revolution H. Kao and K. K. Mei, University of California, Berkeley, CA	61
4. Scattering by a Hemisphere P. L. E. Uslenghi, University of Illinois, Chicago IL and V. Daniele, CESP, Torino, Italy	62
5. An Efficient Approach for Computing Fresnel-Zone Fields A. M. Rushdi and R. Mittra, University of Illinois, Urbana IL and V. Galindo-Israel, Jet Propulsion Lab, Pasadena, CA	63
6. Nearfield Scattering by a Finite Dielectric Rod G. Tricoles, R. A. Hayward and E. L. Rope, General Dynamics Electronics Division, San Diego, CA	64
7. Radar Cross Section of Loop Antennas Above Finite Conducting Half-Space A. S. Abulkassem and D. C. Chang, University of Colorado, Boulder, CO	65
8. Uses of the Nonlinear Optimization in Field and Scattering Problems Y. L. Chow and S. K. Chaudhuri, University of Waterloo, Waterloo, Canada	66
9. Scattering by Material Bodies of Revolution with a Metallic Core S. K. Chang. EMtec Engineering, Inc., Berkeley, CA	67
10. On Electrically Thick Cylindrical Antennas of Finite Length L. Rispin and D. C. Chang, University of Colorado, Boulder, CO	68

SESSION B-4 (b)
TUESDAY PM 1:30-5:00
HUB AUDITORIUM

WAVES IN RANDOM MEDIA II

Chairman: I. M. Besieris
Virginia Polytechnic Institute and State University
Blacksburg, VA

	<u>Page</u>
1. A Functional Path-Integral Approach to Stochastic Wave Propagation I. M. Besieris, Virginia Polytechnic Institute and State University, Blacksburg, VA	70
2. Propagation in a Two-Mode Randomly Perturbed Waveguide Werner Kohler and S. Patsiokis, Virginia Polytechnic Institute and State University, Blacksburg, VA	71
3. An Intensity Probability-Density Function of Plane Waves Propagated Through Random Media M. Tateiba, Nagasaki University, Nagasaki, Japan	72
4. Coherrent Wave Propagation and the Foldy-Twersky Integral Equation G. S. Brown, Applied Science Associates, Inc., Apex, NC	73
5. An Analytical Theory of Pulse Wave Propagation in Turbulent Media K. Furutsu, Radio Research Laboratories, Tokyo, Japan	74
6. Backscattering of a Picosecond Pulse from a Dense Scattering Medium K. Shimizu, A. Ishimaru and A. P. Bruckner, University of Washington, Seattle, WA	78

SESSION B-5
THURSDAY AM 8:30-12:00
KANE HALL 120

TRANSIENTS

Chairman: F. M. Tesche
Science Applications Inc.
Berkeley, CA

	<u>Page</u>
1. Transients on Lossy Transmission Lines A. H. Mohammadian and C. T. Tai, University of Michigan, Ann Arbor, MI	80
2. The Response of a Transmission Line Illuminated by Lightning- Induced Electromagnetic Fields H. J. Price, A. K. Agrawal, H. M. Fowles, and L. D. Scott, Mission Research Corporation, Albuquerque, NM	81
3. On the Low Frequency Asymptotic Behavior of SEM-Derived Equivalent Circuits for Wire Antennas C. W. Streable, Bell Laboratories, Holmdel, NJ and L. W. Pearson, K. A. Michalski, University of Kentucky, Lexington, KY	82
4. Transient Electromagnetic Field of a Vertical Dipole Located on a Dissipative Earth Surface H. A. Haddad and D. C. Chang, University of Colorado, Boulder, CO	83
5. A Geometric Theory of Natural Oscillation Frequencies in Exterior Scattering Problems A. Q. Howard, Jr., University of Arizona, Tucson, AZ	84
6. Is Prony's Method an Ill Posed Problem and Pencil-of-Function Method a Well Posed Problem in System Identification? T. K. Sarkar, Rochester Institute of Technology, Rochester, NY	85
7. Pulse Response Waveforms of Aircraft D. L. Moffatt and K. A. Shubert, The Ohio State University ElectroScience Laboratory, Columbus, OH	86
8. EMP Interaction of a Low-Altitude Missile with an Inhomogeneous Plasma Plume S. K. Chang and F. M. Tesche, LuTech, Inc., Berkeley, CA	87
9. Resolution of Closely Spaced Point Targets G. S. Sandhu, Teledyne Brown Engineering, Huntsville, AL and N. F. Audeh, The University of Alabama in Huntsville, Huntsville, AL	88

SESSION B-6
THURSDAY PM 1:30-5:00
KANE HALL 120

ANTENNAS II

Chairman: W. V. T. Rusch
University of Southern California
Los Angeles, CA

	<u>Page</u>
1. Vector Secondary Patterns of Non-Parabolic Reflectors---Some Novel Observations Y. Rahmat-Samii, P. Cramer and V. Galindo Israel, Jet Propulsion Lab, Pasadena, CA	90
2. Comparisons Between Different Methods for Subreflector Analysis N. Chr. Albertsen and K. Pontoppidan, TICRA ApS, Copenhagen, Denmark	91
3. Design of Cluster Feed for Multibeam Reflector Antennas P. Cramer and K. Woo, Jet Propulsion Lab, Pasadena CA and S. W. Lee, University of Illinois, Urbana IL	92
4. Generalized Geometrical Optics R. Mittra and A. M. Rushdi, University of Illinois, Urbana, IL	93
5. On the Validity of Thin-Wire Theory C. D. Taylor, Mississippi State University, Mississippi State, MS	94
6. Analysis of a Monopole Near the Edge of a Half-Plane D. M. Pozar and E. H. Newman, Ohio State University, Columbus, OH	95
7. Effect of Taper Profile on Performance of Dielectric Taper Antennas S. T. Peng, Polytechnic Institute of New York, Brooklyn, NY and F. Schwering, U.S. Army Communication Research and Development Command, Ft. Monmouth, NJ	96
8. Maximizing the Gain-Bandwidth Product of a Lossy Linear Antenna R. M. Bevensee, Lawrence Livermore Lab, Livermore, CA	97
9. Experimental Investigation of the Radiated Fields of a Buried Antenna F. Vaziri, S. A. Long and L. C. Shen, University of Houston, Houston, TX	98
10. Optimized Launching of the Ground Wave: A New Look at the Beverage Antenna D. C. Chang and E. F. Kuester, University of Colorado, Boulder, CO	99

SESSION B-7
FRIDAY AM 8:30-12:00
KANE HALL 120

GUIDED WAVES

Chairman: K. Casey
Kansas State University
Manhattan, KS

	<u>Page</u>
1. Leaky Modes on Open Dielectric Waveguides A. A. Oliner and S. T. Peng, Polytechnic Institute of New York, Brooklyn, NY	101
2. Coupling Between Triangular Optical Waveguides P. L. E. Uslenghi, University of Illinois at Chicago Circle, Chicago, IL	102
3. Junction Effect of Two Thin, Coaxial Cylinders of Dissimilar Radius D. C. Chang, University of Colorado, Boulder, CO	103
4. Waveguide Modes with One-Dimensional Transverse Inhomogeneities W. A. Davis, Virginia Polytechnic Institute and State University, Blacksburg, VA and R. B. Kaplan, Wright-Patterson AFB, OH	104
5. On Using the I. Q. of Waveguides Intelligently D. L. Jaggard, University of Utah, Salt Lake City, UT	105
6. Propagation Characteristics of a Two-Layer Dielectric Wave- guide with an Azimuthal Asymmetry T. C. K. Rao, Florida Atlantic University, Boca Raton, FL	106
7. Scattering of Surface Waves by a Notch in a Perfectly Conduct- ing Ground Plane Covered by a Dielectric Slab R. D. Nevels, Texas A&M University, College Station, TX and C. M. Butler, University of Mississippi, University, MS	107
8. Integral Operator Analysis of Coupled Dielectric Optical Waveguide System - Theory and Application S. V. Hsu, E-System Inc., Dallas, TX and D. P. Nyquist, Michigan State University, East Lansing, MI	108
9. Dielectric-Lined Metal Rectangular Waveguide R. Chatterjee, Indian Institute of Science, Bangalore, India and G. K. Deb, Electronics and Radar Development Establish- ment, Bangalore, India	109
10. Scalar Wave Approach for Single-Mode Inhomogeneous Fiber Problems W. P. Brown and C. Yeh, Hughes Research Laboratories, Malibu, CA	110

AP/B POSTER SESSION A
 TUESDAY PM 1:30-5:00
 KANE HALL - WALKER AMES ROOM

ANTENNAS

Chairman: C. M. Butler
 University of Mississippi
 University, MS

	<u>Page</u>
1. Some Considerations to the Divergence Problem of Antenna Integral Equation Solutions G. Greving, Technische Hochschule Aachen, Aachen, West Germany	112
2. Current on Thick Cylindrical Antennas. Improved Solution of the Generalized Boundary Condition Integral Equation by Le Foll's Algorithm J. Ch. Bolomey, S. El Habiby, F. Hillaire, D. Lesselier, C.N.R.S. -E.S.E. Gif-sur-Yvette, France	112
3. GTD Solution of the Input Admittance of a Slot on a Cone E. K. Yung Hong Kong Polytechnic, Hung Hom, Hong Kong, S. W. Lee, and R. Mittra, University of Illinois, Urbana, IL	112
4. Shaped Beam Reflector Feed Network for Clutter Reduction and Angle Estimation C. F. Winter, Raytheon Company, Wayland, MA	112
5. Study of Batwing Radiator of the Superturnstile Antenna for TV Broadcasting R. W. Masters, Antennas Research Associates, Inc. Beltsville, MD and G. Sato, H. Kawakami, and M. Umeda, Sophia University, Tokyo, Japan	112
6. The Characteristics of a Modified Duoconical Monopole with Curved Surface Transition K. Fukuzawa and R. Sato, Tohoku University, Sendai, Japan	112
7. Best Possible Thermal Noise Sensitivity of Electrically Small Loop Antennas M. Dishal, ITT Avionics, Nutley, NJ	112
8. Dual-Beam Waveguide Slot Array for Monopulse Application G. A. Hockham and R. I. Wolfson, ITT Gilfillan, Van Nuys, CA	112
9. Peak Cross Polarization of Reflectors with Surface Errors S. I. Ghobrial, University of Khartoum, Khartoum, Sudan	112
10. A Multimode Dielectric Coated Horn For Circularly Polarized Elliptical Beam S. H. J. Quboa, S. C. Gupta, University of Mosul, Mosul, Iraq	112
11. Horn-Reflector Antenna Performance at 2 GHz with Simultaneous Operation in the 4, 6 and 11 GHz Bands J. E. Richard, Bell Telephone Laboratories, Inc., North Andover MA	112

AP/B POSTER SESSION A

ANTENNAS (cont.)

	<u>Page</u>
12. Astigmatic Correction by a Deformable Subreflector W. Y. Wong and S. von Hoerner, National Radio Astronomy Observatory, Green Bank, WV	113
13. A Decoupled Antenna System with a Lossless Network H. Iwasaki, Y. Mikuni, and K. Nagai, Toshiba Research and Development Center, Kawasaki, Japan	113
14. Performance of Reflector Antennas with Absorber-Lined Tunnels R. B. Dybdal, H. E. King, The Aerospace Corporation, Los Angeles, CA	113
15. Sidelobe Reduction with Horn-Antennas F. M. Landstorfer, R. R. Sacher, Technical University of Munich, Munich FRG.	113
16. Radiation by Microstrip Patches N. G. Alexopoulos and I. Rana, University of California, Los Angeles, Los Angeles, CA, and N. K. Uzunoglu, National Technical University of Athens, Athens, Greece	113
17. Microstrip Antennas for Airborne Radar Systems A. W. Biggs, University of Kansas, Lawrence, KS	114
18. A Microstrip Analysis Technique E. H. Newman and P. Tulyathan, The Ohio State University ElectroScience Laboratory, Columbus, OH	115
19. A Circularly Polarized Microstrip Resonator Antenna J. Vandensande, H. Pues, E. Van Lil, A. Van de Capelle Katholieke Universiteit Leuven, Heverlee, Belgium	116
20. The RN^2 Multiple Beam Array Family and the Beam Forming Matrix J. L. McFarland, Lockheed Missiles and Space Company, Sunnyvale, CA	113
21. Frequency Selection for Reliable, Low-Cost Satellite Links P. F. Christopher, The MITRE Corporation, Bedford, MA	113
22. Far-Field Antenna Pattern Calculation From Near-Field Measurements Including Compensation for Probe Positioning Errors L. E. Corey and E. B. Joy, Georgia Institute of Technology, Atlanta, GA	113
23. A Maritime Communications Subsystem (MCS) for Intelsat V Satellites W. J. English, INTELSAT - Space Segment Engineering, Washington, DC	117
24. Automated Probing for Outdoor Antenna Ranges S. M. Sanzgiri, G. Crain, and R. C. Voges, Texas Instruments Inc., Dallas, TX	113

AP/B POSTER SESSION A

ANTENNAS (cont.)

	<u>Page</u>
25. On the Accuracy of the Transmission Line Model of the Folded Dipole G. A. Thiele, E. P. Ekelman, Jr., and L. W. Henderson, The Ohio State University ElectroScience Laboratory, Columbus, OH	113
26. A Circularly Symmetric Dual-Reflector-Type Multibeam Antenna H. Kumazawa, Nippon Telegraph and Telephone Public Corp., Yokosuka, Japan, and M. Mizusawa, Mitsubishi Electric Corp., Kamakura-City, Japan	113
27. Air Launch Cruise Missile Instrumentation Antennas R. E. Lantagne, J. P. Grady and G. E. Miller, Boeing Aerospace Company, Seattle, WA	113

AP/B POSTER SESSION B
WEDNESDAY PM 2:00-5:30
KANE HALL - WALKER AMES ROOM

WAVE PHENOMENA

Chairman: C. M. Butler
University of Mississippi
University, MS

	<u>Page</u>
1. On Convergence of the Method of Moments T. K. Sarkar, Rochester Institute of Technology, Rochester, NY	118
2. The Non Uniqueness of Inverse Problems and Partial Coherence B. J. Hoenders, State University at Groningen, Groningen, The Netherlands, H. P. Baltes, L. G. Z. Landis, and G. Zug, Zentrale Forschung und Entwicklung, Zug, Switzerland	118
3. Exact and Approximated Time-Domain Deductive Reconstruction of Conducting Multilayer Slabs D. Lesselier, C.N.R.S. - E.S.E., Gif-sur-Yvette, France	118
4. Multiple Wavelength Aperture Synthesis for Passive Sensing of the Earth's Surface E. Schanda, University of Berne, Berne, Switzerland	118
5. The Backward Transform of the Near Field for Reconstruction of Aperture Fields J. D. Hanfling, G. V. Borgiotti, and L. Kaplan, Raytheon Co, Bedford, MA	118
6. A Study of Adaptive Sidelobe Canceller C. A. Chuang, Harris Government Communications System Division, Melbourne, FL	118
7. To Theory Wave Propagation in W-Fiberguides with Rectangular Core V. V. Cherny, University of California, Berkeley, Berkeley, CA	118
8. SEM Characteristics of a Log-Periodic Dipole Array K. D. Rech, K. J. Langenberg, Universitat des Saarlandes, Saarbrucken, FRG	118
9. SEM Investigation of Transient Acoustic Scattering from a Fixed Finite Rotationally Symmetric Body G. Bollig, K. J. Langenberg, Universitat des Saarlandes, Saarbrucken, FRG	118
10. Doppler Spectrum of Extended Objects J. B. Andersen, Aalborg University Centre, Aalborg, Denmark	118
11. Measured and Calculated Field Within Partitioned One and Two- Port Coaxial Cavities M. G. Harrison, USAF Weapons Laboratory, Kirtland AFB, NM C. M. Butler, University of Mississippi, University, MS	118
12. A Dual Polarization Broad-Band Waveguide J. Tourneur, Thomson-CSF, Malakoff, France	119

AP/B POSTER SESSION B
WEDNESDAY PM 2:30-5:30
KANE HALL - WALKER AMES ROOM

WAVE PHENOMENA

Chairman: C. M. Butler

Page

13. Resonance, Phase Front and Polarization-Independence
Constraints of Inhomogeneous Fabry-Perot Interferometers 119
S. Raz, University of Houston, Houston, TX and Y. Leviatan,
Technion-Israel Institute of Technology, Haifa, Israel

AP/B POSTER SESSION C
THURSDAY PM 1:30-5:00
KANE HALL - WALKER AMES ROOM

SCATTERING

Chairman: C. M. Butler
University of Mississippi
University, MS

	<u>Page</u>
1. Coupling of Electromagnetic Waves to a Cable Through Long Slots T. C. Tong, TRW Defense and Space Systems Group, Redondo Beach, CA	120
2. A New Surface-Current Model for Metallic Scattering Surfaces A. Mendelovicz, Hughes Aircraft Company, Canoga Park, CA	120
3. Design of Cylindrical Shields: An Application of the Uniform Geometrical Theory of Diffraction B. S. M. C. Galvao and C. S. Pereira, Instituto de Pesquisas Espaciais, Sao Jose dos Campos, Brazil	120
4. Radiation by Sources on Perfectly Conducting Convex Cylinders with an Impedance Surface Patch L. Ersoy and P. H. Pathak, The Ohio State University Electro-Science Laboratory, Columbus, OH	120
5. An Interpretation of Variation in the Slot Electric Field of a Slot-Perforated Dielectric-Slab-Covered Infinite Conducting Screen R. D. Nevels, Texas A&M University, College Station, TX and C. M. Butler, University of Mississippi, University, MS	121
6. Reflection and Transmission Characteristics of Multilayered Lossy Periodic Strips T. K. Wu, Lockheed Missiles and Space Company, Sunnyvale, CA	122
7. Surface-Wave Excitation on a Bonded Mesh K. F. Casey, Dikewood Corporation, Los Angeles, CA	123
8. Edge Behavior for a Thick Half Plane V. Daniele and I. Montrosset, Politecnico di Torino, Italy and P. L. E. Uslenghi, University of Illinois at Chicago Circle, Chicago, IL	124
9. An Angle Filter Containing Three Periodically Perforated, Metallic Layers E. L. Rope and G. Tricoles, General Dynamics Electronics Division, San Diego, CA	120
10. On the Response of a Terminated Twisted-Wire Cable Excited by a Plane Wave Electromagnetic Field C. D. Taylor, Mississippi State University, Mississippi State, MS and J. P. Castillo, Air Force Weapons Laboratory, Kirtland AFB, NM	125
11. New Quasistatic Representation for Sommerfeld Integrals J. N. Brittingham, G. J. Burke, Lawrence Livermore Laboratory, Livermore, CA	126

AP/B POSTER SESSION C
 THURSDAY PM 1:30-5:00
 KANE HALL - WALKER AMES ROOM

SCATTERING (continued)

	<u>Page</u>
12. Cross Polarization Discrimination Characteristics During Multipath Fading at 4 GHz S. Sakagami and K. Morita, Nippon Telegraph and Telephone Public Corporation, Yokosuka-shi, Japan	120
13. Boundary Conditions for a Thin Resistive Elliptic Cylinder R. K. Ritt, Illinois State University, Normal, IL	128
14. A Differential-Integral Method for Scattering Calculations H. C. H. Chen, University of Utah, Salt Lake City, UT M. A. Morgan, University of Mississippi, University, MS and P. W. Barber, University of Utah, Salt Lake City, UT	129
15. Receiving and Transmitting Properties of Some Reflecting Surfaces K. M. Romberg, R. L. Fante, Rome Air Development Center, Hanscom AFB, MA	120
16. Aperture Excitation of a Wire in a Rectangular Cavity W. A. Johnson, University of Mississippi, University, MS and D. G. Dudley, University of Arizona, Tucson, AZ	130
17. Space-Time Integral Equation Solution for Scattering by Thin Flat Surfaces C. L. Bennett and H. Mieras, Sperry Research Center, Sudbury, MA	120
18. An Update on Naval Vessel Identification D. L. Moffatt and C. M. Rhoads, The Ohio State University ElectroScience Laboratory, Columbus, OH	131
19. Simple Theory of Electromagnetic Shielding of Enclosures K. S. H. Lee, Dikewood Corporation, Los Angeles, CA	132
20. Loading/Imaging Effects on Resonance Region Scattering N. A. Howell, Technology Service Corporation, Santa Monica, CA	120
21. The Thickness Criterion for Single-Layer Radar Absorbents E. F. Knott, Georgia Institute of Technology, Atlanta, GA	120
22. Half-Plane Diffraction at Oblique Incidence of an Electromagnetic Plane Wave of Arbitrary Polarization G. A. Deschamps and S. W. Lee, University of Illinois, Urbana, IL	133
23. Predicting Average/Median-Value Scattering from Cylinders N. A. Howell, Technology Service Corporation, Santa Monica, CA	120

SESSION C-1
MONDAY PM 1:30-5:00
HUB 106B

HIGH TIME-BANDWIDTH PRODUCT SIGNALS: THEORY AND APPLICATIONS

Chairman: R. Price
Sperry Research Center
Sudbury, MA

	<u>Page</u>
1. Reduction of Out-of-Band Splatter of Pseudonoise Spread Spectrum C. R. Cahn, Magnavox Government and Industrial Electronics Company, Torrance, CA	135
2. Design and Application of Large Time-Frequency Coded Signal Sets G. R. Cooper, Purdue University, W. Lafayette, IN	136
3. Large Time-Bandwidth Product Signals for Spread-Spectrum Multiple-Access Communications M. B. Pursley, University of Illinois, Urbana, IL	137
4. Pseudo-Noise Matched Filters in Adaptive Arrays M. P. Ristenbatt and E. K. Holland-Moritz, University of Michigan, Ann Arbor, MI	138
5. Surface-Acoustic-Wave Convolvers for Processing Spread-Spectrum Signals R. C. Williamson, Lincoln Laboratory, Lexington, MA	139
6. Applications of Chirp Transform Networks Based on Large TB Saw Reflective Array Filters T. W. Bristol, Hughes Aircraft Company, Fullerton, CA	140
7. Chebyshev-Low Pulse Compression Sidelobes Via a Nonlinear FM R. Price, Sperry Research Center, Sudbury, MA	141

SESSION C-2
TUESDAY AM 8:30-12:00
HUB 106B

NEW SATELLITE SYSTEMS FOR THE 80's AND BEYOND

Chairman: H. Staras
RCA Laboratories
Princeton, NJ

	<u>Page</u>
1. Large Active Satellite Antennas Based on <u>Solar-Microwave Array</u> Technology (SMART) F. Sterzer, RCA Laboratories, Princeton, NJ	143
2. The Effects of Rain Attenuation on 18/30 GHz Communications Satellite Systems D. O. Reudink, Bell Laboratories, Holmdel, NJ	144
3. Some Factors that Influence EHF Satcom Systems L. J. Ricardi, MIT Lincoln Laboratory, Lexington, MA	145
4. Large Aperture Solid State Antenna for Space-Radar D. Staiman, RCA, Moorestown, NJ	146
5. A Closed Form Solution to the Problem of Adaptive Jammer Nulling H. Waldman, RCA Laboratories, Princeton, NJ	147
6. Global Planning in the Fixed-Satellite Service H. J. Weiss, COMSAT, Washington, D.C.	148

COMBINED SESSION C/E
MONDAY AM 8:30-12:00
HUB ROOM 106B

TELECOMMUNICATION SYSTEMS IN NON-GAUSSIAN ENVIRONMENTS

Chairman: J. M. Morris
Naval Research Laboratory
Washington, D.C.

	<u>Page</u>
1. Asymptotic Performance of Nonlinear Demodulators in Impulsive Noise D. F. Freeman, GTE Sylvania, Needham Heights, MA	150
2. Estimation of Mean and Standard Deviation from Quantities in Interference Modeling D. B. Sailors, Naval Ocean Systems Center, San Diego, CA	151
3. Robust Signal Detection for Asymmetric Departures from the Gaussian Noise Density S. A. Kassam and J. G. Shin, University of Pennsylvania, Philadelphia, PA	152
4. Antenna Superresolution Revisited R. L. Fante and R. V. McGahan, RADC, Hanscom AFB, MA	153
5. High Frequency Communications Enhancement Study Using Spatial Filtering Techniques P. M. Hansen and G. J. Brown, Naval Ocean Systems Center, San Diego, CA	154
6. Effects of High-Order Phase Errors on Synthetic-Aperture Radar Performance W. D. Brown, Sandia Laboratories, Albuquerque, NM	155
7. A Demodulation Method for Use in Computer Simulation of Communication System Characteristics J. M. Kelso, Honeywell, Inc., Annapolis, MD	156
8. Higher-Order Data Processing Algorithms Realizable in Optics F. P. Carlson, Oregon Graduate Center, Beaverton, OR, and R. E. Francois, Jr., Lincoln Laboratories, Lexington, MA	157
9. Measurement of Signal Strengths Transmitted by a Portable VLF Antenna at 3.125 kHz R. J. Dinger, W. D. Meyers and J. A. Goldstein, Naval Research Laboratory, Washington, D.C.	158

SESSION E
TUESDAY PM 1:30-5:00
HUB ROOM 106B

CHARACTERIZATION AND MEASUREMENT OF NOISE

Chairman: A. D. Spaulding
Office of Telecommunications
Boulder, CO

	<u>Page</u>
1. The Radio Environment at 800 km as Viewed by a DMSP Satellite C. M. Rush, R. K. Rosich and C. Mellecker, U.S. Department of Commerce, Boulder, CO	160
2. Simultaneous Radio Observations of Auroral Electrons from Satellite and Ground-Based Stations S. Y. Peng, Hughes Aircraft Co., Fullerton CA and J. S. Kim, State University of New York, Albany, NY	161
3. Rate Statistics for Radio Noise from Lightning D. M. Le Vine and R. Meneghini, NASA Goddard Space Flight Center, Greenbelt MD and S. A. Tretter, University of Maryland, College Park, MD	162
4. Amplitude Probability Distribution Measurements and Noise Excision Studies of 0.5-4.5 kHz Ambient Noise R. J. Dinger, J. R. Davis, W. D. Meyers and J. A. Goldstein, Naval Research Lab, Washington, D.C.	163
5. Distribution Pattern of Polar VLF Hiss Emission Observed by Polar Orbital Satellites T. Yoshino, University of Electro-Communications, Tokyo, Japan and H. Fukunishi, National Institute of Polar Research, Tokyo, Japan	164
6. Rocket and Balloon Observation of Power Line Radiation Over Japanese Islands T. Yoshino, I. Tomizawa and T. Shibata, University of Electro- Communications, Tokyo, Japan	165
7. Prediction of Solar Induced Currents and Effects on Power Transmission Systems in Central Canada W. R. Goddard, University of Manitoba, Winnipeg, Canada and W. M. Boerner, University of Illinois at Chicago Circle, Chicago, IL	166

SESSION F-1
MONDAY AM 8:30-12:00
KANE HALL 110

SCATTERING BY TURBULENCE

Chairman: T. E. VanZandt

NOAA, Boulder, CO

	<u>Page</u>
1. Precision of Tropospheric/Stratospheric Wind Measurements N. J. Chang, SRI International, Menlo Park, CA	168
2. Continuous Measurement of Upper Atmospheric Winds and Turbulence Using a VHF Doppler Radar: Preliminary Results W. L. Ecklund, D. A. Carter, and B. V. Balsley, NOAA, Boulder, CO	169
3. Radar Measurements of the Vertical Component of Wind Velocity in the Troposphere and Stratosphere V. L. Peterson, Centennial Sciences, Inc., Colorado Springs, CO B. B. Balsley, NOAA, Boulder, CO	170
4. Early Results from the Poker Flat MST Radar B. B. Balsley, W. L. Ecklund, D. A. Carter, P. E. Johnston, NOAA, Boulder, CO	171
5. High Resolution Wind Measurements Using the High Powered Radar at Kwajalein R. K. Crane, Environmental Research and Technology, Corcord, MA G. Weiffenbach, M.I.T. Lincoln Laboratories, Lexington, MA	172
6. An Improved Model for the Calculation of Profiles of Mean Turbulence Parameters from Background Profiles of Wind, Temperature, and Humidity T. E. VanZandt, K. S. Gage, and J. M. Warnock, NOAA, Boulder, CO	173
7. Measurements of the Phase Structure Function at 35 GHz on a 28-KM Path R. R. Rogers, McGill University, Montreal, Quebec and R. W. Lee and A. T. Waterman, Stanford University, Stanford, CA	174
8. Comstar and CTS Angle of Arrival Measurements R. A. Baxter, D. M. J. Devasirvatham, and D. B. Hodge, The Ohio State University ElectroScience Laboratory, Columbus, OH	175
9. Simultaneous Measurements of Angular Scattering and Intensity Scintillation in the Atmosphere W. A. Coles and R. Frelich, University of California at San Diego La Jolla, CA	176
10. Effect of Meteorological Variables on Radiometric Sensing of Atmospheric Temperature P. Basili, P. Ciotti, and D. Solimini, Universita di Roma, Rome, ITALY	177

COMBINED SESSION AP-S/F-2
MONDAY PM 1:30-5:00
KANE HALL 110

JOHN W. WRIGHT MEMORIAL SESSION ON RADIO OCEANOGRAPHY

Chairman: C. T. Swift
NASA Langley Research Center
Hampton, VA

	<u>Page</u>
1. Introduction C. T. Swift, NASA Langley Research Center, Hampton, VA	179
2. Review of Collaborative Efforts with Jack on Ocean Surface Physics and Radar Return O. H. Shemdin, California Institute of Technology, Pasadena, CA	180
3. Remote Sensing of the Air-Water Interface: The Legacy of John W. Wright W. J. Plant and W. C. Keller, U.S. Naval Research Laboratory Washington, DC	181
4. SAR Imaging of the Ocean Surface - an Asymtotic Eulerian Formulation G. R. Valenzuela, Naval Research Laboratory, Washington, DC	182
5. Electromagnetic Scattering Patterns from Sinusoidal Surfaces A. K. Jordan and R. H. Lang, Naval Research Laboratory, Washington, DC	183
6. Tank Measurements of Radar Return from Oil-Covered and Rain- drop Impacted Water R. K. Moore, A. K. Fung, G. J. Dome, K. Soofi and Y. S. Kim, The University of Kansas, Lawrence, KA	184
7. Modulation of Radar Backscatter by Ocean Waves W. L. Jones and A. E. Cross, NASA Langley Research Center, Hampton, VA and W. J. Plant and W. C. Keller, Naval Research Center, Washington, DC	185
8. Aircraft Radar Doppler Spectrometer and Dual Frequency Backscatter Wave Spectrometer for the Measurement of Ocean Surface Spectrum D. E. Weissman, Hofstra University, Hempstead, NY and J. W. Johnson, NASA Langley Research Center, Hampton, VA	186

SESSION F-3
TUESDAY AM 8:30-12:00
KANE HALL 110

PROPAGATION WITHIN THE EARTH

Chairman: R. G. Olsen
Washington State University
Pullman, WA

	<u>Page</u>
1. Remote Sensing of Dielectric Medium S. Coen and K. Mei, University of California, Berkeley, CA	188
2. Electromagnetic Scattering from an Earth with a Buried Cylindrical Inhomogeneity S. F. Mahmoud, Cairo University, Giza, Egypt and S. M. Ali, Military Technical College, Cairo, Egypt	189
3. Induction Sounding Response of Finite Buried Conducting Models E. A. Quincy and M. M. Rahman, University of Wyoming, Laramie WY and J. H. Richmond, Ohio State University, Columbus, OH	190
4. In Situ Microwave Measurements of Lossy Dielectrics R. J. King, C. D. Kim and J. B. Beyer, University of Wisconsin, Madison, WI	191
5. Electromagnetic Response of Ore Deposits M. Cauterman, P. Degauque and R. Gabillard, Lille University, Villeneuve d'Ascq, France	192
6. An Improvement on a Microwave Technique to Locate Economically Producibile Hydrocarbons in a Drill Hole G. S. Huchital, Schlumberger-Doll Research Center, Ridgefield, CT	193
7. Comparison of Loop and Dipole Antennas in Leaky Feeder Commu- nication Systems D. A. Hill and J. R. Wait, U.S. Department of Commerce, Boulder,CO	197
8. Bounding the Propagation Characteristics of TEM Modes in Tunnels of Arbitrary Shape D. L. Jaggard and M. F. Iskander, University of Utah, Salt Lake City, UT	198
9. Surface Transfer Impedance of a Loosely Braided Coaxial Cable R. S. Tomar and A. Paul, Indian Institute of Technology, Kanpur, India	199
10. Reconstruction Algorithms for Geophysical Applications in Noisy Environments R. D. Radcliff and C. A. Balanis, West Virginia University, Morgantown, WV	200

SESSION F-4
TUESDAY PM 1:30-5:00
KANE HALL 110

SCATTERING FROM ROUGH SURFACES

Chairman: R. H. Lang
George Washington University
Washington, D.C.

	<u>Page</u>
1. Backscattering from a Vegetated Half Space R. H. Lang, George Washington University, Washington, D.C.	202
2. Multiple Scattering Effects on Backscattering of a Pulse from Terrain A. Ishimaru, University of Washington, Seattle, WA	203
3. Polarized and Cross Polarized Scattering by an Inhomogeneous Layer with a Slightly Irregular Interface A. K. Fung and H. J. Eom, University of Kansas, Lawrence, KS	204
4. Experimental Data Matching for Active and Passive Microwave Remote Sensing J. A. Kong, M. Zuniga, L. Tsang and R. Shin, MIT, Cambridge, MA	205
5. Theoretical Models and Approaches for Active and Passive Microwave Remote Sensing J. A. Kong, L. Tsang, M. Zuniga and R. Shin, MIT, Cambridge, MA	206
6. A Radar Clutter Model: Average Radar Backscatter from Land, Sea, Snow, and Sea Ice R. K. Moore, K. Soofi and S. M. Purduski, University of Kansas Lawrence, KS	207
7. New Effects in Forward Scattering from Water Waves C. I. Beard, Naval Research Lab, Washington, D.C.	208
8. On the Role of Shadowing in Forward Scatter from the Sea at Extreme Grazing Angles L. B. Wetzel, Naval Research Lab, Washington, D.C.	209
9. Effects of Scatter Depolarization on Optical and Microwave Holographic Image Degradation H. Ghandeharian, University of British Columbia, Vancouver, Canada and W. M. Boerner, UICC, Chicago IL and University of Manitoba, Winnipeg, Canada	210
10. The Effect of Salt Solubility and Salinity on the Response of a Microwave Remote Sensor R. P. Jedlicka, New Mexico State University, Las Cruces, NM	211
11. Microwave Remote Sensing of Saline Seeps K. R. Carver, New Mexico State University, Las Cruces, NM	212

SESSION F-5
WEDNESDAY PM 2:00-5:30
KANE HALL 110

EARTH-SPACE PROPAGATION

Chairman: D. C. Cox
Bell Labs
Holmdel, NJ

	<u>Page</u>
1. A Summary of Rain Attenuation Experiments on Earth-Satellite Paths in Georgia and Illinois S. H. Lin, J. H. Bergmann and M. V. Pursley, Bell Labs, Holmdel, NJ	214
2. COMSTAR 19-GHz Beacon Reception at Spaced Locations in Tampa, Florida D. D. Tang and D. Davidson, GTE labs, Waltham MA and S. C. Bloch University of South Florida, Tampa, FL	215
3. Observations of Orientation-Dependent Depolarization of 19 GHz Earth-Space Signals by Atmospheric Hydrometeors H. W. Arnold, D. C. Cox, H. H. Hoffman and R. P. Leck, Bell Labs, Holmdel, NJ	216
4. Update of the Results of the 28.56 GHz COMSTAR Experiment at Wallops Island, Virginia J. Goldhirsh, Johns Hopkins University, Laurel, MD	217
5. Measurement of Rain Attenuation and Depolarization of the CTS Satellite Beacon Signal at Holmdel, New Jersey A. J. Rustako, Jr., Bell Labs, Holmdel, NJ	218
6. Depolarization Measurement at Various Locations Across Canada Using the 11.7 GHz CTS Beacon J. J. Schlesak, J. I. Strickland and W. L. Nowland, Communications Research Centre, Ottawa, Canada	219
7. Some Measurement of CTS 11.7 GHz Cross Polarization Comparing a Fixed and an Adjustable Polarization Receiver W. J. Vogel, University of Texas, Austin, TX	220
8. CTS Beacon Rain Attenuation Measurements D. Davidson and O. G. Nackoney, GTE Labs, Waltham MA	221
9. Summary of 1978 Attenuation and Depolarization Measurements Made with the CTS (11.7 GHz) and COMSTAR (19.04 and 28.56 GHz) Beacons C. W. Bostian, W. L. Stutzman, E. A. Muus, P. H. Wiley, R. E. Marshall and P. Santago, Virginia Polytechnic Institute and State University, Blacksburg, VA	222
10. Cumulative Statistics of 11.7 and 28.56 GHz Rain Attenuation From CTS and COMSTAR Satellite Beacon Measurements L. J. Ippolito, NASA Goddard Space Flight Center, Greenbelt, MD	223

SESSION F-6
 THURSDAY AM 8:30-12:00
 KANE HALL 110

PART I: PROPAGATION ABOVE THE SURFACE: MODES AND RAYS

Chairman: R. J. King
 University of Wisconsin
 Madison, WI

	<u>Page</u>
1. Zenneck-Like Wave for the Spherical Earth K. Mano, Deputy for Electronic Technology RADC, Hanscom AFB, MA	225
2. An Experimental Study of Surface Wave Propagation on a Low Permittivity Medium J. Appel-Hansen, Technical University of Denmark, Lyngby, Denmark and R. J. King, University of Wisconsin, Madison WI	226
3. RF Ray Tracing in an Atmospheric Ducting Environment F. T. Wu, W-M P. Yu and A. Shlanta, Naval Weapons Center, China Lake, CA	227
4. Hybrid Ray-Mode Formulation of Propagation in a Tropospheric Duct S. H. Cho, G. Migliora and L. B. Felsen, Polytechnic Institute of New York, Farmingdale, NY	228
5. A Numerical Study of Tropospheric Ducting at HF C. L. Goodhart and R. A. Pappert, Naval Ocean Systems Center, San Diego, CA	229
6. A New Set of Solutions for the Modal Equation for Propagation in a Trilinear Tropospheric Duct R. H. Ott, U.S. Department of Commerce, Boulder, CO	230

PART II: SCATTERING BY SNOW AND ICE

1. Measurement of the Microwave Properties of Sea Ice at 90 GHz and Lower Frequencies B. E. Troy, J. P. Hollinger, R. M. Lerner and M. M. Wisler, Naval Research Lab, Washington, D.C.	231
2. Aircraft Microwave Radar and Radiometric Measurements of the Electromagnetic Properties of Lake Ice C. T. Swift, R. F. Harrington, J. C. Fedors and W. L. Jones, NASA Langley Research Center, Hampton, VA	232
3. Experimental Evaluation of the Microwave Response to Snow F. T. Ulaby and W. H. Stiles, University of Kansas, Lawrence KS	233
4. Characterization of Polar Terrain Features Through Satellite Microwave Radiometry S. R. Rotman, A. D. Fisher and D. H. Staelin, MIT, Cambridge, MA	234
5. Emission from a Snow Layer with a Slightly Irregular Interface A. K. Fung and M. F. Chen, University of Kansas, Lawrence, KS	235

SESSION F-7
THURSDAY PM 1:30-5:00
KANE HALL 110

RADIOOCEANOGRAPHY

Chairman: J. R. Apel
NOAA
Seattle, WA

	<u>Page</u>
1. Radar Altimetry for Use in Measuring Sea Surface Slope H. M. Byrne, NOAA, Seattle, WA	237
2. The SEASAT Radar Altimeter - A Study of Wave Height Measurements L. S. Fedor and J. A. Leise, NOAA, Boulder, CO	238
3. The Computation of Wind Speed and Wave Heights from GEOS 3 Data N. Mognard, JISAO, Seattle, WA and B. Lago, GRGS-CNES, Toulouse, France	239
4. Air Sea Temperature Difference Effects on Microwave Scattering W. C. Keller and W. J. Plant, Naval Research Lab, Washington, DC	240
5. Double-Modulation Experiments on Ocean Wave Systems Using a Dual-Frequency Microwave Radar D. L. Schuler and W. J. Plant, Naval Research Lab, Washington, DC	241
6. Side-Looking Radar Images of Dispersive, Homogeneous Waves R. O. Harger, University of Maryland, College Park, MD	242
7. Measurement of Surface Roughness from Nadir Using Dual Frequency Correlation and Spatial Resolution with a S.A.R. Chirped Signal D. E. Weissman, Hofstra University, Hempstead, NY, J. W. Johnson and W. L. Jones, N.A.S.A. Langley Center, Hampton, VA, and W. F. Townsend, N.A.S.A. Wallops Flight Center, Wallops, VA	243
8. Synthetic Aperture Radar Imagery of Moving Ocean Waves C. L. Rufenach, NOAA, Boulder, CO and W. R. Alpers, University of Hamburg & Max-Planck-Institute of Meteorology, Hamburg, West Germany	244
9. SeaSat-A Synthetic Aperture Radar Imagery of Ocean Waves F. I. Gonzalez, R. A. Schuchman, D. R. Ross, J. F. R. Gower, and C. Rufenach, NOAA, Seattle, WA and Boulder, CO	245
10. Synthetic Aperture Radar Observations at Various Aspects of Ocean Waves J. F. Vesecky and H. Assal, Stanford University, Stanford, CA and R. H. Stewart, University of California, La Jolla, CA	246

SESSION F-8
FRIDAY AM 8:30-12:00
KANE HALL 110

PROPAGATION MODELING

Chairman: W. J. Vogel
University of Texas
Austin, TX

	<u>Page</u>
1. Effective Path Length and the Frequency Scaling of Rain Attenuation H. N. Kheirallah, Carleton University, Ottawa, Canada and R. L. Olsen, Communications Research Centre, Ottawa, Canada	248
2. The Impact of Uncertainties in Rain Fade Estimates on the Design of 20/30 GHz Satellite Communication Systems R. R. Persinger, Hughes Aircraft Co., Los Angeles, CA and W. L. Stutzman, Virginia Polytechnic Institute and State University, Blacksburg, VA	249
3. Prediction of Rain-Induced Fades Along Earth-Space Millimeter Wave Links W. L. Stutzman, Virginia Polytechnic Institute and State University, Blacksburg, VA and R. R. Persinger, Hughes Aircraft Co., Los Angeles, CA	250
4. Global Rain Attenuation Model R. K. Crane, Environmental Research & Technology, Inc., Concord, MA	251
5. Measurement of Cloud Liquid Content Using the 28 GHz COMSTAR Beacon J. B. Snider, NOAA, Boulder, CO	252
6. Phase and Amplitude Dispersion for Earth-Space Propagation in the 20 to 30 GHz Frequency Range D. C. Cox, H. W. Arnold and R. P. Leck, Bell Labs, Holmdel, NJ	253
7. Microwave Depolarization of an Earth-Space Path T. S. Chu, Bell Labs, Holmdel, NJ	254
8. Multiple Scattering of Millimeter Waves in Rain R. L.-T. Cheung and A. Ishimaru, University of Washington, Seattle, WA	255
9. Effect of Adverse Sand-Storm Media on Microwave Propagation H. T. Al-Hafid and S. C. Gupta, Mosul University, Mosul, Iraq and K. Buni, Iraqi Ministry of Telecommunications, Baghdad, Iraq	256
10. QPM-Digital Signal Multipath Fading H. S. Hayre, University of Houston, Houston, TX	257

SESSION G-1
MONDAY PM 1:30-5:00
HUB 309A

DIAGNOSTICS, EFFECTS, AND MODIFICATIONS OF THE IONOSPHERE

Chairman: E. J. Fremouw
Physical Dynamics Inc.
Bellevue, WA

	<u>Page</u>
1. Which Ionospheric Parameters can we Really Measure with Incoherent Scatter Radar? J. B. Hagen, National Astronomy and Ionosphere Center, Arecibo, Puerto Rico	259
2. Long-Term Observation of Polar D-Region Ionization W. J. Helms, University of Washington, Seattle, WA and A. S. Chandler, John Fluke Manufacturing Company, Mountlake Terrace, WA	260
3. Backscatter Inversion in Spherically Asymmetric Ionosphere R. E. DuBroff, Phillips Petroleum Company, Bartlesville, OK and N. N. Rao and K. C. Yeh, University of Illinois at Urbana-Champaign, Urbana, IL	261
4. Specific Properties of Backscattering of Radio Waves on Magneto-Oriented Ionospheric Irregularities at Frequencies below Critical Frequency S. A. Namazov, Institute of Radioengineering and Electronics, Moscow, USSR, and Yu. A. Kravtsov, The Moscow Lenin State Teacher's Training Institute, USSR	262
5. Effects of Magnetospheric Disturbances on the Geoelectric Field in Sub-Auroral Regions and its Interaction with HV-DC/AC Electrical Power Lines W. M. Boerner, U.I.C.C., Chicago, IL and University of Manitoba, Winnipeg, Canada, J. Cole, U.I.C.C., Chicago, IL, D. E. Olson, University of Minnesota, Duluth, MN, W. R. Goddard, and D. H. Hall, University of Manitoba, Winnipeg, Canada	266
6. An Update of the Program to Assess the Impact of the Operation of the Satellite Power System C. M. Rush, U. S. Department of Commerce, Boulder, CO	267

SESSION G-2
TUESDAY AM 8:30-12:00
HUB 309-A

TRANSMISSION AND IN-SITU MEASUREMENTS OF NATURAL AND ENHANCED
IONOSPHERIC IRREGULARITIES

Chairman: C. Rino
Stanford Research Institute
Menlo Park, CA

	<u>Page</u>
1. On the Ratio of Intensity and Phase Scintillation Indices E. J. Fremouw, Physical Dynamics, Inc., Bellevue, WA	269
2. Longitudinal Sensitivity of Equatorial Scintillation as Discovered in the 1978 Equatorial Scintillation Campaign J. P. Mullen, H. E. Whitney, J. Aarons, Air Force Geophysics Laboratory, Hanscom AFB, MA and K. C. Yeh, University of Illinois, Urbana, IL	270
3. Observations of Ionospheric Bubbles at the Magnetic Equator C. H. Liu, K. C. Yeh, University of Illinois, Urbana, IL and H. Soicher, U. S. Army Communication Research and Development Command, Fort Monmouth, NJ	271
4. Direct Comparison of In-Situ Plasma Density and VHF/UHF Phase Scintillation Measurements M. Kelley, Cornell University, Ithaca, NY, D. L. Knepp, Mission Research Corporation, Santa Barbara, CA and K. D. Baker, Utah State University, Logan UT	272
5. On the Signal Statistics of Scintillation E. J. Fremouw, Physical Dynamics, Inc., Bellevue, WA	273
6. Signal Coherence Properties Obtained from Wideband Satellite Data D. L. Knepp, Mission Research Corporation, Santa Barbara, CA	274
7. Some Characteristics of Phase and Intensity Scintillation in Alaska E. J. Fremouw and J. M. Lansinger, Physical Dynamics, Inc., Bellevue, WA	275

SESSION G-3
TUESDAY PM 1:30-5:00
HUB 309-A

POLARIZATION EFFECT AND LARGE-SCALE STRUCTURES OF THE IONOSPHERE

Chairman: J. Aarons
Air Force Geophysics Laboratory
Hanscom AFB, MA

Page

1. Distortion and Depolarization by the Ionosphere of L. Band Signals Coded by Phase Reversals: Full Wave Solutions
E. Bahar and B. S. Agrawal, University of Nebraska, Lincoln, NE 277
2. Antenna Polarization Considerations for HF Broadcast Systems Near the Geomagnetic Equator
P. M. Hansen, W. J. Fay, Naval Ocean Systems Center, San Diego, CA 278
3. A New Approach Based on Physical Optics for Computing Field Strengths in the Region of a Caustic with a Comparison with Full Wave Theory in the Region of the Ionospheric Skip
H. Hoogasian, GTE Sylvania, Needham, MA, D. B. Odom and T. I. S. Boak, III, Raytheon Company, Wayland, MA 279
4. Concave-Mirroring by Curved Field-Aligned Irregularities in the F Region
J. A. Ferguson, Naval Ocean Systems Center, San Diego, CA and H. G. Booker, University of California, San Diego, La Jolla, CA 280
5. Estimation of the Effects of Horizontal Gradients in Refractive Index on Ionospheric Propagation Parameters
S. Silven, GTE Sylvania Incorporated, Mountain View, CA 281
6. A Study of the Propagation and Dispersion of Traveling Ionospheric Disturbances
K. A. Ballard and M. G. Morgan, Dartmouth College, Hanover, NH 282

SESSION H
WEDNESDAY PM 2:00-5:30
HUB 106-B

OBSERVED AND PREDICTED PHENOMENA IN LABORATORY AND NATURAL PLASMAS

Chairman: F. W. Crawford
Stanford University
Stanford, CA

	<u>Page</u>
1. A Method for the Evaluation of Solar Coronal Plasma Propagation Speeds by Radio Occultation of Space Probes E. Luneburg, Institut fur Hochfrequenztechnik, Oberpfaffenhofen, West Germany, P. B. Esposito, Jet Propulsion Laboratory, Pasadena, CA	284
2. Some Features of Pararesonance (PR) Whistlers M. G. Morgan, Dartmouth College, Hanover, NH	285
3. Dispersion Characteristics of Plasma Wave- Packets R. J. Vidmar and F. W. Crawford, Stanford University, Stanford, CA	286
4. Transmission and Reflection of Waves from a Magnetoplasma by an Invariant Method H. C. Chen, Ohio University, Athens, OH	287
5. Resonant Absorption of Radiation in the Sheath of a Cold Plasma Surrounding a Wire Carrying a Prescribed Periodic Driving Current M. P. H. Weenink and S. Nagarajan, Technische Hogeschool Eindhoven, The Netherlands	288
6. Electromagnetic Pulse (EMP) Propagation Through a Plasma R. N. Carlile, A. Cavalli, W. L. Cramer, M. E. Dunham, and W. A. Seidler, University of Arizona, Tucson, AZ	289
7. Fluid Theory of Plasma Double-Layers J. S. Levine and F. W. Crawford, Stanford University, Stanford, CA	290
8. Nonlinear Effects in Waveguide Excitation of Lower Hybrid Waves R. W. Motley and W. M. Hooke, Princeton University, Princeton, NJ	291
9. Amplitude and Phase Modulation of a Wave due to Nonlinear Wave-Wave Interactions Y. C. Kim and E. J. Powers, University of Texas at Austin, Austin, TX	292

SESSION NL-1
THURSDAY AM 8:45-11:50
HUB ROOM 106B

NONLINEAR ELECTROMAGNETICS I

Plenary Session, Co-Sponsored by AP-S, URSI COMMISSIONS B, D, and H
and the Bioelectromagnetics Society

INVITED PAPERS

Organizer: P. L. E. Uslenghi

Chairman: N. Marcuvitz
Polytechnic Institute of New York
Farmingdale, NY

	<u>Page</u>
1. Introductory Remarks P. L. E. Uslenghi, University of Illinois at Chicago Circle, Chicago, IL	294
2. History of the Solitary Wave A. C. Scott, University of Wisconsin, Madison, WI	295
3. Solitons as Particles and as Collective Excitations D. W. McLaughlin, University of Arizona, Tucson AZ	296
4. Quasiparticle Method in Nonlinear Wave Propagation N. Marcuvitz, Polytechnic Institute of New York, Farmingdale, NY	297
5. Lagrangian Methods in Nonlinear Plasma Wave Interaction F. W. Crawford, Stanford University, Stanford, CA	298
6. Nonlinear Interactions Between Electromagnetic Waves and Biological Materials in the Frequency Range Below 10GHz F. S. Barnes, University of Colorado, Boulder, CO	299

SESSION NL-2

(Co-sponsored by B and BEMS)

THURSDAY PM 1:30-5:00

HUB 106B

NONLINEAR ELECTROMAGNETICS II

Co-chairmen: F. S. Barnes, University of Colorado, Boulder, CO
W. R. Adey, Veterans Administration, Loma Linda, CA

	<u>Page</u>
1. Biological Sensors for the Detection of Electric and Magnetic Fields A. J. Kalmijn, Woods Hole Oceanographic Institution, Woods Hole, MA	301
2. The Sensitivity of Biochemical Reactions to Weak Oscillating Stimuli L. K. Kaczmarek, California Institute of Technology, Pasadena CA	302
3. Low Frequency Electromagnetic Induction of Electrochemical Information at Living Cell Membranes: A New Tool for the Study and Modulation of the Kinetics of Cell Function A. A. Pilla, Columbia University, New York, NY	303
4. Nonlinear Impedance and Low Frequency Resonance of Polyelectrolyte Under High Sinusoidal Fields C. J. Hu, University of Colorado, Boulder, CO	304
5. Neuronal Membranes as Detectors of RF Fields H. Wachtel, Duke University, Durham, NC	307
6. A Nonlinear Microwave Radiation Effect on the Passive Efflux of Sodium and Rubidium from Rabbit Erythrocytes R. B. Olcerst, New York University Medical Center, New York, NY	308
7. Induction of Calcium Ion Efflux from Brain Tissue by R. F. Radiation: Effect of Sample Number and Modulation Frequency on the Field-Strength Window C. F. Blackman, S. G. Benane, J. A. Elder, D. E. House, J. A. Lampe and J. M. Faulk, US Environmental Protection Agency Research Triangle Park, NC	309
8. Nonlinear Mechanisms in Electrical Transductive Coupling at Nerve Cell Membranes A. R. Sheppard and W. R. Adey, VA Medical Center, Loma Linda, CA and Loma Linda University School of Medicine, Loma Linda, CA	310

SESSION NL-3
 (Cosponsored by AP-S and B)
 FRIDAY AM 8:30-12:00
 HUB 106B

NONLINEAR ELECTROMAGNETICS III
 Organizer: P. L. E. Uslenghi
 Chairman: A. C. Scott
 University of Wisconsin
 Madison, WI

	<u>Page</u>
1. Analysis of Mild Nonlinearities in Electromagnetic Systems Using the Volterra-Series Approach T. K. Sarkar, Rochester Institute of Technology, Rochester, NY and D. D. Weiner, Syracuse University, Syracuse, NY	312
2. Nonlinearly Loaded Antennas G. Franceschetti, University of Illinois at Chicago Circle and University of Naples, Italy	313
3. The Characteristics of a Traveling-Wave, Linear Antenna with a Nonlinear Load M. Kanda, National Bureau of Standards, Boulder, CO	314
4. A Time-Domain Computer Code for Nonlinear Circuits and Thin- Wire Antennas J. A. Landt, Los Alamos Scientific Laboratory, Los Alamos, NM	315
5. Transient Corona Effects on Long Wire Antennas K. C. Chen, J. P. Castillo, C. E. Baum and H. A. Goodwin, Air Force Weapons Laboratory, Kirtland AFB, NM and P. S. Book, Kaman Sciences Corporation, Colorado Springs, CO	316
6. The Inverse Problem for a Nonuniform and Nonlinear Transmission Line C. Q. Lee, B. C. Phan and P. L. E. Uslenghi, University of Illinois at Chicago Circle, Chicago, IL	317
7. Bispectral Study of Nonlinear Wave-Wave Interactions E. J. Powers and Y. C. Kim, University of Texas at Austin, Austin, TX	318
8. Solitons in Randomly Inhomogeneous Media I. M. Besieris, Virginia Polytechnic Institute and State University, Blacksburg, VA	319
9. The Effects of Dielectric and Soil Nonlinearities on the Electromagnetic Transient Response of Cables Lying on the Surface of the Earth R. A. Perala and R. B. Cook, Electro Magnetic Applications, Inc., Golden, CO	320
10. Variation of the Internal Electric Field in a Steel Cylinder Resulting from an Impulse Surface Current W. J. Croisant and P. Nielsen, U.S. Army Construction Engineering Research Laboratory, Champaign, IL	321

SESSION NL-3
FRIDAY AM 8:30-12:00
HUB 106B

NONLINEAR ELECTROMAGNETICS III (continued)

	<u>Page</u>
11. The Geometric Optics in Non-Linear Wave Theory A. B. Shvartsburg, IZMIRAN, Academgorodok, Moscow Region, USSR	322
12. The Non-Linear Resonances in the Lower Ionosphere A. B. Shvartsburg, IZMIRAN, Academgorodok, Moscow Region, USSR	323

SESSION BEMS - 1
MONDAY AM 8:30-10:00
HUB AUDITORIUM

OPENING SESSION

Chairperson: A. W. Guy
University of Washington
Seattle, WA

Page

WELCOMING REMARKS

- | | | |
|----|---|-----|
| 1. | A. W. Guy, Chairman, Technical Program Committee | 325 |
| 2. | R. Baird, Chairman, Commission A. USNC/URSI | 325 |
| 3. | E. L. Alpen, President, The Bioelectromagnetics Society | 325 |

ADDRESSES

- | | | |
|----|---|-----|
| 1. | Keynote Address, W. A. Goeffrey Voss
From Mice to Man | 325 |
| 2. | USA-USSR EM Research Exchange Program: Progress Report,
D. I. McRee, USA
M. G. Shandala, USSR | 325 |
| 3. | EM Research Program: Institute of Biological Physics,
Academy of Sciences, USSR
I. G. Akoev, USSR | 325 |

SESSION BEMS - 2
MONDAY AM 10:20-11:50
HUB AUDITORIUM

THERMOREGULATION

Chairperson: D. R. Justesen
Veterans Administration Medical Center
Kansas City, MO

	<u>Page</u>
L. Metabolic and Physical Scaling in Microwave/Radiofrequency Bioeffects Studies Sol M. Michaelson and Shin-Tsu Lu, University of Rochester School of Medicine and Dentistry, Rochester, NY	327
2. Differential Heating of the Cortex, Hypothalamus and Rectum in Three Species by 2450-MHz Microwaves Virginia Bruce-Wolfe, Dennis L. Reeves and Don R. Justesen, Veterans Administration Medical Center, Kansas City, MO	328
3. Thermal Effects on Colonic and Regional Brain Temperature in Unanesthetized Rats Exposed to 2450 MHz CW Microwaves W. M. Williams, Shin-Tsu Lu, and S. M. Michaelson, University of Rochester School of Medicine and Dentistry, Rochester, NY	329
4. Modification of Microwave Biological End-Points by Increased Resting Metabolic Heat Load in Rats Shin-Tsu Lu, Nancy Lebda, Sue Pettit, and Sol M. Michaelson, University of Rochester School of Medicine and Dentistry, Rochester, NY	330
5. Microwave Modification of Thermoregulatory Behavior: Threshold and Suprathreshold Effects Eleanor R. Adair, John B. Pierce Foundation Laboratory and Yale University, New Haven, CT	331
6. Microwaves Affect Thermoregulatory Behavior in Rats S. Stern, L. Margolin, B. Weiss, S.-T. Lu, S. M. Michaelson School of Medicine and Dentistry, University of Rochester, Rochester, NY	332

SESSION BEMS - 3
MONDAY PM 1:30-3:00
HUB AUDITORIUM

NERVOUS SYSTEM

Chairperson: R. H. Lovely
University of Washington
Seattle, WA

	<u>Page</u>
1. Microwave Effect on the Parameters of the Model Synaptic Membrane O. V. Kolomitkin, V. I. Kuznetsov, and I. G. Akoev, Institute of Biological Physics, USSR Academy of Sciences, Pushchino Moscow Region 142292, USSR	334
2. Evidence of Neuropathology in Chronically Irradiated Hamsters by 2450 MHz Microwaves at 10mW/cm ² Ernest N. Albert, George Washington University Medical Center, Washington, DC	335
3. Elimination of Microwave Effects on the Vitality of Nerves After Active Transport Has Been Blocked Donald I. McRee, National Institute of Environmental Health Sciences, Research Triangle Park, NC and Howard Wachtel, Duke University, Durham, NC	336
4. Effects of Radio Frequency Fields on the EEG of Rabbit Brains Shiro Takashima and Herman P. Schwan, University of Pennsylvania Philadelphia, PA	337
5. In Vitro Study of Microwave Effects on Calcium Efflux in Rat Brain Tissue W. W. Shelton, Jr., Florida Institute of Technology, Melbourne, FL and J. H. Merritt, USAF School of Aerospace Medicine, Brooks AFB, TX	338
6. Retinal Ganglion-Cell Activity Induced by ELF-Fields P. Lövsund, P. A. Öberg and S. E. G. Nilsson, Linköping University, Linköping, Sweden	339

SESSION BEMS - 4
MONDAY PM 3:20-4:50
HUB AUDITORIUM

PHYSIOLOGY

Chairperson: J. A. Elder
Environmental Protection Agency
Research Triangle Park, NC

	<u>Page</u>
1. Bioeffects at the Impact of Low Level Electromagnetic Micro-wave Field of 9400 MHz Yu. D. Dumansky, N. G. Nikitina, I. P. Loss, L. A. Tomashewskaya, E. R. Holyavko, L. G. Andrienko, S. A. Lyubchenko, S. V. Zotov Kieve A. N. Marzeev Scientific Research Institute of General and Communal Hygiene, Kieve, USSR	341
2. Microwave Short-Time Exposure Effect on Gonads A. Ch. Achmadieva, E. N. Smirnova, and I. G. Akoev, Institute of Biological Physics, USSR Academy of Sciences, Pushchino Moscow Region 142292, USSR	342
3. Changes in the Electrocardiograms of Rats and Dogs Exposed to DC Magnetic Fields C. T. Gaffey and T. S. Tenforde, Lawrence Berkeley Laboratory, University of California, Berkeley, CA	343
4. Cardiovascular Response of Rats Exposed to 60-Hz Electric Fields D. I. Hilton and R. D. Phillips, Pacific Northwest Laboratory, Richland, WA	344
5. Dual Actions of Microwaves on Serum Corticosterone in Rats Shin-Tsu Lu, S. Pettit and S. M. Michaelson, University of Rochester School of Medicine and Dentistry, Rochester, NY	345
6. Endocrine Function in Rhesus Monkeys and Rats Exposed to 1.29 GHz Microwave Radiation W. G. Lotz, Naval Aerospace Medical Research Laboratory, Naval Air Station, Pensacola, FL	346

SESSION BEMS - 5
TUESDAY AM 8:30-10:00
HUB AUDITORIUM

THEORETICAL/EXPERIMENTAL DOSIMETRY (I)

Chairperson: R. A. Tell
Environmental Protection Agency
Las Vegas, NEV

	<u>Page</u>
1. Measurements of the RF Power Absorption in Human and Animal Phantoms Exposed to Near-Field Radiation J. F. Iskander, H. Massoudi, C. H. Durney, University of Utah, Salt Lake City, Utah and S. J. Allen, U.S.A.F. School of Aerospace Medicine, Brooks Air Force Base, TX	348
2. Real Time Measurement of RFR Energy Distribution in the Macaca Mulatta Head J. G. Burr and J. H. Drupp, USAF School of Aerospace Medicine, Brooks Air Force Base, TX	349
3. A Method of Calculating Electromagnetic Absorption Under Near-Field Exposure Conditions I. Chatterjee, O. P. Gandhi, M. J. Hagmann, and A. Riazi, University of Utah, Salt Lake City, UT	350
4. Near-Field Irradiation of Cylindrical Models of Humans and Animals C. K. Han, M. F. Iskander, C. H. Durney, and H. Massoudi, University of Utah, Salt Lake City, UT	351
5. Experimental and Analytical Study on Interaction Between Near-Zone EM Field of CB-Radio Antenna and Human Body K. Karijullah, D. P. Nyquist, and Kun-Mu Chen, Michigan State University, East Lansing, MI	352
6. A Thermal Model of the Human Body Exposed to an Electromagnetic Field D. M. Deffenbaugh, R. J. Spiegel, and J. E. Mann, Southwest Research Institute, San Antonio, TX	353

SESSION BEMS - 6
TUESDAY AM 10:20-11:50
HUB AUDITORIUM

THEORETICAL/EXPERIMENTAL DOSIMETRY (II)

Chairperson: J. C. Mitchell
USAF School of Aerospace Medicine
Brooks AFB, TX

	<u>Page</u>
1. Far-Field Microwave Dosimetry in a Rhesus Monkey Model R. G. Olsen, T. A. Griner, and G. D. Prettyman, Naval Aerospace Medical Research Laboratory, Pensacola, FL	355
2. A System for Determining the Radiofrequency Absorption Coefficient of the Human Body in the High Frequency Band D. A. Hill, Defence Research Establishment, Ottawa, Canada H. M. Assenheim, G. W. Hartsgrove, National Research Council of Canada, Ottawa, Canada and G. A. Grant, Scientific Consultant LTD, Ottawa, Ontario	356
3. Electromagnetic Absorption in Multilayered Cylindrical Models of Man H. Massoudi, C. H. Durney, P. W. Barber, and M. F. Iskander, University of Utah, Salt Lake City, UT	357
4. Electromagnetic Interaction with Human Phantom Models; Applications to Mobile Radios L. H. Belden, Major Appliance Laboratories, Louisville, KY and J. A. Bergeron, Corporate Research and Development, Schenectady, NY	358
5. Modification of the Extended Boundary Condition Method for Models of Man at and Above the Resonant Frequency M. J. Hagmann, F. S. Stenger, and P. W. Barber, University of Utah, Salt Lake City, UT	359
6. Electric and Magnetic Field Intensities and Associated Induced Body Currents in Man in Close Proximity to a 50 kW AM Standard Broadcast Station R. A. Tell and E. D. Mantiplly, Electromagnetic Radiation Analysis Branch, Las Vegas, NV, C. H. Durney and H. Massoudi, University of Utah, Salt Lake City, UT	360

SESSION BEMS - 7
WEDNESDAY PM 2:00-4:35
HUB AUDITORIUM

BLOOD BRAIN BARRIER

Chairperson: E. L. Hung
Walter Reed Army Institute of Research
Washington, DC

	<u>Page</u>
1. Is the Blood-Brain Barrier Altered by RF Irradiation? D. H. Spackman, V. Riley, Pacific Northwest Research Foundation and Fred Hutchinson Cancer Research Center, Seattle, WA A. W. Guy and C. K. Chou, The University of Washington, Seattle, WA	362
2. Cerebrovascular Permeability to ¹⁴ C-Sucrose in the Rat Following 2450 MHz CW Microwave Irradiation E. Preston and G. Prefontaine, Division of Biological Sciences, National Research Council of Canada, Ottawa, Canada	363
3. Studies on Microwave and Blood-Brain Barrier Interactions J. C. Lin and M. F. Lin, Department of Electrical Engineering and Department of Physical Medicine and Rehabilitation, Wayne State University, Detroit, MI	364
4. Effect of Low-Level Microwave Irradiation on the Uptake of Horseradish Peroxidase by Synaptosomes L. M. Irwin, J. L. Lords and C. H. Durney, Departments of Biology and Electrical Engineering, University of Utah, Salt Lake City, UT	365
5. Drug Studies of MWR Effects on the Blood Brain Barrier R. M. Lebovitz, Department of Physiology, University of Texas, Dallas, TX	366
6. Effects of Low Power Microwaves on the Local Cerebral Blood Flow of Conscious Rats K. J. Oscar, U.S. Army Mobility Equipment Research and Development Command, Fort Belvoir, VA and Department of Physics, American University, Washington, DC S. P. Gruenau, M. Folker, Behavioral Sciences Department, Naval Medical Research Institute, Bethesda, MD S. I. Rapoport, Laboratory of Neurosciences, National Institute on Aging, Gerontology Research Center, Baltimore City Hospital, Baltimore, MD	367
7. Ultrastructural Neuropathology in Areas of Increased Blood-Brain Permeability after Microwave Irradiation E. N. Albert, Department of Anatomy, George Washington University Medical Center, Washington, DC	368
8. Microwave Fever: An Attempt to Transfer Pneumococcal Antibody Across the Cerebrospinal-Fluid (CSF) Barrier G. R. Hodges, S. E. Worley, D. L. Reeves, Veterans Administration Medical Center, Kansas City, MO D. R. Justesen, University of Kansas School of Medicine, Kansas City, KS	369

SESSION BEMS - 7
WEDNESDAY PM 2:00-4:35
HUB ADUITORIUM

BLOOD BRAIN BARRIER (Continued)

Page

9. The Effect of Power Deposition Rate on Blood-Brain Barrier Disruption
C. H. Sutton, Q. Balzano, F. B. Carroll, University of Miami School of Medicine, Miami, FL and Motorola, Inc., Plantation, FL

370

SESSION BEMS - 8
THURSDAY AM 8:30-10:15
HUB AUDITORIUM

DIELECTRIC PROPERTIES: PHYSICAL MEASUREMENT

Chairperson: J. C. Lin
Wayne State University
Detroit, MI

	<u>Page</u>
1. Tissue Impedance Measurements Using the Microwave Network Analyzer J. R. Schepps, K. R. Foster, Department of Bioengineering/D2, University of Pennsylvania, Philadelphia, PA A. W. Friend, Jr., Naval Medical Research Institute, Bethesda, MD	372
2. Microwave Dielectric Absorption of Muscle Tissue: Evidence for Multiple Absorption Mechanisms between 1 and 18 GHz K. R. Foster, J. L. Schepps, H. P. Schwan, Department of Bioengineering/D2, University of Pennsylvania, Philadelphia, PA	373
3. Electromagnetic Dosimetry: Development of Analysis and Measurement Techniques for Three-Dimensional Complex-Shaped Dielectric Bodies E. C. Burdette, F. L. Cain, and J. J. Wang, Electromagnetic Effectiveness Division, Georgia Institute of Technology, Atlanta, GA	374
4. Automated Dielectric Measurements with a Small Monopole Impedance Probe T. W. Athey, Bureau of Radiological Health, Rockville, MD	375
5. A Temperature Monitor for Microwave Bioeffects Research and Electrothermia Therapy R. R. Bowman, Vitek, Inc., Boulder, CO	376
6. Measurement of Electric and Magnetic Field Strengths from Industrial Radiofrequency (6-38 MHz) Plastic Sealers D. L. Conover, W. E. Murray, Jr., E. D. Foley, J. M. Lary, and W. H. Parr, National Institute for Occupational Safety and Health, U.S. Department of Health, Education, and Welfare, Cincinnati, OH	377
7. Electromagnetic Hazards in Safety Zone of Radio- and TV Transmitters H. R. Korniewicz, Centralny Instytut Ochrony Pracy, Warszawa, Poland	378

SESSION BEMS - 9
THURSDAY AM 10:35-11:50
HUB AUDITORIUM

SPECIAL TOPICS

Chairman: E. N. Albert
George Washington University
Washington, DC

	<u>Page</u>
1. Immunological Effects of Low Microwave Exposure M. G. Shandala, M. I. Rudnev, G. I. Vinigradov, N. G. Belonozhko, N. M. Gonchar, Kieve Research Institute of General and Municipal Hygiene after A. N. Marzeev, Kiev, USSR	380
2. Microwave Effect on Lipid Bilayer Modified by Polyene Anti- biotics V. V. Tyashelov, S. I. Alekseev, and V. I. Mirutenko, Institute of Biological Physics, USSR Academy of Sciences, Pushchino Moscow Region, USSR	381
3. The Biological Effects of the Low Frequency Electromagnetic Field (50 Hz) M. G. Shandala, Yu. D. Dumansky, Ye. V. Prohvatilo, I. P. Loss, L. A. Tomashewskaya, S. A. Lyubchenko, I. S. Bezdolnaya, Yu. I. Vasilenko, Kieve A. N. Marzeev Scientific Research Institute of General and Communal Hygiene, Kiev, USSR	382
4. The Possible Mechanisms of the Biological Effects of the Electromagnetic Fields of Low Frequency G. I. Evtushenko and F. A. Kolobub, Kharkov Research Institute of Labour Hygiene and Occupational Diseases, Kharkov, USSR	383
5. Microwave Gastric Ulcer V. V. Tyazhelov, V. P. Safronov, and B. K. Gavriliuk, Institute of Biological Physics, USSR Adademy of Sciences, Pushchino Moscow Region 142292, USSR	384

SESSION BEMS - 10
FRIDAY AM 8:30-10:00
HUB AUDITORIUM

ROUND TABLE: CELLULAR EFFECTS, RAMAN SPECTRA AND MILLIMETER WAVES		<u>Page</u>
Moderator:	O. P. Gandhi University of Utah Salt Lake City, UT	385
Panel:	T. W. Athey Bureau of Radiological Health Rockville, MD	385
	K. H. Illiger Tufts University Medford, MI	385
	S. Motzkin Polytechnic Institute of New York Brooklyn, NY	385
	L. M. Partlow University of Utah Salt Lake City, UT	385
	J. P. Sheridan Naval Research Laboratory Washington, DC	385

SESSION BEMS - 11
FRIDAY AM 10:20-11:50
HUB AUDITORIUM

MEDICAL APPLICATIONS

Chairperson: S. M. Michaelson
University of Rochester
Rochester, NY

	<u>Page</u>
1. Dynamics of Organism Behavioral Reactions Changes Caused by Microwave Radiation M. I. Rudnev, M. A. Navakatikian, Kiev A. N. Marzeev Scientific Research Institute of General and Communal Hygiene, Kiev, USSR	387
2. Measurements of Electromagnetic Activities of the Human Body in the Frequency Region 1 KHz - 2 GHz B. Enander and G. Larson, Royal Institute of Technology, Stockholm, Sweden	388
3. Microwave Diathermy Treatment of the Human Thigh: The Simultaneous Measurement of Muscle Blood Flow (MBF) and Temperature of the Human Thigh During Microwave Diathermy K. M. Seknins, A. F. Emery, Department of Mechanical Engineering, University of Washington, Seattle, WA J. F. Lehmann, D. Dundore, Department of Rehabilitation Medicine, University of Washington, Seattle, WA W. B. Nelp, Department of Nuclear Medicine, University of Washington, Seattle, WA	389
4. Immunologic Aspects in Cancer Treatment by Microwave Hyperthermia W. Roszkowski, S. Szmigielski, and M. Janiak, Center for Radiobiology and Radioprotection, Warsaw, Poland	390
5. Microwave Effects on Energy Levels of Brain and Malignant Brain Tumor A. P. Sanders, D. J. Schaefer and W. T. Joines, Department of Radiology and Department of Electrical Engineering, Duke University, Durham, NC	391
6. Electrical Stimulation of Alveolar Bone D. B. Harrington, T. A. Chen, P. Mollica and F. Davis, School of Dentistry, Fairleigh Dickinson University, Hackensack, NJ	392

SESSION BEMS - 12
FRIDAY PM 1:30-3:00
HUB AUDITORIUM

REPRODUCTION, GROWTH, AND DEVELOPMENT (1)

Chairperson: Z. R. Glaser

National Institute for Occupational Safety and Health
Rockville, MD

	<u>Page</u>
1. <u>In Vivo</u> Study of 60 Hz Electric Field Effects D. M. Koltun, S. N. Ackerman, D. M. Weissfeld, J. M. Seto, Y. J. Seto, Electrosience and Biophysics Research Laboratories, Tulane University, New Orleans, LA	394
2. Growth of Rats and Mice Exposed to 60-Hz Electric Fields R. D. Phillips, J. H. Chandon, D. I. Hilton and R. L. Sheldon, Biology Department, Pacific Northwest Laboratory, Richland, WA	395
3. Effects of Exposure to 60 Hz Electric Fields on Growth and Development in the Rat L. D. Montgomery, L. G. Smith, and M. R. Sikov, Pacific Northwest Laboratory, Richland, WA	396
4. Chronic Exposure of Rats to 100-MHz (CW): Assessment of Biological Effects R. J. Smialowicz, E. Berman, S. J. Bursian, J. B. Kinn, C. G. Liddle, L. W. Reiter and C. M. Weil, Experimental Biology Division (MD-72), Research Triangle Park, NC	397
5. The Effect of Prenatal Microwave Exposure on the Development of Behavioral Responses in the Mouse J. C. Monahan, Bureau of Radiological Health, Rockville, MD	398
6. Development Alterations in Rats Following In-Utero Exposure to 500 $\mu\text{w}/\text{cm}^2$, 2450-MHz Microwaves S. J. Y. Mizumori, R. H. Lovely, R. B. Johnson and A. W. Guy, Departments of Rehabilitation Medicine and Psychology, University of Washington, Seattle, WA	399

SESSION BEMS - 13
FRIDAY PM 3:20-5:05
HUB AUDITORIUM

REPRODUCTION, GROWTH, AND DEVELOPMENT (II)

Chairperson: M. L. Shore
Bureau of Radiological Health
Rockville, MD

	<u>Page</u>
1. The Effect on the Heart Rate of Embryonic Quail of 2450 MHz Electromagnetic Waves P. E. Hamrick and D. I. McRee, Department of Health, Education, and Welfare, National Institute of Environmental Health Sciences, Research Triangle Park, NC	401
2. Teratogenicity of 27.12 MHz Radiofrequency Radiation in Rats J. M. Lary, D. L. Conover, E. D. Foley, and P. L. Hanser, National Institute for Occupational Safety and Health, U.S. Department of Health, Education, and Welfare, Cincinnati, OH	402
3. Studies Concerning the Effects of Non-Thermal Protracted Prenatal 2450 MHz Microwave Irradiation on Prenatal and Postnatal Development in the Rat R. P. Jensch, W. H. Vogel, J. Ludlow, T. McHugh, and R. L. Brent, Departments of Anatomy, Pharmacology, and Radiology, Thomas Jefferson University, Philadelphia, PA	403
4. Exposure of Pregnant Mice to 2.45 GHz Microwave Radiation D. I. McRee, P. Nawrot, National Institute of Environmental Health Sciences, Research Triangle Park, NC	404
5. Teratogenic Effects of RF Radiation on Mice J. C. Nelson, J. C. Lin, Department of Electrical and Computer Engineering, Wayne State University, Detroit, MI E. Ekstrom, Department of Comparative Medicine, Wayne State University, Detroit, MI	405
6. Observations of Rat Fetuses after Irradiation with 2.45 GHz (CW) Microwaves E. Berman, H. B. Carter, U.S. Environmental Protection Agency, Health Effects Research Laboratory, Research Triangle Park, NC D. House, U.S. Environmental Protection Agency, Statistics and Data Management Office, Research Triangle Park, NC	406
7. Teratology in Rats Exposed to 2450 MHz Microwaves at Intense and Intermediate Dose Rates M. E. Chernovetz, University of Tulsa, Tulsa, OK D. L. Reeves and D. R. Justesen, Kansas City Veterans Administration Medical Center, Kansas City, MO	407

BEMS POSTER SESSION A
 TUESDAY PM 1:30-4:50
 HUB 108 WEST LOUNGE

Co-Chairperson: P. Kramar
 University of Washington
 Seattle, WA

Co-Chairperson: W. A. G. Voss
 University of Alberta
 Edmonton, Alba., Canada

MEDICAL APPLICATIONS (Paper Nos. 1 - 15)
 DOSIMETRY (Paper Nos. 16 - 24)
 CELL BIOLOGY (Paper Nos. 25 - 36)
 BEHAVIOR (I) (Paper Nos. 37 - 48)

Page

- | | |
|--|-----|
| 1. A Microwave Diathermy Applicator | 409 |
| M. A. Stuchly, Health and Welfare Canada, Ottawa, Ont.,
S. S. Stuchly, University of Ottawa, Ottawa, Ont., G. Kantor,
U. S. Dept. of Health Education and Welfare, Rockville, MD | |
| 2. Measured Patterns of Stray Radiation Produced by Therapeutic
Microwave Applicators When Applied to Tissue-Substitute
Models and Human Subjects | 410 |
| J. F. Lehmann, A. W. Guy, and J. Wallace, University of
Washington, Seattle, WA | |
| 3. Comparative Study of 2450 MHz and 915 MHz Diathermy Applicators
with Phantoms | 411 |
| G. Kantor and D. M. Witters, FDA, Rockville, MD | |
| 4. Evaluation of 915-MHz and 2450-MHz Direct Contact Diathermy
Applicators | 412 |
| J. Wallace, A. W. Guy, J. A. McCougall, and J. F. Lehmann,
University of Washington, Seattle, WA | |
| 5. Microwave Diathermy Treatment of the Human Thigh: The
Experimental Measurement of the Muscle Blood Flow Response
and the Numerical Simulation of the Tissue Temperature
Response | 413 |
| A. F. Emery, K. M. Sekins, D. Dundore, J. F. Lehmann,
P. W. McGrath, and W. B. Nelp, University of Washington,
Seattle, WA | |
| 6. A Broadband and Compact Applicator for Deep Tissue Heating
Using Focused Microwaves | 414 |
| J. F. Iskander, C. H. Durney, D. A. Christensen, and A. Riazzi,
University of Utah, Salt Lake City, UT | |
| 7. Deep Visceral Hyperthermia in Man Without Surface Tissue Injury | 415 |
| F. K. Storm, W. H. Harrison, R. W. Elliott, D. L. Morton,
University of California School of Medicine, Los Angeles, CA
and Veterans Administration Hospital, Sepulveda, CA | |

	<u>Page</u>
8. Localized RF Hyperthermia on Hamster Cheek Pouch Carcinoma D. P. Colvin, B. S. Burgess, and A. L. Patra, Becton, Dickinson Research Center, J. D. Doss, Los Alamos Scientific Laboratory, Los Alamos, NM, and B. R. Marsh and J. K. Frost, Johns Hopkins University Medical Center, Baltimore, MD	416
9. Localized Microwave Hyperthermia at X-Band on External Tumors in Mice A. Feldman, University of Hawaii, Honolulu, HI, and L. H. Piette, Cancer Center of Hawaii, Honolulu, HI	417
10. Localized Hyperthermia in Dog Brain Using an Invasive Microwave Probe D. DeSieves, B. S. Trembly, R. Matic, Thayer School of Engi- neering, D. W. Roberts, Dartmouth College Medical School, J. W. Strohbehn, E. B. Double, S. Brown, Thayer School of Engineering and Dartmouth College Medical School, and P. Runstadler, Creare, Inc., Hanover, NH	418
11. Electrical Properties of Tissue Equivalent Bolus for Microwave Hyperthermia A. Y. Cheung, G. H. Harrison and L. S. Taylor, University of Maryland, College Park, MD, and P. D. Hrycak, Westinghouse Electric Corp., Baltimore, MD	419
12. A System for Producing Localized Hyperthermia in Brain Tumors Through Magnetic Induction Heating of Ferromagnetic Implants P. R. Stauffer, T. C. Cetas, R. C. Jones, and M. R. Manning, University of Arizona, Tucson, AZ	420
13. Validation of Microwave Pulmonary Edema Detection by Isolated Lung and Phantom Measurements M. F. Iskander, C. H. Durney, B. H. Ovard, and D. G. Bragg University of Utah, Salt Lake City, UT	421
14. Technical Aspects of Electromagnetic Techniques for Recovering Cryogenically-Preserved Large Organs J. Toler, J. Seals, and E. McCormick, Georgia Institute of Technology, Atlanta, GA	422
15. Influence of Microwave-Induced Temperature Gradients on the Uptake of Chemotherapeutic Agents by Experimental Brain Tumors in Mice C. H. Sutton and F. B. Carroll, University of Miami School of Medicine, Miami, FL, and Q. Balzano, Motorola, Inc., Plantation, FL	423
16. Tensor Integral Equation Method Combined with Iteration Technique for Quantifying Induced EM Fields in Biological Systems K.-M. Chen and S. Rukspollmuang, Michigan State University, East Lansing, MI	424
17. Surface Integral Equation Method for Interaction of Microwave with Biological Body J.-H. Lee and K.-M. Chen, Michigan State University, East Lansing, MI	425

	<u>Page</u>
18. Specific Absorption Rates in Mice Exposed to 918 and 2450 MHz Circularly Polarized Guided EM Fields A. W. Guy, C. K. Chou, J. F. Lehmann, W. Farnham, and J. A. McDougall, University of Washington, Seattle, WA	426
19. Specific Absorption Rates Measured in Rats and Mice Exposed to 2450, 425 or 100 MHz Radiofrequency Radiation J. B. Kinn, U.S. Environmental Protection Agency, Research Triangle Park, NC	427
20. Waveguide Dosimetry Data on Mice, In Vivo, 2.5 - 4.2 GHz R. Turner, W. A. G. Voss, W. R. Tinga, P. Fisher and R. Rajotte, University of Alberta, Edmonton, Alberta	428
21. A Study of the Heating Pattern of a Biological Body Inside a Rectangular Waveguid J. J. H. Wang, Georgia Institute of Technology, Atlanta, GA and L. E. Larsen, Walter Reed Army Institute of Research, Washington, DC	429
22. Estimation of Internal Power Absorption by Human Heads in Presence of Electromagnetic Radiation K. Quboa, H. T. Al Hafid and S. C. Gupta, University of Mosul, Mosul, Iraq.	430
23. Energy Absorption from Small Radiating Probes in Lossy Media M. L. Swicord, Bureau of Radiological Health, Rockville, MD and C. C. Davis, University of Maryland, College Park, MD	431
24. Numerical Solutions for Microwave Power Absorptions in Body-of-Revolution Models of Man T.-K. Wu, Lockheed Missiles & Space Company, Sunnyvale, CA	432
25. Experimental Model for Detecting and Amplifying Subtle RF Field-Induced Cell Injuries V. Riley, D. H. Spackman, M. A. Fitzmaurice, A. W. Guy, and C. K. Chou, Pacific Northwest Research Foundation, Fred Hutchinson Cancer Research Center, and the University of Washington School of Medicine, Seattle, WA	433
26. Differential Consequences of Biological System Exposure to Pulsed- and Continuous-Wave Electromagnetic Fields J. Toler, J. Seals, and E. McCormick, Georgia Institute of Technology, Atlanta, GA, and R. Vogler and L. Winton, Emory University School of Medicine, Atlanta, GA	434
27. The Differentiation (Retransformation) of Neuroblastoma Cells as an Indicator of the Biologic Activity of Pulsed Magnetic Radiation. The Non-Thermal Effects of Pulsed Electromagnetic Fields on Tumor Growth and <u>In Vitro</u> Mouse Palatal Development and Neuroblastoma Differentiation W. Regelson, B. West, R. Carchman, D. End, D. DePaola, and R. Lieb, Medical College of Virginia, Richmond, VA, and A. Pilla, Columbia University, New York, NY	435
28. Effect of Long-Term Low-Level Microwave Exposure on Development and Growth of Chemically/3,4-Benzopyrene and Di-Ethyl-Nitrosoamine/Induced Neoplasms S. Szmigielski, A. Pietraszek, and M. Bielec, Center for Radiobiology and Radioprotection, Warsaw, Poland	436

	<u>Page</u>
29. Effects of A.C. Magnetic Field on Lymphoma Cells S. Batkin and F. L. Tabrah, University of Hawaii School of Medicine, Honolulu, HI	437
30. Effects of 1.07 GHz RF Fields on Microbial Systems E. Moody, C. McLerran, J. W. Frazer, and V. A. Segreto, University of Texas Health Science Center, San Antonio, TX	438
31. Microwave-Induced Increase of Water and Conductivity in Submaxillary Salivary Gland of Rats H. Mikolajczyk, Institute of Occupational Medicine, Poland	439
32. Further Studies of Testis Cytology in Mice Irradiated with 2450-MHz Microwaves A. B. Cairnie and R. K. Harding, Defence Research Establish- ment Ottawa, Ottawa, Ontario, Canada	440
33. Heat-Induced Cataracts in the Rat Lens <u>In Vitro</u> P. J. Stewart-DeHaan, M. O. Creighton, W. M. Ross, and J. R. Trevithick, University of Western Ontario, London, Ontario, Canada	441
34. Effect of D.C. Magnetic Fields on Ca ²⁺ Transport in Isolated Muscle Microsomes E. M. Ettienne, P. A. Hoenig, and R. B. Frankel, MIT, Cambridge, MA, and University of Massachusetts Medical School, Worcester, MA	442
35. Effects of Pulsed Electrical Fields on Erythrocyte Membranes S. F. Cleary, Virginia Commonwealth University, Richmond, VA	443
36. Enhanced Repopulating Capacity of a Bone Marrow Cell Suspension after Microwave Irradiation <u>In Vitro</u> D. Rotkowska and A. Vacek, Institute of Biophysics, Czechoslovakia	444
37. Chronic Exposure of Rats to 100-MHz (CW): Assessment of Operant Behavior M. I. Gage, J. D. Edwards, and R. J. Pettinelli, U.S. Environ- mental Protection Agency, Research Triangle Park, NC	445
38. Chronic Exposure of Rats to 2450-MHz Microwaves at 5 mW/cm ² Defining Frequency Dependent Dose-Determinate Effects R. H. Lovely, S. J. Y. Mizumori, R. B. Johnson, and A. W. Guy, University of Washington School of Medicine, Seattle, WA	446
39. Effects on Behavior of Long Term Exposure to Low Level MWR R. M. Lebovitz and R. L. Seaman, University of Texas Health Science Center, Dallas, TX	447
40. The Effect of 9.31 GHz Pulsed Microwave Irradiation on the Lever Press Behavior of Operantly Responding Rhesus Monkeys R. D. McAfee, VA Medical Center, New Orleans, LA, and University of New Orleans, New Orleans, LA, and R. Bishop and S. T. Elder, University of New Orleans, New Orleans, LA	448
41. Vigilance Behavior in Rats Exposed to 1.28 GHz Microwave Irradiation J. O. de Lorge and C. S. Ezell, Naval Aerospace Medical Research Laboratory, Pensacola, FL	449

	<u>Page</u>
42. Microwave-Induced Conditioned Taste Aversions in Rats at 987 MHz G. R. Sessions, Walter Reed Army Institute of Research, Washington, DC	450
43. Alteration of Repeated Acquisition in Rats by Microwave Radiation J. Schrot, J. R. Thomas, and R. A. Banvard, Naval Medical Research Institute, Bethesda, MD	451
44. Changes in Temporal Aspects of Behavior by Low Levels of Pulsed Microwaves J. R. Thomas and R. A. Banvard, Naval Medical Research Institute, Bethesda, MD	452
45. Modulation of Pentobarbital Effects on Timing Behavior in Rats by Low-Level Microwaves G. Maitland, Naval Medical Research Institute, Bethesda, MD	453
46. Attempts to Cue Successful Escape from a Highly Intense Microwave Field by Photic Stimulation A. M. Grove and D. M. Levinson, University of Missouri, Kansas City, MO, and D. R. Justesen, Veterans Administration Medical Center, Kansas City, MO	454
47. Motor Coordination or Balance Differences Between Rats Exposed or Sham Exposed to 60 Hz Electrical Fields A. H. Frey and D. Meles, Randomline, Inc., Huntingdon Valley, PA	455
48. Modification of Tail Pinch Consummatory Behavior by Microwave Energy Exposure A. H. Frey and L. S. Wesler, Randomline, Inc., Huntingdon Valley, PA	456

BEMS - POSTER SESSION B
 THURSDAY PM 1:30-4:50
 HUB 180 WEST LOUNGE

Co-chairperson: O. P. Gandhi
 University of Utah
 Salt Lake City, UT

Co-chairperson: C.-K. Chou
 University of Washington
 Seattle, WA

CELLULAR EFFECTS: RAMAN SPECTRA AND MILLIMETER WAVES (Paper Nos. 1-12)
 IMMUNOLOGY (Paper Nos. 13-23)
 ELF/H - FIELD EFFECTS (Paper Nos. 24-31)
 PROBE INSTRUMENTATION (Paper Nos. 32-38)
 SPECIAL TOPICS (Paper Nos. 39-46)

	<u>Page</u>
1. Millimeter-Wave Radiation Fails to Induce Lambda Phage Expression T. W. Athey and B. A. Krop, Bureau of Radiological Health, Rockville, MD	458
2. Studies of Microwave Absorption in Liquids by Phase Fluctuation Optical Heterodyne Spectroscopy C. C. Davis, Electrical Engineering Department, University of Maryland, College Park, MD M. L. Swicord, Bureau of Radiological Health, Rockville, MD	459
3. Millimeter Wave CW Cells Irradiation Studies: I. Microwave Aspects. Colicin Induction in E. Coli S. Motzkin, L. Birenbaum, S. Rosenthal, C. Rubenstein, S. Davidow, R. Remily, R. Melnick, Departments of Life Sciences and Electrical Engineering, Polytechnic Institute of New York, Brooklyn, NY	460
4. Millimeter Wave CW Cells Irradiation Studies: II. Membrane Transport in Mitochondria and Erythrocytes R. Melnick, S. Motzkin, C. Rubenstein, S. Davidow, L. Birenbaum, S. Rosenthal, Departments of Life Sciences and Electrical Engineering, Polytechnic Institute of New York, Brooklyn, NY	461
5. Sensitivity of C. Albicans Cells to Frequency of Modulation in the 72-74 GHz Band L. Dardanoni, M. V. Torregrossa, Institute of Hygiene, University of Palermo, Palermo, Italy C. Tamburello, L. Zanforlin, Institute of Electrotechnics and Electronics, University of Palermo, Palermo, Italy.	462
6. Millimeter Wave Absorption Spectra of Biological Samples R. A. Lee, M. J. Hagmann, O. P. Gandhi, I. Tanaka, D. W. Hill, and L. M. Partlow, Departments of Bioengineering, Electrical Engineering, Microbiology, and Pharmacology, University of Utah, Salt Lake City, UT	463

	<u>Page</u>
7. A Search for Frequency-Specific Bioeffects Caused by Microwave Irradiation L. M. Partlow, L. G. Bush, L. J. Stensaas, D. W. Hill, A. Riazi, and O. P. Gandhi, Departments of Pharmacology, Microbiology, Physiology, and Electrical Engineering, University of Utah, Salt Lake City, UT	464
8. Raman Spectroscopy of Mammalian Cells A. Riazi, O. P. Gandhi, Department of Electrical Engineering, University of Utah, Salt Lake City, UT J. R. Duffey, Department of Physics, University of Utah, Salt Lake City, UT D. W. Hill, Department of Microbiology, University of Utah, Salt Lake City, UT	465
9. A Theoretical Basis for Microwave and RF Field Effects on Excitable Cellular Membranes, C. A. Cain, Department of Electrical Engineering, University of Illinois, Urbana, IL	466
10. Vibrational Spectra of <u>In Vivo</u> Biological Systems K. H. Illinger, Department of Chemistry, Tufts University, Medford, MA	467
11. Molecular Level Effects of Microwaves on Natural and Model Membranes: A Raman Spectroscopic Investigation J. P. Sheridan, B. P. Gaber, F. Cavatorta, and P. E. Schoen Naval Research Laboratory, Washington, DC	468
12. Effect of Microwaves on Red Blood Cell Components: Investigations at the Molecular Level B. P. Gaber and J. P. Sheridan, Naval Research Laboratory, Washington, DC	469
13. Microwave Effects on Human Colony Forming Marrow Cells M. J. Ottenbreit, S. Inoue, and M. Fracassa, Department of Pediatrics, Wayne State University, Detroit, MI J. C. Lin, Department of Electrical Engineering, Wayne State University, Detroit, MI	470
14. Primary Immune Response of Mice Exposed to Continuous or Pulsed Wave 425-MHz Radiofrequency Radiation R. J. Smialowicz, M. M. Riddle, P. L. Brugnolotti, K. L. Compton and J. B. Kinn, Environmental Protection Agency, Experimental Biology Division, Research Triangle Park, NC	471
15. Growth of Human Bone Marrow Cells in Agar Culture under the Influence of Electrical Currents J. Bojsen and B. T. Mortensen, The Finsen Laboratory and Medical Department, The Finsen Institute, Copenhagen, Denmark	472
16. Effects of Hyperthermia and Microwave Induced Hyperthermic Shock on HPC Cells W. A. G. Voss, Division of Biomedical Engineering and Applied Sciences, Surgical Medical Research Institute, University of Alberta, Edmonton, Canada A. Kennedy, A. Fontaine, B. Hall, Department of Biology, University of Victoria, Victoria, British Columbia, Canada J. Van Netten, Royal Jubilee Hospital, Victoria, British Columbia, Canada	473

	<u>Page</u>
17. The Effects of 9-GHz Pulsed Microwaves on Circulating Antibody Titers of Mice C. G. Liddle, J. P. Putnam, J. Y. Lewis, B. Bell, M. W. West, and O. L. Huey, Environmental Protection Agency, Experimental Biology Division, Research Triangle Park, NC	474
18. The Effect of Radio Frequency (148 MHz) Electromagnetic Field Exposures on Hypersensitivity Responses in Mice J. A. Majde, Office of Naval Research, Chicago, IL J. C. Lin, Department of Electrical Engineering, Wayne State University, Detroit, MI	475
19. Immunologic and Hematopoietic Alterations by 2450 MHz Radiation A. T. Huang and N. Mold, Division of Hematology-Oncology, Department of Medicine, Duke University Medical Center, Durham, NC	476
20. Influence of Pulsed Microwave Radiation on the Lymphocytes of Rats J. Pazderova-Vejlupkova, Department of Occupational Diseases, University Hospital, Charles University of Prague, Prague, Czechoslovakia	477
21. Kinetics and Mechanisms of the Induction of an Increase in Complement Receptor Positive (CR ⁺) Mouse Spleen Cells Following a Single Exposure to 2450 MHz Microwaves C. Schlagel, A. Ahmed, Naval Medical Research Institute, Bethesda, MD K. Sulek, Military School of Medicine, Warsaw, Poland H. Ho and W. Leach, Bureau of Radiological Health, FDA, Rockville, MD	478
22. Altered In Vivo Lymphocyte Migration Following Whole-Body RFR Exposure: Differential Effects on T- and B-Lymphocytes R. P. Liburdy, Radiation Sciences Division, USAF School of Aerospace Medicine, Brooks Air Force Base, TX	479
23. Serum and Lymphocytes from Microwave Exposed Mice Enhance Cell-Mediated Effector Function: Increased Lymphocyte-Mediated Cytotoxicity During Allograft Rejection of EL-4 Lymphoma Cells R. P. Liburdy, Radiation Sciences Division, USAF School of Aerospace Medicine, Brooks Air Force Base, TX	480
24. A Behavioral Procedure and 60 Hertz Exposure System for Determining Field Detection by Rats S. Stern, V. G. Laties, C. Stancampiano, G. B. Inglis, E. Carstensen, S. M. Michaelson, M. W. Miller, Department of Radiation Biology and Biophysics, University of Rochester, Rochester, NY and J. O. de Lorge, Naval Aerospace Medical Research Laboratory, Pensacola, FL	481
25. Effects of 60 Hz Environmental Electric Fields on the Central Nervous System of Laboratory Rats S. M. Bawin, I. Sabbot, B. Bystrom, P. M. Sagan, W. R. Adey, V.A. Medical Center, Loma Linda, CA and Departments of Physiology and Surgery, Loma Linda University, Loma Linda, CA	482

	<u>Page</u>
26. Effects of Chronic Exposure to an Electric Field on Subsequent Discrimination of Electric Fields D. L. Hjeresen, Biology Department, Pacific Northwest Laboratory, Richland, WA	483
27. Effects of High Intensity 60 Hz Electric Fields on Primate Behavior Exposure Facility, Field Measurement Techniques, and Individual Performance C. S. Feldstone, R. T. Smith, H. F. Barsun, E. Bronaugh, R. Spiegel, J. Polonis, E. E. Dean, K. St. Mary, A. D. Smith, Southwest Research Institute, San Antonio, TX	484
28. Navigational Compass in Magnetotactic Bacteria R. B. Frankel, Francis Bitter National Magnet Laboratory, MIT, Cambridge, MA R. P. Blakemore, Department of Microbiology, University of New Hampshire, Durham, NH Ad. J. Kalmijn and C. R. Denham, Woods Hole Oceanographic Institution, Woods Hole, MA	485
29. Threshold Values for Magneto- and Electrophosphenes - A Comparative Study P. Lövsund, P. Å. Öberg, and S. E. G. Nilsson, Departments of Biomedical Engineering and Ophthalmology, Linköping University, Linköping, Sweden.	586
30. Studies of Mutagenic Effects of Magnetic Fields in Bacteria S. C. Causey and F. P. Hungate, Biology Department, Pacific Northwest Laboratory, Richland, WA	487
31. Short-Term Exposure of Rhesus Monkeys to 20,000 Gauss Steady Magnetic Field J. H. Battocletti, A. Sances, Jr., Research Service, Veterans Administration Medical Center, Wood, WI and Department of Neurosurgery, The Medical College of Wisconsin, Milwaukee, WI S. Salles-Cunha, R. E. Halbach, F. J. Antonich, Department of Neurosurgery, The Medical College of Wisconsin, Milwaukee, WI J. Nelson, J. Mykelbust, Research Service, Veterans Administration Medical Center, Wood, WI	488
32. An Improved Implantable Electric Field Probe for Microwave Dosimetry H. Bassen, K. Franke, S. Neuder, Food and Drug Administration, Bureau of Radiological Health, Rockville, MD E. Aslan, Narda Microwave Corporation, Plainview, NY	489
33. A Nonperturbing Temperature Probe System Designed for Hyperthermia Monitoring D. A. Christensen and R. J. Volz, Department of Bioengineering and Department of Electrical Engineering, University of Utah, Salt Lake City, UT	490
34. An Optical Non-Perturbing Probe for Temperature Measurements in Biological Materials Exposed to Microwave Radiation F. Cavatorta, P. E. Schoen, J. P. Sheridan, Naval Research Laboratory, Washington, DC	491

	<u>Page</u>
35. Commercial Microwave Hazard Meters: A Laboratory Evaluation W. A. Herman and D. M. Witters, Jr., Bureau of Radiological Health, FDA, Rockville, MD	492
36. A High-Sensitivity, Ultra-Broadband Radiation Probe S. Hopfer and Z. Adler, General Microwave Corporation, Farmingdale, NY	493
37. Dosimetric Use of Schottky Diodes W. A. Herman, Bureau of Radiological Health, FDA, Rockville, MD	494
38. Power Density Flux Measurements T. M. Babij, H. Trzaska, Institute of Telecommunications and Acoustics, Technical University of Wroclaw, Wroclaw, Poland	495
39. Considerations and Criteria for a Recommended Standard for Occupational Exposure to Radiofrequency and Microwave Fields R. F. Boggs and Z. R. Glaser, National Institute for Occupa- tional Safety and Health, Rockville, MD R. F. Cleveland and J. K. Kielman, Equitable Environmental Health, Inc., Rockville, MD	496
40. Development of Occupational Exposure Recommendations: Observations on the Uses of RF/Microwave Energy Z. R. Glaser, R. F. Cleveland, J. K. Kielman, and R. F. Boggs, National Institute for Occupational Safety and Health, Rockville, MD and Equitable Environmental Health, Inc., Rockville, MD	497
41. Measured Modulation Waveform of Leakage Radiation from Micro- wave Ovens H. S. Ho and W. P. Edwards, U.S. Department of Health, Education, and Welfare, FDA, Rockville, MD	498
42. Microwave-Induced Pressure Waves in a Model of Biological Tissue R. G. Olsen and W. C. Hammer, Naval Aerospace Medical Research Laboratory, Pensacola, FL	499
43. Electromagnetic Exposure Effects on the Visual System of a Flying Insect S. S. Sandler and W. Peros, Department of Electrical Engineering and Biology, Northeastern University, Boston, MA	500
44. Radiation of Open Waveguides Application to Biomedical Probes J. Audet, J. Ch. Bolomey, Ch. Pichot, Groupe d'Electromagnetisme, Laboratoire des Signaux et Systemes, Gif-sur-Yvette, France	501
45. A Corrugated Waveguide Applicator Q. Balzano and O. Garay, Motorola, Inc., Miami, FL C. H. Sutton, School of Medicine, University of Miami, Miami, FL	502
46. Measured Internal Electric Field in Phantom Human Heads Exposed to Leakage Radiation from Microwave Ovens H. S. Ho, W. P. Edwards, and H. Bassen, U.S. Department of Health, Education and Welfare, FDA, Rockville, MD	503





PLENARY SESSION
JOINT USNC/URSI - AP-S - BEMS
WEDNESDAY AM 9:00-11:30
KANE HALL 130

Chairman: A. Ishimaru
University of Washington
Seattle, WA

Plenary 1

RAYS AND MODES IN GUIDED PROPAGATION

L. B. Felsen
Polytechnic Institute of New York
Route 110, Farmingdale, N. Y. 11735

Various physical environments permit guiding of high-frequency signals. Examples are provided by tropospheric, ionospheric or oceanic ducts formed by refractive index inhomogeneities or by interfaces separating regions with different material properties. Guiding also occurs along concave surfaces and in dielectric waveguides. The propagation characteristics of a signal radiated in such an environment may be analyzed either in terms of rays or in terms of guided modes. In many instances, the required number of multiply reflected rays or of modes may be exceedingly large, thereby making calculation cumbersome and necessitating truncation of either the ray series or the modes series. Quantitative estimates of the truncation error have generally not been available. We shall demonstrate that the truncation in either case can be accounted for by a hybrid ray-mode field formulation. This judiciously chosen mixture of rays and modes may be interpreted in two ways: a certain number of guided modes accounts for rays omitted from a truncated ray series, while a certain number of rays accounts for modes omitted from a truncated mode series. Appealing physical criteria determine the proper ray-mode combination. Numerical advantages accrue since the number of rays and modes required in the hybrid formulation is far less than when either the ray series or the mode series is used individually. The utility of the hybrid approach is demonstrated in various examples. (T. Ishihara, L. B. Felsen and A. Green, *IEEE Trans. Ant. Prop.*, AP-26, 757-767, Nov. 1978; L. B. Felsen and T. Ishihara, *J. Acoust. Soc. Am.* (to be published)).

THE INTERFEROMETER ARRAY IN RADIO ASTRONOMY

G. W. Swenson, Jr.

Departments of Electrical Engineering and Astronomy
University of Illinois at Urbana-Champaign
Urbana, Illinois 61801

Modern interferometer arrays (or correlator arrays), as used for radio-astronomical research, differ in several fundamental respects from "phased" antenna arrays as used in radar and broadcasting services. The interferometer arrays are used for receiving only, and are non-reciprocal. They depend upon the incoherent nature of cosmic radio waves and would be of limited usefulness for receiving coherent signals from man-made transmitters. However, they represent the most powerful method for study of natural cosmic radio emitters at very high angular resolution.

In this paper the basic theory of the correlator interferometer is derived from first principles, and the basic "transfer-function" method of array design is described. Existing arrays of both "connected-element" and "independent-local-oscillator" (VLBI) types are illustrated.

Plenary 3

HISTORICAL OVERVIEW AND STATE OF THE ART ON QUANTITATION OF EM BIO-EFFECTS

Arthur W. Guy, Ph.D.

Department of Rehabilitation Medicine
University of Washington, Seattle, WA 98195

Investigations of EM Bio-effects beginning with the work of physician-physiologist d'Arsonval have dealt principally with the heating of tissues. The character of the heating became better understood with the characterization of dielectric properties of various tissues as a function of frequency between 1927 and the mid-1950s. The EM fields and associated heating patterns in exposed tissue were first analyzed in the early 1950s with the use of simple models consisting of plane layers of muscle, subcutaneous fat, and skin. Analyses after 1960 on prolate spheroid tissue models using static solutions to determine low-frequency quasi-static field coupling and spheres using the Mie theory to determine plane wave field coupling characteristics with the bodies of humans indicated that the absorption cross section varies markedly with frequency, displaying sharp minima and maxima.

In the mid-1960s experimental phantom models of various tissues were developed and used for experimentally verifying the theoretical analyses and determining field coupling and absorption characteristics for more complex tissue structures not amenable to theoretical analysis. From the late 1960s until the present, thermography has played a powerful role in measuring the EM field induced temperature changes in both phantom and actual biological tissues allowing for a rapid and accurate quantitation of the absorbed energy and electric field distributions within the tissues. Both theoretical work and the development of new instrumentation increased substantially in the 1970s. Complex spherical models of the human head consisting of a core of brain tissue and spherical shells simulating the skull and the scalp indicated that hot spots or localized regions of high energy absorption could occur in the center of the brain with magnitudes much higher than observed at the surface of the head due to the focusing of energy by the high dielectric constant and spherical shape of the head. More extensive analyses using spherical, prolate spheroidal, and ellipsoidal models has recently created a much better understanding of the absorbed energy patterns in the bodies of man and animals exposed to EM fields. Theoretical work is being backed up by careful experiments utilizing special temperature sensing probes composed of microwave transparent materials such as fiber optics and miniature leads of low electrical conductivity. Finite difference techniques and other numerical methods are being used for calculating EM field and associated heating patterns in arbitrarily shaped bodies more closely simulating man.

Plenary 4

SATELLITEBORNE SYNTHETIC APERTURE RADAR

K. Tomiyasu
General Electric Company
P.O. Box 8555
Philadelphia, Pa. 19101

The principles of operation of a synthetic aperture radar (SAR) will be briefly reviewed, and examples of SAR borne by satellites will be discussed. The SAR comprises a pulsed transmitter, an antenna, and a phased coherent receiver. SAR operation requires relative motion between the radar and the scene. The antenna beam axis is oriented typically at right angle to the satellite velocity vector. The amplitude and phase of the received signals are collected for the duration of an integration time after which the signal history is processed to produce a high resolution two-dimensional image of the scene. High resolution in azimuth is achieved by focusing with a signal processing technique, an extremely long antenna that is synthesized from the coherent phase history.

In 1978 NASA launched the SEASAT satellite which carried and L-Band SAR. From this highly successful experiment, numerous images of oceanic, polar ice and terrestrial surfaces were produced. For the Shuttle era, SAR sensors are being planned for flight, and these Shuttle Imaging Radars are referred to as SIR-A and SIR-B. A wide swath SAR employing an electronically scanned phased array is being configured to map the polar ice caps. A SAR has been configured to operate from a satellite in a 24-hour, inclined and eccentric orbit. This SAR in geosynchronous orbit can map the United States every 4.5 hours with 100-meter resolution. By using separate transmitting and receiving antennas in two satellites a bistatic radar can be configured, and by mapping the same scene from different orbits a holographic or bistatic SAR image can be produced.

Plenary 5

The Activities of the Antenna Society
of the Chinese Electronics Institute

Mao Yu-Kuan
Department of Electromagnetic Engineering
Northwest Telecommunication Engineering Institute
Xian, Shanxi, People's Republic of China

BREMMER SESSION
WEDNESDAY PM 2:00-5:30
KANE HALL 120

BREMMER BIRTHDAY CELEBRATION SESSION

Chairman: J. R. Wait
ERL/NOAA
Boulder, CO

GROUND WAVE THEORY VIA NORMAL MODES - AN HISTORICAL PERSPECTIVE
A Tribute to Professor H. Bremmer on His 75th Birthday

James R. Wait, ERL/NOAA, U.S. Dept. of Commerce, Boulder, Colo. 80303

Ever since the pioneering work by Zenneck [*Ann. Phys.*, 23, 846-866, 1907] and Sommerfeld [*Ann. Phys.*, 28, 665-737, 1909; 81, 1135-1153, 1926], the propagation of radio waves along the earth's surface has captured the fancy of theoreticians. The subject reached a state of some maturity in the 1930-1940 period when Van der Pol and Bremmer [*Phil. Mag.*, 24, 141-176, 1937; 25, 817-834, 1938; 26, 261-275, 1939] exposed a general theory for the diffraction of a dipole field by a finitely conducting spherical earth. Their approach also reached a pinnacle of complexity because they wished to retain mathematical generality. But they did clearly identify the nature of a number of approximations that led to simplified working formulae (i.e., *the residue series*) that have been used by many for numerical studies. This subject is very clearly and exhaustively described by Bremmer [*Terrestrial Radio Waves*, Elsevier, 1949]. Benefiting by hindsight a series of papers by Fock [*JETP*, 15, 480-490, 1945; *EM Propagation and Diffraction Problems*, Pergamon, 1965] and his Soviet colleagues appeared about this same time that essentially rederived the Van der Pol-Bremmer theory by introducing various physical approximations at the outset rather than at the end of the analysis. In a parallel development based on wartime research in the early 1940s, Booker and Walkinshaw [*Meteorological Factors in Radio Prop.*, Physical Society, London, 1946] showed that the residue series representations were really nothing more than a sum of normal modes. When the problem was formulated in this fashion for a perfectly conducting earth, the modal spectrum was discrete and no need arose to introduce a continuous spectrum of modes. Sommerfeld was apparently very conversant with this approach [e.g., see Sommerfeld, *Partial Diff. Equs. in Phys.*, Academic Press, 1949].

Here we present an exposition of the normal mode approach to ground wave propagation over a spherical earth when excited by either a vertical or a horizontal antenna. The derivation incorporates the essential features of prior analyses without becoming embroiled in the mathematical niceties of improper poles, branch cuts and intricate (and tricky) deformations of integration contours in the complex wave number planes. Previous papers that deal generally with the topic are as follows: Wait, [*J. Math. Phys.*, 8, 920-925, 1967], Cho and King [*IEEE Trans.*, GE-10, 96-105, 1972], Zucker [*Antenna Theory*, Chap. 21, McGraw-Hill, 1969], Wait [*Proc. IEEE*, 62, 1061-1072, 1974], Bahar [*Radio Science*, 5, 1069-1076, 1970], King, et al, [*IEEE Trans.* AP-22, 551-556, 1970], Wait [*J. Math. Phys.*, 11, 2851-2860, 1970], Spies and Wait [*IEEE Trans.*, AP-14, 515-517, 1966], Wait [*EM Probing in Geophysics*, 163-207, Golem, 1971], and King and Wait [*Symposia Mathematica*, 18, 107-208, Academic Press, 1976]. Many of these papers also contain additional references. Here we will deal explicitly with an airless earth since the physics of the diffraction process is not changed when a smooth gravitationally stratified atmosphere is allowed for [Bremmer, *Jour. Res. NBS*, 63D, 75-86, 1959; loc. cit. 1965; Wait, *EM Waves in Stratified Media*, 2nd Ed. Pergamon, 1972]. However, this can be regarded as a convenient starting point in the more elaborate analysis of tropospheric ducting [Bremmer, *Handbuch der Phys.*, 16, 423-639, 1958; and Fock, loc. cit, 1965]. A further natural extension deals with the laterally varying tropospheric duct where mode conversion plays a significant role [S.H. Cho and J.R. Wait, *Pure and Appl. Geophys.* 116, 1118-1142, 1978]. A closely related problem that we call attention to is VLF transmission in the earth-ionosphere via waveguide modes and/or wave hops [e.g., see J.R. Wait, *Reviews of Geophys. and Space Phys.*, 16, 320-726, 1978].

PROPAGATION ALONG CONCAVE SURFACES

L. B. Felsen

Polytechnic Institute of New York
Route 110, Farmingdale, N. Y. 11735

High frequency propagation along concave surfaces cannot be analyzed by geometrical optics when rays from the source to the observation point experience too many reflections. It is then necessary to account for these multiply reflected rays in some other manner. Various alternative field representations, which include whispering gallery modes, rays and continuous spectrum integrals, have been developed to describe the propagation phenomena. These results are reviewed for previously investigated cases in two and three dimensions when source and observation points are both on the boundary (T. Ishihara, L. B. Felsen and A. Green, IEEE Trans. Ant. Prop., vol. AP-26, 757-767, Nov. 1978). Substantial modifications are encountered when the source, the observer or both move off the boundary. Numerical results demonstrate the utility of the various field formulations.

Bremmer 3

SPECKLE INTERFEROMETRY FOR A PARTIALLY-COHERENT SOURCE

By

Ronald L. Fante
Rome Air Development Center
Hanscom AFB, MA 01731

Speckle interferometry is a technique developed to circumvent the deleterious effects of turbulence on the imaging of incoherent sources. In this paper we will demonstrate that this method is also applicable to partially coherent sources, and will obtain results for the generalized frequency transfer function. We will examine this transfer function in the limit of high and low spatial frequencies, and show that it reduces to previous results in the limiting case when the source is completely incoherent.

A WIGNER-DISTRIBUTION MATRIX FOR A STOCHASTIC MEDIUM

H. Bremmer

Emeritus Professor Technical University Eindhoven (Netherlands)

Abstract

Wigner distribution functions $W(\vec{r}, t; \vec{k}, \omega)$ describe the distribution of the local energy density of waves over the propagation directions (\vec{k} spectrum) and the frequencies ω . "transport equations" give the rate of change of these functions in the direction of the \vec{k} vector considered. The paper concerns a time dependent medium with a stochastic permittivity. Its Wigner functions fix a tensor the elements W_{jk} of which concern the product of two special electric-field components. After having derived wave equations for the corresponding correlation functions, a statistical averaging is performed, based on two assumptions: a normal distribution of the permittivity fluctuations, and a coherence scale much smaller than the mean free path for scattering. By a Fourier transform the resulting equations pass into corresponding ones for the Wigner tensor. The latter are simplified by forward-scattering approximations, while the medium fluctuations should be slow enough. The final equations thus obtained for the W_{jk} 's indicate resonance effects interpretable in terms of Bragg reflections against periodic structures generated by the travelling waves contained in the $k\omega$ spectrum of the fluctuations. The vectorial treatment involves transport equations in which all W_{jk} elements appear coupled. The neglect of all cross correlations between the field components reduces the main transport equations into a single one that has been presented in (M.S. Howe, Phil. Trans. Roy. Soc., 274A, 523-549, 1973), using a scalar treatment for a stochastic medium depending on a Helmholtz equation instead of our Maxwell equations.

WAVES IN RANDOM MEDIA: LIMITING IRRADIANCE DISTRIBUTION

D. A. de Wolf
 RCA Laboratories
 Princeton, N.J. 08540

As the light path through a weakly-scattering medium of small, random, dielectric fluctuations is increased, it seems intuitively clear that the irradiance of a propagating bundle of light must tend to an exponential distribution. Calculations of irradiance moments, even in a limit procedure of increasing cumulative randomizing of a light beam, are difficult when the Fresnel length $(\lambda L)^{1/2}$, defined by pathlength L and wavelength λ , is sandwiched between the two extreme scales of turbulence. The second moment has been analyzed for beams in Kolmogorov turbulence (M. H. Lee, et al., J. Opt. Soc. Am., 66, 1389-1392, 1976), and all higher-order moments have been shown by selective summation of diagrams to yield an exponential distribution for plane waves (D. A. de Wolf, J. Opt. Soc. Am., 63, 171-179, 1973). However, the error analysis of disregarded terms is difficult. We now utilize a recently developed formalism to write the irradiance moments as formal solutions of operator integro-differential equations. Relatively simple, straightforward, mathematical approximations can then be shown to yield the moments corresponding to an exponential distribution. The procedure is easily expanded to spherical waves, hence also to beams under reasonably nonrestrictive conditions. The analysis of the approximation is simplified because it rests upon the cluster-separation property that the $2N$ point correlation of electric fields $\langle u(r_1), u^*(r_2), \dots, u(r_{2N-1}), u^*(r_{2N}) \rangle$ separates into $\langle u(r_m) u^*(r_n) \rangle$ times the remaining $(2N-2)$ point correlation whenever r_m and r_n are distant from the other points. The wave structure function is utilized to define a decorrelation distance for this separation. The expansion parameter then is shown to be the expected $\sigma^2 c_n^2 k^7/6 L^{11/6}$ for Kolmogorov turbulence (i.e. as $\sigma^2 \rightarrow 0$, one may expect irradiance moments to tend to those of an exponential distribution). The analysis can also be utilized to see why, in general, it is so difficult to predict an irradiance probability distribution for large but finite values of σ^2 .

FORWARD SCATTER THEORY AND DIFFUSION THEORY
FOR WAVES IN RANDOM MEDIA

Akira Ishimaru
Department of Electrical Engineering
University of Washington
Seattle, Washington 98195

The scale sizes of atmospheric turbulence are usually so large compared with a wavelength that the angular broadening is small and the forward-scatter theory is applicable. For waves in scatterers such as clouds and fog, the particle sizes are comparable to a wavelength and the diffusion phenomena become dominant at relatively short optical distances. The paper reviews recent progress in the study of the two distinct states of propagation and scattering in random media: Forward scatter and diffusion. In forward scatter region, backscattering is negligible compared with forward scattering while there is as much backscattering as forward scattering in diffusion region. The forward scatter theory is based on parabolic approximation where the scattering is confined in a small forward angular region. In contrast, the diffusion theory is based on an approximation where the angular spectrum is almost uniform. They are two asymptotic theories which can be derived from a general radiative transfer equation. This paper presents formulations and some approximation solutions in these two regions for both cw and pulse cases. For a line-of-sight problem, the diffusion solution is seen to be applicable for optical scattering distance of greater than one. The transmitted flux, the angular spectrum and the pulse broadening are obtained. For backscattering, the diffusion solution is still applicable except for a short initial time. This is to be expected as the diffusion theory is not applicable near the boundary. This paper also outlines some outstanding theoretical problems in this area.

SESSION A-1
THURSDAY AM 8:30-12:00
HUB 309A

MEASUREMENTS OF ELECTROMAGNETIC PARAMETERS AND MATERIALS

Chairman: D. G. Dudley
University of Arizona
Tucson, AZ

A COAXIAL LINE TECHNIQUE FOR ONE-SIDED NONDESTRUCTIVE MATERIAL MEASUREMENTS

Fred E. GARDIOL, Jean-Claude E. BESSON, Juan R. MOSIG
Ecole Polytechnique Fédérale
Chemin de Bellerive 16
CH-1007 LAUSANNE SWITZERLAND

ABSTRACT: *The permittivity of materials can be determined in a nondestructive and non-invasive manner with the help of an open-ended coaxial line terminated by a flat metallic flange placed in close contact with the material to be measured. The coaxial line provides the possibility of very broad frequency range analysis and consequently, investigations can be made at variable depth into the material being tested.*

The relationship linking the complex permittivity of the material with the reflection factor measured in the line are obtained from a theoretical analysis of the fields near the aperture. An extension of the theory given by J. GALEJS (Antennas in inhomogeneous media, Oxford 1969, pp 39-44) over the higher-order evanescent modes generated in the aperture plane (discontinuity) is used. A computer program was elaborated to carry out the necessary calculations.

A probe was built and the first measurements are in good accordance with the numerical results.

The electromagnetic field injected by the probe within the material tested can be calculated at the same time: it is possible in this manner to determine the heating pattern produced by a coaxial diathermy applicator.

TM CYLINDRICAL CAVITY MEASUREMENT
OF DIELECTRIC CONSTANT AND LOSS TANGENT

D. G. Dudley, University of Arizona, Tucson, AZ 85721; J. A. Fuller, Engineering Experiment Station, Georgia Institute of Technology, Atlanta, GA 30332; R. G. Semelsberger, Science Applications, Inc., Tucson, AZ 85711.

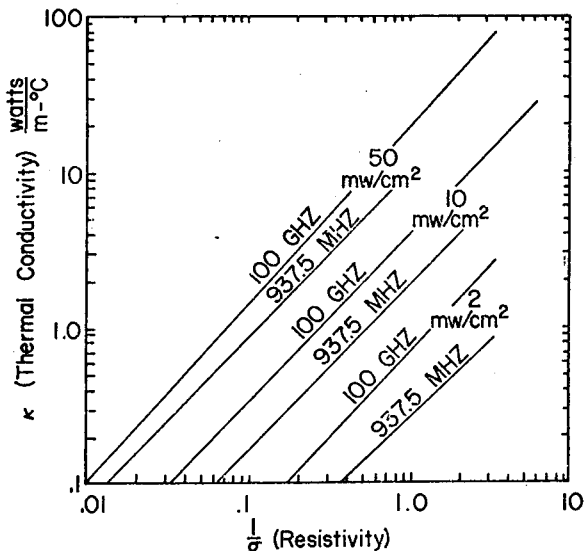
The measurement of the electrical properties of a dielectric sample that is thin compared to a wavelength continues to be a difficult problem. In our application, we require the material to be sprayed on a metallic plate. To measure the electrical properties, we use the material-covered plate as an end plate in a circular cylindrical cavity excited in the lowest TM mode. We perform a modal analysis to determine the fundamental limitations on measurement accuracy and give supportive measurement results over a wide range of dielectric constants. Finally, we discuss applications to dielectric covers for antenna arrays.

APPLICATIONS OF THE INFRARED DETECTION OF SURFACE CURRENTS

R.W. Burton and C.V. Stewart, Department of Electrical Engineering
 U.S. Air Force Academy, CO 80840

A method has been developed that permits the rapid measurement of the magnitudes of charge and surface current distributions using an infrared scanner (R.W. Burton and J.D. Selim, Proc of the 1977 Intl Microwave Symposium). Thermal distributions due to I'R heating are detected and displayed on a color video monitor. Not all surfaces and materials, particularly metals, are sufficiently emissive in the infrared region to be useful. The figure illustrates the regions of acceptable thermal conductivity vs electrical resistivity as a function of the frequency and power density of the incident field.

The technique described here should be particularly useful in research concerned with the reduction of aircraft radar cross sections or EMP effects. The feasibility of using these methods on scale model aircraft and composite materials is explored.



Regions of acceptable parameters of surface preparations for current detection on a perfect conducting surface

ANALYSIS OF THE QUANTUM LIMITED DC SQUID
MAGNETOMETER AND VOLTAGE AMPLIFIER

Claudia D. Tesche
LuTech, Inc.

P.O. Box 1263, Berkeley, CA 94701

Superconducting Quantum Interference Devices (SQUIDS) are now the most sensitive detectors of changes in magnetic flux available. Commercially available rf SQUIDS employing a single Josephson junction are widely used as magnetometers, gradiometers and voltage amplifiers, with applications in such diverse fields as magnetotellurics and magnetocardiology. However, recent advances in thin film Josephson tunnel junction technology now permit development of even more sensitive double junction dc SQUIDS. A careful analysis of the noise sources in the dc SQUID is presented, which indicates that a shot noise limited voltage preamplifier could now be fabricated with a noise temperature, T_N , approaching the minimum value consistent with the uncertainty principle, $T_N \gtrsim hf/k_B$.

The voltage at the SQUID output as a function of the input applied flux is determined by the development in time of the quantum mechanical phase differences across the Josephson junctions. A set of coupled, non-linear, partial differential equations for the phases is presented. Two white random noise sources, corresponding to either thermal or shot noises, are explicitly included. The equations are integrated stepwise in time on a computer, and the device forward transfer function and voltage and current noise spectral densities determined. In addition, a simple thermal-activation model solution is presented.

The device characteristics are used to compute the noise temperature of the SQUID coupled inductively to an input circuit. Optimization of the noise temperature in terms of the SQUID and input circuit parameters is discussed. For an untuned input circuit with source resistance R_i in series with an inductance L_i coupled to the SQUID, the optimal source resistance at frequency ω_0 is $R_i \approx 1.4 \omega_0 L_i$. The optimal noise temperature for the amplifier operated at 4.2K with presently available Johnson noise limited dc SQUIDS is $T_N \approx 5.9 \times 10^{-7} (f/1\text{ Hz})\text{K}$. This corresponds to $R_i \approx 9\Omega$ and $T_N \approx 5.9 \text{ mK}$ for $f = 10^4 \text{ Hz}$ and $L_i = 10^{-4} \text{ H}$. The noise temperature can be reduced by a factor of 8 at the expense of bandwidth by tuning the input circuit. Optimization of the SQUID itself would yield $T_N \sim 17 hf/k_B$ in the shot noise limit. For magnetometer applications, an untuned input circuit with a solenoid pick-up coil of length 0.2m and radius 0.05m would have a magnetic field resolution over a bandwidth Δf , of $B_0 \approx 10^{-16} (\Delta f/1\text{ Hz})^{1/2} T$ in the Johnson noise limit and $B_0 \approx 3 \times 10^{-18} (B/1\text{ Hz})^{1/2} T$ in the shot noise limit.

SESSION A-2
THURSDAY PM 1:30-5:00
HUB 309A

MEASUREMENTS OF RADAR CROSS SECTIONS, ANTENNA PROPERTIES,
AND ELECTROMAGNETIC EMISSIONS

Chairman: C. F. Stubenrauch
National Bureau of Standards
Boulder, CO

PERFORMANCE OF BROAD-BAND RADAR SCATTERING MEASUREMENT
SYSTEM USING AMPLITUDE AND PHASE POST PROCESSING TECHNIQUES

E.K. Walton
The Ohio State University
ElectroScience Laboratory
Electrical Engineering Department
Columbus, Ohio

An experimental system for the broad band measurement of the complex radar scattering from targets in an anechoic chamber has been developed at the Ohio State University. The measurements yield absolute radar cross-section magnitudes as well as the absolute phase (with respect to a particular point in space) of the signal scattered from the target. A vector calculation method is used for calibration. In this system, measurements of the amplitude and phase of the radar return are made over a broad band of frequencies for the target in question, for a calibration sphere, and for the background (target support pedestal empty). The background data at each frequency is then subtracted (vector components) from the target and the sphere. Finally, the sphere data in conjunction with theoretical values for the sphere are used to calibrate the target data in absolute magnitude and absolute phase (relative to the center of the sphere in this case).

A discussion of the specific problem areas for this type of system and the solutions developed is presented. Details of the performance for a known target (sphere) are given over a frequency ranging from one to 16GHz. Errors are discussed with respect to their origin and mitigation.

BROAD BAND SCATTERING
SIGNATURES OF CONE-LIKE OBJECTS

E.K. Walton and J.D. Young
The Ohio State University ElectroScience Laboratory
Department of Electrical Engineering
Columbus, Ohio 43212

The radar cross section amplitude and phase of a group of cone and cone-like objects was measured at each of 59 harmonically related frequencies. At the fundamental frequency, the wavelength ranged from 17 to 33 times larger than the base diameter of the various cones, and was well into the Rayleigh region. The highest frequency, at 60 times the fundamental, was well into the resonance region for each cone. The system used a bistatic angle of 20 degrees, with aspect angles of 0, 10, 20, and 30 degrees. Both vertical and horizontal polarizations were used. The measurement system used a unique vector subtraction technique to remove effects of system background and system distortion. The data presented will be compared with GTD results in the frequency domain before conversion to the time domain.

Using an FFT, transient scattering signatures can be generated from these data. Time-domain, impulse, step and ramp response waveforms are defined and illustrated for these targets. Transient signature features related to body geometry and specific scattering phenomena are discussed. A comparison of measured and calculated transient waveforms is presented.

USE OF ORBITING WIRE FOR CALIBRATION OF CIRCULARLY POLARIZED
RADAR RETURNS *

Hitoshi Inada
M.I.T. Lincoln Laboratory
Lexington, MA. 02173

An orbiting wire will be examined for a possible candidate to be used as an external object to calibrate left (principal) PP - and right (orthogonal) OP - circularly polarized radar return. The Haystack LRIR (Long-Range Imaging Radar) was used in this investigation. However, this type of calibration may be used for any radar with circular polarization. The backscattering characteristics of a long thin wire illuminated by a circularly polarized wave will be discussed. For a long thin wire when ka is less than 0.05 (a is the radius of wire), the ratio of OP to PP RCS (radar cross section) assumes unity (0 dB) at normal incidence. For LRIR, almost all orbiting wires have $ka=0.166$, for which the theory for an infinitely long cylinder indicates that the OP RCS exceeds the PP RCS by 1.36 dB at normal incidence. Accurately calibrated PP and OP RCS would be useful in estimating target size, shape, orientation and motion.

CW data on a wire in orbit were recorded by LRIR during several tracks. The wire is a TIROS despin cable with a length of 3 m (100 wavelengths long). Over a data interval of 1 minute, approximately 25 broadside speculars at normal incidence were observed and the average value of (OP/PP) RCS is 1.27 dB with a standard deviation of 0.2 dB. In addition, the peak RCS of normal incidence is 49 degrees with a standard deviation of 9.7 degrees. The phase difference is somehow related to the wire orientation. Measured wire RCS at normal incidence is compared with those obtained by using Ufimtsev's solutions for a long thin wire. The calculated and measured X-band RCS are in good agreement to an accuracy within 1 dB and the initial results support the conclusion that the wire in orbit may be used as a relative (OP to PP) RCS calibration target as well as an absolute OP and PP RCS calibration target.

*This work was sponsored by the Space and Missile Systems Organization (SAMSO) of the Air Force.

"FAR-FIELD ESTIMATION FROM NEAR-FIELD MEASUREMENTS
TAKEN ALONG A STRAIGHT LINE SEGMENT"

MARCO TULLIO MARTINS DA SILVA - FINEP/BRAZIL

ANTONIO R. PANICALI - UNIV. DE S. PAULO, FINEP/BRAZIL

This work describes a method of estimating antenna far-field characteristics from near-field data measured along a straight line segment oriented along the direction at which the far-field is desired.

A truncated series of base functions is used to expand the antenna field outside the volume containing the sources; the series coefficients are then estimated by requiring the series to be a constrained least squares approximation to the measured data. The approach can be described as a near-field synthesis where power constraining was found necessary in order to avoid the ill-posedness of the problem.

The method has been numerically tested for circular apertures up to 60 wavelengths (λ) with a great variety of aperture distributions; in all cases fields were computed at 101 points uniformly distributed between 360λ and 600λ ; independent random errors within $\pm 1\%$ were added to the real and imaginary parts of the computed near-field in order to simulate a real experiment; expression (21) in "M.M. Rabello, S.L.G. Nobili, Radio Science, 8, 677-680, 1973" with $n = 0$ and $D = 6\lambda, 12\lambda, \dots, 60\lambda$, were used as base functions. In all cases the main beam gain could be estimated within $\pm 0,27$ dB, with 99.7% probability.

THE USE OF KING-TYPE CURRENT PROBES FOR BROADBAND
TRANSIENT MEASUREMENTS, L. Wilson Pearson, Y. M. Lee,
Department of Electrical Engineering, University of
Kentucky, Lexington, KY 40506

A miniature balanced loop current probe fabricated from semi-rigid coaxial tubing is described by King (R.W.P. King, The Theory of Linear Antennas, 1956) and has been used with great success in time harmonic current probing. The Air Force Weapons Laboratory has, more recently, developed a family of transient sensors comprising the so-called B-dot and D-dot probes. These probes offer excellent bandwidth. They are, however, fixed station probes.

The present work stems from an attempt to gain the position agility offered by the King probing scheme in a transient measurement application. The probe is to be used, ultimately in transient data collection for extraction of the SEM description of a scatterer as reported by Pearson and Roberson at the January 1978 National Radio Science Meeting.

The first constraint placed on the design by the transient application is the need to maintain a flat 50 ohm transmission line from the probe gap to the instrumentations. This is readily achievable by means of using a continuous section of 0.020" semi-rigid coax for fabrication of the probe and its feed. The transition from 0.020" cable to a subminiature connection is observed to be the only significant source of mismatch.

In this presentation, we describe the probe as it is applied in transient measurements. The calibration of the probe by means of transient techniques in a transmission line section is described and analyzed and specimen results are given. The possibility of using the probe as an excitor as well as a sensor is discussed.

SESSION B-1
MONDAY AM 8:30-12:00
KANE HALL 120

HIGH FREQUENCY SCATTERING

Chairman: Y. Rahmat-Samii
Jet Propulsion Laboratory
Pasadena, CA

APPLICATION OF THE UNIFORM GTD TO THE
DIFFRACTION BY AN APERTURE IN A THICK SCREEN

Roberto Tiberio
University of Florence
Florence, Italy

Robert G. Kouyoumjian
The Ohio State University
Columbus, Ohio

A uniform GTD solution is presented for the diffraction of a plane wave normally incident on a slit in a perfectly-conducting thick screen. This problem involves the diffraction of ray-optical fields, as well as fields which do not exhibit a ray-optical behavior. The diffraction of the ray-optical fields is determined by means of the uniform GTD (Kouyoumjian and Pathak, Proc. of IEEE, 62, 1448-1461, 1974) together with slope diffraction. However, the rays doubly-diffracted at grazing incidence from the two thick edges of the slit are treated by means of a recent extension of the uniform GTD (Tiberio and Kouyoumjian, 1977 USNC/URSI meeting at Stanford University). In this case the transition region fields incident on the trailing edges are represented by a superposition of inhomogeneous, cylindrical waves whose diffraction can be determined by the uniform GTD alone. In addition, approximate closed-form expressions are found for the interaction between the two thick edges. This interaction is obtained from doubly- and triply-diffracted rays which may also be multiply reflected.

Illumination by both TE and TM plane waves is considered and results are given for the diffracted near and far fields. An integral occurs in the near field for the TM case which cannot be evaluated in closed form, except in the forward direction; however, it can be evaluated numerically without difficulty. Calculations of the transmission coefficient and radiation patterns are compared with numerical results from a moment method solution provided by R. F. Harrington.

HIGH FREQUENCY ELECTROMAGNETIC FIELDS ON PERFECTLY CONDUCTING
CONCAVE SURFACES

E. Topuz L.B. Felsen
Polytechnic Institute of New York

This investigation deals with high frequency fields on the concave surface of a perfectly conducting circular cylindrical segment excited by an arbitrarily oriented magnetic dipole located on the surface.

The vector fields are derived from two scalar Green's functions which are constructed as contour integrals and evaluated asymptotically in two alternative ways. In one representation an appropriate number of geometrical optics rays is extracted to provide canonical remainder integrals with highly improved convergence characteristics. In the second approach a properly determined combination of rays together with E and H type angularly guided (whispering gallery) modes is utilized. It is found that this latter hybrid field representation developed and applied previously to scalar problems (T. Ishihara, L.B. Felsen, IEEE Trans. AP, AP.26, 757-767, 1978) retains advantages also for vector fields in that it furnishes much higher computational efficiency together with a better understanding of the underlying physical phenomena.

Extensive numerical results are presented to exhibit the relevant vector features of the fields. Magnitude and polarization have been investigated as functions of dipole orientation and observation point location. As for the planar boundary the magnitudes of the surface fields are sensitive to the source orientation with respect to the geodesic to the observation point. However, the polarization with respect to geodesic may differ markedly from that for the planar case. The results are interpreted in terms of the physical models implied by the various field representations.

Scattering by Resistive Strips

Thomas B.A. Senior, Radiation Laboratory
The University of Michigan, Ann Arbor
Michigan, 48109

For an E- or H-polarized plane wave incident on a resistive strip of electrical width kw , a high frequency asymptotic technique is used to derive expressions for the far field amplitude through second order terms. The results are valid for all angles of incidence and scattering other than grazing, and can be cast in terms of functions analogous to those appearing in the uniform expressions derived by Fialkovskiy (Radio Eng. Elect. 2 (150) 1966) and Khaskind and Vainshteyn (Radio Eng. Elect. 10 (1492) 1964) for E- and H-polarizations respectively in the special case of perfect conductivity. It is shown that each function is directly related to the diffracted portion of the relevant current on a half plane, and using representations for the currents valid for all angles of incidence, uniform expressions for the far field amplitude of the strip are obtained which hold even at grazing angles. In the particular case of edge-on backscattering, the contribution from the rear edge of the strip is proportional to the square of the current at the corresponding point on a half plane. The constant of proportionality involves the 'split' function produced by the Wiener-Hopf method of solution of the half plane problem and, for E-polarization and real resistivities, differs by no more than 6 percent from the constant empirically derived by the author (National Radio Science Meeting, Boulder, 1978).

RAY-OPTICAL THEORY OF COUPLING BETWEEN AND RADIATION
FROM ADJACENT PARALLEL PLATE WAVEGUIDES

Peter F. Driessen and Edward V. Jull
Department of Electrical Engineering
University of British Columbia
Vancouver, B.C., Canada V6T 1W5

The coupling between two immediately adjacent semi-infinite parallel plate waveguides (Fig. 1) is calculated by ray-optical methods. The procedure of Yee et al (SIAM J.Appl.Math (29)1,164-175), which avoids shadow boundary singularities by using line source diffraction, is employed. Both single and multiple diffraction terms are calculated. Numerical values of the coupling coefficient using only single diffraction terms provide the average behaviour. Adding the multiple diffraction terms reveals a fine structure with minima near cutoff of the waveguide modes.

The radiation pattern of a small array of coupled waveguides (Fig.2) is calculated using a combination of ray-optical methods and the known exact radiation pattern for a single guide. The coupling coefficient between two adjacent guides in the array may be modified to take into account the presence of the other guides in the array. Radiation from the edges of the waveguide not implicitly included in the radiation from the feed and parasitic guides can also be added to yield the total radiation pattern.

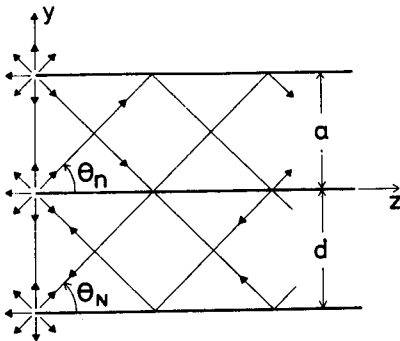


Fig. 1

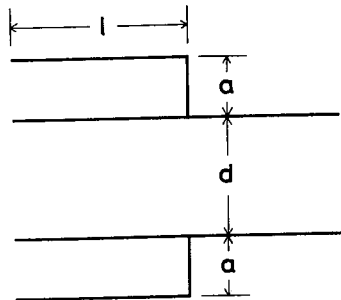


Fig. 2

Edge Currents on Rectangular Plates

Valdis V. Liepa, Radiation Laboratory
The University of Michigan, Ann Arbor MI 48109

The back scattering from a rectangular plate at edge-on incidence is due essentially to individual contributions of edge currents on the front and rear edges. The behavior of the current on the front edge is analogous to that on a finite length wire excited by a plane electromagnetic wave, but the current on the rear edge is entirely determined by the current waves along the sides. Quantitative behavior of the currents on the plate has been measured and described by Knott et al for a case of fixed frequency and plate size (T-AP, Nov. 71, 788-789), but here the currents measured at various points along the edges as a function of frequency are presented. From these data relatively simple formulae are then deduced to characterize these currents.

It is shown that the current on the front edge can be considered as consisting of the half-plane edge current and the reflected waves from the corners. Along the sides the current consists of a component transmitted from the front around the front corner and one excited directly by the incident wave. The currents at the rear edge result from the side edge current transmitted around rear corners.

SCATTERING FROM A CORNER FORMED BY TWO LINE ELEMENTS

K. M. Mitzner and S. A. Sloan, Aircraft Group,
Northrop Corporation, Hawthorne, CA 90250

In a recent paper (IEEE Trans. on Antennas and Propagation, AP-25, 406-409, 1977), Knott showed how to calculate the radar cross section of the dihedral corner formed by two intersecting plates.

In this paper, we present a similar study for another kind of reflecting corner, the corner formed by two intersecting straight line elements. The elements, which may be wires or may be the edges of a body, are of finite length and are assumed to be sufficiently long so that resonances can be neglected.

For an obtuse corner angle, there are no directions of retrodirectivity. For a 90° corner angle and incidence in the plane which contains the two elements, the scattering is retrodirective just as for the analogous dihedral corner. For a given acute corner angle, there is a locus of directions of incidence for which the corner is retrodirective. Only two points on this locus lie in the plane containing the elements.

By working with incremental length diffraction coefficients we develop a simple formulation in which the double bounce contribution is given by a one-dimensional integral. We then evaluate the integral asymptotically to get a simple but accurate closed form approximate solution. We use this solution to study the reduction in backscatter as either the corner angle or the direction of observation is changed from a value which gives retrodirectivity.

The approach is readily extended to bistatic scattering.

RADIATION FROM SOURCES ON SMOOTH CONVEX
SURFACES WITH EDGES — A SPECTRAL DOMAIN APPROACH

S. Safavi-Naini and R. Mittra
University of Illinois
Electrical Engineering Department
Urbana, Illinois 61801

In this paper, we consider the problem of radiation from sources on a finite, smooth, convex surface, e.g., a truncated cylinder. The problem of deriving an asymptotic solution for the surface currents excited by a magnetic dipole placed on the surface of an infinite cylinder has recently been investigated by Lee and Safavi-Naini [IEEE Trans. Ant. Prop., pp. 539-598, 1978] and a solution has been derived in a convenient, closed form. This solution has been verified to be accurate for cylinders of large radius ($ka > 10$). In this paper, we use these known currents to derive the far-field pattern of the source, taking particular account of the edge contributions at the ends of the truncated cylinder. We employ an approach based on STD - the spectral theory of diffraction - and show that it circumvents the difficulties associated with GTD when applied to the same problem. The GTD edge-diffraction formula for the finite cylinder problem is derived using a diffraction coefficient for a right-angle wedge, one of whose faces is a plane tangent to the surface of the cylinder. The GTD diffraction coefficient is singular at certain observation angles and is therefore non-uniform. In the STD method, the radiated field is associated with the spectrum of the surface current induced on the finite cylinder. The surface current consists of two parts - one is the excess current due to the edge, and the other is derived by truncating the induced current on an infinite cylinder excited by the given source. Because of the curvature of the cylindrical surface, the second component of the current is substantially different in character than the corresponding one in GTD for the wedge with planar surfaces. In addition, this current produces finite fields everywhere in space and is therefore uniform. The excess current on the cylinder due to edge diffraction also radiates uniform fields which are readily derivable through a simple modification of the GTD formulas. To effect this modification, one merely subtracts out the far-field contribution of the fictitious semi-infinite, physical optics type of half-plane current used in the GTD formula and identifies the remainder as the contribution of the excess edge current. The physical optics current contribution is next replaced by the far-fields derived from the curved-surface currents on the infinite cylinder excited by the given source. Thus, while the simplicity of GTD formulas is essentially preserved in the spectral approach, the STD formula does not suffer from the difficulties at certain observation angles and is more accurate as well. The paper presents illustrative numerical results and also discusses a method for circumventing the difficulties along the caustic directions using the STD approach.

EVANESCENT WAVE TRACKING IN A SLAB WAVEGUIDE
WITH TRANSVERSE AND LONGITUDINAL
REFRACTIVE INDEX VARIATION

G. Jacobsen* and L. B. Felsen
Polytechnic Institute of New York
Route 110, Farmingdale, N. Y. 11735

The theory of evanescent waves has previously been applied to determine the high frequency behavior of modal fields guided in slab waveguides with transversely varying refractive index, (S. Choudhary and L. B. Felsen, J. Acoust. Soc. Am. 63, 661-666 1978). The method, which involves the tracking of local evanescent plane waves along parallel phase path trajectories and avoids the caustic correction problems inherent in conventional ray-optical or WKB procedures, provides systematically the asymptotic expansions for the modal propagation coefficients and field amplitudes in inverse powers of the large wavenumber k . The present study generalizes the method to waveguides with gradual transverse and longitudinal refractive index variations, the latter being characterized by a perturbation parameter δ . A local orthogonal curvilinear coordinate system is employed to describe in terms of δ either the deformed phase paths or the deformed contours of constant refractive index. From the resulting eikonal and transport equations, one may determine the profile shape to match a specified modal field or the modal field perturbation caused by a specified index variation. To the lowest order in δ , the contours of constant refractive index are found to coincide with the perturbed phase paths, but deviations are encountered to higher orders in δ . The tracking procedure is illustrated for transitions from uniform to tapered waveguides, for different "smoothness" conditions at the junction. Numerical results will be presented for various profile shapes.

*On leave from the Electromagnetics Institute, Technical University of Denmark, Lyngby, Denmark.

ON THE ASYMPTOTIC THEORY OF INHOMOGENEOUS WAVE TRACKING
AND ITS RELEVANCE TO THE INVERSE SCATTERING
OF GAUSSIAN BEAMS

P. Einziger

The Technion-Israel Institute of Technology
Department of Electrical Engineering

and S. Raz

The Technion-Israel Institute of Technology
Department of Electrical Engineering
Currently on Sabbatical Leave
At The University of Houston,
Department of Electrical Engineering

This work presents alternative formulations of the asymptotic, inhomogeneous wave tracking theory (IWT) initially proposed by Felsen and Choudhary [IEEE Trans. Antennas & Prop., AP-21, 827-842, 1973], and investigates the basic analytical features of the ensuing operators. The outstanding deviations from classical ray theory are traceable to the fact that the generalized system of equations is of the quasi-linear, elliptical type. Consequently, representation via an initial value formulation, standardly posed by geometrical optics (and, in the quasi-homogeneous limit, by IWT) must be approached with caution and an appropriate boundary value formulation should be considered. Questions of existence, uniqueness, stability and locality are discussed and related to the problem of inverse scattering of Gaussian beams. The following alternative, but by no means equivalent, formulations are considered:

- (a) A first order, quasi-linear system of equations cast into a canonical form, the existence, uniqueness (but not the stability) of whose solution are ensured by the Cauchy-Kowalewsky conditions.
- (b) A quasi-linear, second order, elliptical differential equation subject to Dirichlet boundary conditions and to the requirements of elliptic uniformity.
- (c) As (b), but posed as a two-dimensional variational problem.
- (d) Quasi-linear, second order, phase trajectory equation obtained from (b) via the, so called, Hodograph Transformation.

GTD ANALYSIS OF THE NEAR-FIELD
PATTERNS OF PYRAMIDAL HORNS

M. S. Narasimhan and K. Sudhakar Rao
Centre for Systems and Devices
Indian Institute of Technology
Madras-600036, India

A novel technique of analysing the principal plane near-field amplitude and phase patterns of pyramidal horns excited in the dominant mode for $0 \leq |\theta| \leq 180^\circ$ based on the UTD (Uniform Theory of Diffraction) [1] and its Modified Slope Diffraction (MSD) version [2], which have been shown to closely follow the most rigorous Spectral Theory of Diffraction for simple GTD calculations involving a line source and a straight edge [3], is presented in this paper. The geometrical optics field is derived by approximating the horn as a quasi-pyramidal horn-waveguide [4]. While the E-plane near-field (amplitude and phase) pattern is derived by considering only diffraction by the E-plane edges, the H-plane near-field (amplitude and phase) pattern is calculated taking into account the diffracted field contributions from the E-plane edges also for $0 \leq |\theta| \leq \theta_H$ and $(\pi - \theta_H) < |\theta| \leq \pi$, where θ_H is the semiflare angle of the horn in the H-plane. Numerical computations of the near-field patterns, taking into account both singly and doubly diffracted fields, based on the GTD technique detailed here well correlate with the measured patterns of a typical pyramidal horn (with $r_H = 13.1\lambda$; $r_E = 13.77\lambda$; $\theta_E = 17.5^\circ$ and $\theta_H = 16.5^\circ$, where r is the flare-length in the particular plane and θ_E is the E-plane semi-flare angle) for several near-field distances of observation.

References

- [1] R. G. Kouyoumjian and P. H. Pathak, 'A uniform geometrical theory of diffraction for an edge in a perfectly conducting surface,' Proc. IEEE, Vol. 62, pp. 1448-1461, 1974.
- [2] Y. M. Hwang and R. G. Kouyoumjian, 'A dyadic coefficient for an electromagnetic wave which is rapidly varying at an edge,' URSI 1974 Annual Meeting, Boulder, Colorado.
- [3] Y. Rahmat-Samii and R. Mittra, 'A spectral domain analysis of high frequency diffraction problems,' coordinated science lab., Report R-770 May 1977, Univ. of Illinois, USA.
- [4] M. S. Narasimhan, 'Eigenvalues of a class of spherical wave functions,' IEEE Trans. Antennas and Propagation, Vol. AP-20, No. 1, Jan. 1973, pp. 8-14.

SESSION B-2
MONDAY PM 1:30-5:00
KANE HALL 120

WAVES IN RANDOM MEDIA I

Chairman: D. deWolf
RCA David Sarnoff Lab
Princeton, NJ

DEPOLARIZATION AND SCATTERING OF ELECTROMAGNETIC WAVES
BY IRREGULAR BOUNDARIES FOR ARBITRARY INCIDENT
AND SCATTER ANGLES--FULL WAVE SOLUTIONS

E. Bahar and G. G. Rajan
Electrical Engineering Department
University of Nebraska, Lincoln, Nebraska 68588

ABSTRACT

Explicit expressions are presented for the radiation fields scattered by rough surfaces. Both electric and magnetic dipole sources are assumed, thus excitations of both vertically and horizontally polarized waves are considered. The solutions are based on a full wave approach which employs complete field expansions and exact boundary conditions at the irregular boundary. The scattering and depolarization coefficients are derived for arbitrary incident and scatter angles. When the observation point is at the source these scattering coefficients are related to the backscatter cross section per unit area.

Solutions based on the approximate impedance boundary condition are also given, and the suitability of these approximations are examined.

The solutions are presented in a form that is suitable for use by engineers who may not be familiar with the analytical techniques and they may be readily compared with earlier solutions to the problem. The full wave solutions are shown to satisfy the reciprocity relationships in electromagnetic theory and they can be applied directly to problems of scattering and depolarization by periodic and random rough surfaces.

SCATTERING AND ABSORPTION SPECTRA FOR
PLATELIKE HYDROMETEORS

H. Weil and C. M. Chu
Dept. of Electrical and Computer Engineering
The University of Michigan
Ann Arbor, Michigan 48109

To obtain information on polarization and orientation influences on scattering and absorption of electromagnetic waves by platelike hydrometeors or aerosols the individual particles are modeled as flat circular absorptive discs of thickness much less than a wavelength. An integral equation for the current density (including the transverse component) induced in the disc by an incident wave is solved by a partly analytic, partly numerical method which is a hybrid of the finite element and moment methods. The procedure is tailored to be efficient for thin discs of radius to wavelength ratio in the range of roughly $1/5$ to 2 . The current densities thus determined can be used to compute all elements of the bistatic scattering or Stokes matrices as well as total scattering absorption and extinction cross-sections for both the individual particles or polydispersions. The latter is possible because arbitrary directions and elliptical polarizations for the incident waves are handled by the theory and the computational program and this is the chief difference between the present work and an earlier effort (C. M. Chu and H. Weil, *J. Comp. Phys*, **22**, 111-124, 1976) where only the cases of broadside and edge-on incidences with plane polarization parallel to the flat disc surface were developed. The present procedure also models the physics more accurately in computing the circumferential components of the induced current density and so gives more accurate as well as more extensive results.

Curves of the matrix elements and cross-sections for a single disc of ice with fixed radius to wavelength ratio are given as wavelength, and hence complex refractive index, is varied through the infrared. Effects of variation in incident wave directions and polarizations are explored.

NEAR-FORWARD MULTIPLE SCATTERING BY A
RANDOM SLAB OF LARGE PARTICLES

Essam A. Marouf, Center for Radar Astronomy, Stanford University,
Stanford, CA 94305 and University of Alexandria, Egypt

For large particles, direct numerical solution of the equation of transfer is hampered by the need for a highly accurate integration scheme to compute the rapidly varying intensity component in near-forward directions. It is possible, however, to separate this component analytically. The solution is an infinite series sum, with each term representing a successive order of scattering and expressed as the product of an angular function and a weighting function that depends only on the optical depth of the random slab. The solution is sometimes referred to as Hartel's multiple scattering theory. Analytic evaluation of the angular functions requires expanding the phase function of a single particle in spherical harmonics, resulting in considerable increase in computational complexity for large particles. Using the convolutional properties of these angular functions, an explicit sum of the infinite series is derived in the Hankel transform domain. The closed form solution for the intensity transform is identical to a solution obtained by Ishimaru. In general, a numerical inverse transform is needed to recover the intensity. However, the analytical approach is further pursued by modeling the phase function of a spherical particle by its forward diffraction pattern plus an isotropic component chosen so as to satisfy the normalization condition of the phase function. The model leads to good approximate formulas for the variation of the directly transmitted intensity and the width of the forward lobe as a function of optical depth of the slab.

EFFECTS OF ANISOTROPIC IRREGULARITIES ON PHASE SCINTILLATIONS

R. Woo and J. W. Armstrong
Jet Propulsion Laboratory,
California Institute of Technology

There has been considerable interest in phase scintillations in the solar wind because they contain information over a wide range of electron density scale sizes and are invaluable for probing the solar wind. The purpose of this paper is to investigate the effects of anisotropy in the density irregularities on phase scintillations. A closed form solution is obtained for the phase scintillations using the Rytov approximation for fluctuation frequencies lower than the frequency corresponding to the Fresnel zone size (scale size larger than the Fresnel zone size). It is seen that anisotropy causes the phase scintillations to increase over those in the isotropic case. It is also shown that the effects of anisotropy on phase scintillations (large scale sizes) are similar to those on spectral broadening (small scale sizes). As a result, simultaneous observations of phase scintillations and spectral broadening will not provide a means of measuring the anisotropy of the electron density fluctuations. The effects of velocity fluctuations on phase scintillations will also be discussed.

HIGH-ALTITUDE TURBULENCE MEASUREMENTS FOR OPTICAL PROPAGATION PREDICTIONS

Curt A. Levis and John P. Serafin, The Ohio State University
ElectroScience Laboratory, 1320 Kinnear Road, Columbus, OH 43212

Much progress has been reported on the propagation of coherent electromagnetic waves through turbulent media in recent years, but relatively little information is available on the turbulence properties of the atmosphere, particularly in the presence of orographic effects and at high altitudes. This paper reports on measurements of turbulence at high altitudes from aircraft using hot-wire anemometers to measure the temperature structure parameter and to infer from it the refractive-index structure parameter.

It is shown that under typical conditions it is not easy to distinguish between temperature structure and velocity structure. The reason is that the instrument responds not to the ambient air but to the stagnated air surrounding the probe, which has been compressively heated by the aircraft motion. In the process, velocity fluctuations are converted to equivalent temperature fluctuations, resulting in a higher temperature (and therefore refractive-index) parameter value than that actually existing in the ambient medium. A method utilizing two probes heated to different temperatures (L.S.G. Kovaszny, J. Atmos. Sci., 7, 565-584, 1950) was translated into the spatial frequency domain to avoid noise problems and used, thus modified, to separate the two effects.

The results of one flight are discussed in detail and are compared with data taken over the past three years under a variety of conditions in a continuing effort to create a data base for high-altitude optical propagation predictions.

DETECTION EFFECTS ON HIGHER ORDER STATISTICS OF
LIGHT FLUCTUATIONS DUE TO ATMOSPHERIC TURBULENCE

A. Consortini and L. Ronchi
Istituto di Ricerca sulle Onde Elettromagnetiche of CNR
Firenze, Italy

A number of phenomena related to the detection process can alter the statistics of amplitude fluctuations of a laser beam after a path in the atmosphere, giving rise to a "detected signal" whose statistics can be substantially different from that of the signal under study. These alterations become particularly evident when higher order moments are concerned with.

The averaging effects of the collecting aperture, when the aperture is larger than the correlation area of the phase fluctuations, and the non-linearity of the detecting system, in particular of the recorder, are the main responsible of the alteration of the statistics.

In the present communication a procedure is described by which one can deduce from the statistics of the detected signal the parameters of the statistics of the incident signal, by taking into account the above effects. Cases when the statistics of the revealed signal does not allow to deduce in an univocal way the statistics of amplitude fluctuations are presented.

The results are also described of a practical application of the procedure to several sets of experimental data.

RESOLUTION THROUGH THE ATMOSPHERE
OF OPTICAL ADAPTIVE SYSTEMS

A. Consortini, F. Pasqualetti and L. Ronchi
Istituto di Ricerca sulle Onde Elettromagnetiche of CNR
Firenze, Italy

The results are described of a theoretical investigation on the resolution through the atmospheric turbulence of an adaptive optical system. Both cases of long and short exposures are examined. The phase correction introduced by the adaptive system is taken into account by assuming that the phase structure function $D(r)$ of the wave after correction be a fraction α of the phase structure function $D'(r)$ impinging on the system after propagation through the atmosphere:

$$D(r) = \alpha D'(r)$$

where $0 \leq \alpha \leq 1$. The case $\alpha = 0$ corresponds to a perfect correction of phase fluctuations, the case $\alpha = 1$ implies no correction.

For generality purposes possible corrections of amplitude have been also examined.

The atmospheric turbulence is assumed to be described by a modified Karman model which allows one to take into account the effects of both inner and outer scale of turbulence.

Numerical results are described and discussed.

BACKSCATTERED PULSE SHAPE DUE TO SMALL-ANGLE MULTIPLE SCATTERING
FROM A SLAB OF RANDOM MEDIUM

Akira Ishimaru, Department of Electrical Engineering,
University of Washington, Seattle, WA
Kirk J. Painter, Lockheed Missiles and Space Co.,
Sunnyvale, CA

This paper presents calculations for the pulse-envelope shape of a wave backscattered from a turbulent or discrete random medium. The results are given in terms of dimensionless variables; hence they may be applied to a broad class of physical situations and may provide a means for characterizing random media by remote sensing techniques.

The cumulative forward-scatter single-backscatter (CFSB) approximation discussed by deWolf (IEEE Trans., AP-19, 254-262, 1971) and others is applied to a plane wave incident upon a slab for calculation of the backscattered two-frequency mutual coherence function, from which the backscattered pulse shape is found by Fourier transformation. The response to a general pulse may then be obtained by convolution. To employ this technique, the forward-propagating two-frequency mutual coherence function is expressed as the solution to a parabolic equation. Multiple scattering effects are included, under the restrictions of small angular-spread of the wave and a narrow-bandwidth envelope for the incident pulse. The governing parameters for the pulse shape are the depth of the medium measured by the optical distance τ , the albedo W_0 and a parameter which is inversely related to the angular width of the averaged scattering pattern of the medium. When the scattering pattern is a Gaussian function, the latter parameter is $\gamma = \ell^2 k_0^2 / 4$, where ℓ is the scale length of the correlation function of refractive index fluctuation and k_0 is the wave number. The range of validity of the CFSB approximation is found to be approximately $\tau < (2\theta_0/3)^2 \gamma / W_0$ where θ_0 is the maximum allowable angular-spread within the medium. Although the overall temporal pulse width is always approximately $2L/c$, where L is the actual depth of the slab and c is the velocity of propagation, the pulse shape is best preserved when the time scale is normalized to $2L/c\tau$. The effect of non-unity albedo is to hasten attenuation. The effect of γ is surprisingly weak, as drastic increases in γ serve only to sharpen the leading and trailing edges of the overall pulse shape. Thus, asymptotic solutions may be valuable, and a closed-form solution as $\gamma \rightarrow \infty$ is presented. When scattering is instead characterized by a Kolmogorov process, the characteristic parameter $k_0 L_0$ is introduced, where L_0 is the outer scale length. The resulting pulse shape differs greatly from the pulse shape for a Gaussian spectrum. In this case the range of validity for the CFSB approximation is found to be $\tau \leq (k_0 L_0)^{5/3} \theta_0^{5/3} / 12W_0$. The effect of changing $k_0 L_0$ is quite pronounced; however a closed-form asymptotic solution for the pulse shape as $k_0 L_0 \rightarrow \infty$ is found, which in extreme conditions of short wavelength of a large outer scale size may be a good approximation to actual behavior.

SESSION B-3
TUESDAY AM 8:30-12:00
KANE HALL 120

ANTENNAS I (ARRAYS)

Chairman: K. G. Balmain
University of Toronto
Toronto, Canada

LINEAR ARRAY SYNTHESIS USING PRONY'S METHOD*

E. K. Miller and G. J. Burke
University of California
Lawrence Livermore Laboratory
Post Office Box 5504
Livermore, CA 94550

Prony's Method has found an increasing variety of applications in electromagnetics. This is because it provides a straightforward way to obtain the poles and residues of functions which are sums of complex exponentials. Such functions occur commonly in physics, particularly in areas which involve wave phenomena. These include acoustics, structural behavior and, of course, electromagnetics.

Electromagnetic applications range from characterizing spectral and temporal responses to representing bistatic scattering and radiation patterns. The latter area is the one of concern in this presentation, which addresses the specific problem of antenna synthesis. As shown earlier (E. K. Miller and D. L. Lager, "Radiation Field Analysis and Synthesis Using Prony's Method," Electronics Letters, March 16, 1978, Vol. 14, No. 6, pp. 180-182.) the patterns of linear source distributions can be processed using Prony's Method to either determine the actual discrete source array which produced the pattern (i.e., to image the source distribution) or to develop an equivalent discrete array which matches the original pattern (to synthesize a source distribution).

Our attention is focused specifically on antenna synthesis. However, in contrast to our previous work where the pattern being synthesized was derived from a prescribed continuous aperture distribution, we now start from the prescribed pattern itself. This distinction is important, because there is no a priori assurance that an arbitrarily prescribed pattern will be realizable with the exponential source-field relationship required both by Prony's Method and physical reality.

Results are given here for several pattern types to demonstrate the outcome of using Prony synthesis. A pattern found to be especially useful is one given by $\sin^N(\theta)$ where $N \sim 100$ gives a half power beamwidth ~ 10 degrees. The performance of an actual (computer modeled) array of wire dipoles designed to radiate a given pattern is illustrated, and its sensitivity to errors in electrical and mechanical parameters is discussed.

*Work performed under the auspices of the U.S. Department of Energy by the Lawrence Livermore Laboratory under contract number W-7405-ENG-48.

AN ARRAY THINNING TECHNIQUE

De Yuan Ho and Bernard D. Steinberg
Valley Forge Research Center
Moore School of Electrical Engineering
University of Pennsylvania
Philadelphia, Pennsylvania 19104

Random deployment of antenna elements in large arrays permits element thinning by many orders of magnitude without suffering the consequences of grating lobes. Nevertheless the poor sidelobe characteristics of random arrays tend to limit the dynamic range of targets or sources that can be resolved. An ad hoc technique is described which appears to offer an additional order of magnitude of thinning.

The concept is to adjust the element weights during scanning so that nulls are fixed in the directions of the largest responses. By comparing the output scans before the nulls are modified, it appears possible to separate the target responses of the array from the sidelobe responses even though the sidelobe responses to the large targets are huge compared to the smaller targets. In the examples shown a target dynamic range of nearly 40 dB is accommodated by an array with a peak sidelobe level of -7 dB.

ON THE CURRENT DISTRIBUTION ON
PRINTED PARASITIC THIN WIRE ARRAYS

I. E. Rana and N. G. Alexopoulos
Electrical Sciences and Engineering Department
University of California
Los Angeles, CA 90024

The problem of thin wire arrays printed on grounded dielectric substrates is addressed. It is shown that by considering Pocklington's integral equation with the method of moments, it is possible to solve for the current distribution on printed wire arrays, including parasitic elements. The Green's function employed in this analysis results from the solution of a printed Hertzian dipole on the substrate. The results to be shown correspond to printed wires of arbitrary length and interelement separation.

ANALYSIS OF A PHASED ARRAY OF DIPOLES PRINTED ON
PERIODIC DIELECTRIC SLABS OVER A GROUND PLANE

Ruey-Shi Chu

Ground Systems Group, Hughes Aircraft Co., Fullerton, Ca. 92634

Shii-Shyong Wang

The Aerospace Corporation, El Segundo, Ca. 90234

Phased arrays of dipoles printed on periodic dielectric slabs standing over a ground plane with the feeding network printed on the same dielectric board extending behind the ground plane have been used in several practical radar antenna systems. A solution for the active array impedance of this phased array is presented. By using the regular E and H modes with respect to the direction along the periodicity of the dielectric-slab array, we obtain the field solutions in the region containing the array of dielectric slabs. Then we use the E-type and H-type modes with respect to the direction transverse to that of periodicity to describe the transverse fields in a unit cell in both the free space and the periodic dielectric slab regions. Transmission-line equations in a unit cell with excitation due to the printed dipole source and with termination at the ground plane can be set up for the modal coefficients. By matching the boundary conditions at the interface between the two regions, all the modal coefficients can be obtained and thus the active array impedance is solved.

PERIODIC-STRUCTURE-RAY APPROACH TO ANALYSIS
OF ARRAYS ON CONCAVE SURFACESH. Ahn, B. Tomasic and A. Hessel
Polytechnic Institute of New York

This paper will discuss the principles of a rapidly convergent ray approach to analysis of mutual coupling in large arrays on concave surfaces. The prototype configurations employed are uniformly spaced arrays of aperture elements on circular cylindrical conducting surfaces. The high frequency asymptotic evaluation of exact expressions for coupling coefficients gives rise to a variant of GTD, termed the Periodic Structure Ray Method, because the relevant canonical problems are associated with planar periodic arrays, rather than with conducting surfaces. The straight line periodic-structure-ray trajectories are identical with those for the case of an unperforated concave array support surface. In passing from the excited to the receiving element, the ray fields are weighted by the angle dependent launching, reception, and reflection coefficients. These no longer correspond to a planar conducting surface, but to planar periodic arrays appropriate to the respective environments of the transmitting, the receiving element, or the point of reflection on the concave surface. The two former are proportional to the transmitting and receiving element pattern values in the ray direction. The periodic structure ray field expressions are valid in the far zone of the excited element; for elements close to the source, a transition function has been obtained. In the case of three dimensional cylindrical arrays, a stationary phase evaluation of both the ray field and the transition function expressions is required. The advantages of the Periodic-Structure-Ray Approach are:

1. The results are generalizable to variable curvature and/or periodicity.
2. Inversion of large matrices is not required (in contrast to modal analysis or to the usual GTD evaluation); the method employs planar phased array solutions as canonical problems, and exploits the associated computer programs.
3. It provides physical explanation of numerical results

The basis of the approach was presented at the URSI General Assembly in Helsinki, but only two-dimensional (slit) arrays were discussed. After a suitable background, the paper will describe the modifications necessary to derive the ray formalism applicable to infinite-stacked-ring arrays of rectangular waveguide elements in a concave geometry. A comparison of numerical results with those of modal analysis in two and three dimensional arrays will be given.

CURRENTS ON A YAGI STRUCTURE OF INCLINED DIPOLES

Walter K. Kahn*
Naval Research Laboratory
Washington, D.C. 20375

Excitation of one element of a uniform (Yagi) array of parasitic dipoles gives rise to currents on the parasitic elements which are conveniently dissected into surface-wave and radiative components. A network formulation from which characteristics of the surface wave component was found has been presented. This formulation, which exhibits the close connection between the properties of the array of parasitic dipoles and those of the same structure when all elements are excited as in a phased array, has been extended to yield also the radiative components of the currents. For dipoles inclined at an angle $\theta_0 = \arctan \sqrt{2}$ to the array axis, the expressions simplify remarkably, and the complete solution is obtained by function theoretic techniques. The relative amplitude of the surface wave and radiative component is computed, and the decay of the radiative component with distance from the source element is found.

* Professor of Engineering and Applied Science
George Washington University, Washington, D.C. 20052

RESONANCE PHENOMENA ON YAGI ARRAYS

J.M. Tranquilla
Department of Electrical Engineering
University of New Brunswick
Fredericton, N.B. Canada

K.G. Balmain
Department of Electrical Engineering
University of Toronto
Toronto, Ont. Canada

ABSTRACT

The Yagi antenna has been studied experimentally and theoretically and a class of resonance phenomena has been found to occur in a narrow range of kh values (where k is the free space number and $2h$ is the dipole length) immediately below the dipole array cutoff frequency. This resonant behaviour is characterized in the swept frequency radiation patterns by a very narrow-band reduction in the front-to-back ratio and in the input impedance pattern by very rapid fluctuations in both the real and imaginary impedance components. The dispersion characteristics of arrays of dipole elements are used to show that a design procedure may be developed which prevents the occurrence of such resonances.

ANALYSIS OF THE LOOP-COUPLED LOG-PERIODIC DIPOLE ARRAY

J.M. Tranquilla
Department of Electrical Engineering
University of New Brunswick
Fredericton, New Brunswick, Canada

K.G. Balmain
Department of Electrical Engineering
University of Toronto
Toronto, Ontario, Canada

ABSTRACT

A model is described to analyse the loop-coupled log-periodic dipole antenna. Both theoretical and experimental data are presented to investigate such properties as the far-field radiation, input impedance and dispersion characteristics for a wide range of antenna parameters. It is shown that a class of resonances characterized in the swept-frequency radiation pattern by a sudden narrow-band loss in front-to-back ratio and involving sets of adjacent elements exists on the loop-coupled array and that in most cases these resonances are dependent upon the nature and location of the feedline termination. A simple model is proposed to permit optimization of the gain by adjustment of the dipole-to-feedline coupling and experimental results on several antennas indicate that the front-to-back ratio may be simultaneously optimized.

THE INFLUENCE OF A BOREHOLE ON THE MUTUAL IMPEDANCE OF AN ARRAY OF
COPLANAR LOOPS

R. G. Olsen and N. A. Sanford
Department of Electrical Engineering
Washington State University
Pullman, WA 99164

It is well known that the mutual impedance between loops carrying high frequency currents can be used to determine the conductivity and permittivity of the infinite media in which they are immersed (J. A. Fuller and J. R. Wait, Proceedings of the IEEE, 60, 993-994, 1972). However, when this technique is used to determine the electrical properties of the earth, the loops are surrounded by a cylindrical borehole which has been drilled in the earth. Further, it is not always possible to know the electrical characteristics of the material which fills the borehole. It is therefore important to determine the conditions for which the borehole can be neglected. Under these conditions, simple formulas for the mutual impedance can be used and the presence of the borehole does not introduce significant error into the determination of the earth's conductivity and permittivity.

The case for electromagnetic coupling between coaxial loops in a borehole has been investigated (J. A. Fuller and J. R. Wait, Radio Science, 8, 453-457, 1973). It was found that under most conditions the coupling is independent of the borehole's presence.

In this paper the effect of the borehole on the mutual impedance between coplanar loops is investigated. The coplanar array is of interest for two reasons. First, at lower frequencies it is more sensitive than a coaxial array to planar discontinuities azimuthally. Thus it can be used to determine the direction to an anomaly.

For simplicity the loops are modelled as magnetic dipoles. A closed form expression for the mutual impedance between two horizontal magnetic dipoles in a vertical borehole is derived which can be examined to determine conditions for which the borehole can be neglected.

AN ANALYSIS OF THE MUTUAL COUPLING BETWEEN ANTENNAS
ON A SMOOTH CONVEX SURFACE.

P.H. Pathak and N.N. Wang
The Ohio State University ElectroScience Laboratory
Columbus, Ohio 43212

A compact, approximate high frequency solution is developed in this paper for the electromagnetic surface fields excited by infinitesimal electric or magnetic current sources which are placed on a smooth, perfectly conducting, arbitrary convex surface. A knowledge of the surface fields is essential in the calculation of the mutual coupling between a pair of antennas on a smooth convex surface. In the present solution the surface fields propagate along Keller's surface ray paths, and their asymptotic description is uniformly valid along the ray including the immediate vicinity of the source. Furthermore, as the curvature of the surface becomes vanishingly small, this result recovers the known, exact result for the fields on a planar, perfectly-conducting surface. The development of this solution is heuristically based upon the form of the asymptotic solutions for the surface fields which are first obtained for the canonical circular cylinder and spherical geometries. The heuristic generalization of these canonical solutions is that the arbitrary convex surface case then follows via local properties of wave propagation at high frequencies. The effect of torsion associated with the surface rays is clearly identified in this result through the presence of a factor T/K which appears in the expressions for the surface fields. Here, T denotes the surface ray torsion and K denotes the surface curvature along the ray direction. Numerical calculations for the mutual coupling between a pair of slots in cylinders and cones will be indicated along with measurements, or with calculations based on exact model series solutions, to illustrate the accuracy of the present solution.

The work reported in this paper was supported in part by the Joint Services Electronic Programs (Contract N00014-78-C-0049) and by contract N62269-76-C-0554 between the Naval Air Development Center and the Ohio State University Research Foundation.

SESSION B-4 (a)
TUESDAY PM 1:30-5:00
KANE HALL 120

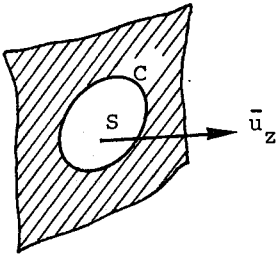
FIELD PENETRATION AND SCATTERING

Chairman: R. F. Harrington
Syracuse University
Syracuse, NY

"FIELD PENETRATION THROUGH SMALL APERTURES :
THE FIRST-ORDER CORRECTION"

J. Van Bladel

Laboratorium voor Elektromagnetisme en Acustica
Rijksuniversiteit Gent, Gent, Belgium



At sufficiently low frequencies (i.e. for λ large compared with the aperture's dimensions), an iterated solution can be obtained by expanding fields in power of $jk = j \frac{2\pi}{\lambda}$. Typically

$$\underline{E} = \underline{E}_0 + jk\underline{E}_1 + \dots$$

The zero-order terms are well-known. They are of a "static" nature. We are concerned with

$\underline{E}_1, \underline{H}_1$. The basic unknown of the problem is the equivalent magnetic current density in the aperture, which we write as

$$\underline{K}_s = 2(\underline{E} \times \underline{u}_z) = \text{grad}_{xy} \Gamma + \underline{u}_z \times \text{grad}_{xy} \theta$$

where

$$\begin{cases} \theta = 0 & \text{on } C \\ \frac{\partial \Gamma}{\partial n} = 0 & \text{on } C \end{cases}$$

Iterated integral and integro-differential equations are derived for $\theta_0, \theta_1, \Gamma_1$ etc...

For example :

$$\left\{ \begin{array}{l} \frac{1}{4\pi} \nabla_{xy}^2 \iint_S \theta_1(\underline{r}') \frac{1}{|\underline{r} - \underline{r}'|} dS' = -\underline{u}_z \cdot \underline{E}_1 + \frac{1}{4\pi} \int_C \frac{\partial \Gamma_1}{\partial c'} \frac{1}{|\underline{r} - \underline{r}'|} dc' \\ \theta_1 = 0 \quad \text{on } C \end{array} \right.$$

The general theory is applied to plane-wave incidence (normal or oblique). Formulas are obtained for the dipole and quadrupole moments, through which the far-field can be expressed. The formulas are applied to the circular aperture, the results checking with those obtained previously by Bouwkamp by other methods.

DIFFRACTION BY A NARROW SLIT IN AN IMPEDANCE PLANE

R. A. Hurd, Division of Electrical Engineering,
National Research Council of Canada,
Ottawa, Ontario, Canada, K1A 0R8.

A study is made of diffraction by a narrow slit in a plane which has a reactive boundary condition on one side and a second (possibly different) reactive boundary condition on the other side. An incident field, comprising both a space plane wave and a bound surface wave, is assumed. See Fig. 1. Owing to lack of symmetry, the formulation of the problem leads to a pair of coupled integral equations. These are solved by assuming that the slit width is small with respect to the wavelength, and making quasi-static approximations. The integral equations are then replaced by a sequence of simpler, uncoupled equations which can be solved successively. The first two terms of the expansion (in powers of kd , where $2d$ is the slit width) are obtained, and expressions derived for the scattered fields. The latter are of two types: surface waves generated at the slit on both sides and space waves above and below the screen. The amplitudes of the waves are computed. It is found that the magnitudes of the oppositely-directed surface waves on the top are equal; and are in general different from the (equal) magnitudes of the bottom surface waves. The amplitudes of the scattered space waves turn out to be ϕ -dependent, with a maximum in the broadside direction and with a possible secondary maximum for a certain range of X_j . This contrasts with the uniform pattern obtained when $X_j = 0$. Finally the field in the slit is computed and it is found that the components normal to the edges are singular as $R^{-\frac{1}{2}}$.

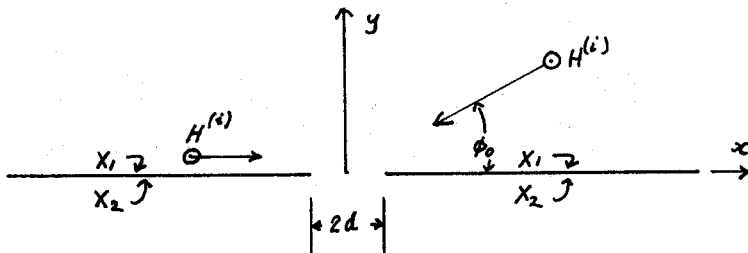


FIG. 1.

PENETRATION AND SCATTERING OF EM FIELDS BY
ADVANCED COMPOSITE BODIES OF REVOLUTION

H. Kao and K. K. Mei

Department of Electrical Engineering and Computer Sciences
and the Electronics Research Laboratory
University of California, Berkeley, California 94720Abstract

The solution to a large class of radiation and scattering problems are readily accessible by the unimoment method. The computational utility of the unimoment method is demonstrated in the solution of EM field penetration and scattering by advanced composite bodies of revolution. The region of space is mathematically divided into interior and exterior region. The interior region completely encloses the scatterer. With the anisotropic properties of the advanced composite characterized by a permittivity tensor, a finite-element algorithm is generated for the interior solution. The scattered field in the exterior region is analytically represented by a series expansion having unknown coefficients. With appropriate enforcement of continuity conditions, the solution to the EM field penetration and scattering problem is obtained.

Research sponsored by the National Science Foundation Grant ENG-76-22296.

SCATTERING BY A HEMISPHERE

P.L.E. Uslenghi
 Communications Laboratory
 Department of Information Engineering
 University of Illinois at Chicago Circle
 Chicago, Illinois 60680
 and
 V. Daniele
 CESP, Politecnico di Torino, Italy

Acoustic and electromagnetic scattering by a hemisphere of radius $r = a$ occupying the angular region $0 \leq \theta \leq \pi/2$ is studied by modal matching. The space surrounding the hemisphere is divided into two regions ($r \leq a$, $\pi/2 \leq \theta \leq \pi$) and ($r > a$, $0 \leq \theta \leq \pi$); in both regions, the field is represented in terms of spherical modes. By imposing the continuity of the field and its normal derivative (in the scalar case) or of the tangential components of the field (in the vector case) at the surface ($r = a$, $\pi/2 \leq \theta \leq \pi$), we eliminate the coefficients a_n of the spherical modes in the region $r \leq a$, thus obtaining an infinite system of linear equations in the unknown coefficients b_n of the spherical modes in the region $r \geq a$. By imposing the boundary conditions at the surface ($r = a$, $0 \leq \theta \leq \pi/2$), we obtain another system of infinite linear equations in the unknowns b_n .

In both infinite systems, it is possible to express the even coefficients b_{2n} in terms of the odd coefficients b_{2n+1} , and viceversa. This property allows us to eliminate either the even or the odd coefficients, thus obtaining a system which does not present the property of relative convergence (Mittra and Lee, 1971); therefore, an approximate solution of such a system is easily obtained by matrix truncation. However, the system obtained has another interesting property which may lead to an exact solution of the scattering problem.

The infinite matrix M formed with the coefficients of the unknowns b_{2n} (or b_{2n+1}) can be written as the sum of two matrices $M = C + D$. The matrix C is a compact operator, while D is the matrix which is obtained by applying mode matching to the scattering from the disk ($0 \leq r \leq a$, $\theta = \pi/2$). The inverse matrix $M^{-1} = (1 + D^{-1}C)^{-1} D^{-1}$, where D^{-1} is known, whereas $(1 + D^{-1}C)^{-1}$ may be calculated by an extension of Fredholm's theory of integral equations of the second kind to infinite systems of linear equations. This research was supported in part under grant AFOSR-77-3253, and in part under a joint program between NSF and the Italian CNR.

AN EFFICIENT APPROACH FOR COMPUTING FRESNEL-ZONE FIELDS

A. M. Rushdi, R. Mittra and V. Galindo-Israel†
 University of Illinois, Urbana, Illinois and
 Jet Propulsion Laboratory
 California Institute of Technology, Pasadena, California

The determination of Fresnel-zone fields from aperture antennas and reflecting surfaces is an important problem and arises in many applications, e.g., antenna measurements and design of beam waveguides. The computation of these fields is extremely time-consuming, even more so than the determination of the corresponding far-field patterns. Recently, an efficient series method (Galindo-Israel and Mittra, IEEE Trans. AP-25, 631-641, 1977) based on the use of Jacobi polynomials, was introduced for efficient computation of far-field (Fraunhofer) patterns from reflector and aperture antennas. In this paper we show how the series method can also be employed for the determination of Fresnel region fields from planar aperture antennas and parabolic reflectors. We begin by expressing the magnetic field in the Fresnel region due to a given surface current distribution \vec{J}_s on a surface Σ :

$$\vec{H}(\vec{r}) = -jk \frac{e^{-jkr}}{4\pi r} [\hat{r} \times (\vec{A}_0 + 2\vec{A}_1 + j\vec{A}_2) + \vec{A}_3]$$

where $\vec{A}_0 = \iint_{\Sigma} \vec{J}_s(\vec{r}') e^{jk\vec{r}' \cdot \hat{r}} ds' =$ Far field term

and the Fresnel region contributions are given by the higher-order terms \vec{A}_1 , \vec{A}_2 , and \vec{A}_3 . We show that these higher-order terms can be expressed in terms of \vec{J}_s and \vec{A}_0 as

$$\vec{A}_1 = \frac{1}{r} \iint_{\Sigma} (\vec{r}' \cdot \hat{r}) \vec{J}_s e^{jk\vec{r}' \cdot \hat{r}} ds'$$

$$\vec{A}_2 = -\frac{k}{2r} \iint_{\Sigma} (r'^2 - (\vec{r}' \cdot \hat{r})^2) e^{jk\vec{r}' \cdot \hat{r}} ds'$$

$$\vec{A}_3 = -(1/r) \iint_{\Sigma} \vec{r}' \times \vec{J}_s e^{jk\vec{r}' \cdot \hat{r}} ds'$$

The principal contribution of this work is to demonstrate that, once \vec{J}_s is expanded in a Jacobi-polynomial series, the coefficients of the series can be employed to not only compute the integral \vec{A}_0 , but the higher-order integrals as well. Consequently, this series procedure represents a considerable time-saving over the conventional methods which require repeated numerical integrations of highly oscillatory nature for each observation point.

†The order of the authors is arbitrary. V. Galindo-Israel is with JPL.

NEARFIELD SCATTERING BY A FINITE DIELECTRIC ROD

G. Tricoles, R. A. Hayward, E. L. Rope
General Dynamics Electronics Division
P. O. Box 81127, San Diego, CA 92138

The fields distributions near finite dielectric rods illuminated with plane electromagnetic waves give useful information for applications like radome analysis. The fields also are of interest in electromagnetic scattering by dielectric particles and structures. This paper gives theoretical, numerical, and experimental results for scattering by finite length circular cylinders. The theory is a form of the moment method. It utilizes volume integrals for polarization currents (J. H. Richmond, IEEE Trans., AP-13, pp 334-341, 1965); however, it differs from earlier work because the rod is subdivided into thin discs. The theory includes the divergence of the polarization charges. We describe calculations for wave polarization either parallel or perpendicular to the rod length, but incidence is normal to rod length. The computed field distributions are compared with measured values for distances of 0.5, 1.0, and 1.5 wavelengths from a rod, dielectric constant 2.6 and length 1.5 wavelength.

RADAR CROSS SECTION OF LOOP ANTENNAS
ABOVE FINITE CONDUCTING HALF-SPACE

Ahmed S. Abulkassem and David C. Chang
Electromagnetics Laboratory
Department of Electrical Engineering
University of Colorado
Boulder, Colorado 80309

The problem concerning the scattering cross section of a thin wire loop antenna located in air above a dissipative earth is of interest in radar target identification and direction finding. In many situations when the circumference of the loop is comparable to the free space wavelength, scattering pattern of a loop near resonance can be significantly different from that of a loop of smaller radius. The problem is further complicated by the interaction between the loop and the earth surface when the loop is oriented in a different direction. In this paper, we shall discuss in detail the difference in scattering cross-section of a horizontal and vertical loop. We begin first by an integral equation formulation for the induced currents on the two loops taking into account the interaction between the loop and the earth via the well known Sommerfeld integrals for an electric dipole of arbitrary orientation. A Fourier Series expansion of the induced current is then used to convert the integral equation to a matrix equation for the current components, which is subsequently solved by numerically computing all matrix elements. For a resonant loop, we have shown that scattering cross-section of a horizontal loop is typically larger than that of a vertical loop. Going from perfectly conducting ground to a finite conducting earth, substantial difference cross section exists mainly because the field incident onto the loop is now greatly modified by the reflection of the plane wave from the earth surface. For loop height greater than free space wavelength, the interaction between the loop and earth can be ignored.

USES OF THE NONLINEAR OPTIMIZATION IN FIELD AND SCATTERING PROBLEMS;
Y.L. Chow and S.K. Chaudhuri, Department of Electrical Engineering,
University of Waterloo, Waterloo, Ontario N2L 3G1, Canada.

An optimization subroutine minimizes an objective function by iteratively adjusting its function variables. The objective function can be the sum of the squared errors of the constant terms of a set of simultaneous equations derived from a numerical or analytical method. If the equations are linear, they can be solved by matrix inversions. If the equations are transcendental, they cannot be solved in any usual manner, however they can still be solved by the nonlinear optimization subroutine.

Many problems in fields and scattering can be quite simple when a set of transcendental simultaneous can be used. We shall discuss three examples in this paper.

The first example is the capacitance and field around two oppositely charge conducting spheres (Y.L. Chow and C. Charalambous, URSI Meeting, Boulder, CO., Jan. 1978 and IEE Proc. in press). By placing simulated charge images in the spheres with strength and locations to be optimized, a rapid convergence of two charge images per sphere is obtained giving the same boundary accuracy as that of eight charge images in the well known successive images method (W.R. Smythe, "Static and dynamic electricity", 3rd. Ed., McGraw-Hill, 1968, pp. 128-129). The latter, of course, is still faster convergent than the point matching moment method.

The second example is the scattering cross section of one or more conducting spheres (Y.L. Chow and C. Charalambous, URSI Meeting, Boulder, CO., Nov. 1978). By placing three pairs of electric and magnetic dipoles images inside one conducting sphere and optimizing, the scattering cross section calculated is accurate, up to $ka = 2.2$ (i.e. far into the resonant region). With only a small number of dipole images thus obtained, the near field around the sphere can be obtained very easily and just as accurately as the scattering cross section.

The third example is different from the first two in studying the back scattering impulse response of ellipsoids. An application of the physical optics condition and the first four moment conditions (E.M. Kennaugh and D.L. Moffatt, Proc. IEEE, Vol. 53, 1965, pp. 893-901), leads to a set of transcendental equations which is then solved by a nonlinear optimization subroutine.

Based on these three examples, interesting points in other examples and the actual use of the optimization subroutines are discussed.

SCATTERING BY MATERIAL BODIES OF REVOLUTION
WITH A METALLIC CORE

S.K. Chang

EMtec Engineering, Inc., Box 679, Berkeley, CA 94701

Electromagnetic scattering from material bodies with a metallic core is of interest in many practical problems. This paper applies the unimoment method (Mei, IEEE AP-22, Nov. 1974) to solve the scattering by a composite of rotationally-symmetric lossy dielectric and perfectly conducting bodies of arbitrary cross sectional profiles. The coupled azimuthal potentials

$\psi_1 = k_o \rho e_\phi$ and $\psi_2 = k_o \rho h_\phi$ (Morgan, Chang, Mei, IEEE AP-25, May 1977) in the material are solved by the variational finite element method. The boundary conditions of the potentials are $\psi_1 = 0$ and $\partial\psi_2/\partial n = 0$ on the conducting surface. The technique is useful in solving the scattering by objects up to several wavelengths in dimension.

ON ELECTRICALLY THICK CYLINDRICAL ANTENNAS
OF FINITE LENGTH

Lawrence Rispin and David C. Chang
Electromagnetics Laboratory
Department of Electrical Engineering
University of Colorado
Boulder, Colorado 80309

The finite length tubular cylinder is often used as a basis in modeling similar physical structures. At low frequencies, thin wire antenna theory is adequate for estimating the axially-directed current on the cylinder due to a plane wave incident field. At higher frequencies, however, this simplified approach is not applicable and more sophisticated methods of analysis are necessary. Numerical techniques such as Kao's (Rad. Sci., 5, 853-859) and the approximate analytical solution of King, et al. (Interact. Note 633, AFWL, Kirtland AFB, N.M.) prove successful in predicting the current densities on the cylinder for both E and H polarization of the plane wave, but are formulated only for normal incidence. Employing the Wiener-Hopf technique, expressions for the current densities on a semi-infinite tubular cylinder of arbitrary radius due to an arbitrarily polarized plane wave incident at an arbitrary angle may be derived. For those radii where waveguide modes in the interior region of the cylinder are still under cut-off, one can show that the angular current as well as the non-uniform component of the axial current decay away from the end of the cylinder, while the uniform axial current reflects and propagates away from the end. Using these expressions, the axially and circumferentially directed current distributions on a finite length cylinder antenna are constructed by summing the multiple reflections from the ends with due attention also being given to the conversions between the axial and circumferential current densities near the ends. Numerical computation of the current distribution for various angles of incidence and polarizations are given, the normal incidence data being consistent with existing theories. In addition, since the reflection of the current wave from the end of a transmitting antenna can be obtained from an incident wave near grazing, one can also investigate a thick cylindrical antenna with an excitation that may be uniform or varying about the cylinder.

SESSION B-4 (b)
TUESDAY PM 1:30-5:00
HUB AUDITORIUM

WAVES IN RANDOM MEDIA II

Chairman: I. M. Besieris
Virginia Polytechnic Institute and State University
Blacksburg, VA

A FUNCTIONAL PATH-INTEGRAL APPROACH TO STOCHASTIC
WAVE PROPAGATION

Ioannis M. Besieris
Department of Electrical Engineering
Virginia Polytechnic Institute and State University
Blacksburg, Virginia 24061

Conrad M. Rose
Naval Surface Weapons Center
Dahlgren, Virginia 22448

Because of the restrictive assumption of zero correlation length along the range, it is well known that Tatarskii's and Klyatskin's pure Markovian random process approximation [cf. Izv. VUZ., Radiofiz. 13, 1061 (1970); 14, 1400 (1971)] allows formally the derivation of exact equations for coherence functions of any order when used in conjunction with the stochastic complex parabolic equation; even in this case, however, the integration of the equations for the fourth- and higher-order coherence functions presents basic difficulties. [These difficulties become more pronounced in the case of the integration of the equations for multifrequency coherence functions (quantities intimately linked to pulse statistics)].

One of the reasons why the aforementioned approach has not yielded sufficient information in connection with higher-order coherence functions is that the study of these functions based on their governing local equations is a nontrivial problem. In contrast, recently formulated methods based on functional (or path) integration [cf. P. L. Chow, J. Math. Phys. 13, 1224 (1972); J. Stat. Phys. 12, 93 (1975); Indiana U. Math. J. 25, 609 (1976); R. Dashen, Stanford Research Inst. Tech. Rept. JSR-76-1 (May 1977); V. U. Zavorotnyi *et al.*, Zh. Eksp. Teor. Fiz. 73, 481 (1977); C. M. Rose and I. M. Besieris, J. Math. Phys. (May 1979)] have the distinct advantage that they work on a global rather than a local level making, thus, easier the algorithmic derivation of asymptotic solutions to higher-order moments.

Our intent in this exposition is twofold: (1) to assess the importance of the path-integral technique as an asymptotic tool in stochastic wave propagation; (2) to present a series of new results dealing with n th-order multifrequency coherence functions in the presence of a deterministic profile, dispersion, and with allowance for finite longitudinal (range) decorrelations.

PROPAGATION IN A TWO-MODE RANDOMLY
PERTURBED WAVEGUIDE

Werner Kohler

Department of Mathematics

Virginia Polytechnic Institute and State University
Blacksburg, Virginia 24061

Stelios Patsiokis

Department of Electrical Engineering

Virginia Polytechnic Institute and State University
Blacksburg, Virginia 24061

In describing the flow of energy in randomly perturbed waveguides, coupled power and coupled fluctuation equations represent a commonly used approximation (c.f. Light Transmission Optics, D. Marcuse, Van Nostrand Reinhold, New York 1972.) These equations, arising from a neglect of backscattering, have also found application in the study of underwater acoustic propagation (c.f. L.B. Dozier and F.D. Tappert, J. Acoust. Soc. Am., 63, 353 and 533).

In this work, our intent is to determine how the coupled power and coupled fluctuation equations emerge from an analysis of the full terminated guide problem. This basic problem is a stochastic 2-pt. boundary value problem in which full multiple scattering effects are included. A model two-mode randomly perturbed guide (matched at generator and load) is studied. The coupled power and coupled fluctuation equations are found to emerge as the leading order terms of a perturbation expansion of the full problem solution when the random fluctuations have a long correlation length in the propagation direction. First order corrections are also obtained. The results are compared to computer simulations and the predictions of a 2-mode transport theory.

AN INTENSITY PROBABILITY-DENSITY FUNCTION
OF PLANE WAVES PROPAGATED THROUGH RANDOM MEDIA

Mitsuo TATEIBA

Department of Electronics, Nagasaki University
1-14 Bunkyo-machi, Nagasaki 852, Japan

Abstract

The $2n$ th-order moment equation determines the statistical properties of successively forward-scattered (SFS) waves in random media. It, however, has not been exactly solved except the case (K. Furutsu, J. Opt. Soc. Amer., 62, 240-254, 1972) that the correlation function $B(\mathbf{r}, z)$ of the refractive index can be approximately expressed as $B(\mathbf{r}, z) = a_0(z) + a_2(z)r^2$, while usually $B(\mathbf{r}, z) = a_0(z) + a_2(z)r^2 + a_4(z)r^4 + \dots$. In $B(\mathbf{r}, z)$, only the r^2 term gives rise to such an idealized spot dancing that each intensity of SFS waves has the same form, and the arrival position displaces randomly (M. Tateiba, IEEE Trans., AP-23, 493-497, 1975). Other terms r^{2n} ($n \neq 0, 1$) yield the random deformation of the intensity (M. Tateiba, *ibid.*).

This paper presents an exact solution of the moment equation for a plane incident wave in a special case $B(\mathbf{r}, z) = a_0(z) + a_2(z)r^2 + a_4(z)r^4$ by the application of Fourier transform technique and operational calculus. The solution leads to the result that the logarithm of the intensity of a plane wave is specified by a normal density function with the mean and the variance determined uniquely by $a_4(z)$ and the propagation length z . The process of solution may suggest that the log-normal density function of the plane wave intensity is caused by only the r^4 term in $B(\mathbf{r}, z)$.

It is found on the basis of perturbation theory that intensity fluctuations of a plane wave due to the r^{2n} ($n = 3, 4, \dots$) terms in $B(\mathbf{r}, z)$ are negligible as compared with the fluctuation due to the r^4 term, if $z/l \ll kl$ and $B(0, 0)(z/l)^3 \ll 1$ where k is the wave number in free space and l the correlation length of $B(\mathbf{r}, z)$. Accordingly, these conditions show the limits of applicability of the exact solution and the log-normal density function. Besides, they indicate that the intensity fluctuation is very weak, and, in general, wave-form distortion occurs slightly. Therefore, the aforementioned spot dancing also is observable under the conditions.

COHERENT WAVE PROPAGATION AND THE
FOLDY-TWERSKY INTEGRAL EQUATION

Gary S. Brown
Applied Science Associates, Inc.
Apex, North Carolina 27502

The general problem of coherent wave propagation in discrete random media requires the inclusion of all orders of multiple scattering or interaction between particles. When the multiple scattering is negligible and the particle number density is small, the problem is adequately formulated by the Foldy-Twersky integral equation. Unfortunately, there are no general rules as to when multiple scattering is important and one must therefore exercise caution in the use of the Foldy-Twersky integral equation. Conversely, one should not ignore solutions of this equation just because they appear to be representative of potentially strong multiple scattering situations.

Solutions of the Foldy-Twersky integral equation have been previously found for isotropic scattering particles (Foldy) and for a slab of large, nearly transparent particles (Twersky). In this paper, we consider the problem of coherent wave propagation in an unbounded medium of discrete scatterers and show that a solution can be obtained without resorting to the so called far-field approximation. This solution requires accurate knowledge of the average field inside the particles and so it is most amenable to a collection of either Rayleigh-Gans or Rayleigh particles. For Rayleigh particles, the solution for the propagation constant of the coherent field appears to exhibit a "built-in" restriction in terms of the fractional volume occupied by the particles, the dielectric constant, and the shape of the particles. This restriction seems to imply a necessary (but not sufficient) condition for the application of the Foldy-Twersky integral equation. The solution therefore comprises a low frequency asymptotic result which is applicable when multiple scattering is negligible.

Under the assumption that multiple scattering is negligible, a heuristic discussion will be presented on the extension of these results to include both electromagnetically small and large scale particles. The application of this theory to coherent wave propagation through forested environments will be briefly mentioned.

AN ANALYTICAL THEORY OF PULSE WAVE PROPAGATION
IN TURBULENT MEDIA

K. Furutsu

Radio Research Laboratories, Koganei-shi, Tokyo 184, Japan

Most of the theoretical works on the pulse wave propagation in turbulent media have been achieved by use of the two-frequency mutual coherence functions and, except the work by Sreenivasiah et al. (1), also by numerically solving their equations, followed by the numerical integration over the frequency difference for the Fourier inversion. The analytical works also have been tried by use of a method similar to the Rytov approximation, although their results are applicable only to the cases of short optical distances (2), (3)

In this paper, the basic equation is chosen to be the space-time transport equation for the angular-frequency distribution function of wave, since the equation has a symmetrical form in space and time, and it is then subjected to the forward-scattering approximation.

In the space-time coordinate system (ρ, t) where ρ denotes the three-dimensional space coordinates and t the time, the conventional transport equation is given in the form

$$\begin{aligned} & [\Omega \cdot \partial/\partial \rho + c^{-1} \partial/\partial t + \gamma(\Omega, \omega)] I(\Omega, \omega; \rho, t) \\ & = \int_{-\infty}^{\infty} d\omega' \left\{ d\Omega' \delta(\Omega, \omega | \Omega', \omega') I(\Omega', \omega'; \rho, t) + J_c(\Omega, \omega; \rho, t) \right\}, \end{aligned} \quad (1)$$

where Ω is the three-dimensional unit vector, ω the angular frequency, and $I(\Omega, \omega; \rho, t) = I(\Omega, -\omega; \rho, t)$ is the angular-frequency distribution function at (ρ, t) . In the following where the forward scattering is assumed to be essential as in the typical case of light-wave propagation in turbulent media, we shall use the spatial coordinate system $(\rho) = (\xi, z)$ with the z -axis taken in the main direction of wave propagation, and also put $(\Omega) = (\Omega_1, \Omega_2)$ where $\Omega_2 = (1 - \Omega_1^2)^{1/2} \sim 1 - \frac{1}{2} \Omega_1^2$. Then, (1) yields the equation of the angular-frequency distribution function in the form [$J_c = 0$]

$$\begin{aligned} & [\Omega_2 \cdot \partial/\partial \xi + (1 - \frac{1}{2} \Omega_1^2) \partial/\partial \eta + c^{-1} \partial/\partial t + \gamma] I(\Omega_2; \omega; \xi, \eta, t) \\ & = \int_{-\infty}^{\infty} d\omega' \int_{-\infty}^{\infty} d\Omega_1' \delta(\Omega_2 - \Omega_1', \omega - \omega') I(\Omega_1', \omega'; \xi, \eta, t). \end{aligned} \quad (2)$$

In order to solve (2), it is most convenient to make the Fourier transformation with respect to Ω_2 and ω according to

$$I(x, \tau; \xi, \eta, t) = \int_{-\infty}^{\infty} d\omega \int_{-\infty}^{\infty} d\xi I(\xi, \omega; \xi, \eta, t) \quad (3)$$

$$\times \exp[i\{\omega\tau - k\xi \cdot x\}],$$

with $\Delta\omega = \omega - \omega_0$ and $k = \omega_0/c$. Hence, when the turbulent media are moving with a constant velocity v , the equation of $I(x, \tau; \xi, \eta, t)$ in the new coordinate system t, x and $z = ct - z$ is given in the form

$$[c^{-1}\partial/\partial t + i k^{-1}\partial/\partial x \cdot \partial/\partial \xi - \frac{1}{2}(k^{-1}\partial/\partial x)^2 \partial/\partial z + k V(x - vt)] I(x, \tau; \xi, \eta, t) = 0, \quad (4)$$

where

$$V(x) = \beta |k x|^\alpha. \quad (5)$$

Here, β is a non-dimensional constant, and $\alpha = 2$ or $5/3$ according as the turbulence spectrum is of Gaussian or of Kolmogorovian, respectively. Note that (4) is exactly the same as the equation derived by use of the equation of two-frequency mutual coherence function which has been exclusively used by previous authors.

In the case of plane wave pulses, the solution of (4) becomes independent of ξ and, when $\tau = 0$, is given by the integral of the form

$$I(x; z, t) = (2\pi)^{-1} \int_{-\infty}^{\infty} du e^{iuz} \tilde{I}(\xi, \eta). \quad (6)$$

Here

$$\xi = (2k\beta/iu)^{1/(d+2)} kx, \quad \eta = (iu/2k\beta)^{d/(d+2)} 2k\beta ct, \quad (7)$$

and $\tilde{I}(\xi, \eta)$ is the solution of

$$(\partial/\partial \eta + H) \tilde{I}(\xi, \eta) = 0, \quad H = \frac{1}{2} [-(\partial/\partial \xi)^2 + |\xi|^2]^{d/2}. \quad (8)$$

Although the new coordinates ξ are complex according to (7), the effective way to solve (8) is to construct the eigenfunctions of H , which are defined by the eigenvalue equation

$$H \psi_A(\xi) = A \psi_A(\xi). \quad (9)$$

Here, when ξ is real, the operator H is hermitian and also self-adjoint and therefore the eigenvalues A are real and the eigenfunctions $\psi_A(\xi)$ are orthogonal.

All the above properties of the eigenvalues and eigenfunctions remain to be valid even when the coordinates ξ are changed from real to complex ones given by (7) in so far as the eigenfunctions are analytically continued. In the case of $d = 2$, the operator H is exactly the same as the Hamiltonian of two-dimensional linear quantum oscillator and therefore $A = 2n + 1$, $n = 0, 1, 2, \dots$; also $\Psi_A(\xi)$ can be exactly obtained and $\Psi_A(\xi) \rightarrow 0$ as $|\xi| \rightarrow \infty$ for the complex ξ of (7). This is the case also for other cases of $d < 2$.

When the initial wave at $t = 0$ is a perfectly coherent plane wave pulse and has the form of $\delta(\zeta)$, Eqs. (6) - (8) give the expression of the total intensity $I(\zeta, t) = I(\zeta; \zeta, t)|_{\zeta=0}$ as follows:

$$I(\zeta, t) = \sum_A I_A(\zeta, t), \quad \phi = (2\kappa\beta ct)(2\kappa\beta z)^{-d/(d+2)}, \quad (10)$$

$$I_A(\zeta, t) = C_A (\pi\zeta)^{-1} \sum_{m=1}^{\infty} \frac{1}{m!} \Gamma[1 + d(d+2)^{-1}m] \sin[2\pi m(d+2)^{-1}] (A\phi)^m \quad (11)$$

$$\sim C_A (2\zeta)^{-1} \left\{ \frac{d+2}{\pi} \right\}^{1/2} \left\{ d(d+2)^{-1} A\phi \right\}^{(1+d/2)/2} \times \exp[-(2/d) \{ d(d+2)^{-1} A\phi \}^{1+d/2}], \quad A\phi \gg 1, \quad \zeta > 0. \quad (12)$$

Here, the asymptotic expressions of A and C_A for large eigenvalues are given by

$$A \sim \frac{1}{2} \left\{ \pi(n+1/2)d / B(1/2, 3/2) \right\}^{2d/(d+2)}, \quad n = 0, 1, 2, \dots, \quad (13)$$

$$C_A \sim (-)^n (2d)^{1/2} \pi / B(1/2, 1/2), \quad B(\nu, \mu) = \Gamma(\nu)\Gamma(\mu) / \Gamma(\nu+\mu).$$

Note that both expressions of A and C_A give the exact values $A = 2n + 1$ and $C_A = (-)^n 2$ in the case $d = 2$ of Gaussian spectrum, in spite of the fact that (13) is valid only in the asymptotic sense.

The convergence of the series (10) with (11) - (13) is very good for $\phi \gtrsim 1$ or in the beginning stage of pulse wave, whereas the convergence becomes poor for $\phi \ll 1$. In the latter case, $I(\zeta, t)$ can be expressed by another series of good convergence, given by

$$I(\zeta, t) = (2/d)^{1/2} (2/\phi)^{1/2} \zeta^{-1} \sum_{n=0}^{\infty} (-)^n F(c_n), \quad (14)$$

where, with $\nu = 2d/(d+2)$,

$$F(c_n) = \sum_{\ell=0}^{\infty} (-)^{\ell} \Gamma[2(\ell+1)/\nu] [\ell!(2\ell+1)!]^{-1} c_n^{2\ell+1} \quad (15)$$

$$\sim (2\pi)^{-1} \nu \sum_{m=1}^{\infty} (m!)^{-1} \Gamma(1+m\nu/2) \Gamma(1+m\nu) \sin\{\pi(1-\nu)m\} c_n^{-m\nu-1}, \quad (16)$$

$$c_n \gg 1, \quad \alpha < 2.$$

Here, in the special case of $\alpha = 2$, (15) becomes

$$F(c_n) = c_n \exp[-c_n^2], \quad (17)$$

which used in (14) gives the series obtained in Ref. 1.

Curves shown in Fig. 1 were obtained by use of (10) - (13), and show a good agreement with those shown by previous authors who solved (4) by a numerical method for $\alpha = 5/3$ and used the series (14) with (17) for $\alpha = 2$, the latter convergence being very poor for $\phi \gg 1$ or in the beginning stage of pulse wave. In Fig. 2 are shown the tail parts of the same pulses, which decrease exponentially for $\alpha = 2$ and with the factor

$\zeta^{-16/11}$ for $\alpha = 5/3$. The pulse moments $\langle \zeta^p \rangle$ associated with the pulse wave width were also analytically obtained, and show that, when $\alpha = 5/3$, $\langle \zeta^p \rangle = \infty$ for $p > 5/11$. [To be published in J. Math. Phys., April, 1979]

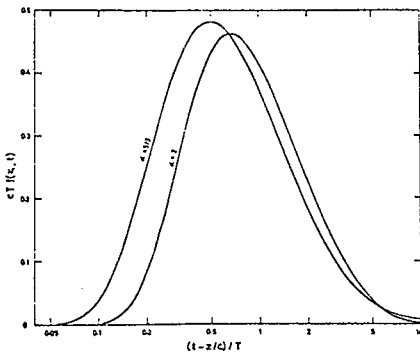


Fig. 1

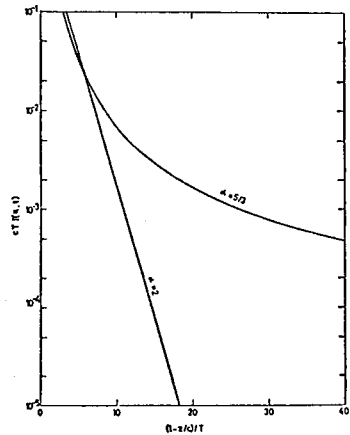


Fig. 2

- (1) I. Sreenivasiah, A. Ishimaru, and S.T. Hong, Radio Sci., 11, 775 (1976).
- (2) C.H. Liu, A.W. Wernik, and K.C. Yeh, IEEE Trans. AP-22, 624 (1974).
- (3) A. Ishimaru and S.T. Hong, Radio Sci., 10, 637 (1975).
- (4) L.C. Lee and J.R. Jokipii, Astrophys. J., 196, 695 (1975); 201, 532 (1975).

BACKSCATTERING OF A PICOSECOND PULSE FROM
A DENSE SCATTERING MEDIUM

Koichi Shimizu and Akira Ishimaru
Department of Electrical Engineering
Adam P. Bruckner
Department of Aeronautics and Astronautics
University of Washington
Seattle, Washington 98195

Diffusion of a short pulse in a dense scattering random medium has previously been studied using the time-dependent equation of transfer and its diffusion approximation (A. Ishimaru, *JOSA*, **68**, 1045-1050, 1978). This paper presents a diffusion solution for a beam wave incident upon a slab of a dense scattering medium. The backscattered pulse shapes are calculated from the theory and compared with the experimental data. The experimental system was constructed by modifying the laser range-gating system (A. P. Bruckner, *Appl. Opt.*, **17**, 3177-3183, 1978). Using high power laser pulses ($\sim 500 \text{ MW/cm}^2$) and an ultrafast shutter (CS_2 between two crossed polarizers), it is capable of recording backscattered pulse shapes in a picosecond range. A beam of pulses with the pulse width of approximately 10 picoseconds at $\lambda = 0.53 \text{ }\mu\text{m}$ is incident upon an aqueous solution containing latex microspheres. The latex spheres have diameters ranging from 0.5 to 50 μm and their concentrations are in the range of 0.1 to 30% in weight. The backscattered pulse shapes are digitized and stored for statistical processing. The pulse broadening for a 10% solution is a few picoseconds, while the broadening for a 1% solution is approximately 5 to 10 picoseconds. The pulse broadening increases as the concentration is decreased and for a 0.1% solution, the pulse broadening extends to several tens of picoseconds. The general pulse shape is characterized by a sharp rise time and a slow tail. When the scatterers are absorbing, the tail part tends to suffer attenuation. The diffusion solutions are calculated using parameters obtained from the Mie solution and the known concentration. It is demonstrated that the theoretical predictions and the experiments agree well not only in the pulse shape and broadening, but in the relative magnitudes of the pulse height for different particle sizes and concentrations as well.

SESSION B-5
THURSDAY AM 8:30-12:00
KANE HALL 120

TRANSIENTS

Chairman: F. M. Tesche
Science Applications Inc.
Berkeley, CA

Transients on Lossy Transmission Lines

A. H. Mohammadian and C. T. Tai
Radiation Laboratory, University of Michigan
Ann Arbor, Michigan

Transients on lossy transmission lines have previously been studied by Jeffreys and Kuznetsov. Jeffreys examined the case of a semi-infinite line. His solution is expressed in a series of modified Bessel functions. Kuznetsov examined the semi-infinite line and a line terminated by a series R-L impedance. His solution is expressed in terms of Lommel functions. In this work we have proved the identity between these two formulations. Based on Kuznetsov's theory we have also examined the R-L terminated line with no restrictions placed on the values of R and L as imposed by Kuznetsov. The case of a parallel G-C termination is also studied in detail.

An approximate solution based on a perturbation in the Laplace transform domain is obtained for lines with low loss. Although the method can not be justified rigorously numerical results based on this simple method show good agreement with the exact solution for low loss lines.

THE RESPONSE OF A TRANSMISSION LINE ILLUMINATED BY
LIGHTNING-INDUCED ELECTROMAGNETIC FIELDS

Harold J. Price, Ashok K. Agrawal, Howard M. Fowles and Larry D. Scott
Mission Research Corporation, Albuquerque, NM 87108

This paper presents the theory and procedures used to estimate the voltages and currents induced on long transmission lines by cloud-to-cloud lightning. A model for the cloud-to-cloud lightning phenomena is presented, and the theory necessary to calculate the electromagnetic fields created by the lightning stroke is derived.

Unlike the method used by Uman (M. A. Uman, et al, Am. Jo. of Physics, January 1975) for vertical lightning strokes, we formulate the problem in terms of a Cartesian coordinate system, for ease in integration of the vector fields. In addition, to increase the speed of numerical computation, the vertical derivative of the electric field is used to compute the horizontal electric field close to the ground. The static fields which occur prior to the lightning discharge are also included, since they impose a nonzero initial condition on the transmission line.

The time-domain transmission line equations are derived from Maxwell's equations in the presence of external electromagnetic fields. Similar formulations in the frequency domain are contained in a note by Taylor (C. D. Taylor, et al, IEEE Trans. AP, 13, November 1965); however, it was not pointed out that (in terms of sources) there are two equivalent formulations of the equations. The source terms appear quite differently in the two formulations.

In this paper we derive the time-domain transmission line equations in a convenient form, where source terms appear only in one equation. Furthermore, the source does not contain time derivatives of the impressed fields which results in a considerably easier numerical computation. A time-domain formulation is more convenient, if in the future nonlinear effects are to be included.

Finally, the results of sample calculations, using finite difference techniques for the solution of the transmission line equations, are presented.

ON THE LOW FREQUENCY ASYMPTOTIC BEHAVIOR OF SEM-DERIVED EQUIVALENT CIRCUITS FOR WIRE ANTENNAS, G. W. Streeble, Bell Laboratories, Holmdel, NJ, L. Wilson Pearson, K. A. Michalski, Department of Electrical Engineering, University of Kentucky, Lexington, KY 40506

The first two authors presented terminal equivalent circuit derivations for the straight-wire and the wire loop antennas derived by means of the singularity Expansion Representation for these objects at the 1978 National Radio Science Fall Meeting. The circuits derived demonstrate a transient response which agrees well with that of the object in question except in the early time - roughly one transit time across the objects. The present paper demonstrates that this departure of results is attributable to the quasi-static influence of the reactance which one neglects when the formal SEM circuit is truncated to a finite number of elements for computation or realization. Bucci and Franceschetti found it necessary to include the net static capacitance of a spheroidal antenna in an approximate equivalent circuit for that structure (O.M. Bucci and G. Franceschetti, IEEE Trans. Ant. & Prop., v. AP-22, pp. 526-535, 1974). Their conclusion is essentially the same as ours particularized to simply-connected objects. The important consequence of this result is that one must compute the asymptotic reactance of a given structure apart from the SEM representation. The reactance of the truncated equivalent circuit must be adjusted with additional element(s) so as to match that of the object in the asymptotic limit. The entry of this phenomenon into the SEM equivalent circuit formalism is described. The means whereby the asymptotic reactance is computed apart from SEM is reported as well as the means of merging the two results. Computed data demonstrating the phenomenon at play are presented.

TRANSIENT ELECTROMAGNETIC FIELD OF A VERTICAL DIPOLE
LOCATED ON A DISSIPATIVE EARTH SURFACE

Hussain A. Haddad[†] and David C. Chang
Electromagnetics Laboratory
Department of Electrical Engineering
University of Colorado
Boulder, Colorado 80309

Transient response of an elementary dipole in the presence of a finitely conducting earth is evaluated in terms of the singularities of the time-harmonic fields in the complex frequency domain for the case when both the source and observation points are located on the interface. The transient field is found to consist of two kinds of wave; one of these arrives early via propagation in air and the other arrives later via propagation in the earth medium. Decomposition into this manner allows us to express the double infinite integrals into single integrals of finite extent that can be easily evaluated numerically.

Waves arriving via the ground medium, usually are found to be several orders smaller than those arriving from air for a typical earth environment. Provided this is the case, effect of the Zenneck wave in the frequency-domain and the finite ground conductivity are seen to produce the equivalence of an image current propagating along a vertical channel away from the air-earth interface with a varying speed as well as an effective wave number of the surrounding medium. Extensive numerical computations are made for an impulse current source and for various observation distances and ground conductivities, and compared with some known approximate analytical solutions. In general, it is found that the static and induction field is mainly important in the late-time portion of the response. The dispersive effect due to finite conductivity of earth is predominant in the determination of the early time response. For an impulse current source, the electric field strength at a fixed observation distance, remains relatively stable initially after the arrival of the first waves in air via a direct path between the source and observation points. Then it goes through a rapid change of polarity before the static situation is reached at a later time. As a rule, this change of polarity occurs sooner when the ground conductivity is higher, or observation distance shorter.

[†]Now with Northrop Corp. Aircraft Div., Hawthorne, CA.

A Geometric Theory of Natural Oscillation
Frequencies in Exterior Scattering Problems

A. Q. Howard, Jr.
Department of Electrical Engineering
University of Arizona, Tucson, AZ

The representation of the transient electromagnetic response of finite size smooth perfectly conducting objects in terms of a complex exponential series is the central ingredient of the singularity expansion method (SEM). The exponential terms correspond to the complex natural frequencies associated with the object geometry. That such a simple series can predict the response of complicated objects begs the question "is there not a corresponding more direct method to compute the natural frequencies in exterior scattering problems".

To partially answer this question a geometric ray optics method, which because of its asymptotic nature is particularly suited to compute the higher order resonances, is described.

The idea is, in general terms, to consider a smooth convex object with a surface impedance boundary condition. Using a local geodesic coordinate system, the ray orbits are determined which have extremal electrical path lengths.

The electrical path length however depends upon the local principal radii of curvature of the surface. The primary result of the work to be described is that a generalized WKB method can be employed to account for both the curvature and the impedance boundary conditions.

The method when applied to a sphere is shown to reduce to the well known uniform asymptotic expansion of the spherical Hankel functions. In this example a comparison of the asymptotic and exact results for the natural oscillation frequencies of a sphere is given.

IS PRONY'S METHOD AN ILL POSED PROBLEM AND
 PENCIL-OF-FUNCTION METHOD A WELL POSED
 PROBLEM IN SYSTEM IDENTIFICATION?

Tapan Kumar Sarkar
 Department of Electrical Engineering
 Rochester Institute of Technology
 Rochester, New York 14623

Abstract:

Suppose the problem of interest is to identify/approximate the transfer function of a system by its poles and residues when the noise contaminated input and output are specified. Then a well posed problem in system identification is one in which the poles remain relatively stable as the order of the approximation is increased. Secondly, the identification process should not become unstable as the sampling frequency is increased above the Nyquist rate. In this presentation it will be shown:

- (1) that the pencil-of-function method uses an onto mapping in a Hilbert space, where the location of the poles remain invariant as the system order is increased. This is not guaranteed in Prony's method, Wiener filters, maximum entropy and other least square methods.
- (2) that a similar development as in the pencil-of-function could be made using the successive integrals of the functions using a difference equation as in Prony's method. But this method (Carr's method) may not yield any error bounds on the location of the poles. This shows the fundamental mathematical difference between a difference equation type of approach and the pencil-of-function method.
- (3) that there is no justification in choosing any of the coefficients a_i to be unity in a difference equation approach (such as Prony's).¹ Yet each choice yields a completely different set of poles. In the pencil-of-function method each of the coefficients of the polynomial equation is calculated uniquely.
- (4) that as the sampling frequency is increased Prony's method becomes highly unstable. This is in contrast to the pencil-of-function method. This is because in Prony's method, various vectors which span the signal space are related to each other by the shift operator ($\mathcal{Z} = \exp[-j2\pi\Delta tf]$) whereas in the pencil-of-function method the vectors are related by the integral operator (1/S).

PULSE RESPONSE WAVEFORMS OF AIRCRAFT

D.L. Moffatt and K.A. Shubert
The Ohio State University ElectroScience Laboratory
Department of Electrical Engineering
Columbus, Ohio 43212

Swept frequency measurements of five fighter aircraft (F-4, F-5, F-104, (2 versions), F-15, and MIG-21) at simulated frequencies spanning 27.8 MHz to 55.6 MHz have been obtained. The measurements are for polarization perpendicular to the plane of flight and nominal aspects (bistatic) spanning nose-on to tail-on. The reflectivity measurement system is really a discrete swept arrangement whereby calibration and background subtraction is achieved every 0.139 MHz across the band. The measurement system will be briefly described.

From these measured data, synthetic pulse response waveforms are produced. The principal purpose of these pulse responses was to demonstrate that: 1) the dominant scatterers in this range of frequencies are the vertical and horizontal tail stabilizers and 2) that high-Q natural or free oscillation frequencies could be associated with the stabilizer substructures. Only the first of these postulates is confirmed by the data and both these responses and those which fail to confirm the second postulate are illustrated. Related measurements (55.6 MHz to 105.6 MHz) and pulse response waveforms of a long pencil-type shape with an attached rectangular cavity are used to demonstrate that the position of a shorting plate within the cavity can be deduced.

Finally, it is demonstrated that a stable multiple aspect difference equation can be obtained for the pencil-type target with an attached vertical stabilizer. The coefficients of the difference equation are a distinct function of the height of the vertical stabilizer. Consequently the pencil-type target is identifiable on the basis of the stabilizer substructure. It is postulated that a similar identification of the fighter aircraft is feasible.

EMP INTERACTION OF A LOW-ALTITUDE MISSILE
WITH AN INHOMOGENEOUS PLASMA PLUMES.K. Chang and F.M. Tesche
LuTech, Inc., P.O. Box 1263, Berkeley, CA 94701

ABSTRACT

An in-flight missile at a low altitude is usually trailed with a long, inhomogeneous plasma plume. The plume may substantially affect the electromagnetic pulse (EMP) induced current on the missile. In order to study the effect of the plume on the EMP response of the missile, a new integral equation solution for the missile and plume current has been developed. An equivalent impedance of the inhomogeneous plume section is obtained by solving an approximate differential equation which describes the fields in the inhomogeneous plume. An additional modification of the integral equation is included to compensate for the gradual radius change in the plume.

The conductivity of the plume is obtained from the electron density and collision frequency by using the cold plasma approximation. Dual plume boundaries, which include the plume-air interface and a current sheet at the position of maximum plume current, are used in the integral equation calculations. The transient responses of the currents are obtained from the frequency domain calculations, with the use of a fast Fourier transformation (FFT).

This paper will describe in more detail the above theory and will present some sample transient data for simple cylindrical shapes which resemble a missile.

RESOLUTION OF CLOSELY SPACED POINT TARGETS

G. S. Sandhu, Principal Engineer, Teledyne Brown Engineering,
Huntsville, Alabama 35807

N. F. Audeh, Professor of Electrical Engineering and Dean of
Graduate Studies, The University of Alabama in Huntsville,
Huntsville, Alabama 35807

This paper considers the measurements of the distance between two point targets by means of a pulsed radar. Upon reception of the transmitted pulse, each point target produces a pulse of known shape with a peak amplitude depending upon the radar cross section (RCS) of the target. The pulse returned from the second target is delayed because of the spacing between the targets which also produces an electrical phase difference with respect to the first pulse. In the receiver the two individual pulses add to form a complex function of time.

Baum (IEEE Trans. Vol. AES-11, No. 6, 1975 pp. 1260-1268) introduced an algorithm for measuring the distance between the two point target by utilizing only the absolute value of the complex function of the time namely RCS. The underlying concept is the method of moments estimation provided that certain inequality relating to the target characteristics is satisfied. Baum's algorithm outperforms earlier methods (Maximum Likelihood Estimation, Threshold and Peak-Picking Methods) described in the literature. However, it exhibits singularity conditions for certain class of targets.

In this paper, we modify the method of moments estimation and derive targets separation in the closed form. It will be shown that Baum's algorithm is a special case of the results presented. The algorithm singularity, which results in erroneous estimates for certain class of targets, is removed. We derive the algorithm through a much simplified approach using transformation of moments. Further, by utilizing moments estimation in the frequency domain, the targets separation, their unknown scatter strength and random phase difference are formulated in the closed form. Complete simulation is carried out to demonstrate the feasibility of the working models as compared with Baum's results.

SESSION B-6
THURSDAY PM 1:30-5:00
KANE HALL 120

ANTENNAS II

Chairman: W. V. T. Rusch
University of Southern California
Los Angeles, CA

VECTOR SECONDARY PATTERNS OF NON-PARABOLIC
REFLECTORS - - SOME NOVEL OBSERVATIONS

Y. Rahmat-Samii, P. Cramer and
V. Galindo-Israel
Jet Propulsion Laboratory
California Institute of Technology
Pasadena, CA 91103

Application of large reflector antennas for space and satellite communication has revived considerable attention among researchers to develop new computational schemes for synthesizing and analyzing reflector antennas in an accurate and efficient manner. Design requirements such as reduction of blockage, increasing aperture efficiency, shaping the far field patterns, reducing sidelobes, etc., have guided researchers to use more complicated structures, e.g., shaped offset reflector antennas. In synthesis, one customarily arrives at the design of dual-shaped reflectors based on the laws of geometrical optics. In order to fully assess the degree of achievement obtained by shaping the reflectors, one must study their radiation characteristics from a vector-diffraction viewpoint. Typically in a dual-shaped antenna configuration, the subreflector is convex with a broad pattern and the main reflector is concave with a pencil beam shaped pattern. A study of an arbitrary shaped subreflector can be found in the literature where the geometrical theory of diffraction (GTD) is used as the basic analytical tool. In this presentation, our emphasis will be focused only on the main reflector.

It has been found that although the physical optics radiation integral provides a very accurate solution for predicting the far field of reflector antennas, it can have the drawback of being excessively time-consuming. The difficulty stems from the fact that for large reflectors and wide observation angles the integrand of the radiation integral oscillates rapidly and is therefore hard to evaluate accurately. In this paper, the vector radiation integral is first constructed for an offset non-parabolic reflector illuminated by an arbitrary source. A novel procedure is then discussed for rearranging the integrand which makes it possible to use the 'biconvergent' form of the Bessel-Jacobi polynomial series expansion, which is related also to the asymptotic evaluation of the integral. The successful applications of this series have already been demonstrated for symmetric and offset parabolic reflectors. Extensive numerical results are presented for different reflector configurations and feed locations and comparisons are made with other available data. In particular, a detailed study of the pattern degradation versus a perturbation parameter, which brings a parabolic reflector to a spherical reflector, is presented. Some novel observations are made on the polarization dependence of the far field patterns of symmetrical non-parabolic reflectors.

COMPARISONS BETWEEN DIFFERENT METHODS
FOR SUBREFLECTOR ANALYSIS

N.Chr.Albertsen and K.Pontoppidan,
TICRA ApS, Kronprinsensgade 13,
DK-1114 Copenhagen K, Denmark

The analysis of reflector antennas is often based upon the physical optics method (PO). For space applications frequency re-use by means of orthogonal polarizations pose severe demands on the accuracy of the predicted results, both for the co-polar and for the cross-polar components. The PO approach is very efficient for a main reflector with an approximately uniform phase distribution in the aperture plane. However, for the sub-reflector scattered field in a dual reflector antenna system PO is disadvantageous in relation to computer time. The present paper compares the PO method to other alternative methods such as the geometrical theory of diffraction (GTD) which is attractive due to its high speed. For rotational symmetric structures the results are also compared to moment method solutions.

The calculated results have shown that the co-polar component is well predicted by all the methods whereas for the cross-polar component significant differences may occur. For a subreflector with a relatively high edge illumination (-10 dB or above) it has been found that GTD provides a more accurate solution than PO for the cross-polar field. When the excitation is strongly tapered and the edge illumination therefore low the GTD solution will contain almost only the geometrical optics reflected field. In this case recent results seem to indicate that PO is preferable with respect to the cross-polar component.

The performance of the methods will be discussed for both rotational symmetric and for offset subreflector configurations.

DESIGN OF CLUSTER FEED FOR MULTIBEAM REFLECTOR ANTENNAS

P. Cramer and K. Woo
Jet Propulsion Laboratory, Pasadena, California
S. W. Lee
University of Illinois, Urbana, Illinois

Multibeam antennas are finding increasing applications in today's communication systems. From the cost and reliability viewpoint, a most attractive multibeam antenna is a reflector type with a feed array of identical elements, each of which produces an independent beam in space. The performance of the antenna may seriously deteriorate, however, when the number of beams is large. This is due to the fact that some of the feed elements are unavoidably placed far away from the focus of the reflector. The beams produced by them usually have relatively low gains and high side lobes. An effective way for reducing this problem is to adjust the excitations of surrounding elements for compensating the feed displacement from the focus. In this manner, a beam is controlled by a cluster of elements, instead of a single element. A systematic way to design the excitation in a cluster was first reported by Galindo-Israel, Lee, and Mittra (IEEE Trans. Antennas Propagat., AP-26, pp. 220-228). That result was restricted to a rotationally symmetrical parabolic reflector.

In this paper, we extend the cluster design to a general offset reflector antenna. By studying the effective aperture distribution of the main reflector, we introduce a performance index which is a weighted average of aperture phase error, aperture efficiency, and illumination taper. Because the calculation of the index is very simple, the cluster excitation can be optimized by trial and error. Our results show that, at large scan angle (25 beamwidths or more), a good cluster design can improve the weighted phase error across the reflector aperture by 10 to 20%, and increase the illumination taper from around 3 db (large spillover loss) to 10 or more. Typically, the magnitudes of currents in the surrounding elements in the cluster vary from 10 to 40% of that in the center. The use of complex currents (controlling both magnitude and phase of the excitation) does not seem to improve significantly the cluster design.

GENERALIZED GEOMETRICAL OPTICS

R. Mittra and A. M. Rushdi
University of Illinois, Urbana, Illinois 61801

In certain applications involving reflection from smooth convex surfaces, the ray optical method is not sufficiently accurate. However, no formulas for higher-order correction terms are available in the literature, and one is typically forced to carry out the physical optics integration numerically to derive a more accurate result. The purpose of this paper is to generalize the concepts of ray optics by combining it with the diffraction theory, and derive closed-form expressions for the first few higher-order terms for the scattered field. This task is accomplished by effecting a Fresnel transformation of the fields between the two planes Σ_0 and Σ_1 , shown in Figure 1. We show that if the field on Σ_0 at $z = z_0$, which can be expressed in the neighborhood of the specular point Q in terms of the incident field and local surface properties at Q, is written as a function of the coordinates (x_0, y_0) of the surface Σ_0 as:

$$f(x_0, y_0) = \left[\sum_{m, n=0}^{m+n \leq 2} A_{mn} x_0^m y_0^n \right] \cdot \exp(-jkz_0) \cdot \exp \left[-j(k/2) \rho_0^T \bar{Q}_0 \bar{\rho}_0 \right].$$

Then, within the Fresnel approximation, the field on Σ_1 at $z = z_1$ is expressible in terms of the following convenient, closed-form formula as a function of the principal coordinates (x_1, y_1) of Σ_1

$$f_1(x_1, y_1) = \left[\sum_{m, n=0}^{m+n \leq 2} A_{mn} a^{m+1} x_1^m d^{n+1} y_1^n \right] -j(z_1 - z_0)k^{-1} \cdot \left[a^2 A_{20} + d^2 A_{02} \right] \cdot \exp(-jkz_1) \cdot \exp -j(k/2) \rho_1^T \bar{Q}_1 \bar{\rho}_1 \right].$$

The constants a and d are related to R_1 and R_2 , the radii of curvature of the wavefront, by the formulas $a = \sqrt{(R_1 + z_0)/(R_1 + z_1)}$ and $d = \sqrt{(R_2 + z_0)/(R_2 + z_1)}$. The dominant term, viz., A_{00} , is found to be identical to that given by conventional ray optics, and the higher-order terms, particularly those involving A_{02} and A_{20} are useful for computing improved GO results at P. We also show that the search for the specular point P can be bypassed and the field computation with the generalized GO may be carried out very efficiently by using a method recently developed by the authors.

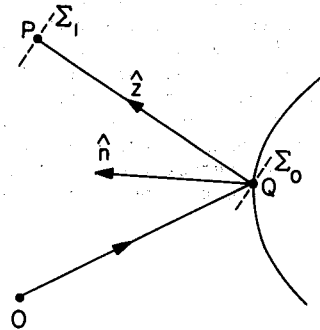


Figure 1

ON THE VALIDITY OF THIN-WIRE THEORY

Clayborne D. Taylor
Mississippi State University
Mississippi State, MS 39762

For thin-wire scatterers both measurement (V. V. Liepa, National Radio Science Meeting, November 1978) and computation (P. Tulyathan and E. H. Newman, IEEE Trans. Ant. Prop., AP-27, 46-50, 1979) reveal significant circumferential variation in the axial current density. Because the thin-wire approximation does not account for this circumferential variation the validity of the much used thin-wire theory has been questioned. However it is shown that thin-wire theory is indeed valid and that the circumferential variation of the axial current is simply related to the magnetostatic solution. Questions of antenna efficiency and transient response are also addressed.

ANALYSIS OF A MONOPOLE NEAR THE EDGE OF A HALF-PLANE

D.M. Pozar and E.H. Newman
The Ohio State University ElectroScience Laboratory
Department of Electrical Engineering
Columbus, Ohio 43212

A problem which is of continued interest is that of antennas mounted on finite conducting bodies. The authors have previously presented (E.H. Newman and D.M. Pozar, IEEE Trans., Vol. AP-26, Nov. 1978, pp. 784-789) a surface patch moment method solution for geometries involving wires and plates, including wire/plate junctions. Wire/plate junctions were restricted to be 0.2λ or more from a plate edge. This paper discusses computation of the currents and input impedance for an antenna mounted near the edge of a half-plane via three methods.

The first method (the most rigorous) uses the exact half-plane Green's function in a hybrid moment method solution with piecewise-sinusoidal (PWS) expansion and testing modes on the wire. An important feature of this solution is that the geometrical optics terms (which include source singularities) are separated off, so that the input impedance is expressed as a sum of the input impedance of a monopole on an infinite ground plane plus a correction term, ΔZ , which accounts for the edge effect.

The second solution is similar to the first except that the Geometrical Theory of Diffraction is used to compute the edge diffracted field and ΔZ . This MM/GTD hybrid solution agrees very well with the more rigorous solution for antennas as close as $.2\lambda$ to the edge.

The third method is a modification to the above referenced surface patch/wire solution. It uses results from the canonical problem of an infinitesimal dipole near the edge of a half-plane to construct suitable expansion modes.

The input impedances of the three methods are compared for a $\lambda/4$ monopole vs. distance from the half-plane edge.

EFFECT OF TAPER PROFILE ON PERFORMANCE
OF DIELECTRIC TAPER ANTENNAS

S. T. Peng

Polytechnic Institute of New York
Brooklyn, New York 11201

and

F. Schwering

U. S. Army Communication Research and Development Command
Fort Monmouth, New Jersey 07703

It has been well known that the gain of a dielectric rod as an end-fire antenna may be increased greatly by tapering the radiating end. Because of theoretical difficulties in solving this type of boundary value problem and also because of practical convenience, only tapers of linear profile have been analyzed and used in the past. While linear tapering may have improved the performance of dielectric rod antennas, the effect of taper profile on radiating characteristics has not been well understood. By introducing the staircase approximation for a continuous profile and then placing the dielectric antenna in a metallic waveguide (of large dimensions) to discretize the spectrum, we have analyzed the radiation of a dielectric taper antenna in terms of the wave scattering by a series of step discontinuities between piecewise uniform regions. This approach yields a clear physical picture of wave scattering by a dielectric taper and relates the antenna performance to the change in physical dimensions as well as the slope of the taper profile. Specifically, the performance of tapers with linear, parabolic and elliptic profiles is analyzed in detail and criteria for the design of dielectric tapers to optimize the antenna performance are suggested.

MAXIMIZING THE GAIN-BANDWIDTH PRODUCT
OF A LOSSY LINEAR ANTENNA*

R. M. Bevensee

Lawrence Livermore Laboratory

Maximization of the G-BW product of the general 2-port antenna will be discussed. An expression for the maximum product at driving port 1 will be derived, assuming optimized 2-port network parameters and reactive loading at port 2. The maximum product is inversely proportional to rate of change of input reactance relative to frequency at port 2 (with port 1 open circuit). The energy theorem is invoked to relate this to stored energy. A lower bound on stored energy is derived by assuming each closed contour of energy around the antenna is related to the real power flow (constant) by the factor c , the velocity of light. The effective volume of stored energy is estimated for practical antennas from some unpublished work of the author.

The result of the analysis is an expression for the maximum G-BW product in terms of the unloaded antenna parameters. The expression shows a critical dependence on the input resistances at both ports.

*This work was performed under the auspices of the U.S. Department of Energy by the Lawrence Livermore Laboratory under contract number W-7405-ENG-48.

Experimental Investigation of the Radiated
Fields of a Buried Antenna

Faramarz Vaziri, Stuart A. Long and Liang C. Shen
Department of Electrical Engineering
University of Houston
Houston, Texas 77004

The problem of determining the radiated fields when both the transmitter and receiver are near the interface between air and a lossy medium has numerous applications in subsurface communications. To aid in the understanding of this problem a systematic experimental investigation was undertaken to measure the radiated fields near a transmitting antenna which was buried in the earth. The radiator was close enough to the surface so that the dominant field was the lateral wave along the interface rather than the direct wave through the lossy earth. To excite this lateral wave more efficiently an eccentrically insulated, traveling wave type antenna was chosen as the radiator. It was buried at a depth of 40 cm and its transmitter and source of power buried even deeper. The antenna radiated approximately 0.9 watt at 144 MHz. The resulting fields were then measured just above ground level. All three orthogonal polarizations were recorded both as a function of the radial distance and the azimuthal angle. Soil samples were taken and the conductivity and dielectric constant determined. Using these material constants the theoretical attenuation rates for the electric fields with distance were calculated for an electrically short dipole. The corresponding experimental results for each component of the field versus radial distance were then compared with the theoretical ones with reasonable agreement being obtained. The field patterns in the azimuthal plane were compared with measurements made for similar antennas submerged in lake water.

OPTIMIZED LAUNCHING OF THE GROUND WAVE:
A NEW LOOK AT THE BEVERAGE ANTENNA

David C. Chang and Edward F. Kuester
Electromagnetics Laboratory
Department of Electrical Engineering
University of Colorado
Boulder, Colorado 80309

Recent interest in ground radar systems has led to new studies on the efficient excitation of electromagnetic waves near the earth's surface--the so-called ground wave (D.A. Hill and J.R. Wait, Radio Science 13, 969-977, 1978). While the latter reference concentrates on vertically distributed sources (apertures), we shall focus on an old and venerable means of exciting low-angle radiation: the Beverage antenna (H.H. Beverage et al., Trans. AIEE 42, 215-266, 1923). This antenna consists of a long horizontal wire above a finitely conducting earth. This system behaves much like a transmission line and is excited with a current wave

$$I(z) = I_0 e^{ik_0 \alpha_p z - i\omega t}$$
 (where α_p is a normalized complex propagation constant in the neighborhood of unity) and terminated in an appropriate impedance to suppress reflection of this wave. The resulting endfire pattern is usually treated quite approximately by a plane wave approximation, but here we start from a rigorous Sommerfeld integral formulation to find the ground-wave of this antenna. It is found that by adjusting the position of α_p in the complex

α -plane, it is possible to emphasize the ground-wave at the expense of the other portions of the field. The classical Beverage antenna already has an α_p in the neighborhood of one, and so is a good, endfire, ground-wave radiator. Further enhancement is attained by moving α_p closer to the "propagation constant" of the ground wave. This enhancement can be accomplished by variations on the classical antenna, such as changing the surface impedance of the horizontal wire. Dielectric coated wires (Goubau lines) or leaky coaxial cables are two such variations, and can be shown to provide flexibility in the tailoring of a ground-wave pattern.

SESSION B-7
FRIDAY AM 8:30-12:00
KANE HALL 120

GUIDED WAVES

Chairman: K. Casey
Kansas State University
Manhattan, KS

LEAKY MODES ON OPEN DIELECTRIC WAVEGUIDES

A. A. Oliner and S. T. Peng
Polytechnic Institute of New York
333 Jay Street
Brooklyn, New York 11201

Open dielectric waveguides have become increasingly important within the past few years, particularly in connection with the areas of integrated optics and millimeter wave integrated circuits. Examples of these waveguides are strip and indiffused waveguides for the optical and infrared wavelengths, and dielectric image lines and inverted strip guides for millimeter waves. These waveguides are associated with either a substrate or a ground plane; we are not concerned here with fiber waveguides of circular cross section.

It is not generally known that most modes on most of these waveguides can be leaky, instead of being purely bound, as is customarily assumed. The tacit assumption that these modes are completely bound is based largely on published theoretical propagation characteristics, which are obtained from approximate analyses that neglect those features which lead to the leakage effects. More careful analyses reveal that under appropriate conditions leakage is indeed possible. We shall show, from simple and general considerations, how to determine when leakage is present. We can determine which classes of waveguide may leak and which will never leak, which modes will do the leaking and which will not, and we can prescribe how to modify the waveguiding structure to avoid leakage, or alternatively to produce leakage when we wish to.

The leakage, when it occurs, is due to the coupling between the constituent TE and TM waves produced at the waveguide sides when these waves bounce back and forth in the central guiding region, as part of the guiding process. This coupling mechanism is not applicable to circular dielectric fibers, and the leaky modes discussed here in fact form a new class of such modes.

COUPLING BETWEEN TRIANGULAR OPTICAL WAVEGUIDES

P.L.E. Uslenghi
Communications Laboratory
Department of Information Engineering
University of Illinois at Chicago Circle
Chicago, Illinois 60680

The coupling between two triangular dielectric waveguides of identical cross section embedded in a common dielectric substrate is considered. The cross section of both guides has one 90° angle, while the other two angles are either 60° and 30° , or both equal to 45° .

The modes which can propagate in each individual guide are determined by ray-tracing techniques, following a method previously employed by the author (Uslenghi and Wiiken, 1978; Uslenghi and Yun, 1979). The results obtained are verified by a field-theory treatment similar to that employed by Marcatili (1969) for the rectangular dielectric waveguide.

In the case of single-mode propagation, power transfer between the two guides is studied using the strong-coupling theory of Uslenghi and Kazkaz (1976, 1978). The results predicted by the weak-coupling theory of Miller and Marcatili are obtained as particular cases of our results, for large separation between guides and long coupling distance. Design criteria for a directional coupler are discussed. This research was performed under NSF grant Eng 77-06544.

JUNCTION EFFECT OF TWO THIN, COAXIAL CYLINDERS OF DISSIMILAR RADIUS

David C. Chang
 Electromagnetics Laboratory
 Department of Electrical Engineering
 University of Colorado
 Boulder, Colorado 80309

In many antenna practices such as the design of a sleeve antenna, one encounters the need of joining together two thin-wire, coaxial cylinders of different radius. Since such a junction presents a step discontinuity to the flow of current, it is important to know the amount of reflection, as well as transmission caused by the junction. On the other hand, if loading at the junction can be modified to produce an open circuit, current transmission can be substantially reduced. A reactively loaded junction thus can be utilized to effectively provide a "choke" in isolating a dipole antenna from its feed system in some application.

In this work, the problem of a coaxial system consisting of a semi-infinite outer conductor of radius b and an infinite inner conductor of radius a is analyzed. Based upon a thin-wire assumption and use of the Wiener-Hopf technique, analytical expressions for the reflected and transmitted current both inside and outside the coaxial region are obtained in closed-form, in terms of the antenna parameters $k_0 a$, $k_0 b$ where k_0 is the wave number, and the coaxial parameter, $\ln b/a$. By terminating the coaxial-line with an adjustable short-circuit, various loadings at the junction can be achieved. In the case of a short-circuit, the junction presents itself as a small voltage generator in producing a current $I_{a,b}$ on cylinder a and b when a current wave $I_0 \exp(\pm i k_0 z)$ is incident onto the junction at $z=0$:

$$I_{a,b} = \pm I_0 Z [u_{\pi}^{a,b}(|z|)/u_{\pi}^{a,b}(0)]; \quad Z = [u_{\pi}^b(0) - u_{\pi}^a(0)]/[u_{\pi}^a(0) + u_{\pi}^b(0)] \quad (1)$$

$$\text{where } u_{\pi}^v(|z|) = [2C_w^v + i\pi + \Omega(2k_0|z|)]^{-1} e^{i k_0 |z|} \quad (2)$$

$$C_w^v = -(\ln k_0 v + 0.5772); \quad \Omega(x) = 0.5772 - i \pi/2 + \exp(-ix) E_1(-ix) + \ln x \quad (3)$$

and E_1 is the exponential integral of order one. We have also chosen a cylindrical coordinate so that conductor b extends from 0 to ∞ , while conductor a from $-\infty$ to ∞ . On the other hand, for an open-circuit junction, the amount of current transmitted to the second cylinder is shown to be

$$I_{a,b} = \pm I_0 \Omega(2k_0|z|) u_{\pi}^{a,b}(|z|) \quad (4)$$

which vanishes at $z=0$, and is small overall because $|u_{\pi}^{a,b}| \ll 1$ under a thin wire assumption. Thus, an open-circuit junction can now effectively act like a choke to minimize the presence of the second conductor in such a system.

WAVEGUIDE MODES WITH ONE-DIMENSIONAL TRANSVERSE INHOMOGENEITIES

William A. Davis
 Virginia Polytechnic Institute and State University
 Blacksburg, Virginia
 Lt. Ruth B. Kaplan
 AMRL/MEA, Wright-Patterson AFB, Ohio

Classical methods of solving the problem of transverse inhomogeneities are standard boundary-value techniques or optical type techniques using the WKB approximation. The latter is most applicable to slowly-varying, continuous inhomogeneities while the former is best-suited to discontinuous inhomogeneities. Several authors have solved the boundary-value problem using an optimization procedure which begins with a given boundary condition, integrates the fundamental differential equations to the remaining boundary, compares boundary conditions, and repeats the process with a new parameter using optimization. In waveguide problems, the parameter of optimization is the wave number in the longitudinal direction of the guide.

This paper presents a modified procedure which has the advantage of designating the desired mode of evaluation. Previous methods have been based on the integration of the field quantities such as the electric or magnetic field intensities. In doing so, the only method of determining the order of the mode is to observe the number of nulls and peaks occurring in the amplitude of the field quantity as the waveguide is traversed. The alternate approach taken in this paper is to define the transverse impedance function given by E_x/H_y for an x-directed TM wave with z-directed inhomogeneities. The primary difficulty of using this function as it stands is the problem of zeroes and infinities in the impedance function. To avoid this difficulty, a new function u may be defined which is given by $\tan^{-1}(\xi Z)$, where ξ is a scaling factor to speed convergence of the optimization routine. A first order differential equation for u is obtained from Maxwell's equations which may be solved by integration. The equation depends on the wavenumber which results in different final values for u . Since the value of u is fixed by the boundary condition, the parametric wavenumber must be optimized until an appropriate solution for u is obtained.

A trivial example of this technique is the homogeneous, parallel-plate waveguide. For simplicity, ξ is chosen as $j\omega\epsilon/k_z$. The equation that results is $du/dz = k_z$, where k_z is given by the square root of $(k^2 - k_x^2)$. For perfectly conducting boundaries at zero and a , the boundary conditions are $u(0) = 0$ and $u(a) = m\pi$. Iterating the solution for u to obtain $m\pi$ at a , k_z is found to be $m\pi/a$ as expected. In this same manner, the technique can be used to obtain the desired m th mode in inhomogeneous cases.

ON USING THE I.Q. OF WAVEGUIDES INTELLIGENTLY

D. L. Jaggard
 Department of Electrical Engineering
 University of Utah
 Salt Lake City, Utah 84112

The isoperimetric quotient (I.Q.) of closed planar figures has its origin in the legend concerning Dido's problem. In this problem, the goddess Dido desires to know the maximum area A that can be enclosed by a planar figure of perimeter P . The I.Q. of such a figure is defined by the relation

$$\text{I.Q.} = 4\pi A/P^2.$$

As was known since 300 B.C., the planar figure which solves Dido's problem is the figure with maximum I.Q., namely the circle. One is then lead immediately to the inequality

$$\text{I.Q.} \leq 1.$$

Two auxiliary parameters, the inner radius $r_{in} = (A/\pi)^{1/2}$ and the outer radius $r_{out} = P/2\pi$ are related to the I.Q. by

$$r_{in}^2 / r_{out}^2 = \text{I.Q.} \leq 1.$$

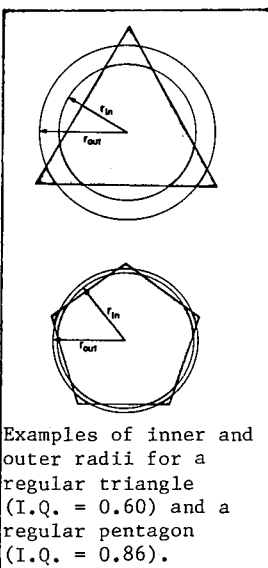
The I.Q. and related parameters play a role in describing the eigenvalues of the Helmholtz equation as noted by Lord Rayleigh and others. In this presentation we use these quantities to approximate and bound the cutoff wave numbers of metallic waveguides with arbitrary cross section. We find that as the I.Q. of a convex waveguide is increased, the fundamental TE cutoff wave number μ also increases, whereas the fundamental TM wave number γ decreases. Through this fact and the knowledge of the fundamental cutoff wave numbers of a circular waveguide, we find that the following inequalities hold for waveguides in the shape of regular polygons.

$$1.841/r_{out} \leq \mu \leq 1.841/r_{in}$$

$$2.405/r_{in} \leq \gamma \leq 2.405 r_{out}/r_{in}^2$$

See the figure for typical inner and outer radii.

Other bounds are presented for the cutoff wave numbers of convex metallic waveguides of arbitrary cross section and for the cutoff wave numbers of fiber optical waveguides.



PROPAGATION CHARACTERISTICS OF A TWO-LAYER
DIELECTRIC WAVEGUIDE WITH AN AZIMUTHAL ASYMMETRY

T. C. K. RAO
Department of Electrical Engineering
Florida Atlantic University
Boca Raton, Florida 33431

Guided electromagnetic wave propagation over an infinitely long dielectric cylinder asymmetrically surrounded by a second dielectric cylinder is examined. The problem is formulated by choosing the appropriate expansion functions satisfying the wave equation in different regions and matching the fields at various interfaces making use of orthogonality relations and Graf's Addition Theorem for the cylindrical functions. The resulting characteristic equation is numerically solved for the first TM and TE modes. By means of a perturbation analysis, various propagation characteristics such as the attenuation and phase constants, phase velocity and decay coefficient and their variation with the degree of asymmetry are discussed. Certain limiting cases of the structure like the asymmetrical forms of the coaxial line, the Goubau line and the modified Goubau line are also briefly dealt with in light of the approximations made.

SCATTERING OF SURFACE WAVES BY A NOTCH
 IN A PERFECTLY CONDUCTING GROUND PLANE
 COVERED BY A DIELECTRIC SLAB

R.D. Nevels, Electrical Engr. Dept., Texas A&M University, College Station, Texas.

C.M. Butler, Electrical Engr. Dept., University of Mississippi, University, Mississippi.

We consider here a dielectric-slab-covered ground plane of infinite extent containing a notch of infinite length and finite width (ℓ) and depth (w) as shown in the figure below. A TM mode surface wave is assumed to be propagating in the dielectric slab. Also for generality the electromagnetic parameters are assumed to be different in each of the three regions - the notch, the dielectric slab and the space above the dielectric slab (see Fig.1).

In this paper we present an integral equation solution for the unknown tangential electric field at the interface of the notch and the dielectric slab. The 'notch' problem is investigated with the objective of studying the scattering properties of surface waves guided by a dielectric slab over a ground plane which encounter surface discontinuities in the ground plane. An S-parameter (scattering matrix) representation is presented as a means of describing the system of incident, transmitted and scattered fields about the notch.

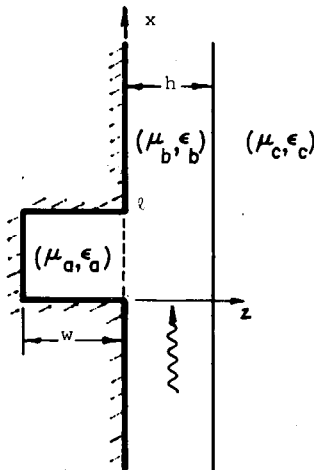


Fig. 1. TM surface wave excitation of a 'notch' in a ground screen covered by a dielectric slab

INTEGRAL OPERATOR ANALYSIS OF COUPLED DIELECTRIC OPTICAL WAVEGUIDE SYSTEM - THEORY AND APPLICATION

Shuhui V. Hsu, Antenna Department, E-System Inc.,
Garland Division, P.O. Box 226118, Dallas, TX 75222
Dennis P. Nyquist, Department of Electrical Engineering and
Systems Science, Michigan State University, East Lansing, MI 48824

An integral-operator technique is described as an alternative to the conventional boundary-value analysis for wave propagation in a coupled system of cladded, dielectric waveguides. The heterogeneous region, i.e., the core, of each optical waveguide is replaced by an equivalent current distribution which maintains a scattered field in the otherwise uniform, infinite cladding. Total electric field in each dielectric waveguide consists of scattered fields maintained by all waveguides in the coupled system superposed upon an impressed excitatory field.

A coupled system of volume electric-field integral equations (EFIE's) for the unknown equivalent currents (electric fields) in each core is formulated. When applied to two coupled slab waveguides, having $\exp(-j\beta z)$ propagation dependence, two 1-d EFIE's are obtained, leading to the same characteristic equation for β as obtained by the conventional method. Integral equations for natural mode fields e_1 and e_2 in coupled slabs of thickness d_1 and d_2 separated by distance s are obtained as,

$$e_1(x) \frac{(k_1^2 - k_2^2)}{2\gamma_1} \int_0^{d_1} e_1(x') e^{-\gamma_1 |x-x'|} dx' - \frac{(k_1^2 - k_2^2)}{2\gamma_2} \int_s^{s+d_2} e_2(x') e^{-\gamma_2 |x-x'|} dx' = 0$$

for $0 < x < d$

$$e_2(x) \frac{(k_1^2 - k_2^2)}{2\gamma_2} \int_s^{s+d_2} e_2(x') e^{-\gamma_2 |x-x'|} dx' - \frac{(k_1^2 - k_2^2)}{2\gamma_1} \int_0^{d_1} e_1(x') e^{-\gamma_1 |x-x'|} dx' = 0$$

for $s < x < s+d$

where $\gamma_{1,2}$ are characteristic parameters depending upon $\beta_{1,2}$.

Several advantages of this integral-operator analysis for a coupled, dielectric waveguide system are: 1) coupling coefficients between degenerate or non-degenerate modes in the multi-waveguide system can be obtained, 2) it is adaptable to core cross sections of arbitrary shape, and 3) general core index profiles for each core can be accommodated. Applications to coupled degenerate and non-degenerate modes on a slab-waveguide system and simple modes on coupled circular fibers are studied.

DIELECTRIC-LINED METAL RECTANGULAR WAVEGUIDE

R. Chatterjee
Department of Electrical Communication Engineering
Indian Institute of Science
Bangalore-560012, India

Major G. K. Deb
Electronics and Radar Development Establishment
Highgrounds, Bangalore-560001, India

Using the concept of equivalent artificial dielectric, it has been shown that the dielectric-lined rectangular metal waveguide can support LSE and LSM modes. The phase constant, cut-off frequency, and attenuation constant for both types of mode have been evaluated. Experimental verification of cut-off frequency and guide wavelength has been made.

SCALAR WAVE APPROACH FOR SINGLE-MODE INHOMOGENEOUS FIBER PROBLEMS

W. P. Brown and C. Yeh
Hughes Research Laboratories
Malibu, California 90265

It has been universally accepted that the full set of Maxwell equations resulting in the vector wave equation must be used to treat waveguides supporting single mode. This requirement confines the analytical treatment to only a few simple structures. The advent of optical fiber guides as viable communication links as well as the dawn of small, high bandwidth integrated optical circuits demand that the analytical horizon be expanded. It is recognized that many more problems can be solved if only the scalar wave equation needs be considered. The purpose of this paper is to investigate in depth the conditions under which the scalar wave equation can be used instead of the vector wave equation and to demonstrate, with concrete examples, the validity of the scalar wave approach in providing accurate results for the graded index fiber guide.

It is shown that if certain limiting conditions are satisfied the scalar wave approach will yield valid results for single mode structures. These limiting conditions are usually satisfied by many practical single-mode inhomogeneous fiber or IOC structures.

AP/B POSTER SESSIONS
KANE HALL - WALKER AMES ROOM

Chairman: C. M. Butler
University of Mississippi
University, MS

SESSION A - ANTENNAS
TUESDAY PM 1:30-5:10

SESSION B - WAVE PHENOMENA
WEDNESDAY PM 2:00-5:30

SESSION C - SCATTERING
THURSDAY PM 1:30-5:00

AP/B POSTER SESSION A
TUESDAY PM 1:30-5:00
KANE HALL - WALKER AMES ROOM

ANTENNAS

Chairman: C. M. Butler
University of Mississippi
University, MS

The following papers belong to the IEEE AP-S Symposium and the summaries are included in the IEEE AP-S Digest under AP/B Poster Session A.

1. Some Considerations to the Divergence Problem of Antenna Integral Equation Solutions
G. Greving, Technische Hochschule Aachen, Aachen, West Germany
2. Current on Thick Cylindrical Antennas. Improved Solution of the Generalized Boundary Condition Integral Equation by Le Foll's Algorithm
J. Ch. Bolomey, S. El Habiby, F. Hillaire, D. Lesselier, C.N.R.S.-E.S.E. Gif-sur-Yvette, France
3. GTD Solution of the Input Admittance of a Slot on a Cone
E. K. Yung Hong Kong Polytechnic, Hung Hom, Hong Kong, S. W. Lee, and R. Mittra, University of Illinois, Urbana, IL
4. Shaped Beam Reflector Feed Network for Clutter Reduction and Angle Estimation
C. F. Winter, Raytheon Company, Wayland, MA
5. Study of Batwing Radiator of the Superturnstile Antenna for TV Broadcasting
R. W. Masters, Antenna Research Associates, Inc., Beltsville, MD and G. Sato, H. Kawakami, and M. Umeda, Sophia University, Tokyo, Japan
6. The Characteristics of a Modified Duoconical Monopole with Curved Surface Transition
K. Fukuzawa and R. Sato, Tohoku University, Sendai, Japan
7. Best Possible Thermal Noise Sensitivity of Electrically Small Loop Antennas
M. Dishal, ITT Avionics, Nutley, NJ
8. Dual-Beam Waveguide Slot Array for Monopulse Application
G. A. Hockham and R. I. Wolfson, ITT Gilfillan, Van Nuys, CA
9. Peak Cross Polarization of Reflectors with Surface Errors
S. I. Ghobrial, University of Khartoum, Khartoum, Sudan
10. A Multimode Dielectric Coated Horn for Circularly Polarized Elliptical Beam
S. H. J. Quboa, S. C. Gupta, University of Mosul, Mosul, Iraq
11. Horn-Reflector Antenna Performance at 2 GHz with Simultaneous Operation in the 4, 6 and 11 GHz Bands
J. E. Richard, Bell Telephone Laboratories, Inc., North Andover, MA

AP/B POSTER SESSION A
TUESDAY PM 1:30-5:00
KANE HALL - WALKER AMES ROOM

ANTENNAS (cont.)

12. Astigmatic Correction by a Deformable Subreflector
W. Y. Wong and S. Von Hoerner, National Radio Astronomy
Observatory, Green Bank, WV
13. A Decoupled Antenna System with a Lossless Network
H. Iwasaki, Y. Mikuni, and K. Nagai, Toshiba Research and
Development Center, Kawasaki, Japan
14. Performance of Reflector Antennas with Absorber-Lined Tunnels
R. B. Dybdal, H. E. King, The Aerospace Corporation, Los
Angeles, CA
15. Sidelobe Reduction with Horn-Antennas
F. M. Landstorfer, R. R. Sacher, Technical University of
Munich, Munich FRG.
16. Radiation by Microstrip Patches
N. G. Alexopoulos and I. Rana, University of California,
Los Angeles, Los Angeles, CA, and N. K. Uzunoglu, National
Technical University of Athens, Athens, Greece
20. The RN^2 Multiple Beam Array Family and the Beam Forming Matrix
J. L. McFarland, Lockheed Missiles and Space Company,
Sunnyvale, CA
21. Frequency Selection for Reliable, Low-Cost Satellite Links
P. F. Christopher, The MITRE Corporation, Bedford, MA
22. Far-Field Antenna Pattern Calculation From Near-Field
Measurements Including Compensation for Probe Positioning
Errors
L. E. Corey and E. B. Joy, Georgia Institute of Technology,
Atlanta, GA
24. Automated Probing for Outdoor Antenna Ranges
S. M. Sanzgiri, G. Crain, and R. C. Voges, Texas Instruments
Inc., Dallas, TX
25. On the Accuracy of the Transmission Line Model of the Folded
Dipole
G. A. Thiele, E. P. Ekelman, Jr., and L. W. Henderson, The
Ohio State University ElectroScience Laboratory, Columbus, OH
26. A Circularly Symmetric Dual-Reflector-Type Multibeam Antenna
H. Kumazawa, Nippon Telegraph and Telephone Public Corp.,
Yokosuka, Japan, and M. Mizusawa, Mitsubishi Electric Corp.,
Kamakura-City, Japan
27. Air Launch Cruise Missile Instrumentation Antennas
R. E. Lantagne, J. P. Grady and G. E. Miller, Boeing Aerospace
Company, Seattle, WA

MICROSTRIP ANTENNAS FOR AIRBORNE
RADAR SYSTEMS

Albert W. Biggs
University of Kansas
Lawrence, Kansas 66045

Arrays of circular and rectangular microstrip antennas are described for a Side Looking Airborne Radar (SLAR) antenna and a Short Pulse Ice Thickness Radar (SPITR) antenna. The SLAR antenna is located on the side of a C-130 airplane, and the SPITR antenna is located in a helicopter or a wide bottom aircraft.

Theoretical and experimental antenna patterns are presented for square and circular microstrip antennas. Design information is also presented for their fabrication. Curves of relative coupling indicate the criteria for spacing of elements for the microstrip antenna arrays.

The SPITR antenna is a stripline feed log periodic dipole array. The bandwidth provides use of a 2 nanosecond gaussian shaped pulse for probing depths of Arctic ice.

A MICROSTRIP ANALYSIS TECHNIQUE

E.H. Newman and P. Tulyathan
The Ohio State University ElectroScience Laboratory
Department of Electrical Engineering
Columbus, Ohio 43212

A microstrip antenna consists of a metallic patch on an electrically thin dielectric slab over a ground plane. The patch is fed by either a coaxial cable through the ground plane, or by a microstrip transmission line from the side. Microstrip antennas are finding increasing application in aircraft, spacecraft and missiles since they are lightweight, easy and inexpensive to fabricate, while maintaining good impedance and radiation characteristics over a few percent bandwidth.

The solution is based on a surface patch moment method technique, employing the sinusoidal reaction formulation, (E.H. Newman and D.M. Pozar, IEEE Trans., Vol. AP-26, Nov. 1978, pp. 784-789) for wires, rectangular plates, and wire/plate junctions. Trapezoidal surface patch modes, instead of the previous rectangular surface patch modes, are introduced so that microstrip patches of arbitrary shape can be treated. An effective dielectric constant is used to account for the dielectric slab. Results will be presented for a non-rectangular microstrip antenna using only three modes (1 wire, 1 surface patch, and 1 attachment mode).

A CIRCULARLY POLARIZED MICROSTRIP RESONATOR ANTENNA.

J.Vandensande, H.Pues, E.Van Lil, A. Van de Capelle, K.U.Leuven, Dept. of Electrical Engineering, Div.M.I.L. B-3030 Heverlee, Belgium.

In view of future satellite applications there exist a need to develop high gain circularly polarized antenna arrays. Traveling wave circularly polarized arrays on microstrip were already treated by Wood, Hall and James ("Design of Wideband Circularly Polarized Microstrip Antennas and Arrays", Intern. Conf. Ant. Prop., Nov. 78, London). A serious drawback of this kind of arrays is their low efficiency, about 30%.

Synthesizing arrays with a greater efficiency implies that one has at one's disposal a circularly polarized radiating element. In this paper one presents an analysis of a square microstrip resonator antenna. This antenna can be made circularly polarized by exciting two orthogonal modes of the antenna with signals 90° out of phase. J.Q. Howell has already mentioned this idea ("Microstrip Antennas", Trans. Ant. Prop., Jan. 75), but until now there are no data available about the performance of this antenna.

The resonator antenna was designed for a resonance frequency of 3 GHz. The 3-dB bandwidth was 296 MHz. We were primarily interested in the variation of the polarization state within the 3-dB bandwidth of the antenna. It was found that the circular polarization ratio (C.P.R.) was lower than -15 dB (or an ellipticity lower than 3 dB) between the 3 dB frequencies (fig. 1). The sense of rotation was left-handed, measured in accordance to the IEEE standard.

To meet the requirements of the CCIR, it is necessary to obtain a C.P.R. lower than -25dB (or greater than 25 dB for right-handed sense) in the broadside direction. This is only met for a 30 MHz frequency band. The reason why this requirement is not met lies in the unequal power division between the orthogonal modes. Nevertheless it seems possible to design a feed network that maintains an equal power division over the entire frequency band of operation of the antenna.

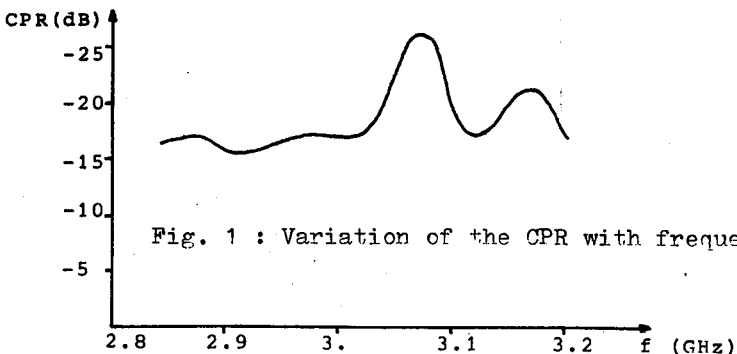


Fig. 1 : Variation of the CPR with frequency.

A MARITIME COMMUNICATIONS SUBSYSTEM
(MCS) FOR INTELSAT V SATELLITES

Dr. William J. English
INTELSAT - Space Segment Engineering
490 L'Enfant Plaza, S.W.
Washington, D.C. 20024

This paper describes the engineering design of the maritime communications subsystem (MCS) which will be incorporated into the INTELSAT V satellites. In January, 1979, the INTELSAT Board of Governors approved the MCS for the INTELSAT V F-5, F-6, F-7 spacecraft. The MCS will be part of a second generation global coverage maritime communications satellite system to be utilized by the International Maritime Satellite Organization (INMARSAT) during the 1980's.

The MCS provides four global coverage beams. Two are at C-band for shore-satellite links and two are at L-band for satellite-ship links. Thirty maritime voice channels are available.

The MCS design constraints which are discussed include:

- (1) no interference to the existing INTELSAT V antenna coverage beams. There are 14 communications beams and 11 different antenna structures.
- (2) minimize modifications to existing spacecraft design. The initial INTELSAT V's are to be launched later this year. This includes operating within the present spacecraft power budget and maximum use of INTELSAT V hardware.
- (3) preserve original delivery schedule for the spacecraft modified by the MCS.
- (4) insure compatibility with three potential launch vehicles--Atlas/Centaur, Ariane and Space Shuttle. This includes limiting to 40 kg. the incremental mass associated with the MCS.
- (5) define operating modes of the MCS and 14/11 GHz spot beam subsystem in terms of their combined power and thermal balance requirements.
- (6) accommodate $\pm 2^\circ$ spacecraft pitch bias required for optimizing existing coverages for different orbital locations.

Notable design features which result include:

- (1) a deployable L-band array antenna which can be pitch biased.
- (2) solid state high power L-band amplifier modules.
- (3) the use of orthogonally polarized ports of two existing C-band global coverage horns.

AP/B POSTER SESSION B
WEDNESDAY PM 2:00-5:30
KANE HALL - WALKER AMES ROOM

WAVE PHENOMENA

Chairman: C. M. Butler
University of Mississippi
University, MS

The following papers belong to the IEEE AP-S Symposium and the summaries are included in the IEEE AP-S Digest under AP/B Poster Session B.

1. On Convergence of the Method of Moments
T. K. Sarkar, Rochester Institute of Technology, Rochester, NY
2. The Non Uniqueness of Inverse Problems and Partial Coherence
B. J. Hoenders, State University at Groningen, Groningen,
The Netherlands, H. P. Baltes, L. G. Z. Landis, and G. Zug,
Zentrale Forschung und Entwicklung, Zug, Switzerland
3. Exact and Approximated Time-Domain Deductive Reconstruction of
Conducting Multilayer Slabs
D. Lesselier, C.N.R.S. - E.S.E., Gif-sur-Yvette, France
4. Multiple Wavelength Aperture Synthesis for Passive Sensing of
the Earth's Surface
E. Schanda, University of Berne, Berne, Switzerland
5. The Backward Transform of the Near Field for Reconstruction
of Aperture Fields
J. D. Hanfling, G. V. Borgiotti, and L. Kaplan, Raytheon Co,
Bedford, MA
6. A Study of Adaptive Sidelobe Canceller
C. A. Chuang, Harris Government Communications System Division,
Melbourne, FL
7. To Theory Wave Propagation in W-Fiberguides with Rectangular
Core
V. V. Cherny, University of California, Berkeley, Berkeley, CA
8. SEM Characteristics of a Log-Periodic Dipole Array
K. D. Rech, K. J. Langenberg, Universitat des Saarlandes,
Saarbrucken, FRG
9. SEM Investigation of Transient Acoustic Scattering from a Fixed
Finite Rotationally Symmetric Body
G. Bollig, K. J. Langenberg, Universitat des Saarlandes,
Saarbrucken, FRG
10. Doppler Spectrum of Extended Objects
J. B. Andersen, Aalborg University Centre, Aalborg, Denmark
11. Measured and Calculated Field Within Partitioned One and Two-
Port Coaxial Cavities
M. G. Harrison, USAF Weapons Laboratory, Kirtland AFB, NM
C. M. Butler, University of Mississippi, University, MS

AP/B POSTER SESSION B
WEDNESDAY PM 2:00-5:30
KANE HALL - WALKER AMES ROOM

WAVE PHENOMENA (cont.)

12. A Dual Polarization Broad-Band Waveguide
J. Tourneur, Thomson-CSF, Malakoff, France
13. Resonance, Phase Front and Polarization-Independence
Constraints of Inhomogeneous Fabry-Perot Interferometers
S. Raz, University of Houston, Houston, TX and Y. Leviatan
Technion-Israel Institute of Technology, Haifa, Israel

AP/B POSTER SESSION C
THURSDAY PM 1:30-5:00
KANE HALL - WALKER-AMES ROOM

SCATTERING

Chairman: C. M. Butler
University of Mississippi
University, MS

The following papers belong to the IEEE AP-S Symposium and the summaries are included in the IEEE AP-S Digest under AP/B Poster Session C.

1. Coupling of Electromagnetic Waves to a Cable Through Long Slots
T. C. Tong, TRW Defense and Space Systems Group, Redondo Beach, CA
2. A New Surface-Current Model for Metallic Scattering Surfaces
A. Mendelovicz, Hughes Aircraft Company, Canoga Park, CA
3. Design of Cylindrical Shields: An Application of the Uniform Geometrical Theory of Diffraction
B. S. M. C. Galvao and C. S. Pereira, Instituto de Pesquisas Espaciais, Sao Jose dos Campos, Brazil
4. Radiation by Sources on Perfectly Conducting Convex Cylinders with an Impedance Surface Patch
L. Ersoy and P. H. Pathak, The Ohio State University Electro-Science Laboratory, Columbus, OH
9. An Angle Filter Containing Three Periodically Perforated, Metallic Layers
E. L. Rope and G. Tricoles, General Dynamics Electronics Division, San Diego, CA
12. Cross Polarization Discrimination Characteristics During Multipath Fading at 4 GHz
S. Sakagami and K. Morita, Nippon Telegraph and Telephone Public Corporation, Yokosuka-shi, Japan
15. Receiving and Transmitting Properties of Some Reflecting Surfaces
K. M. Romberg, R. L. Fante, Rome Air Development Center, Hanscom AFB, MA
17. Space-Time Integral Equation Solution for Scattering by Thin Flat Surfaces
C. L. Bennett and H. Mieras, Sperry Research Center, Sudbury, MA
20. Loading/Imaging Effects on Resonance Region Scattering
N. A. Howell, Technology Service Corporation, San Monica, CA
21. The Thickness Criterion for Single-Layer Radar Absorbents
E. F. Knott, Georgia Institute of Technology, Atlanta, GA
23. Predicting Average-Median-Value Scattering from Cylinders
N. A. Howell, Technology Service Corporation, Santa Monica, CA

AN INTERPERTATION OF VARIATIONS IN THE
SLOT ELECTRIC FIELD OF A SLOT-PERFORATED
DIELECTRIC-SLAB-COVERED INFINITE CONDUCTING
SCREEN

R.D. Nevels, Electrical Engr. Dept., Texas A&M University, College
Station, Texas.

C.M. Butler, Electrical Engr. Dept., University of Mississippi,
University, Mississippi.

An integral equation solution for the problem of a dielectric-slab-covered infinite conducting screen perforated by a slot or slots of infinite extent was reported at the URSI and URSI/APS meetings in 1978. The method of moments was utilized to find the unknown tangential slot electric field due to illumination of the slot by a TE- or TM- polarized wave at an arbitrary angle of incidence. Results were presented as a function of the thickness of a dielectric slab covering the shadow side of the screen.

One result of the above mentioned investigation was an interesting regular variation noted in the slot tangential electric fields, particularly evident in the wider slot cases. Such a variation in the slot tangential electric field has been observed in both the case in which a slot-perforated-conducting screen is situated in a homogeneous medium and in the case in which a slot-perforated-conducting screen separates half spaces with different electromagnetic properties (two-media case) (C.M. Butler and K.R. Umashankar, Radio Sci., 11, 611-619, 1976). Such phenomena are attributed to an interference pattern created by the diffraction of the illuminating field from the edges of the slot. In the case of a dielectric-slab-covered screen, however, the interference pattern is much more distinct than has been observed in either the homogeneous or two-media case. In this case evidence is presented which indicates that, for the present case, variations in the tangential slot electric field are due to the interaction of surface waves that are excited at both edges of the slot in the dielectric slab by the incident illuminating fields.

REFLECTION AND TRANSMISSION CHARACTERISTICS OF
MULTILAYERED LOSSY PERIODIC STRIPS

Te-Kao Wu
Lockheed Missiles & Space Company
P.O. Box 504
Sunnyvale, CA 94086

The scattering from multilayered lossy periodic strips has been analyzed by Tsai, et al. (IEEE T-AP, 26, 257-260, 1977) with normally incident TM plane waves. However, one needs to know whether their conclusions are still valid when the incident plane wave is changed from broadside or with a different polarization. In this paper, a more generalized method is developed by considering both TM and TE plane waves with an arbitrarily incident angle. The formulation employs the impedance sheet approximation and Floquet's theorem. The solution yields the current densities on each layer as well as the transmitted and reflected fields. Typical examples are given for the applications to phase-delay type artificial dielectric lenses and coupling grids for far-infrared lasers, etc. It is found that the refraction index of the artificial dielectric lenses is independent of the incident angle of the plane wave excitations. However, the transmitted and reflected fields of a two - layer periodic strip are strongly dependent on the incident angles. Current plots are also presented for structures up to nine layers. The advantage of this method is that the computation time is relatively small since the matrix fill involves no numerical integration and no special functions. Moreover, it also allows not only the quantitative examination of the ~~losses~~ losses in artificial dielectrics but also the refraction index sensitivity to substrate thickness. It is believed by the author that this method may be extended to analyze the three-dimensional lattice or mesh structure.

SURFACE-WAVE EXCITATION ON A BONDED MESH

K.F. Casey, Dikewood Corporation, Los Angeles, California

A wire mesh with bonded junctions is capable of supporting a single proper surface wave, although the characteristic equation based on an equivalent sheet impedance representation of the mesh also admits an improper solution. In this paper we discuss the excitation of the proper surface wave by a magnetic line source, employing a technique related to that of Karp and Karal (Comm. Pure Appl. Math., 12, 435, 1959). An equivalent sheet impedance operator is used to describe the mesh, so that the analysis is valid when the mesh dimensions are small in comparison to the wavelength.

It is found that the tangential magnetic field, which itself satisfies a mixed boundary condition at the mesh surface, is expressible as the solution of a second-order linear inhomogeneous differential equation whose driving function satisfies the Dirichlet condition on the mesh surface. The proper choice of the driving function and the evaluation of the arbitrary constants from the differential equation yield a simple expression for the electromagnetic field radiated by the source. The surface-wave excitation efficiency is then easily calculated. The method may also be applied to the analysis of surface-wave excitation on structures capable of supporting several proper surface waves.

Numerical results are presented to illustrate the behavior of the radiated field and the surface-wave excitation efficiency as functions of frequency and mesh geometry. It is found that in the frequency range where the equivalent sheet impedance representation is valid, the surface-wave excitation efficiency is low. The surface wave excitation problem is also briefly discussed for the case in which a more nearly exact analysis of the currents on the mesh wires is employed.

EDGE BEHAVIOR FOR A THICK HALF PLANE

V. Daniele and I. Montrosset
 Politecnico di Torino, Italy
 and

P.L.E. Uslenghi
 Communications Laboratory,
 Department of Information Engineering
 University of Illinois at Chicago Circle
 Chicago, Illinois 60680

The problem of the behavior of the electric and magnetic field components near the two edges of a perfectly conducting thick half plane is considered. The half plane is occupying the region $(0 < x \leq s, y \geq 0)$ of the (x,y) plane, with edges at the origin and at $(x = s, y = 0)$. The behavior of the field at the edges changes from that of a 90° wedge when s is large to that of a thin half plane when $s = 0$. In the intermediate region ($s \neq 0$ but small compared to the wavelength $\lambda = 2\pi/k$), the two edges interact in a complicated fashion which we examine by conformally mapping the portion of the $z = x + jy$ plane that is exterior to the thick half plane onto the upper half of the $w = u + iv$ plane. The appropriate conformal transformation is

$$Z = \frac{ks}{\pi} \{ (\xi-1)(2\xi-\xi^2)^{\frac{1}{2}} + \sin^{-1}(\xi-1) \} + \frac{ks}{2}$$

where $Z = kz$, $\xi = w/a$ and a is a positive constant. The edges at $z = 0$, s are respectively mapped onto the points $w = 0, 2a$. Extensive numerical solutions are presented, and comparisons with previous approaches are performed. Approximate analytical solutions are also given for the case $ks \ll 1$, and for both E and H polarizations. This research was supported in part by grant AFOSR-77-3253 and in part by a cooperative scientific program between NSF and the Italian CNR.

ON THE RESPONSE OF A TERMINATED
TWISTED-WIRE CABLE EXCITED BY A
PLANE WAVE ELECTROMAGNETIC FIELD

Clayborne D. Taylor*
J. Philip Castillo**
*Mississippi State University
Mississippi State, MS 39762
**Air Force Weapons Laboratory
Kirtland AFB, NM 87117

In this paper a formulation is presented for predicting termination currents of an arbitrarily terminated twisted-pair cable with general nonuniform illumination. Specific results are obtained for a cable under plane wave illumination with the electric field directed parallel to the axis of the cable. Comparisons are made with the corresponding responses of the cable in an untwisted configuration to determine the dependence of the "cable-induced" noise upon the twisting.

For convenience a few assumptions are made in the analysis. First, it is assumed that the configuration of the twisted-pair is an ideal bifilar helix. Second, it is assumed that the pitch of the turns is much greater than the wire separation. With these assumptions various termination configurations are considered and a comparison is made with measured data.

NEW QUASISTATIC REPRESENTATION FOR
SOMMERFELD INTEGRALS*

James N. Brittingham
Gerald J. Burke
Lawrence Livermore Laboratory
Livermore, California 94550

Abstract

In the past a procedure called the solution space method ["Bivariate Interpolation Approach to Efficiently and Accurately Modeling Antennas Near A Half Space," J. N. Brittingham, E. K. Miller, J. T. Okada, Electronic Letters, November 10, 1977, Vol. 13, No. 23, pp. 690-691] has been used to quickly and accurately find values of the Sommerfeld integrals for lossy earths. The solution space method uses bivariate interpolation on a grid of prestored values when the integral functions are well behaved. Near $\rho=0$ and $z=0$, where the integrals are singular a series representation ["A New Series Solution for Sommerfeld Integrals in a Two Media Problem," J. N. Brittingham and J. T. Okada, URSI, National Radio Science Meeting January 1978] was used. The variables ρ and z are the distance along the interface and the sum of the field-point plus the source-point heights above the interface, respectively. If a function could be found to represent the singularity, then this function could be removed from the solution space method. A previous method ["Quasi-Static Fields of Dipole Antenna Located Above the Earth's Surface," P. R. Bannister, Radio Science, Vol. 2, No. 9, September 1967, pp. 1096-1103] finds the quasistatic representation by setting a propagation constant in the kernel to zero, then evaluating the remaining integral. This procedure does not have a rigorous justification.

This paper presents a rigorous method to find the quasistatic representation for the Sommerfeld integrals. This new quasistatic representation has some differences from the previously presented term. The new method to find the quasistatic representation consist of separating the Sommerfeld's kernel into two parts whose sum equals the original Sommerfeld integral for all values of ρ and z . On investigating these integrals, it is found that one integral is bounded as ρ and z approach zero while the other integral dominates over the other integral for small ρ and z , one identifies the singular integral as the quasistatic representation. This new quasistatic integral is a constant times a free space Green's function located a $\rho=0$ and $z=0$.

*This work was performed by the U.S. Department of Energy by the Lawrence Livermore Laboratory under contract number W-7405-ENG-48.

This new quasistatic representation is then used to improve the solution space method used in the study of practical antennas over an interface. The improvement consists of storing a better behaved function to be used in the bivariate interpolation. The function that is now stored on the solution space grid is the actual Sommerfeld integral divided by the new quasistatic representation of the point of interest. As in the past a bivariate interpolation will be used to find function values not on the grid. Once the interpolated function has been found it is multiplied by the new quasistatic value to obtain the original integral. This new function permits the use of interpolation up to the singular point $\rho=0$ and $z=0$, therefore eliminating the need for the series representation.

Boundary Conditions for a Thin Resistive Elliptic Cylinder

R.K.Ritt

Illinois State University, Normal, IL, 61761

The two dimensional problem of diffraction of a monochromatic plane electromagnetic wave by a homogeneous isotropic cylinder is known to be solvable, in principle, by matching the tangential components of the interior fields to those of the exterior fields at the boundary. For both electric and magnetic polarizations, this leads to an exterior scalar wave equation, with a boundary condition of the form:

$$u(x) = -r \int_C G(k, x, y) \frac{\partial u}{\partial \bar{n}}(y) ds,$$

in which r is a dimensionless constant, C is the cylinder boundary, $G(k, x, y)$ is the Green's function for the interior Neumann problem, and k is the interior wave number.

In the present paper, C is an elliptic cylinder with major axis a and minor axis b ; $k^2 = k_0^2(1 + i\sigma Z_0 k_0^{-1})$ in which k_0 is the free space wave number, Z_0 is the free space impedance, and σ is the conductivity. The integral is evaluated asymptotically, for $\sigma \gg 1$, $\sigma b = \text{constant}$, and $k_0 a \gg 1$.

A DIFFERENTIAL-INTEGRAL METHOD FOR SCATTERING CALCULATIONS

H. C. H. Chen, Department of Bioengineering
University of Utah, Salt Lake City, Utah 84112
M. A. Morgan, Department of Electrical Engineering
University of Mississippi, University, Mississippi 38677
P. W. Barber, Department of Electrical Engineering
University of Utah, Salt Lake City, Utah 84112

The unimoment method has recently been used to obtain numerical solutions for electromagnetic scattering problems involving inhomogeneous nonspherical objects. The approach uses the finite-element method (FEM) to obtain expressions for the fields within a spherical mesh region which encloses the inhomogeneous body. The incident and scattered fields outside the enclosing sphere are expanded in spherical harmonics and the boundary conditions at the surface of the sphere are used to couple the interior and exterior field expansions and obtain a solution.

Although the unimoment method is applicable to problems involving general inhomogeneous nonspherical scatterers, it is quite inefficient if the scatterer is elongated, due to the large number of extra interior mesh elements which are required in the homogeneous region between the enclosing sphere and the scatterer. This drawback can be overcome by replacing the enclosing sphere with a properly selected spheroid (or other minimum enclosing surface). This has the advantage of greatly reducing the number of required mesh elements. While the usual spherical harmonic expansion can no longer be used directly in the external region, there is an integral equation method which can be used in the external region. The extended boundary condition method (EBCM) is known to provide an efficient and stable solution for scattering problems involving smooth 3-D surfaces. In particular, in the present problem it is possible to write the external fields (in terms of spherical harmonic expansions) using the EBCM and then couple exterior incident and scattered fields to the internal FEM solution at the surface. A further advantage of this combined approach is that it is no longer necessary to expand the internal fields in spherical harmonics as is usually done with the EBCM (this requirement results in restrictions on the interior region, i.e., it must be homogeneous or consist of layered homogeneous regions).

The hybrid method which will be described here utilizes the best features of both the FEM and EBCM approaches to eliminate the drawbacks of each and thereby make it possible to efficiently solve a large variety of electromagnetic scattering problems.

APERTURE EXCITATION OF A WIRE IN A RECTANGULAR CAVITY

William A. Johnson
Department of Electrical Engineering
University of Mississippi
University, Mississippi 38677

and

Donald G. Dudley
Department of Electrical Engineering
University of Arizona
Tucson, Arizona 85721

This paper addresses the problem of determining the current on a straight, thin-wire situated in a rectangular cavity excited by an exterior source coupling through a full aperture in one of the cavity walls. The cavity wall containing the aperture is assumed to have an infinite, perfectly conducting, planar flange on it. The frequency domain problem is formulated in terms of a linear system of integral equations for unknown aperture fields and wire currents. Once the frequency domain problem is solved, a time domain solution may be given by numerical inverse Fourier transform.

The major difficulties encountered in this problem are (1) rapid numerical summation of cavity potential dyads as the distance between source and observation points becomes small and (2) efficient numerical solution of the system of integral equations. The first difficulty has been overcome in the works (D. B. Seidel, IEEE Trans. MTT-26, No. 11, pp. 908-914, 1978) and (W. A. Johnson and D. G. Dudley, URSI Meeting, Boulder, Nov. 1978). An efficient numerical solution to the aperture field integral equations may be obtained by use of shifted subdomain field expansions and a finite difference scheme (D. R. Wilton and A. W. Glisson, AP-S Symposium, Amherst, Oct. 1976).

Numerical results for frequency domain wire currents and aperture fields will be given. Finally a transient problem will be considered.

AN UPDATE ON NAVAL VESSEL IDENTIFICATION

D.L. Moffatt and C.M. Rhoads
The Ohio State University ElectroScience Laboratory
Department of Electrical Engineering
Columbus, Ohio 43212

The purpose of this paper is to give an update on a matched-filter type identification procedure for naval vessels. The basic method and a multiple-frequency reflectivity measurement system used to obtain the requisite scattering data were recently reported (1978 International IEEE/AP-S Symposium USNC/URSI Spring Meeting). The harmonic measurements were initially confined to bow-on, abeam and stern-on aspects for seven model ships (hull length $\approx 1.5\lambda$ at fundamental). It was found that the frequencies of free oscillation (or natural resonances) as extracted from these measured data via matched filter waveforms were distinctly different for the widely spaced viewing aspects for any ship. It was postulated at that time that the extracted resonances were actually quasi-invariant in that essentially the same resonances would hold over some range of aspects in the neighborhood of the well-defined aspects (bow-on, stern-on, etc.).

In this paper, measured harmonic data and extracted natural resonances are presented which basically confirm this postulate. Measured bi-static scattering data (elevation angle $\approx 29^\circ$, bi-static angle $\approx 13^\circ$ and vertical polarization) have now been obtained for two model ships. For each ship, data at eleven additional aspects were obtained corresponding to $\pm 5^\circ$ and $\pm 10^\circ$ from the previous aspects. Tests on these data yield excellent identification results over the increased aspect ranges. These results and a slightly modified test procedure are described.

In addition to the discrete frequency measurements, initial results on swept frequency measurements for these same targets will be presented. These additional measurements are desirable in that they are useful in constructing chirp-type pulse response waveforms. It is anticipated that these measurements will point to narrower frequency ranges containing useful target identification data thereby removing harmonic scattering data as an identification requirement.

SIMPLE THEORY OF ELECTROMAGNETIC SHIELDING OF ENCLOSURES

K.S.H. Lee, Dikewood Corporation, Los Angeles, California

Electromagnetic energy can penetrate into a metallic enclosure by means of diffusion through the enclosure's wall. The diffusive penetration comes about because the conductivity of the wall, albeit high, is not infinite. It is common knowledge that at low frequencies the diffusion mechanism provides an effective means for penetration by magnetic field, while penetration by the electric field is negligible by comparison.

In this paper we first review the low-frequency electromagnetic shielding theory of Latham and Lee (Canad. J. Phys., 46, pp.1745 - 1752, 1968), in which the effect of the enclosure's wall on the penetrant field is duplicated by a set of boundary conditions for the magnetic scalar potentials. From these boundary conditions we derive a simple perturbation procedure for good shields to calculate the penetrant field. Finally, we apply the theory to certain canonical enclosure shapes and obtain frequency- and time-domain solutions for the penetrant pulse. Based on these solutions we deduce simple engineering formulas for determining the wave shape and peak value of the penetrant pulse. We then show how these simple formulas can be generalized to enclosures of arbitrary shape.

HALF-PLANE DIFFRACTION AT OBLIQUE INCIDENCE OF AN ELECTROMAGNETIC PLANE WAVE OF ARBITRARY POLARIZATION

G. A. Deschamps and S. W. Lee
 Department of Electrical Engineering
 University of Illinois, Urbana, Illinois 61801

The solution to this classical problem is cast in a simple coordinate-free form by introducing operators of rotation about the edge of the half-plane. The vector t being along the edge, a rotation through the angle α will be denoted by t^α , which is appropriate because $t^\alpha t^\beta = t^{\alpha+\beta}$. The field $F = (\vec{E}, \vec{H})$ resulting from an incident planewave $F_1 = (\vec{E}_1, \vec{H}_1)$ of arbitrary polarization and direction is

$$F(\vec{r}) = F_1(\vec{r})F(\tau_1) + g(kr)(t^{\psi_1} - t^0)F_1(0) + (1\rightarrow 2) \quad (1)$$

where (1 \rightarrow 2) means the first two terms with 1 replaced by 2,

$$F(\tau) = \pi^{-1/2} \int_{\tau}^{\infty} \exp(i\tau^2 - \frac{\pi}{4}) dt, \quad g(x) = (8\pi x)^{-1/2} \exp(i(x + \frac{\pi}{4}))$$

F_2 is the field image of F_1 under reflection through the plane of the screen, τ_1 and τ_2 are the detour parameters for the fields F_1 and F_2 , ψ_1 and ψ_2 are the angles of rotations that bring the incident and reflected rays on the diffracted ray through \vec{r} , $r = |\vec{r}|$ the origin for \vec{r} being the point of diffraction on the edge. The exact diffracted field, obtained by subtracting the geometrical optic field from F , is

$$F_D(\vec{r}) = V(\tau_1) e^{ikr} F_1(0) + g(kr)(t^{\psi_1} - t^0)F_1(0) + (1\rightarrow 2) \quad (2)$$

where $V(\tau) = (\text{sgn } \tau) \bar{e}^{i\tau^2} F(|\tau|)$. When τ_1 and τ_2 are large, F_D reduces to the GTD diffracted field

$$F_d(\vec{r}) = F_{d1} + F_{d2} = \frac{1}{\sin \beta} \chi_1 g(kr) t^{\psi_1} F_1(0) + (1\rightarrow 2) \quad (3)$$

where $\chi_1 = \text{cosec}(\psi_1/2)$ and β is the angle of the incident ray with the edge. Expressions (1) and (2) can be used to compare the two uniform theories: Theory A (Ahluwalia, Lewis, Boersma, Lee and Deschamps) and Theory B (Kouyoumjian and Pathak). According to Theory A, applied to the present problem, the total field is

$$F_A(\vec{r}) = [F(\tau_1) - \tilde{F}(\tau_1)] F_1(\vec{r}) + F_{d1} + (1\rightarrow 2) \quad (4)$$

while according to Theory B the diffracted field is

$$F_B(\vec{r}) = [V(\tau_1)/\tilde{V}(\tau_1)] F_{d1} + (1\rightarrow 2) \quad (5)$$

The tildes over functions F and V indicate large argument asymptotic expression. It is verified that Theory A recovers the exact solution of the present problem, while Theory B does not (a fact also observed by J. Boersma). An explicit expression for the error of Theory B can be derived and shows that the error might be significant near the edge.

SESSION C-1
MONDAY PM 1:30-5:00
HUB 106B

HIGH TIME-BANDWIDTH PRODUCT SIGNALS: THEORY AND APPLICATIONS

Chairman: R. Price
Sperry Research Center
Sudbury, MA

REDUCTION OF OUT-OF-BAND SPLATTER
OF PSEUDONOISE SPREAD SPECTRUM

C. R. Cahn, Magnavox Government and Industrial
Electronics Company, Torrance, CA 90503.

The simplest form of pseudonoise (PN) spread spectrum is generated via biphas shift keying (BPSK) with the bits of pseudorandom binary sequence. The spectrum of unfiltered BPSK is that of a rectangular pulse shape and decreases at the rate of 6 dB/octave out-of-band. Unfortunately, filtering with the intent of further reducing the out-of-band spectral splatter for electromagnetic compatibility is defeated by hard limiting to restore the signal to a constant envelope. Minimum shift keying (MSK) is a quadriphase version of PN which has a constant envelope and a spectrum decreasing at the rate of 12 dB/octave, corresponding to a cosine pulse shape. MSK is very similar to staggered (or offset) quadriphase shift keying (SQPSK), except that SQPSK has the same spectrum as BPSK. However, when SQPSK is filtered and hard limited, the out-of-band spectrum remains low, in contrast to BPSK. This is a consequence of having completely avoided 180° phase transitions in the staggered waveform.

An analytical computation of the spectrum of filtered and hard-limited SQPSK is not available, but extensive computer simulations with Butterworth filters have been carried out. Empirically, it is found that an optimum number of poles exists, as a function of the filter bandwidth. The effect places a floor on the achievable out-of-band spectrum reduction by this simple and practical modulation technique for generating pseudonoise spread spectrum.

Recently, a new phase-modulation technique has been discovered which yields a further reduction in the out-of-band spectrum of a constant envelope signal. This technique is called tamed frequency modulation (TFM), and can best be described as frequency modulation by a polybinary waveform. Interestingly, from this point of view, SQPSK can be described as a duobinary frequency modulation, and (as is well known) MSK as a conventional binary frequency modulation. TFM exploits constraints extending over several bits and, thereby, exceeds what can be done purely by a pulse shaping modification to MSK. The out-of-band spectrum of TFM can be obtained by analytical approximation, and also by computer simulations. These show the spectrum is 100 dB down at approximately 1.5 times the total bit rate (i.e., the null-to-null bandwidth for SQPSK), with a smoothly decreasing auto-correlation function.

**DESIGN AND APPLICATION OF LARGE
TIME-FREQUENCY CODED SIGNAL SETS**

George R. Cooper, School of Electrical Engineering
Purdue University, W. Lafayette, IN 47907

A method for designing large sets of time-frequency coded signals having uniformly small crosscorrelation properties is described and typical computed crosscorrelation functions are shown. It is demonstrated that such signals possess properties that are reasonably close to the theoretical limits that can be expected. Furthermore, the number of such signals having a specified time-bandwidth product can be made extremely large, although the ultimate limit remains an unsolved theoretical problem at this time.

Although large time-bandwidth product signals are not normally considered to be spectrally efficient, there are some circumstances in which they provide greater efficiency than orthogonal signals. A particular situation that has been analyzed in some detail is that of cellular communication systems such as are being proposed for land-mobile radio service. In this case, the large bandwidth provides frequency diversity that minimizes the effects of frequency-selective rapid fading and the large time-bandwidth product makes it possible to suppress interference from other users in the same geographic area. The result is a system that has greater spectral efficiency than narrowband cellular systems and also provides more consistent speech quality, privacy and more flexible blocking properties under overload conditions. A brief discussion of the application of the time-frequency coded signal set to cellular systems and the resulting spectral efficiency is provided.

LARGE TIME-BANDWIDTH PRODUCT SIGNALS FOR
SPREAD-SPECTRUM MULTIPLE-ACCESS COMMUNICATIONS

Michael B. Pursley
Coordinated Science Laboratory
University of Illinois
Urbana, Illinois 61801

As suggested by their name, spread-spectrum communications systems require the use of signals with large time-bandwidth products. For a spread-spectrum system with only one transmitter, the main requirement for these signals is that they have good autocorrelation properties. For a spread-spectrum multiple-access (SSMA) communications system, however, the number of large time-bandwidth-product signals needed is at least the number of transmitters in the system. Furthermore, these signals must have not only good autocorrelation properties but also good crosscorrelation properties. For SSMA applications, the large time-bandwidth-product signals are usually derived from periodic sequences which are often referred to as signature sequences. Examples of classes of signature sequences which have been considered for SSMA communications systems are the maximal-length sequences (m-sequences), the Gold sequences, and the Kasami sequences.

In this paper, the selection of signals with large time-bandwidth product for use in SSMA systems is discussed. Several families of signature sequences are considered such as m-sequences of periods 31, 63, 127, and 255; Gold sequences of periods 31, 127, and 255; and Kasami sequences of period 255. Techniques are described for the selection of optimal sets of sequences from these families, and numerical results are presented. Several different correlation parameters are considered including the peak periodic and odd autocorrelation and crosscorrelation, the mean-squared aperiodic and partial autocorrelation and cross-correlation, and the signal-to-noise ratio parameter defined in (M. B. Pursley, IEEE Trans. Commun., vol. COM-25, 795-799, 1977).

In addition to the above results for specific families of signature sequences, identities and bounds are presented which relate various correlation parameters for general complex-valued periodic sequences. A survey of previously known identities is given along with new results on the partial correlation.

Acknowledgement. This paper draws upon recent results from an ongoing research project supported by the National Science Foundation (ENG 78-06630) and the Army Research Office (DAAG 29-78-G-0114). Some of the results presented were obtained in joint work with Professor D. V. Sarwate, D. W. Gahutu, F. D. Garber, and H. F. A. Roefs obtained the numerical data.

PSEUDO-NOISE MATCHED FILTERS IN ADAPTIVE ARRAYS

M. P. Ristenbatt, E. K. Holland-Moritz,
Cooley Electronics Laboratory, University
of Michigan, Ann Arbor, Michigan 48109

Large time-bandwidth (TW) product signals are often formed with random-appearing binary sequences called pseudo-noise (PN). The interference rejection available with such signals can be combined with the interference rejection capability of adaptive arrays (see, e.g., R. T. Compton, Jr., "An Adaptive Array in a Spread-Spectrum Communication System," Proc. IEEE, Vol. 66, No. 3, March 1978, pp. 289-298). Adaptive antennas have been studied for some time in radar applications to reject sidelobe interference of large phased array antennas.

The first part of this presentation overviews, in a coarse engineering fashion, the methods studied thus far for combining the two techniques, including their gross implementation implications. In those closed-loop methods where the array-processing precedes the PN collapsing, the spatial processing is serial in nature, and one has to deal with a transient response. If an open-loop arrangement is used, the transient response can be replaced by decision algorithms.

The second part of this presentation describes the general concept of using PN matched-filters ahead of either closed-loop or open-loop spatial processing. This appears to exploit the rapid processing speed of large-scale-integrated (LSI) correlation devices, such as CCD's and SAW's. Other important aspects are: (1) parallel spatial processing is available; (2) after synchronization, interference-only samples can be separated from signal-plus-interference samples.

SURFACE-ACOUSTIC-WAVE CONVOLVERS
FOR PROCESSING SPREAD-SPECTRUM SIGNALS

R. C. Williamson

Lincoln Laboratory, Massachusetts Institute of Technology
Lexington, Massachusetts 02173

The technology of surface-acoustic-wave convolvers has advanced to the point where these devices provide an attractive means for programmable matched filtering of spread-spectrum signals with bandwidths (chip rates) of 100 MHz or more. The most highly developed type of convolver utilizes a nonlinear acousto-electric interaction. Such a device consists of a strip of silicon held in close proximity ($\approx 0.3 \mu\text{m}$) to the surface of a LiNbO_3 substrate. Counterpropagating surface acoustic waves are launched on the LiNbO_3 substrate and the piezoelectric fields generated by these waves interact with the carriers in the adjacent semiconductor. A distributed mixing action takes place and the mixing products are spatially integrated in a capacitor plate metallized on the back of the silicon, thus yielding the convolution of the two counterpropagating waves. By time-reversing one input (the reference), the desired correlation between the reference and a counterpropagating received signal is obtained. Devices of this type have been developed to demodulate wide-bandwidth spread-spectrum signals and obtain correlation gains in excess of 30 dB. A fast synchronization system utilizing acoustoelectric convolvers has been constructed. Synchronization to within a fraction of a chip is obtained by the end of a synchronization preamble consisting of only 13 bits.

Surface-acoustic-wave convolvers are well suited for processing spread-spectrum waveforms in which the chips are MSK or PSK modulated and data is encoded as DPSK modulation of successive bits (each consisting of several hundred chips). Such devices are also naturally adapted to matched filtering of continuously changing codes because the device symmetry ensures that reference codes may be entered with the same bandwidth as an incoming signal.

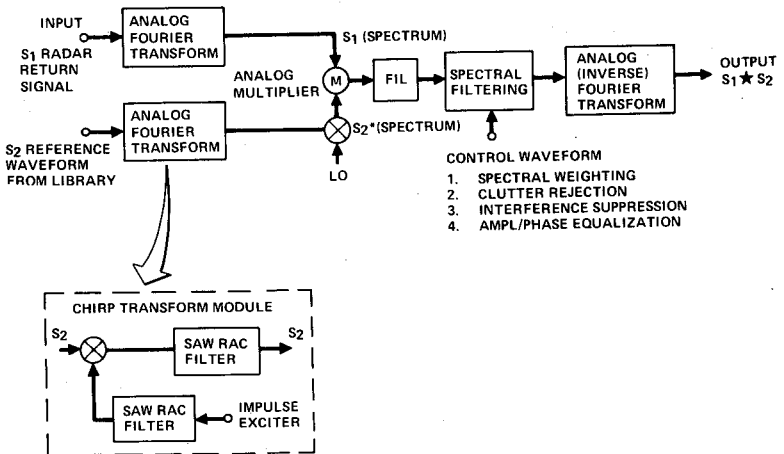
Another type of convolver depends on elastic and piezoelectric nonlinearities in a surface-wave substrate (usually LiNbO_3). The mixing products generated by counterpropagating waves are integrated in a metallized strip deposited on the substrate. Such monolithic convolvers have operated at bandwidths up to 30 MHz with correlation gains up to 25 dB. Because of their simplicity, ruggedness and projected low cost, this type of convolver is currently the subject of renewed interest.

APPLICATIONS OF CHIRP TRANSFORM NETWORKS
 BASED ON LARGE TB SAW REFLECTIVE ARRAY FILTERS

T. W. BRISTOL, Hughes Aircraft Company, Fullerton, California, 92634

The recent development of high quality linear FM surface acoustic wave (SAW) filters has resulted in the realization of real-time Fourier transformations of large bandwidth signals. The basis is the SAW implementation of the chirp transform (CT) algorithm which is depicted below. Maximum signal bandwidth and frequency resolution are controlled by the performance capabilities of the SAW filters used for the pre-multiply chirp waveform generation and chirp convolution filter. Recent advances in SAW reflective array (RAC) allows up to a few hundred MHz bandwidth and resolution of down to 10 kHz.

This paper will describe applications of CT processors to spectrum analysis and programmable signal cross-correlation systems. Performance capabilities of RAC filters will be reviewed. This will be followed by examples of the microscan (compressive) receiver, which is basically a single chirp transform module. Development of the generalized signal correlator shown below will then be described. Three CT modules are used to provide the cross-correlation of arbitrary signals S_1 , and S_2 , subject only to the constraints that they have bandwidth ≤ 60 MHz and duration ≤ 60 usec. Examples of correlation of chirp, PSK and pulsed CW signals will be given.



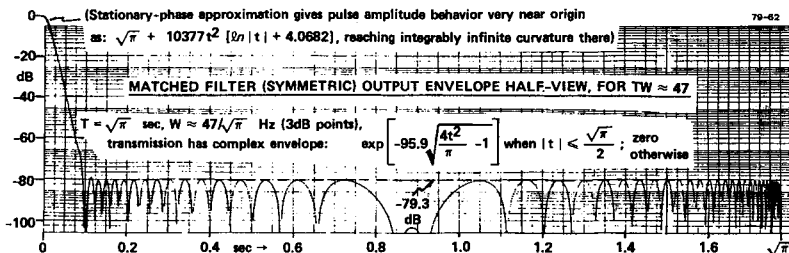
CHEBYSHEV-LOW PULSE COMPRESSION SIDELOBES VIA A NONLINEAR FM

R. Price, Sperry Research Center, Sudbury, MA 01776

Pulse compression as applied during $|t| \leq T/2$ within a T-second long rectangular-envelope sensor transmission, employs carrier phase modulation $\phi(t)$ or FM ($=d\phi/dt$) to spread the emitted 3dB bandwidth $W \gg 1/T$ (in Hz). At large enough TW's, stationary-phase design via nonlinear FM time-trajectory (Key et al, 1961 IRE Int. Conv. Rec., pt.4, 146) enables close control over the receiver's compressive matched-filter output pulse. Indeed, in the instance of FM by $(\gamma/T)\tan(\pi t/T)$ no sidelobes whatever exist for any γ (\approx affine to TW); here, however, nonintegrabilities inflict infinitely many modulation cycles near both edges of the transmitted pulse.

Intuitively, no finite-cycle, rectangular-magnitude modulating pulse can with $TW \gg 1$ be, at matched filter output, free of potentially target-resolution impairing sidelobes; still, an infinite-swinging but integrable FM might yet offer escape from the snr-penalizing practice of suppressing them by filter mismatching. Candidates are C. Cook's $(\gamma/T)\arctanh(2t/T)$ and our "circle- ϕ " (" ϕ "): $\gamma(d/dt)\sqrt{1-(2t/T)^2}$. Zero-Doppler, exact evaluations show the latter as quite unique among various stationary-phase syntheses, in yielding near-Chebyshev sidelobe envelope (below). Moreover, even for modest TW's the relative level is nicely low, and decreases as γ^{-2} , e.g., being ideally -52.5 dB for the $TW \approx 10$, SAW implemented case (Worley, Proc. IEEE, 59, p.1618, 1971; U.S. Pat. 3,753,166).

The found behavior is explained by temporarily imagining the " ϕ " extended as an analytic function to $\pm\infty$, so as to have exponentially fast transmitter envelope decay outside $(\pm T/2)$; analysis then proves entire sidelobe absence. When $\gamma \gg 1$, this unimodal compression fits well to $2\gamma|t|K_1(2\gamma|t|/T)$, in Bessel-given proportion to the cosine transform of the stationary-phase-approximate, scaled signal energy density $(4\gamma^2 + \omega^2 T^2)^{-3/2}$ out of the matched filter. (Spectral radian-parameter ω and FM instantaneous frequency of course lie opposite in domain.) The actual, Lommel-peak-magnitude sidelobes are thus seen as created by the convolution of the original, truncated modulating pulse, against the impulse-pair-like disparity of its real part from that of its analytic continuation.



SESSION C-2
TUESDAY AM 8:30-12:00
HUB 106B

NEW SATELLITE SYSTEMS FOR THE 80's AND BEYOND

Chairman: H. Staras
RCA Laboratories
Princeton, NJ

LARGE ACTIVE SATELLITE ANTENNAS BASED ON
SOLAR-MICROWAVE ARRAY TECHNOLOGY (SMART)

F. Sterzer
RCA Laboratories
Princeton, NJ 08540

Advances in low-cost space transportation systems and in microwave integrated circuits will make it feasible in the next decade to deploy large active antennas in space. A promising technology to realize such antennas is SMART (Solar-Microwave Array Technology). In SMART, arrays of miniaturized solid-state modules are integrated into a large sheet antenna. Each module is a self-contained microwave receiver and transmitter with its own independent photovoltaic power supply.

The paper will describe a specific approach to realizing SMART modules based on GaAs technology. Use of such modules in communications satellites and solar power satellites will be discussed.

THE EFFECTS OF RAIN ATTENUATION ON 18/30 GHZ
COMMUNICATIONS SATELLITE SYSTEMS

D. O. Reudink
Bell Laboratories
Crawford Hill Laboratory
Holmdel, New Jersey 07733

New configurations for satellite systems using the 18 to 30 GHz frequency bands can be considered, assuming by the time that these frequencies are used in commercial satellites, the space shuttle will be the primary launch vehicle. This provides an opportunity to re-examine system performance in anticipation of high technology satellites with large mass and physical dimensions launched by the space shuttle, and in light of accurate measured attenuation data obtained from over two years of continuous recording of the 18 and 30 GHz satellite beacons measured from the COMSTAR satellites.

A very large aperture antenna is possible using the nearly 15' diameter of the shuttle bay, and indeed such an antenna could provide gain in excess of 60 dB at 20 GHz in a 3 dB beam of width on the order of a quarter degree. Assuming designs supporting spot beams with this gain or using a scanning spot beam concept, and also assuming several hundred watt power levels that might reasonably be expected in shuttle launched communications satellites, large margins would be available for earth station antenna diameters of modest size. Rain attenuation margins at 20 GHz in excess of 20 dB might be available under the right set of assumptions. In this paper we compare margins available with the shuttle technology to margins required for various outage objectives. We present cumulative probability distributions for two years continuous data at Crawford Hill and compare them with cumulative distributions for the hours from 9 a.m. to 5 p.m. to determine what, if any, advantages might occur for satellite systems whose primary use is for communications during the working day. The data show that margins in excess of 40 dB would be required to achieve 99.99% availability. However, if the reliability requirement is relaxed an order of magnitude, the margin required drops by 30 dB.

In addition to the attenuation probability distributions, numbers of fading events and additional statistics are provided. Curves are given which show the number of occurrences when the signal fades below a certain level. Additionally, histograms of the time length of these events are also presented. These data are also plotted considering only the eight-hour working day.

SOME FACTORS THAT INFLUENCE EHF SATCOM SYSTEMS *

Leon J. Ricardi
M.I.T./Lincoln Laboratory
Lexington, MA 02173

Frequency management problems, scarcity of orbital position assignment and resistance to interfering signals are projected to become serious problems for satellite communications (SATCOM) systems operating below about 15 GHz. International frequency allocations in the 15-50 GHz range permit SATCOM system operation with increased frequency bandwidth and hence may eliminate significant frequency management problems. This paper addresses some of the salient factors that influence SATCOM systems operating over the range 7-50 GHz. Propagation losses, frequency variation of a terminal's EIRP, spatial discrimination, and bandwidth available for spread spectrum AJ are presented as a guide to choosing the operating frequency of an EHF SATCOM system.

* This work was sponsored by the Defense Communications Agency.

"The views and conclusions contained in this document are those of the contractor and should not be interpreted as necessarily representing the official policies, either expressed or implied, of the United States Government."

LARGE APERTURE SOLID STATE ANTENNA FOR SPACE-RADAR

Dr. David Staiman
RCA
Missile and Surface Radar Division
Moorestown, New Jersey

The capability to place large regions of the earth within the viewing angle of a single spacebased radar makes it highly attractive for satisfying demanding strategic and tactical radar mission requirements. The advent of the Space Transportation System (Shuttle) makes feasible the deployment of large structures in space suitable for the large antenna apertures needed. Concurrently, the continued rapid development of microwave integrated circuits suitable for lightweight RF transceiver modules makes an active element phased array antenna a promising candidate for a spacebased radar antenna, offering the advantages of inertialess scanning, highly efficient prime power utilization, low voltage requirements, and large inherent redundancy.

The interactions between the system requirements of a spacebased radar and its antenna design parameters are manifold. The long ranges encountered in spacebased radar require large power aperture products for high probability detection of targets. As a consequence of limited energy resources in the space environment, it is advantageous to use large apertures, optimizing to achieve minimum energy consumption. The narrow beamwidths of large apertures also serve to provide significant clutter rejection. Additionally, the large apertures can be more resistant to ECM by providing a rapid falloff of sidelobes away from the main beam direction. The phased array approach enables rapid surveillance and tracking over large coverage regions, a severe limitation for mechanically-scanned antennas.

The transfer-lens array has been determined to be the most suitable antenna for the successful utilization of the solid state modules in a phased array. It is the least resistant to tolerance in the radiating element position. An important physical consideration in the antenna design is the F/D ratio. Although it is preferable from structural and deployment considerations to minimize this ratio, it is apparent that electrical performance parameters favor large F/D ratios. For example, it may be shown that the performance of an array degrades rapidly for radial expansions with F/D ratios less than one, a significant consideration for a spaceborne system.

The transceiver modules required for the space-based radar will demand extensions in technology to aid in reducing their size and weight. These modules are to incorporate circuits for power amplification of the transmitted signal, low noise amplification of the received signal, 4-bit phase shifting of signals for collimation and beamsteering, logic circuitry for transmit-receive switching and a threshold detector circuit to decode individual module commands. The weight of these modules is to be in the neighborhood of 1 to 10 grams.

A CLOSED FORM SOLUTION TO THE PROBLEM
OF ADAPTIVE JAMMER NULLINGHarvey Waldman
RCA Laboratories
David Sarnoff Research Center

This paper describes a method of calculating the complex element weights required in a phased array to null potential jammers while maintaining the largest possible gain in a desired direction. The antenna pattern generated by using these weights is the best that can be obtained by beamforming. Therefore, they may be used to mathematically evaluate a proposed antenna configuration prior to the design of adaptive circuitry and/or construction of the array. The case of multiple jammers is analyzed to the point where the weights may be obtained by straightforward calculation on a digital computer. In addition, the cases of one and two jammers are solved in detail. It is assumed that the jammer and desired signal directions are known and the elements are non-interacting.

GLOBAL PLANNING IN THE FIXED-SATELLITE SERVICE

Hans J. Weiss
COMSAT, Washington, D.C.

Abstract

The utilization of the geostationary orbit-spectrum resource by the fixed-satellite service is constrained by the need for electromagnetic compatibility between systems.

Concerns with a progressive preemption of the orbit, especially at frequencies below 10 GHz, to the detriment and possible exclusion of later claimants might make the adoption of an orbit assignment plan, such as that developed for geostationary broadcasting satellites, attractive as a means to guarantee the latecomer access to the resource.

It is argued that such rigid prior planning would not only limit the potential "yield" of the resource but would retard its development. Moreover, by foreclosing many implementation and operating options, it would greatly if not fatally diminish the utility of any access guarantee, particularly to the latecomer.

To avoid premature preemption of the geostationary orbit-spectrum and to alleviate the difficulties of coordination in an increasingly congested environment, there are a number of options which administrations could invoke at the upcoming WARC. These options are of a technical/regulatory nature, but they may require some departure from the historical allocation practices.

If planning were seen to be the only acceptable means of protecting future claims to the resource, it should be open-ended, dynamic and synergic rather than rigid, and it should provide the same kind of guarantee a rigid a-priori plan would offer. Principles of a dynamic planning approach are outlined.

COMBINED SESSION C/E
MONDAY AM 8:30-12:00
HUB ROOM 106B

TELECOMMUNICATION SYSTEMS IN NON-GAUSSIAN ENVIRONMENTS

Chairman: J. M. Morris
Naval Research Laboratory
Washington, D.C.

ASYMPTOTIC PERFORMANCE OF NONLINEAR DEMODULATORS
IN IMPULSIVE NOISE

David F. Freeman
GTE SYLVANIA
Electronic Systems Group
Eastern Division
77 "A" Street
Needham Heights, Mass. 02194

ABSTRACT

We present a technique for calculating the bit error rate performance of non-linear demodulators operating in impulsive noise in the limit of large time-bandwidth products. We give the asymptotic limit and the first order correction; higher order corrections are possible, but computationally burdensome. We calculate bit error rates with two non-linearities, a band pass limiter and a low pass limiter; we find that the two give very similar results. The computational technique is applicable to all noise distributions. We present results for two distributions, an analytic continuation of the Hall model and a truncated Hall model. The models yield significantly different results.

ESTIMATION OF MEAN AND STANDARD DEVIATION
FROM QUANTILES IN INTERFERENCE MODELING

David B. Sailors, Naval Ocean Systems Center
San Diego, CA 92152

In computing the electromagnetic compatibility of communication systems, it is often desirable to have estimates of the mean and standard deviation of relevant parameters. But often only a few quantiles are available to represent the parameter—usually the median and the upper and lower deciles. This paper reviews techniques for estimating the mean μ and the standard deviation σ from quantiles and compares these results to that obtained from estimating the sample means and standard deviations from data samples of man made radio noise and of oblique incidence MOF and LOF.

The use of a few quantiles from a very large sample as a basis for an estimate of the mean μ and standard deviation σ was first considered by K. Pearson (Biometrika, 13, 113-132, 1920) and was much later discussed by F. Mosteller (Ann. Math. Statist., 17, 377-408, 1946), F. Bensen (J. Royal Statist. Soc., Series B, 11, 91-100, 1949), and I. Eisenberger and E. C. Posner (Am. Statist. Assoc. J., 60, 97-133, 1965). Optimal estimators are obtained by choosing quantile points that minimize the variance in the estimate of the parameter, assuming normality. F. Bensen also has shown how bias in the estimates, due to the assumption of normality, can be minimized. E. S. Pearson and J. W. Tukey (Biometrika, 52, 533-546, 1965) have presented a technique for estimating μ and σ from quantiles which is more robust in that normality is not assumed. The technique due to Zacharisen and Crow (Radio Science, 5, 1307-1315, 1970) for determining the degrees of freedom of a Chi-square distribution, using the median and upper and lower deciles, can be used to estimate μ and σ for a skewed distribution.

The mean can be estimated from a single quantile, the median. A more efficient estimate is $\mu = 0.416 [50\%] + 0.292 ([15.9\%] + [84.1\%])$ where $[15.9\%]$, $[50\%]$, and $[84.1\%]$ are quantiles located at the 15.9, 50.0, and 84.1 percentile points respectively. A slightly less efficient estimate is $\mu = 0.514 [50\%] + 0.243 ([10\%] + [90\%])$. Pearson and Tukey use the 5, 50, and 95 percentile points to obtain a robust estimate.

To estimate σ at least two quantiles are needed. The optimum two quantile estimate is $\sigma = 0.337 ([93\%] - [5.9\%])$. A somewhat less efficient estimator is $\sigma = 0.39 ([90\%] - [10\%])$. The bias due to assuming normality can be minimized using $\sigma = 0.289 ([95\%] - [5\%])$. The robust estimator due to Pearson and Tukey utilizes quantiles at the 2.5, 5, 95, and 97.5 percentile points.

ROBUST SIGNAL DETECTION FOR ASYMMETRIC DEPARTURES
FROM THE GAUSSIAN NOISE DENSITY

Saleem A. Kassam and Jung Gil Shin
University of Pennsylvania
The Moore School of Electrical Engineering
Department of Systems Engineering
Philadelphia, PA. 19104

Robust procedures maximizing worst-case detection performance for signals in noise which has a mixture of an unknown symmetric contamination and a nominal Gaussian density have been considered by several investigators. The robust detectors are typically based on nonlinearities which act as hard limiters for large observations.

In this paper we consider a mixture, or contamination, model for nominally Gaussian noise which allows arbitrary asymmetric non-Gaussian tail behavior for the noise density function and a symmetric contaminated Gaussian central region. This model is of much greater practical significance than the symmetric-contamination model. Some recent results (Collins: Ann. Stat., vol. 4, pp. 68-85, 1976) suggest the structure of the robust (minimax) detector for this noise model. Specifically, we show that a nonlinearity which completely ignores large observations (a "noise-blanker") is robust for performance in terms of asymptotic efficiency. The noise-blanking characteristic is required to result in a consistent test. Numerical results on relative performance show the advantage of this detection structure.

We also show that in a related problem of robust quantization of signals for detection applications, a minimax solution can be found which is robust for the general asymmetric contamination model for the nominal Gaussian noise density.

ANTENNA SUPERRESOLUTION REVISITED

By

Ronald L. Fante

Robert V. McGahan

Rome Air Development Center

Hanscom AFB, MA 01731

It has long been known that a portion of a bandlimited function can be uniquely extrapolated by analytic continuation. Thus if there were no noise or other error sources one could obtain extremely high resolution even with a relatively small aperture. Based on the aforementioned principle a number of techniques have been developed for extrapolating signals, or equivalently, estimating their spectra. These include the autoregressive method and maximum entropy technique and an algorithm for adaptive extrapolation developed by Papoulis (IEEE Trans CAS-22, 737-742, 1975). Unfortunately the effect of noise and other errors on the applicability of these techniques has not been explored, and in the case of the Papoulis algorithm noise can be shown to cause divergence of the results. In this paper we will evaluate the possibility of aperture extrapolation using the stochastic approximation method employed by Kashyap and Blaydon (Proc. IEEE 54, 1127-29, 1966). The results obtained with this method can be shown to converge with probability one and in the square sense, even in the presence of considerable noise corruption. We will compare functions, and their spectra, extrapolated by this method with the correct results for a number of different noise levels, and will comment on the applicability to antenna superresolution.

HIGH FREQUENCY COMMUNICATIONS ENHANCEMENT STUDY
USING SPATIAL FILTERING TECHNIQUES

Dr. Peder M. Hansen and Gary J. Brown
Naval Ocean Systems Center
271 Catalina Blvd.
San Diego, California 92152

Conventional communications in the hf (2 MHz to 30 MHz) frequency band are often disrupted or degraded due to unintentional other user interference. This study evaluates the effectiveness of an adaptive antenna array to achieve interference suppression by spatial filtering at hf. This approach is evaluated for both the short range groundwave path and long haul skywave communications using simple interference models based on actual interference measurements. The results are interpreted in terms of communication system operating characteristics, system communication reliability, and achievable communication range.

EFFECTS OF HIGH-ORDER PHASE ERRORS
ON SYNTHETIC-APERTURE RADAR PERFORMANCEWarren D. Brown
Sandia Laboratories, Albuquerque, New Mexico

The formalism presented expresses the pointing angle error, the quadratic, cubic, and quartic components of the phase errors, and an integrated sidelobe ratio in terms of weighted integrals over the power spectral density function of the phase errors. Expressions for the ensemble-averaged antenna pattern with the linear, quadratic, cubic, and quartic components of the phase errors removed are derived in terms of both the autocorrelation function and the structure function of the phase errors. Antenna patterns for a power-law phase-error spectrum are computed and compared for the cases in which components of the phase errors are removed through second and fourth orders. Implications for removing phase errors induced by propagation through the troposphere and ionosphere are discussed.

A DEMODULATION METHOD FOR USE IN COMPUTER SIMULATION
OF COMMUNICATION SYSTEM CHARACTERISTICS

John M. Kelso, Signal Analysis Center, Honeywell Inc.,
Annapolis, Maryland 21404

During the development of a repeater for radio-relay links, a determination of the character and extent of the signal distortions imposed by repeated filtering was needed. In the particular case, a T1 digital carrier was used to frequency-modulate a carrier frequency (seen as 70 MHz in the intermediate-frequency stage where the filtering was performed). Although part of the desired process could be carried out analytically, it appeared impractical to complete the solution in this fashion. Thus, recourse to computer simulation was taken.

A typical portion of a T1 data stream was expanded in a truncated Fourier series, and the resulting expansion was used to compute samples of the frequency-modulated waveform, using a sample rate consistent with the sampling theorem. This sampled waveform was translated into the frequency domain by an FFT computation. After repeated multiplications by the sampled transform function of the filter (a 5-pole linear phase filter with 0.5 degree equiripple), the multiply-filtered waveform was transformed back to the time domain by an inverse FFT, yielding a set of equally-spaced samples of the filtered waveform.

A demodulation process based on the Prony method (c. 1795) for exponential interpolation was developed for use in this problem. Over one or two cycles, the FM waveform remains essentially as a nearly-pure sinusoid with an instantaneous frequency whose departure from the carrier frequency is proportional to the instantaneous modulating frequency. The instantaneous wave frequency can, in principle, be determined from three equally-spaced samples of the waveform, through use of the Prony technique, although it is convenient to use more than three samples in practice. This process provides the necessary demodulation technique.

It will also be shown that the demodulation method can be extended to include amplitude modulation as well as frequency modulation (and, thus, phase modulation also), or a combination of the modulation types.

Submitted for Commission C

HIGHER-ORDER DATA PROCESSING ALGORITHMS
REALIZABLE IN OPTICS

F. Paul Carlson and Robert E. Francois, Jr.

Oregon Graduate Center, 19600 N.W. Walker Road, Beaverton, OR 97005
Lincoln Labs, MIT, 991 Massachusetts Ave., Lexington, MA 02173

In large-array data reduction problems questions concerning optimum algorithms for signal recognition are still being posed. Specifically there is a need to incorporate known spectrum functions. In addition, the possibility of interarray correlations is raising the question of using fourth-order statistical measures such as developed in the Hanbury-Brown Twiss intensity interferometer.

In this paper the realizability and minimal system configurations for such systems are investigated from the point-of-view of using coherent optical data processors for this data reduction problem. The primary motivation stem from the resultant high data rates for these higher-order algorithms and the case of interchanging spectral and temporal data formats as inputs to the system processor.

MEASUREMENT OF SIGNAL STRENGTHS
TRANSMITTED BY A PORTABLE VLF ANTENNA AT 3.125 KHZ

R. J. Dinger, W. D. Meyers, and J. A. Goldstein, Communications Sciences Division, Naval Research Laboratory, Washington, DC 20375

For some applications a short range low data rate communication system with a carrier frequency in the vicinity of the 3 kHz earth-ionosphere waveguide cutoff is advantageous. In order to investigate the feasibility of a portable 3 kHz antenna, a 165 m wire was suspended from a 350 m tower to simulate a balloon-borne antenna, and the element was driven as a monopole by a 1.0 kw power amplifier and compact (0.35 m^3) 5 henry tunable matching inductor. The transmitter bandwidth was 40 Hz. A current of 1.0 A rms and a CW frequency of 3.125 kHz were used. Measurements of the radiated transverse magnetic field strength were made at ranges of 10, 50, 94, and 187 km; at 187 km the measured field strength was -169 dB//1A/m. The measured variation of field strength with distance compared favorably with the equation derived from a source with images reflected about perfectly conducting earth and ionospheric boundaries, except for the value at 50 km. The 50 km field value was possibly distorted by local geological inhomogeneities. The daytime ionospheric reflecting height, derived by fitting the image theory equation to the experimental field values, was 67 km. Limited measurements of the signal strength change during the sunset transition were made at 187 km, and qualitative agreement with the image theory equation was found. The transmitter dipole moment was measured to be 50 A-m rms, which is 40% less than the expected 83 A-m rms value. The difference is attributed to pattern distortion caused by the nearby support tower. Extrapolation of the test results to a system using differential phase-shift keying modulation in the presence of typical mid-latitude daytime noise indicates a communication range of at least 500 km at a 1.0 baud data rate.

SESSION E
TUESDAY PM 1:30-5:00
HUB ROOM 106B

CHARACTERIZATION AND MEASUREMENT OF NOISE

Chairman: A. D. Spaulding
Office of Telecommunications
Boulder, CO

THE RADIO ENVIRONMENT AT 800 KM AS VIEWED BY A DMSP SATELLITE

C. M. Rush, R. K. Rosich, and C. Mellecker
U. S. Department of Commerce
National Telecommunications and Information Administration
Institute for Telecommunication Sciences
Boulder, CO 80303

For over one year an orbiting Air Force satellite has been making continuous measurements of the HF radio environment at the satellite height. The satellite, which is part of the Air Force's Defense Meteorological Satellite Program, is equipped with an HF receiver that provides measurements continuously between 1.2 and 13.9 MHz in 100 kHz steps. The satellite is in a near circular orbit at 800 km and the orbit is essentially sun-synchronous in the dawn-dusk plane.

Observations made along the satellite orbit have been used to develop world maps of the electromagnetic environment at 800 km. The maps have been constructed from observations averaged over time periods ranging from three months to one day. The discussion of the results will center on how the radio environment varies as a function of frequency with particular emphasis being paid to describing the degree to which the results are in concert with what would be expected if the signals reaching the satellite were due to ground-based high-powered transmissions.

SIMULTANEOUS RADIO OBSERVATIONS OF
AURORAL ELECTRONS FROM SATELLITE AND
GROUND-BASED STATIONS

S. Y. Peng, Hughes Aircraft Company, Fullerton, CA. 92670
and
J. S. Kim, State University of New York, Albany, NY 12222

Abstract

A new systematic method is proposed in this paper for the measurement of radio noise from auroral electrons. The proposed method uses both satellite and ground-based stations, simultaneously, to observe auroral radio noise. The advantage of using multiple observation station approach is to minimize or eliminate some of the possible ambiguities in realizing electron energy and pitch angle distributions. Four observation stations have been chosen in the analysis for the proposed method. Three of them are satellites located above the north pole at $\lambda = 90^\circ\text{N}$ (latitude), $R = 2.0 R_E$ (earth radius), and $\lambda = 90^\circ\text{N}$, $R = 3.0 R_E$; and above equator at $\lambda = 0^\circ$, $R = 6.6 R_E$. The other is a ground-based station located at $\lambda = 66.7^\circ\text{N}$ and $R = 1.0 R_E$. Radio frequencies of interest are from 0.1 MHz to 30 MHz. The calculation of auroral radio noise is based on a helical motion synchrotron radiation model. Electron energies considered are ranging from 100 eV to 7 MeV. Several electron energy and pitch angle distributions were used in the calculation. These distributions are based on the measured values by Westerlund (*J. Geophys. Res.*, 74, 351-354, 1969) and Vette (*NASA Spec. Publ.*, No. 3024, 1966), and two assumed isotropic and $\sin \alpha$ pitch angle distributions. The calculated radio noise spectra show distinct different shapes at different observer locations, and vary with electron altitudes and energy and pitch angle distributions. These results lend themselves to the possibility of realizing electron energy and pitch angle distributions through the comparison of the measured radio noise spectra to that calculated. For the ground-based station, the measured and calculated radio noise spectra were compared with good agreement. For the satellite observers, such comparison is not possible due to the lack of the measured data. It is recommended that future programs should be undertaken in developing and implementing such an observation network which will provide invaluable information on auroral electron distributions.

RATE STATISTICS FOR RADIO NOISE FROM LIGHTNING

D. M. Le Vine and R. Meneghini, Microwave Sensors Branch, Goddard Space Flight Center, and S. A. Tretter, Department of Electrical Engineering, University of Maryland

Radio frequency noise from lightning was measured at several frequencies in the HF - VHF range during the Thunderstorm Research International Project (TRIP) at the Kennedy Space Center, Florida. The data was examined to determine flashing rate statistics during periods of strong activity from nearby storms. It has been found that the time between flashes is modelled reasonably well by a random variable with a lognormal distribution.

Initially, the hypothesis that the occurrences of lightning flashes is a Poisson point process was tested using a uniform conditional test with Durbin's transformation and the Kolmogorov-Smirnov statistic. However, the Poisson hypothesis failed for the measured data. This results mainly from a lack of small time intervals, which we believe is a consequence of the finite duration of lightning flashes. This hypothesis has been tested by simulation, using a compound process in which the intervals between lightning flashes is assumed to be exponentially distributed and each flash is assumed to have a duration given by another independent random variable. Assuming flash rates and durations consistent with data, and that the flash duration has a fixed minimum of the order of the measuring system's resolution, the lognormal distribution consistently fit the simulated data.

AMPLITUDE PROBABILITY DISTRIBUTION MEASUREMENTS
AND NOISE EXCISION STUDIES OF 0.5-4.5 KHZ AMBIENT NOISE

R. J. Dinger, J. R. Davis, W. D. Meyers, and J. A. Goldstein,
Communications Sciences Division, Naval Research Laboratory,
Washington, DC 20375

Coordinated measurements of ambient atmospheric and ionospheric noise from 0.5 to 4.5 kHz have been taken at Giglio Island, Italy, and Tromsø, Norway. Measurements were taken for 24 days in March, 1978, and 25 days in June, 1978. Both sites had identical instrumentation: three air core loop antennas, a tape recorder, strip chart recorders, and a real-time amplitude probability distribution (APD) computer. The measured noise spectral densities ranged from a low of $-190 \text{ dB}/1\text{A}/\text{m}/\sqrt{\text{Hz}}$ (Norway, winter) to a high of $-145 \text{ dB}/1\text{A}/\text{m}/\sqrt{\text{Hz}}$ (Italy, summer). Very good agreement is obtained between the APDs and the two parameter noise model of Field and Lewinstein. Good agreement is also obtained with the more complicated four parameter Middleton noise model.

The decrease in the RMS noise level possible by clipping the largest atmospheric noise impulses was investigated. A clipping bandwidth of 130 Hz was found to be sufficient at a frequency of 3 kHz; a larger bandwidth gave only a marginal decrease in the effective noise level. The noise reduction due to clipping was highly variable. In one special instance in Norway the high noise level produced by a small localized nearby thunderstorm was reduced by 27 dB in amplitude by clipping. More typically the improvement in Norway was 3 to 5 dB and had only a slight seasonal dependence. Clipping produced larger decreases in the effective noise level in Italy than in Norway because of the larger impulsive component from nearby thunderstorms. In Italy a reduction of 6 to 9 dB was typical in winter; in the summer the reduction was 4 to 7 dB. Broadband ionospheric hiss emissions were observed in Norway during both measurement periods. No improvement by clipping was possible during these emissions because of their Gaussian APD. The emissions were not observable in Italy, except possibly for a strong emission that occurred on 26 March 1978.

DISTRIBUTION PATTERN OF POLAR VLF HISS EMISSION
OBSERVED BY POLAR ORBITAL SATELLITES

Takeo Yoshino
Univ. of Electro-Communications,
Chofushi, Tokyo 182, Japan.

Hiroshi Fukunishi
National Institute of Polar Research,
Kaga, Itabashiku, Tokyo 173, Japan.

The polar orbital satellites "KYOKKO" (EXOS-A), ISIS-1 and 2 data (1976 to 78) that received at Syowa Station, Antarctica, are being used to the study the distribution of VLF hiss emission in the polar cap region. The results show that the satellite altitude (800Km - 2600Km) in the polar cap region is virtually filled with VLF hiss emission around the higher invariant geomag. latitude side of auroral oval in the region from 8:00 AM till 3:00 AM LT via day through dusk and mid-night. But the area around geomagnetic pole of higher than approximately 80°S of invariant latitude and the area continuing to dawn side (3:00 AM to 8:00 AM) have been never observed the any kind of VLF emission.

These distribution pattern in the polar cap region gives a very good agreement to the polar plasma current injection pattern and related the aurora activity at the auroral oval. The saucer emission appears the lower latitude side of VLF hiss emission distribution pattern, and these location shows a good agreement to the pattern of polar return current belt.

ROCKET AND BALLOON OBSERVATION OF POWER LINE
RADIATION OVER JAPANESE ISLANDS

Takeo Yoshino, Ichiro Tomizawa and Takashi Shibata
University of Electro-Communications,
Chofushi, Tokyo 182, Japan.

By the results of satellite observation data analysis on the power line radiation (PLR) by Stanford University Group, the PLR over Japan in 1967 was consistently lower than the other industrial complexes of the world. Also, the same group published their observation results about the amplified power line harmonics and related triggered VLF emissions in the magnetospheric duct between central Canada and Siple, Antarctica.

For the basical research of PLR, the first balloon experiment have been operated to observe the intensity spreading of PLR in to Pacific Ocean at Sanriku Balloon Range of ISAS of Tokyo University, Tohoku Japan, in 26th September 1978. By the results of this experiment, PLR signal could be detected over threshold noise level even over 600 Km from coast.

The first rocket for the observation of the vertical intensity distribution of PLR over Japan have been launched at Kagoshima Space Center of the ISAS of University of Tokyo, in 31st January 1979 by No. 5 of S-310 type single stage sounding rocket. This rocket reached to 180 Km altitude at apex, and the PLR signal intensity at this apex point was detected as approximately 50 mV/m or more higher. The intensity gradient between ground to apex was slightly continued to approximately same levels except below first 1 Km.

PREDICTION OF SOLAR INDUCED CURRENTS AND EFFECTS ON POWER
TRANSMISSION SYSTEMS IN CENTRAL CANADA

W.R. Goddard, Department of Electrical Engineering,
University of Manitoba, Winnipeg, Canada R3T 2N2

W.M. Boerner, Department of Information Engineering,
University of Illinois at Chicago Circle,
Chicago, Illinois 60680 U.S.A.

The extensive use of the hydro-electric generating capacity in Northern Manitoba requires long HV-DC/AC transmission lines to serve the southern part of Manitoba and neighbouring U.S. power companies. The auroral-electroject zone covers three-quarters of the province and consequently, solar storms strongly affect these transmission systems. Harmonics are generated at transformers due to the saturation of their cores by induced currents, and the level of harmonics produced will cause malfunction of control relays, and yield unacceptable distortions in normal AC waveforms. The objective of our study is to determine the expected affects on long AC transmission systems, and in particular, effects on a 500 KV line to be built from Winnipeg to Minneapolis-St. Paul.

We have used power spectral analyses and histograms of events with rate of change and duration of rate as variables, and these were derived from induced current records at Manitoba Hydro's La Verendrye station and magnetograms from Thompson, Island Lake and Whiteshell (in the IMS magnetometer chains in Manitoba). These analyses and results of Campbell's work (W.H. Campbell, Pure & Applied Geophys., 116, 1978.) on the Alaska pipeline induction problem were used for prediction of periodic and surge currents in the transmission line. The double exponential method (G.L. Siscoe, J. Geophys. Res., 81, 4782-4784, 1976, and D.B. Fleming and G.V. Keller, Report for Bonneville Power Admin., 1972), was applied to six sub-storm records to obtain an initial estimate of the probability of occurrence of very large storms during the lifetime of the power system. The results of our work show that, a surge current of 300 Amperes will occur on the average of once per 2 years, and a surge of 800 Amperes once per 20 years. A study performed by Manitoba Hydro, showed that harmonics produce unacceptable waveforms when a voltage of 6 V/km is applied along the 500 KV line.

We conclude that surge currents will produce significant levels of harmonics and serious operating problems during magnetic storms. Two approaches to avoid these problems will be described.

SESSION F-1
MONDAY AM 8:30-12:00
KANE HALL 110

SCATTERING BY TURBULENCE

Chairman: T. E. VanZandt
NOAA
Boulder, CO

PRECISION OF TROPOSPHERIC/STRATOSPHERIC
WIND MEASUREMENTS

Norman J. Chang
SRI International
Menlo Park, California 94025

ABSTRACT

The results of detailed comparisons of radar-derived wind profiles using the Chatanika radar with a series of 12 rawinsondes launched at approximately 45-minute intervals during 6 April 1978 at Poker Flat, Alaska are presented. Radar-derived wind profiles are generally in good agreement with rawinsonde-derived wind profiles, but significant differences are found occasionally. The significance of these differences and the precision of the radar measurements are discussed. Particular attention is given to the propagation of errors from radar line-of-sight measurements to resolved velocities.

CONTINUOUS MEASUREMENT OF UPPER ATMOSPHERIC WINDS AND TURBULENCE
USING A VHF DOPPLER RADAR: PRELIMINARY RESULTS

W. L. Ecklund, D. A. Carter, and B. B. Balsley
Aeronomy Laboratory
National Oceanic and Atmospheric Administration
Boulder, Colorado 80303

During February 1978 and again in the winter of 1978-1979 a 50MHz Doppler radar was operated at Platteville, CO, as a prototype for a much larger system in the auroral zone at Poker Flat, AK. The antenna consists of 100 x 100m arrays of coaxial linear antennas, with one array phased to point 15° to the north and another, 15° to the east. The average transmitted power was 200W.

In this paper are presented tropospheric and stratospheric results up to about 20km and daytime mesospheric results between about 73 and 82km. In particular, continuous hourly tropospheric and stratospheric profiles for a two week period are presented.

RADAR MEASUREMENTS OF THE VERTICAL
COMPONENT OF WIND VELOCITY
IN THE TROPOSPHERE AND STRATOSPHERE

Vern L. Peterson*
Ben B. Balsley**

Three techniques have been developed of using a Doppler Radar for deducing the vertical component of the wind velocity in the troposphere and stratosphere. These correspond to three different modes of operation: scanning along almucantar circles (azimuth scans), scanning along vertical circles (elevation scans), and fixed observations at the zenith. Observations made in October 1976 with the Chatanika, Alaska radar facility indicate that all three techniques give reliable results for the lower altitudes. The elevation scan and azimuth scan techniques, however, become increasingly subject to inhomogeneities in the wind field with the greater altitudes. For these data, the elevation scan data gave unreliable vertical winds above about 10 km; the corresponding altitude for the azimuth scan data was about 5 km.

* Centennial Sciences, Inc., 4445 Northpark Drive, Suite 200
Colorado Springs, Colorado 80907

**Aeronomy Laboratory, National Oceanic and Atmospheric Administration
Boulder, Colorado 80302

EARLY RESULTS FROM THE POKER FLAT MST RADAR

B. B. Balsley, W. L. Ecklund, D. A. Carter, and P. E. Johnston
Aeronomy Laboratory
National Oceanic and Atmospheric Administration
Boulder, Colorado 80303

A 50MHz MST (Mesosphere-Stratosphere-Troposphere) pulsed Doppler radar was installed at Poker Flat, AK, in February 1979. The antenna consists of two 100 x 100m arrays of coaxial colinear antennas, with one array phased to point 15° to the north of the zenith and the other, 15° to the east. The average transmitted power was 350W for each direction. This radar is the first stage of a much larger system (200 x 200m, 5600W).

In early results echoes are obtained and winds and turbulence are measured in the troposphere and stratosphere up to about 20km and in the mesosphere during the daytime from about 60 to 70km. This height range of echoes in the mesosphere is about 10km lower than in middle latitude winter (Miller et al., Geophys. Res. Lett., 5, 939-942, 1978; Ecklund et al., J. Atmos. Terrest. Phys., submitted, 1979). The effects of particle precipitation on the echoes will be discussed.

HIGH RESOLUTION WIND MEASUREMENTS
USING THE HIGH POWERED RADARS AT KWAJALEINR.K. Crane, Environmental Research & Technology, Inc.
G. Weiffenbach, MIT Lincoln Laboratory*

The high powered UHF and L-band radars at the Kwajalein Missile Range were used for high spatial and velocity resolution measurements of wind profiles in the equatorial troposphere and lower stratosphere. As operated, the radars had a resolution volume smaller than 240 m on a side, a velocity resolution of 0.1 m/s, and a C_n^2 detection sensitivity of better than $10^{-19} \text{ m}^{-2/3}$ at a height of 15 km.

Analysis of data from two different days has revealed a wide range of results. On one day with strong gravity wave activity, C_n^2 values as high as $10^{-14} \text{ m}^{-2/3}$ were detected at heights up to 8 km. On the other day, values of less than 10^{-18} were detected at the same height. The detailed wind observations reveal simultaneous observations of components of the wind separated by more than 20 percent of the magnitude of the wind from within the same resolution volume. These measurements are interpreted in terms of the detailed turbulent mixing process within a shear layer.

*Present Affiliation - Johns Hopkins Applied Physics Laboratory

AN IMPROVED MODEL FOR THE CALCULATION OF PROFILES OF
MEAN TURBULENCE PARAMETERS FROM BACKGROUND PROFILES OF
WIND, TEMPERATURE, AND HUMIDITY

T. E. VanZandt, K. S. Gage, and J. M. Warnock
Aeronomy Laboratory
National Oceanic and Atmospheric Administration
Boulder, Colorado 80303

In previous publications (VanZandt et al., Radio Sci., 13, 819-829, 1978; Gage and Balsley, Bul. Am. Meteorol. Soc., 59, 1074-1093, 1978) we developed a model for the calculation of mean vertical profiles of the turbulence energy dissipation rate ϵ and the radio refractivity structure constant C_n^2 from background profiles of wind, temperature, and humidity. The calculated profiles of C_n^2 agreed remarkably well with profiles of C_n^2 measured nearly simultaneously by Doppler radar. The model suffered, however, from conceptual difficulties, which may also have restricted its range of validity. In the present paper some of these difficulties are resolved.

The basis of the new model is the calculation of the probability distribution of turbulent layer thicknesses due to random fluctuations or "fine structure" in the vertical wind shear and stability. This distribution is calculated as a function of the background parameters, measured by radar or balloon. The resulting C_n^2 profiles are compared with radar-measured C_n^2 profiles.

MEASUREMENTS OF THE PHASE STRUCTURE FUNCTION
AT 35 GHz ON A 28-KM PATH

R. R. Rogers, Meteorology Dept. McGill Univ.;
R. W. Lee and A. T. Waterman, Radioscience Lab., Stanford Univ.

The phase structure function $D_p(\rho) = \overline{[\phi(\rho + \rho_0) - \phi(\rho_0)]^2}$ where ρ is the separation between receiving antennas, has been measured on a 28-km line-of-sight path at 35 GHz, under weak-scattering conditions. Theory indicates that, for a Kolmogorov atmospheric turbulence spectrum, in the inertial subrange, this structure function should vary as a power of the separation ρ : $D_p(\rho) = B\rho^b$, with $b = 5/3 = 1.67$. Measurements made under a variety of meteorological conditions show values of b which fluctuate but lie for the most part between 1.4 and 1.5. These values correspond to a turbulence spectrum exponent between $-9/3$ and $-10/3$ (instead of the Kolmogorov $-11/3$). On only two occasions did b significantly exceed 1.6. In an attempt to account for the discrepancy, the influence of various factors was examined: noise, measurement uncertainties, non-uniform distribution of C_n along the path, and size of the outer scale of turbulence. None, except possibly the last, offers a reasonable explanation. The implication is that the turbulence spectral slope is flatter than that given by the Kolmogorov model.

COMSTAR AND CTS ANGLE OF ARRIVAL MEASUREMENTS

R.A. Baxter, D.M.J. Devasirvatham, and D.B. Hodge
ElectroScience Laboratory
The Ohio State University
Columbus, Ohio 43212

Measurements of angle of arrival and attenuation along several Earth-space paths are discussed. These data were gathered using four geosynchronous satellite beacons at the Ohio State University ground station in Columbus, Ohio.

The 11.7 GHz beacon of the Communications Technology Satellite (CTS) was observed from April to August, 1976 and from December, 1976 to June, 1978 at an elevation angle of 32° . Comstar D1 and D2 28.56 GHz beacons were observed in August, 1978 at elevation angles of 25° and 42° , respectively. Currently, the Comstar D3 28.56 GHz beacon is under observation at an elevation angle of 43° .

The satellite beacon signals are received by a four-element, self-phased, square array with 1 m spacing between 0.6 m parabolic dishes. The beamwidth of each element sufficiently covers the diurnal motion of the satellite. Also, a second-order phase-locked loop compensates for the Doppler shift associated with the satellite's diurnal motion.

Phase differences between pairs of elements are measured. These differential phase measurements are used to calculate the apparent angle of arrival of the incoming wave.

Short term fade events as well as long term angle of arrival and attenuation statistics are presented.

Invited paper for USNC/URSI special sessions on propagation above 10 GHz

SIMULTANEOUS MEASUREMENTS OF ANGULAR SCATTERING AND INTENSITY SCINTILLATION IN THE ATMOSPHERE. W.A. Coles and R. Frellich, University of California, San Diego, La Jolla, CA 92093.

Measurements have been made on a horizontal path 1.5 m above a superheated surface at various ranges from 150 to 1500 m. The angular scattering is measured with a telescope using film as an integrating and recording medium. The film is digitized, calibrated, and Fourier transformed to determine the mutual coherence function (MCF). The integrated phase structure function, $D(\vec{s})$, is estimated by $-\ln(\text{MCF})$. The dynamic range of the $D(\vec{s})$ measurement is extended by using data from both long and short ranges (as $D(\vec{s})$ is linearly proportional to range). The intensity scintillations are measured simultaneously with an array of PIN photodiodes. The spatial and temporal statistics of intensity are computed and compared with calculations based on the measured $D(\vec{s})$. Data taken using a HeNe laser transmitter with a divergent beam are compared with those taken using an incoherent source (an incandescent lamp). The effects of source size on the intensity correlation is shown. It is shown that in the case of strong scattering, where the width of the angular spectrum is more than $100 \mu\text{rad}$, that the structure function follows a square law. However under weaker conditions a Kolmogorov slope, $D(\vec{s}) \propto s^{5/3}$, is a better description. In our experiments the change occurred in the vicinity of $s = 2 \text{ mm}$, suggesting that viscous damping is becoming important in this range.

EFFECT OF METEOROLOGICAL VARIABLES
ON RADIOMETRIC SENSING OF ATMOSPHERIC TEMPERATURE

P. Basili, P. Ciotti, and D. Solimini

Istituto di Elettronica, Facoltà di Ingegneria, Università di Roma
Via Eudossiana 18, 00184 Rome, Italy.

Accuracy of low altitude temperature profiles retrieved by inversion of ground-based radiometric data is affected by several factors: some are inherent in the measuring equipment and procedures, but others are related to the relevant meteorological variables.

A first source of error in retrievals originates from the uncertainty in estimating the radiative transfer kernels and therefore the weighting functions to be used in the inversion process. Indeed, when infrared measurements are considered, both water vapor density distribution and the nature and altitude variation of aerosols can significantly affect the radiative transfer. Season, time of day, local climate and meteorological conditions are therefore able to modify the weighting functions. To gain quantitative information on such variations, radiosonde data acquired in different seasons both at night and during the day have been used to calculate the weighting functions for different bands in the infrared. These results are also compared with those obtained using standard model atmospheres instead of actual radiosoundings.

A second source of error proceeds from the eventual non-stationarity of the atmosphere during the radiometric measurements. The random space-time fluctuations of the meteorological variables which control the radiative transfer produce both irregularities of the weighting functions and change of the profiles under measure. The variations of these variables appear to exhibit characteristic patterns which seem to depend on the atmospheric stability and, according to this latter, can affect differently the accuracy of the temperature retrievals. The different types of irregularities that have been observed by radiometric means, as connected with the various classes of atmospheric stability, are briefly reviewed.

Finally, the robustness of some present inversion techniques against the mentioned sources of errors are investigated.

COMBINED SESSION AP-S/F-2
MONDAY PM 1:30-5:00
KANE HALL 110

JOHN W. WRIGHT MEMORIAL SESSION ON RADIO OCEANOGRAPHY

Chairman: C. T. Swift
NASA Langley Research Center
Hampton, VA

Introduction

C. T. Swift
NASA Langley Research Center
Hampton, VA

REVIEW OF COLLABORATIVE EFFORTS WITH JACK ON
OCEAN SURFACE PHYSICS AND RADAR RETURN

O. H. Shemdin
Jet Propulsion Laboratory
California Institute of Technology
4800 Oak Grove Drive
Pasadena, California 91103

The collaborative efforts with Jack began a decade ago when he was still a radar physicist unfamiliar with ocean wave dynamics but rather curious about radar return signatures from the water surface. The problem faced with at that time was the measured low energy levels in the wave frequency bands in the capillary-gravity range near the point of minimum phase speed. The energy level in those bands increased rapidly beyond a critical wind-speed. Those observations were later explained by the difference in group velocity properties of capillary waves and short gravity waves.

The continuity of stress across the air-sea interface was the next subject to receive much attention. Jack was able to obtain phase speeds of short waves with his radar observations. Explanation of his results required careful investigation of the near-surface shear flow layer below the interface. These investigations were followed by studies on the modulation of short waves by long waves which he conducted in the University of Florida wind and wave tank. He once noted "those two weeks I spent working in Florida were the two most scientifically productive weeks of my career."

The laboratory investigations on wave induced modulation were followed by similar investigations in the field. The West Coast experiment was the site of extensive field activity on this subject. The preliminary results are illuminating even though the analysis has not been exhausted.

REMOTE SENSING OF THE AIR-WATER INTERFACE:
THE LEGACY OF JOHN W. WRIGHT

W. J. Plant and W. C. Keller
U.S. Naval Research Laboratory
Washington, DC 20375

The death of John W. Wright in an automobile accident on November 20, 1978 was an enormous loss not only for his family and personal friends, but also for the scientific community working in the area of radio oceanography. Jack was a leader in this field for many years and his novel insights will be greatly missed. This paper will attempt to convey an idea of the magnitude of Jack's contributions to the field as well as a sense of his directions of thought at the time of his death. Many of the concepts which Jack pioneered or elaborated are now widely accepted and employed in the study of the air-water interface. Among these are the principles of Bragg scattering as applied to water waves, the composite surface scattering model, the effects of scatterer motion on synthetic aperture radar imagery of waves, the dual-frequency technique for sensing long ocean waves, and the relaxation-time model for the modulation of short waves by long. His conviction that microwaves present a unique method of interrogating the air-water interface and his many wavetank studies of the interface have done much to promote the acceptance of remote sensing methods for oceanographic applications. Much of the information he obtained by these methods was difficult, or indeed impossible, to obtain by other means. At the time of his death, Jack was involved in oceanographic experiments on the Outer Banks of North Carolina, in the Gulf of Mexico, and in the North Sea. His efforts were directed toward a better understanding of the parameters affecting the air-water interface and their determination from space. Results of these efforts and their implications for the future will be presented.

SAR IMAGING OF THE OCEAN SURFACE
- AN ASYMPTOTIC EULERIAN FORMULATION

G.R. Valenzuela
Naval Research Laboratory
Washington, DC 20375

An analytic framework to aid in the interpretation (prediction) of SAR images of the dynamical ocean surface is developed. As is well known two basic mechanisms contribute to the formation (distortion) of synthetic radar maps of the ocean. These are amplitude effects involving the "modulation" and "tilting" of the short Bragg scattering waves by the longer (dominant) gravity waves of the ocean, and fluid motion effects from local currents, velocities, accelerations and velocity strains which distort the phase history of the return signal. The final SAR image depends on the interplay of these two processes.

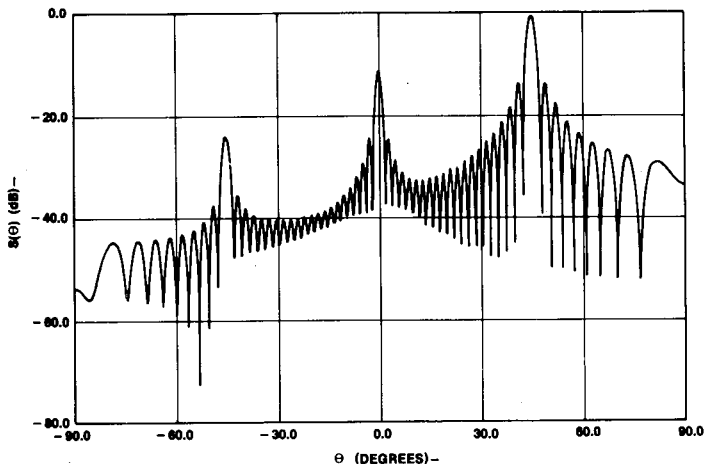
In this work we provide analytical structure to the ideas advanced previously (Larson et al, IEEE Trans., AP-24, 393-394, 1976) in regard to synthetic image formation of nonstationary distributed scatterers. Starting with a simplified expression (polarization independent) for the backscattered fields from the ocean and using an Eulerian specification for the fluid motion asymptotic results are readily obtained for the processed signals by "stationary phase" integration. The physical significance of the results is clear, SAR images from the ocean represent a "map" of the "stationary points" of the ocean surface as interpreted with the SAR system.

Our results suggest that a treatment similar to that of "Optical Aberrations" should provide the best means for interpreting SAR images of ocean waves.

ELECTROMAGNETIC SCATTERING PATTERNS FROM
SINUSOIDAL SURFACES

A. K. Jordan and R. H. Lang*
 Naval Research Laboratory
 Washington, D.C. 20375

In this paper we present an analysis and calculation of scattering from sinusoidal surfaces. An exact space-harmonic representation is used for the field on the surface and, as a result, the calculation includes the effects of shadowing, diffraction, and multiple scattering. An asymptotic evaluation has been employed to obtain an exact expression for the scattering pattern as a product of the space-harmonic scattering coefficients times the corresponding pattern functions. The formula obtained has been simplified for illuminated areas that are many wavelengths long and plotted for a variety of surface parameters. The present method for scattering pattern calculations can be considered to be complementary to methods using physical-optics and point-matching techniques. In addition to the scattering pattern calculations the exact Bragg backscattering amplitudes have been computed and compared to their Rayleigh approximations. The figure shows an example of the pattern of scattered energy density $S(\theta)$ for second-order Bragg scattering; angle of incidence $\theta_0 = -45^\circ$, scattering angle = θ



* Also, Department of Electrical Engineering and Computer Science, George Washington University, Washington, D.C.

TANK MEASUREMENTS OF RADAR RETURN FROM
OIL-COVERED AND RAINDROP IMPACTED WATER

R.K. Moore
A.K. Fung
G.J. Dome
K. Soofi
Y.S. Kim

Remote Sensing Laboratory
The University of Kansas
Lawrence, Kansas 66045

Measurements have been made of the radar return from wind-driven waves in a small wave tank over the frequency range from 8-18 GHz and a range of incidence angles from 10° - 70° . Measurements from the undisturbed wave surface are compared with those from the surface covered with a thin oil layer and the surface impacted by rains of various intensities. The expected large reduction in backscatter from the oil-covered surface was found, and the amount of this effect is reported as a function of frequency and angle of incidence. When raindrops impact the surface, the effect ranges from a significant increase in backscatter for small wind speeds to a negligible effect for large wind speeds and all but the heaviest rain rate.

This work was supported by a grant from NASA Langley Research Center, Grant number NSG 1397.

Modulation of Radar Backscatter by Ocean Waves

W. Linwood Jones and Aubrey E. Cross
NASA Langley Research Center
Hampton, VA 23665

William J. Plant and William C. Keller
Naval Research Laboratory
Washington, D.C. 20375

Recent analyses of radar images of the ocean have indicated the potential for remote sensing directional ocean wave spectra. At off-nadir viewing angles, the imaging radar senses the modulation of the ocean surface reflectivity caused by the interaction of long waves with the predominant radar scatters, the short gravity/capillary waves. However, before quantitative measurements of ocean wave spectra can be derived by radar, the transfer function between modulating long waves and the radar scatterers must be determined. To this end, experiments have been conducted in the open ocean from piers and towers using CW Doppler radars operating at 1.5 and 9.4 GHz. The ocean wave-radar modulation transfer functions were measured for vertical polarization at approximately 50° incidence angle under a range of wind speeds up to 10 m/s and ocean wave periods from 2-18 seconds. Results are compared to a relaxation-time model and possible wave-wave modulation mechanisms are presented.

AIRCRAFT RADAR DOPPLER SPECTROMETER AND DUAL
FREQUENCY BACKSCATTER WAVE SPECTROMETER FOR THE
MEASUREMENT OF OCEAN SURFACE SPECTRUM

D. E. Weissman, Hofstra University, Hempstead, NY 11550
and J. W. Johnson and W. L. Jones, N.A.S.A. Langley
Research Center, Hampton, VA 23665

An experimental program is in progress using an aircraft platform. Backscattered microwave signals are analyzed to measure the dominant ocean surface wavelength and directional spectrum. The basis for this approach is the modulation of the local scattering coefficient along the large gravity waves. The principal being exploited here is that it is not necessary to have a very high spatial resolution (less than the longest wavelengths) when the surface features have periodic or quasi-periodic oscillations. The information to be extracted by a remote sensing system for ocean waves pertains to the spectral functions and their parameters.

Three techniques are being studied, all involve a scatterometer type instrument: large illumination area, encompassing many of the largest waves with narrow bandwidth signals. The signal processing involves statistical techniques to determine correlation and spectrum functions, whose parameters and features are related to the spatial wavelengths of the surface waves. The horizontal velocity of the aircraft platform is also an important parameter in these signal products. The Wave Modulation Doppler Spectrometer concept is based on the Doppler information backscattered to a "point" moving radar. In this method the difference in the Doppler frequency between any two scattering "patches" stays approximately constant as the moving radar sweeps by waves which have periodic variations in the local scattering coefficient. Analysis has shown that an envelope detector will cause these separated Doppler frequencies to mix together to produce pronounced features in its power spectral density and autocorrelation functions. The Dual Frequency Wave Spectrometer technique utilizes the matching of the "beat" electromagnetic wavelength (at the difference frequency) to a surface wavelength to sense the relative strength of this wavelength in the total surface spectrum.

The results that have been obtained with laboratory and flight experiments will be presented and discussed.

SESSION F-3
TUESDAY AM 8:30-12:00
KANE HALL 110

PROPAGATION WITHIN THE EARTH

Chairman: R. G. Olsen
Washington State University
Pullman, WA

REMOTE SENSING OF DIELECTRIC MEDIUM

Shimon Coen, Engineering Geoscience, University of California, Berkeley

Kenneth Mei, Electrical Engineering and Computer Sciences,
University of California, Berkeley

Abstract

This paper presents an active remote sensing technique for the estimation of the dielectric and conductivity profile of an inaccessible stratified half-space. The data is the reflected power from the inaccessible region, due to normally incident plane waves at various discrete frequencies. The problem is posed as a non-linear Fredholm equation where the dielectric and conductivity profile of the inaccessible half-space is sought. The equation is solved approximately by developing a Quasi-Newton method in functional space. The Backus and Gilbert resolving power theory is used to estimate the resolution and certainty of the results. Results are given for the reconstruction of various dielectric and conductivity profiles from an artificial data, together with resolving kernels and local average estimates.

Research sponsored by the National Aeronautics and Space Administration Grants NCA2-OR050-704 and NSG-5093 and the National Science Foundation Grant ENG-76-22296.

ELECTROMAGNETIC SCATTERING FROM AN
EARTH WITH A BURIED CYLINDRICAL INHOMOGENEITY

Samir F. Mahmoud
E.E. Dept., Cairo Univ., Giza, Egypt.
and

Sami M. Ali
E.E. Dept., Military Tech. College, Cairo, Egypt

The electromagnetic wave scattering from a long cylinder of general electric and magnetic properties and which is buried in a lossy half-space, is considered. The fields of the primary source are assumed to have their most general form as a spectrum of travelling waves along the direction of the cylinder's axis.

It is shown that, under the condition that the product of the radius of the cylinder and the transverse wave number in the surrounding medium is considerably smaller than unity, the scattered fields can be obtained from a set of equivalent sources. The latter contain electric and magnetic line sources plus electric and magnetic two-dimensional dipoles. The amplitudes of these sources are determined from the boundary conditions, and hence they fully account for the multiple scattering occurring between the cylinder and the plane interface.

For the special case of a highly conducting non-permeable cylinder, it is shown that the only significant equivalent source is the electric line source. However, when the highly conducting cylinder is coated with a dielectric tube the magnetic line source, and possibly the electric and magnetic dipoles, will also have a considerable contribution.

Numerical examples on the influence of the buried cylinder on the wave tilt and earth's surface impedance are presented for two cases of primary excitation,

- a) a plane wave incident from the upper half-space, and
- b) an electric line source.

The present problem is believed to have important applications in the remote sensing of buried cables, pipes, tunnels ... etc. using electrical methods.

INDUCTION SOUNDING RESPONSE OF FINITE BURIED CONDUCTING MODELS

E. A. Quincy and M. M. Rahman
Department of Electrical Engineering
University of Wyoming, Laramie, WY 82071
J. H. Richmond
Department of Electrical Engineering
The Ohio State University, Columbus, OH 43212

Experimentation with technique of underground coal gasification has presented the challenge for remote delineation of underground burn regions utilizing induction sounding techniques. Previous research (E. A. Quincy, et al., Abstracts of National Radio Science Meeting, 196, Nov. 1978, Boulder, CO) employed statistical procedure for model fitting of induction sounding data taken over underground coal burns at Hanna, WY. These results discussed responses of specific finite buried conducting models at 1kHz. These metallic models with approximate dimensions of 60 ft. x 70 ft. x 30 ft., were buried in a conducting medium of 0.001 mhos/meter up to depths of 275 ft.

Finite induction models do not usually have responses that are obtainable as closed form expressions. Consequently, numerical results are presented here parametrically as families of response with dimensions normalized to wavelength of the sounding frequency. Responses are shown for perfectly conducting models buried in a medium of finite conductivity. The geometries considered are rectangular boxes, elliptical cylinders and spheres. This parametric presentation lends itself to a wide range of applications.

The loop-loop induction sounding system is modeled as vertical magnetic dipoles over a conducting body. The secondary (scattered) magnetic field intensity normalized to the primary (direct) magnetic field intensity, is computed as the coplanar loops are moved in line with fixed spacing, across the conducting body. For computational purposes the continuous metal body is replaced by a wire grid model (J. H. Richmond, IEEE Trans. on Antennas and Propagation, 14, 782-786, 1966) of straight-line segments. A system of linear equations is generated by enforcing the boundary conditions at the center of each wire segment of the grid. Currents on the segments are obtained from these equations via solution on a digital computer. The secondary magnetic field is readily calculated once each of the grid currents is known.

Families of responses in terms of the normalized magnetic field are shown for rectangular boxes, elliptical cylinders and spheres. The effect of size, depth, loop spacing, frequency and the conductivity of the medium are shown. The trade-off between computation time and accuracy is obtained by varying the number of wire grid segments.

IN SITU MICROWAVE MEASUREMENTS OF LOSSY DIELECTRICS

R.J. King, C.D. Kim and J.B. Beyer
Department of Electrical and Computer Engineering
University of Wisconsin-Madison 53706

A simple homodyne system for in situ measurement of the complex dielectric constant of large lossy bodies is described. Two techniques appear promising. Both involve measurement of the complex propagation constant, $\gamma = \alpha + j\beta$, which can be used to find the dielectric constant and loss tangent, depending upon the geometry.

The first technique involves propagating a wave (4.6GHz) normally into the medium which is assumed to be several skin depths thick. By drilling a small hole and inserting a tiny modulated scattering loop, the attenuation and wavelength can be measured. Design criteria for the loop are minimum size, maximum scattering cross-section and relatively low Q (i.e. broadband). Several designs are discussed and the results for soil, sand and cement will be given.

The second method still under development is nondestructive and requires no hole. It uses a transmission line mode guided along the medium interface using a single conductor, e.g. a bare ribbon laid directly on the interface to enhance coupling with the lossy medium. Again, a modulated scattering probe can be moved along the guiding conductor to measure attenuation and wavelength.

Both techniques have application in in situ measurement of various solids such as soil, rock, cement, minerals and of liquids.

Homodyne systems are well known for their simplicity, good sensitivity and accuracy; but more importantly, they are phase sensitive. Use of a modulated scatterer readily permits measuring the phase of the propagating wave as well as attenuation, without requiring a separate RF receiving antenna and its associated cables.

ELECTROMAGNETIC RESPONSE OF ORE DEPOSITS

M. CAUTERMAN, P. DEGAUQUE and R. GABILLARD, Lille University, Electronics Dept., B.P. 36, 59650 VILLENEUVE D'ASCQ, France

Ore deposits can often be considered as a horizontal sheet, or at least, the length parallel to the air-ground interface is much greater than the other sides. To simulate the electromagnetic response of such an anomaly, the first step could be the use of a two-dimensional model. The limit of validity of this approach has been outlined by Wait and Hill who have calculated analytically the response of a conducting cylinder situated in an infinite homogeneous medium (Radio Sci., 12, 1169-1176, 1973).

In this paper, we first consider a "theoretical" example to point out the behaviour of the anomaly response. For that, we assume that an anomaly is situated in a dissipative half space ($\sigma=10^{-3}$ mho/m), the excitation being a line source placed on the earth surface ($f=10$ kHz). The cross section of the anomaly is 4 m^2 , its roof being at a depth of 4 m. Furthermore, to compare the results to those obtained by Wait and Hill for a perfectly conducting cylinder, we suppose a very conducting anomaly ($\sigma=1$ mho/m). This configuration is suitable since it is possible to increase the length of the heterogeneity so that it could be much greater than its depth. Using numerical models that we have previously described (Radio Sci., 2, 371-378, 1978), we give the variation of the amplitude and phase of the induced current in the anomaly as a function of its length ($10 \text{ m} < l < 100 \text{ m}$). Since the resistivity ratio is important, we remark in this example that the induced current nearly vanish at the ends of the anomaly. Then we show the variation of the secondary field and we compare its value to the one obtained with a two dimensional model.

In the second part of this paper, a sulfure deposit is simulated. In order to know what is the most efficient configuration, we consider successively various types of transmitter : such as magnetic and electric dipoles, both transmitter and receiver being situated on the ground surface. At last experimental results will be given.

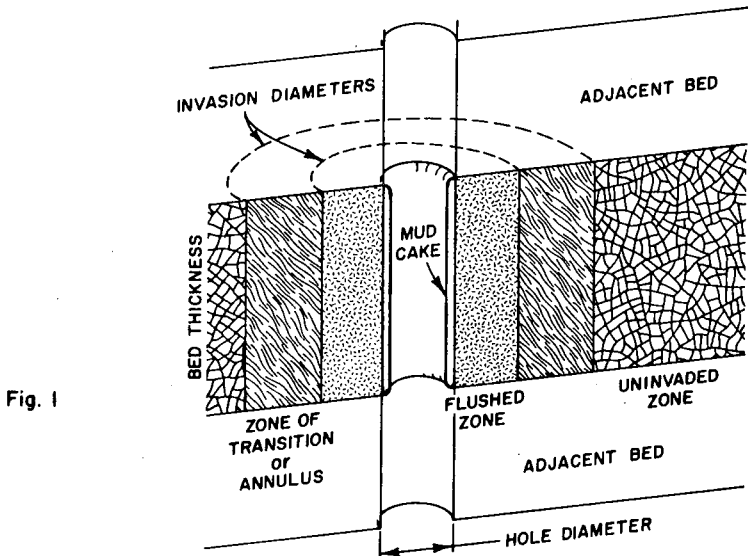
AN IMPROVEMENT ON A MICROWAVE TECHNIQUE
TO LOCATE ECONOMICALLY PRODUCIBLE
HYDROCARBONS IN A DRILL HOLE

by

G. S. Huchital
Schlumberger-Doll Research Center,
Ridgefield, Connecticut

A recent addition to the devices used to locate hydrocarbons in a borehole is an electromagnetic measurement system operating in the microwave region.¹⁻³ This device measures the propagation velocity and attenuation of a 1.1 GHz wave. From these measurements, the dielectric constant and conductivity of the rock formation can be determined. A recent paper⁴ has discussed the interpretation of these results in terms of hydrocarbon content in the sedimentary formations surrounding the drill hole. The question to which this paper will address itself is a technique intended to reduce the effects of borehole conditions on the electromagnetic measurements.

Figure 1 is representative of the borehole conditions in which the measurements must be performed. The device is lowered into the borehole and measurements are made as the tool is raised to the surface.



The fluid in the borehole is usually conductive. Therefore in order to perform measurements on the surrounding rocks, the device is forced against one side of the hole. The wall may be covered by a firm cake of drilling mud, up to one inch thick. Due to the conductive nature of the environment, the investigation depth of the device is only on the order of inches; therefore the mud cake can severely distort the measurements.

The measurements are made by launching a 1.1 GHz wave from a transmitter and detecting the propagated wave at receivers spaced 8 and 12 centimeters away. All three antennas are cavity-backed slots. The received signals are compared as to their phase and level, thus yielding measurements of the wave's attenuation and velocity of propagation. These measurements can be interpreted in terms of the dielectric constant and the conductivity of the formation rock.

The cavity-backed slot antennas have been modeled as magnetic line sources and placed in a layered medium shown in Figure 2. The effect of a mud cake on the predicted dielectric constant is shown by the dashed curves in Figure 3.

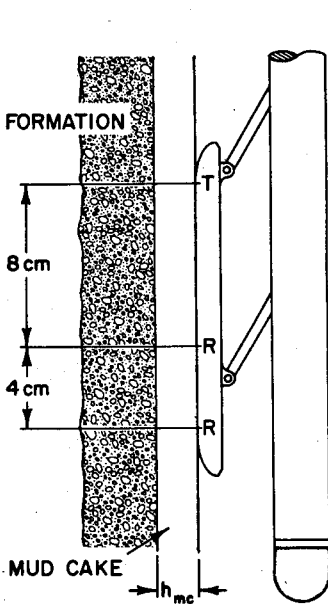


Fig. 2

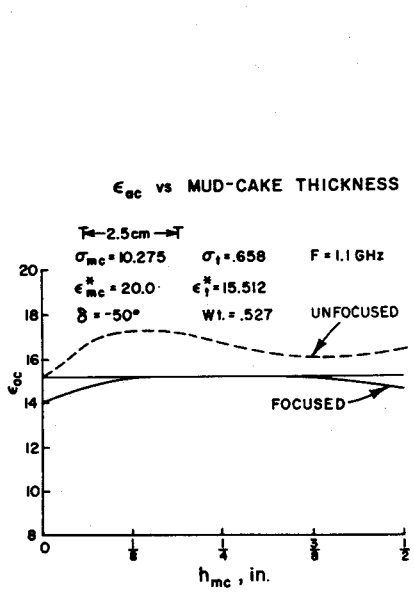


Fig. 3

It should be possible to reduce this effect through the use of an additional transmitter. This transmitter is placed between the main transmitter and the closest receiver. Its purpose is to form a small broadside array with the main transmitter and thus direct a greater portion of the signal into the formation and less into the mud cake. The medium into which this array is placed is lossy, and the spacings involved are less than or on the order of a wave length. Theoretical computations show that a broadside array can be formed by proper weighting, placement, and phasing of the secondary transmitter with respect to the main transmitter. A typical array pattern is shown in Figure 4. For display purposes, the array shown is a three-transmitter array. The transmitter below the main transmitter is not necessary for the improved operation.

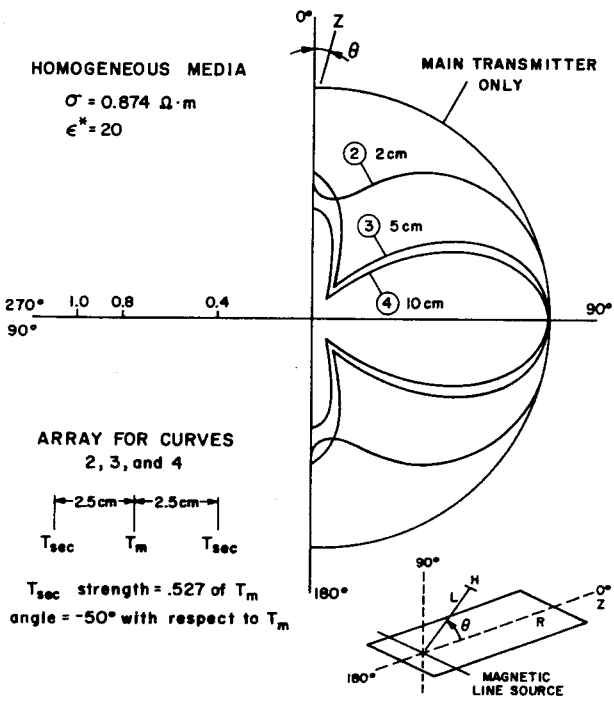


Fig. 4

The proper parameters for a broadside array are medium-dependent. For the layered-media environment of the drill hole, optimum reduction of the mud cake effect is achieved by choosing the array parameters for the broadside array in a homogeneous medium whose properties are similar to the mud cake. The solid curve in Figure 3 displays the improvement in the response of the device when the two-transmitter array is used rather than the unfocused one-transmitter array now in use.

These results show that it is possible to reduce the "mud cake effect" on a high-frequency (1.1 GHz) electromagnetic measurement system which has been placed in a drill hole to locate economically producible hydrocarbons. The approach to be used is to construct a small (two-transmitter) broadside array in the lossy, layered medium of the borehole.

References

- [1.] T. J. Calvert, R. N. Rau, and L. E. Wells, "Electromagnetic propagation... a new dimension in logging", presented to the Society of Petroleum Engineers of the AIME, April 1977.
- [2.] T. J. Calvert, "Microwave logging apparatus having dual processing channels", U.S. Patent No. 3,849,721, Nov. 19, 1974.
- [3.] R. N. Rau, "Method and apparatus utilizing microwave electromagnetic energy for investigating earth formations", U.S. Patent No. 3,944,910, Mar. 16, 1976.
- [4.] G. S. Huchital, "Oil exploration and the use of dielectric mixture theories", presented at the AP-S/URSI Conference, College Park, Maryland, 1978.

COMPARISON OF LOOP AND DIPOLE ANTENNAS
IN LEAKY FEEDER COMMUNICATION SYSTEMS

David A. Hill and James R. Wait
ITS/NTIA
U.S. Department of Commerce
Boulder, CO. 80303

The leaky-feeder technique for mine communications has been investigated recently in several theoretical and experimental studies (e.g. Special Issue of Radio Science, 11, April 1976). The leaky transmission line is usually a coaxial cable, and the energy is coupled into or out of the channel by antennas in the vicinity of the transmission line (Special Issue of Radio Electronic Engr., 45(5), 1975). Both electric dipole and magnetic dipole (small Toop) antennas have been used.

Here we analyze an idealized leaky-feeder channel which consists of a uniform leaky coaxial cable located at an arbitrary position within a uniform circular tunnel. General expressions for the mutual impedance between a pair of electric or magnetic dipoles of arbitrary orientation and location are derived by matching the tangential fields at the tunnel wall and applying a series impedance condition at the coaxial cable. When the dipoles are widely spaced, the mode of lowest attenuation provides the dominant contribution to the mutual impedance. In most cases, the "bifilar" mode, which has strong fields inside the cable and weak leakage fields outside, has the lowest attenuation.

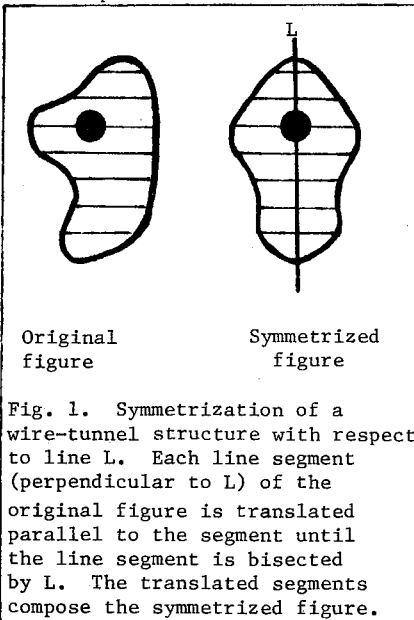
By letting the two dipoles coincide, the mutual impedance formulation also yields the input impedance. The input resistance is of particular importance since the near field losses due to the lossy tunnel walls can be quite large.

Once the input impedance and the mutual impedance are known, the total transmission loss can be calculated. This is the quantity of most interest to the systems engineer. Calculations have been performed for frequencies from 1 MHz to 50 MHz for both electric and magnetic dipole antennas. A broad minimum in transmission loss is generally observed somewhere between 2 MHz and 10 MHz. In this frequency range, the transmission loss is somewhat lower for magnetic dipoles because they have a smaller near-field loss than electric dipoles.

BOUNDING THE PROPAGATION CHARACTERISTICS OF TEM MODES
IN TUNNELS OF ARBITRARY SHAPE

D. L. Jaggard and M. F. Iskander
Department of Electrical Engineering
University of Utah
Salt Lake City, Utah 84112

Due to the growing interest in the propagation of waves along wires in tunnels or mines, recent attention has been focused on the electrical characteristics of wire-tunnel configurations with arbitrary cross section [D. B. Seidel and J. R. Wait, *J. Appl. Phys.* 49 (November 1978); E. F. Kuester and D. B. Seidel, National Radio Science Meeting, Boulder, Colorado (November 6-9, 1978)]. It has been shown that in the low-frequency regime, the governing equation for the TEM propagation constant depends on the capacitance of the wire-tunnel structure. Therefore, the propagation characteristics can in principle be determined numerically by calculating the capacitance. Alternatively one can sandwich the exact solution between bounds. For this task we use the method of symmetrization [G. Pólya and G. Szegő, *Isoperimetric Inequalities in Mathematical Physics*, Princeton University Press (1951)] which has been used successfully in bounding the solutions of other problems in electromagnetics [see, e.g., D. L. Jaggard and C. H. Papas, *Appl. Phys.* 15, 21 (1978)]. The sketch in Fig. 1 demonstrates the symmetrization of a wire-tunnel configuration with respect to the line L.



In this report the propagation characteristics of the wire-tunnel structure are bounded. These bounds depend on simple geometric quantities such as area and perimeter and are valid in the long wavelength approximation. In addition, the above considerations place in evidence the change in the relevant characteristics as the cross-sectional area is topologically transformed. Furthermore, these bounds point the way to optimize wire-tunnel configurations. Since many of the bounds are stationary about the values for a symmetrically placed wire in a circular tunnel, this configuration may be used as a first approximation to other configurations involving a wire in a tunnel.

SURFACE TRANSFER IMPEDANCE OF A LOOSELY BRAIDED COAXIAL CABLE

R. S. Tomar and Alakananda Paul
Electrical Engineering Department
Indian Institute of Technology
Kanpur-208016, India

ABSTRACT

Loosely braided coaxial cables are extensively used for communication in mines and tunnels. The most important parameter of a leaky coaxial cable is its surface transfer impedance, which determines the behavior of the cable in a complicated environment. The surface transfer impedance of a leaky coaxial cable is defined as the ratio of the axial electric field to the discontinuity in the azimuthal magnetic field at the sheath. The fields have been calculated on the basis of a rigorous electromagnetic analysis given by Wait (J. R. Wait, IEEE Trans., MTT-24 (9), 547-553, Sept. 1976). The numerical computation of fields involves doubly infinite series. However, expressions can be simplified considerably for radiating cable at UHF. Wait's analysis has been extended to derive and calculate the surface transfer impedance of some standard loosely braided coaxial cables and results have been compared with those obtained by other available approximate methods. The results show some definite trends of variation with different cable parameters which can be clearly explained in terms of basic electromagnetic theory. In comparison, some other published results of surface transfer impedance calculated by approximate methods do not seem to follow any particular pattern (P. P. Delogne and M. Safak, The Radio and Electronic Engineer, 45 (5), pp. 233-240, May 1975).

RECONSTRUCTION ALGORITHMS FOR GEOPHYSICAL APPLICATIONS
IN NOISY ENVIRONMENTS

Roger D. Radcliff and Constantine A. Balanis
Department of Electrical Engineering
West Virginia University
Morgantown, WV 26506

A system for remote determination of underground structures or voids would prove to be of great value in many areas of geophysical exploration. It is shown that mapping such an environment by transmission of electromagnetic radiation between boreholes involves the solution of a system of equations made inconsistent by the necessary assumption of straight-line propagation through the area of interest. When straight-line algorithms successfully used in other applications prove to be unacceptable due to errors in the measured data. After investigating the relative performance of previous reconstruction methods with large amounts of noise in the data, it was found that a modified version of the conventional Algebraic Reconstruction Technique (ART) displayed superior reconstruction quality. An Underground Coal Gasification (UCG) process was taken as an example to illustrate the performance of the modified ART algorithm.

SESSION F-4
TUESDAY PM 1:30-5:00
KANE HALL 110

SCATTERING FROM ROUGH SURFACES

Chairman: R. H. Lang
George Washington University
Washington, D.C.

BACKSCATTERING FROM A VEGETATED HALF SPACE

Roger H. Lang
 George Washington University
 Washington, D.C. 20052

A vegetated terrain is modelled by a random collection of lossy dielectric scatterers. The scatterers are arbitrarily shaped dielectric bodies whose scattering amplitudes are assumed to be known. The bodies have random placement as well as random orientation so that averages over position and alignment can be made. The backscattering coefficients are computed for the scalar and vectors problems by employing the distorted Born approximation.

The problem is solved in two stages. First, the mean field due to an obliquely incident plane wave is found approximately by employing the method of smoothing in the low density limit. The technique follows closely the discrete scatter treatments of Twerky and Keller. Initially equivalent propagation constants are found for the case of aligned scatterers and then averages over alignment are made.

The backscattered field can now be calculated by employing the Born or single scattering approximation in the equivalent medium. This is justified when the absorption cross section of an individual particle is much larger than its scattering cross section. Simple formula for the backscattering coefficients, σ_{hh}° , σ_{hv}° , σ_{vh}° and σ_{vv}° are obtained for aligned bodies and then averaged over alignment.

In contrast to existing results in terrain backscatter, the cross polarized backscattering coefficients, σ_{hv}° and σ_{vh}° do not disappear in the single scattering approximation. This is because of the depolarizing effect of the individual scatterers. The scattering coefficients have been calculated for spheres and discs that are small compared to a wavelength. As expected the depolarization terms disappear in the case of spherical scatterers.

MULTIPLE SCATTERING EFFECTS ON BACKSCATTERING
OF A PULSE FROM TERRAIN

Akira Ishimaru
Department of Electrical Engineering
University of Washington
Seattle, Washington 98195

The backscattering characteristics of terrain are dependent upon the surface roughness, the nature of the volume scattering and the roughness of the bottom ground surface. This paper is primarily concerned with the volume scattering characteristics of a pulse incident upon the terrain. Among various parameters which can be used to characterize the volume scatterers, there are three essential quantities: the extinction coefficient, the albedo and the mean cosine of the scattering pattern (phase function). The Henyey-Greenstein phase function depends only on these three numbers and it approximates many actual phase functions of scatterers with size distributions. This paper first outlines the general characteristics of the transmitted and reflected fluxes from a medium characterized by the Henyey-Greenstein formula. Even though the radiative transfer equation can be solved numerically or by the Monte Carlo technique, a useful and convenient technique is the diffusion approximation. We have obtained diffusion solutions which agree well with the Monte Carlo solutions. The pulse scattering from the volume scatterers can be analyzed by using the two-frequency mutual coherence function. The approximate solution is then obtained by solving the diffusion equation, and the backscattered pulse is shown to depend greatly on the diffusion time $(C_{tr}c)^{-1}$, where C_{tr} is the transport coefficient and c is the velocity of light. The transport coefficient C_{tr} is given by $C_{tr} = b(1 - \bar{\mu}) + a$, where b is the scattering cross-section, $\bar{\mu}$ is the mean cosine of the phase function and a is the absorption cross-section. However, further study is needed to take into account the polarization effect and the anisotropic phase functions.

POLARIZED AND CROSS POLARIZED SCATTERING BY AN INHOMOGENEOUS LAYER
WITH A SLIGHTLY IRREGULAR INTERFACE

A.K. Fung and H.J. Eom
Remote Sensing Laboratory
University of Kansas
Lawrence, Ks. 66045

The scattering coefficients of a homogeneous layer containing Rayleigh scatterers and possessing a slightly irregular interface have been computed with the matrix doubling method reported by Howell and Jacobowitz. For the case considered substantial simplification can be achieved by recognizing that the first two modified Stokes parameters are even functions in the azimuth angle while the third Stokes parameter is odd. In addition, there is no coupling between the first three and the fourth Stokes parameters. Thus, a 3 x 3 instead of an 8 x 8 phase matrix is sufficient. The effect of the layer boundary was not considered by Howell and Jacobowitz. To include the rough boundary effect the technique used by Leader for a plane layer has been generalized. To account for the slightly rough interface effect on volume scattering both modified Fresnel reflection coefficients and the first-order rough surface scatter and transmission coefficients have also been computed. To illustrate the results of this theory, theoretical backscattering coefficient curves are computed and compared with some snow measurements. Computations have also been carried out using only the first two Stokes parameters. For the cases considered the difference between using 3 versus 2 Stokes parameters is within 1 dB.

EXPERIMENTAL DATA MATCHING FOR ACTIVE AND PASSIVE
MICROWAVE REMOTE SENSING

J. A. Kong, M. Zuniga, L. Tsang and R. Shin
Department of Electrical Engineering and
Computer Science and Research Laboratory
of Electronics
Massachusetts Institute of Technology
Cambridge, MA 02139

Theoretical results obtained from the models of random medium and discrete scatterer characterization of earth terrain are used to match experimental data collected from vegetation and snow-ice fields. In matching active remote sensing data with the random medium model, we find that for vegetation the horizontal correlation length ℓ_{ρ} is smaller than the vertical correlation length ℓ_{ρ} and for snow-ice field $\ell_{\rho} > \ell$ indicating the more laminar structure of the snow layer. It is interesting to note that the vertically polarized backscattering cross-section σ_{vv} is always stronger than the horizontally polarized backscattering cross-section σ_{hh} for a half-space random medium. In order to account for the effect of $\sigma_{hh} > \sigma_{vv}$ we must resort to a two-layer random medium where more horizontally polarized wave components may be available for backscattering by the random medium due to the fact that there are more horizontally polarized components being reflected by the bottom boundary. The same random medium model is also used to match passive remote sensing data obtained from different snow fields. We also compared snow fields that are characterized by models having $\ell_{\rho} = \ell$ with the corresponding discrete scatterer models and showed they yield essentially the same results. The spectral dependence of the brightness temperature due to diurnal change is explained by changing the dielectric properties of a top thin layer to account for possible melting effects in the afternoon hours compared to the morning hours. The basic approach in the data matching exercise is to come up with one model characterizing an area that matches all data sets obtained in the same area and plotted as functions of frequency, angle, and polarization.

THEORETICAL MODELS AND APPROACHES FOR ACTIVE
AND PASSIVE MICROWAVE REMOTE SENSING

J. A. Kong, L. Tsang, M. Zuniga, and R. Shin
Department of Electrical Engineering and
Computer Science and Research Laboratory
of Electronics
Massachusetts Institute of Technology
Cambridge, MA 02139

To account for volume scattering effects in the microwave remote sensing of earth terrain, we make use of two theoretical models: (1) a random medium with a variance δ , a horizontal correlation length ℓ_h , and a vertical correlation length ℓ_v , (2) a homogeneous dielectric containing discrete scatterers. The radiative transfer (RT) approach to the solution of layered random medium has been proven to be the simplest and most useful in the interpretation of experimental data collected from snow-ice field, vegetation canopy and culture targets. The radiative transfer theory for random media is a consequence of the solution to the Bethe-Salpeter equations under the ladder approximation which accounts for constructive interference among ray optical paths. To account for constructive interference among phase fronts in a wave picture, we need to develop a wave radiative transfer (WRT) theory that includes more terms than required by the ladder approximation. This is different from another modified radiative transfer (MRT) theory that accounts for coherent interactions between the top and bottom boundaries. The wave approach to random medium is carried out with an iterative procedure to calculate the backscattering cross-sections. The depolarization effect is shown to arise from a second order term in albedo under the Born approximation. In applying the wave approach to scattering by discrete scatterers, we attempt the use of a generalized molecular optics approach that regards a medium as consisting of discrete scattering objects. The total wave field is expressed as the sum of incident and scattered multipole fields from the object characterized by a scattering matrix.

A RADAR CLUTTER MODEL: AVERAGE RADAR BACKSCATTER
FROM LAND, SEA, SNOW, AND SEA ICE

R.K. Moore
K. Soofi
S.M. Purduski
Remote Sensing Laboratory
The University of Kansas
Lawrence, Kansas 66045

Average radar backscatter curves have been developed for a wide range of targets over the frequency range from 1-18 GHz and an angular range from vertical form:

$$\sigma_{dB}^0 = A + B\theta + cf \quad f > 6 \text{ GHz (land), } f > 8 \text{ GHz (ice, snow)}$$

$$\sigma_{dB}^0 = A + B\theta + cf + Df\theta \quad f < 6 \text{ GHz, } 8 \text{ GHz}$$

The average levels for the land data were obtained from the measurements made with the 13.9 GHz SKYLAB radiometer-scatterometer; these have been extended in frequency and angle by use of data collected in the years 1974-1976 by Professor F.T. Ulaby and co-workers over agricultural terrain. The snow measurements used were also collected by Professor Ulaby during the winter of 1977. Sea ice measurements were made near Barrow, Alaska, in the spring of 1977 and 1978. The oceanographic model is more complicated because of the need to accommodate wind speed variations, and is based on a theoretical model developed by Professor A.K. Fung with the aid of experimental data from SKYLAB and NASA Langley Research Center aircraft measurements analyzed at the University of Kansas.

This is believed to be the first time that such an extensive model of frequency and angular behavior of radar backscatter has been made because measurements of the type used to develop the model have only recently become available.

This work was supported by Rome Air Development Center through the RADC Post-Doctoral Program under subcontract P.O. 5ST83417 from Syracuse University through prime contract F30602-75-C-0121.

NEW EFFECTS IN FORWARD SCATTERING
FROM WATER WAVES

C. I. Beard

Naval Research Laboratory, Washington, D.C. 20375

Further analysis of previous data of forward scattering from the ocean and from a water wave tank brings forth new relations in the coherent and incoherent fields: (1) A new spherical wave effect of incoherent field scattering by the transverse correlation length. (2) A trend between the surface probability density and the coherent field strength.

There does not appear to be an established theory for the forward scattered field for "roughnesses" above 0.1. However, Beckmann's [1967] spherical wave theory of the coherent reflected field, evaluated for wave tank conditions, actually closely follows the over-ocean data. Comparison of sphericity parameters for wave tank and ocean geometries indicates that they are comparable, and thus the spherical wave scattering effects should be as measurable in ocean forward scattering as in the wave tank. Incoherent field scattering in the horizontal plane by the transverse scale length (L_y) is an effect of spherical wave fronts, and is demonstrated quantitatively for the first time in the wave tank. Conversely, in principle, at least, this offers a method for obtaining L_y by forward scattering. As Beckmann's coherent field expression is a function of L_x , the scale length along the path, a way is offered, in principle, of finding L_x by forward scattering. Thus, the two-dimensional scale lengths of the surface are, in principle, obtainable from coherent and incoherent field scattering data.

Arranging the theories of different authors in a sequence shows that, the more the surface probability density departs from a Gaussian, the more the coherent field curve departs upward from the Gaussian surface theory (Ament's).

ON THE ROLE OF SHADOWING IN FORWARD SCATTER FROM THE
SEA AT EXTREME GRAZING ANGLES

L. B. Wetzel

Naval Research Laboratory, Washington, D.C. 20375

In microwave propagation at very small grazing angles over a surface of any appreciable roughness, most of the surface will be in shadow. This observation is often overlooked when plotting the measured specular reflection coefficient ρ against the roughness parameter $r = (\sigma/\lambda)\sin\psi$ (σ is the rms surface height, λ the incident wavelength and ψ the grazing angle.) As a consequence, ambiguous interpretations of experimental data can result. Shadowing has two competing effects on the coefficient ρ : (1) ρ goes to zero with the grazing angle (not to 1, as often assumed); (2) the value of ρ is raised by decreases in effective surface roughness as the deeper parts of the surface are occulted. These effects are illustrated by using data calculated for representative sea surfaces to plot two families of curves of ρ vs. r , one for a sequence of grazing angles from 0.1° to 4° , the other for a sequence of ratios (σ/λ) from 1 to 12. These curves demonstrate that the roughness parameter can not be used to characterize specular reflection at low grazing angles, since the behavior of ρ vs. r will depend upon how the variations in r were produced experimentally. Other implications of surface shadowing are noted, such as the role of diffraction, and how the loss of a reflecting surface affects the duct models generally used to explain extended propagation in the evaporative layer over the sea.

EFFECTS OF SCATTER DEPolarIZATION ON OPTICAL
AND MICROWAVE HOLOGRAPHIC IMAGE DEGRADATIONHossein Ghandeharian⁽¹⁾ and Wolfgang-M. Boerner^(2,3)

(1)Elect.Eng.Dept.,UBC,Vancouver,BC. V6T 1W5; (2)Inform.Eng.Dept.,
UICC,Chicago, IL 60680;(3)Elect.Eng.Dept.U.Man.,Winnipeg,Can.R3T 2N2

The effects on image quality due to polarization changes of the illuminating beam after scattering by an object are analyzed. These effects include a decrease in signal-to-noise ratio (decrease in fringe visibility) of the hologram and for an extended object, a loss of information of those segments of the object that have large curvature (edges, discontinuities, etc.). The autocorrelation function of the transmittance of a nonlinearly recorded hologram of a diffuse object is obtained. It is shown that the change of polarization of the illuminating beam by the object not only reduces the signal-to-noise ratio but it also fortifies the distortion of the images due to the nonlinearity of the recording medium. This new distorting effect, which can be identified as a multiplicative holographic factor, is dependent on the irradiance distribution of the object's cross-polarized component. Simple procedures of decreasing the above-mentioned degradation effects in the optical and microwave cases are suggested.

THE EFFECT OF SALT SOLUBILITY AND SALINITY
ON THE RESPONSE OF A MICROWAVE REMOTE SENSOR

Russell P. Jedlicka
Physical Science Laboratory
New Mexico State University
Las Cruces, New Mexico 88003

Soil permittivity is an important factor in such earth resource microwave remote sensing endeavors as soil moisture investigations and remote sensing of saline seeps. Complex permittivities of soils are known to be strongly dependent on soil moisture. It is this dependence which allows soil moisture to be remotely sensed. Similarly the dependence of the complex permittivity on salinity allows highly saline areas such as saline seeps to be located.

Results reported herein show a significant dependence on solubility as well as salinity. For a given salt, therefore a given solubility, the imaginary part of the complex permittivity is shown to increase with an increase in salinity. For a given salinity level the imaginary part of the complex permittivity is shown to increase when the salt solubility is increased. It is therefore seen that the amount of salt which goes into solution is the determining factor.

The effects of these phenomena on the microwave sensor response are considered. Measured brightness temperatures for a saline sand are reported as a function of salinity. The brightness temperature is seen to show a marked decrease with increasing salinity level for a given physical temperature.

MICROWAVE REMOTE SENSING OF SALINE SEEPS

Keith R. Carver
Physical Science Laboratory
New Mexico State University
Las Cruces, New Mexico 88003

In June, 1978 an experiment in microwave remote sensing of saline seeps was carried out in Harding County, South Dakota where the incidence of these very saline local discharge areas is high. Aircraft data was taken by the NASA/JSC C-130 aircraft and consisted of L-band and C-band radiometer and scatterometer data, along with red-band and thermal-IR band imagery from the multi-spectral scanner. In addition, Zeiss 9"x9" color-IR imagery was taken along with thermal-IR temperatures via a Barnes PRT-5 IR radiometer. The test area was 200 m in width by 2 km in length (along the flight line) and included both smooth and plowed bare fields, plowed fields with a 30" stand of winter wheat, and two major saline seep zones. Ground truth samples were taken from 1000 - 1400 hrs local time (centered on the noon flight time) and consisted of soil moisture measurements at 0-2 cm, 2-5 cm, and 0-5 cm. In addition, soil salinity measurements were made over the 0-5 cm depth and bulk density samples were taken. Approximately 2500 soil samples were processed for the above ground truth data.

The data were collected on a single day and after a period of several days heavy to intermittent rainfall. As a result, the average gravimetric soil moisture was greater than 20%. Soil salinities ranged from 0.2 o/oo to 20 o/oo depending on spatial location.

The saline seep areas along the flight line were found to be clearly evident on both the passive and active microwave data profiles. The optimum active response was obtained from the L-band scatterometer at an incidence angle of 20° . For this frequency and angle, the largest seep showed in increase of approximately 20 dB in σ^0 over the background radar scattering coefficient of -12 dB. The optimum angle at C-band was approximately 15° , although the seeps were not as pronounced at the higher frequency. The radiometric data showed a strong sensitivity to the seeped areas and a stronger response to surface roughness changes than did the radar data.

This initial experiment suggests that soil salinity can be reliably detected by microwave remote sensors at the lower frequencies and that data should be acquired when the soil is wet in order to differentiate salinity-caused responses from those caused by soil moisture.

**SESSION F-5
WEDNESDAY PM 2:00-5:30
KANE HALL 110**

EARTH-SPACE PROPAGATION

**Chairman: D. C. Cox
Bell Labs
Holmdel, NJ**

A SUMMARY OF RAIN ATTENUATION EXPERIMENTS
ON EARTH-SATELLITE PATHS IN GEORGIA
AND ILLINOIS*

S. H. Lin, H. J. Bergmann and M. V. Pursley

Rain attenuation experiments on earth-satellite paths terminating in Georgia and Illinois at 19 and 28 GHz have been carried out for a two-year period (July 1976-August 1978) using the COMSTAR Beacon signals. Passive radiometer experiments at these locations have been operational for four years (73-75, 77 & 78) at 13.6 GHz and two years (73-75) at 17.8 GHz. These data have been analyzed and a summary is presented for the cumulative attenuation distributions, the fade duration distribution, the diversity improvement factor, the frequency dependence, the seasonal and diurnal variations and the dynamic rain attenuation behavior. These long term data support a simple empirical model for the prediction of the long term rain attenuation distribution derived from the long term distribution of five-minute point rain rates.

* Invited paper for USNC/URSI special sessions on Propagation above 10 GHz.

COMSTAR 19-GHZ BEACON RECEPTION AT SPACED LOCATIONS
IN TAMPA, FLORIDA

D. D. Tang, GTE Laboratories, Waltham, MA 02154
D. Davidson, GTE Laboratories, Waltham, MA 02154
S. C. Bloch, University of South Florida, Tampa, FL 33620

A full rainy season's experience with three receiving terminals in the Tampa area (baselines 11, 16, and 20 km) reveals considerably different diversity results from month to month. These results will be discussed and compared with regional rainfall characteristics. Attenuation is largely coincident with local rain at each site because of the high elevation angles employed to receive COMSTAR beacons D-2 and D-3.

Invited paper for USNC/URSI special sessions on propagation above 10 GHz.

OBSERVATIONS OF ORIENTATION-DEPENDENT DEPOLARIZATION OF
19 GHz EARTH-SPACE SIGNALS BY ATMOSPHERIC HYDROMETEORS

H. W. Arnold, D. C. Cox, H. H. Hoffman and R. P. Leck
Bell Laboratories
Crawford Hill Laboratory
Holmdel, New Jersey 07733

Depolarization along earth-space paths is produced by the alignment of non-spherical atmospheric hydrometeors in wind, gravity or electric fields. This depolarization is minimized when the incident polarizations are aligned with the average symmetry axes of the hydrometeors. Observations of a 19 GHz COMSTAR beacon yield the angular statistics of these symmetry axes (in the plane perpendicular to the propagation path) as functions of depolarization and attenuation. The average orientation of the symmetry axes is shown to be nearly vertical and horizontal during heavy rainstorms, but may deviate significantly from this orientation during periods dominated by ice depolarization. The observed behavior of the resulting minimum depolarization with copolarized attenuation will be shown along with observed depolarization-attenuation relations for several other fixed incident polarizations.

When the incident polarizations are aligned for minimum depolarization, the observed copolarized differential phase and differential attenuation are maximized. The observed relations between copolarized attenuation, differential phase and differential attenuation provide additional information on the distribution of hydrometeors along earth-space propagation paths.

Invited paper for USNC/URSI Special Sessions on Earth-Space Propagation
Above 10 GHz

UPDATE OF THE RESULTS OF THE 28.56 GHz COMSTAR
EXPERIMENT AT WALLOPS ISLAND, VIRGINIA

Julius Goldhirsh
Applied Physics Laboratory
The Johns Hopkins University
Laurel, Maryland

The results to date of the COMSTAR experiment at Wallops Island, Virginia, are presented. There are several aims to this experiment and these are: (1) To test the ability for predicting rain attenuation at 28.56 GHz using radar and ground disdrometer measurements, (2) To correlate radar reflectivity levels along the earth-satellite path with those cross polarization phenomena which occur at low fade levels, and (3) To arrive at a multi-year data base of fade statistics at 28.56 GHz.

In this paper the results pertaining to (1) and (2) are described for the 1978-79 period. With regard to (1), the radar predicted fades are compared with directly measured levels on a case by case basis as well as statistically. Preliminary results for the 1978-79 period show excellent agreement between radar predicted and directly measured fades.

With regard to (2), a Faraday rotation switch is situated at the front end of the COMSTAR receiving system enabling both the co- and cross-polarization at 28.56 GHz to be continuously sampled at a rate of once per second. During selected periods of low fade levels, simultaneous radar reflectivity measurements are made along the path using the high resolution S-band radar (3 GHz, 0.4° beamwidth, 1 μ sec pulsewidth). The reflectivities due to both rain and high altitude ice crystals are subsequently correlated with the measured cross polarization levels.

NOTE: Invited paper for USNC/URSI special session on propagation above 10 GHz.

MEASUREMENT OF RAIN ATTENUATION AND
DEPOLARIZATION OF THE CTS SATELLITE
BEACON SIGNAL AT HOLMDEL, NEW JERSEY

A. J. Rustako, Jr.
Bell Telephone Laboratories
Holmdel, New Jersey 07733

ABSTRACT

An experimental measurement of attenuation and depolarization, primarily due to rain, of the 12 GHz Communications Technology Satellite (CTS) beacon is being made at Crawford Hill, Holmdel, New Jersey. The measurement system uses a 6-meter-aperture, fully steerable, horn reflector antenna fitted with a dual-sense, circular polarized feed. The amplitudes of the copolarized and cross-polarized signal components are measured with a two-branch, stable, narrowband, frequency tracking receiver.

Measurement results of copolarized signal attenuation and cross-polarization discrimination for a 3 year period beginning April 1976 are described.

NOTE: This is an invited paper for the USNC/URSI special sessions on propagation above 10 GHz.

DEPOLARIZATION MEASUREMENTS AT VARIOUS LOCATIONS
ACROSS CANADA USING THE 11.7 GHz CTS BEACON

J.J. Schlesak, J.I. Strickland, and W.L. Nowland, Department of Communications, Communications Research Centre, Ottawa, Canada, K2H 8S2

To evaluate the characteristics of earth-space propagation for the next generation of Canadian domestic communications satellites, an experiment to measure attenuation and depolarization at 11.7 GHz was performed using the circularly polarized beacon transmission from the Communications Technology Satellite (CTS).

A special receiver was designed which measures the amplitude of the horizontal and vertical linear components of the received signal and the phase angle between them. This equipment was installed at four locations across Canada - St. John's, Newfoundland; Halifax, Nova Scotia; Toronto, Ontario; and Vancouver, British Columbia. A summary of the results derived from the data collected at these locations for the period May to December 1978 is presented in this paper.

The measurements at all locations show that, when rain is the dominant depolarization mechanism, the circular cross polarization discrimination (XPD) of the received signal decreases logarithmically with increasing co-polar attenuation (CPA). This result is compared with theoretical predictions based on calculations using the Pruppacher and Pitter form raindrop and the Laws and Parsons drop-size distribution. In addition to depolarization observations associated with precipitation, fluctuations in XPD down to 15 dB were sometimes observed in the absence of significant co-polar attenuation both as isolated events and just before and after some rainstorms. Depolarization of this type is attributed to differential phase shifts caused by ice crystals present in clouds.

Invited paper for USNC/URSI special session on propagation above 10 GHz.

SOME MEASUREMENTS OF CTS 11.7 GHz CROSS
POLARIZATION COMPARING A FIXED AND AN
ADJUSTABLE POLARIZATION RECEIVER

W. J. Vogel
Electrical Engineering Research Laboratory
The University of Texas at Austin

Data collected in Austin, Texas indicate that equal probability levels of attenuation A (dB) and cross polarization isolation CPI (dB) of the CTS beacon are related by $CPI = 41 - 20.6 \log A$ for A above about 5 dB. At a 10 dB fade margin, isolation is expected to be less than 21 dB, thus making a frequency reuse system isolation limited. A receiver with fully adjustable polarization has been built. By changing its polarization it can reject unwanted crosstalk caused by a depolarizing atmosphere or by inaccurate pointing of the receiving antenna. The data to be presented will allow some preliminary conclusions about whether a receiver with adaptive polarization can change the constants in the above equation sufficiently to make system performance attenuation limited and therefore more predictable.

CTS BEACON RAIN ATTENUATION MEASUREMENTS

D. Davidson, GTE Laboratories, Waltham, MA
O. G. Nackoney, GTE Laboratories, Waltham, MA

Over two years of propagation measurements using the 11.7 GHz CTS beacon have been collected at GTE Laboratories at Waltham, Massachusetts. Beacon measurements are made over a 20-dB dynamic range with a 3-meter linearly polarized antenna at a 24° elevation angle. Rain-rate data is also collected at the site using a tipping-bucket rain gauge.

The paper will present attenuation and rain-rate statistics together with the seasonal and annual variations observed. Empirical relationships between attenuation and local rainfall statistics useful for prediction purposes will be discussed. Also to be discussed are general observations concerning the character of fade events, including observed signal enhancement.

SUMMARY OF 1978 ATTENUATION AND DEPOLARIZATION
MEASUREMENTS MADE WITH THE CTS (11.7 GHz) AND
COMSTAR (19.04 AND 28.56 GHz) BEACONS

C. W. Bostian, W. L. Stutzman, E. A. Manus,
P. H. Wiley, R. E. Marshall, and P. Santago
Electrical Engineering Department
Virginia Polytechnic Institute and State University
Blacksburg, Virginia

This paper summarizes attenuation, depolarization, and rain rate data collected during the 1978 calendar year on the CTS and COMSTAR downlinks. It discusses the statistical relationships between attenuation and rain rate and between attenuations measured at different frequencies. Regression equations relating cross polarization isolation to the logarithm of attenuation are presented.

Note: This is an invited paper for the USNC/URSI Special Sessions on Propagation Above 10 GHz.

CUMULATIVE STATISTICS OF 11.7 AND 28.56 GHZ
RAIN ATTENUATION FROM CTS AND COMSTAR
SATELLITE BEACON MEASUREMENTS

Dr. Louis J. Ippolito
NASA Goddard Space Flight Center
Greenbelt, Maryland 20771

Abstract

Continuous observations of the 11.7 GHz CTS beacon and the 28.56 GHz COMSTAR beacon have been in progress at the Goddard Space Flight Center, Greenbelt, Maryland, since June of 1976 and October of 1978, respectively. Cumulative statistics of ground (point) rain rate and path attenuation have been developed for monthly, seasonal and annual periods. Coincident attenuation and rain rate measurements are combined to derive the effective path length for the monthly, seasonal and annual periods. Time of day and fade duration statistics are developed for the rain attenuation data, and attenuation ratio statistics between the 11.7 and 28.56 GHz links are compared.

Long term rain rate and 11.7 GHz attenuation distributions are compared with analytical distributions and with published empirical prediction models. The prediction models evaluated include those of CCIR (Rep. 564-1), Rice-Holmberg, Dutton-Dougherty, CCIR SPM (Doc. F5/003), and the GSFC effective path length model. The measured distributions are also compared with similar measurements from other locations in the U.S. and Canada. The paper concludes with a summary of recommended power margin requirements and link availability constraints for earth-space communications systems operating in climate regions similar to the Greenbelt, Maryland, area.

NOTE: Invited paper for USNC/URSI special sessions on propagation above 10 GHz.

SESSION F-6
THURSDAY AM 8:30-12:00
KANE HALL 110

PART I: PROPAGATION ABOVE THE SURFACE: MODES AND RAYS

Chairman: R. J. King
University of Wisconsin
Madison, WI

ZENNECK-LIKE WAVE FOR THE SPHERICAL EARTH

Koichi Mano
Electromagnetic Sciences Division
Deputy for Electronic Technology
Rome Air Development Center
Hanscom AFB, Massachusetts 01731

We model the problem by assuming that the earth is a solid sphere of finite radius with homogeneous electromagnetic property which is immersed in an infinitely vast and homogeneous medium. We then examine the propagation of waves where there exists symmetry around the polar axis of the spherical coordinate system in such a way that the magnetic field is perpendicular to the meridian plane while the electric field lies in it. We seek the Zenneck-type solution for this problem which means that the differential equation for the magnetic field that follows from Maxwell equations has to be separated for each variable. The boundary conditions for such a solution, however, are very difficult to satisfy, preventing us from drawing a conclusion regarding the existence of Zenneck wave for a sphere.

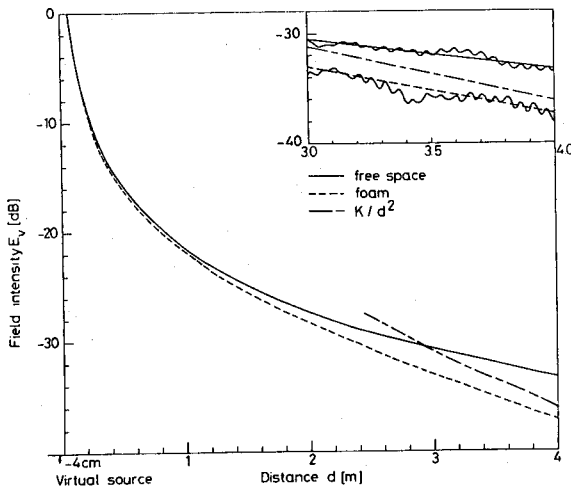
For this reason we consider instead the case of a sphere with extremely, but not quite infinitely, large radius. Guided by the known solution for Zenneck wave for a flat interface we can obtain Zenneck-like approximate solution for the present case in the form of the product of a direct analog of the flat-interface solution and a correction factor.

SURFACE WAVE PROPAGATION ON A
LOW PERMITTIVITY MEDIUM - AN EXPERIMENTAL STUDY

J. Appel-Hansen Electromagnetics Institute
Technical Univ. of Denmark 2800 Lyngby, Denmark
R. J. King Dept. of Electrical & Computer Engineering
Univ. of Wisconsin - Madison, WI. 53706

Significant experimental evidence has been obtained which supports the contention [R. J. King and J. R. Wait, *Symposia Mathematica*, XVIII, Academic Press, 133-161, 1976] that a Norton surface wave can exist on a medium having a dielectric constant near unity. Unlike a trapped surface wave which is slow and decreases exponentially with height, the present wave is actually an asymptotic ground wave. It propagates at the speed of light with an attenuation factor of d^{-1} in addition to the free-space spreading factor and merges into the free-space field with height. As such, it is indistinguishable from the free-space field except for grazing incidence where the direct and surface-reflected waves cancel; moreover, it is closely akin to the lateral wave (up-over and down mode) observed in propagation through or above dense vegetation.

The figure shows some experimental data for vertical polarization taken at 3 GHz for propagation over 4 meters of polystyrene foam situated in an anechoic chamber. The source and receiver antennas were open-ended wave guides laid directly on the foam surface. The inset shows how the raw data was averaged for $3 < d < 4$ meters. For comparison, the free-space field was measured to show its d^{-1} dependence, and a curve showing a d^{-2} dependence is also shown. Clearly, the field on the foam surface is asymptotically approaching the predicted d^{-2} behavior of a Norton surface wave. Similar results were obtained for perpendicular polarization. The full



text of this paper is available in *Electronics Letters*, 15(4), 1979.

RF RAY TRACING IN AN
ATMOSPHERIC DUCTING ENVIRONMENTFrank T. Wu
Wai-Mao P. Yu
Alexis ShlantaNaval Weapons Center
China Lake, California

It is well established that radio frequency (RF) wave propagation in the atmosphere can be greatly affected by atmospheric refractivity. In general, RF radiation tends to propagate in the direction towards a denser region of the atmosphere. As a result, ray bending phenomena such as reflection and refraction are commonly observed and are taken into consideration in modern communications and radar applications. Long range over the horizon radar detection due to the extreme case of atmosphere refraction, namely ducting effects, is limited in quantitative treatment. In this analysis, it is usually assumed that the atmosphere is a stratified medium that is horizontally homogeneous and the index of refraction of the atmosphere varies only as a function of height. As an augmentation of current treatment, a simplified ray tracing (geometrical optics) model in a ducting environment is presented that can use stratified atmospheric profiles obtained by measurement. Grazing angle, depression angle, and horizontal range related to RF wave propagation in an atmospheric duct are calculated in terms of refractivity profile, duct height, wave length, target height, and the thickness of the duct. It has been found in this work that the radar detection horizon can be effectively extended when larger grazing angles and depression angles, associated with the RF rays propagating inside a duct, are considered.

HYBRID RAY-MODE FORMULATION OF
PROPAGATION IN A TROPOSPHERIC DUCT

S. H. Cho, G. Migliora and L. B. Felsen
Polytechnic Institute of New York
Route 110, Farmingdale, N. Y. 11735

Electromagnetic wave propagation in an elevated tropospheric duct is analyzed by a new method involving an appropriate mixture of ray-optical fields and whispering gallery mode fields guided by the concave side of the duct boundary. This formulation quantifies in terms of ray fields the remainder term when a guided mode series is truncated or, alternatively, in terms of guided modes the omission of higher order reflected rays in a ray representation. To explore the new method on a simple example, the duct is modeled by a single cylindrical boundary separating an interior higher refractive index region from an exterior region with lower index. The electric line source is located at the boundary and the corresponding Green's function is first derived in terms of whispering gallery modes plus a continuous spectrum contribution, and then converted to the hybrid ray-mode form. It is shown that the number of modes and rays required in the hybrid formulation is far less than when the field is expressed solely either in terms of modes or in terms of rays. Furthermore, one can avoid the difficulties associated with higher order reflected rays having incidence angles near grazing since these rays are replaced by a few low-loss whispering gallery modes in the hybrid scheme. A numerical example for typical tropospheric conditions indicates that a few of the lowest-loss modes are adequate to describe the field when the source and observation points are on the boundary, rendering the ray contribution to the total field insignificant. However, ray-fields are expected to play a more important role when the observation point, source point, or both are located inside duct. Calculations for this case are in progress.

A NUMERICAL STUDY OF TROPOSPHERIC DUCTING AT HF

C. L. Goodhart, Naval Ocean Systems Center, San Diego, CA 92152

R. A. Pappert, EM Propagation Division, Code 532, Naval Ocean Systems Center, San Diego, CA 92152

Path loss calculations for frequencies between 4 and 32 MHz will be compared with Hansen's (P. Hansen, Radio Sci., 12, 397-404, 1977) recent measurements on a 235 km over-ocean southern California path. The calculations involve standard waveguide theory along with available radiosonde data and show convincingly that signal enhancement, relative to that expected on the basis of ground wave theory, observed on frequencies greater than 20 MHz was due to superrefractive environments.

Commission F

F6 I - 6

A new set of solutions for the modal equation for propagation in a trilinear tropospheric duct

R. H. Ott
 U. S. Department of Commerce
 NTIA/ITS
 Boulder, Colorado 80303

A new set of solutions of the modal equation near $\arg(t) = -\pi/3$, where t is the conventional modal parameter in addition to the Whispering Gallery modes and earth-waveguide modes are found. These are identified physically as intra-waveguide modes. The modal equation for a trilinear troposphere is given by

$$t^{3/2} - \frac{3}{2} D_0 x_2 t^{1/2} - \frac{3\pi}{2} (m-1) e^{i\frac{\pi}{2}(4k-1)} = 0; m = 1, 2, \dots$$

with x_2 proportional to the electrical thickness of the duct, $D_0 = (1 - a_1 S_0)^{1/3}$ and a_1 the height of the duct, s_0 the slope of the first segment in the trilinear model, and $k=0$ for the intra-waveguide roots and $k=1$ for the Whispering Gallery roots.

It is shown that the intra-waveguide roots have imaginary parts comparable with higher-order roots of the earth-waveguide modes and may be important when calculating fields with the source removed from the duct and coupling energy into the duct.

MEASUREMENT OF THE MICROWAVE PROPERTIES
OF SEA ICE AT 90 GHZ AND LOWER FREQUENCIES

B. E. Troy, J. P. Hollinger, R. M. Lerner, and M. M. Wisler
Advanced Space Sensing Applications Branch
Space Science Division
Naval Research Laboratory
Washington, D. C. 20375

Passive microwave measurements of sea ice were made in the Greenland Sea from an aircraft at an altitude of approximately 300 M in April 1977. The experiment package included a 90 GHz microwave imager, and fixed nadir-looking radiometers at 31, 19 and 14 GHz. The microwave brightness temperatures and emissivities at these frequencies are computed for various ice types observed over a latitude range of approximately 77-85 North. Identification of sea ice type for comparison with the microwave measurements is made from photography and from the records of experienced ice observers accompanying the flight. Distribution curves of number of pixels versus brightness temperature derived from the 90 GHz imagery clearly show peaks corresponding to different ice types. Percentage cover of first-year and multi-year ice determined from these curves agrees with that of the ice observers as a function of position along the flight path.

AIRCRAFT MICROWAVE RADAR AND RADIOMETRIC MEASUREMENTS
OF THE ELECTROMAGNETIC PROPERTIES OF LAKE ICE

C.T. Swift, R. F. Harrington, J. C. Fedors, and
W. L. Jones
NASA Langley Research Center
Hampton, Virginia 23665

An experimental program was initiated in March 1978, joint between NASA Langley and NASA Lewis to remotely sense the characteristics of lake and Arctic ice utilizing active and passive microwave remote sensing techniques. The Langley sensors consisted of a 13.9 GHz scatterometer with a mechanically scanned antenna and a nadir viewing radiometer which was operable within selective bands of the 4.5 - 7.2 GHz frequency range. Both instruments were mounted on the NASA C-130 aircraft. On March 3, the aircraft flew back and forth along a planned 40 mile stretch of Lake Erie from Cleveland to the vicinity of Detroit. Holes were drilled into the ice at five points along this track in order to measure thickness, which varied from 40 cm near Cleveland to 140 cm near Detroit. The radiometer trace exhibited a general increase in brightness temperature with increasing ice thickness, and a rather predominant increase in brightness occurring each time the instrument over-flew a refrozen lead. When the scatterometer was pointed at nadir, the received power decreased with increasing ice thickness. This increase was quite dramatic when the refrozen lead was in the radar field of view. On subsequent passes, the scatterometer was pointing away from nadir, and the refrozen lead was not detectable. This data is indicative that attenuation predominates over volume scattering. The analysis of the radiometric data also indicates that the absorption of the refrozen lead is in excess of 8 dB/m, which is substantially higher than the values given in the published literature. The radiometer was tuned in frequency to determine if changes in emissivity occurred as a result of standing waves within the ice slab. No gross changes in emissivity were observed, possibly because of suppression by roughness at the air on water interface. It is planned to repeat the mission in March 1979, with much more accompanying ground truth than was available in 1978.

EXPERIMENTAL EVALUATION OF THE MICROWAVE
RESPONSE TO SNOW

Fawwaz T. Ulaby and William H. Stiles
University of Kansas Center for Research, Inc.
Remote Sensing Laboratory
Lawrence, Kansas 66045

ABSTRACT

Experimental measurements of the backscattering coefficient σ^0 and apparent radiometric temperature T_{ap} of snow are used to develop simple empirical models relating σ^0 and T_{ap} to snow wetness and to water equivalent. The data were acquired by truck-mounted sensors, covering the 1-35 GHz band in the case of σ^0 and at 10.7, 37 and 94 GHz for T_{ap} . It is observed that σ^0 's sensitivity to wetness increases with angle of incidence away from nadir, while T_{ap} 's sensitivity is almost angle independent, and for both active and passive sensors, the sensitivity to wetness increases with microwave frequency. For dry snow, σ^0 increases and T_{ap} decreases, both exponentially, as a function of snow depth.

CHARACTERIZATION OF POLAR TERRAIN FEATURES THROUGH
SATELLITE MICROWAVE RADIOMETRY

S. R. Rotman, A. D. Fisher, and D. H. Staelin
Research Laboratory of Electronics
Massachusetts Institute of Technology
Cambridge, Massachusetts 02139, U.S.A.

The Scanning Microwave Spectrometer (SCAMS) on the Nimbus-6 Satellite mapped the entire earth's surface up to latitudes of 80° at the two microwave frequencies of 22.235 and 31.65 GHz during 1975 and 1976. The observations in the Antarctic and Greenland areas were used to obtain such geophysical parameters as snow accumulation rates, relative extent of ice packs, and differentiation between winter and pack ice. Microwave radiometric techniques have been used previously to track the movements of the polar ice cap and the relative amounts of first year and old ice in the Arctic and Antarctic regions (Gloersen et al., Boundary-Layer Meteorology, 13, 339-359, 1978). Furthermore, a relation has been found between the accumulation rate of dry snow and microwave emissivity from its surface (H. J. Zwally, Journal of Glaciology, Vol. 18, No. 79, 195-215, 1977).

In the present study, a semi-empirical relation was derived from the Antarctic observations which connected the snow accumulation rates to surface emissivity and sub-surface temperature. Using this relation, contour maps of snow accumulation were then prepared for both Antarctica and Greenland which not only showed excellent agreement with previous maps obtained from ground surveys but also extended their range. In addition, seasonal changes in the microwave brightness temperature of the snow were noted and related, through multi-frequency measurements, to physical temperature gradients in the firn.

The satellite observations also showed clearly distinguishable differences in the variation of surface brightness temperature with scan angle for new ice, old ice and dry snow. New ice apparently acts as a homogeneous dielectric with almost no internal scattering so that its emissivity is controlled almost entirely by the Fresnel reflections from its surface. Old ice shows largely isotropic scattering due to numerous air voids which are left after drainage of brine. The relative percentages of ice and sea water in a given region can be resolved on the basis of differences in their relative reflectivities. In contrast to ice, dry snow appears to form horizontal layers which cause the scattering to become highly anisotropic. These discriminants can all be used to characterize regional differences in polar terrains and to monitor their seasonal changes.

EMISSION FROM A SNOW LAYER WITH
A SLIGHTLY IRREGULAR INTERFACE

A.K. Fung and M.F. Chen
Remote Sensing Laboratory
University of Kansas
Lawrence, Ks. 66045

A layer of snow above the ground surface is modelled as a layer of Rayleigh scatterers above a plane ground surface with a slightly irregular air-snow interface. The radiative transfer method is then applied to the snow medium to compute the upward brightness temperature assuming a constant ground surface and snow temperature. The assumption of a slightly irregular air-snow interface requires the computations of the modified Fresnel reflection coefficients and the first-order bistatic scatter and transmission coefficients of the interface. Note that the use of the modified Fresnel reflection coefficients is necessary to obtain energy conservation to the first-order. Comparison between the plane and the irregular air-snow boundary cases indicates that for nadir angles near vertical a smaller and flatter angular response is obtained in the presence of the irregular boundary which permits better trend agreement with some measurements.

SESSION F-7
THURSDAY PM 1:30-5:00
KANE HALL 110

RADIOOCEANOGRAPHY

Chairman: J. R. Apel
NOAA
Seattle, WA

RADAR ALTIMETRY FOR USE IN MEASURING SEA SURFACE SLOPE

H. Michael Byrne Pacific Marine Environmental Laboratory

During September 1978 the SeaSat satellite orbit was placed in a repeat ground track configuration. For the month beginning 8 September the subsatellite track repeated itself exactly over three transects of the Kuroshio. During this time a hydrographic survey was performed along the subsatellite track in coincidence with the satellite overpass. An intercomparison was made between the relief of the sea surface topography measured with the 10 cm altimeter on the SeaSat spacecraft and that deduced from the standard oceanographic data. Additional comparisons were made between the total flow field deduced from NOAA-5 infrared data and velocity vectors deduced from the altimetric data.

A detailed comparison with surface topographies generated using the GEOS-III data show the radar altimeters capable of measuring surface slopes at accuracies useful for oceanographic calculations.

The SEASAT Radar Altimeter -
A study of Wave Height Measurements

by

L. S. Fedor and James A Leise
Wave Propagation Laboratory
National Oceanic and Atmospheric Administration
Boulder, Colorado 80302

The SEASAT ocean monitoring spacecraft was placed into earth orbit on June 27, 1978. On board was a 13.5 GHz radar altimeter which was used to measure spacecraft height above mean sea level, the significant waveheight, and the radar backscatter cross section to infer winds. The high resolution radar was designed to measure altitude to ± 10 cm and waveheights from 1 to 20 meters with an accuracy of $\pm 10\%$ or 0.50 meters whichever is larger. An algorithm for estimating waveheights is presented and the effect of preprocessing the data by filtering is discussed. Spectral plots of the significant waveheight determined along the satellite track are presented to show the spatial resolution of the altimeter and determine dominant spatial features. Comparisons are made with surface determined data.

THE COMPUTATION OF WIND SPEED AND WAVE HEIGHTS FROM GEOS 3 DATA

NELLY MOGNARD, J.I.S.A.O., 3711 15th AVENUE N.E., SEATTLE, WA.
98105 AND BERNARD LAGO, G.R.G.S.-C.N.E.S., 18 AVENUE E. BELIN
31055 TOULOUSE CEDEX FRANCE

We have processed radar altimeter data from more than 100 GEOS 3 passes. The statistical analysis of the stretching of the leading edge of the return radar pulses gives us an estimate of the significant wave heights. Moreover, the AGC level measurements of the reflected power provide an evaluation of the wind speed. The wave height and wind speed estimates are in favorable agreement with the meteorological information obtained from weather maps used as sea truth, thus resulting in interesting complementarities.

AIR SEA TEMPERATURE DIFFERENCE EFFECTS ON MICROWAVE SCATTERING

W.C. Keller and W.J. Plant
Ocean Sciences Division
Naval Research Laboratory
Washington, DC 20375 USA

The modulation of short gravity-capillary waves, and thus radar cross-section, by long ocean waves is an important mechanism in remote sensing of the sea surface by microwave radars. Previous measurements reported the modulation transfer function (MTF) as a function of long wave frequency and windspeed (W.J. Plant et al, J. Geophys. Res., 83, 1347-1352, 1978, and Wright et al, submitted to J. Geophys. Res., 1979).

We will present results from the Panama City Experiment II (Nov - Dec 1978) where the passage of significant cold fronts provided a wide range in the air-sea temperature difference. Radar cross-section and the MTF were measured at 9.375 GHz using a CW Doppler radar at short range, a depression angle of 45 degrees and vertical polarization. Air temperature changes up to 22 C deg within a 24 hour period were recorded with hourly changes up to 7 C deg.

DOUBLE-MODULATION EXPERIMENTS ON OCEAN WAVE SYSTEMS
USING A DUAL-FREQUENCY MICROWAVE RADAR

Dale L. Schuler and William J. Plant
Naval Research Laboratory
Washington, D.C. 20375

A new application of the dual-frequency microwave radar technique has been developed and tested through field experiments. Previous work (D. L. Schuler, Radio Science, Vol. 13, no. 2, 321-31, 1978) has indicated that directional gravity wave spectra and surface currents may be studied using the dual-frequency approach. Recent field-experiments in coastal waters of the Atlantic Ocean, and from a site overlooking the Pacific Ocean, have shown that the utility of the dual-frequency system as a remote-sensing probe of long wavelength waves is, perhaps, greater than was previously conceived.

A pulsed, L-band, dual-frequency radar has been used successfully as a probe for sensing the modulation of 3-30 meter waves by longer wind waves and swell. In particular, simultaneously measured single-frequency and dual-frequency outputs yield information on 1) directional orbital velocity spectra (and concomitantly wave height spectra) as well as 2) the modulation transfer function for selectable wave-wave interactions. The wave-wave interactions that can be examined involve a long wavelength modulating wave and a dual-frequency Bragg resonant wave of wavelength 3-30 meters. The technique is based upon the use of short transmitted pulses (0.1 μ s) and relatively coarse azimuthal (13°) resolution to create long, slender, illumination cells on the surface. Because these scattering cells have small total area, 1) the dual-frequency resonance peak/background ratio may be optimized and, 2) the orbital velocity spectrum of the long wavelength waves becomes directional.

Experimental results of preliminary double-modulation experiments will be given as well as an analytical interpretation of the results.

SIDE-LOOKING RADAR IMAGES OF
DISPERSIVE, HOMOGENEOUS WAVES

Robert O. Harger, Electrical Engineering Department,
University of Maryland, College Park, Md. 20742

The image produced by a side-looking--e.g., synthetic aperture-radar system is derived for a time-varying scene characterized by a time-variant reflectivity density. Application to the image of the so-called two-scale sea surface model motivates a collateral consideration of the image of a time-varying scene described by a reflectivity density that satisfies a dispersive, homogeneous wave equation. It is shown that there exists a distortion--most simply a scaling and skewing--inherent in any side-looking technique: the latter's specifics--most simply--modify the (true) wave-number spectrum.

MEASUREMENT OF SURFACE ROUGHNESS FROM NADIR
USING DUAL FREQUENCY CORRELATION AND
SPATIAL RESOLUTION WITH A S.A.R. CHIRPED SIGNAL

D.E. Weissman, Hofstra University, Hempstead,
N.Y., 11550, J.W. Johnson and W.L. Jones,
N.A.S.A. Langley Research Center, Hampton, Va.,
23665, W.F. Townsend, N.A.S.A. Wallops Flight
Center, Wallops Island, Va. 23337

The measurement of the root-mean-square height of a randomly rough surface from an elevated platform can be approached from either the measurement of the time dispersion of a short pulse or the decorrelation of the amplitudes of two narrow band backscattered signals separated by a variable difference frequency. The latter method has been considered in this study. The variation in the height of the scatterers within an illuminated area produces phase differences among the backscattering elements that are not identical at the two different carriers. The correlation between the resultant signals, over an ensemble of surfaces, will decrease with an increase in the rms surface roughness and the separation frequency. In order to limit this decorrelation to surface roughness effects and minimize the range spreading caused by off-nadir beam illumination, high spatial resolution near nadir is required. With a very high altitude platform (aircraft or spacecraft) this can be achieved with the chirped signal used in a synthetic aperture radar. The spectrum of the transmitted energy is sufficiently broad to be separated into adjacent bands that are capable of providing both the spatial resolution (with matched filtering) and the frequency separation, Δf . The fluctuating amplitudes of the outputs of the matched filters are cross correlated to infer the surface roughness. An analysis has been performed to determine the dependence of the cross correlation on the statistical parameters of the matched filter output signals. These results will be discussed from the viewpoint of determining ocean wave heights from an aircraft or satellite.

Measured results obtained with the Dual Frequency Correlation Radar taken during the West Coast Experiment will be discussed and compared with simultaneous radar altimeter measurements.

SYNTHETIC APERTURE RADAR IMAGERY OF MOVING OCEAN WAVES

C. L. Rufenach
NOAA/ERL/Wave Propagation Laboratory
Boulder, Colorado 80303

W. R. Alpers
Institute of Geophysics
Univ. of Hamburg & Max-Planck-Institute of Meteorology
Hamburg, W. Germany

The theory developed by Swift and Wilson, and Alpers and Rufenach describing the intensity modulation in Synthetic Aperture Radar SAR imagery caused by ocean wave motion is extended. The restrictive approximation $\hat{\omega}T \ll 1$ used in their work is removed where $\hat{\omega}$ is the long ocean wave angular frequency and T is the radar coherent integration time. This generalization, valid for all $\hat{\omega}T$, is significant since the integration time associated with L-band radars is sufficiently long $T=2$ sec. that the restriction $\hat{\omega}T \ll 1$ is only appropriate for the longer ocean wavelengths. Calculations show that the $\hat{\omega}T \ll 1$ theory is valid for wavelengths greater than 400m for all waveheights of interest and for wavelengths greater than about 250m for the lower waveheights, say $H_{1/3} < 3$ m. Radar and surface measurements off the Florida coast during December 1975 are consistent with the theory.

The effects of ocean wave motion on SAR imagery under a variety of sea states will be discussed including the detectability of azimuth traveling ocean waves from the SEASAT satellite.

SEASAT-A SYNTHETIC APERTURE RADAR IMAGERY OF OCEAN WAVES

F. I. Gonzalez	Pacific Marine Environmental Laboratory/NOAA
R. A. Shuchman	Environmental Research Institute of Michigan
D. B. Ross	Sea-Air Interaction Laboratory/NOAA
J. F. R. Gower	Institute of Ocean Sciences
C. L. Rufenach	Wave Propagation Laboratory/NOAA

An analysis of the ocean wave imaging capabilities of the Seasat-A Synthetic Aperture Radar (SAR) has been performed. Five SAR passes collected during the NOAA-sponsored Gulf of Alaska SeaSat Experiment (GOASEX) were examined. Ocean wave surface truth consisted of two-dimensional power spectra acquired by Pitch-Roll buoy, one-dimensional spectra from NOAA data buoys, and X- and L-band airborne SAR imagery. Optical Fourier Transforms (OFT's) of the Seasat SAR imagery yielded data which agreed to within about $\pm 10\%$ and $\pm 20^\circ$ of surface truth wavelength and direction measurements, respectively. Wavelengths of 100 m to 300 m were imaged and significant waveheights of about 1 to 3.5 m were recorded by surface truth; within this limited range, there appears to be an improvement of wave image quality with increasing wavelength and significant wave height.

SYNTHETIC APERTURE RADAR OBSERVATIONS
AT VARIOUS ASPECTS OF OCEAN WAVES

John F. Vesecky and Hany Assal, Center for Radar Astronomy
Stanford University, Stanford, CA 94305
Robert H. Stewart, Scripps Institution of Oceanography,
University of California, La Jolla, CA 92093

On March 25, 1975 a very interesting set of synthetic aperture radar (SAR) images of the ocean were collected by the Jet Propulsion Laboratory (JPL) in deep water some 20 miles WSW of Pt. Arguello, CA. A concurrent ground truth (wave rider buoy) wave spectrum was also obtained. The aircraft carrying the L-band SAR viewed a single area of ocean from eight different directions. The imaged area contained waves driven by approximately 25-30 kt winds blowing over a 300-400 mile fetch for some hours before the observations. SAR images of one or two 6 x 6 km areas along each flight leg have been digitized and geometrically corrected to obtain an undistorted image. We have estimated the directional ocean wave spectrum $\Psi(k, \theta)$, from these corrected images on the basis of a very simple assumption, namely that the SAR image density fluctuations are proportional to ocean surface height fluctuations. Near the peak in the wave spectrum (wave period ~ 10 s.) the SAR estimates of Ψ and ground truth correspond reasonably well. However, away from the peak the SAR estimates of Ψ tend to fall more rapidly than the buoy spectrum at both larger and smaller periods. Further, the SAR estimates from flight paths at differing angles with respect to the dominant wave direction are significantly different in that the spread of wave direction varies as the waves are viewed from different aspects. A priori knowledge of the dominant wave direction allows first order correction for the variable response of the radar to waves viewed from varying angles.

SESSION F-8
FRIDAY AM 8:30-12:00
KANE HALL 110

PROPAGATION MODELING

Chairman: W. J. Vogel
University of Texas
Austin, TX

EFFECTIVE PATH LENGTH AND THE FREQUENCY
SCALING OF RAIN ATTENUATION

H.N. Kheirallah, Department of Electronics, Carleton University, Ottawa, Canada, K1S 5B6 and R.L. Olsen, Department of Communications, Communications Research Centre, Ottawa, Canada, K2H 8S2

A common method of predicting rain attenuation along an earth-space path is to multiply the specific attenuation obtained from point rainrate measurements by an empirical effective path length. Implicit in this method is the assumption that the effective path length is independent of frequency. In this paper it is shown theoretically and numerically that the effective path length is actually frequency dependent. This dependence is due to the inhomogeneity of the rain along the path in combination with the nonlinear relation between specific attenuation and rainrate, and to cloud effects. In order that effective path length data obtained at different frequencies may be appropriately combined, the use of a normalized effective path length is proposed. Finally, a new method of frequency scaling rain attenuation statistics is presented. Comparison with existing methods shows that it gives better results for the small percentages of time of greatest interest. Two-frequency attenuation statistics measured in both the USA and Japan are employed in the analysis.

THE IMPACT OF UNCERTAINTIES IN RAIN
FADE ESTIMATES ON THE DESIGN OF
20/30 GHZ SATELLITE COMMUNICATION SYSTEMS

R. R. Persinger
Hughes Aircraft Co.
Space and Communications Group
Los Angeles, California 90009

W. L. Stutzman
Virginia Polytechnic Institute and State University
Department of Electrical Engineering
Blacksburg, Virginia 24061

The design of 20/30 GHz multiple zone coverage for service in the continental U.S. requires accurate rain fade estimates. Existing data from 20/30 GHz rain attenuation measurements is insufficient for drawing statistically meaningful conclusions. Also, the number of sites for which data is available is limited. Therefore, the system design engineer must rely on predictive techniques. In the 20 and 30 GHz frequency ranges the rain fades are much larger than at lower frequencies. Thus, modeling uncertainties can lead to relatively large fade value uncertainties, which have a significant effect on communication system design and cost.

Single site rain fade predictions using current predictive models are presented in this paper, together with measured data. The resulting differences in rain fade margin estimates are given, and reasons for these modeling uncertainties are discussed.

Site diversity is an important mechanism for increasing system reliability. Prediction methods for estimating the performance of site diversity systems are discussed.

The impact of single and dual site rain fade uncertainties on system design and cost will be presented.

PREDICTION OF RAIN-INDUCED FADES
ALONG EARTH-SPACE MILLIMETER WAVE LINKS

W. L. Stutzman
Virginia Polytechnic Institute and State University
Department of Electrical Engineering
Blacksburg, Virginia 24061

R. R. Persinger
Hughes Aircraft Co.
Space and Communications Group
Los Angeles, California 90009

Millimeter wave signals experience attenuation when precipitation occurs along a satellite-earth propagation path. In this paper a simple model is presented for prediction of rain-induced fades on slant path millimeter wave links. A synthetic storm model coupled with specific attenuation values permits easy calculation of total attenuation. Point rainfall accumulation data is combined with the model to provide predictions of rain attenuation statistics.

The sensitivity of rain fade predictions to specific attenuation values as a function of elevation angle, polarization, etc. is discussed. Scaling of attenuation values to different frequencies is also discussed.

Comparisons between predicted results and measured data at several locations are presented for 11, 20, and 30 GHz.

GLOBAL RAIN ATTENUATION MODEL

Robert K. Crane
Environmental Research & Technology, Inc.
696 Virginia Road
Concord, Massachusetts 01742

A global rain model has been developed for the estimation of rain attenuation distributions for terrestrial and for earth-space paths. The attenuation estimation procedure employs empirical point rain rate distributions together with models to provide path averaged attenuation or rain rate along a horizontally inhomogeneous slant path through the atmosphere. The procedure has been designed for ready application to design problems using rainfall distribution maps and a pocket calculator.

The model was developed using meteorological data describing the horizontal and vertical variation of rain intensity. It has been verified by comparison with empirical attenuation distribution estimates obtained from terrestrial path and slant path measurements.

MEASUREMENT OF CLOUD LIQUID CONTENT USING
THE 28 GHZ COMSTAR BEACON

J. B. Snider
Environmental Radiometry
Wave Propagation Laboratory
Environmental Research Laboratories
National Oceanic & Atmospheric Administration
Boulder, CO 80303

Since October 1978, we have been measuring the liquid content of clouds in Colorado. Our instrument, a switched bandwidth receiver radiometer, simultaneously measures:

1. Absorption of the 28.5 GHz coherent signal transmitted by the COMSTAR D-3 satellite, and
2. The associated increase in brightness temperature radiated by the absorbing clouds.

By combination of the two quantities, the line integral of liquid through the cloud is determined. The system operates unattended and continuously, collecting data on clouds that drift through the satellite-earth propagation path.

Initial results are extremely encouraging and we believe the instrument provides quantitative data on cloud liquid content with greater accuracy than previously known. After a description of the receiving system, some of the more interesting absorption events are presented.

PHASE AND AMPLITUDE DISPERSION FOR EARTH-SPACE PROPAGATION
IN THE 20 TO 30 GHz FREQUENCY RANGE

D. C. Cox, H. W. Arnold and R. P. Leck
Bell Laboratories
Crawford Hill Laboratory
Holmdel, New Jersey 07733

The 28 GHz beacon on the COMSTAR Satellite at 95°W longitude was modulated to produce ±264 MHz sidebands coherent with the carrier. Phase and amplitude measurements of the sidebands and carrier determine the phase and amplitude dispersion at the center and edges of a 528 MHz bandwidth. Phase and amplitude measurements of the coherent 19 and 28 GHz beacon carriers provide dispersion information over a much wider frequency range.

A 9 month data set has been comprehensively searched for evidence of phase dispersion. For all propagation events, the change in average sideband to carrier phase is less than the measurement uncertainty of about ±3° for attenuation up to 45 dB. Phase fluctuations are consistent with signal-to-noise ratios over the 45 dB attenuation range. The change in average 19 to 28 GHz phase is on the order of 60° over a 30 dB attenuation range at 28 GHz. This average phase change appears to be due only to the average dispersive properties of the water in the rain along the path. There is no evidence of multipath type dispersion.

Attenuation in dB at 28 GHz is 2.1 times greater than that at 19 GHz for attenuations up to 20 dB at 19 GHz. The small spread observed in the relationship between 19 and 28 GHz attenuations is consistent with the absence of significant phase dispersion over the 528 MHz bandwidth.

Invited paper for USNC/URSI Special Sessions on Earth-Space Propagation
Above 10 GHz

MICROWAVE DEPOLARIZATION OF AN EARTH-SPACE PATH

T. S. Chu
Bell Laboratories
Crawford Hill Laboratory
Holmdel, New Jersey 07733

Both rain and ice particles contribute to microwave depolarization on an earth-space path. Extrapolation of the terrestrial rain model provides only part of a complete picture which is hampered by the lack of physical data of ice clouds. However, analysis may establish a theoretical framework to organize the experimental data and to yield functional dependence of cross polarization on frequency, polarization, elevation angle and rain rate. Agreement will be shown between measured depolarization data and theoretical results which are independent of details of ice clouds.

In particular, a linear relation has been found between cross polarization amplitude and frequency practically throughout the centimeter wavelength range. The dependence of depolarization on orientation of an arbitrary linear polarization is relatively insensitive to the mean canting angle of hydrometeors except within about ten degrees of the vertical or horizontal direction. Depolarization data for paths of various elevation angles, θ , are well governed by an approximate factor of $\cos^2\theta$ for the differential propagation constant.

MULTIPLE SCATTERING OF MILLIMETER WAVES IN RAIN

Rudolf Lap-Tung Cheung and Akira Ishimaru
Department of Electrical Engineering
University of Washington
Seattle, Washington 98195

Above 10 GHz, the multiple scattering due to rain may become significant depending upon the precipitation rate, the thickness of the rain layer, and the observation angle. This paper considers the problem of a wave normally incident upon a plane-parallel rain region. The scattered wave is observed on the ground as a function of the elevation angle and polarizations, and it is calculated for 10, 30 and 120 GHz at the precipitation rate of 12.5 mm/hr with the rain layer thicknesses of 1 km and 3 km. The scattering characteristics of raindrops are calculated using the Mie solution and the Laws-Parson distribution. Both the first order multiple scattering theory and the radiative transfer theory are used and the results are compared. It is shown that at 10 GHz, these two methods yield almost identical results. However at 30 GHz and 120 GHz, the first order scattering is smaller than that obtained from the radiative transfer theory, indicating the effects of higher-order scattering. It is also shown that the horizontal polarization is in general greater than the vertical polarization due to the scattering characteristics of raindrops. As the angle from the zenith increases, the scattering in horizontal polarization increases while that in vertical polarization decreases at 10 and 30 GHz. However at 120 GHz, the scattering in both polarizations decreases with the angle, indicating the effect of forward scattering. Based on the above study, the incoherent (fluctuating) intensity for a receiver with a given field of view or the receiving angle can be calculated.

For example, with the receiver beamwidth of 5° and the rain thickness of 3 km, the incoherent intensity is approximately 50 db down from the coherent intensity at 10 GHz, but it is 20 db down at 120 GHz. The incoherent intensity for the rain thickness of 1 km is about 5 db less than that for the rain thickness of 3 km.

EFFECT OF ADVERSE SAND-STORM MEDIA ON
MICROWAVE PROPAGATION

H. T. AL-HAFID,* S. C. GUPTA* and
K. BUNI**

* Mosul University, Mosul, Iraq.

** Iraqi Ministry of Telecommunications,
Baghdad, Iraq.

ABSTRACT

Theoretical and experimental study is being made to study the possible effects of dust-storms on the performance of microwave links. The sand and dust particles scatter or absorb electromagnetic energy at microwave frequencies and results in attenuation of signal. A laboratory model is developed, simulating the actual conditions. Theoretically the attenuation constant for microwave energy is estimated. The total cross-section due to absorption and scattering of EM waves by spherical particle after simplification for ($K \ll 1$, the dimensions of particles are small compared to wavelength), is,

$$A_s = \frac{\lambda_0^2}{2\pi} K^3 (C_1 + C_2 K^2 + C_3 K^3)$$

where C_1 and C_2 are estimated due to absorption and C_3 due to scattering of EM waves.

The total attenuation is given by

$$\mathcal{L} \text{ (Neper/Unit Length)} = N A_s$$

where N is the number of particles per unit volume.

Attenuation about 0.085 dB/Km for concentration of 2.0×10^{-5} gm/cm³ for sand is obtained. Experimentally attenuation of MW signal at 11.0 GHz VS concentration and visibility in storms were plotted. It was observed that median level of signal drops by 2 dB to 4 dB and the fading spikes having a duration of less than 15 seconds, drops the level by 10 dB or more under severe dust storm period of two months. During the severe sandstorms periods, when horizontal visibility is shortened by 100 meters to 200 meters, the variation in received signal level were recorded. Meteorological data during the period were also recorded.

QPM-DIGITAL SIGNAL MULTIPATH FADING

Prof. H. S. Hayre, E. E. Dept. - Wave Prop. Lab.
University of Houston
Houston, TX 77004

Since quaternary coherent phase shift keyed control and guidance system of a given bandwidth uses a maximum information bite rate per hertz compatible with the carrier to noise ratio for an acceptable performance degradation in terms of bit error rates (BER) for a fixed channel separation, any multipath fading caused by intervening environment/objects between the transmitter and the receiver increases the spill over into the adjacent channel for multichannel systems or increase the BER for a single channel. In this case such a digital system operating at 12 GHz at an airport, where the runways separate the receiver and transmitter locations, and all types of aircraft fuselage causes multipath is ultrasonically simulated in water at 2.25mhz signal utilizing linear wavelength scaling. Both theory and simulated results are presented to show the degradation of the BER due to various types of aircraft. Furthermore an attempt will be made to collect full scale data for comparison with simulated results at the conference. Preliminary results seem to confirm the usefulness of the ultrasonic simulation technique, and further show that the usual forms of noise distribution functions, assumed in communication problems, don't simulate this aircraft multipath case adequately.

SESSION G-1
MONDAY PM 1:30-5:00
HUB 309A

DIAGNOSTICS, EFFECTS, AND MODIFICATIONS OF THE IONOSPHERE

Chairman: E. J. Fremouw
Physical Dynamics, Inc.
Bellevue, WA

WHICH IONOSPHERIC PARAMETERS CAN WE REALLY
MEASURE WITH INCOHERENT SCATTER RADAR?

Jon B. Hagen, National Astronomy and Ionosphere
Center, Arecibo, Puerto Rico, 00612

Least square fits of topside ionosphere data to theoretical spectra yield estimates of O^+ , He^+ , and H^+ concentrations as well as electron and ion temperatures. Strong correlations between the various parameters can and do make the estimation of some parameters impossible or ambiguous while estimates of other parameters can be reliable even with quite noisy data. A graphical presentation of error ellipses is useful to visualize the ambiguous regions of the parameter space.

LONG-TERM OBSERVATIONS OF POLAR D-REGION IONIZATION

Ward J. Helms
Department of Electrical Engineering
University of Washington
Seattle, Washington 98195

Alan S. Chandler
John Fluke Manufacturing Company
P.O. Box 43210
Mountlake Terrace, Washington 98043

Long-term observation of the polar D-region at Byrd Station, Antarctica utilizing a Very Low Frequency Ionospheric Sounder has indicated that background ionization is related to magnetospheric processes and is not strongly affected by solar radiation.

Large increases in production are seen to be directly related to solar proton fluxes with an apparent modulation of the loss process by photo detachment. New evidence is presented linking D-region production and natural VLF signals suggesting triggering of the precipitation by electromagnetic signals.

BACKSCATTER INVERSION IN SPHERICALLY
ASYMMETRIC IONOSPHERER. E. DuBroff*, N. Narayana Rao⁺ AND K. C. Yeh⁺

*Phillips Petroleum Company, Bartlesville, OK 74004

⁺Department of Electrical Engineering
University of Illinois at Urbana-Champaign
Urbana, IL. 61801

It is well known that various diurnal and morphological features of the ionosphere reveal substantial departures from the normally simplified assumption of spherical symmetry at certain times of the day or at certain geographic locations. A radio ray passing through such an ionosphere must bear information about its horizontal gradients. The leading edge of a backscatter ionogram is formed by obliquely propagated radio rays of minimum time delay and hence is useful in deducing information about the ionospheric horizontal gradients. In this regard, the ionospheric electron density distribution is modeled by a locally quasi-parabolic layer with six parameters consisting of the critical frequency, base radius, and peak radius and their horizontal gradients. This six-parameter space is known as the "ionostate". Our object is to seek the "best" ionostate in the sense that the corresponding mean square error in the minimum group delay is minimized. A computer technique to carry out this procedure is described and a number of sample calculations are presented and discussed.

SPECIFIC PROPERTIES OF BACKSCATTERING OF RADIO WAVES ON
MAGNETO-ORIENTED IONOSPHERICAL IRREGULARITIES AT FREQUEN-
CIES BELOW CRITICAL FREQUENCY.

S.A.NAMAZOV

Institute of Radioengineering
and Electronics Ac.Sci.USSR.
Moscow.

YU.A.KRAVTSOV

The Moscow Lenin State
Teacher's Training
Institute. USSR.

I. High resolution ionospheric sounding.

To obtain higher resolution of ionospheric irregularities linear frequency modulated (LFM) signal and pulse compression technique were used. LFM signal has a large product $T \cdot \Delta f$ with $\Delta f \approx 100$ Kcps band width and $T \approx 400$ msec pulse duration. The time resolution (after pulse compression by means of matching filter) was about $10 \mu\text{sec}$.

An increased resolution enables one to investigate fine structure of the signals, diffusely scattered from weakly disturbed ionosphere when ordinary sounding technique doesn't register these perturbations (weak F-spread) [1] .

2. Experimental results.

Diffuse scattering of radio waves was observed over wide frequency band from 1,7 to 7,1 Mcps as a rule during sunset time. The scattered signal usually consisted of many discrete pulses. Time delays of these pulses were stable enough during two-minute intervals, but their amplitudes changed considerably. One or two (in the case of magneto-ionic splitting) pulses with the largest amplitude were distinguished during practically the entire period of observation.

Essential amplitude variations as well as considerable fluctuation of time delay were registered for the pulses, reflected from the maximum of the F-layer [1].

The discrete structure of the scattered signals is in a good qualitative agreement with experimental results obtained by means of antennae with narrow beam width under natural and artificial F-spread conditions [2,3].

The statistical processing of experimental data at eight frequencies from 1,7 to 7,1 Mcps was carried out. The mean envelopes $\langle A(\tau) \rangle$, the most probable amplitudes, the intervals between pulses in diffuse group and other parameters were determined. The mean envelope $\langle A(\tau) \rangle$ of diffusely scattered signals at frequencies 1,7; 6,6 (O-mode) and 7,1 Mcps (X-mode) versus time delay τ are described in Fig 1. One may see from Fig 1, that envelope $\langle A(\tau) \rangle$ has asymmetrical form at low frequency 1,7 Mcps (curve 1) and that at high frequencies $\langle A(\tau) \rangle$ changes abruptly when $\langle A(\tau) \rangle \approx 0,6 + 0,7 \langle A_{max} \rangle$ (curves 2,3).

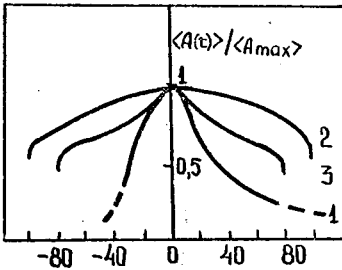


Fig 1

- 1 - $f = 1,7$ Mcps
- 2 - $f = 6,6$ Mcps
- 3 - $f = 7,1$ Mcps

3. Theoretical consideration.

a) Four channels of scattering. There are two rays arriving in each point of irregularities ionosphere, thus providing for four possible ways ("channels ") of scattering $I \rightarrow I$, $I \rightarrow 2$, $2 \rightarrow I$ and $2 \rightarrow 2$, shown in Fig 2. The signals, corresponding to channel $I \rightarrow 2$ and $2 \rightarrow I$ are coherent for one-position measurements.

b) Enhancing of backscattering in caustic zone. The rays 1 and 2 coincides at caustics, so that four channels are coherent inside caustic zone. As a result, backscattering irradiance becomes $4 \times 4 = 16$ times greater than for one-channel case. Another reason of enhancing of backscattering is focusing effect at caustic which increase backscattering cross-section by factor $\left[(KH)^{1/6} \right]^4 = (KH)^{2/3}$ where $H \sim \epsilon \left| \frac{\partial \epsilon}{\partial z} \right|^{-1}$ is

ionospheric scale, $k = \omega/c$ is a wave number.

c) Aspect sensitivity. Backscattering cross-section has a maximal value on the "aspect" surfaces, where the vector $\vec{q} = \vec{k}_{inc} - \vec{k}_{scatt}$ is orthogonal to static magnetic field \vec{H} . In general case, there are three aspect surfaces corresponding to vectors \vec{q}_{11} , $\vec{q}_{12} = \vec{q}_{21}$ and \vec{q}_{22} , shown in Fig 2.

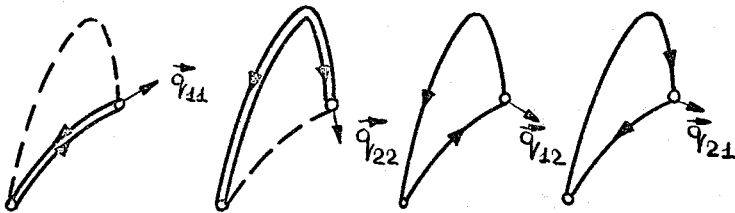


Fig 2

d) The zone of the greatest scattering. Both aspect and caustic zones have a limited thickness. We presume that their intersection gives the most of the backscattered signals. Comparatively short initial part of function $\langle A(\tau) \rangle$ at low frequencies (see curve I in Fig I) may be caused by scattering in North direction where ray meet aspect points before reflection and where aspect zone is a short extension. At high frequencies (curve 2 and 3 at Fig I) function $\langle A(\tau) \rangle$ has a slowly decaying tail due to backscattering in W - E direction where aspect and caustical zone almost coincide over long distances.

e) Overlapping of different part of signals. Calculations for linear layer model show that time delay of obliquely incident wave may be less than delay of vertically sounding ray. This results in overlapping of different scattered impulses and in a more complicated $\langle A(\tau) \rangle$ form. In particular, this phenomenon may cause a "flattening" of dependence $\langle A(\tau) \rangle$ when signal frequency approaches a critical value ($f=6,6$ and $7,1$ Mcps, Fig I).

4. Numerical analysis. To analyse aspect surfaces, numerical method of ray path calculation was used in the case of spherically layer anisotropic ionosphere. Only surfaces $\vec{Q}_{11} \perp \vec{H}$ and $\vec{Q}_{22} \perp \vec{H}$ were considered. Contrary to VHF, when aspect surface is in the north direction only aspect surface at frequencies below critical value has a complicated dome-like form with a large E - W extention and with strong asymmetry in the plane of geomagnetic meridian [4]. Time delay of diffuse signals was up to 10 msec for above model of ionosphere. Further analysis of azimuthal distribution of backscattered signals would allow to reveal some important properties of the magneto-oriented ionospheric irregularities.

References

1. S.A.Namzov, T.E.Ryzhkina, "Rasprostranenie radiovoln" (Wave propagation), M,Nauka, pp 262 - 290.
2. G.D.Brownlie, L.G.Dryburgh, J.D.Whitehead, J.Atmos. Terr. Phys., 35, 2147, 1972.
3. E.M.Allen, G.D.Thome, P.B.Pao, Rad. Sci., 9, 905, 1974.
4. S.A.Namzov, V.V.Korobeishchikov, "Radiotekhnika i Elektronika", 23, II2I, 1978.

EFFECTS OF MAGNETOSPHERIC DISTURBANCES ON THE GEOELECTRIC
FIELD IN SUB-AURORAL REGIONS AND ITS INTERACTION WITH
HV-DC/AC ELECTRICAL POWER LINES

W-M. Boerner^{1,3}, J. Cole¹, D.E. Olson², W.R. Goddard³, D.H. Hall³
(1) Communications Laboratory, UICC, Chicago; (2) Geoelectric
Observatory, U. Minn, Duluth; (3) AEM Laboratory, U. Man, Winnipeg

There is a strong evidence that magnetic disturbances affect the *earth-ionospheric potential*. Potential variations of about $\pm 20\%$ have been observed to correlate with the sunspot cycle. Among the various mechanisms proposed are wind-driven inhomogeneities in the ionospheric plasma giving rise to a dynamo effect, stratospheric intrusion into the troposphere acting as a charge separation mechanism, solar induced and fluctuations in atmospheric columnar resistance, particularly at higher altitudes. Of particular importance are substorms of class $K_p \approx 5$ and higher which can be observed and analyzed in Central to Southern Manitoba and Northern Minnesota.

Recently it has been found that VLF harmonics radiated from HV-AC electric power transmission systems have a non-negligible effect on the magnetosphere. The extension of HVDC lines into auroral and sub-auroral regions may possibly introduce another parameter into the complex interactions between atmospheric electric potential and geomagnetism.

There exists the possibility that HVDC transmission systems may produce local geoelectric fluctuations which might somehow be amplified to couple with other electro-magnetospheric effects and give rise to weather perturbations greater than would be expected from their primary amplitude alone.

An interinstitutional study addressing some of the basic problems will be described.

AN UPDATE OF THE PROGRAM TO ASSESS THE
IMPACT OF THE OPERATION OF THE SATELLITE POWER SYSTEM

Charles M. Rush
U. S. Department of Commerce
National Telecommunications and Information Administration
Institute for Telecommunication Sciences
Boulder, CO 80303

At the November 1978 meeting of URSI a special session was devoted to explaining the potential effects on the ionosphere and telecommunications systems due to the operation of the Satellite Power System (SPS). At that session, it was pointed out that numerous studies must be undertaken in order to provide a full assessment of the potential impact of the SPS on the ionosphere. The purpose of this discussion is to provide an updated description of the ionospheric assessment portion of the SPS program. The specific programs of experimental and theoretical studies planned for 1979 will be described. The manner in which these studies are to be used in determining the impact of SPS operation on the ionosphere will be discussed.

SESSION G-2
TUESDAY AM 8:30-12:00
HUB 309A

TRANSMISSION AND IN-SITU MEASUREMENTS OF NATURAL
AND ENHANCED IONOSPHERIC IRREGULARITIES

Chairman: C. Rino
Stanford Research Institute
Menlo Park, CA

ON THE RATIO OF INTENSITY AND PHASE SCINTILLATION INDICES

E. J. Fremouw
Physical Dynamics, Inc.
Bellevue, WA 98009

Among the earliest characteristics of complex-signal scintillation noted from the DNA-002 Wideband Satellite Experiment (Fremouw et al, Rad. Sci., 13, 167-187, 1978) was a sizeable difference in the ratio of the intensity scintillation index, S_4 , to the phase scintillation index, σ_ϕ , when measured at mid-latitude (Stanford), auroral-zone (Poker Flat), and equatorial (Ancon) stations. It has been found that two equatorial stations, Ancon and Kwajalein, consistently show a larger S_4/σ_ϕ ratio than does Poker Flat (Alaska), for conditions of nonsaturated intensity scintillation. Records from the aforementioned four receiving stations were carefully inspected to find data segments that show reasonable statistical stationarity over at least 20 sec (60 km of F-layer scan) and are well distributed in elevation angle and scintillation level. A plot of S_4 vs σ_ϕ for 62 VHF data sets so selected shows essentially linear relationships up to a saturation regime beginning near $S_4 = 0.8$ and approaching $S_4 = 1.0$ asymptotically for three of the stations. Curves for the two equatorial stations coincide and display a decidedly steeper linear portion than that for the auroral-zone curve. The mid-latitude data points show much more scatter than do those from the other stations.

The phase-screen theory for production of scintillation in a power-law random medium has been reviewed to determine the relationship of the S_4/σ_ϕ ratio to properties of the medium in the non-saturated regime (weak to moderate intensity scintillation). It is possible to separate four factors as an aid to physical interpretation. In this paper, the behavior of two of the factors is explored for models describing both sheetlike and rodlike plasma-density irregularities. The analysis permits rejection of the effects of static diffraction by field-aligned irregularities (whether rodlike or sheetlike) at substantially the same altitude as the factor controlling the different behaviors observed. It is shown, on the other hand, that geometrical control of the effective outer scale imposed by detrend filtering in the presence of highly anisotropic irregularities can readily explain the observed behavior. It is concluded, further, that other factors may contrive to mitigate the effect of the controlling factor identified, which otherwise might produce even more marked differences in behavior at the various stations.

It is stressed that detrending effects are not to be viewed merely as experimental artifacts. Such effects arise in virtually all experiments and operational systems in the presence of a power-law spectrum with a very large outer scale, and they are important in controlling the quantitative relationship between phase and intensity scintillation.

LONGITUDINAL SENSITIVITY OF EQUATORIAL SCINTILLATION
AS DISCOVERED IN THE 1978 EQUATORIAL SCINTILLATION
CAMPAIGN

by

John P. Mullen
Herbert E. Whitney
Jules Aarons
Air Force Geophysics Laboratory
Hanscom Air Force Base, MA 01731

K. C. Yeh
University of Illinois
Urbana, IL 61801

Between 27 February - 13 March 1978, a campaign of intensive observations of VHF and UHF radio wave scintillation was pursued at Ancon and Huancayo, Peru, Natal, Brazil, Ascension Island and Accra, Ghana. High levels of scintillation were observed at each station; those in Peru permitted estimating the lifetime as well as drift velocities as a function of time. Drift velocities measured at Ancon were found similar to those measured at Natal. Scintillation measurements found at the stations are compared and found generally similar except for those of Ascension which showed marked differences, which are attributed to geometry. The occurrence of scintillation during the intensive period of observations is compared for each site using histograms of scintillation levels for the MARISAT and LES-9 satellites. Power spectra of Ancon and Accra scintillations are presented.

OBSERVATIONS OF IONOSPHERIC BUBBLES
AT THE MAGNETIC EQUATORC. H. Liu*, H. Soicher[†] and K. C. Yeh**Department of Electrical Engineering,
University of Illinois, Urbana, IL 61801[†]Center for Communication Systems US Army Communication
Research & Development Command Fort Monmouth, NJ 07703

Recent data collected near the magnetic equator depict one kind of ionospheric perturbations in the evening hours variously as bubbles or plumes. Theoretical studies show that the under-side of the ionosphere is subject to Rayleigh - Taylor instabilities which, when triggered, will cause a region of depleted ionization to rise as bubbles. When such regions are traversed by a probing radio wave, the associated Faraday effect is expected to show depletions of the electron content. This paper describes some experimental results obtained at Natal, Brazil (35.23°W, 5.85°S, dip-9.6°) by monitoring radio signals transmitted by the geostationary satellites MARISAT 1 and GOES 1. Using ionization depletions as indications of bubbles, statistical studies of occurrence, size and magnitude of perturbations are carried out. The most probable depletions for the propagation path under study have values in the range 1.5 to 3.0×10^{16} electrons per meter², but depletions as large as 1.5×10^{17} electrons per meter² have also been observed. The experimental data further show that the scintillation rate may increase suddenly when these bubbles either form along or drift across the propagation path. This result suggests a new look at the scintillation mechanism is needed since the current theories do not seem to be able to explain this sudden change in the fading rate.

DIRECT COMPARISON OF IN-SITU PLASMA DENSITY AND
VHF/UHF PHASE SCINTILLATION MEASUREMENTS

Michael Kelley
CORNELL UNIVERSITY
Ithaca, New York 14853

Dennis L. Knepp
MISSION RESEARCH CORPORATION
735 State Street, P.O. Drawer 719
Santa Barbara, CA 93102

K. D. Baker
UTAH STATE UNIVERSITY
Logan, Utah 84322

In this paper we report the results of an active experiment to study scintillation effects of ionospheric irregularities. Several large barium ion clouds (48 kg) were released in the mid-latitude ionosphere. The clouds developed plasma density variations (striations) and, some tens of minutes after the release, sounding rockets were successfully flown through the cloud to determine the intensity and character of the striations (K.D. Baker and J.C. Ulwick, Geophys. Res. L 5, 723-726, 1978.) Simultaneously, a receiving station onboard an aircraft measured the phase and amplitude variations of signals transmitted from a geostationary satellite through the same scattering volume. The electron density power spectra obtained from the sounding rocket data is compared to that deduced by numerically back-propagating the signal to the barium cloud location. Estimates of the outer scale and spectra index are given and compared.

ON THE SIGNAL STATISTICS OF SCINTILLATION

E. J. Fremouw
Physical Dynamics, Inc.
Bellevue, WA 98009

The general nature of the statistics that best describe optical and radio signals that have been scattered by random refractive-index structure has been an open question for some time, with different models being used close to the medium (log-normal) and far from it (Rician). Signal behavior in the intermediate zone, which is the relevant distance regime for radiowave propagation through the structured ionosphere, has been difficult to characterize in a systematic way. Multifrequency, coherent satellite transmitters, however, recently have made available signals suitable for developing and testing general models. In this work, data from the DNA-002 Wideband Beacon have been applied to this task.

Detailed analysis has been performed of approximately 100 carefully selected (on the basis of visual inspection for statistical stationarity) VHF, UHF, and L-band data sets from equatorial, mid-latitude, and auroral-zone receiving stations to establish the statistical behavior of scintillating signals over a wide range of scattering strength, Fresnel-zone size, and observing geometry. Histograms of intensity and phase were compared, by means of chi-square testing, with probability density functions derived from four leading signal-statistical hypotheses: log-normal, generalized Gaussian (of which Rice statistics are a special case), two-component (which invokes the log-normal and generalized Gaussian hypotheses in different regimes of the signal fluctuation spectrum), and Nakagami-m (which is an approximation to generalized Gaussian statistics addressing only the behavior of signal intensity).

The analysis disclosed the expected efficacy of log-normal statistics in the near zone, limited to conditions of weak intensity scintillation, and a tendency toward generalized-Gaussian statistics approaching the far zone, limited to a modulo- 2π description of phase. It clearly demonstrated, however, that log-normal statistics do not provide a generally valid description of intensity scintillation and that the generalized-Gaussian model does not characterize the overall behavior of complex-signal scintillation. The two-component model was found to be generally efficacious for describing all aspects of signal behavior in all regimes, providing a systematic transition between the two classical models.

A strong conclusion is reached in support of the Nakagami-m distribution as a general descriptor of intensity fading and of the normal distribution for describing phase behavior, the first-order statistics of which appear to be altered little in post-scattering propagation. At present, however, there is no underlying signal-statistical hypothesis that leads to both joint Nakagami-normal behavior and an accounting for correlation between intensity and phase fluctuations, which is commonly observed.

SIGNAL COHERENCE PROPERTIES OBTAINED FROM
WIDEBAND SATELLITE DATA

Dennis L. Knepp
MISSION RESEARCH CORPORATION
735 State Street, P.O. Drawer 719
Santa Barbara, CA 93102

Data taken by SRI, International on the Defense Nuclear Agency (DNA) Wideband satellite experiment during a period of intense UHF scintillation is examined in detail to obtain amplitude and phase cross-correlation coefficients between frequencies of 379 and 390 MHz. Results from analysis of a 10 second period when the scintillation amplitude statistics are approximately Rayleigh show that rapid phase changes during deep fades can dramatically influence values of the phase cross-correlation coefficient. Results for the phase cross-correlation coefficients are shown to depend on the location of the deep fades and the signal behavior during these fades. This behavior indicates that the phase cross-correlation coefficient is of little value in determining signal coherence properties during severe amplitude fading conditions.

SOME CHARACTERISTICS OF PHASE AND
INTENSITY SCINTILLATION IN ALASKAE. J. Fremouw and J. M. Lansinger
Physical Dynamics, Inc.
Bellevue, WA 98009

The VHF (138 MHz) signal received at Poker Flat, Alaska, in the auroral zone ($L = 5.5$) from the Wideband coherent beacon on satellite P76-6 has been analyzed to determine morphological characteristics of complex-signal scintillation and of the ionospheric irregularities that produce it. Twenty-second values of the standard deviation, σ_{ϕ} , of VHF dispersive phase (measured relative to S Band) and of the normalized standard deviation, S_4 , of VHF intensity (square of amplitude) are employed as scintillation indices. To date, results have been obtained from analysis of 21 months of data, collected from launch through February of 1978. Data from 697 satellite passes were selected by means of rather stringent data-quality criteria and have been sorted against a number of variables. The processed results have been interpreted in terms of a phase-screen scattering model containing a description of three-dimensionally anisotropic irregularities.

Initial results strongly support the idea that plasma-density irregularities in the auroral ionosphere (at least in the region of diffuse particle precipitation) characteristically take the form of sheets aligned along L shells rather than of axially symmetric rods. The results disclose, on the other hand, that irregularities in the daytime subauroral ionosphere are axially symmetric, elongated along the magnetic field. This difference causes the geometric behavior of the transionospheric communication channel at moderately high latitudes to differ significantly between day and night.

SESSION G-3
TUESDAY PM 1:30-5:00
HUB 309A

POLARIZATION EFFECT AND LARGE-SCALE STRUCTURES OF THE IONOSPHERE

Chairman: J. Aarons
Air Force Geophysics Laboratory
Hanscom AFB, MA

DISTORTION AND DEPOLARIZATION BY THE IONOSPHERE
OF L BAND SIGNALS CODED BY PHASE REVERSALS:
FULL WAVE SOLUTIONS

E. Bahar and B. S. Agrawal
Electrical Engineering Department
University of Nebraska, Lincoln, Nebraska 68588

ABSTRACT

The distortion and depolarization of L-Band transient signals that propagate through an inhomogeneous anisotropic model of the ionosphere are investigated using a full wave approach. The dispersive and anisotropic properties of the ionosphere impede the decoding at the receiver of the two orthogonally polarized signals which are independently coded at the transmitter. Thus in addition to determining the signal delays and the phase shifts of the transmitted signals, features that distinguish between the depolarized and nondepolarized signals are also identified.

ANTENNA POLARIZATION CONSIDERATIONS FOR HF BROADCAST SYSTEMS
NEAR THE GEOMAGNETIC EQUATOR

P. M. Hansen

W. J. Fay

Naval Ocean Systems Center
San Diego California 92152

Under certain conditions, ionospheric propagation at hf may be limited to the ordinary or extraordinary mode only. The characteristic or limiting polarization of these modes may be linear, elliptical, or circular of either sense depending upon the angle between the ray path and earth's magnetic field at the ionospheric entry point.

The ordinary and extraordinary modes are complementary such that if one mode is not strongly excited due to polarization mismatch between the mode and antenna, the other mode will be strongly excited. However, if only one mode propagates, then there can be regions of poor coverage depending upon propagation path and antenna polarization. This effect has been examined for locations at and near the geomagnetic equator by calculation of the polarization mismatch factors for vertical and horizontal antennas, and regions of potential poor coverage have been plotted. In addition, antenna polarization requirements in order to avoid possible long term nonreciprocity are discussed.

A NEW APPROACH BASED ON PHYSICAL OPTICS FOR
COMPUTING FIELD STRENGTHS IN THE REGION OF A
CAUSTIC WITH A COMPARISON WITH FULL WAVE
THEORY IN THE REGION OF THE IONOSPHERIC SKIP:

H. Hoogasian, GTE Sylvania, 189 B Street, Needham,
Massachusetts 02194 and D. B. Odom, T.I.S. Boak, III,
Raytheon Company, Wayland, Massachusetts 01778.

The widely used geometric-optics method of estimating the fields of signals reflected from an arbitrary ionosphere becomes inaccurate when ray focusing is large and is singular when neighboring rays converge. Well-known examples are the skip distance and horizon ray focusing, where geometric-optics cannot be used and a higher order theory must be applied.

A new method, based on physical optics, removes the singularities inherent in the geometric-optics approach. The method defines a central Fresnel zone on the wavefront at the observation point. Standard ray tracing methods find the image of the zone in a Poynting sphere about the source. The ratio of the area of the zone to that of its image determines the divergence of a tube of rays leaving the transmitter and thus the spreading loss. Since the Fresnel Zone area is never zero, this method avoids singularities.

Computations by the physical-optics method for a concentric ionosphere were compared to geometric-optics fields and the Bremmer's full-wave solution. The physical-optics fields compare favorably with the Bremmer fields in the vicinity of the skip distance and converge to the geometric-optics field beyond the skip.

Concave-mirroring by Curved Field-aligned Irregularities in the F Region

by

Jerry A. Ferguson
Naval Ocean Systems Center
San Diego, CA

and

Henry G. Booker*
University of California, San Diego
La Jolla, CA

Abstract

The theory of spread F by Booker and Ferguson (1978) employing back-scattering from long field-aligned irregularities of ionization in the F region can be adapted for transequatorial propagation in the VHF band. The theory involves scattering by irregularities in planes perpendicular to the earth's magnetic field, combined with coherent behavior along the length of each field line. For specular reflection in a North-South vertical plane from field-aligned irregularities, curvature of the field-lines causes concave-mirroring that creates caustics and foci. For field-lines whose height above the earth's surface at the equator is between 400 and 1000 km, a caustic intersects the earth's surface for a ground-based transmitter whose magnetic latitude (North or South) is between about 10° and 20° . The caustic intersection is in the opposite hemisphere but is not in general at a location conjugate to the transmitter. It is suggested that the convergence effect associated with curvature of field-aligned irregularities is a significant feature of transequatorial propagation in the VHF band.

*Supported by NSF Grant ATM 78-02625

ESTIMATION OF THE EFFECTS OF
HORIZONTAL GRADIENTS IN REFRACTIVE INDEX
ON IONOSPHERIC PROAGATION PARAMETERS

Saul Silven
GTE Sylvania Incorporated
Mountain View, California 94042

Formulas are derived for the purpose of providing estimates of certain effects on ionospheric radio propagation due to the existence of horizontal gradients in refractive index. The estimates are derived as first-order variations from nominal values; the latter being computed on the basis of zero-gradient. The requirement for the estimation formulas is based on the desirability to avoid the use of expensive and time-consuming 3-dimensional ray tracing computer simulations. This is particularly desirable when such simulations cannot be justified in view of the uncertainties in the manner in which actual gradients can be modeled and parameterized.

Tabulated results are presented showing comparisons between values calculated from the formulas and those calculated via a 3-D ray tracing simulation, for given values of gradient in ionospheric critical frequency. The values calculated are angular deviations in azimuth and elevation and perigee altitudes for rays of nominal one-hop ground-to-ground paths.

A STUDY OF THE PROPAGATION AND DISPERSION OF TRAVELING
IONOSPHERIC DISTURBANCES

K.A. Ballard and M.G. Morgan

Radiophysics Laboratory, Thayer School of Engineering
Dartmouth College, Hanover, New Hampshire 03755

Traveling ionospheric disturbances (TID's) appear as large-scale transverse waves in the F-region, with frequencies of the order of 0.01 cycle per minute, which propagate horizontally over hundreds or even thousands of kilometers. These disturbances have been observed by various techniques over the past thirty years and, with C. O. Hines's classic paper in 1960 (Can. J. Phys. 38, 1441), are now generally accepted as being the manifestation, in the ionized medium, of internal atmospheric gravity waves. Dartmouth College operated a three-station ionosonde network in Vermont and New Hampshire from 1968 to 1974, in which one ionogram was taken at each station every two minutes. Seven large TID's in the 1969 data have been studied extensively. Two theoretical models which predict the propagation of gravity waves have come to our attention: one envisions the gravity wave energy as trapped in a thermally stratified atmosphere and propagating horizontally in a duct; the other describes the gravity wave as freely propagating and reaching the observer via direct and ground-reflected paths where lower frequencies travel to greater distances from the source. In light of these two models, we have reexamined the seven TID's from 1969 with particular attention given to the spectral composition of each disturbance. Fourier decomposition at a single station yields the spectral content as a function of height, while cross-spectral analysis yields coherence functions and the dispersion of the TID. By overlaying the coherence functions and power spectral densities it is possible to discriminate between the frequency composition of the TID and the statistical variations of the ionospheric background. Our preliminary results show some spectral shifting with height which is in qualitative agreement with the freely propagating model. We are presently re-activating the three-station ionosonde network in northern New England together with a fourth sounder in Bermuda. In view of their preponderant travel towards the south southeast, it is anticipated that large TID's observed in northern New England will also be observed in Bermuda and that a more definitive study of their propagation characteristics can be completed. We anticipate that some preliminary results will be available for this meeting.

SESSION H
WEDNESDAY PM 2:00-5:00
HUB 106B

OBSERVED AND PREDICTED PHENOMENA IN LABORATORY AND NATURAL PLASMAS

Chairman: F. W. Crawford
Stanford University
Stanford, CA

A METHOD FOR THE EVALUATION OF SOLAR CORONAL PLASMA PROPAGATION SPEEDS BY RADIO OCCULTATION OF SPACE PROBES

E. Lüneburg, Deutsche Forschungs- und Versuchsanstalt für Luft- und Raumfahrt E.V., Institut für Hochfrequenztechnik,
8031 Oberpfaffenhofen, W.-Germany
P.B. Esposito, Jet Propulsion Laboratory, Pasadena, Ca. 91103

As a new application of radio tracking data of spacecrafts undergoing solar occultations a method for the experimental determination of the radial speed of propagating solar plasma disturbances using single station, two-way, coherent S-Band Doppler data is described. The method exploits the spatial separation of the up- and downlink of the telemetry link between Earth station and space probe due to their different relative velocities w.r.t. the line-of-sight between Earth and probe. Solar plasma disturbances intersecting the up- and downlink at approximately the point of closest approach between the ray path and the Sun (p) embed a signature on the signal which is propagated to the receiving station directly along the downlink and time retarded along the detour path via the PLL probe transponder. The location of the resulting peak in the autocorrelation function of the Doppler residuals combined with a precise orbital determination program determines the propagation speed near p. The analysis makes use of the retarded Rytov solution for the propagation of the CW signal through the turbulent solar wind.

Data acquired from the sun probe Helios 2 during the time period April-June 1976 covering a p-region from several to about 60 solar radii in the ecliptic plane have been analysed. The spatial separation of up- and downlink at p is about 20.000 km. Generally a high or a low propagation speed has been observed varying from 600 to 1000 km/sec or 200-400 km/sec. The power spectra of the integrated Doppler residuals (phase) indicate a Kolmogorov spectrum for the electron density fluctuations in the solar wind (R. Woo et al, AP.J. 210, 568-574, 1976).

SOME FEATURES OF PARARESONANCE (PR) WHISTLERS

M.G. Morgan

Radiophysics Laboratory, Thayer School of Engineering
Dartmouth College, Hanover, New Hampshire 03755

Pararesonance (PR) whistlers, observed in the topside ionosphere by the Dartmouth receiver on Ogo 6, are examined. The study extends that of Walter and Angerami (J. Geophys. Res., 74, 6352, 1969) to higher frequencies and shows that the upper cutoff frequency of PR whistlers closely follows a $1/L^4$ dependence from 6 to 100 kHz (at $L = 2.90$ to 1.37 , respectively). Most PR whistlers are attached to paralongitudinal (PL) whistlers due, presumably, to intermode coupling. The 'walking trace', or unattached PR whistler reported by Walter and Angerami is evidently unusual. The upper cutoff frequency follows $1/L^4$ whether attachment occurs or not. Rising sawtooth appendages at the upper cutoff frequency are frequently seen on PR whistlers and an extension of the theoretical iso-frequency curves, plotted in travel time vs. observing latitude by Walter and Angerami, has been devised to produce this signature. The significance of the extension, in terms of ray tracing in Walter and Angerami's model, is left for a future undertaking. The terms pararesonance (PR) and paralongitudinal (PL) are suggested as preferable to preresonance and pralongitudinal which have been previously used.

DISPERSION CHARACTERISTICS OF PLASMA WAVE-PACKETS

by R. J. Vidmar and F. W. Crawford, Institute for Plasma Research, Stanford University, Stanford, CA 94305

The dispersion characteristics of plasma waves are typically expressed by dispersion diagrams, showing the frequency variation (ω , real) with wavenumber (k , real), from which inferences concerning phase and group velocities are drawn. Although this generally suffices for propagation in lossless plasmas, difficulties arise if the plasma is absorptive or unstable: the group velocity may be infinite or complex. In this paper a consistent definition of group velocity is used for lossless, absorptive and unstable plasmas, based on the saddle-point method of describing the propagation of wave-packets. It is suggested that an observational dispersion diagram is useful which effectively describes the results of complex ω, k measurements on wave-packets. The form of this dispersion relation and its dependence on the source exciting the wave-packets are established. The results have application to ionospheric ray tracing and instabilities in inhomogeneous plasmas.

TRANSMISSION AND REFLECTION OF WAVES FROM A MAGNETOPLASMA
BY AN INVARIANT METHOD

Hollis C. Chen
Department of Electrical Engineering
Ohio University
Athens, Ohio 45701

Based on the eigenvectors of a wave matrix, an invariant method is presented in this paper to unify and systematize the analysis of transmission and reflection of waves from a magnetoplasma. The incident wave may have any polarizations. The results, all in invariant forms, include (1) the dispersion equation of a magnetoplasma, (2) the directions of field vectors, (3) the Booker quartic equation, and (4) the transmission and reflection coefficient matrices. The distinct advantage of the invariant method over the conventional one is that the former eliminates the necessity of coordinate systems. The results thus obtained are therefore general and easily correlated to experiments.

RESONANT ABSORPTION OF RADIATION IN THE SHEATH OF A
COLD PLASMA SURROUNDING A WIRE CARRYING A PRESCRIBED
PERIODIC DRIVING CURRENT;

M.P.H.WEENINK and S.NAGARAJAN
Technische Hogeschool Eindhoven
The Netherlands

A straight conducting wire along the z -axis carries a prescribed periodic current proportional to $\exp j(kz - \omega t)$. This current excites transverse electromagnetic waves and a longitudinal wave in the cold plasma in which the wire is embedded. The plasma is taken inhomogeneous in the radial direction. The driving frequency ω is such that it is resonant with the local plasma frequency in the inhomogeneous region (the sheath). The energy of the plasma wave is partially resonantly absorbed by the same mechanism as described by Sedláček, Barston, Crawford, Weenink and Abels. The energy loss is exactly calculated. The conversion of the absorbed energy into heat and other modes is considered in detail.

ELECTROMAGNETIC PULSE (EMP)
PROPAGATION THROUGH A PLASMA

R.N. Carlile, A. Cavalli, W.L. Cramer, M.E. Dunham,
and W.A. Seidler*, University of Arizona.

We have pursued an experimental investigation of the propagation of an EMP through a plasma in order to determine the ability of the so-called swarm model (moments of the Boltzmann equation) to predict the details of propagation. This model has been used traditionally by the Air Force to predict EMP generation and propagation due to a nuclear detonation. We are conducting a series of experiments in which an EMP-type pulse is propagated down a plasma filled waveguide.

We find that for an input EMP duration of 3 nanoseconds, that the pulse emerging from the output persists for nearly an order of magnitude longer in time, and then develops a ringing character. The swarm theory also predicts this general qualitative behavior. Quantitatively, however, we find experimentally that there is much more energy absorption by the plasma from the pulse than is predicted theoretically. We shall discuss reasons for this important discrepancy.

*Permanent address: Jaycor Corp., Del Mar, CA.

FLUID THEORY OF PLASMA DOUBLE-LAYERS

by J. S. Levine and F. W. Crawford, Institute for
Plasma Research, Stanford University, Stanford, CA 94305

A double-layer consists of two oppositely-charged space-charge layers in close proximity, and may occur in space or laboratory plasmas. In this paper, we use a fluid model to analyze the double-layer constituting the transition region between two homogeneous semi-infinite plasmas of different densities and temperatures. Four populations of particles are accounted for: electrons transmitted through the double-layer from Plasma 1 (at potential $\phi = 0$) to Plasma 2 (at potential $\phi = \phi_0 > 0$), ions transmitted from Plasma 2 to Plasma 1, and ions in Plasma 1 and electrons in Plasma 2 that are reflected from the double-layer. Self-consistent relations are established between the particle streaming velocities, temperatures and densities, and the double-layer length and potential step. Comparisons are made between predictions of the theory and data available from space and laboratory experiments on double-layers.

NONLINEAR EFFECTS IN WAVEGUIDE EXCITATION
OF LOWER HYBRID WAVES

R.W. Motley and W.M. Hooke
Princeton University, Plasma Physics Laboratory
Princeton, New Jersey 08540

Radio frequency heating of toroidal plasmas near or above the lower hybrid frequency possesses distinct technical advantages over other types of RF heating: high power sources in the gigahertz range already exist; phased waveguide arrays should present minimal interference with the cooling and shielding functions of a reactor blanket. Both low power tests and experiments on Tokamaks have demonstrated efficient wave launching and wave absorption, provided the wavelengths satisfy the accessibility criterion and the frequency is near the lower hybrid frequency, $\omega_{LH} = \omega_{pi} / (1 + \omega_{pe}^2 / \omega_{ce}^2)^{1/2}$.

The viability of this heating method will depend to a large extent on the magnitude of the wave power that can pass unattenuated through the surface plasma layers and thereby on the nonlinear properties of the plasma near the throat of the waveguide. To heat plasmas in a toroidal reactor will require a power flux in excess of 1 kW/cm^2 . In several heating experiments on Tokamaks this figure has already been exceeded; these experiments have also demonstrated a breakdown of the linear coupling theory, in that the wave reflection becomes independent of the phasing between adjacent waveguides.

In this paper we report results of high power lower hybrid wave excitation in a test plasma in which the linear theory has been extensively studied and verified. Short pulses (1-5 μ s) of power (up to 8kW) at 2.5 GHz are applied to two elements of a 4-waveguide array placed at the surface of an overdense ($n/n_c \sim 20$), magnetically confined (<15kG) plasma column. At this power level $E^2/8\pi n k T \approx 1$ at the $\omega = \omega_{pe}$ layer where the electrostatic waves are generated.

At low power the predictions of linear theory are recovered; i.e., optimum coupling efficiency (>90%) occurs if the waveguides are excited 180° out of phase. First measurements at high power show that the reflectivity becomes less dependent on waveguide phasing and that a plasma crater, perhaps 2 or 3 mm deep, is created in the plasma near the mouth of the waveguide.

AMPLITUDE AND PHASE MODULATION OF A WAVE
DUE TO NONLINEAR WAVE-WAVE INTERACTIONS

Y.C. Kim and E.J. Powers
Department of Electrical Engineering
and
Electronics Research Center
University of Texas at Austin
Austin, Texas 78712

When a large amplitude wave propagates in a nonlinear dispersive medium, one of the most significant consequences of nonlinearity is the appearance of amplitude dependence in a dispersion relation which results in a nonlinear frequency shift, i.e., the wave undergoes modulation in amplitude and phase. Therefore, the experimental determination of the amplitude and phase modulation of the carrier wave is an important problem with respect to understanding the physics of nonlinear wave modulation. We have investigated the relationship between the characteristics of the modulation spectrum and the physics of the nonlinear wave interaction as described by a coupling coefficient. When the coupling coefficient has a weak dependence on the wavenumber, the ratio of amplitude to phase modulation indices is proportional to a variation of the coupling coefficient with respect to the wavenumber. It also turns out that when the coupling coefficient is an increasing function of the wavenumber, the amplitude of lower sidebands are larger than those of the upper sidebands, and vice versa. Furthermore, when the lower sidebands are dominant compared to the upper sidebands, the amplitude modulation is completely out of phase with respect to the nonlinear frequency shift (which is just the negative time derivative of the phase modulation). The experimental observation of nonlinear modulation of an ion wave in an rf-excited weakly ionized plasma is found to be in a good agreement with the theoretical predictions.

SESSION NL-1
THURSDAY AM 8:30-12:00
HUB ROOM 106B

NONLINEAR ELECTROMAGNETICS I

Chairman: N. Marcuvitz
Polytechnic Institute of New York
Farmingdale, NY

NLI - 1

Introductory Remarks

P. L. E. Uslenghi
University of Illinois at Chicago Circle
Chicago, IL

HISTORY OF THE SOLITARY WAVE

A. C. Scott
Department of Electrical and Computer Engineering
University of Wisconsin
Madison, Wisconsin 53706

The course of solitary wave studies is traced from the original hydrodynamic investigations of Russell (1834) and the nerve impulse measurements of Helmholtz (1850) and Bernstein (1868) through the development of the soliton concept by Zabusky and Kruskal (1965) to the recent proliferation of solitary wave research in applied mathematics, solid state physics, hydrodynamics, nonlinear optics, neurodynamics, plasma waves, nonlinear acoustics, meteorology, and the structure of elementary particles.

Solitons as Particles and as Collective Excitations

by

D. W. McLaughlin*

Program in Applied Math
University of Arizona
Tucson, Arizona 85721

Solitons are described from two alternative points of view - as particles and as collective excitations. Concrete physical examples of each viewpoint will be emphasized.

Particle properties of solitons include their localization in space, their stability, their dynamical response to exterior forces, and their statistical behavior. This analogy with particles leads to rather simple calculations which describe the dynamical and statistical behavior of solitons.

Alternatively, solitons are collective excitations of the underlying micro-structure. The collective properties of solitons include their internal degrees of freedom and their decay into different types of solitons and into radiation. This collective interpretation of solitons leads to their complete description by a mathematical transform known as the inverse spectral transform.

Finally, some very recent results from the theory of the inverse spectral transform are mentioned.

*D. W. McLaughlin is supported, during the academic year 1978-79, by the United States Dept. of Defense, T-Division, Los Alamos Scientific Laboratory.

QUASIPARTICLE METHOD IN NONLINEAR WAVE PROPAGATION

N. Marcuvitz
Polytechnic Institute of New York
Long Island Center
Farmingdale, New York 11735

Abstract

Wave propagation in nonlinear media is characterized by both fast and slow space-time behavior. In several methods of analysis the fast behavior is averaged out and propagation properties are calculated from the slow space-time dependence of the wave fields. The latter are often decomposable into wavepackets representative of the "mode types" comprising the overall field. Single mode type wavepackets represent a concentration of momentum and energy that can be viewed as a system of quasiparticles. A quasiparticle is described at time t by its position $x(t)$, momentum $k(t)$, and energy $\omega(k,x,t)$ with the latter defined by the dispersion relation descriptive of the relevant mode type. The average space-time dependent amplitude, wavenumber, frequency, etc., characteristics of a propagating wavepacket can then be inferred from corresponding dynamical properties of the quasiparticle system. The latter properties can be defined either kinetically or fluid dynamically and permit the determination of the average space-time dependent density, momentum, energy, etc., indicative of the above mentioned wavepacket characteristics. Features of such quasiparticle analyses peculiar to nonlinear wave propagation will be described with emphasis on physical significance and adaptability to computer graphing.

LAGRANGIAN METHODS IN NONLINEAR PLASMA WAVE INTERACTION

by F. W. Crawford, Institute for Plasma Research,
Stanford University, Stanford, CA 94305

Analysis of nonlinear plasma wave interactions is usually very complicated, and simplifying mathematical approaches are highly desirable. The application of averaged Lagrangian methods offers a considerable reduction in effort, with improved insight into synchronism and conservation (Manley-Rowe) relations. This paper will illustrate how suitable Lagrangian densities have been defined, expanded, and manipulated to describe nonlinear wave-wave and wave-particle interactions in the microscopic, macroscopic and cold plasma models. Recently, further simplifications have been introduced by the use of techniques derived from Lie algebra. These and likely future developments will be reviewed.

NONLINEAR INTERACTIONS BETWEEN ELECTROMAGNETIC WAVES
AND BIOLOGICAL MATERIALS IN THE FREQUENCY RANGE BELOW 10 GHz

Invited Paper

Frank S. Barnes
Department of Electrical Engineering
University of Colorado
Boulder, Colorado 80309

This paper will review four categories of nonlinearities which may affect the biological characteristics of the interaction between microwaves or radio frequency waves and biological materials. In particular, we will present both theoretical and experimental data with respect to the following four nonlinearities: (1) Barriers or membranes which may possess either nonlinear resistance or reactive characteristics; (2) Nonlinearities associated with the alignment of long chain molecules and structures with dielectric properties different than their surroundings; (3) Associated with thermal changes in both the resistivity and the dielectric constant; (4) Quantum phenomena, in particular with respect to saturation of quantum transitions as a function of the frequency and the concentration. Multiple quantum transitions will also be considered.

In the first case, we will review theoretical predictions for nonlinear characteristics of membranes and the possibility of nonlinear reactive components. An attempt will be made to indicate the correspondence to the work of Seamen and Wachtel on the ganglion pacemaker of *Aplysia*.

In the second case, we will examine theoretically the forces for alignments of dielectric bodies of different dielectric constants from their surroundings, threshold phenomena for the alignment and transit time for their orientation along field lines. In addition to that, the implication of this in solutions vis-a-vis the Wien effect and selection of some new phenomena related to a resonance in the nonlinearity of the resistance at approximately 4 kilocycles will be discussed. Also included will be the effects of the nonlinear viscosity for the movement of very large molecules through a fluid.

The effect of changes in temperature in both the resistivity and the dielectric properties of materials will be briefly examined and implications discussed in terms of changes in viscosity of fluids and biochemical reactions. Additionally, some unexplained experimental results on the disappearance of membranes when exposed to high field pulses will be discussed as a portion of the mechanisms associated with tissue damage. These results include some nice electron micrographs of neuroblastoma cells which have been exposed to microsecond pulses at 2.7 GHz and fields of 2 KV/cm where some of the membranes have disappeared. The calculated temperature rise is less than 4°C.

Elementary Quantum phenomena will be reviewed with particular emphasis on the nature of experiments which need to be performed to illuminate this phenomena. The effects of power levels on saturation as a function of the density of the resonant molecules and their line widths will be discussed. The probability for multiple quantum transitions and the required signal levels will also be reviewed. Some very brief speculation will be given to possible ideas of this mechanism being involved in the power window effects observed by Ross Adey and Fred Rosenbaum in their experiments on calcium shift at the surface of membranes and in the generation of genetic defects in corn meal worms.

SESSION NL-2
(Co-sponsored by B and BEMS)
THURSDAY PM 1:30-5:00
HUB 106B

NONLINEAR ELECTROMAGNETICS II

Co-chairmen: F. S. Barnes, University of Colorado, Boulder, CO
W. R. Adey, Veterans Administration, Loma Linda, CA

BIOLOGICAL SENSORS FOR THE DETECTION
OF ELECTRIC AND MAGNETIC FIELDS

Ad. J. Kalmijn, Woods Hole Oceanographic Institution, Woods Hole, Massachusetts 02543.

Marine sharks, skates, and rays are endowed with a keen electric sense, enabling them to detect dc and low-frequency voltage gradients as low as $0.01 \mu\text{V}/\text{cm}$. The pertinent receptors are the ampullae of Lorenzini, located in the protruding snouts of these ancient fishes. In predation, they use their electric sense to cue in on the bioelectric fields emanating from the prey as has been demonstrated in both laboratory and field experiments. When drifting with ocean currents, they may sense the upstream and downstream directions by detecting the electric fields induced by the water flowing through the earth's magnetic field. In addition, they may sense their magnetic compass headings by detecting the fields they induce by actively swimming through the earth's magnetic field. The animals' ability to orient relative to uniform electric and magnetic fields of natural strengths has recently been established in successful training experiments.

The main groups of freshwater fishes sensitive to dc and low-frequency voltage gradients are the weakly electric fishes, the catfishes, and the lower bony fishes (e.g., the sturgeon and the paddlefish). While these freshwater species are less sensitive than the marine sharks, skates, and rays, the fields they encounter are correspondingly stronger. Again, the bioelectric fields play a role in predation, whereas the inanimate fields are used for orientation. In the freshwater habitat, however, the prevailing abiotic fields are of electrochemical rather than electromagnetic origin. Besides the low-frequency sensory system, the weakly electric fishes have higher-frequency receptors, tuned to the detection of their own electric-organ discharges. With this higher-frequency system they not only signal and detect each other, but they also probe their physical environment electrically, sensing nearby objects as impedance non-uniformities.

Regarding the recently discovered ferromagnetic orientation mechanism, see abstract "Navigational Compass in Magnetotactic Bacteria" by Frankel *et al.* in this volume.

Ad. J. Kalmijn, in: Handbook of Sensory Physiology, Vol. III/3 pp. 147-200, A. Fessard ed. Springer-Verlag: New York 1974.
Ad. J. Kalmijn, in: Animal Migration, Navigation, and Homing, pp. 347-353, K. Schmidt-Koenig and W.T. Keeton, eds. Springer-Verlag: New York 1978.

This project has been conducted under the auspices of the Office of Naval Research.

THE SENSITIVITY OF BIOCHEMICAL REACTIONS TO
WEAK OSCILLATING STIMULI

L. K. Kaczmarek
Division of Biology
California Institute of Technology
Pasadena, CA 91125

The sensitivity of biochemical reactions to external stimuli will be considered from two points of view. The first concerns the behavior of a radiolabeled tracer in a biochemical system that oscillates either because of non-linearities in the kinetics of the reactions or because of coupling to an external oscillator. It can be shown by both analytical methods and numerical computations that the rate of flux of a labeled tracer through a reaction step whose rate is oscillating is a function of the amplitude of the oscillation. In general, the flux of the tracer is greater for an oscillating state than for a stationary steady state system which maintains the same mean concentrations, mean total metabolite flux and overall affinity as the oscillating system. These findings imply that measurement of metabolite fluxes by radiolabeled tracers is a sensitive method of detecting oscillations induced in a reaction scheme by external stimuli, particularly when the oscillations are of a frequency that precludes the determination of metabolite concentrations at each time point in a single cycle.

The second aspect concerns the frequency sensitivity of non-linear reaction schemes to external perturbations. A model biochemical system that is particularly sensitive to external perturbations over a restricted range of frequencies has been studied by numerical computation. The basis of the model resides in the interaction of oscillating stimuli with a limit cycle generated by non-linearities in the reaction kinetics.

Both of these topics will be discussed in the light of experimental observations of altered fluxes in cerebral calcium ion binding during exposure to amplitude modulated VHF fields.

LOW FREQUENCY ELECTROMAGNETIC INDUCTION OF
ELECTROCHEMICAL INFORMATION AT LIVING CELL MEMBRANES:
A NEW TOOL FOR THE STUDY AND MODULATION
OF THE KINETICS OF CELL FUNCTION

Arthur A. Pilla
Bioelectrochemistry Laboratory, Orthopaedic Research Laboratories
College of Physicians and Surgeons
and
Department of Applied Chemistry and Chemical Engineering
Columbia University
New York, New York 10032

The manner by which living cells can respond in real time to the induction of low level, low frequency pulsating current has been proposed to be via transient electrochemical surface processes. The cell may then exhibit a non-linear response if there is a net change in the rate of a given functional process. Modeling and verification of the impedance of living membranes in which surface coupled transport processes are taken into account indicates the possibility that electrochemical surface steps are involved in the regulation of some cell functions. This has allowed the definition of a family of induced current waveforms which have been shown to be effective in in vitro and in vivo experiments. Pulsating currents configured to excite either surface of surface coupled transport have been chronically applied to affect the "de-differentiation" of amphibian red blood cells, Ca^{++} kinetics in isolated embryonic chick limb rudiments, rate of healing of artificially induced bone fractures in the rat, and the healing of recalcitrant bone fractures in the human.

NONLINEAR IMPEDANCE AND LOW FREQUENCY RESONANCE
OF POLYELECTROLYTE UNDER HIGH SINUSOIDAL FIELDS

Chia-Lun J. Hu
Department of Electrical Engineering
University of Colorado
Boulder, Colorado 80309

ABSTRACT

This paper reports a new method of studying the complex impedance of a biological or polyelectrolytic solution under high sinusoidal voltages, and some new results under these high voltages, namely, a nonlinear effect at about 1000 V/cm and a low frequency resonance effect at around 4 KC. The medium we used is sodium polystyrene-sulfonate (NaPSS). The method we employed is a novel "thin-film" i-v sampling scheme. With this method, we can avoid the Ohmic heat damage and therefore, the results are reproducible. The complex impedance and the nonlinearity of the sample can be calculated by the reproducible curves shown on an oscilloscope. A summary of these results is included in the text. A preliminary theory explaining these phenomena and possible applications to, say, low frequency safety standards, are proposed.

SUMMARY

This paper reports some new experimental results of nonlinear and resonance phenomena we observed when a high, sinusoidal voltage is applied to a biological or polyelectrolytic solution. Using sodium polystyrenesulfonate (NaPSS) as samples, we found a significant nonlinear effect of impedance at about 1000 volt/cm (peak-to-peak) with frequency below 1 KC, and a sharp resonance effect of impedance near 4 KC. The method we used for applying the high sinusoidal voltage which cuts down significantly the thermal damage due to Ohmic heating is a novel one - we used a pair of "thin-film" electrodes with a narrow gap of 2 mm between them for applying the high voltages. We then deposited a thin layer of NaPSS solution across these electrodes as shown in Figure 1. This thin layer structure of solution makes the highly conductive sample highly resistive because its cross section is very small. Therefore, it suppresses significantly the Ohmic heat. The small heat generated in this thin layer of sample can then be conducted away efficiently by means of the aluminum electrodes and the contacting glasses. With this method, our sinusoidal high voltage experiments can be reproduced without significant thermal damage.

The impedance measuring method we used is a current-voltage sampling scheme as shown in Figure 1. In Figure 1, because the resistance (10 ohms) of the current sampling resistor r is much smaller than that of the thin-film sample (10 K Ω to 100 K Ω), the current flowing through r will be about the same as that flowing through the sample as if there were no r connected in. Therefore, monitoring the voltage drop across this r by means of a dual trace

oscilloscope will give us the wave form of the current flowing through the sample. On the other hand, monitoring the voltage drop across the voltage source will approximately give us the wave form of the voltage across the sample. From these two wave forms displayed on the oscilloscope, we can not only calculate both the phase and magnitude of the complex impedance of the sample, but also detect the occurrence of the nonlinearity of the sample by observing the appearance of the non-sinusoidal current wave form on the scope. Sweeping the frequency, we can then obtain an "impedance spectrum" * of this sample. A typical nonlinear effect of NaPSS under high voltage is shown in Figure 2 and a typical impedance spectrum of NaPSS under high voltage is shown in Figure 3. It is seen that a resonance effect under high field is obvious near 4 KC where $|Z|$ is maximum and $\angle Z$ is zero. It is also seen that the nonlinearity decreases as frequency increases. These nonlinear and resonance effects are not observed when a saline sample is used.

A preliminary theory using tank circuit resonance property with inertia of polyions taken into account is proposed. A detailed literature search (with 70 references found from 1929 to present) in both fields of electrochemistry and bioelectrical engineering has been carried out which shows that the method and results reported here are unique.

Applications of this study may be the following:

1. Identify the dangerous low frequency zones of bio-mediums under high fields due to the resonance effect. Determine the threshold field strength.
2. Study the nonlinear movements of the giant molecules under high fields.
3. Determine molecular weights and nonlinear mobilities of polyions by means of the resonance data obtained at low frequencies.

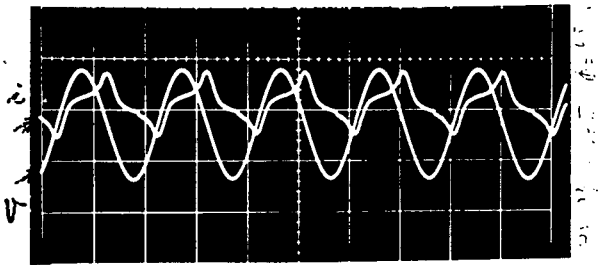


Figure 2. i, v curves for a polymer sample

Figure 2.1: $f = 0.1$ KC, vertical scales 10 V/cm for V and 0.02 V/cm for i (or 2 ma/cm, $V_r = 10\Omega$ (see Figure 1)

* Impedance under non-sinusoidal i is defined by calculating the phase difference and the magnitude ratio between two peak points of the i, v curves shown on the oscilloscope.

NEURONAL MEMBRANES AS DETECTORS OF RF FIELDS

H. Wachtel
Department of Biomedical Engineering
Duke University
Durham, North Carolina 27706

The effects of RF, or microwave, fields on the firing pattern of nerve cells often resembles that produced by low frequency fields (0-10 kHz) or by the application of low frequency currents directly across the neuronal membrane. We have noted such similarities in our studies of the response of endogenously firing (pacemaker) *Aplysia* neurons to microwaves (at 1.5 and 2.45 GHz) and to ELF fields (0.1 to 1000 Hz) as well as to transmembrane currents injected via intracellular microelectrodes. Since the ambient firing rates of these particular neurons is extremely steady, small perturbations in response to fields, or intracellular current injection, can be taken as definite indicators of a "threshold" effect. In terms of ELF current densities, such thresholds are observed at about 10^{-8} amps/cm² for intracellular currents and as low as 10^{-6} amps/cm² for ELF fields of optimal direction and frequency. For microwave fields, thresholds for analogous effects (which are not thermally based) are seen at an S.A.R. of about 1 Watt/kg which, for *Aplysia* neural tissue, implies a microwave current density of about 10^{-3} amps/cm². The effects of either the microwave or the ELF fields can be directly offset by simultaneously applying an opposing intracellular current through the recording microelectrode. Thus it appears that roughly 0.1% of the microwave current is "detected" as an equivalent ELF current and about 1% of this amount is effectively acting as a net transmembrane current. The overall microwave detection efficiency is therefore of the order of 10^{-5} --a small value, but one that is sufficient to account for the observed changes in firing pattern.

The most likely site of this detection process is the membrane itself which is known to have highly nonlinear electrical characteristics at low frequencies. The rectification efficiency of neuronal membranes falls off sharply for RF currents but, as recent models have indicated, it may be adequate to explain these microwave effects. Alternatively the detection process may be based on more complex "cooperative" interactions between the RF field and the functional state of the membrane. In either case, it appears that a small, but significant, amount of RF energy is converted to ELF currents (by an essentially nonlinear detection process) and it is these currents which are actually producing the firing pattern changes.

A NONLINEAR MICROWAVE RADIATION EFFECT ON THE PASSIVE
EFFLUX OF SODIUM AND RUBIDIUM FROM RABBIT ERYTHROCYTES

Robert B. Olcerst*
New York University Medical Center
Institute of Environmental Medicine

The passive efflux rates of sodium-22 and rubidium-86 from the red cells of male New Zealand white rabbits were measured in vitro after one hour irradiations at 2.45 GHz. The temperature of the samples and the power absorbed were controlled. Arrhenius plots of measurements made in the absence of radiation exposure revealed that both the sodium and rubidium efflux have four separate linear regions with transitions at 8-13, 22.5 and 36°C. The efflux rates with microwave exposure were identical to the control rates, except at the critical temperatures, where irradiation increased the efflux of both cations. This response was examined at the 22.5°C phase transition at three specific absorption rates (100, 190, 390 mW/gm). At all three levels the cation efflux was statistically greater than one would predict from a strictly thermal response. The response does not increase monotonically as a function of absorbed power. Similar increased cation efflux was also observed near the 36°C and 8-13°C transitions. The data suggest that the existence of two phases within the membrane is necessary for the observation of the increased efflux. Mechanistic interpretations of these observations are discussed.

* Present address: IBM, P.O. Box 390, Department 348,
Building 224, Poughkeepsie, NY 12602.
All correspondence should be sent to
this address.

INDUCTION OF CALCIUM ION EFFLUX FROM BRAIN TISSUE BY
R.F. RADIATION: EFFECT OF SAMPLE NUMBER AND
MODULATION FREQUENCY ON THE FIELD-STRENGTH WINDOW

C.F. Blackman, S.G. Benane, J.A. Elder,
D.E. House, J.A. Lampe, and J.M. Faulk
Experimental Biology Division (MD-72)
Health Effects Research Laboratory
US Environmental Protection Agency
Research Triangle Park, NC 27711

We have reported changes in calcium ion binding to brain tissue exposed *in vitro* to a specific field-strength (0.75 mW/cm^2) of 147-MHz radiation, amplitude modulated by a 16-Hz sine wave. We report here three extensions of that work. The original finding has been replicated under more rigorous conditions: the results of each exposure condition were paired with the results of sham-exposures conducted at the same time.

To more precisely define the range of effective field-strengths, two different numbers of samples were treated in our Crawford cell with 147-MHz radiation, sinusoidally modulated at 16-Hz; in one series, four brain tissues were exposed at a time, while in the other series, four brain tissues and six dummy loads were exposed at a time. Unlike the narrow field-strength-window found for four samples, the ten pseudo-sample configuration resulted in a broader field-strength-window similar to that recently described by Adey *et al.*, who used a far field exposure situation. The reason for the sample-number dependence is unknown.

The ten pseudo-sample configuration was also used to test for the presence of the field-strength-window at a sinusoidal modulation frequency of 9-Hz. Preliminary findings indicate a response curve essentially identical to the one found for 16-Hz sine-wave modulation.

NONLINEAR MECHANISMS IN ELECTRICAL TRANSDUCTIVE
COUPLING AT NERVE CELL MEMBRANES

A. R. Sheppard and W. R. Adey
VA Medical Center, Loma Linda, CA 92357 and Depts. Physiology
and Surgery, Loma Linda University School of Medicine, CA 92350

Surfaces of cell membranes are the site of immunological and endocrine interactions and electrochemical events in nervous excitation. This broad range of biological signaling is typified by focal events at specific receptor sites and spread of altered molecular organization to remote points. Ca ions are essential in all these sequences, mediating altered molecular organization in membrane surface glycoprotein strands, which serve both as receptor sites and as signaling devices to adjacent similar strands and to intracellular elements, including microfilaments. Binding and release of Ca in cerebral tissue mirrors nonlinearities in transductive coupling of weak EM fields. Ca triggers its own release and release of amino acid transmitter GABA from awake cerebral cortex in a highly nonlinear fashion, suggesting a cooperative interaction. Response to an increment of 0.5 mM is within a factor of two to that from a 20 mM increment. Stimulation of awake cerebral cortex with low frequency gradients of 50 mV/cm (similar to EEG) increases $^{45}\text{Ca}^{2+}$ and ^3H -GABA efflux by almost 20% for a stimulating gradient of less than 1.0 μV across synaptic terminals 0.5 μm in diameter. Stimulation of isolated chick cerebral hemisphere with 147 or 450 MHz fields inducing similar tissue gradients (10-100 mV/cm) also raises $^{45}\text{Ca}^{2+}$ efflux, but only with field amplitude modulation at frequencies from 6-20 Hz. There is also an intensity "window" for this RF field effect between 0.1 and 1.0 mW/cm^2 , with tissue gradients centered around 50 mV/cm. Strong nonlinearities in this $^{45}\text{Ca}^{2+}$ response pattern occur with respect to tissue H^+ and HCO_3^- concentrations. La blocks transmembrane movement of Ca, and persisting field effects are interpreted as arising at a class of cell-surface field sensitive Ca binding sites. Neuronal and neuroglial membrane potentials fall linearly with temperature at 1-2 mV/c between 37 and 33C, but decrease exponentially below this level. Pentobarbital or urethane anesthesia prevent this depolarization down to 25C. Topical 20 mM Ca solutions also prevent the depolarization of transient cooling, suggesting action at membrane sites common to those binding these anesthetic substances. Cooperativity is suggested in step-like decreases in membrane potential during repeated cortical cooling and in binding processes at immunoreceptor sites on lymphocytes in patching and capping. In smooth muscle, accumulation of Na^+ and K^+ with changing external K^+ concentration is step-like between 12 and 17C and fits a model of cooperative interaction between nearest neighbor cytoplasmic binding sites. Cooperative reactions occur in systems in which, by the expenditure of energy, one parameter is held far from equilibrium. Structurally defined domains with raised energy levels distinguish the cooperative region from its surround. By partitioning into phases, entire subsystems could be affected by a trigger which may be at or below the full spectrum kT noise level. Highly nonlinear energy dependence of tunneling probabilities suggests that quantum mechanically switched ionic fluxes into cooperative domains trigger the membrane and cellular responses. Supported by FDA (BRH) Contract 1 R01FD-678-01 and ONR Contract N0014-76-C-0421.

SESSION NL-3
(Co-sponsored by AP-S and B)
FRIDAY AM 8:30-12:00
HUB 106B

NONLINEAR ELECTROMAGNETICS III

Chairman: A. C. Scott
University of Wisconsin
Madison, WI

ANALYSIS OF MILD NONLINEARITIES IN ELECTROMAGNETIC
SYSTEMS USING THE VOLTERRA-SERIES APPROACH

Tapan K. Sarkar
Department of Electrical
Engineering
Rochester Institute of Technology
Rochester, New York 14623

Donald D. Weiner
Department of Electrical
Engineering
Syracuse University
Syracuse, New York 13210

Abstract: The Volterra-series approach differs from conventional time-domain solutions in that individual frequency components in the output can be determined directly without the need to perform a fast Fourier transform on the total time domain solution. This is an important advantage when frequency components are of small magnitude compared to the total waveform. In this method the response at any intermodulation frequency is obtained by solution of the linearized equivalent network in which the nonlinearities appear as known excitations. The paper will illustrate how this method can be used

- (1) for scattering analysis of nonlinearly loaded antennas in the presence of an imperfectly conducting ground (APS, March 1976, pp 125-131 & EMC, May 1978, pp 278-288)
- (2) for analyzing nonlinear microwave circuits using the scattering matrix technique.

NONLINEARLY LOADED ANTENNAS

Giorgio Franceschetti
 Communications Laboratory,
 University of Illinois at Chicago Circle
 and Department of Electrical Engineering,
 University of Naples, Italy

Nonlinearly loaded wire or loop antennas are usually studied by solving the nonlinear integral equation

$$(1) \quad v(t) = v_g(t) - \int h(t - t')i[v(t')] dt'$$

where $v_g(t)$ is the voltage at the antenna terminals, $v(t)$ the voltage across the load and $h(t)$ the unit response of the antenna (Fourier transform of input impedance). Successive iterations of (1) and rearrangement of terms lead to a Volterra-type series (Volterra, 1930), which has been applied to lumped circuits by several authors (Wiener, 1942, 1958; George, 1960; Zames, 1960; Parente, 1966). Criteria for convergence have been discussed by Flake (1963) and Krasnov, Kiselev and Makarenko (1971).

Application to antenna problems is more recent and has been performed assuming a purely resistive nonlinear load. In the first part of this paper we relax this hypothesis by considering reactive nonlinearity (above 700 MHz the effect of nonlinear capacitance becomes dominant for hot-carrier diodes). Basic limitations of the Volterra-series method are outlined: analytical description of the nonlinearity, acceptable truncation of the resulting series only in the mildly nonlinear range.

In the second part of the paper we present a different method (PHB method, Baily, 1968) which is based on the representation of all state variables in Fourier series and on solving for the coefficients of the expansion with a minimizing square-root algorithm. Application of this method to lumped circuits (Nakhla and Vlach, 1976) makes use of the gradient method, thus still postulating an analytical description of the nonlinearity. We introduce a different method, based on the Fibonacci golden-section rule, which allows for the inclusion of arbitrary nonlinearities. The excellent performance of our method is illustrated by applications to wire and spiral antennas. This research was performed under grant AFOSR-77-3253.

THE CHARACTERISTICS OF A TRAVELING-WAVE, LINEAR ANTENNA
WITH A NONLINEAR LOAD

Motohisa Kanda
Electromagnetic Fields Division
National Bureau of Standards
Boulder, Colorado 80303

Abstract

This paper discusses the characteristics of a traveling-wave, linear antenna with a nonlinear load. The theoretical technique used for analyzing the antenna is the time-stepping, finite-difference equation method with the Newton-Raphson technique. Differential equations are solved using the time-stepping, finite-difference equation method, whereas the nonlinear effect is treated by the Newton-Raphson iteration technique.

A beam lead Schottky barrier diode, which is used as a nonlinear load, is modeled by a nonlinear resistance R_n and a nonlinear junction capacitance C_j , as well as by a linear series resistance R_s , a linear package capacitance C_p , and a lead inductance L . The nonlinear resistance R_n can be described by the diode i - V characteristics, modeled as:

$$i = i_s(e^{\alpha V} - 1),$$

where i is the current (amperes), V is the voltage (volts) across the diode junction, i_s is the saturation current (amperes) which is assumed to be 2×10^{-9} A, and $\alpha \cong 38 \text{ V}^{-1}$. The nonlinear capacitance C_j is represented by:

$$C_j(V) = \frac{C_j(0)}{(1 - V/V_b)^{1/2}},$$

where $C_j(0)$ is the zero bias junction capacitance, typically 1 pf, and V_b is the built-in potential, typically 0.45eV for the beam lead Schottky barrier diode.

The dynamic range and the transfer function of the traveling-wave antenna with a beam lead Schottky barrier diode used as a nonlinear load are evaluated. Physical insight into the nonlinear response of the antenna will be given by a qualitative discussion of the effects of skewness and distortion of detected time-domain electromagnetic (EM) waves.

A TIME-DOMAIN COMPUTER CODE FOR NONLINEAR CIRCUITS
AND THIN-WIRE ANTENNAS

Jeremy A. Landt
Los Alamos Scientific Laboratory
Los Alamos, NM 87544

The response of a system consisting of antennas and circuit elements is typically found by considering the antenna response and the circuit response separately. Subsequently, these two responses are combined using the parameters of each determined at the terminals where the antenna and circuit are connected. These techniques can employ experimental as well as analytical methods. Here, an alternate technique is presented. The antenna portion of the network is treated by application of the method of moments to a time-domain, thin-wire electric-field integral equation. The circuit portion of the network is analyzed by time-domain nodal equations. Combination of these two types of equations allows a self-consistent solution to be obtained directly in the time domain. Nonlinear circuit elements are easily accommodated and wideband responses are economically calculated.

The numerical procedure is an addition to the technique developed by Miller, et al. (J. Comput. Phys., 12, 24-48, 1973). Development of the numerical procedure is followed by a discussion of code limitations and guidelines. The paper concludes with several examples that illustrate the technique's capability. One of these is given in Fig. 1, which compares the tuned and untuned performance of a voltage doubler connected to a quad loop antenna illuminated by a sinusoidal plane wave.

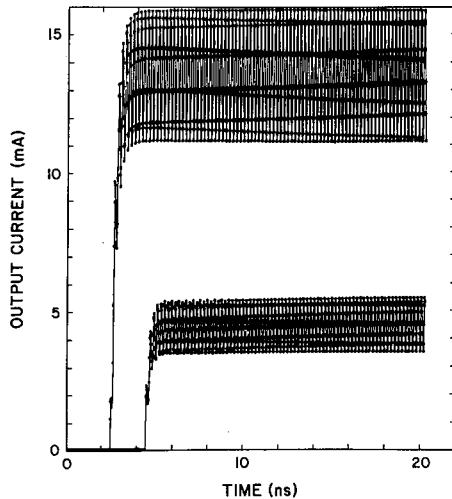


Fig. 1. Output current of a voltage doubler attached to a quad loop antenna (lower curve) is increased by tuning the diode junction capacitance with a coil placed across the antenna feed-point (upper curve).

TRANSIENT CORONA EFFECTS ON LONG WIRE ANTENNAS

K. C. Chen, J. P. Castillo,
C. E. Baum, H. A. Goodwin
Air Force Weapons Laboratory
Kirtland AFB, NM 87117
and
P. S. Book
Kaman Sciences Corporation
Colorado Springs, CO 80933

Military aircraft, such as TACAMO and Airborne Command Post, employ long VLF trailing wire antennas. These antennas are required to survive exposure to nuclear electromagnetic pulse environment. During such an exposure the electric field on the trailing wire antenna can be considerably greater than the breakdown electric field of the air, which results in corona around the wire. As a first step in understanding wires with corona, the Air Force Weapons Laboratory set up a wire over a copper wire mesh ground plane facility at Kaman Sciences Corporation. A high voltage pulser is used to drive this transmission line up to 90 Kv. Baum's electric and magnetic field sensors are situated on the ground plane to measure the corona effect.

The recorded signals clearly show the onset of corona which is characterized by a dip in the measured data. Corona data for different wire types, e.g., Aluminum, Copper; for a range of voltage levels; and for both polarities; have been collected. Linear and nonlinear corona models are developed to interpret this data.

SOLITONS IN RANDOMLY INHOMOGENEOUS MEDIA

Ioannis M. Besieris

Department of Electrical Engineering
Virginia Polytechnic Institute and State University
Blacksburg, Virginia 24601

One of the most significant accomplishments in the area of mathematical physics during the past twelve years has been the development of the inverse scattering method [C. S. Gardner et al., Phys. Rev. Lett. 19, 1095 (1967); P. D. Lax, Comm. Pure Appl. Math. 21, 467 (1968); V. E. Zakharov and A. B. Shabat, Zh. Eksp. Teor. Fiz. 61, 118 (1971)], whereby initial and boundary value problems for nonlinear wave systems are solved exactly by the successive application of linear techniques. Such solutions consist of solitons [cf. A. C. Scott et al., Proc. IEEE 61, 1443 (1973)] - nonlinear wave packets emerging from collisions with similar packets with unaltered shape and speed by virtue of the balance of various physical mechanisms (e.g., nonlinearity and dispersion).

An important nonlinear partial differential equation which arises in electromagnetic propagation and is amenable to the "inverse method" is the nonlinear complex parabolic equation, wherein nonlinear corrections to the index of refraction are assumed to exhibit a pronounced Kerr effect, i.e., they are proportional to the field intensity (irradiance). Within the framework of the quasi-optical description, it models exceedingly well the self-interaction of light beams, which may lead to self-focusing, self-modulation, etc.

There exist physical situations (e.g., graded lightguides, laser-induced plasmas, etc.) which require that one take into account the presence of randomly perturbed spatial profiles in addition to nonlinearities and dispersion. A model stochastic nonlinear complex parabolic equation incorporating all these effects is studied in this exposition.

The statistical technique expounded here is based on a fundamental ansatz [cf. I. M. Besieris, J. Math. Phys. 19, 2533 (1978)]. This ansatz constitutes essentially an embedding process: Through a transformation, the nonlinear stochastic parabolic equation is brought into an one-to-one correspondence with the nonlinear parabolic equation characterizing the unperturbed (deterministic) medium, together with a set of stochastic nonlinear ordinary differential equations. The basic statistical analysis of the original stochastic nonlinear partial differential equation is thus simplified considerably since one can now combine the results of the inverse scattering technique with the already highly developed theory of stochastic ordinary differential equations. Many physically interesting averaged observables can be calculated by this approach. Specifically, we shall report on the stability of single-envelope solitons in the presence of randomly perturbed spatial gradients.

THE EFFECTS OF DIELECTRIC AND SOIL NONLINEARITIES
ON THE ELECTROMAGNETIC TRANSIENT RESPONSE
OF CABLES LYING ON THE SURFACE OF THE EARTH

R. A. Perala
R. B. Cook
Electro Magnetic Applications, Inc.
P. O. Box 8
Golden, Colorado 80401

ABSTRACT

In this paper, the effects of soil and dielectric breakdown upon the response of insulated cables lying on the earth's surface illuminated by a transient electromagnetic wave are examined. The insulated cable response is solved by using a time domain finite difference model of a three conductor TEM transmission line. The three conductors are the reference at infinity, the soil dielectric interface, and the cable conductor. Voltages (and thus electric fields) can then be solved explicitly in the dielectric and soil regions. The treatment of the dielectric breakdown is to simply set the dielectric voltage to zero after it exceeds the specified breakdown level. The soil breakdown is somewhat more complex. When the dielectric punctures, an arc occurs between the cable conductor and the earth, and a current is injected into the earth. This current will induce a potential on the earth's surface which will ionize part of the earth. This ionized region is roughly the shape of a thin disc, because the surface breakdown of soil (250-500 kV/m) is much less than that of the bulk soil medium. Therefore, the ionized region tends to extend along the earth's surface instead of into it. The soil nonlinearity is therefore modelled by a time dependent nonlinear conductance and capacitance of a disc.

Several predictions were made of both linear and nonlinear responses in order to compare the effects. It was found that the effect is to greatly increase the late-time short circuit current, and to limit the possible open circuit voltage.

The effect on systems is thus that if the system is low impedance, more current can be injected into it, and thus a greater threat results. If the system is high impedance, a lesser threat may result because the voltage is reduced. However, if the voltage is large enough to cause something in the system to break down and become low impedance, then a greater threat results in this case also.

VARIATION OF THE INTERNAL ELECTRIC
FIELD IN A STEEL CYLINDER RESULTING
FROM AN IMPULSE SURFACE CURRENT

William J. Croisant and Paul Nielsen
U.S. Army Construction Engineering Research Laboratory
Champaign, Illinois 61820

When an axially directed current pulse is injected along the outer surface of an electrically conducting cylinder, the fields eventually diffuse through the walls of the cylinder and result in a transient electric field inside the cylinder. This paper considers the transient electric field response resulting from pulses of such a duration that they can be regarded as impulses.

For essentially nonmagnetic materials such as copper and aluminum, the material properties are constant and the response is linear. This linearity has two important consequences:

1. The magnitude of the transient electric field is directly proportional to the injected charge.
2. The time variation of the transient electric field is independent of the injected charge; e.g., the peak occurs at the same time regardless of the magnitude of the injected charge.

Thus, if the response is determined for a unit impulse (i.e., an impulse of unit charge), then the impulse response for some other charge level can be determined by simple linear scaling. Experimental results of impulse tests on aluminum cylinders illustrate this linearity.

The permeability of a ferromagnetic material such as steel is field dependent. As the applied magnetic field strength is increased from zero, the permeability typically starts from an initial value, increases to some maximum value, and then decreases to the permeability of free space as the material becomes saturated at high field levels. Experimental results of impulse tests on a steel cylinder (a commercial thin wall electrical conduit) exhibit a nonlinear behavior as the applied pulse is increased:

1. The peak electric field does not scale linearly with charge. Measured values at high pulse levels were found to be significantly lower than those which would have been predicted from a linear extrapolation of results at low pulse levels.
2. The shape of the transient electric field does not remain the same. The peak electric field has been observed to occur later in time as the charge level is increased.

THE GEOMETRIC OPTICS IN NON-LINEAR WAVE THEORY

A. B. Shvartsburg
IZMIRAN, Academgorodok, P./O. 142092
Moscow Region, USSR

The new approach in non-linear theory of localized wave pulse non-stationary evolution is developed. This approach is connected with non-linear geometric optics of dispersive media, based on hydrodynamical analogy with non-linear optics. Many classes of exact analytical solutions of intense limited wave pulses self-action equations are constructed in non-linear geometric optics. Unlike the widely known soliton-like pulses and numerical solutions, these new solutions are represented in a simple algebraic form of the eigen-functions, connected with many-dimensional Laplace equations in a special amplitude-phase space. These solutions illustrate the essential dependence of pulse evolution dynamics upon the initial pulse envelopes. The theory is applied to the following problems:

- 1) The perspectives of controlled simultaneous evolution of different parameters of the pulse, containing the pulse duration decrease, the spectrum broadening, and the pulse front's formation.
- 2) The role of initial envelopes in the development of two types of non-linear self-action regimes: the monotonous regime, connected with the pulse self-constriction, and the non-monotonous one, connected with the pulse self-stratification.
- 3) The possibilities of non-linear wave processes modeling, associated with the similarity of these new solutions for the waves of different physical nature, governed by the non-linear Schrödinger equation.

References

- Shvartsburg, A.B. 1974, "Phys. Lett.," 48A, p. 257.
Shvartsburg, A.B. 1976, "Opto-Electronics," 8, p. 393.
Shvartsburg, A.B. 1976, "J.E.T.P.," 70, p. 1640.

THE NON-LINEAR RESONANCES IN THE LOWER IONOSPHERE

A. B. Shvartsburg
IZMIRAN, Academgorodok, P./O. 142092
Moscow Region, USSR

The new class of ionospheric modification experiments, based on resonant properties of the ordinary polarized middle frequency radiowaves in the lower ionosphere, are suggested. The complex of non-linear plasma radiophysical phenomena in this region is connected with an essential dependence of magnetoactive plasma dispersive properties upon the electron-neutral collision frequency. This dependence, typical for the lower ionosphere, shows the possibility of considerable electron heating in this region, due to Langmuir electron resonance and resonant localization of the radiowaves' Joule absorption in a thin ionospheric layer. Unlike the effects of non-resonant wave heating in HF and LF ranges, the MF energy is dissipated in a thin resonant plasma layer, whose thickness may become less than 1 km. The appearance of this peculiarity is not connected with any ionospheric profile irregularities, but this phenomenon is resonant wave effect only. The main part of wave energy is dissipated in this resonant layer; therefore, the electron temperature growth in this layer may become especially considerable (the transmitter power $Q < 0.5$ MWt may lead to temperature increases of 8 - 10 times). The following perspectives of such effects are discussed:

- 1) The selective wave heating of thin plasma layer with the controlled localization in MF range ($0.4 \text{ MHz} < f < 1 \text{ MHz}$).
- 2) The possibilities of resonant local diagnostic of electron-neutral collisions.
- 3) Resonant temperature anomaly of Joule absorption in E-layer.

References

- Shvartsburg, A.B. 1974, "Soviet Physics - Uspechi," 113, p. 735.
Shvartsburg, A.B. 1976, "Phys. Lett.," 57A, p. 435.

BIOELECTROMAGNETICS SYMPOSIUM

Co-sponsors:

- I) USNC/URSI Commission A and B (See the front for officers' names)
II) Bioelectromagnetics Society

President

E.L. Alpen

Vice President

E.N. Albert

Secretary-Treasurer

E.L. Hunt

Editor

E. Postow

Executive Director

T.C. Rozzell

Directors

C.F. Blackman

S.F. Cleary

A.H. Frey

A.W. Guy

K.H. Illinger

J.L. Lords

C.D. Lytle

R.G. Medici

F.J. Rosenbaum

R.W. Rosenthal

M.A. Stuchly

C.H. Sutton

Technical Program Committee

A.W. Guy, Chairman

E.N. Albert

F.L. Cain

C.K. Chou

J.A. Elder

O.P. Gandhi

Z.R. Glaser

E.L. Hunt

D.R. Justesen

J.C. Lin

R.H. Lovely

S.M. Michaelson

J.C. Mitchell

P.O. Kramar

M.L. Shore

D.H. Spackman

R.A. Tell

W.A.G. Voss

SESSION BEMS - 1
MONDAY AM 8:30-10:00
HUB AUDITORIUM

OPENING SESSION

Chairperson: A. W. Guy
University of Washington
Seattle, WA

WELCOMING REMARKS

1. A. W. Guy, Chairman, Technical Program Committee
2. R. Baird, Chairman, Commission A, USNC/URSI
3. E. L. Alpen, President, The Bioelectromagnetics Society

ADDRESSES

1. Keynote Address, W. A. Geoffrey Voss
From Mice to Man
2. USA-USSR EM Research Exchange Program: Progress Report,
D. I. McRee, USA
M. G. Shandala, USSR
3. EM Research Program: Institute of Biological Physics,
Academy of Sciences, USSR
I. G. Akoev, USSR

SESSION BEMS - 2
MONDAY AM 10:20-11:50
HUB AUDITORIUM

THERMOREGULATION

Chairperson: D. R. Justesen
Veterans Administration Medical Center
Kansas City, MO

METABOLIC AND PHYSICAL SCALING IN MICROWAVE/RADIOFREQUENCY
BIOEFFECTS STUDIES*

Sol M. Michaelson and Shin-Tsu Lu
Department of Radiation Biology and Biophysics
University of Rochester School of Medicine and Dentistry
Rochester, New York 14642

Research on the biological effects of microwaves is primarily related to the problem of hazard assessment for exposure to man. To reach an objective, scientifically valid solution to the hazard assessment problem, two complex, integrative tasks must be systematically accomplished. One of these is the determination of the absorbed energy required to cause deleterious changes in body functions of experimental animals; this requires a quantitative evaluation and comparison of the many experiments that have been conducted. The second task is extrapolation of the results of animal experiments to the exposure conditions of man.

Data obtained on dogs, rabbits and rats exposed to 2830 MHz and 1280 MHz, Pulsed and 200 MHz CW have been reevaluated in the light of more recent concepts related to Specific Absorption Rates (SAR). These results will be integrated with recently published data for 2450 MHz CW exposure of rats and non-human primates to provide a basis for establishing extrapolation factors for human exposure.

*This paper is based on work performed under contract with the U.S. Department of Energy at the University of Rochester Department of Radiation Biology and Biophysics and has been assigned Report No. UR-3490-1561.

DIFFERENTIAL HEATING OF THE CORTEX, HYPOTHALAMUS AND RECTUM
IN THREE SPECIES BY 2450-MHz MICROWAVES

Virginia Bruce-Wolfe, Dennis L. Reeves and Don R. Justesen
Veterans Administration Medical Center
Kansas City, Missouri 64128

To assess the relationship between rectal temperature and superficial and deep brain temperatures after microwave induced hyperthermia, four rabbits, four guinea pigs and six rats were anesthetized with sodium pentobarbital (30mg/kg) and were stereotaxically implanted with 22-gauge Teflon microcatheters aimed at the preoptic area of the hypothalamus. In addition, a small opening (1-mm in dia) was burred through the calvarium to expose the dura, which allowed placement of another microwave thermocouple on the cortex. Animals were radiated in a 2450-MHz field at dose rates of 30 to 40 mW/g until rectal temperature reached a level between 42.5 and 43.0 °C. After radiation, rectal, hypothalamic and cortical temperatures were recorded at 30-sec. intervals for five minutes, 1-min. intervals for 10 minutes, and at 2-min. intervals for 15 minutes. In all three species, baseline cortical and hypothalamic temperatures were reliably lower than rectal temperatures. An analysis of variance confirmed that after microwave-induced hyperthermia, cortical temperature fleetingly exceeded rectal temperature ($p < .01$). Cortical temperature was significantly higher than hypothalamic temperature in guinea pigs and rats, but not in rabbits. These data indicate that the rectum, cortex and hypothalamus are differentially heated within and among differing species during microwave radiation. The degree of elevation of cerebral temperatures during whole-body irradiation in a multi-path field is believed to depend on a number of factors 1) the lower heat capacity of the brain due to its high lipid content 2) part-body resonant absorption by the head; and 3) anatomical, physiological and pharmacological differences among species.

THERMAL EFFECTS ON COLONIC AND REGIONAL BRAIN TEMPERATURE
IN UNANESTHETIZED RATS EXPOSED TO 2450 MHz CW MICROWAVES*

W. M. Williams, Shin-Tsu Lu, and S. M. Michaelson
Departments of Anatomy and Radiation Biology and Biophysics
University of Rochester School of Medicine and Dentistry
Rochester, New York 14642

Perturbations of the blood-brain barrier in rats have been reported to occur following exposure to microwaves. To more clearly define microwave effects on the brain, colonic temperature, as well as temperature within cerebral cortex, hypothalamus, cerebellum, and medulla oblongata have been monitored in unanesthetized rats either sham-exposed or exposed in the far field for 30 or 90 minutes to 2450 MHz CW microwaves at a field intensity of 65 mW/cm^2 . Brain temperatures were determined with a YSI series 524 hypodermic thermistor manually inserted through nylon screws having a 0.025 mm center-drilled hole, and stereotaxically implanted in the skull.

Comparison of regional brain temperature with individual colonic temperatures, expressed as $\Delta T = t^{\circ}\text{C}_{\text{brain}} - t^{\circ}\text{C}_{\text{colonic}}$, revealed a consistent pattern of variation in both sham-control groups and in animals exposed to microwaves. While temperatures measured in cerebral cortex and cerebellum were somewhat lower than colonic temperature, those measured in hypothalamus and medulla were comparatively higher.

Regional brain and colonic temperatures of rats exposed to microwaves for 30 and 90 minutes were increased significantly ($U = 0$; $P = .001$) over sham exposed animals.

Deviation below colonic temperature was greatest for cerebral cortex and cerebellum in animals exposed to microwaves. This deviation differed significantly ($P = .048$ for cerebral cortex and $P = .018$ for cerebellum) from sham-controls only after animals had been exposed to microwaves for 90 minutes. Deviation of hypothalamic temperature above colonic, for animals exposed to microwaves was somewhat less than that noted for sham-controls, while temperature of the medulla varied inversely between sham and control groups. Differences between groups in these two regions were not statistically significant.

Regional brain and colonic temperatures will also be compared in animals exposed for 30, 90, and 180 minutes to microwaves having an I.P.D. of 20 mW/cm^2 . The relationship between colonic and regional brain temperature in rats exposed to a microwave field will be discussed.

*This paper is based on work performed under contract with the U.S. Department of Energy at the University of Rochester Department of Radiation Biology and Biophysics and has been assigned Report No. UR-3490-1567.

MODIFICATION OF MICROWAVE BIOLOGICAL END-POINTS BY INCREASED
RESTING METABOLIC HEAT LOAD IN RATS*

Shin-Tsu Lú, Nancy Lebda, Sue Pettit, and Sol M. Michaelson
Department of Radiation Biology and Biophysics
University of Rochester School of Medicine and Dentistry
Rochester, New York 14642

The aims of this experiment were to modify biological end-points by an increase in the resting metabolic heat load and unveil the thyroidal stimulatory effect of microwave thermalization. Triiodothyronine (T3) was administered subcutaneously to rats daily for 5 days at 4 µg/100 g body weight. Microwave (MW) was 2.45 GHz (CW) far-field exposure at 40 mW/cm² for 2 hours. Four protocols were used: (A) sham-T3-injection-sham-MW-exposure; (B) sham-T3-injection-MW-exposure; (C) T3-injection-sham-MW-exposure; and (D) T3-injection-MW-exposure. Results indicated that T3 injection could increase resting metabolic rate by 30%. This increase in resting metabolic heat load could increase base-line colonic temperature significantly. Microwave exposure could increase colonic temperature in sham-T3-injected and T3-injected rats. Triiodothyronine injections did not alter increases in colonic temperature induced by MW exposure; the magnitude of increases were similar for T3- or sham-T3-injected rats. Triiodothyronine injection did not affect base-line corticosterone (CS) levels. Microwave exposure could significantly increase CS in Sham-T3 or T3-injected rats. Triiodothyronine could also exaggerate CS responses induced by microwave exposure. Both T3 injection and microwave exposure could significantly reduce serum thyrotropin levels. Microwave exposure did stimulate T3-inhibited thyroxine secretion.

*This paper is based on work performed under contract with the U.S. Department of Energy at the University of Rochester Department of Radiation Biology and Biophysics and has been assigned Report No. UR-3490-1565.

MICROWAVE MODIFICATION OF THERMOREGULATORY
BEHAVIOR: THRESHOLD AND SUPRATHRESHOLD EFFECTS

Eleanor R. Adair, John B. Pierce Foundation Laboratory
and Yale University, New Haven, CT 06519

Temperature changes, whether environmental or internal, will elicit both behavioral and autonomic responses in endotherms that are directed toward the maintenance of a constant internal body temperature. Unlike infrared radiation, which does not penetrate the skin, microwaves can be absorbed in complex patterns below the skin surface; they thus have the potential to alter thermoregulatory responses through thermal stimulation of both peripheral and deep body thermosensitive sites. My primary experimental objective was to determine the minimal incident microwave energy that will modify the ongoing thermoregulatory behavior of squirrel monkeys, the nature of the modification, and the degree to which the effect may be attributed to heating of the skin. A secondary objective was to assess the impact of suprathreshold energy levels on the ability of the animals to thermoregulate behaviorally. Adult male squirrel monkeys were restrained in the far field of a horn antenna inside a 6' x 6' x 8' anechoic chamber that was heated and cooled by forced convection. The animals were highly trained to control the temperature of the air circulating through the anechoic space by selecting between two preset air temperatures, 15° and 55°C. At specific times during the experiments they were exposed to 10-min periods of 2450 MHz CW microwaves (E Polarization). Incident power densities ranged from 1 to 22 mW/cm². The corresponding specific absorption rate (SAR), derived from temperature increments in saline-filled phantom models, ranged from 0.15 to 3.25 W/Kg. Controls included exposure to infrared radiation of equivalent incident energy and no radiation exposure. Normal thermoregulatory behavior produces tight control over environmental and body temperatures; most monkeys select an air temperature of 34-36°C. Brief exposures to 2450 MHz CW microwaves at an incident power density of 6-8 mW/cm² stimulated the animals to select a lower environmental temperature. This threshold energy level represents a whole-body SAR of 1.1 W/Kg, roughly 20% of the resting metabolic heat production of the monkey. The efficiency of thermoregulatory behavior was high even at 22 mW/cm² where the preferred air temperature was lowered by as much as 4°C and skin and rectal temperatures remained stable. No comparable reduction in selected air temperature below control levels occurred during infrared radiation of equal incident energy. These results suggest that changes in thermoregulatory behavior triggered by absorbed microwaves result from stimulation of internal thermoreceptors whereas responses to infrared radiation result primarily from stimulation of receptors in the skin. (Supported by AFOSR Grant 77-3420.)

MICROWAVES AFFECT THERMOREGULATORY BEHAVIOR IN RATS *

S. Stern, L. Margolin, B. Weiss, S.-T. Lu, S. M. Michaelson: Department of Radiation Biology and Biophysics, and Environmental Health Sciences Center, School of Medicine and Dentistry, University of Rochester, Rochester, New York 14642

Rats, with their fur clipped, pressed a lever to turn on an infrared lamp while in a cold chamber. When 2450 Megahertz continuous wave microwaves were presented for 15 minutes, the rate of turning on the infrared lamp decreased as a function of the microwave power density, which ranged between 5 mW/cm^2 and 20 mW/cm^2 . This result indicates that behaviorally significant levels of heating occur at exposure durations and intensities that do not produce reliable changes in either colonic temperature or other behavioral measures. Further study of how microwaves affect thermoregulatory behavior may help us understand phenomena such as reported "non-thermal" behavioral effects of microwaves.

* This report is based on work supported in part by postdoctoral fellowship F22 ESO1804 (awarded to S.S.) and grant ES-01247 both from the National Institute of Environmental Health Sciences, and in part by a contract with the U.S. Department of Energy at the University of Rochester Department of Radiation Biology and Biophysics and has been assigned Report No. UR-3490-1556.

SESSION BEMS - 3
MONDAY PM 1:30-3:00
HUB AUDITORIUM

NERVOUS SYSTEM

Chairperson: R. H. Lovely
University of Washington
Seattle, WA

BEMS 3 - 1

MICROWAVE EFFECT ON THE PARAMETERS
OF THE MODEL SYNAPTIC MEMBRANE

O.V. Kolomitkin, V.I. Kuznetsov, and I.G. Akeov
Institute of Biological Physics
USSR Academy of Sciences
Pushchino Moscow Region 142292
USSR

EVIDENCE OF NEUROPATHOLOGY
IN CHRONICALLY IRRADIATED HAMSTERS
BY 2450 MHz MICROWAVES AT 10mw/cm²

Ernest N. Albert
Department of Anatomy
George Washington University Medical Center
Washington, D.C. 20037

This is an extension of studies reported previously (Albert and DeSantis 1975, 1976). Adult Chinese hamsters were exposed to 2450 MHz microwaves (CW) at 10 and 25 mw/cm² power densities for 14 hours/day for 70 days. Sham irradiated animals were treated exactly in the same manner as experimentals except for exposure to microwaves.

Immediately following the final exposure the animals were anesthetized with pentobarbital (IP), perfusion fixed with buffered formalin via the left ventricle, and the brains were dissected out and processed for neuropathological examination using standard and special stains for dendritic spines, axons, bouton terminals, glia and neurons.

Microscopic examination of serial sections revealed that brains of some experimental animals exposed to 10 mw/cm² power density had fewer dendritic spines, axonal swelling, axonal beading, hyperchromatic neurons, and cytoplasmic swelling of neurons in some parts of the brains. There was no evidence of gliosis, hemorrhage or pyknosis. While no recovery studies were performed, it is this investigator's opinion that all of the above observed morphological changes are probably reversible.

Animals exposed to 25 mw/cm² showed similar histological alterations as those irradiated at 10 mw/cm². There was some evidence that quantitatively the effects may be greater in the 25 mw/cm² group. During the first 7 - 14 days of exposure animals exposed to 25 mw/cm² were decidedly more irritable but appeared to become acclimatized as judged by external behavior.

Details of exposure conditions and histopathological procedures will be presented at the symposium.

Albert, E.N. and DeSantis, M. Do microwaves affect central nervous system structure? A light and electron microscopic study. *Annals N.Y. Acad. Sci.* 247:87-108, 1975.

Albert, E.N. and DeSantis, M. Histological observations on central nervous system. In *Biological Effects of Electromagnetic Waves*. Eds.: C. Johnson and M. Shore. HEW Publication (FDA) 77-8010, pp. 299-310, 1975.

ELIMINATION OF MICROWAVE EFFECTS ON THE VITALITY OF NERVES
AFTER ACTIVE TRANSPORT HAS BEEN BLOCKED

Donald I. McRee
National Institute of Environmental Health Sciences
Research Triangle Park, North Carolina 27709

Howard Wachtel
Duke University
Durham, North Carolina

We have previously reported that exposure to fairly low level microwave fields (an SAR of 10 W/kg at 2.45 GHz CW) would consistently lower the survival time of isolated frog sciatic nerves stimulated at high repetition rates (50 pulse pairs per sec.). The time course of the loss of excitability of the exposed nerve (as compared to its unexposed contralateral mate) is reminiscent of that seen when the active transport of sodium (Na) and potassium (K) is blocked by certain agents - such as the cardiac glycoside ouabain. In order to assess the role that microwaves may be having in interfering with, or counteracting, active transport we have performed a series of experiments in which the active Na-K pump has been substantially blocked by ouabain prior to microwave exposure. Our waveguide exposure and thermal control system is the same as that described previously and allows us simultaneously to observe the "run down" of a pair of nerves from opposite legs of the same frog, only one of which is exposed to the 10 W/kg microwave SAR. In order to achieve the fastest and most complete blockade of Na-K pump the paired nerves were soaked for 5 minutes in a high concentration (10^{-3} g/l) of ouabain, prior to stimulation at 50 ppps. The "rundown time course" was, as expected, accelerated in all ouabain treated nerves, but the microwave exposed nerve showed no significant further shortening of its survival time (out of 8 experiments, 3 showed slightly longer survival times for the exposed nerve, 2 for the unexposed nerve and 3 others were too close to call). An additional 3 control experiments on ouabain treated nerves, but without microwaves, showed essentially the same results - i.e., no significant difference in vitality between the paired nerves.

We have also repeated these experiments at a lower stimulation rate (5 ppps) wherein the survival time more closely approximates that of the untreated nerves stimulated at 50 ppps (1 or 2 hours versus 30 minutes or less for ouabain treated nerves stimulated at 50 ppps). Results at these lower stimulation rates indicate that there is still no significant difference in the survival time of paired nerves. These results lend support to the view that the relative loss of excitability in microwave exposed nerves is related to an interference with, or counteraction of the Na-K pump.

EFFECTS OF RADIO FREQUENCY FIELDS
ON THE EEG OF RABBIT BRAINS

Shiro Takashima and Herman P. Schwan
Department of Bioengineering D2, University of Pennsylvania
Philadelphia, Pennsylvania 19104
U.S.A.

Previously we reported that chronic exposure of rabbits to RF energies produced abnormal EEGs. We further reported that the type of abnormal EEG depended on the intensity of RF fields. Namely, increase of slow waves with moderate RF intensities and appearance of fast waves with low intensity fields.

We repeated previous experiments using similar conditions and confirmed the appearance of abnormal EEGs. In particular, after long irradiation at low intensities (100-200 V/M), the EEG is characterized by the presence of spindle-like signals with a frequency about 14-16 Hz. These spindles have large amplitudes and appear with a mean interval of 20-30 seconds. These abnormal EEGs persist for several weeks even after the termination of irradiation.

In order to locate the source of abnormal spindles, we used three intracranial electrodes in the posterior regions of both hemispheres and the ground electrode in the anterior region on the midline. Using these electrodes we found that the spindles are originating from the posterior region of the right hemisphere. This observation indicates that the lesion caused by RF is limited to a small region of the brain.

The effects of acute irradiation on EEGs were reinvestigated using an improved technique. RF pulses (1 ms with an interval of 1 second) were applied to animal heads. EEG recordings were initiated immediately after the end of each pulse and continued until the arrival of another stimulus. We found that RF pulses eliminated the normal patterns and replaced them with low amplitude fast waves with frequencies 15-25 Hz. These abnormal patterns are transient and disappear in several minutes if the field is terminated. In spite of these observations, these experiments failed to detect a well defined time locked evoked signal as a consequence of RF stimuli.

IN VITRO STUDY OF MICROWAVE EFFECTS
ON CALCIUM EFFLUX IN RAT BRAIN TISSUE

W. W. Shelton, Jr.
Dept. of Electrical & Computer Engineering
Florida Institute of Technology
Melbourne, Florida 32901

J. H. Merritt
Radiation Sciences Division
USAF School of Aerospace Medicine
Brooks Air Force Base, Texas 78235

Considerable experimental evidence has been presented identifying adverse central nervous system response to electromagnetic radiations, the severity of response being a function of such variables as power density, frequency, exposure duration and facilitating factors (e. g., drugs, stress). Despite the safety standards currently observed (e. g., maximum power densities of 10 mW/cm^2 in the U.S. and $10 \text{ } \mu\text{W/cm}^2$ in the Soviet Union), much research remains to be performed in identification of minimal values of these variables (or combinations of variables) for which threats to biological well-being are clearly posed.

The research reported herein addressed the prospect of pulsed-microwave induced alteration of $^{45}\text{Ca}^{++}$ -efflux in brain tissue at low values of pulse repetition frequency (PRF) and power density under in vitro experimental conditions. Rat cerebral samples were incubated for 30 minutes in $^{45}\text{Ca}^{++}$ -treated medium and then transferred to fresh, $^{45}\text{Ca}^{++}$ -free solution (efflux medium) for a 20-minute exposure to far-field pulsed-microwave irradiation according to one of several PRF-power density schemes: 16 Hz at 0.5, 1.0, 2.0, and 15.0 mW/cm^2 , and 32 Hz at 1.0 and 2.0 mW/cm^2 . Measurements of radioactivity in the tissue samples and in aliquots of the efflux media at post-irradiation were used to calculate a $^{45}\text{Ca}^{++}$ -efflux value for each sample. Control samples were then processed in an identical fashion with the exception that power was not applied to the irradiation chamber.

Preliminary statistical treatment of the data reveals no significant differences between irradiated and control sample efflux values.

RETINAL GANGLION-CELL ACTIVITY INDUCED BY ELF-FIELDS

P. Lövsund, P.Å. Öberg and S.E.G. Nilsson
Departments of Biomedical Engineering and Ophthalmology,
Linköping University, S-581 85 Linköping, Sweden.

The influence of ELF magnetic field on peripheral nerves can be studied by recording the electrical activity of the ganglion cell in the frog retina following magnetic field exposure. The preparations are exposed to a magnetic flux density of the same magnitude and frequency known to produce magnetophosphenes on volunteers (0-80 mT, 10-50 Hz).

The electrical activity from the ganglion OFF-, ON-OFF- and ON-cells is recorded during exposure and immediately after the field is switched off.

The response from the ganglion cells varies to a large extent with the magnetic flux density used and the field frequency. Similar to the response of light stimulus the ganglion cells respond only to ON-OFF changes in the magnetic field.

From this material we cannot determine the detailed mechanisms behind the phosphene generation in the retina. However, the comparison of the responses from the two different types of stimulus (light, magnetic field) give raise to interesting questions.

SESSION BEMS - 4
MONDAY PM 3:20-4:50
HUB AUDITORIUM

PHYSIOLOGY

Chairperson: J. A. Elder
Environmental Protection Agency
Research Triangle Park, NC

BIOEFFECTS AT THE IMPACT OF LOW LEVEL ELECTRO-
MAGNETIC MICROWAVE FIELD OF 9400 MHZ

Yu.D.Dumansky, N.G.Nikitina, I.P.Less, L.A.Tomashevskaya,
E.R.Holyavko, L.G.Andrienko, S.A.Lyubchenko, S.V.Zotov

/Kiev A.N.Marzeev Scientific Research Institute of Gene-
ral and Communal Hygiene, Kiev, USSR/

To study the biological effects of EM pulsed field with frequency of 9400 MHz (λ - 3 cm) engineering-technical approach was used enabling to create the uniform EM microwave field distribution in the laboratory experimental conditions.

Medico-biological experiment was carried out with 1200 white rats at constant irradiation of pulsed field at PD 5 to 115 $\mu\text{W}/\text{cm}^2$ during six months (4 months - factor effects, 2 months - aftereffects study), 12 hours a day.

During the whole experiments (period of exposure) physiological, immunological, hematological, biochemical, generative, pathomorphological and other functional animal state indices were studied.

The results of the investigations have shown that EM microwave fields with the frequency of 9400 MHz appeared to be biologically active. At PD of 25 to 115 $\mu\text{W}/\text{cm}^2$ statistically true changes in a number of functional organism state indices of the animals were found. No effects were observed at lower PD.

BEMS 4 - 2

MICROWAVE SHORT-TIME EXPOSURE EFFECT ON GONADS

A.Ch. Achmadieva, E.N. Smirnova, and I.G. Akoev
Institute of Biological Physics
USSR Academy of Sciences
Pushchino Moscow Region 142292
USSR

CHANGES IN THE ELECTROCARDIOGRAMS OF RATS AND
DOGS EXPOSED TO DC MAGNETIC FIELDS

C.T. Gaffey and T.S. Tenforde
Lawrence Berkeley Laboratory, University of
California, Berkeley, California 94720

An evaluation of cardiovascular performance in magnetic fields (MF) is being undertaken. Exposure of experimental animals to D.C. MF is achieved at the Magnetic Testing Facility (MTF) at Berkeley. The MTF permits the bioassay of MF from 0.5 to 22,000 gauss. Cardiovascular performance is evaluated as a function of the MF strength. Since the vector characteristics of MF may be a factor influencing cardiovascular function, the position of animals in a MF is being tested. In practice, each test animal is inserted between the poles of a magnet in a selected orientation that locates the heart in the center of the MF. The electrocardiogram (ECG) is measured with platinum needle electrodes attached to each animal. ECG is recorded before, during and following the application of a MF. The interval between summits of the R waves allows the average heart rate to be obtained. The average respiratory rate is measured from the baseline shifts in the ECG trace. The amplitudes of the P, Q, R, S and T waves are taken from the ECG records, as well as the P-Q intervals. Rectal temperature is measured with a non-magnetic thermistor.

The major change in the ECG pattern induced by a MF is an increase in the amplitude of the T wave of rats and dogs. In our rat study a 20,000 gauss field increased the T wave by about 450 percent; the dog's T wave was increased 750 percent by a 16,000 gauss field. The biomagnetic effects appear to be reversible. Our experiments were designed to test for the presence of a magnetic strength threshold (MST) to evoke T wave enhancement. MST is defined as the minimum number of gauss to produce a measurable change in the T wave amplitude. The MTS is 3.0 kgauss for rats and 0.9 kgauss for dogs. These are average MST values from experiments on 12 adult rats and 2 adult dogs. In experiments with newborn rats from 3 to 7 days old, augmentation of the T wave was found to be greatest when the lines of the MF were perpendicular to the long axis of the body and least when parallel. Hence, the orientation of the subject in the MF influences the ECG profile.

CARDIOVASCULAR RESPONSE OF RATS
EXPOSED TO 60-HZ ELECTRIC FIELDS

D. I. Hilton and R. D. Phillips
Biology Department
Pacific Northwest Laboratory
Richland, WA 99352
Operated by
Battelle Memorial Institute

Recent studies have shown that exposure to high strength electric fields can influence ECG patterns, heart rates and blood pressures in various species of animals. Our studies were designed to evaluate these reported effects and to help clarify some of the conflicting reports in the literature. Various cardiovascular parameters were measured in rats exposed to 60-Hz, 80 or 100 kV/m fields for periods up to and including 4 month durations. In addition, physiological reserve capabilities were measured in rats exposed to 100 kV/m for 1 month and then subjected to cold stress. No significant differences in heart rates, ECG patterns, blood pressures or vascular reactivity measurements were found between exposed and sham exposed rats after 8 hours, 40 hours, 1 month or 4 months of exposure. Electric field exposure did not alter the animals' physiological response to cold stress. While our studies cannot be directly compared to the work of other investigators, our failure to detect any cardiovascular changes is probably the result of eliminating secondary field effects such as microcurrent shocks, corona and ozone formation.

DUAL ACTIONS OF MICROWAVES ON SERUM CORTICOSTERONE IN RATS*

Shin-Tsu Lu, Sue Pettit, and Sol M. Michaelson
Department of Radiation Biology and Biophysics
University of Rochester School of Medicine and Dentistry
Rochester, New York 14642

Fifty-eight male, young adult Long-Evans rats acclimated to experimental procedures were exposed to 2.45 GHz CW microwaves for 4 hours at 0, 0.1, 1, 10, 25 and 40 mW/cm². They were sacrificed immediately after exposure at 1530 hours. The time of sacrifice is the mid-course of circadian increase of serum corticosterone (CS). While the CS levels in the shams (25.0 ± 2.1 µg/dl, S.E., n = 18) was not different from shams obtained previously (23.7 ± 4.3 µg/dl; S.E., n = 6), a significant lower CS was observed in groups exposed to 0.1 mW/cm² (16.4 ± 2.8 µg/dl; S.E., N = 8) and 1 mW/cm² (16.4 ± 3.1 µg/dl; S.E., n = 8). Significant adrenal stimulation was noted in rats exposed to 40 mW/cm² (41.8 ± 6.8 µg/dl; S.E., n = 8). Power densities of 10 and 25 mW/cm² did not induce any changes in the CS levels. A dual action of microwave on the CS is thus demonstrated. However, the lower CS levels in the 0.1 or 1 mW/cm² is still higher than the sham at 1230 hours. Thus, this can only be viewed as an inhibition of the expected circadian elevation of the CS levels. In the present study, colonic temperature was higher than shams in rats exposed to 10 mW/cm² or higher.

Evidence was obtained in 4 hour microwave exposed rats that there was a decreased CS dependence on the body temperature from the normal relation between CS and colonic temperature of sham-exposed rats between 1230 to 1930 hours. Therefore, the same degree of temperature increase in the microwave exposed rats may be less stressful than would be expected from the daily oscillation of biologic activity, if CS increase is considered to be indicative to a reaction to a stressor.

*This paper is based on work performed under contract with the U.S. Department of Energy at the University of Rochester Department of Radiation Biology and Biophysics and has been assigned Report No. UR-3490-1566.

ENDOCRINE FUNCTION IN RHESUS MONKEYS AND RATS
EXPOSED TO 1.29 GHz MICROWAVE RADIATION

W. Gregory Lotz
Naval Aerospace Medical Research Laboratory
Naval Air Station
Pensacola, Florida 32508

Adult, male rhesus monkeys (6-8 kg) and male, Long-Evans rats (350-450 gm) were exposed to 1.29 GHz pulsed microwave radiation in an anechoic chamber in the far-field zone of a horn antenna. Blood samples were drawn from both species via chronically indwelling venous catheters. During the experiments the monkeys were restrained in a Styrofoam chair and the rats were housed unrestrained in Styrofoam cages. For the rhesus monkeys, blood samples were drawn hourly before, during, and after an eight-hour microwave exposure within a total experimental time of 24 hr. Plasma was analyzed for growth hormone, cortisol, and thyroxine concentrations. In addition, rectal temperature was monitored continuously over the 24 hr period. Average incident power densities of 28 and 38 mW/cm² were used in the rhesus monkey experiments. Three monkeys were each exposed to each field intensity three times. In addition, corresponding sham-exposed sessions were conducted an equal number of times with each animal. In the rat experiments, blood samples were taken every 15 min before and during 90 min exposures to 15 mW/cm² over a total period of 150 min. Samples of rat plasma were assayed for corticosterone concentration. Separate groups of rats were used for exposed and sham-exposed experiments.

In the rhesus monkeys, rectal temperature increases during the microwave exposure averaged 0.6°C and 1.5°C, respectively, for 28 and 38 mW/cm² exposures, compared to the corresponding temperature during a sham-exposure. In spite of the considerable increase in rectal temperature noted during these exposures, no changes in circulating levels of any of the three hormones measured in the monkeys were observed at any time during or after the exposure. In the rats, however, plasma corticosterone levels began to rise after 30 min of exposure to 15 mW/cm², as compared to sham-exposed rats. This corticosterone elevation increased to a level 6-8 times that of sham-exposed rats after 75 to 90 min of exposure. These results indicate that rat adrenocortical function is stimulated at a lower power density at 1.29 GHz than had previously been observed for similar experiments using 2.45 GHz radiation. These studies also raise the possibility that rhesus monkey neuroendocrine function may be more stable during even highly thermogenic microwave exposure than is rat neuroendocrine function.

SESSION BEMS - 5
TUESDAY AM 8:30-10:00
HUB AUDITORIUM

THEORETICAL/EXPERIMENTAL DOSIMETRY (1)

Chairperson: R. A. Tell
Environmental Protection Agency
Las Vegas, NEV

MEASUREMENTS OF THE RF POWER ABSORPTION IN HUMAN AND
ANIMAL PHANTOMS EXPOSED TO NEAR-FIELD RADIATION

M. F. Iskander, H. Massoudi, C. H. Durney
Department of Electrical Engineering
University of Utah
Salt Lake City, Utah 84112

S. J. Allen
Radiation Physics Branch, Radiobiology Division
U.S.A.F. School of Aerospace Medicine
Brooks Air Force Base, Texas 78235

ABSTRACT

With the availability of significant data about the specific absorption rate (SAR) for plane wave irradiation, attention has been recently focused on near-field exposure conditions. In this paper we present experimental results for the average SAR and the SAR distribution in scaled phantoms of human and animal models exposed to near-field radiation. Prolate spheroidal models are used to evaluate the average SAR values, while realistic (figurines) models are used to measure the SAR distribution. Phantoms of different sizes (using different scale factors) for each model were used to obtain results over a broad frequency range while limiting the radiation frequency band to between 400 and 800 MHz. Furthermore, to control the exposure conditions, simple sources of known radiation characteristics, such as a short electric dipole, were used. Suitable electric- and magnetic-field probes are constructed, calibrated in the TEM cell and used to measure the radiation fields. The accuracy of the results is evaluated by making several average SAR measurements in the far-field exposure case. The obtained results are found to be in good agreement with those available in the *Radiofrequency Radiation Dosimetry Handbook*. Near-field SAR measurements will be presented as a function of frequency and the separation distance from the source. In these measurements emphasis is placed on locations and levels of possible SAR enhancements and the generation of new hot spots due to the near-field exposure conditions.

REAL TIME MEASUREMENT OF RFR ENERGY
DISTRIBUTION IN THE MACACA MULATTA HEAD

John G. Burr and Jerome H. Krupp
Radiation Sciences Division
USAF School of Aerospace Medicine
Brooks Air Force Base, Texas 78235

Temperature increases due to absorption of 2.5 and 1.2 GHz, CW, 70 to 100 mW/cm², RF energy, were measured in 3.3 cm radius homogeneous muscle equivalent spheres, M. mulatta cadaver heads (detached from body and attached to body) and living, anesthetized M. mulatta heads. Temperatures were measured using the Vitek, Inc., Model 101, Electrothermia Monitor which has a response time constant of less than 0.02 sec., short term stability, better than 0.01°C, absolute temperature accuracy of ±0.02°C, and a maximum RF-induced line heating error of 0.005°C for a heating rate of 1°C/min. Temperature distributions were compared to theoretical predictions from a computer program developed by the Data Sciences Division of the School of Aerospace Medicine.

The results show that (1) the computer model accurately predicts the temperature distribution in the muscle equivalent sphere, (2) the computer model predicts the distribution of temperature in the detached head but fails to predict the absolute temperature rise, (3) the temperature distribution in the detached head of a cadaver varies markedly with exposure orientation and polarity, i. e., facing forward, backward or to the side, (4) for the same frequency, temperature distribution in the head of a complete cadaver is very much different from that in a detached head, and (5) head temperature distribution in the living, anesthetized animal becomes more uniform due to removal of excess heat by cerebral blood flow.

The animals involved in this study were procured, maintained, and used in accordance with the Animal Welfare Act of 1970 and the "Guide for the Care and Use of Laboratory Animals" prepared by the Institute of Laboratory Animal Resources - National Research Council.

A METHOD OF CALCULATING ELECTROMAGNETIC ABSORPTION
UNDER NEAR-FIELD EXPOSURE CONDITIONS

I Chatterjee, O. P. Gandhi, M. J. Hagmann, and A. Riazi
Department of Electrical Engineering
University of Utah
Salt Lake City, Utah 84112

ABSTRACT

The rapidly expanding use of electromagnetic heating in domestic ovens as well as industrial and biomedical applications is exposing an ever increasing fraction of the society to exposure to such radiation in near-field conditions. When the source and operator are tightly coupled, the computations of dose must allow for the coupling by using coupled integral equations or iterative methods. A multitude of different near-field situations exist in real life, so the computations must be repeated, even if possible, for each individual circumstance. This paper describes a numerical method which allows considerable generalization, but is limited to situations with negligible coupling.

We have used the following procedure for near-field problems: First, a Fourier analysis of the incident field is used to give an equivalent distribution of plane waves. Then, the propagation of the individual plane waves into the target is calculated. Finally, the plane waves are vectorially added within the target and the distribution of energy deposition is determined. The use of the fast-Fourier transform (FFT) contributes to the high efficiency of our computations.

Calculations for the two-dimensional problem of an infinite slab of muscle in the presence of a slot source having infinite length have shown several interesting results. Absorption in the muscle slab is limited to an area comparable to the cross section of the source. Evanescent waves, associated with fields stored in the source, are prominent for small slot widths. Coupling of fields into the dielectric tends to be weak when the electric vector of the incident field is parallel to the surface of the dielectric.

Numerical results will be presented with some corresponding experimental tests made with biological phantom models.

NEAR-FIELD IRRADIATION OF CYLINDRICAL MODELS
OF HUMANS AND ANIMALS

C. K. Han, M. F. Iskander, C. H. Durney, and H. Massoudi
Department of Electrical Engineering
University of Utah
Salt Lake City, Utah 84112

ABSTRACT

With the acquisition of significant data about average specific absorption rate (SAR) for free-space planewave irradiation, enough is now known about that case to make reasonable estimates of dosimetry. A remaining important problem, however, is obtaining similar information about the SAR resulting from near-field and partial-body irradiation. Toward solving that problem, this paper describes the calculation of the SAR in infinitely long cylindrical models of humans and animals irradiated by the near fields of short dipoles. The analysis includes the calculations of the internal fields produced in a lossy dielectric cylinder located in the near fields of a short dipole, which has not been previously done.

Cylindrical models have been found previously to be useful for calculating the average SAR in humans and animals in the frequency range where the wavelength is small compared to the length of the absorber. In the near-field case, the cylindrical model is expected to be even more useful because of the more localized nature of the near-field exposure, which minimizes the end effects that cause the principal error in the planewave calculations.

The method of solution involves expanding the fields internal and external to the cylinder as well as the fields radiated by a short dipole in terms of the electric and magnetic Hertzian potentials. Expressions for the expansion coefficients are then obtained by matching the tangential fields across the surface of the cylinder. Although a similar formulation is available in the literature (see G. N. Tsandoulas, AP-16, 1968, p. 324; and R. Woo and A. Ishimaru, AP-12, 1969, p. 488), the numerical calculations of the near and internal fields have not been done. In the latter case, difficulties due to the infinite integration and summation involving the arguments of the Hankel functions were overcome numerically by expanding the integral in terms of Hermite polynomials. Numerical results of SAR distribution for a dipole at a distance equal to a wavelength from the cylinder were computed and found to be in good agreement with those for the planewave case. The SAR for different cylindrical models of humans and animals as a function of frequency, incident power density, and electric and magnetic energy densities will be presented.

EXPERIMENTAL AND ANALYTICAL STUDY ON INTERACTION BETWEEN
NEAR-ZONE EM FIELD OF CB-RADIO ANTENNA AND HUMAN BODY

Khalid Karimullah, Dennis P. Nyquist, and Kun-Mu Chen
Department of Electrical Engineering and Systems Science
Michigan State University
East Lansing, Michigan 48824

Near-field coupling between a CB-radio antenna and the human body of its operator in near proximity is investigated experimentally and analytically. The potential biological hazard associated with CB-radio EM radiation at 27 MHz has recently become a public concern due to the vast number of CB-radio operators and evidence that some CB antennas are operated with high input power. Although the EM field excited in a biological body by impressed plane-wave illumination has been successfully quantified, the interaction between the nonuniform near-zone field of a radiating element and such a body is not well understood. The electric field excited in a human-body model due to its coupling with a CB antenna as well as the antenna current and impedance are studied.

A simultaneous pair of coupled, tensor integral equations is developed for the unknown current excited in a CB antenna and the electric field induced in a human-body model located close to the antenna in its near-zone field. These equations are solved numerically by the method of moments for various antenna-body configurations. Accuracy of the analytical solution for a monopole antenna coupled with a rectangular-cylindrical body model is confirmed by good agreement between the induced body fields and antenna impedances predicted analytically and measured experimentally with phantom material and saline body models.

Coupling between antenna and body is found to be strongly dependent upon antenna-body proximity and environmental effects such as conducting ground. 3.5% of the input power to a quarter-wavelength monopole is coupled into a human-body model over conducting ground at 20 cm separation. In this case, antenna input power of 235 watts excites the same maximal induced field in the human body as a 10 mW/cm^2 impressed plane wave. Very tight coupling is demonstrated to occur when the CB radio and its antenna are in direct, capacitively-coupled contact with the outstretched arm of a simplified human-body model. Under these circumstances, 77% of the antenna input power is coupled into the body and relatively intense fields and SAR's are excited, particularly near the contact point between CB radio and body extremity. Extensive experimentally-measured and analytically-predicted induced fields, antenna currents, and impedances confirm the capability of the numerical solution for predicting antenna-body coupling with adequate accuracy.

A THERMAL MODEL OF THE HUMAN BODY EXPOSED TO
AN ELECTROMAGNETIC FIELD

D.M. Deffenbaugh, R.J. Spiegel, and J.E. Mann
Southwest Research Institute
San Antonio, Texas 78284

The human body was modeled by numerical procedures to determine the thermal response under varied electromagnetic exposures. The basic approach taken was to modify the governing heat transfer equations for man in air to account for thermal loading due to the energy absorbed from the electromagnetic field. The human body was represented in an electromagnetic model by a large number of small cubical cells of varying tissue properties, and the energy density was determined for each cell. This information was used as input to a thermal response model. The thermal response model consisted of solving a series of two-dimensional transient conduction equations with internal heat generation due to metabolism and shivering, internal convection heat transfer due to blood flow, external interaction by convection and radiation, and cooling of the skin by sweating and evaporation. This model represented the human body by a series of cylindrical segments in which each radius and length was determined independently by comparing the height and weight of the subject to the statistical 2.5%, 50%, and 97.5% man.

These two codes were combined in a number of different ways, and the results are shown to indicate the effect of different methods for distributing the electromagnetic heat deposition. The output of the combined code gives the local temperature of 61 discrete locations as well as the thermoregulatory responses of vasoconstriction, vasodilation, shivering, and sweating. This code was then used to determine local "hot spots" and overall thermoregulatory response to a number of electromagnetic field intensities and frequencies both at resonant and nonresonant conditions.

SESSION BEMS - 6
TUESDAY AM 10:20-11:50
HUB AUDITORIUM

THEORETICAL/EXPERIMENTAL DOSIMETRY (II)

Chairperson: J. C. Mitchell
USAF School of Aerospace Medicine
Brooks AFB, TX

FAR-FIELD MICROWAVE DOSIMETRY IN A RHESUS MONKEY MODEL

Richard G. Olsen, Toby A. Griner, and George D. Prettyman
Naval Aerospace Medical Research Laboratory
Pensacola, Florida 32508

ABSTRACT

Microwave dosimetry at 1.29 GHz was conducted in a full-size rhesus model in the sitting position. The phantom model was composed of muscle-equivalent material supported by a polyurethane foam mold. Far-field irradiations were conducted in a microwave-anechoic chamber illuminated with pulsed microwave energy from a type AN/TPS-1G radar set.

Several kinds of temperature probes were used in the calorimetric determination of specific absorption rate (SAR) at eight locations of the phantom. These probes included the liquid crystal optical fiber (LCOF) device and a 4 lead, high resistance thermistor. Thermographic imaging techniques were also employed to produce two-dimensional records of the microwave absorption in the monkey model.

Results of the initial dosimetry show a front-surface heating for several measured locations similar to the initial measurements in a man-size model. Some locations in the sitting primate model, however, showed a different heating pattern such as an internal "hot-spot" effect where the embedded region of high absorption exhibited an SAR of approximately three times the observed front-surface value.

A SYSTEM FOR DETERMINING THE RADIOFREQUENCY ABSORPTION COEFFICIENT OF THE HUMAN BODY IN THE HIGH FREQUENCY BAND

Douglas A. Hill¹, Harry M. Assenheim²,
George W. Hartsgrrove², and George A. Grant³

- 1 Protective Sciences Division, Defence Research Establishment Ottawa, Ottawa, Canada K1A 0Z4
- 2 Microwave & Radiofrequency Section, Division of Biological Sciences, National Research Council of Canada, Ottawa, Canada K1A 0R6
- 3 G.A. Grant Scientific Consultants Ltd.,
46 Crystal Beach Dr., Ottawa, Ontario, K2H 5M9

A system has been constructed for measuring radio-frequency absorption in the human body resulting from exposure to 10-26 MHz electromagnetic radiation. Both free-space and grounded conditions can be simulated. The subject is positioned between the vertical septum and outer wall of a 12.2 m long x 7.3 m wide x 6.1 m high rectangular coaxial TEM cell (1). An exceptionally precise, stable and low-noise measurement system has been constructed. The final precision in the power absorption measurement, after computer averaging, is $\pm 0.05\%$ of incident power (± 0.002 dB in insertion loss). The E and H fields in the cell are measured by a small dipole and circular loop antenna, respectively. From 20-30 MHz the TEM mode field pattern is altered by the TE₀₁ and TE₁₀ travelling modes and various resonant standing wave patterns in all three components of E and H. The largest field gradient is the 50-60% change in the septum-to-wall direction over the 1.8 m length of a subject lying in the EKH (ellipsoid-equivalent) orientation.

We have made 17 preliminary measurements on 3 volunteers at 23.25 MHz. The absorption results are reproducible for any one subject but differ between subjects. With 400 W of incident power, producing a nominal power density of 1 mW/cm², the subject absorbs only 0 to 2 W. Volunteers in the EKH orientation absorb more than when in the KEH orientation. The EKH absorption is significantly more than predicted by the ellipsoid model. We have yet to evaluate the three main corrections to our measurement required to reduce it to a free-space uniform-plane-wave-equivalent value. Therefore, such a value is not given at this time.

ELECTROMAGNETIC ABSORPTION IN MULTILAYERED
CYLINDRICAL MODELS OF MAN

H. Massoudi, C. H. Durney, P. W. Barber, and M. F. Iskander
Departments of Electrical Engineering and Bioengineering
University of Utah
Salt Lake City, Utah 84112

ABSTRACT

An important question in docimetry is whether the skin-fat muscle layers and other inhomogeneities in the body are important factors in calculating the specific absorption rate (SAR), or is a homogeneous model adequate.

To help answer this question, the absorption characteristics of multilayered cylindrical models of man irradiated by a normally incident electromagnetic plane wave are described in this paper. Numerical calculations for a specific skin-fat-muscle cylindrical model of man predict a layering resonance at 1.2 GHz with an average specific absorption rate (SAR) about double that calculated for the corresponding homogeneous model. The layering resonance frequency is found to be the same for incident waves polarized parallel and perpendicular to the cylinder axis. The effects of layers on whole-body absorption by man are determined by averaging the effects obtained for many combinations of skin and fat thicknesses. Absorption effects due to clothing are also investigated.

ELECTROMAGNETIC INTERACTION WITH HUMAN
PHANTOM MODELS; APPLICATIONS TO MOBILE RADIOS

L.H. Belden, General Electric Company, Major Appliance Laboratories, Louisville, Ky. 40225.

J.A. Bergeron, General Electric Company, Corporate Research and Development, Schenectady, N.Y. 12301.

ABSTRACT:

Transient thermographic measurements have been performed using full size human head phantom models (containing muscle equivalent material) irradiated by a quarter wave monopole above a ground plane. The antenna was excited by 100 watts at 456.65 MHz. Results describe the effect of model position and orientation on the deposited power. Corrections for thermal diffusion during and after irradiation of the model are applied. Peak specific absorption rates (SAR) for worst case conditions are presented.

MODIFICATION OF THE EXTENDED BOUNDARY CONDITION METHOD FOR
MODELS OF MAN AT AND ABOVE THE RESONANT FREQUENCY

M. J. Hagmann, F. S. Stenger, and P. W. Barber
Departments of Electrical Engineering,
Mathematics, and Bioengineering
University of Utah
Salt Lake City, Utah 84112

ABSTRACT

The extended-boundary-condition method (EBCM) has been used with prolate spheroid models of man and animals to generate much of the theoretical data used in the current dosimetry handbook.

When large a/b ratios (typical of man) or large magnitude permittivities are used with the EBCM, the matrix becomes ill-conditioned, thus disallowing calculations above a certain maximum frequency. Solutions for prolate spheroidal man models are therefore restricted to frequencies somewhat below whole-body resonance. An earlier attempt to solve the problem of ill-conditioning was not completely successful.

The standard mathematical procedure for inverting an ill-conditioned matrix is singular value decomposition, such as with Householder transformations. We have followed the algorithm of Golub and Reinsch to develop a FORTRAN program for inversion of ill-conditioned complex matrices. The routine appears to be significantly more stable than standard matrix inversion procedures. We are currently applying our new inversion routine to EBCM and will present results showing how much of an extension in frequency range is allowed for dosimetry calculations with man and animals.

Householder transformations, as used in our program, serve to transform the matrix for solution relative to a new basis having improved conditioning. Previous applications have shown that consideration of the new basis often provides insight allowing reformulation for a new procedure that is not inherently ill-conditioned. We will follow this direction and attempt to present a description of a Meta-EBCM method especially suitable for use with models of man at and above the resonant frequency.

ELECTRIC AND MAGNETIC FIELD INTENSITIES AND ASSOCIATED INDUCED
BODY CURRENTS IN MAN IN CLOSE PROXIMITY TO A 50 KW AM STANDARD
BROADCAST STATION

R. A. Tell and E. D. Mantiply
U.S. Environmental Protection Agency
Electromagnetic Radiation Analysis Branch
P.O. Box 15027
Las Vegas, Nevada 89114

C. H. Durney and H. Massoudi
The University of Utah
Departments of Electrical Engineering and Bioengineering
Salt Lake City, Utah 84112

Measurements of the electric and magnetic fields which exist in the immediate proximity of a 50 kW AM standard broadcast radio station and the associated induced body currents flowing in man are reported. The data illustrate the potentially intense exposure fields which can occur near high power monopole radiators and represent a novel method for validating theoretically derived values of radiofrequency currents in man. Such validation is important since actual measurements of specific absorption rates (SAR) in full sized humans are difficult to perform at medium wave frequencies. Field measurements were performed at a local radio station operating on 720 kHz and using a single 0.25λ height monopole radiator. Electric (E) and magnetic (H) field strengths up to 300 V/m and 5.5 A/m rms respectively were observed at a distance of about 2 m from the monopole and values of the ratio of E and H, or the wave impedance, were examined from 2 m to approximately 20 km. It was found that the wave impedance dropped to less than half of the far field value of 377 ohms at distances less than 150 m. The current induced in the body of man immersed in these fields was examined via determining the current flowing from the body to ground by standing a person on a small ground plane 15 cm above the earth ground and measuring the voltage drop occurring across a known resistor between the ground plane and earth. A narrow band, tuned technique was used to measure the resulting voltage drop which permitted a very high sensitivity in detecting body currents. It was found that body current was linearly related to the electric field intensity parallel to the long axis of the body and was in the range of 260-290 (μ A)/(V/m) rms depending on height of the person. The measured body current data was compared with theoretically computed values which would flow in a prolate spheroidal model of man standing on a high conductivity ground plane. Excellent agreement between the measured data and the theoretical calculations suggests that theoretical results can accurately account for potentially hazardous currents flowing in man at medium wave frequencies.

SESSION BEMS - 7
WEDNESDAY PM 2:00-4:35
HUB AUDITORIUM

BLOOD BRAIN BARRIER

Chairperson: E. L. Hunt
Walter Reed Army Institute of Research
Washington, DC

IS THE BLOOD-BRAIN BARRIER ALTERED BY RF IRRADIATION?

Darrel H. Spackman, Vernon Riley, *Arthur W. Guy, and *C.K. Chou, Pacific Northwest Research Foundation and Fred Hutchinson Cancer Research Center, Seattle, WA 98104, and *The University of Washington, Seattle, WA 98195.

In previous studies from other laboratories, it was reported that RF radiation at low power densities produced an increased permeability in the blood-brain barrier (BBB) in rats. We have studied this phenomenon in mice, using as test compounds (T-cpds), fluorescein (FCN) and amino acids not normally found in mice. Following i.p. injection of the T-cpds, the animals were bled, killed, perfused, and the brains removed. Clear deproteinized extracts of plasma and of brain homogenates were analyzed for FCN with a Turner spectrofluorometer, and for amino acids with a Beckman amino acid analyzer. The concentration of T-cpds in the brain and plasma of RF-irradiated and other experimental animals was compared to that of non-treated controls.

Following exposure to CW or pulsed RF radiation at 918 MHz and at average power densities ranging from 2.5 to 132 mW/cm² (ave SAR = 0.22 W/kg per 1 mW/cm² incident power density), no significant increase in the BBB permeability could be detected. Subsequent experiments have been directed toward assessing the susceptibility or sensitivity of the mouse BBB as a system for testing RF radiation-induced biological changes. In substitution for RF radiation, the effects of whole-body heating and of i.p. injections of glycerol, urea, metaraminol (a pressor agent), and dimethyl sulfoxide (DMSO) have been examined with respect to any resulting changes in BBB penetration in mice. In the heating experiment, mice were placed in an incubator at 50° for 22 to 25 minutes. In the experiments using the various pharmacological agents, a pretested, maximally-tolerated dose of the compound was injected i.p. In none of the experiments, except those using DMSO were we able to demonstrate an increase in BBB permeability. With DMSO, we observed a significant increase in BBB permeability for the first time in treated mice.

Since several investigators have reported RF radiation-induced increases in BBB permeability in rats, we are now comparing the responses of rats with those of mice under closely controlled, comparable conditions, to determine whether there is a fundamental BBB difference in these two widely used experimental animals.

CEREBROVASCULAR PERMEABILITY TO ^{14}C -SUCROSE IN THE RAT
FOLLOWING 2450 MHz CW MICROWAVE IRRADIATION

Edward Preston and Gabrielle Prefontaine, Division of Biological
Sciences, National Research Council of Canada, Ottawa K1A 0R6

To evaluate whether microwaves alter the blood-brain barrier, permeability-area products (PA) have been measured for passage of ^{14}C -sucrose from the bloodstream into brain. Sprague-Dawley rats (450-500 g) were anesthetized with Nembutal and the femoral artery was cannulated. Each rat was placed singly in a prone position in the quiet zone of an anechoic chamber (8x3x3m) with its head facing a horn antenna located 5 m away. Each rat was irradiated with 2450 MHz CW microwaves for 30 min with a power density of either 1 or 10 mW/cm², or was sham-irradiated. Linear polarization was used with the E-field vertical. About 10 min after irradiation, 15 μCi of ^{14}C -sucrose was injected intravenously, and small serial samples of arterial blood removed for the next 25 min. After the final blood sample at 25 min, the rat was decapitated and the brain was dissected into 5 regions. Using techniques for liquid scintillation counting, the following values were determined for each rat: C_{brain} (dpm ^{14}C /g for medulla, cerebellum, midbrain, diencephalon and cortex); C_{blood} (dpm ^{14}C /ml for the last sample at 25 min); $\int_0^{25} C_{\text{plasma}} dt$ (integral of the plasma level-time curve in which dpm/ml plasma, obtained from blood samples throughout 25 min, were plotted against time). Permeability-area products were calculated from the following equation:^{1,2}

$$\text{PA} = (C_{\text{brain}} - (C_{\text{blood}} \times \text{BVS})) \div \int_0^{25} C_{\text{plasma}} dt$$
 The term BVS represents blood volume space in brain (ml/g) and is used to correct C_{brain} for intravascular sucrose. Regional brain BVS values were estimated from separate experiments using the method of reiterative calculations described earlier,^{1,2} and were found to range from 0.0133 to 0.0206. Mean PA values ($\times 10^6$) for brain regions from the sham-irradiation group (n=7 rats) ranged from 11.99 ± 0.61 (SEM) to $14.47 \pm 0.82 \text{ sec}^{-1}$. For the 10 mW/cm² group (n=7) mean PA values ranged from 11.96 ± 1.73 to $13.70 \pm 1.76 \text{ sec}^{-1}$, and for the 1 mW/cm² group (n=5 rats to date) mean PA values ranged from 11.15 ± 0.91 to $12.19 \pm 0.56 \text{ sec}^{-1}$. An effect of microwave treatment on barrier permeability cannot be concluded at this point, and the results support negative findings reported earlier in which Brain Uptake Index measurements were used.³

¹ Ohno, K. et al. Am J. Physiol. 235: H299-H307, 1978

² Rapoport, S.I et al. Brain Research 150; 653-657, 1978

³ Preston, E. et al. Brain Research (in Press), 1979

STUDIES ON MICROWAVE AND BLOOD-BRAIN BARRIER INTERACTIONS

James C. Lin and Mei F. Lin
Department of Electrical Engineering
and
Department of Physical Medicine and Rehabilitation
Wayne State University
Detroit, Michigan 48202

ABSTRACT

Although the effects of microwave exposure on blood-brain barriers have been studied extensively in laboratory animals, reports of the effects have been varied and sometimes contradictory. Much of this confusion arises from the technical difficulty of controlling microwave exposure and of measuring the absorbed microwave energy distribution in as complex a structure as the brain. An exposure method was developed using a direct contact applicator that allows it to be positioned at a number of sites on the animal's head thereby establishing a different absorbed energy distribution inside the brain at each location. In addition to greatly simplifying the dosimetry, it helps to correlate any observed blood-brain barrier change to the distribution of microwave energy inside the brain. In this experiment, adult Wistar rats were anesthetized with sodium pentobarbital i.p. Indwelling catheters were placed in the femoral vein and in the left external carotid artery. Two ml/kg of 2 percent Evans blue in isotonic saline was used as a visual indicator of barrier opening. Exposure to pulsed 2450 MHz radiation for 20 min. at average power densities of 5, 20 or 40 mW/cm², or approximate SAR's of 3.5, 14 or 28 mW/g in the brain did not produce staining, except in the pineal body, pituitary gland and the choroid plexus, regions in which there appears to be no barrier. Staining was also absent in the brains of sham-exposed animals. Hypertonic urea infusion into the internal carotid artery via the external carotid catheter produced extensive Evans blue staining of the ipsilateral brain regions.

EFFECT OF LOW-LEVEL MICROWAVE IRRADIATION ON THE
UPTAKE OF HORSERADISH PEROXIDASE BY SYNAPTOSOMES

L. M. Irwin, J. L. Lords and C. H. Durney, Departments of
Biology and Electrical Engineering, University of Utah

Synaptosomes isolated from whole rat brain were incubated at 30°C in physiological saline medium which contained horseradish peroxidase (HRP), an extracellular tracer. Synaptosome preparations were either incubated for 70 minutes in 5 mM K⁺ medium (control), depolarized by incubation in 50 mM K⁺ medium for 30 minutes, or irradiated at 960 MHz (absorbed power ~ 1.5 mW/g) for 30 minutes in 5 mM K⁺ medium. K⁺ stimulation and irradiation were both followed by a 40 minute "rest" in 5 mM K⁺ medium. The synaptosomes were then fixed, incubated with H₂O₂ and diaminobenzidine, and prepared for electron microscopy. Thin sections were examined and photographed at random.

There is a significantly higher frequency of synaptosome profiles with 2 or more HRP-labeled vesicles and vacuoles in the K⁺ depolarized preparations. There is a small nonsignificant difference between the irradiated and control preparations, the irradiated synaptosomes showing a slightly higher level of uptake than the controls.

DRUG STUDIES OF MWR EFFECTS ON THE
BLOOD BRAIN BARRIER

Robert M. Lebovitz, Ph.D.
Department of Physiology
University of Texas, Health Science Center at Dallas

Rats weighing from 150-250 grams were exposed in a circularly polarized waveguide chamber to pulse modulated MWR at 1.3 GHz for 2-3 weeks. Exposure was for 3 hours per day at specific dose rates (SAR) of from 0 to 2.6 mW/g. The zero exposure group served as control. Other laboratories have shown significant changes in the blood brain barrier (BBB) following MW irradiation at non-thermal levels. To examine this possibility, the animals were tested for their rate of absorption of the anesthetic sodium barbital.

Since the slow onset of barbital anesthesia is due to slow passage through the BBB, then if MWR had altered this barrier, we would expect the irradiated animals to show a more rapid onset of the anesthetic. Immediately after the final exposure session each of the experimental and control animals were given an interperitoneal injection of barbital sodium, at a dose of 200 mg/kg (in saline solution). The parameter measured was time taken for loss of the righting reflex. At the SAR's of 0.42, 0.96 and 2.6 mW/g no significant differences between control and experimental animals could be detected.

In another series of experiments, irradiated animals along with matched controls were injected with dopamine (100 mg/kg IP). Normally excluded from the brain by the BBB, an elevation in brain dopamine levels would be expected to yield some evidence of motor dysfunction. After MWR exposure at an SAR of 2.6 mW/g for two weeks, the rats were injected and tested for degree and quality of motor activity on the open field (square crossing, rearing, grooming and defecation). Although there was observed more frequent defecation with regard to the experimental versus the control rats, no significant differences in motor activity were observed.

These data do not support the hypothesis of a significant alteration of the BBB by low level MWR. Further, they suggest that any such alterations, were they in fact induced, were not functionally significant.

EFFECTS OF LOW POWER MICROWAVES ON THE
LOCAL CEREBRAL BLOOD FLOW OF CONSCIOUS
RATS

Kenneth J. Oscar, Steven P. Gruenau*, Michael Folker*,
and Stanley I. Rapoport +
US Army Mobility Equipment Research and Development
Command, Fort Belvoir, VA 22060 and Department of
Physics, American University, Washington DC 20016,*
Behavioral Sciences Department, Naval Medical Re-
search Institute, Bethesda, MD 20014,+ Laboratory of
Neurosciences, National Institute on Aging, Geronto-
logy Research Center, Baltimore City Hospital, Balti-
more MD 21224

Local cerebral blood flow was measured in several different rat brain structures with a radioactive iodoantipyrine technique. Exposure to pulsed microwaves of either $1\text{mW}/\text{cm}^2$ or $15\text{mW}/\text{cm}^2$ average power density increased the local cerebral blood flow in several different brain regions. The iodoantipyrine technique allows the use of conscious rats for both the microwave exposure and the regional determination of brain blood flow. Local cerebral blood flow increases of 10 to 144 percent occurred in 16 of the 20 brain regions sampled in both the $1\text{mW}/\text{cm}^2$ and $15\text{mW}/\text{cm}^2$ microwave exposed rats. The largest statistically significant increases occurred in the pineal, hypothalamus, and temporal cortex in the $1\text{mW}/\text{cm}^2$ exposed rats and in the pineal, temporal cortex, inferior colliculus, and medial geniculate in the $15\text{mW}/\text{cm}^2$ exposed rats. Our experiments demonstrating increased brain flow, along with the Wilson et al. experiments (Brain Res. in press) showing increased glucose consumption, confirm that low-power microwaves can cause metabolic changes in rat brains.

ULTRASTRUCTURAL NEUROPATHOLOGY
IN AREAS OF INCREASED BLOOD-BRAIN BARRIER PERMEABILITY
AFTER MICROWAVE IRRADIATION

Ernest N. Albert
Department of Anatomy
George Washington University Medical Center
Washington, D.C. 20037

Adult Wistar rats and Chinese hamsters were exposed to CW microwave irradiation of 2450 and 2800 MHz at 10 mW/cm^2 for 2 hours. Immediately after the exposure animals were anesthetized and an electron dense protein, horseradish peroxidase, was injected via the femoral vein for identification of areas of brains whose blood-brain barrier had become leaky (Albert 1977,79). The brains were fixed via ventricular perfusion of buffered aldehydes, dissected, incubated in 3'3' diaminobenzidine, dehydrated and prepared for electron microscopic examination.

The following ultrastructural changes associated with the blood-brain barrier alterations were observed. 1) Endothelial cell flooding with horseradish peroxidase indicating increased permeability of the plasma membranes, 2) swelling of astrocytic end feet, 3) myelin figures in dendrites indicating possible degeneration, 4) membranous proliferation in dendrites, 5) occurrence of platelet microthrombi in a few capillaries.

Some of the observed changes could present serious health hazards while others may be of lesser concern. Details of these observations will be discussed.

Albert, E.N. Light and electron microscopic observations on the blood-brain barrier after microwave irradiation. In Symposium on Biological Effects and Measurement of Radio Frequency/Microwaves, HEW Publication (FDA) 77-8026, pp 294-309, 1977.

Albert, E.N. Ultrastructural pathology associated with microwave induced blood-brain barrier permeability. URSI International Symposium on Biological Effects of Electromagnetic Radiation, Helsinki, p. 58, 1978.

MICROWAVE FEVER: AN ATTEMPT TO TRANSFER
PNEUMOCOCCAL ANTIBODY ACROSS THE
CEREBROSPINAL-FLUID (CSF) BARRIER

G.R. Hodges, S.E. Worley
D.L. Reeves, and D.R. Justesen

Veterans Administration Medical Center
Kansas City, Missouri 64128

and

University of Kansas School of Medicine
Kansas City, Kansas 66103

To determine whether the relatively large molecule of an experimentally induced antibody would transfer across the cerebrospinal-fluid (CSF) barrier in animals subjected to an intense microwave field, mature rats were individually subjected to sham radiation ($n = 6$) or 918-MHz radiation ($n = 6$) for 30 minutes in a multi-mode cavity (dose rates 20 to 70 mW/g) 7 days after immunization with Type III pneumococcal polysaccharide vaccine. Rats bled and aspirated for CSF immediately after or 7 days after irradiation, which resulted in an elevation of colonic temperature to 42.5 °C, yielded serum titers of antibody that were only half those of sham-radiated rats, but high variability precluded reliable differences. No evidence of antibody was found in CSF of irradiated rats. Because clinical treatment and natural immunological combat of infections of the CNS are hampered by brain and CSF barriers, additional attempts reversibly to breach the barriers to antibody by microwave hyperthermia will be attempted and reported.

THE EFFECT OF POWER DEPOSITION RATE ON BLOOD-BRAIN
BARRIER DISRUPTION

Carl H. Sutton, M. D., Quirino Balzano, Ph.D., and
Frederick B. Carroll
University of Miami School of Medicine, Miami
Florida, and Motorola, Inc., Plantation, Florida

In order to study the tolerance of brain tissue to microwave irradiation, and to determine the upper limits of time and temperature for the application of microwave energy without the production of damaging side-effects, an experimental model was developed which permitted heating of the rat brain selectively. The microwave field from a type A applicator and a standard Burdick medical microwave diathermy generator at 2,450 MHz was visualized with liquid crystal. The integrity of the blood-brain barrier was studied to determine those temperature dosage levels at which protein might begin to extravasate. Horseradish peroxidase, a basic protein with a molecular weight of 45,000, was employed as a tracer protein, which can be studied enzymatically both morphologically and quantitatively in tissues. It does not penetrate the intact blood-brain barrier, but can demonstrate sites of barrier impairment. Each animal was injected intravenously with horseradish peroxidase prior to heating. While bodycore temperatures were maintained at normal levels, the brains of rats were heated to 40°, 42°, 45°, or 47°C. It was found that the blood-brain barrier to peroxidase could be disrupted by heating the brain excessively with microwaves.

The combinations of time and temperature parameters established with the type A applicator failed to show consistent blood-brain barrier disruption when a dielectric-loaded rectangular waveguide was used as the radiator. The waveguide has a large reflection loss (-3dB or higher) and presents dielectric breakdown when the incident power is higher than 80W. A third applicator has been designed and constructed to further investigate the influence of specific absorption rate on the integrity of the blood-brain barrier. The applicator is a cavity-excited corrugated waveguide, which is more directive than the type A applicator or the rectangular waveguide and has practically no mismatch loss. With the corrugated waveguide applicator it is possible to disrupt blood-brain barrier with the same combinations of temperature and time previously determined. Although further investigation is necessary to establish the threshold parameters, it is concluded at this time that slow microwave heating of brain tissue may not be able to disrupt blood-brain barrier, while rapid heating gives reproducible results.

This research was supported in part by Grant PDT-74 from the American Cancer Society, and grants from the Veterans Administration Hospital, Miami, Florida, and the American Cancer Society, Florida Division.

SESSION BEMS - 8
THURSDAY AM 8:30-10:15
HUB AUDITORIUM

DIELECTRIC PROPERTIES: PHYSICAL MEASUREMENT

Chairperson: J. C. Lin
Wayne State University
Detroit, MI

TISSUE IMPEDANCE MEASUREMENTS
USING THE MICROWAVE NETWORK ANALYZER

Jonathan R. Schepps*, Albert W. Friend, Jr.**,
and Kenneth R. Foster*

*Department of Bioengineering/D2, University of Pennsylvania
Philadelphia, Pennsylvania 19104

**Naval Medical Research Institute, Bethesda, Maryland 20014

Accurate data for the dielectric properties of tissue are needed, both to study the mechanisms of microwave interactions with tissue, and to predict the microwave deposition patterns in irradiated tissue. Well known transmission line methods are used to precisely measure the dielectric properties of liquids at frequencies above 100 MHz. However, the semisolid nature of tissue and its high permittivity and loss at microwave frequencies make dielectric measurements difficult. This paper describes the important prerequisites for such accurate measurements.

We describe the use of the microwave network analyzer for measuring tissue dielectric measurements between 0.1 and 18 GHz, using a modified Roberts-von Hippel technique. Using the analyzer, we measure the reflection coefficient from a tissue sample confined at the end of a short circuited length of precision coaxial line by a thin teflon plug. From this reflection coefficient, after correction for various system errors, the sample dielectric properties are calculated. Using the network analyzer, we measure - and correct for - these small residual errors, which seriously degrade the accuracy of the tissue dielectric measurements.

We now routinely measure dielectric properties of tissues over the range 0.1 to 18 GHz, with estimated errors of the order of 2%. To obtain this accuracy, one must (1) use "tuned" sample lengths of one-quarter of a wavelength where the reflection coefficient is most sensitive to the dielectric properties of the sample, (2) measure the sample thickness to within 0.001 cm, and (3) correct for residual system errors (including reflections from the teflon plug used to confine the sample) using calibration measurements on known terminations to obtain the S matrix of the effective two-port error network. This calibration procedure must be performed each time a tissue sample is measured. Measurements on distilled water, physiological saline, and methanol demonstrate the validity of the technique.

MICROWAVE DIELECTRIC ABSORPTION OF MUSCLE TISSUE:
EVIDENCE FOR MULTIPLE ABSORPTION MECHANISMS BETWEEN 1 AND 18 GHz

Kenneth R. Foster, Jonathan L. Schepps, Herman P. Schwan
Department of Bioengineering/D2, University of Pennsylvania
Philadelphia, Pennsylvania 19104

There has been much debate over the mechanisms for the absorption of microwave energy by tissues. Since each absorption process can be expected to result in a dispersion in the tissue dielectric properties at a frequency characteristic of that process, accurate dielectric measurements on tissues should give much information about the biophysical mechanisms responsible for microwave absorption.

We have measured the dielectric properties of single muscle cells from the giant barnacle, Balanus nubilus, using a microwave network analyzer at frequencies between 0.1 and 18 GHz and at temperatures from 1°C to 38°C. This preparation was chosen over vertebrate muscle tissue because single cells can be removed from the animal immediately before each measurement. The cells are a convenient size (ca. 30 mg) and remain contractile during the measurement, so our data are obtained from physiologically viable tissues. At the lowest temperature, the frequencies of measurement extend to twice the Debye relaxation frequency of water (9 GHz at 0°C), the major constituent of the tissues.

In this frequency range, the dielectric properties of the muscle cells are largely determined by the dielectric relaxation of the intracellular water. Thus the dielectric permittivity slightly decreases, and the conductivity quadratically increases, with frequency above 1 GHz and below the Debye relaxation frequency of pure water. By fitting the dielectric data at the higher end of the measurement range to the simple Debye relaxation equations, we find the Debye relaxation frequency and apparent permittivity of the intracellular water. The relaxation frequency of the major fraction of tissue water appears to be the same as that of pure water at the same temperature.

However, there is evidence of a second relaxation process occurring at frequencies in the 0.5 to 5 GHz region. Because of interference from the large dielectric dispersion occurring at still lower frequencies due to the cell membranes, this second dispersion cannot be clearly resolved. While the mechanisms responsible for this second dispersion are not known, it has a characteristic frequency (ca. 1 GHz) and dielectric increment (ca. 5 dielectric units) comparable to that observed in protein solutions, and traditionally attributed to "bound water." At frequencies between 1 and 3 GHz, this second dispersion accounts for a significant fraction of the total microwave energy absorption in these tissues.

ELECTROMAGNETIC DOSIMETRY: DEVELOPMENT OF ANALYSIS AND
MEASUREMENT TECHNIQUES FOR THREE-DIMENSIONAL
COMPLEX-SHAPED DIELECTRIC BODIES

E.C. Burdette, F.L. Cain, and J.J. Wang
Electromagnetic Effectiveness Division
Engineering Experiment Station
Georgia Institute of Technology
Atlanta, Georgia 30332

Accurate dosimetry analysis and measurement techniques are crucial to the use of electromagnetic energy in beneficial medical applications and in investigations of the biological effects of EM radiation. A generalized numerical model for computing the field distribution and absorbed power within complex-shaped heterogeneous three-dimensional biological bodies has been developed, and a 12-channel temperature measurement system was developed and used to validate the model via laboratory measurements of temperature distribution. The analytical model employs the method of moments to solve a pair of integral equations for the unknown equivalent volume electric and magnetic currents. Pulse functions are used as basis functions and delta functions are used for testing. The model treats both uniform plane wave and complex excitation cases. The complex field excitation can be either the near field of an antenna or an enclosing coil. The temperature measurement instrumentation has the capability to measure over a wide temperature range and provides a multi-channel capability with both analog and digital outputs. Laboratory evaluation of the instrumentation indicated excellent linearity over a wide dynamic temperature range, and EM induced temperature errors were very small.

Laboratory experiments were performed to validate the analytical model used for predicting internal field distributions within heterogeneous lossy dielectric bodies. Several geometrical shapes including cubes, square cylinders, ellipsoids, and rat-shaped models were examined. Both homogeneous and heterogeneous cases were evaluated for the normal incidence of the EM field orientated both parallel and orthogonal to the axis of the model and for the EM field oriented at oblique incidence angles. Analytical convergence tests were conducted for cubes, cylinders, and ellipsoids, and experimental verification of the predicted temperatures were performed in homogeneous cylinders, heterogeneous cylinders, and homogeneous rat-shaped models. The analytical convergence tests yielded good results, and the experimental verification of the computer analysis, which was based upon the agreement of measured and predicted temperature rise, also showed very good agreement between computed and measured temperatures.

AUTOMATED DIELECTRIC MEASUREMENTS WITH A
SMALL MONOPOLE IMPEDANCE PROBE

T. Whit Athey
Bureau of Radiological Health
12721 Twinbrook Parkway
Rockville, MD 20857

Interest is increasing in the use of a small monopole antenna as a probe of the dielectric properties of materials, including in vivo and simulated biological tissues. This approach allows a relatively simple measurement system at the point of contact with the material, eliminating the need for precision sample holders and sample preparation. The probe is simply inserted into, or placed against, the material under study. It has broadband capabilities covering HF through X-band.

There is also considerable current interest in automating the measurement of microwave network parameters. Very expensive systems have been available in the past for this purpose, but low-cost desktop computers and minicomputers which can communicate with instruments over the IEEE-488 Interface Bus have brought this approach into widespread usage. We have developed such a system from existing components which is controlled by a minicomputer.

The use of semi-automated microwave network measurements with the monopole dielectric probe potentially provides an extremely simple and versatile tool for making dielectric measurements. Uncertainties in the measured dielectric properties may be significantly reduced. However, there are unique problems associated with the calibration of a network analyzer when using the impedance probe.

The network analyzer system is normally calibrated at a reference plane where standard connectors are available. However, upon attachment of the monopole probe, the system is no longer completely calibrated because of the added connector and short transmission line. We have developed a solution to this problem utilizing a specially-designed probe which can mate directly to similarly designed impedance standards. This allows calibration of the system at the plane of the monopole.

A detailed description of the probe and network analyzer system is given and an analysis of the residual errors is included. Results obtained on standard materials with the system fall well within the range of values reported in the literature.

A TEMPERATURE MONITOR FOR MICROWAVE BIOEFFECTS RESEARCH
AND ELECTROTHERMIA THERAPY

Ronald R. Bowman
Vitek, Inc.
216 Sentinel Lane, JSR
Boulder, Colorado 80302

A very capable electrothermia monitor has been developed. The probe, which is based on prior work, uses a thermistor connected to four slightly conductive leads. The four leads allow the effects of the large and unstable lead resistances to be effectively eliminated. The probes are typically 30 to 35 cm long and slightly more than 1 mm in diameter. They are stable (typically within 0.1 C per month), rugged, and easy to calibrate.

Thermographs show that the probe-caused field distortions and extra heating are negligible for most situations of interest to researchers or therapists. Some simple analysis predicts these thermographic results for portions of the probe away from the tip. Regarding the tip, any extra heating can be measured by the probe itself; and experimental results show, for example, that the extra heating is less than 0.01 C when the probe is used in simulated brain material at 2 GHz with a heating rate of 1 C per minute.

The electronics provide a digital readout in degrees C as well as a signal for recording. The nonlinearity is less than 0.03 C from 25 to 45 C and less than 0.07 C from 20 to 50 C. Several useful features have been designed into the unit, such as a precision offset capability to aid in recording small temperature differences (changes of 0.01 C can usually be measured). The electronics package is "hardened" against RF interference.

MEASUREMENT OF ELECTRIC AND MAGNETIC
FIELD STRENGTHS FROM INDUSTRIAL
RADIOFREQUENCY (6-38 MHz) PLASTIC SEALERS

D.L. Conover, W.E. Murray, Jr.,
E.D. Foley, J.M. Lary, and W.H. Parr
Physical Agents Effects Branch
Division of Biomedical and Behavioral Science
National Institute for Occupational Safety and Health
Center for Disease Control
Public Health Service
U.S. Department of Health, Education, and Welfare

This paper describes the results of occupational radio-frequency (RF) field strength measurements made by the National Institute for Occupational Safety and Health (NIOSH) and compares the results to the ANSI C95.1-1974 personnel exposure standard. Based on this measurement experience, suggestions are made to reduce and better evaluate potential worker hazards from industrial RF exposure. The RF sealers are characterized according to operating frequency, duty cycle, and nominal power output. The field-strength monitors used in the measurements were constructed and calibrated for near-field exposure measurements for NIOSH by the National Bureau of Standards (NBS) and Narda Microwave Corporation. Near-field measurements were made at distances less than one free space wavelength to the RF sealers because the operator is normally positioned at this location. Results of these measurements showed that at least 60% of the RF sealers emitted electric-field strengths in excess of the ANSI C95.1-1974 guideline (200 V/m). In addition, at least 29% of the RF sealers exceeded the ANSI guideline for magnetic field strength exposure (0.5 A/m). In both instances, the measurements have been corrected for duty cycle. Several valuable observations were also made during the surveys. First, depending on how it is used, shielding can substantially reduce or increase operator exposure. Second, exposure from adjacent sealers can be comparable to that received from the RF sealer being operated. Third, all RF sealers surveyed were operated by women. Fourth, short duty cycles can result in high measured field strengths (i.e. greater than 1000 V/m and 2 A/m) but low duty cycle corrected field strengths (i.e. less than 200 V/m and 0.5 A/m). This situation suggests consideration of maximum field strength values (not duty cycle corrected) since certain biological effects may occur in the absence of measurable heating. Finally, field strengths can be quite different when measured at the same anatomical location using the same operator for the same RF sealer.

ELECTROMAGNETIC HAZARDS IN SAFETY ZONE OF
RADIO- AND TV TRANSMITTERS

Henryk R. Korniewicz
Centralny Instytut Ochrony Pracy
00-950 Warszawa, Tamka 1
Poland

The Polish standards define the safety zone around sources of electromagnetic fields with intensities up to 20 V/m, 7 V/m and 0.1 W/m² respectively for the frequencies 0.1 - 10 MHz, 10 - 300 MHz and 0.3 - 300 GHz.

Results of investigation have shown that metallic constructions placed in the region of the safety zone can receive and accumulate enough electromagnetic energy to cause H.F. electric current hazards, initiation of electric detonators and ignition of flammable vapours.

Metallic construction in the safety zone can also act as a secondary source of strong hazardous EMF.

Results obtained:

1. H.F. electric current hazard (50 mA), in the case of human body contact with the grappling iron of cranes, can occur in the safety zone especially in the frequency range 0.5 - 10 MHz for $E \geq 0.8$ V/m.
2. Initiation of electric detonators (threshold sensitivity 0.2 A) connected with the firing installation can take place in the safety zone of the 0.8 - 45 MHz for $E \geq 1.5$ V/m.
3. Ignition of flammable vapours (threshold sensitivity 0.2 mJ) with H.F. spark discharge at metallic construction can take place in the safety zone especially in the region of medium waves when $E \geq 0.2$ V/m.

SESSION BEMS - 9
THURSDAY AM 10:35-11:50
HUB AUDITORIUM

SPECIAL TOPICS

Chairperson: E. N. Albert
George Washington University
Washington, DC

IMMUNOLOGICAL EFFECTS OF LOW MICROWAVE
EXPOSURE

M.G.Shandala, M.I.Rudnev, G.I.Vinigradev, N.G.Belozhko, N.M.Gonchar

/Kiev Research Institute of General and Municipal Hygiene after A.N.Marzeev, Kiev, USSR/

Low levels microwave exposure to power densities 500, 50, 10, 5 and 1 $\mu\text{W}/\text{cm}^2$ effects on cell immunity state and cytochemical indices of functional state of white blood cells were studied experimentally as a function of impact level and duration.

Cell immunity state was assessed according to the lymphocytes blast transformation reaction and spontaneous rosette formation. Glycogen and alkaline phosphatase contents in peripheric blood neutrophils were studied as cytochemical indices.

Significant inhibition of the functional activity of the most important immunocompetent cells was observed under the 500 and 50 $\mu\text{W}/\text{cm}^2$ microwave exposure. This effect was not caused by levels of 1 and 5 $\mu\text{W}/\text{cm}^2$. Shifts caused by microwave energy of 10 $\mu\text{W}/\text{cm}^2$ are considered as adaptative, the complete restoration of changed functions being observed during three months after the termination of exposure.

MICROWAVE EFFECT ON LIPID BILAYER MODIFIED BY
POLYENE ANTIBIOTICS

V.V. Tyazhelov, S.I. Alekseev, and V.I. Mirutenko
Institute of Biological Physics
USSR Academy of Sciences
Pushchino Moscow Region 142292
USSR

THE BIOLOGICAL EFFECTS OF THE LOW FREQUENCY
ELECTROMAGNETIC FIELD (50 Hz)

M.G.Shandala, Yu.D.Dumansky, Ye.V.Prohvatilo, I.P.Loss,
L.A.Tomashewskaya, S.A.Lyubchenko, I.S.Bezdolnaya,
Yu.I.Vasilenko

/Kiev A.N.Marzeev Scientific Research Institute of General and Communal Hygiene, Kiev, USSR/

The biological effects of 50 Hz electromagnetic field following intermittent long-term (for 4 months) exposure of 400 white random-bred rats were studied. Under different energetic and time conditions 4 series of investigations were performed. Physiologic, immunologic, hematologic, biochemical, pathomorphologic and some other indices of animals organism functional state were taken into account.

The minor changes in some indices at the systematic (80 - 300 min. a day) exposure to the electromagnetic field of 15; 20 kV/m intensities were observed. At the shorter period of exposure and lower field intensities (10 kV/m) functional changes were not found at all.

THE POSSIBLE MECHANISMS OF THE BIOLOGICAL EFFECTS
OF THE ELECTROMAGNETIC FIELDS OF LOW FREQUENCY

G. I. Evtushenko and F. A. Kolodub
Kharkov Research Institute of Labour Hygiene
and Occupational Diseases, Kharkov, USSR

In the experiment with white male rats, we studied the biological activity of the electromagnetic fields (EMF) of solenoid of industrial (50 Hz) and low (5-7 kHz) frequencies of different tensions (10-72000 A/m), expositions (to 6 months), regimes of generation (continuous, interrupted, impulsive).

It was determined that under certain parameters of EMF in animal organisms there were distinct changes in the functional condition of the central nervous system (CNS), and the cardiovascular system. There were observed morphological changes in the nervous system, heart, liver, kidney, endocrine glands (adrenal glands, thyroid glands, testes) and in the blood system.

The biochemical methods show that the basis of the most described changes is the discoordination of the individual links of carbohydrate energetic, nitrous and nucleic metabolism. It is conditioned by the primary influence of EMF on the regular systems (femoral and humeral) as on subcellular and cellular at the organismic level.

The importance of primary physico-chemical effects of interactions of EMF of low frequency with organisms is discussed, in particular, Zeeman's effect, inductional current, ponderomotorial forces in the arising of biological function and structural changes.

BEMS 9 - 5

MICROWAVE GASTRIC ULCER

V.V. Tyazhelov, V.P. Safronov, and B.K. Gavriiliuk
Institute of Biological Physics
USSR Academy of Sciences
Pushchino Moscow Region 142292
USSR

SESSION BEMS - 10
FRIDAY AM 8:30-10:00
HUB AUDITORIUM

ROUND TABLE: CELLULAR EFFECTS, RAMAN SPECTRA AND MILLIMETER WAVES

Moderator: O. P. Gandhi
University of Utah
Salt Lake City, UT

Panel: T. W. Athey
Bureau of Radiological Health
Rockville, MD

K. H. Illinger
Tufts University
Medford, MI

S. Motzkin
Polytechnic Institute of New York
Brooklyn, NY

L. M. Partlow
University of Utah
Salt Lake City, UT

J. P. Sheridan
Naval Research Laboratory
Washington, DC

SESSION BEMS - 11
FRIDAY AM 10:20-11:50
HUB AUDITORIUM

MEDICAL APPLICATIONS

Chairperson: S. M. Michaelson
University of Rochester
Rochester, NY

DYNAMICS OF ORGANISM BEHAVIORAL REACTIONS
CHANGES CAUSED BY MICROWAVE RADIATION

M.I.Rudnev, M.A.Navakatikian

/Kiev A.N.Marzeev Scientific Research Institute of General and Communal Hygiene, Kiev, USSR/

The purpose of this experimental work was to study peculiarities of behavioral reactions changes under chronic exposure to microwaves (frequency 2375 MHz) of different power densities (500, 50, 10, 5 and $1 \mu\text{W}/\text{cm}^2$).

Defensive conditioned reflexes, animal activity, food unconditioned reflexes, shock threshold, ability to work and aggressive behavior were registered as indices of central nervous system state.

Dose dependent changes were found at SHF levels of 500 to $5 \mu\text{W}/\text{cm}^2$. As a rule inhibition of CNS was detected by the end of the exposure time and activation after exposure.

MEASUREMENTS OF ELECTROMAGNETIC ACTIVITIES OF THE HUMAN BODY IN THE FREQUENCY REGION 1 kHz - 2 GHz.

B.Enander and G.Larson, Royal Institute of Technology, Stockholm.

Measurements of electromagnetic fields from the human body have been made extensively in the infrared region and at very low frequencies (around 1 Hz, EEG, ECG, EMG). Recently microwave radiation has been measured using microwave radiometers. The results indicate that the human body is only emitting thermal radiation except at very low frequencies (below 10^4 Hz).

The purpose of our experiments was to cover the frequency region 10^3 - $2 \cdot 10^9$ Hz where very few reliable investigations seem to have been made.

To investigate the emission of electromagnetic waves in this wide frequency range we designed a number of tunable radiometers. The general principle of these was a comparison of the noise power obtained from an antenna connected to some part of the human body with the noise power from a reference impedance. At frequencies above 10^8 Hz the antenna consisted of a loop about 1 cm in diameter connected to a coaxial cable. The loop was placed in close contact with some part of the human body. At frequencies below 10^8 Hz the antenna was a pair of EEG or ECG electrodes.

Our results show that the human body acts as a purely thermal radiator down to about 10^4 Hz. Below 10^4 Hz the high frequency components of EMG and similar signal rise above the thermal level. Many different positions on the body were tried as the head, the chest and the arms. For all positions the radiation temperature was equal to the body temperature at frequencies above 10^4 Hz.

MICROWAVE DIATHERMY TREATMENT OF THE HUMAN THIGH:
THE SIMULTANEOUS MEASUREMENT OF MUSCLE BLOOD FLOW (MBF)
AND TEMPERATURE OF THE HUMAN THIGH DURING MICROWAVE DIATHERMY

by

K.M. Sekins, Dept. of Mechanical Engineering, Univ. of Wash.
A.F. Emery, Dept. of Mechanical Engineering, Univ. of Wash.
J.F. Lehmann, Dept. of Rehabilitation Medicine, Univ. of Wash.
W.B. Nelp, Dept. of Nuclear Medicine, Univ. of Wash.
D. Dundore, Dept. of Rehabilitation Medicine, Univ. of Wash.

Abstract

To date the investigation of local muscle blood flow (MBF) response to diathermy and the measurement of associated tissue temperature fields have been undertaken separately, the link between the two phenomenon being inferred from analyses of experiments performed on different individuals undergoing thermally similar treatment regimes. The present study provides more direct evidence illuminating the temperature-MBF relationship by simultaneously measuring MBF by the Xenon¹³³ clearance technique and monitoring the heated tissue temperatures at various depths with a recently developed, microwave-transparent thermistor probe (Vitek Model 101 electrothermia monitor). These measurements were performed by introducing 16 gauge Teflon cannulae from the side of the thigh in an orientation perpendicular to the microwave field such that the cannulae tips were located at prescribed depths along the centerline of anterior portion of the thigh underlying the microwave applicator. The positions of the cannulae as well as the tissue's geometric distortion due to weight of the applicator on the thigh (e.g. crushing effect on subcutaneous fat and change in shape of the thigh cross-section) were ascertained by X-raying the instrumented leg from both the anterior and lateral aspects. After allowing several minutes for the hyperemic response to the cannulae introduction to subside the Xe¹³³ tracer was injected in 0.1 ml volumes at a position just beyond the end of the cannula tip by means of long, narrow hypodermic needles introduced through the lumen of cannula. Subsequent to this injection the thermistor probes were introduced through the cannulae such that their tips were placed in the location of the Xenon injection depot. The temperature history was monitored throughout the entire diathermy process, in contrast to the MBF measurements which were performed corresponding to various thermal events (e.g. pre-treatment, post cooling, peak temperature and steady temperature phases of the application). The resulting data will be presented and their implication for diathermy treatment, as well as their contribution to the understanding of the MBF-tissue temperature relationship, will be discussed.

IMMUNOLOGIC ASPECTS IN CANCER TREATMENT
BY MICROWAVE HYPERTHERMIA

By

Waldemar Roszkowski, Stanislaw Szmigielski,
and Marek Janiak

Center for Radiobiology and Radioprotection
128 Szaserow, 00-909 Warsaw, Poland

Whole-body and local microwave hyperthermia as applied in cancer treatment changes reactivity of the cell-mediated immunity, although the mechanisms of the phenomenon are still virtually unknown. Still more, the reaction of macrophages and lymphocytes differs significantly at 39-41°C (stimulation) and at 42-44°C (inhibition). Thus, the reaction of cell-mediated immunity to whole-body heating or local hyperthermia of tumorous tissues in vivo may differ significantly.

The following subjects will be presented and discussed:

- I. Whole-body microwave (2450 MHz) hyperthermia in mice (rectal temperature 41 °C):
 1. Damage to cell membranes (inhibition of potassium transport and increased membrane permeability for labelled compounds) in different subpopulations of lymphocytes (splenic, lymph-node and thymic) and in macrophages heated to 40 or 43 °C);
 2. Increased intracellular level of cyclic AMP in heated lymphocytes;
 3. Inhibition of lymphocyte reaction to non-specific mitogens after repeated sessions of microwave hyperthermia.
- II. Local microwave hyperthermia of tumorous tissues (43 °C):
 1. Regression of Guerin carcinoma in rats after local hyperthermia and enhancement of the tumor-inhibiting effect by bacterial immunostimulators (Propionibacteriae);
 2. Stimulation of cell-mediated immunity in vivo (increased reaction of spleen lymphocytes to non-specific mitogens, increased cytotoxicity of spleen lymphocytes for 51-Cr-labelled primary culture tumor cells);
 3. Increased antigenicity of heated tumor cells as measured by cancer lung colony assay in healthy animals.

MICROWAVE EFFECTS ON ENERGY LEVELS OF BRAIN AND
MALIGNANT BRAIN TUMOR

Aaron P. Sanders, Daniel J. Schaefer and William T. Joines
Department of Radiology and Department of Electrical Engineering
Duke University, Durham, N. C. 27710

Brain of male Sprague Dawley rat (150-200g) was exposed via removal of skin and muscle above the skull, and a 5 x 10 mm aperture made through the skull with the dura intact. The brain was sham exposed (controls) or exposed to 591 MHz, 5, or 13.8, or 18, or 60 mW/cm² microwaves for periods of 1/2, 1, 2, 3, or 5 min. Reduced nicotinamide adenine dinucleotide (NADH) relative levels were monitored before and during microwave exposures with a Britton Chance designed time sharing fluorimeter (366 nm excitation light, 460 nm NADH fluorescence, and 366 nm reflectance which varies with changes in hemoglobin in the field). A 5 min control baseline was obtained for reflectance and 460 nm NADH fluorescence prior to microwave exposure. Immediately after initiating the microwave exposure, NADH fluorescence increased, reached a maximum (4-12% of baseline) in 30 sec, decreased toward control level to 3 min and slowly increased from 3-5 min. The 366 nm reflectance trace did not vary over the 5 min exposure. A Faraday shield was used to protect the electronics of the fluorimeter from microwave interference artifacts. These data support the concept of microwave inhibition of the electron transport chain in the mitochondria - due to the increase in NADH fluorescence. If so, this should cause a decrease in ATP (adenosine-5'-triphosphate) and CP (creatine phosphate) levels. At the end of the microwave or sham exposure, the head, neck, and upper thorax of the rat was immediately immersed in liquid nitrogen for 2 min. The frozen head was decapitated and stored in liquid N₂ until time for ATP and CP analyses.

ATP and CP assays were performed on frozen pulverized brain (or brain tumor) by the extraction and enzyme coupling techniques of Lowry and Passoneau, and Lamprecht and Stein. At the 13.8 mW/cm² exposures, brain CP was decreased 39.4, 41.1, 18.2, 13.1, and 36.4% of control at the 1/2, 1, 2, 3, and 5 min exposures respectively, and brain ATP was decreased 25.2, 15.1, 17.8, 7.4 and 11.2% of control at 1/2, 1, 2, 3, and 5 min exposures respectively, with no increase in brain surface temperature being seen over the 5 min exposures. All values are statistically significantly different than controls. The 5 mW/cm² and 60 mW/cm² exposures were significantly decreased at the 2 exposure periods (1/2 and 1 min). No threshold power level was observed.

A malignant astrocytoma tumor transplanted subcutaneously to the rear leg of Fischer 344 rat was similarly studied. Statistically significant decreased CP and ATP levels were observed at 1/2, 1, 3, and 5 min exposures (591 MHz, 20 mW/cm²) with no temperature increase observed in the tumors (surface and center).

ELECTRICAL STIMULATION OF ALVEOLAR BONE

Daniel B. Harrington, Thelma A. Chen,
Philip Mollica and Francis Davis
Fairleigh Dickinson University, School
of Dentistry, Hackensack, New Jersey 07601

While the bioelectric parameters in long bone have been studied in some detail, electrical effects on alveolar bone growth have not been defined. In the present study we have explored the effects of three distinct levels of constant, controlled direct current on alveolar bone regeneration in rabbit mandible, after surgical creation of an intrabony defect. Three experimental groups received current levels of 0.1, 1.0 and 10.0 μ amps, delivered through silver electrodes, to portions of the body of the mandible located deep to the masseter muscle. A cathode was inserted into a surgically created intrabony defect on one side of the mandible and an anode was inserted into a defect on the other side. A constant current electric generator was placed subcutaneously at a point posterior to the cervical vertebrae, and sutured to the fascia of the area. All animals received electric current for 14 days, then were sacrificed. Five hours prior to sacrifice the animals received an injection of tetracycline, a fluorescent antibiotic which unites with the inorganic matrix during the mineralization phase of bone growth. After sacrifice, the mandibles were bisected at the mandibular symphysis, and fixed in 10% formalin for 5 days.

Histological examination of the regions around the intrabony defects showed laydown of bone in regions adjacent to the defect. This new bone appears fluorescent due to incorporation of tetracycline, indicating that this new bone is in an active state of mineralization. The degree of fluorescence appears to be consistent with the degree of osteoid formation.

The data indicate that alveolar bone and long bone respond similarly when stimulated with small amounts of electric current, and that it may be possible to develop a bioelectrical method for regeneration alveolar bone which has been lost through disease or trauma.

Supported by General Research Funds,
Fairleigh Dickinson University, School
of Dentistry, and Howmedica, Inc.
Electric generators supplied by
Ritter Sybron Corp.

SESSION BEMS - 12
FRIDAY PM. 1:30-3:00
HUB AUDITORIUM

REPRODUCTION, GROWTH, AND DEVELOPMENT (I)

Chairperson: Z. R. Glaser
National Institute for Occupational Safety and Health
Rockville, MD

IN VIVO STUDY OF 60 HZ ELECTRIC FIELD EFFECTS

Douglas M. Koltun, Scot N. Ackerman,
David M. Weissfeld, Jane M. Seto, Y. Jo Seto

Electroscience and Biophysics Research Laboratories
Tulane University, New Orleans, LA 70118

ABSTRACT

The results of a year long pilot study which examined effects of chronic exposure on 4 generations of rats to high intensity 60 Hz electric fields will be presented. Sixteen male-female pairs of twenty-one day old Sprague-Dawley rats were continuously exposed to an electric field with an unperturbed strength of 20 kV/m, and an equal number of identical rats were sham-exposed. Offspring from these parental groups were conceived, born, and raised under their respective exposure or sham-exposure conditions. Three filial generations were raised in this manner. Body weight and water consumption were recorded weekly. The adult animals were sacrificed at 15 weeks of age, and the organs were examined for morphological and histological changes. Additionally, blood serum chemistry and hematology specimens were analyzed.

GROWTH OF RATS AND MICE EXPOSED TO 60-HZ ELECTRIC FIELDS

R. D. Phillips, J. H. Chandon, D. I. Hilton and R. L. Sheldon

Biology Department
Pacific Northwest Laboratory
Richland, WA 99352
Operated by
Battelle Memorial Institute

ABSTRACT

Considerable controversy exists concerning possible effects of 60-Hz electric field exposure on growth. Results of past research studies are conflicting; both enhanced and depressed growth have been reported, and none of the reported effects have been confirmed independently by other researchers. We have conducted an extensive series of experiments in an attempt to resolve the current controversy by using an exposure system that has been documented to be free of secondary electric field factors, such as corona, ozone, hum, vibration and spark discharges.

In eight separate experiments, body and organ weights were determined in juvenile (age, 26 days) and young adult (age, 56 days) male and female Sprague Dawley rats and in young adult (age, 60 days) male and female Swiss Webster mice that were exposed or sham exposed to 60-Hz electric fields at 100 kV/m for 30 days or 120 days. A number of other parameters were measured in the various experiments that were related to metabolism and growth, including: daily food and water consumptions; oxygen consumption and carbon dioxide production rates; metabolic rates; circulating concentrations of thyroxin, TSH, and growth hormone; content of liver lipid, protein and glycogen; rates of periosteal and endosteal bone growth; tibia weight; concentrations of blood glucose, blood urea nitrogen and serum triglycerides.

In the studies using rats, there were no reproducible, significant differences between exposed and sham exposed animals in any of the parameters measured. The parameters measured in mice (body and organ weights, food consumption and serum chemistry) were essentially the same for exposed and sham exposed animals. Our failure to confirm the various effects reported by other researchers suggests that such effects may be caused by secondary factors and not by the direct interaction of the electric field with the subject.

EFFECTS OF EXPOSURE TO 60 HZ ELECTRIC FIELDS ON GROWTH AND DEVELOPMENT IN THE RAT

L. D. Montgomery, L. G. Smith, and M. R. Sikov,
Pacific Northwest Laboratory, Richland, Washington

A series of three replicated experiments was performed to determine the effects of exposure to an electric field on reproduction and on fetal or postnatal growth and development in the rat. A system was built for exposing rats to a uniform, 100 kV/m vertical, 60 Hz electric field. Other rats were contemporaneously sham exposed under identical environmental and housing conditions.

Reproductive behavior, fecundity, and fetal development were studied in the first experiment. A 6-day exposure prior to mating and continued exposure during the mating period did not affect the reproductive performance of either males or females. Continued exposure of the mated females through 20 days of gestation did not affect fetal mortality, size, or morphology. The males and unmated females were kept in the field for a total of 30 days. The unmated females were removed from the field and subsequently allowed to mate; no effects on breeding performance, fertility, or fetal development were seen. Evaluations of males indicated no effects on mating behavior or on the morphology and DNA properties of the epididymal sperm.

The second experiment evaluated the postnatal sequelae of prenatal exposure. Females were introduced into the field on the morning following mating, maintained through parturition and removed from the field, with offspring, when the pups reached 8 days of age. The pups were periodically weighed, examined, and subjected to a battery of tests to evaluate reflex development and general neurological status. The only effect observed was a higher percentage of exposed offspring showing motile behaviors and a lower percentage exhibiting righting reflexes at 14 days. Subsequent studies in which randomly selected offspring were mated and re-exposed using the same protocol as in the first experiment did not indicate any significant effect on reproductive behavior, fertility, or fetal development.

A third experiment examined the effects of exposure during late gestation and throughout the suckling period. Exposure or sham exposure began at 17 d.g. and was terminated when the offspring reached 25 days of age, using the same battery of postnatal development measures. The growth curves and various maturational indices were similar to those in the second experiment and again showed no consistent differences between the two groups.

Performed under U.S. Department of Energy contract EY-76-C-06-1830.

CHRONIC EXPOSURE OF RATS TO 100-MHz (CW): ASSESSMENT OF
BIOLOGICAL EFFECTS

R.J. Smialowicz, E. Berman, S.J. Bursian, J.B. Kinn, C.G.
Liddle, L.W. Reiter and C.M. Weil
Environmental Protection Agency
Health Effects Research Laboratory
Experimental Biology Division (MD-72)
Research Triangle Park, N.C. 27711

A multidiscipline approach was employed to assess the possible biological effects of chronic exposure of rats to 100-MHz radio-frequency radiation (RF). A group of 20 time-bred rats were exposed in a transverse electromagnetic mode (TEM) transmission line, to 100-MHz at a forward power of 500 W (50 mW/cm^2) starting on day 6 of pregnancy, under controlled temperature and humidity conditions. Dams were exposed for 4 hours per day 7 days per week. On day one post-partum litters were normalized to 4 male pups and these rats were subsequently exposed following the same regimen as the dams. Specific absorption rates (SARs) for rats of various masses (ages) were determined by twin-well calorimetry. No significant differences in SAR's were observed for rats of different mass or for the position of rats in the 100-MHz chamber. The mean SAR for rats was 2.8 mW/g. An equal number of control rats were simultaneously sham-exposed and handled in the same manner as exposed rats. Growth, neurological development, and locomotor activity of the pups were assessed; no difference was observed for any of these parameters between sham and exposed rats. At 21 and 41 days of age pups from each litter were evaluated for possible changes in hematology and immune function. No difference was observed between sham and exposed rats for complete blood counts, for the mitogen-stimulated response of lymphocytes, for the frequency of T- and B-lymphocytes or for the antibody response to Streptococcus pneumoniae capsular polysaccharide. There was no mutagenic effect on sperm cells caused by exposure of male rats in utero through 90 days of age as determined by the Dominant Lethal Test. There were, however, significant changes in regional brain acetylcholinesterase activities in the brains of rats chronically exposed to 100-MHz.

THE EFFECT OF PRENATAL MICROWAVE EXPOSURE ON THE DEVELOPMENT OF
BEHAVIORAL RESPONSES IN THE MOUSE

John C. Monahan, Bureau of Radiological Health
12709 Twinbrook Parkway, Rockville, Md. 20857

Prenatal exposure to high level microwave radiation has been shown to cause fetal abnormalities including gross morphological changes of the central nervous system. Unfortunately, the effects of low-level microwave exposure to a fetus are less clearly defined. The approach taken in the present investigation focused on functional behavioral changes in the newborn as a consequence of prenatal exposure. Pregnant ICR mice were exposed to 2450 MHz CW radiation in an anechoic chamber from day 7 through day 17 of gestation for 3 hours daily at an ambient temperature of 24°C. The subjects could move freely within a Plexiglas holder during irradiation. Average exposure levels were 10 mW/cm² and the estimated specific absorption rate (SAR) ranged from 5.5 to 9.5 mW/g. A battery of standard behavioral tests to determine both reflexive and neurological development were employed in this study. These included tests such as righting reflex, grasp reflex, crossed extensor reflex, eye opening, walking, etc. Pups from both irradiated and sham irradiated mothers were tested from day 1 through day 21 post partum and all tests were done blind. The results indicate a difference between the two groups in a number of the measured parameters, with exposed pups showing a retardation in the initiation of specific behavioral indices. Some delay in the time necessary for 100 percent of the exposed pups to develop a given response was also evident. It should be emphasized, however, that all exposed pups did eventually display the same neurological development and reflexive behaviors as the sham pups.

DEVELOPMENTAL ALTERATIONS IN RATS FOLLOWING IN-UTERO EXPOSURE
TO 500 $\mu\text{W}/\text{cm}^2$, 2450-MHZ MICROWAVES

Sheri J.Y. Mizumori, Richard H. Lovely, R. Bryan Johnson and
A.W. Guy

Bioelectromagnetics Research Laboratory
Departments of Rehabilitation Medicine and Psychology
University of Washington School of Medicine
University of Washington
Seattle, Washington 98195

Eight pregnant rats were exposed to 500 $\mu\text{W}/\text{cm}^2$, 2450 MHz, circularly polarized guided waves, for twenty hours a day throughout the first nineteen days of gestation. There were no distinct physical characteristics which differentiated exposed from sham- and non-exposed litters at birth. However, during the following two weeks, a series of phenomena emerged which implied some type of in-utero microwave effect. There were seven times as many neonatal deaths in the exposed litters than in the controls. Body weights on day 7 of life were significantly lower in exposed males and females relative to control offspring. The pups exposed prenatally lagged behind by a full day in the initiation of eye openings. In addition, subsets of the treated pups were fostered (F-pups) to naive mothers after being culled from the above mentioned litters, which left the remaining pups (N-pups) with the natural mothers. The F-pups were then exposed or sham-exposed postnatally, two hours daily from day 4-11 of life. The prenatally exposed female F-pups demonstrated a significant inability to retain body heat when sham-exposed postnatally. All prenatally exposed females demonstrated an accelerated growth rate between 49-77 days of age which led to subsequent maintenance of a 10% higher body weight throughout adulthood. As adults, the exposed female N-pups that were tested in a conditioned avoidance task exhibited a facilitation in the acquisition phase, while similarly treated male N-pups did not. On the other hand, prenatally exposed male F-pups, when subjected to cold stress (5°C) as adults, had some difficulty maintaining normal core temperatures relative to controls, while female F-pups showed no such difficulty. These observations strongly suggest the need for further research in the developmental bioeffects of low-level microwave exposure.

SESSION BEMS - 13
FRIDAY PM 3:20-5:05
HUB AUDITORIUM

REPRODUCTION, GROWTH, AND DEVELOPMENT (II)

Chairperson: M. L. Shore
Bureau of Radiological Health
Rockville, MD

THE EFFECT ON THE HEART RATE OF EMBRYONIC QUAIL
OF 2450 MHz ELECTROMAGNETIC WAVES

Philip E. Hamrick & Donald I. McRee
Department of Health, Education, and Welfare
National Institute of Environmental Health Sciences

Abstract

Japanese quail (*Coturnix coturnix japonica*) embryos have been exposed to 2450 MHz electromagnetic waves to determine if any observed changes in heart rate could be associated with the exposure. The embryos were 8 to 13 days old when exposed to specific absorption rates ranging from 0.3 mW/g to 30 mW/g. The heart rate was found to depend greatly on temperature but no effect has been found on heart rate for exposure to either pulsed or CW electromagnetic waves at 2450 MHz. The results of additional studies being made with the blocking agents atropine and propranolol will also be reported.

TERATOGENICITY OF 27.12 MHz
RADIOFREQUENCY RADIATION IN RATS

J.M. Lary, D.L. Conover, E.D. Foley, and P.L. Hanser
Physical Agents Effects Branch
Division of Biomedical and Behavioral Science
National Institute for Occupational Safety and Health
Center for Disease Control
Public Health Service
U.S. Department of Health, Education, and Welfare

Eight groups of 16 to 28 pregnant Sprague-Dawley rats were irradiated at 27.12 MHz in a Radiofrequency (RF) Near-Field Synthesizer facility operating in the dominant magnetic field mode at a magnetic field strength of 55 A/m. The groups were irradiated on gestation days 1, 3, 5, 7, 9, 11, 13, or 15, respectively. Dams were exposed one at a time until their rectal temperature reached $43.0 \pm 0.1^\circ\text{C}$ (about 20 to 40 minutes exposure duration). Eight matching control groups of 10 to 13 pregnant rats were sham-irradiated for 30 minutes at 0 A/m. An additional group of 29 pregnant rats was left untreated in the animal quarters. Sham control groups were combined into early (days 1, 3, 5), middle (days 7, 9, 11), and late gestation (days 13, 15) control groups for statistical comparisons with the experimental groups and untreated control group. All dams were sacrificed on gestation day 20 (sperm day = day 0) and examined by standard teratology procedures. The mean specific absorption rate (SAR) for irradiated animals was 12.5 ± 3.1 mW/g. No significant teratological differences were found between sham-irradiated controls and untreated controls. No significant effects were found in litters irradiated during preimplantation development (days 1, 3, or 5) compared to sham controls except for an increased incidence (3%) of grossly malformed fetuses in rats irradiated on day 3. Rats irradiated during organogenesis (days 7 through 15) had a significant increase in the incidence of gross malformations and significant decrease in fetal weight and fetal crown-rump length. Gestation day 9 appeared to be most sensitive to RF radiation (67% incidence of gross malformations). Postimplantation loss was also increased in rats irradiated on days 7 or 9.

STUDIES CONCERNING THE EFFECTS OF NON-THERMAL PROTRACTED
PRENATAL 2450 MHz MICROWAVE IRRADIATION ON PRENATAL AND
POSTNATAL DEVELOPMENT IN THE RAT.

Jensh, R.P., W.H. Vogel, J. Ludlow, T. McHugh, and R.L. Brent.
Departments of Anatomy, Pharmacology, and Radiology, Thomas
Jefferson University, Philadelphia, Pennsylvania

ABSTRACT: Twenty-four Wistar rats were exposed 8 hours daily throughout pregnancy to a 20 mW/cm^2 dosage level of microwave radiation at a frequency of 2450 MHz (total mean exposure time was 108 hours). Previous initial exposures indicated that dosage levels up to 20 mW/cm^2 did not induce an increase in body temperature as measured by a rectal thermocouple probe. Eight rats served as concurrent controls. On the 22nd day of gestation half of the rats in each group were killed for teratologic evaluation, while the other half were allowed to raise their offspring for postnatal behavioral and physiologic evaluation. Fifty-nine baseline control litters (686 fetuses and neonates) were used to control for operative and environmental conditions (baseline controls). Teratologic studies were performed on 103 irradiated fetuses, 31 concurrent control fetuses, and 314 baseline control fetuses for the following parameters: maternal weight gain, fetal and placental weights, litter size, resorption rates, and abnormality rates. Postnatal studies included: 1. rebreeding of mothers and teratologic evaluation of resultant litters, 2. four reflex tests on F_1 offspring, 3. one neonatal physiologic development test, 4. six adult behavioral tests, and, 5. breeding of the F_1 offspring and analysis of the resultant F_2 litters. The results indicate that a non-thermal dosage level of 2450 MHz microwave radiation does not appear to significantly alter prenatal or postnatal growth and development as determined by the above mentioned parameters.

(Research supported by NIH Grant #ES0-1121)

EXPOSURE OF PREGNANT MICE TO 2.45 GHz MICROWAVE RADIATION

Donald I. McRee

Peter Nawrot

National Institute of Environmental Health Sciences

Research Triangle Park, North Carolina 27709

Pregnant mice (CD-1 strain) were exposed to plane-wave, continuous wave, 2.45 GHz microwave radiation. The power densities used in the experiments were 5 mW/cm², 21 mW/cm², and 30 mW/cm². The specific absorption rates determined by measuring the deep colonic temperature using a non-interacting thermistor probe were 4.3 mW/g, 17.9 mW/g, and 25.5 mW/g, respectively. The mice were exposed 8 hours per day - 4 hours exposure, one hour back in home cages and 4 additional hours of exposure. The 5 mW/cm² group was exposed from day 1 through day 15 of pregnancy. In addition to the exposed group, two groups of controls were placed in the same chamber but out of the microwave field. One control group remained in the home cages the entire period and were not handled. The 21 mW/cm² and 30 mW/cm² groups were each divided into two exposure periods. One group of mice were exposed from days 1 through 6 and a second group was exposed from days 6 through 15 of pregnancy. In addition to the two control groups mentioned above - handled controls and unhandled controls - two additional groups were placed in a second environmental chamber with the appropriate elevated ambient temperature to simulate thermal stress. One of the elevated temperature groups was handled identically to the exposed group while the second elevated temperature group was not handled during the exposure period. On day 18 of pregnancy, the animals were sacrificed and skeletal and visceral teratological examinations were performed on the fetuses.

The results of the experiments can be summarized as follows: (1) A significant decrease in pregnancy rate from 86 percent to 72 percent was measured due only to handling during the early stages of pregnancy (days 1-6). An additional decrease to 65 percent occurred at exposures to 21 mW/cm² (days 1-6) and to 50 percent at 30 mW/cm² (days 1-6). No additional decrease in pregnancy was observed in the elevated temperature groups simulating 21 mW/cm² and 30 mW/cm². (2) A significant decrease in maternal weight gain was measured in all handled groups of animals. No differences were measured between the irradiated handled and temperature handled groups. (3) A significant difference in average fetal weights was measured due to a combination of handling and heating. No significant difference occurred between irradiated handled and temperature handled groups. (4) A significant increase in congenital malformations occurred only at the 30 mW/cm² (6-15 days) exposure condition. An increase from 1.7 percent malformations in the temperature handled groups to 3.1 percent in the irradiated handled group was measured. Two-thirds of the malformations in each case were cleft palate.

TERATOGENIC EFFECTS OF RF RADIATION ON MICE

John C. Nelson, James C. Lin and Merlin E. Ekstrom*

Department of Electrical and Computer Engineering

*Department of Comparative Medicine

Wayne State University

Detroit, Michigan 48202

Investigative results from biological effects research during the last decade have indicated that the mammalian embryo is uniquely sensitive to thermal effects of both microwave and radiofrequency (RF) radiation. With an increasing number of RF sources in the environment a need exists for information regarding specific bioeffects of RF radiation. To study the teratogenic potential (in utero damage of fetuses) of low-level 148 MHz repeated exposures on pregnant mice, three independent experiments were performed. A total of 236 female C₃H mice was timed-mated. The dams were irradiated daily for 1 hour in rectangular coaxial exposure systems from day 1 to day 19 of gestation. The incident power density of the plane wave fields was 0.5mW/cm², corresponding to 0.013 mW/gm. of average rate of energy absorption. Control dams were mock-irradiated in identical nonenergized exposure systems. At the 19th day of gestation, each dam was euthanized and the uterus was removed via Caesarian section. The fetuses were examined for gross abnormalities and then weighed. The percentages of fully resorbed, stillborn, and abnormal fetuses were tabulated. Natural-born fetal weights were recorded at birth and again after allowing the litters to develop to adulthood (60 days). A total of 609 implantations was observed in 63 experimental animals for the three identical experiments. Mean values of fetal and adult weights were analyzed using the t-test. The significance level of the test (p value) was preset at 0.05. For experiments I and II both the Caesarian and natural-born fetal weights differed significantly with $p < 0.05$. There was no difference in Caesarian fetal weights in experiment III, but natural-born fetal weights differed. Adult weights at 60 days of age for the natural born in experiment I were without difference. Representative normal fetuses were selected from each experimental group. Histopathological examination of mid-sagittal sections indicated no substantial difference between control and irradiate organ systems.

OBSERVATIONS OF RAT FETUSES AFTER IRRADIATION
WITH 2.45 GHZ (CW) MICROWAVES

Ezra Berman*, Hershell B. Carter*, and Dennis House**

*U.S. Environmental Protection Agency
Health Effects Research Laboratory
Experimental Biology Division (MD-72)
Research Triangle Park, NC 27711

**U.S. Environmental Protection Agency
Health Effects Research Laboratory
Statistics and Data Management Office (MD-55)
Research Triangle Park, NC 27711

Abstract

Female Sprague-Dawley (CD) rats were exposed to 2.45 GHz frequency (CW) microwave radiation at a power density of 0 or 28 mW/cm² for 100 minutes daily from days 6-15 after breeding. There were 67 sham-irradiated and 70 irradiated females, producing 64 and 66 pregnancies, respectively. When sham and irradiated pregnancies were compared, no significant differences were seen in pregnancy rates; litter mean number of live, resorbed or total fetuses; nor in the incidences of external, visceral, or skeletal anomalies or variations. In a separate experiment, 35% of adult rats exposed under these conditions to a power density of 40 mW/cm² died from hyperthermia. It is concluded that this frequency will not have a strong teratogenic effect in the rat fetus without a very significant maternal thermal hazard.

TERATOLOGY IN RATS EXPOSED TO 2450-MHZ MICROWAVES AT
INTENSE AND INTERMEDIATE DOSE RATES

M.E. Chernovetz
University of Tulsa, Tulsa, Oklahoma

D.L. Reeves and D.R. Justesen
Kansas City Veterans Administration Medical Center
Kansas City, Missouri

Fifty-six female, time-bred, Holtzman-derived Sprague Dawley rats were delivered to the laboratory on day one or two of gestation. Day one is counted as the day during which the animals were sperm positive. Forty of the rats were randomly but equally assorted into four experimental groups, each of which was exposed once to 2450-MHz energy (at 17 or 31 mW/g for 20 min.) on the 8th, 10th, 12th, or 14th day of gestation. Eight of the remaining animals were sham exposed and eight served as passive cage controls. Caesarean section and teratological observation of fetal materials occurred on gestational day 18. The number of implantations and of dead, resorbed, and live fetuses, and the presence of structural abnormalities were recorded as was mass of the fetal body and brain. Two control studies provided information on ΔT s of rectal temperature following 20-min. of irradiation at 31 mW/g. In study one, rectal temperatures were measured after 5, 10, 15, and 20 minutes of irradiation. In study two, temperatures were measured for 40 to 60 minutes at 10-minute intervals following the exposure. Twenty five dams that survived irradiation in the formal study were gravid. Six dams (19%) died during or immediately following a microwave treatment. Reliable increases in numbers of fetal resorptions and abnormalities were observed in dams that had been irradiated at 31-mW/g. Exencephaly was the most frequent abnormality and occurred in association with a treatment on days 8 and 10 of gestation. Fetal mass was lower in association with the 31-mW/g treatment, while fetal-brain mass varied complexly as a function of microwave treatment and the day of gestation during which exposure occurred. Regression analyses showed that both peak temperature and dose rate are inversely related to means of fetal mass and to mean numbers of live fetuses. Peak temperature and dose rate were positively related to the number of resorbed as well as the number of abnormal fetuses. The data provide further evidence that microwave radiation can be teratogenic, but that levels must be so intense as to result in a high incidence of lethality in a given group of dams.

BEMS POSTER SESSION A
TUESDAY PM 1:30-4:50
HUB 108 WEST LOUNGE

Co-Chairperson: P. Kramar
University of Washington
Seattle, WA

Co-Chairperson: W. A. G. Voss
University of Alberta
Edmonton, Alba., Canada

MEDICAL APPLICATIONS (Paper Nos. 1 - 15)
DOSIMETRY (Paper Nos. 16 - 24)
CELL BIOLOGY (Paper Nos. 25 - 36)
BEHAVIOR (I) (Paper Nos. 37 - 48)

A MICROWAVE DIATHERMY APPLICATOR

M.A. Stuchly
Radiation Protection Bureau
Health and Welfare Canada
OTTAWA, Ontario, K1A 0L2

S. S. Stuchly
Dept. of Electrical Engineering
University of Ottawa
OTTAWA, Ontario, K1N 6N5

G. Kantor
Bureau of Radiological Health
U.S. Dept. of Health Education
and Welfare,
ROCKVILLE, MD., 20857 U.S.A.

ABSTRACT

The existence of some indication that microwave induced hyperthermia may be successful in the treatment of certain types of cancer, and the proposed regulation on microwave diathermy devices in Canada and the draft proposed microwave diathermy standard in the U.S. have stimulated an increased interest and progress in the development of new applicators. The main objective of improved applicators is to minimize leakage and optimize the energy deposition.

This paper provides a design method and experimental results for a direct contact circular aperture applicator. The applicator is equipped with a corrugated flange which purpose is twofold, to improve the uniformity of the heating pattern and to limit the leakage. The performance of the applicator operating at 2.45 GHz, has been tested using a short monopole probe and a thermographic camera, and the results obtained by the two methods have been compared.

BEMS POSTER A - 2

MEASURED PATTERNS OF STRAY RADIATION PRODUCED BY
THERAPEUTIC MICROWAVE APPLICATORS WHEN APPLIED TO
TISSUE-SUBSTITUTE MODELS AND HUMAN SUBJECTS

J.F. Lehmann, A.W. Guy, and J. Wallace
Department of Rehabilitation Medicine
University of Washington
Seattle, WA 98195

The patterns of stray radiation produced by two prototype diathermy applicators were measured. Both applicators were used to irradiate four different tissue-substitute models and four human subjects of varying physical size. The applicators were placed at eight anatomical sites on the human subjects. The distances from each diathermy applicator to the $5\text{mW}/\text{cm}^2$ and $10\text{mW}/\text{cm}^2$ power-density levels were recorded as well as the incident power-density at sensitive anatomical sites (i.e., eyes, gonads). The measured power-density levels indicated that neither applicator tested would comply with the proposed Bureau of Radiological Health microwave diatherm performance standard.

COMPARATIVE STUDY OF 2450 MHz and 915 MHz DIATHERMY
APPLICATORS WITH PHANTOMS

G. KANTOR AND D. M. WITTERS

Division of Electronic Products, Bureau of Radiological Health
FDA

5600 Fishers Lane, Rockville, Maryland 20857

In support of the BRH diathermy programs, techniques to evaluate the relative effectiveness and safety of applicators were developed. According to the proposed microwave diathermy standard, a leakage of not more than 10 mW/cm^2 at 5 cm from the phantom-applicator boundary is required. The leakage is determined under conditions in which a Specific Absorption Rate (SAR) of 235 W/kg is delivered to simulated muscle tissue of a phantom beneath its 1 cm or 2 cm fat layer. Three recently developed BRH applicators with chokes, one for 2450 MHz and two for 915 MHz use, meet the requirements of the proposed standard (the smaller 915 MHz applicator has a thin sheet of absorbing material around the exterior choke surface). Analysis of their performance revealed that it is much easier to control leakage at 2450 MHz than at 915 MHz. The 2450 MHz applicator has less than 5 mW/cm^2 leakage for both direct contact and 1 cm spacing between aperture and planar phantom. Both the large and small 915 MHz applicators have less than 5 mW/cm^2 leakage for direct contact. However, for a 1cm spacing between aperture and planar phantom, the leakage exceeds 10 mW/cm^2 for the large 915 MHz applicator and is about 100 mW/cm^2 for the small 915 MHz applicator.

Four microwave hyperthermia applicators of various cancer therapy groups, including RTOG, were evaluated. None of these applicators had special design features to control leakage radiation. They include a 2450 MHz design with three concentric circular tubes and three 915 MHz designs with dielectrically loaded waveguides. A comparison of the heating patterns of all the tested applicators shows that the depth of penetration normal to the fat-muscle interface (defined at a point where half the maximum SAR in muscle tissue exists) is nearly identical for 2450 MHz and 915 MHz. The depth is about 2 cm beneath the fat-muscle interface for both of these ISM frequencies.

To summarize, 915 MHz applicators require much more net power than 2450 MHz applicators to deliver the same SAR to muscle tissue, when not in direct contact. For even a small spacing between aperture and phantom (cm), excessive leakage results. In addition, since depth of penetration is about the same, 2450 MHz applicators seem to be considerably more effective and safe.

EVALUATION OF 915-MHZ AND 2450-MHZ DIRECT
CONTACT DIATHERMY APPLICATORS

J. Wallace, A.W. Guy, J.A. McDougall, and J.F. Lehmann
Department of Rehabilitation Medicine
University of Washington
Seattle, Washington 98195

The design, test, and evaluation of three 915-MHz, circularly polarized direct contact diathermy applicators is discussed. The applicators were developed for the purpose of therapeutically heating biological tissue. The heating patterns produced by the applicators in a bi-layered planar tissue model were measured and compared to the heating patterns produced by a 915-MHz, linearly polarized applicator and a 2450-MHz circularly polarized applicator. Several performance criteria were obtained from the recorded heating patterns, including: peak Specific Absorption Rates (SAR), depth of penetration of energy, and uniformity of SAR in the model.

Each 915-MHz applicator produced greater depths of penetration with significantly less heating of the superficial tissue than was produced by the 2450-MHz applicator. The width of uniform SAR was dependent on the size of the applicator aperture (i.e., as the area of the applicator aperture was increased, the width of the SAR also increased).

MICROWAVE DIATHERMY TREATMENT OF THE HUMAN THIGH:
THE EXPERIMENTAL MEASUREMENT OF THE MUSCLE BLOOD FLOW
RESPONSE AND THE NUMERICAL SIMULATION
OF THE TISSUE TEMPERATURE RESPONSE.

by

A.F. Emery, Dept. of Mechanical Engineering, Univ. of Wash.
K.M. Sekins, Dept. of Mechanical Engineering, Univ. of Wash.
D. Dundore, Dept. of Rehabilitation Medicine, Univ. of Wash.
J.F. Lehmann, Dept. of Rehabilitation Medicine, Univ. of Wash.
P.W. McGrath, Dept. of Nuclear Medicine, Univ. of Wash.
W.B. Neip, Dept. of Nuclear Medicine, Univ. of Wash.

Abstract

The therapeutic effects of diathermy are associated with its ability to increase the tissue temperature and to elevate the local tissue blood flow. This paper reports the results of measurements of muscle blood flow in the anterior thigh treated with a 915 MHz, direct-contact, air cooled microwave applicator. The flow rates were measured by the Xe^{133} clearance method which permits a localized evaluation. The study consisted of a number of separate washout experiments on several volunteers, all of good health and with minimal subcutaneous fat, under a variety of control and treatment protocols designed to demonstrate the behavior of the blood flow while undergoing microwave heating and being simultaneously cooled at the skin surfaces to prevent high temperatures of the fat-muscle interface. Resting blood flow rates of 2 ml/min/100 gm and maximum rates of 32 ml/min/100 gm were recorded, and the particular depths explored were 1.5 and 3.0 cm below the surface. The effective combination of microwave diathermy and surface cooling in focusing the treatment into the deeper muscle tissues was shown by the markedly different blood flow rate histories of the two different depths.

In addition a finite element thermal model of the thigh was developed to predict the local tissue temperatures during the microwave diathermy treatment with surface air cooling. The thermal model includes local temperature dependent metabolism, spatially varying thermal properties and microwave power deposition, a temperature dependent muscle blood flow, and cold-induced subcutaneous fat vasoconstriction. The latter two effects were found to be the most important characteristics in the accurate prediction of tissue temperature as evidenced by a comparison with experimentally measured temperatures. Using measured muscle blood flow rates, the model was used to parametrically study the effects of power deposition rates and cooling protocols. The numerical results show that therapeutically desirable temperatures can be achieved deep within the thigh without undesirable surface temperatures.

A BROADBAND AND COMPACT APPLICATOR FOR DEEP
TISSUE HEATING USING FOCUSED MICROWAVES

M. F. Iskander, C. H. Durney, D. A. Christensen, and A. Riazi
Department of Electrical Engineering
University of Utah
Salt Lake City, Utah 84112

ABSTRACT

An important need in the study of hyperthermia methods in cancer therapy is a focused microwave system that will deliver adequate energy to deep-seated tumors without overheating the intervening normal tissue. This paper describes the design of a broadband (150 MHz to 1100 MHz) microwave applicator that is useful in this regard both as a single applicator and as a radiating element in a focused microwave system.

A broadband applicator is desirable not only to achieve heating at different depths but also to examine the optimum conditions for focusing the microwave radiation. The design procedure utilizes a tapered section of double-ridged waveguide as a broadband feed for a horn section. The waveguide ridges were extended logarithmically up to the aperture of the horn section. This procedure simply allows a smooth and broadband impedance transition between the 50-ohm coaxial input impedance and the 377-ohm free-space impedance. The measured VSWR values at selected frequencies in the operating frequency band were found to be less than 2.0. The double-ridged horn applicator was then filled with a circulating low-loss liquid (formamide, $\epsilon_r = 109$) to achieve both scaling the operating frequency band down by a factor of $1/\sqrt{\epsilon_r}$ and cooling the surface of the overlying tissue. Experimental results describing the measured VSWR, gain, beam width, and heating pattern of the horn as a function of frequency will be presented. This broadband applicator will also be used as a building block in a larger system for focused microwave heating of deep tissue.

DEEP VISCERAL HYPERTHERMIA IN MAN
WITHOUT SURFACE TISSUE INJURY

F. Kristian Storm, William H. Harrison,
Robert S. Elliott, and Donald L. Morton
Division of Oncology, Department of Surgery
University of California School of Medicine
Los Angeles, CA 90024
and
Surgical Service
Veterans Administration Hospital
Sepulveda, CA 91343

There is mounting evidence that radio frequency hyperthermia $\geq 42^{\circ}\text{C}$ is tumoricidal in cell cultures, animal models, and human tumors. Most research has been limited to superficial tumors, since electromagnetic energy is ordinarily preferentially absorbed in surface tissue, causing surface burns.

Our studies on dogs and sheep showed that at least 3 W/cm^2 was necessary to achieve deep internal hyperthermia, and while no preferential heating occurred in any animal normal viscera from $37\text{--}49^{\circ}\text{C}$, surface burns did occur using standard methods.

Surface cooling resulted in efficient internal heating, and with proper dose duty cycling, effective deep hyperthermia was possible in pigs with 3 cm rine. However, in humans with ≥ 1 cm subcutaneous tissue, potentially effective deep hyperthermia resulted in surface burns despite surface cooling to 5°C .

Our development of a fundamentally new radio frequency device which allows uniform heating to any depth without surface injury has allowed evaluation of both superficial and internal tumors. Of 52 human tumors evaluated (25 surface, 27 visceral), temperature $\geq 42^{\circ}\text{C}$ occurred in 42 (81%), $\geq 45^{\circ}\text{C}$ in 23 (44%) and $\geq 50^{\circ}\text{C}$ in 19 (37%), with surface and adjacent normal tissues remaining at physiologic temperatures.

These data suggest that with proper instrumentation, hyperthermic investigation may now safely progress regardless of tumor location.

LOCALIZED RF HYPERTHERMIA ON HAMSTER CHEEK POUCH CARCINOMA

Colvin, D. P.,¹ Doss, J. D.,² Marsh, B. R.,³ Frost, J. K.,³
Burgess, B. S.,¹ and Patra, A. L.¹

¹Becton, Dickinson Research Center

²Los Alamos Scientific Laboratory

³Johns Hopkins University Medical Center

A cooperative program between Becton, Dickinson Research Center, Los Alamos Scientific Laboratory, and Johns Hopkins University Medical Center has been initiated to develop a localized RF hyperthermia probe for transbronchoscopic therapy of early lung cancer. The possible adaptation of a RF hyperthermia system, developed at Los Alamos Scientific Laboratory (LASL), for the treatment of early or unresectable bronchogenic carcinoma is presently under investigation.

The LASL RF hyperthermia system was developed for the treatment of cancer eye in cattle as part of activities related to the Los Alamos Meson Physics Facility (LAMPF). LASL engineers have developed a small, battery-powered, hand-held device which can apply up to 10 watts at 2 Mhz between two electrodes, with the applied power controlled by a thermistor sensor located within one of the electrodes.

An animal model system using DMBA-induced squamous cell carcinoma in hamster cheek pouches is being used to evaluate the potential system at BDRC. A group of experiments were initiated in September using the LASL RF hyperthermia system to heat the cheek pouch carcinomas at 45 to 50°C for 30 to 120 seconds. Results are encouraging with regression within two weeks of treatment of 44 tumors in 15 animals.

LOCALIZED MICROWAVE HYPERTHERMIA AT X-BAND ON
EXTERNAL TUMORS IN MICE

Arnold Feldman, General Science Department, University of Hawaii,
Honolulu, Hawaii 96822 and Lawrence H. Piette, Cancer Center of
Hawaii, 1236 Lauhala Street, Honolulu, Hawaii 96813

Abstract

We have developed a slow-wave structure that can be implanted internally and used to heat tumors. It is a helical coil, operating at 9.3 GHz. It has successfully treated methylcholanthrene-induced fibrosarcomas implanted subcutaneously in the hind leg of BALB/cJ female mice. The tumors range in size from 75mm^3 to 491mm^3 . The coils are wound so as to encompass the tumor and approximately satisfy the relation $\frac{\lambda}{10} \leq 2\pi a \leq \frac{\lambda}{2}$ where $2\pi a$ is the mean diameter and λ is the wavelength in situ.

A single heat dose of $(44.0 \pm 0.4)^\circ\text{C}$. applied for 30 minutes to 34 mice with tumors in the leg resulted in 15 long-term cures (44%), and 4 complete tumor remissions (12%) followed by tumor regrowth within two weeks. In 10 cases (30%), the entire treated tumor was destroyed but tumor regrew in the area adjacent to the treated area. In 26 of 30 untreated controls, a palpable tumor arose within 7 days post-implantation. It never spontaneously regressed and all mice were dead within three months post-implantation. The same heat dose applied to 17 mice with tumors implanted in the footpad - but where the tumor-bearing limb was immersed in a temperature-controlled water bath - resulted in only two long-term cures (12%). All 15 untreated controls grew tumors which never spontaneously regressed and all were dead by three months post-implantation.

LOCALIZED HYPERTHERMIA IN DOG BRAIN USING
AN INVASIVE MICROWAVE PROBE

John W. Strohbehn,^{*,**} Evan B. Douple,^{*,**} David W. Roberts,^{**}
David DeSieves,^{*} B. Stuart Trembly,^{*} Roy Matic,^{*} Stanley Brown,^{*,**}
Peter Runstadler[†]

Thayer School of Engineering,^{*} Dartmouth College;
Dartmouth Medical School;^{**} and Create, Inc.[‡];
Hanover, New Hampshire 03755

In recent years the use of hyperthermia as a modality for cancer therapy has received increased attention and numerous results are beginning to appear with regard to its efficacy in vitro, in animal tumors, and in human trials. Simultaneously many technological alternatives for producing and controlling the heat to cancerous tissue have been proposed and are being evaluated and refined. At present no single technique seems to be able to meet the requirements of providing a prescribed temperature distribution over a variable size volume located anywhere in the body, and hence it is very probable that the research and clinical needs in hyperthermia will be met by a number of technological alternatives for producing heat.

Our group at the Dartmouth Medical School and the Thayer School of Engineering has been investigating the use of invasive microwave antennas (coaxial, quarter-wave monopoles) as a means of providing a localized temperature distribution in regions deep within the body. Such a probe has potential for tumors not accessible by other means, e.g. for glioblastomas located deep within the brain.

In this report we discuss a number of sets of thermal measurements with our invasive microwave antenna system including measurements in (a) dog brain, with and without blood flow, (b) mice, (c) dead human brain, (d) "gel" phantom, and (e) phantom material proposed by Guy. The mouse, dog, and human data was taken with the aid of a carefully constructed mechanical jig which permitted precise measurements (to better than 1 mm) of the radial distribution of temperature.

Theoretical calculations of the temperature distributions in tissue, both with and without blood flow, have been made by numerically solving the heat equation, using a theoretical model for the EM fields produced by our antenna. The results are compared with the measurement data discussed above.

The following conclusions can be made at this time: (a) the heated volume in mouse tumors is about 1 cm, (b) the heated region in the dog brain is about 0.6 cm, being slightly larger without blood flow, (c) the theoretical model compares favorably with the mouse tumor data and with the dog brain data with blood flow, but predicts a much larger heated volume than is observed for dog brain without blood flow, and (d) the volume heated by the present antenna is adequate for re-search investigations in implanted animal tumors but is too small for most human tumors.

ELECTRICAL PROPERTIES OF TISSUE EQUIVALENT
BOLUS FOR MICROWAVE HYPERTHERMIA

A. Y. Cheung*, P. D. Hrycak**, G. H. Harrison and L. S. Taylor***
Department of Radiation Therapy
University of Maryland Hospital, Baltimore, Maryland

*Joint with Institute for Physical Science and Technology
University of Maryland, College Park, Maryland

**Westinghouse Electric Corp., Baltimore, Maryland

***Electrical Engineering Department
University of Maryland, College Park, Maryland

ABSTRACT

Liquid (saline + ethanol) and gel-like (saline + polyethylene + TX150) muscle-equivalent bolus suitable for clinical use in microwave hyperthermia have been developed. Using a combination of techniques, (short-circuited waveguides, and impedance sensing using a short monopole) electrical properties of various mixtures of the above materials have been studied at frequencies ranging from 1-10GHz and temperatures from 25-45°C. Empirical formulation governing the functional dependency on frequency, composition and temperatures for electrical properties of microwave bolus have been derived. The following equations govern the electrical properties of both the liquid and solid materials:

$$\epsilon = (\epsilon_o - P)(1 + (F/F_R)^2)^{-1} + 4.8$$

$$\sigma = \sigma_s + (\%H_2O - 30)(F^3/7.2 \times 10^5)(1 + (F/F_R)^2)^{-1}$$

where

$$\epsilon_o = 78.5(25^\circ C), 77(30^\circ C) \text{ and } 75(35^\circ C)$$

P = Percentage (by weight) of non-water component

$$F_R = 14.5\text{GHz}(25^\circ C), 12.4\text{GHz}(30^\circ C) \text{ and } 11\text{GHz}(35^\circ C)$$

F = Frequency in GHz

and

σ_s = low frequency conductivity due to salinity for gel-like bolus and for liquid bolus, the concentration of ethanol also contributes.

Techniques for measurements, empirical data leading to the above formulation, as well as data describing the temperature dependence of σ_s will be discussed.

A SYSTEM FOR PRODUCING LOCALIZED
HYPERTHERMIA IN BRAIN TUMORS THROUGH MAGNETIC
INDUCTION HEATING OF FERROMAGNETIC IMPLANTS.

P.R. Stauffer, ** T.C. Cetas, ** R.C. Jones **
and M.R. Manning

* Division of Radiation Oncology and ** Department of
Electrical Engineering, University of Arizona, Tucson, AZ

Certain brain tumors, such as glioblastoma multiforme Grade IV which is universally fatal, have been identified as candidates for treatment with hyperthermia combined with ionizing radiation following the usual surgical debulking. This tumor contains radioresistant hypoxic cells which spread into normal brain tissue along microscopic tracts. In vitro data support the hypothesis that hypoxic cells may be particularly sensitive to the combination therapy. Thus, we are developing a magnetic induction system for producing localized hyperthermia in these intracranial tumors. Differential heating is achieved through use of small (1-2 mm diameter) ferromagnetic seeds which can be stereotactically imbedded in residual tumor at the time of craniotomy. The dependence of differential implant heating on the power source frequency has been characterized and indicates use of frequencies below 2MHz. Thermographic analysis of temperature distributions induced in phantom models has been performed for various implant materials, sizes, geometries and array configurations. The thermal conductivity and electrical properties of the phantom brain tissue were verified empirically and were used to construct simple mathematical models. Temperature distributions induced in single seed phantoms are consistent with the theoretically expected dependence on the inverse radial distance from the seed. In particular, Trial 16 showed a temperature differential greater than 4 °C out to five seed radii (1 cm) from the implant site with no significant direct heating of the phantom by the RF field. A description of the coil and system design is provided with special attention to the final impedance matching network. Trials on animals will be followed by application to humans as soon as confidence with the technique and apparatus can be established from these laboratory experiments.

VALIDATION OF MICROWAVE PULMONARY EDEMA DETECTION
BY ISOLATED LUNG AND PHANTOM MEASUREMENTS

M. F. Iskander, C. H. Durney, and B. H. Ovard
Department of Electrical Engineering
D. G. Bragg
Department of Radiology
University of Utah
Salt Lake City, Utah 84112

ABSTRACT

The feasibility of using microwave methods to detect changes in lung water content has previously been demonstrated by measurement on phantoms and live animals. This paper describes how the accuracy of the method for detecting the early stages of interstitial edema was investigated in experiments on isolated lungs of dogs. The isolated lungs were used to eliminate the interference from the extrapulmonary structures, such as the chest wall, which could affect the accuracy of the *in-vivo* measurements. The experimental procedure used to induce the edema in the isolated lungs will be described in detail. The results clearly show that an immediate and direct change in the phase of the microwave transmitted signal occurs as the weight of the lung changes with water content. These results are a strong indication of the accuracy of the microwave method in detecting early stages of pulmonary edema.

Furthermore, the sensitivity of the microwave signal to factors other than the fluid accumulation in the lung was studied experimentally. Physiological and geometrical changes occurring during the development of edema in the *in-vivo* experiment, such as the establishment of a water gradient, and the expansion of the heart and other blood vessels, were first quantified by measurements in a computerized axial tomography (CAT) scanner and then simulated and studied in two-dimensional phantoms. Several phantoms representing typical cross sections of the dog thorax were constructed and the experimental results that were obtained will be presented.

TECHNICAL ASPECTS OF ELECTROMAGNETIC TECHNIQUES FOR
RECOVERING CRYOGENICALLY-PRESERVED LARGE ORGANS

J. Toler, J. Seals, and E. McCormick
Engineering Experiment Station
Georgia Institute of Technology
Atlanta, Georgia 30332

A nation-wide system of banks in which human organs can be stored in readiness for implantation has long been recognized as a capability that would substantially enhance the delivery of health care. Research studies directed to transforming this desired capability into reality have focused on investigating techniques by which organs can be satisfactorily received, typed, stored, and rapidly recovered for implantation. Acceptable techniques for organ receipt and typing are now generally available; consequently, recent research has been concerned with studying the problems associated with organ storage and recovery. Although problems in these two areas are interactive, this paper will focus on recent studies that investigated technical problems involved in using electromagnetic (EM) waves to recover cryogenically-preserved organs.

An a priori knowledge of tissue dielectric properties is essential when using EM waves to recover cryogenically-preserved large organs because these properties influence the interaction between the EM wave and the tissue to be thawed. Electromagnetic instrumentation capable of accurately and reliably measuring dielectric properties at both room and cryogenic temperatures has been assembled. This instrumentation has been used to determine the dielectric properties (dielectric constant, loss tangent, and conductivity) of 36 cryogenically-preserved canine kidneys. These dielectric properties are presented as a function of temperature (-80°C to $+20^{\circ}\text{C}$), cryoprotectant level (0, 5, and 10 percent dimethyl sulfoxide concentrations), frequency (918 MHz and 2450 MHz), and tissue type (medulla and cortex).

Satisfactory thermometry for use under simultaneous conditions of cryogenic temperature and EM waves has been a technical problem. Engineering efforts have now resulted in the assembly of a thermistor-based thermometry system for use under these conditions. Ultra-small thermistors with small diameter wire leads and improved circuits for control purposes have been used to yield temperature values accurate to within 1°C in the presence of EM waves and at cryogenic temperatures. This thermometry system is described and temperature data obtained with the system is presented.

The studies reported in this paper were supported by NSF Grant No. ENG-76-10124.

INFLUENCE OF MICROWAVE-INDUCED TEMPERATURE GRADIENTS ON THE UPTAKE OF CHEMOTHERAPEUTIC AGENTS BY EXPERIMENTAL BRAIN TUMORS IN MICE

Carl H. Sutton, M.D., and Frederick B. Carroll
University of Miami School of Medicine, Miami, Florida
Quirino Balzano, Ph. D.
Motorola, Inc., Plantation, Florida

The effects on uptake by heated glial tumors of two commonly employed antimetabolites were studied by employing temperature gradients induced by microwave power at 2450 MHz. Murine gliomas were heated, while the body core temperatures of the host mice were maintained at either 37° or 28°C. This experimental model was used to study the uptake of tritiated methotrexate and tritiated cytosine arabinoside 45 minutes after intraperitoneal administration, with one flank tumor in each mouse heated to 41°C. Much higher concentrations were achieved in heated tumors using cytosine arabinoside than with metrotrexate. The uptake of cytosine arabinoside by hyperthermic tumors was nearly 2 1/2 greater than that in hypothermic tumors. The highest tumor uptake values for both agents were achieved in animals in which body-core temperatures were maintained at 28°C. These studies demonstrate that the distribution of antineoplastic agents can be affected differently by temperature gradients. The liver was protruted significantly from the uptake of methotrexate by body-core hypothermia, while the kidneys were protected to a lesser extent. These studies also demonstrate a selectively enhanced accumulation of antimetabolites in tumor implants as a result of moderate tumor hyperthermia produced by microwave irradiation. It appears that temperature gradients and, in particular, the microwave heating of tumors to approximately 41°C for periods of 30 to 45 minutes may prove beneficial in the chemotherapy of neoplasms which are sensitive to the agents employed. It is likely that the tumor uptake of other antineoplastic agents may also be influenced in a similar fashion by combining moderate tumor hyperthermia with an appropriate temperature gradient between the heated tumor and the remainder of the body.

This research was supported in part by Grant PDT-74 from the American Cancer Society, and grants from the Veterans Administration Hospital, Miami, Florida, and the American Cancer Society, Florida Division.

TENSOR INTEGRAL EQUATION METHOD COMBINED WITH ITERATION TECHNIQUE
FOR QUANTIFYING INDUCED EM FIELDS IN BIOLOGICAL SYSTEMS

Kun-Mu Chen and Sutus Rukspollmuang
Department of Electrical Engineering and Systems Science
Michigan State University, East Lansing, MI 48824

Abstract

When a numerical method such as the tensor integral equation method (TIEM) is applied to quantify the induced EM fields in an electrically large body, it is necessary to divide the body into a large number of electrically small cells. This will lead to a large number of unknowns in the numerical calculation and it will cause the overloading of computer storage. A scheme has been developed recently which combines an iteration process with the TIEM. This scheme can be used to handle a body consisting of a very large number of cells, while sidestepping the problem of computer storage limitation. This scheme is not a simple numerical average process; it is a process consistent with Maxwell's equations.

This scheme involves the following steps: (1) The body is divided into N cells and the first-order, induced electric fields are obtained by the TIEM. (2) One of the N cells, the m th cell, is subdivided into 8 subcells, and equivalent incident electric fields at the centers of 8 subcells, in the absence of the m th cell, are calculated. (3) The m th cell is then considered as an isolated body irradiated by the equivalent incident electric fields, and the second-order induced electric fields inside the m th cell are calculated by the TIEM. (4) Repeat for each of the N cells. (5) Iteration process can be repeated for more accurate results.

The important advantage of this technique is that since the iteration of the induced electric field of each cell is carried out separately, it does not require the inversion of a large matrix and, thus, computer storage problem is side-stepped.

Examples will be given at the Symposium to show the capability of this scheme and its economical advantage.

SURFACE INTEGRAL EQUATION METHOD FOR INTERACTION
OF MICROWAVE WITH BIOLOGICAL BODY

Jen-Hwang Lee and Kun-Mu Chen

Department of Electrical Engineering and Systems Science
Michigan State University, East Lansing, Michigan 48824

Abstract

In the field of theoretical dosimetry, the quantification of the induced EM field inside an irradiated body has been performed mainly by volume integral equation methods. When a large biological body such as human body is irradiated by an EM wave of microwave range, the body becomes electrically large and the induced EM field concentrates mainly in a thin layer of the body surface. A volume integral equation method then becomes inadequate or inefficient to handle this problem, and it is more efficient to quantify the induced EM field on the body surface based on a surface integral equation method for this case. After the tangential components of the induced electric and magnetic fields on the body surface are determined, the internal EM field can be calculated.

We have recently developed a numerical method to quantify the induced EM field on the surface of an irradiated biological body based on two coupled surface integral equations. The formulation and numerical evaluation of these surface integral equations will be discussed at the Symposium.

To check the accuracy of this method, electrically small bodies are considered first, and results obtained from the surface integral equation method are compared with that obtained from the tensor integral equation method, a volume integral equation method. It was learned that in some cases, the surface integral equation method showed advantages in accuracy and computation cost over the volume integral equation method.

SPECIFIC ABSORPTION RATES IN MICE EXPOSED TO 918 AND 2450 MHZ
CIRCULARLY POLARIZED GUIDED EM FIELDS

Arthur W. Guy, C.K. Chou, J.F. Lehmann,
William Farnham and John A. McDougall
Bioelectromagnetics Research Laboratory
Department of Rehabilitation Medicine
University of Washington
Seattle, Washington 98195

The system previously developed for chronically exposing a large population of rats to 918 and 2450 MHz circularly polarized guided waves has been modified for acutely exposing mice. The exposure waveguide may be used to expose the animals from the top or from the bottom, or may be used to expose the animal from the side. The holding cage is placed one-quarter of the distance from the top or bottom of the waveguide for 2450 MHz exposure. These positions optimize the dual mode (TE_{11} and TM_{11}) coupling of the circular waveguide field to the experimental animals.

The average specific absorption rate (SAR) in mice exposed with an input power of one watt was determined by twin-well calorimetry and found to be 0.69 W/kg with a standard deviation of 0.04 W/kg at 918 MHz and 3.05 W/kg with a standard deviation of 0.32 W/kg at 2450 MHz. A number of photographs were taken of the exposed animals to show typical body orientations as a function of input power. Under low power exposure conditions corresponding to power densities of 30 mW/cm² or less typical orientations of the exposed animals were the same as that for sham exposed animals. Under high power exposure conditions corresponding to 70 mW/cm², the animals would lie on their sides in a curved position. SAR patterns were measured at the surface of exposed animals by thermography for a number of different species. SAR distributions were verified by measurements made just below the surface of the skin in the region of maximum SAR by a Vitek Model 101 Electrothermia monitor temperature probe. The fur from the non-nude mice was removed by use of a depilatory before exposure. The measured results agreed closely for the various species of mice. Thus, it is felt that the thermographic results obtained for naturally nude mice would provide quantitative information in the use of the exposure system for all species of mice. It is significant to note the substantial increase in energy coupling efficiency and uniformity for 2450 MHz as compared to 918 MHz exposure.

SPECIFIC ABSORPTION RATES MEASURED IN RATS AND MICE
EXPOSED TO 2450, 425 or 100 MHz RADIOFREQUENCY RADIATION

James B. Kinn
Experimental Biology Division
Health Effects Research Laboratory
U.S. Environmental Protection Agency
Research Triangle Park, North Carolina

Whole body energy absorption was measured in single mice and rats exposed to 2450 MHz, 425 MHz or 100 MHz radiation. Specific absorption rates (SAR) measurements were made with the twin-well calorimetry technique. SAR were determined for three animal sizes and three orientations. The 2450 MHz exposures were made in an anechoic chamber, whereas the 425 MHz and 100 MHz exposures were made in TEM transmission lines (Crawford Cells). Comparisons were made of the average SAR values to the values determined with theoretical models and a discussion of the differences.

WAVEGUIDE DOSIMETRY DATA ON MICE, IN VIVO, 2.5 - 4.2 GHZ.

R. TURNER, W. A. G. VOSS, W. R. TINGA, P. FISHER AND R. RAJOTTE

Department of Electrical Engineering and Division of Biomedical Engineering and Applied Science, CE 247, University of Alberta Edmonton, Alberta, Canada, T6G 2N7

ABSTRACT

Rectangular and parallel plate waveguide techniques have been used by previous workers to determine the SAR of mice and phantoms of rats. In this paper we have used a normalizing waveguide reflectometer, with a total output power of less than 1 mW, to determine reflection, transmission and, hence, absorption in WR 284 waveguide (i.ds: 7.214 X 3.404 cms) for small, anesthetized mice ($5.30 < w < 16.32$ g, $4.5 < l < 7.7$ cms) over the frequency range 2.5 - 4.2 GHz.

Mice were located centrally in the waveguide with their length parallel to the direction of propagation, facing the incident wave (l parallel to z). It is shown that the absorption does not appear to change for up to 5 hrs after death over the frequency range used. In vivo the position of limbs and, in particular, the attitude of the head affect the resonant frequency under these conditions but SAR changes are small. From data on 24 mice of different sizes, a resonance appears in the reflection response which is frequency dependent according to the relationships $f_R = 6.084 - 0.419l$ (correlation coefficient $r = 0.987$) and $f_R = 4.679 - 0.1266w$ (correlation coefficient $r = 0.952$) where the frequency is in GHz, l is the length of a mouse, centrally located along the waveguide, measured from the nose to the base of the tail (cms) and w is the weight in grams. SARs, computed from the data recorded, show an increased slope through the resonant frequency in all cases. The SAR values, when normalized, are consistent with values reported in the literature at 2.45 GHz.

A number of problems have to be investigated before data from waveguide measurements of SAR can be used to predict free space values. These are discussed.

A STUDY OF THE HEATING PATTERN OF A BIOLOGICAL BODY
INSIDE A RECTANGULAR WAVEGUIDE

Johnson J.H. Wang
Engineering Experiment Station
Georgia Institute of Technology
Atlanta, GA 30332

Lawrence E. Larsen
Department of Microwave Research
Walter Reed Army Institute of Research
Washington, D.C.

ABSTRACT - Research has been conducted to compute and measure the heating patterns inside a three-dimensional arbitrarily-shaped heterogeneous biological body inside a rectangular waveguide. The profile of dissipated power intensity and temperature was determined with satisfactory accuracy. Immediate application of this technique is to provide guidance for the design of microwave applicators for rapid inactivation of enzymes, for which uniform heating is an important consideration. Numerical computation and thermographic measurements were conducted for the case of rectangular-sided blocks. However, the computer program is capable of solving for arbitrary shapes.

The salient features of electromagnetic modeling of this problem has been previously reported (J.J.H. Wang, IEEE MTT Trans. 26, 457-462, 1978). Recently, the calculation and measurement of temperature distribution, which is directly related to the thermal inactivation of enzymes, were successfully conducted. The equivalent heat source due to the dissipation of electromagnetic wave is first determined by the dissipated electromagnetic power density which is then related to the temperature distribution by the heat equation. The experimental results were recorded with thermographic paper and a heat-sensitive camera. Satisfactory agreements were observed between calculation and measurement. A difficulty in the calculation of temperature distribution was experienced near the edge of the test block. This difficulty was overcome by using the heat equation instead of the usual method in which the temperature distribution was related to the dissipated power density with a proportionality constant.

"ESTIMATION OF INTERNAL POWER ABSORPTION BY
HUMAN HEADS IN PRESENCE OF ELECTROMAGNETIC
RADIATION"

K. QUBOA, H. T. AL HAFID AND S. C. GUPTA

Department of Electrical Engineering,
University of Mosul, Mosul - IRAQ.

ABSTRACT

Much data have been accumulated on the interaction of electromagnetic waves with various sphere models, simulating the human head. Here prolate spheroid and ellipsoidal models are used to estimate the power absorption. In order to obtain a quantitative description of the absorbed electromagnetic power distribution with human heads (both adult and infant), a perturbation technique is used to evaluate the internal electric field and then to estimate the time-averaged specific absorbed power and space-averaged specific absorbed power.

Two cases are examined, one is the simulation of an adult head by prolate spheroid and ellipsoid models of an equivalent sphere volume of 10 cms. radius, which represent an idealized adult head. The second case is the simulation of 5 cm. sphere radius by prolate spheroid and ellipsoid models which represent an infant head. Using prolate spheroid models, magnetic, electric and cross polarizations with respect to incident field vectors are used. For ellipsoid model six polarizations like EKH, EHK, KEH, HKE, HEK and HKE are used. The expressions for internal fields, specific time-averaged absorbed power and space-averaged specific absorbed power are derived and are applied further for human adult and infant heads. A comparative study is made with the available experimental results of certain animals. Finally it is concluded that ellipsoidal model is better than spheroid and sphere types. Further discussion is made from human safety point of view, regarding the minimum and maximum power absorption for different polarizations of the incident fields.

ENERGY ABSORPTION FROM SMALL RADIATING PROBES IN LOSSY MEDIA

Mays L. Swicord, Bureau of Radiological Health, 12721 Twinbrook Parkway, Rockville, Maryland 20857

Christopher C. Davis, Electrical Engineering Department, University of Maryland, College Park, Maryland 20742

Theoretical calculations of energy deposition around small antenna probes in lossy media have been made and are reported here. Such small probes have been used or proposed for use in dielectric constant measurements, hyperthermia treatment of small tumors, and microwave spectroscopic investigations of liquids. The results of this investigation are instructive in all of the above cases, but are particularly helpful for those interested in hyperthermia.

The design of probes has varied depending upon the desired use. Basically, these probes are open-ended coaxial lines with the center conductor extending beyond the outer conductor by an amount which is always a small fraction of a wavelength in the medium. The authors' interest in these evaluations stems from the use of this type of probe for coupling microwave energy into dielectric media and the subsequent observation of absorption as a function of frequency with an optical heterodyne technique (Davis and Swicord, companion paper, this conference).

Two theoretical models were used and compared, a short dipole antenna and an open-ended coaxial cable replaced with its equivalent magnetic current. The dipole model yields exact results for the fields. The calculated fields, however, become infinite as one approaches the origin, yielding an infinite value for the total power absorbed in a small sphere or radius R . This method can be used for calculating isopower contours in the far field.

The second theoretical approach follows the far field, free space calculation made by Jordan and Balmain in which the surface separating the inner and outer conductor of the coaxial cable is replaced by an equivalent magnetic sheet. The results must be integrated numerically. An examination of the results by either method indicates that extraction of exact values of the absorption coefficient in the near field of this particular antenna design is at best very difficult if not impossible due to the complexity of the equations. Any attempt to use the results in the far field is also difficult because of the poor microwave induced heating of the liquid in this region. Thus an alternative method is suggested. The fields calculated from the open coax method remain finite in value as one approaches the origin allowing for the calculation of the relative total power absorbed in a sphere of radius R . Such calculations and their implications for hyperthermia will be presented. Isocontour plots of absorbed power for various values of frequency, dielectric constant, loss tangent and antenna dimensions will also be presented.

NUMERICAL SOLUTIONS FOR MICROWAVE POWER ABSORPTIONS
IN BODY-OF-REVOLUTION MODELS OF MAN

Te-Kao Wu
Lockheed Missiles & Space Company
P.O.Box 504
Sunnyvale, CA 94086

In the past, many analytical works have been presented to study the microwave power absorption patterns and total absorption in simple three-dimensional models of man, e.g., spheres, spheroids, and ellipsoids. For realistic models with arbitrarily shaped contours, the integral equation method should prove to be advantageous. In this paper, the internal fields and power absorption in a homogeneous lossy dielectric body of revolution are evaluated using the Surface Integral Equation (SIE) method. The method yields moment method solutions for the induced current densities on the body surface, the interior fields to the body are then evaluated via the reciprocity theorem and the measurement matrix concept. The bulk body power deposition is obtained by the integration of the surface Poynting vector. The method applies for a wide range of dielectric parameters (with ϵ_r from 1.1 to 100 and σ from 0 to 1000 mhos/m). Numerical results for microwave fields and power deposition in a body-of-revolution model of a human torso with height of 1.78 m are evaluated for frequencies of 30, 80, and 300 MHz. It is found that the strongest power deposition in the torso model occurs for fields polarized along the longest dimension and for frequencies near the first resonance (i.e., 80 MHz) of the torso body. Hot spots are also observed in the neck region of the torso body.

AN EXPERIMENTAL MODEL FOR DETECTING AND AMPLIFYING SUBTLE RF FIELD-INDUCED CELL INJURIES.

Vernon Riley, D.H. Spackman, M.A. Fitzmaurice, A.W. Guy* and C.K. Chou* Pacific Northwest Research Foundation, Fred Hutchinson Cancer Research Center, and the University of Washington School of Medicine*.

A combination in vitro/in vivo experimental model utilizing neoplastic target cells, and a special receptive host, is capable of detecting subtle biological effects of non-ionizing, electromagnetic (EM) fields. The experimental findings carry provocative implications concerning the potential biological and pathological influences of radio-frequency (RF) and microwave irradiations, as well as suggesting possible useful applications for EM fields in experimental cancer therapy. Intrinsic, as opposed to hyperthermic, influences of 30 MHz fields upon cancer cells that were exposed in vitro, were detected only when such target cells were reimplanted subcutaneously (sc) in a receptive mouse strain specially selected for its immunocompetent equipoise. The effects of the RF fields on the neoplastic cells were detected by changes in the tumor latent periods, tumor incidence, tumor growth rates, maximum tumor volumes, tumor regressions, and survival times of the hosts. Hyperthermic effects associated with RF field exposure were controlled by: 1) utilization of the Guy cell-exposure apparatus and its sophisticated heat-exchange mechanisms, and 2) by the intentional induction of identical hyperthermias in sham-exposed and RF-exposed neoplastic cells in order to normalize the thermal factor. 3) The possible perturbing effects of thermal gradients were minimized by constantly circulating the cells through the sample chamber so that all cells were exposed to the same average thermal and RF environments. As a result of such controlled exposure of mouse lymphosarcoma cells to 30 MHz fields at 1 to 10 V/cm, a significant number of unexpected tumor regressions was observed. RF-exposed and sham-control neoplastic cells both produced tumors following sc implantation; however, a higher percentage of those tumors derived from cells that had been exposed in vitro to 30 MHz fields subsequently regressed, resulting in host survival. This was in contrast to the sham-exposed and control cells that produced a higher percentage of progressively growing lethal tumors. Mechanisms associated with this model appear to encompass a form of biological amplification that permits the reproducible detection of extremely subtle cell injuries resulting from specific RF field exposures.

These studies have so far been restricted to the single frequency of 30 MHz and electric field strengths of the order of 1, 5, and 10 Volts/cm. These particular field strengths yield average specific absorption rates (SAR) of 31 (± 5), 352 (± 68), and 1805 (± 298) W/kg respectively.

DIFFERENTIAL CONSEQUENCES OF BIOLOGICAL SYSTEM
EXPOSURE TO PULSED- AND CONTINUOUS-WAVE
ELECTROMAGNETIC FIELDS

J. Toler, J. Seals, and E. McCormick
Engineering Experiment Station
Georgia Institute of Technology
Atlanta, Georgia 30332

R. Vogler and L. Winton
Leukemia Research Laboratory
Emory University School of Medicine
Atlanta, Georgia 30322

This paper discusses the engineering and biological aspects of a study that involved exposing BALB/c female mice between the ages of 10 and 14 weeks to pulsed- and continuous-wave electromagnetic environments at frequencies of 432 MHz and 2450 MHz. The following three modulations were used at each frequency:

- Continuous-wave,
- Pulsed-wave with a pulse width of 120 microseconds and a pulse rate of 400 Hz, and
- Pulsed-wave with a pulse width of 12 microseconds and a pulse rate of 4000 Hz.

Power densities were 0.8 mW/cm^2 and 2.14 mW/cm^2 , respectively, for the 432 MHz and 2450 MHz environments. A Compact Range was used as an exposure facility because of its ability to provide a planar wave with a near-uniform amplitude distribution over an area large enough to position 12 mice without detectable interage scattering. Special cages made of Plexiglas and Styrofoam were designed, evaluated, and then used to house the mice during radiation. A total of 366 irradiant and control mice were used during the study. Two different exposure schedules, each providing 60 hours of radiation were used. Analytical dosimetry techniques were verified by experimental studies. The assay system consisted of a highly quantitative, in-vitro liquid assay of granulopoietic stem cells.

At the conclusion of the study, it was concluded that no detectable bioeffects exist in the granulopoietic system of mice exposed to pulsed- and continuous-wave radiation at frequencies of 432 MHz and 2450 MHz. Results supporting this conclusion will be presented as a function of modulation, frequency, and exposure schedule for the various biological parameters.

The study reported in this paper was supported by USAFSAM Contract No. F33615-77-C-0619.

THE DIFFERENTIATION (RETRANSFORMATION) OF NEUROBLASTOMA CELLS AS AN INDICATOR OF THE BIOLOGIC ACTIVITY OF PULSED MAGNETIC RADIATION. THE NON-THERMAL EFFECTS OF PULSED ELECTROMAGNETIC FIELDS ON TUMOR GROWTH AND IN VITRO MOUSE PALATAL DEVELOPMENT AND NEUROBLASTOMA DIFFERENTIATION.

William Regelson, Brian West, Richard Carchman, David End, Dom Depaola, Richard Lieb and Arthur Pilla*. Medical College of Virginia, Richmond, Virginia, 23298.

Pulsed electro-magnetic fields of low frequency have induced clinical bone repair, dedifferentiation of frog erythrocytes and behavioral alterations in monkeys which has led to the concept that both the kinetics and quantity of specific adsorption (binding) and/or membrane transport can be altered by the injection of specific current wave forms.

Neuroblastoma cells were placed in homogeneous time varying magnetic fields (2 gauss average) using 4" air gap coils (Electro-Biology, Inc., Fairfield, N.J.). The induced current wave form (of $\mu\text{A}/\text{cm}^2$ level) were designed to either excite only surface or surface-coupled transport processes. Significant differences in the degree of dendritic outgrowth and surface adhesion vs. multiplication as a function of induced current wave forms were detected which are similar to those reported for calcium ionophores and for polar solvents in inducing differentiation or tumor cell retransformation. Correlations of the above with thymidine uptake, cholinesterase activity and calcium flux are under way.

Based on results using 27 MHz (Diapulse, Lake Success, New York), where growth rates of transplanted Lewis lung tumors, in mice, showed inhibition or acceleration depending on the timing of/and pulsed frequencies used; studies in 14 day old mouse embryo palatal explants were conducted using the Diapulse instrument.

In vitro epithelial destruction or chondrometaplasia was found utilizing low frequency magnetic pulsed radiowaves (27 MHz) administered for 20 minutes to in vitro explants. These effects are non-thermal and establish a biologic role for non-ionizing radiation that deserves further exploration utilizing different wave forms and frequency windows.

The results of our experience stress observations that indicate that non-thermal, electrochemical surface interactions may play a role in cell regulation. If continued observations utilizing neuroblastoma tissue cell lines indicate the sensitivity of this system to pulsed magnetic fields, then we may have a biologic system that could give us quantitative information relevant to the response of cells to varied wave forms. The implications of this for the study of control of tissue differentiation and cancer growth will be discussed.

*Columbia University, New York, New York

EFFECT OF LONG-TERM LOW-LEVEL MICROWAVE EXPOSURE ON
DEVELOPMENT AND GROWTH OF CHEMICALLY (3,4-BENZOPYRENE AND
DI-ETHYL-NITROSO-AMINE) INDUCED NEOPLASMS

Stanislaw Szmigielski, Andrzej Pietraszek and Marian Bielec
Center for Radiobiology and Radioprotection
128 Szaserow, 00-909 Warsaw
Poland

Long-term low-level exposition to microwaves may change the function of the immune systems and thus there exists a possibility that this may lead in turn to different reactivity to carcinogens. Virtually nothing is known about the effect of microwave radiation on the process of carcinogenesis in vivo.

In the present experiments two chemical carcinogens, 3,4-benzopyrene (3,4-BP, leading to development of skin cancer after painting on skin) and Di-Ethyl-Nitroso-Amine (DENA, resulting in development of hepatomas after intraperitoneal injections) were used in BALB/c mice. The following groups of animals were tested:

1. Normal mice exposed to 3,4-BP or DENA;
2. Mice irradiated with microwaves (anechoic chamber, 2450 MHz, field power densities 5 or 20 mW/cm², 2 hours daily, 6 days a week) for 1, 2 or 4 months and then treated with 3,4-BP or DENA;
3. Mice treated with 3,4-BP or DENA and simultaneously irradiated with microwaves as above.

In all mice evaluations of tumor growth and the immune systems functions were performed.

It was found that both the tested carcinogens led to development of neoplasms with immunosuppression in the final stage of tumor growth (last 2 months of observation). Irradiation with microwaves at 20 mW/cm² resulted in quicker appearance of immunosuppression in carcinogen-treated animals and in earlier appearance of neoplasms. On the other side, only slight insignificant differences were found in carcinogen-treated animals exposed to 5 mW/cm² field power density.

EFFECTS OF A.C. MAGNETIC FIELD ON LYMPHOMA CELLS

Stanley Batkin and Frank L. Tabrah
John A. Burns School of Medicine
University of Hawaii
Honolulu, Hawaii 96822

YC-8 mouse lymphoma cells (1×10^6) in tissue culture were exposed to 130 Gauss, 1950 H_z for 48 and 96 hours. Total cell counts were obtained and cell viability determined by the trypan blue staining exclusion method.

- A. In the magnetic field at 48 hours - 31% increase in cell numbers with 85% viability occurred. At 96 hours - 149% increase in cell numbers with 88% viability.
- B. In the control environment at 48 hours - 75% increase in cell numbers with 89% viability. At 96 hours - 318% increase in cell numbers with 84% viability.

The differences in the percentage of cell increase in the two groups suggests a retarding effect of the magnetic field exposure.

In an in vivo experiment using YAC mouse lymphoma cells (2×10^6) two groups were again used. The first group was exposed for 17 days to 1,000 Gauss, 60 H_z and the second control group maintained in a dummy cage in normal laboratory environment. A slower visible and palpable tumor (subcutaneous) onset noted in the first group with average tumor weights being 2.06 grams as compared to 3.1 grams for the control group. Although the magnetic fields were different in the in vitro and in vivo experiments, a retarding effect on the tumor growth occurred in the magnetic groups.

BEMS POSTER A - 30

EFFECTS OF 1.07 ghz RF FIELDS ON MICROBIAL SYSTEMS

E. Moody & C. McLerran (Microbiology), and J.W. Frazer & V.A. Segreto (Diagnosis & Roentgenology) U.T.H.S.C. San Antonio, Texas

Much National discussion of the possibility of long term effects of RF radiation has occurred for a number of years. We aver that any such long term event ultimately depends on producing transcription errors in some somatic cells, and thus have subjected microbial models of transcription systems to analysis.

Strain of E.coli C-600 lac II, with a defect in the tonA locus conferring resistance to bacteriophage T5 has been subjected to 1.07 ghz capacitor fed fields during log phase of growth while suspended in Brain Heart Infusion (BHI) with conductivity approximately 1mho/meter. The system temperature was monitored with a Ramal Liquid Crystal Probe calibrated between each experimental run. Radiofrequency fields were generated by an MCL transmitter with frequency monitored by a Systron Donner frequency counter, input and reflected power monitored by Hewlett Packard 431C power meters coupled via Narda Microline 30db couplers.

It was found that E.coli C-600 became susceptible to infection with non-irradiated bacteriophage T5, as shown both by lysis of E. coli (nearly quantitatively) and production of virus particles, when virus was added immediately post exposure, indicating a membrane receptor site for T5 was uncovered during field application at 42°C.

This strain of E.coli was also more easily inactivated by RF fields than by temperature alone---90 minutes incubation at 48°C produced only a minimal reduction of viable C-600.

By incubating bacteriophage with E. coli during radiation it was shown that the bacteriophage was quantitatively inactivated by fields having little or no effect on E.coli. Field exposure of bacteriophage T5 suspended in BHI resulted in 80% inactivation in two minutes at 37°C. This bacteriophage is normally stable to temperatures in excess of 48°C.

The fields used in this study were at least 5 Vcm^{-1} in solution. The data is consistent with data from whole mammalian cell radiations and effects produced in isolated calf thymus RNA.

MICROWAVE-INDUCED INCREASE OF WATER AND CONDUCTIVITY IN SUBMAXILLARY SALIVARY GLAND OF RATS

Henryk Mikołajczyk, Institute of Occupational Medicine
90-950 Łódź, POLAND

Hyperfunction and hypertrophy of submaxillary salivary gland /SSG/ have been observed in rats subjected to hot environmental conditions. Hypersalivation is an important way of heat dissipation also in rats exposed to acute microwave irradiation.

The water content and conductivity in SSG were investigated in rats exposed to microwaves: 2880 MHz, impulse repetition 1000 Hz and width 1.5 μ s. 20 adult male rats were exposed singly in 25x23x20 cm styrofoam box under 30x30 cm horn antenna for 30 minutes to 25 mW/cm² or 38 mW/cm² of average incident power densities causing energy absorption of 8.4 W/kg or 12.6 W/kg, respectively. There were two parallel control groups each of 10 nonirradiated rats. The power density and absorption was calculated from 0.2 °C and 0.3 °C temperature increase in 300 cc. of 0.85 % NaCl in 10x10x10 cm styrofoam vessel after irradiation within 100 s with the microwave mentioned above. The autopsy of rats was performed immediately after irradiation. Temperature in SSG and in colon was measured with ELLAB thermistor thermometer. The proper resistivity /Ohm x m/ at 20 kHz has been measured with the four electrode probe in excised left lobe of SSG which was subsequently dried to constant weight in convective air of 40 °C. The conductivity was calculated from the measured resistivity: S/m = 1 : Ohm x m. The difference between the weight of fresh and dry SSG indicated the percent of water.

The colonic temperature was 37.8 \pm 0.3 and 38.1 \pm 0.2 °C in rats of control groups and 39.9 \pm 0.4 and 40.9 \pm 0.4 °C in irradiated rats. The SSG was heavier in irradiated than in control animals. This tissue showed 77.3 \pm 2.2 and 80.0 \pm 1.7 % of water and conductivity 0.139 \pm .029 and 0.257 \pm .069 S/m in rats exposed to 25 mW/cm² and 38 mW/cm², respectively, in comparison to 75.0 \pm .65 and 75.6 \pm .8 % of water and conductivity 0.097 \pm .021 and 0.100 \pm .023 S/m in rats of control groups. It is suggested that determination of water content and conductivity in SSG of rats could be used as a sensitive and specific way to test the microwave thermal effect.

FURTHER STUDIES OF TESTIS CYTOLOGY IN MICE
IRRADIATED WITH 2450-MHz MICROWAVES

A.B. Cairnie and R.K. Harding
Defence Research Establishment Ottawa, Ottawa K1A 0Z4,
Canada

Male mice, 10 to 12 weeks old, were housed overnight in an anechoic chamber and exposed to 2450 MHz CW radiation for 0, 2, or 16 h. Up to 10 mice were caged singly in polypropylene cages with food and water and irradiated in a multi-unit cage array located within the 1.8 m diameter quiet zone. Cages were spaced by 3λ to minimise interaction. Power density incident on each cage position depended on its angle relative to the central axis and interaction with neighbouring objects.

In one experiment two groups of 70 B6C3F1 mice were exposed for 4 days, 16 h/day, and were sacrificed at intervals up to 10 weeks for sperm count and percent abnormal sperm. The two groups averaged 20 and 32 mW/cm². We reported last year that immersion of the hindquarters in a waterbath at 40°C for 2 h caused a marked depression of the sperm count and elevation of abnormal sperm from 2 to above 30 per cent from 1½ to 2½ weeks later. Neither of the two microwave-irradiated groups showed any effect on sperm count or percent abnormal sperm.

Another experiment was designed to meet the criticism that our failure to find microwave effects on the testis, as reported last year and this, might be attributed to our choice of the hybrid B6C3F1 mouse which could be particularly resistant to microwave damage. We therefore compared B6C3F1 with three inbred strains, C57B1/6B, C3H/HeB, Balb/c, and a random-bred line, Swiss Webster. Four groups of 10 mice were exposed for 0, 2, or 16 h irradiation in the anechoic chamber (average power density 26 mW/cm²) or the hindquarters in a waterbath at 40°C for 2 h. Five were killed immediately for assay for dark-stained cells in testis, sperm count, and percent abnormal sperm; five were killed 2 weeks later for sperm count and percent abnormal sperm. This time interval was chosen because there was a large effect of heat at this interval (see experiment above). An effect of the heating was demonstrated on all strains, but none showed an effect of microwaves.

Tests of the reproductive effectiveness of male mice irradiated in the anechoic chamber for 4 days (16 h/day) at an average power density of 39 mW/cm² are under way and preliminary results will be available.

HEAT-INDUCED CATARACTS IN THE RAT LENS IN VITRO

P. Jill Stewart-DeHaan, Margaret O. Creighton, William M. Ross, J.R. Trevithick. Biochemistry Department, University of Western Ontario, London, Ontario, Canada N6A 5C1

Microwaves have been shown to produce cataracts in the eyes of whole animals. Since the main effect of microwaves is believed to be heating, it seemed possible that a simple temperature elevation was causing the lens degeneration as indicated by the experiments of Carpenter and Kramar. We, therefore, thought it important to distinguish between the effect of the electromagnetic radiation and the effect of elevated temperature. We studied the effect of temperature on isolated rat lenses incubated in tissue culture medium. Lenses maintain their clarity in medium 199 (M 199) (containing 10% foetal calf serum) for up to two weeks. When ten times the normal serum glucose levels are included in the incubation, opacities and associated globular degeneration of the lens cells developed within one day. Similar loss of transparency occurred after lenses were warmed to 39° or 41° for one hour and then incubated at 37° for 24 hr. Lenses exposed to higher temperatures (60° and 65°) for 1 hour did not become opaque. They had normal transparency probably because they had been "fixed" by a process similar to histological fixation. Scanning electron microscopy revealed subcapsular cortical globular degeneration in the cataractous areas. The degeneration was deepest in the equatorial region. Glucose-induced and temperature-induced cataracts contained spherical bodies up to 20 μ in diameter. Occasionally in temperature-induced cataracts, bodies up to ten times this diameter were found. Lenses were incubated with ³²P in Medium 199 to label membrane phospholipids, and while cataract formation was occurring incorporation proceeded into the major phospholipids, including phosphatidylcholine (PC), phosphatidylethanolamine (PE) and sphingomyelin (SM). In cataractous lenses the specific activity of phosphatidylinositol (PI) was higher. Taken together, these observations suggest that membrane changes may be involved in temperature-induced cataract formation.

Supported by: U.S. Army (DAMD 17-78-G-9449); NIH (EY01927) and MRC of Canada

EFFECT OF D. C. MAGNETIC FIELDS ON Ca^{2+} TRANSPORT
IN ISOLATED MUSCLE MICROSOMES

E. M. Ettienne, P. A. Hoenig and R. B. Frankel, Francis Bitter National Magnet Laboratory*, MIT, Cambridge, MA 02139, and Univ. of Massachusetts Medical School, Worcester, MA 02205

Effects of homogeneous magnetic fields up to 5.5 tesla on cellular contraction and cell mortality have been observed in contractile protozoans following chemical stimulation [1]. These results show that external magnetic fields impose a stress on organisms and that this stress might involve changes in the regulation of intracellular concentrations of Ca^{2+} , which is an important element in cellular metabolism. To test this hypothesis, we have investigated the effects of d. c. magnetic fields on the Ca^{2+} uptake and sequestering function of membranous vesicles isolated from avian pectoralis. Sarcoplasmic reticulum vesicles are obtained from 10-14 day old chick. Microsomes at 4°C are exposed to an 0.7 tesla magnetic field for intervals up to 60 minutes before adding to a reaction mixture containing 5 mM MgCl_2 , 5 mM ATP, 100 mM KCl, 10 mM $\text{K}_2\text{C}_2\text{O}_4$, 10 mM imidazole (to Ph 7.0), 0.2 mM E.G.T.A. and 10 μM free Ca^{2+} . Addition of the microsomes results in ATP energized uptake of Ca^{2+} which is recorded by a Ca^{2+} electrode [2]. Measurements are also made of PO_4^{3-} liberation from ^{32}P -ATP. The results show a monotonic increase in the Ca^{2+} initial uptake rate and in total Ca^{2+} sequestered with increasing exposure time for microsomes exposed to an 0.7 tesla magnetic field. For example, transport rates increase from 800 nmoles of Ca^{2+} /mg/min (controls) to 6000 nmoles/mg/min after 30 minutes exposure and total Ca^{2+} sequestered increases from 175 nmoles/mg to 350 nmoles/mg after 30 minutes. There is a concomitant monotonic decrease of PO_4^{3-} release with increasing exposure time (6.0 nmoles PO_4^{3-} /mg/min (control) to 3.5 nmoles/mg/min after 30 minutes exposure). These results indicate increased Ca^{2+} transport function as a consequence of magnetic field exposure. This could result from changes in lipid-protein interactions due to collective anisotropic diamagnetic properties of the proteins, resulting in aggregation of protein elements (capping) or orientation changes (extrusion).

* Supported by N. S. F.

1. A. Ripamonti, R. B. Frankel and E. M. Ettienne, J. Mag. and Mag. Mats. (1979).
2. E. M. Ettienne and R. H. Singer, J. Membrane Biol. 44, 195 (1978).

EFFECTS OF PULSED ELECTRICAL FIELDS ON
ERYTHROCYTE MEMBRANES

S.F. Cleary
Department of Biophysics
Virginia Commonwealth University
Richmond, VA 23298

The effects of exposure of mammalian erythrocytes to exponential and square wave conductive electric fields have been investigated. The dependent variables investigated, namely Na^+ , K^+ and hemoglobin membrane permeability and cellular osmotic fragility, have been found to be functions of the field strength, pulse duration, inter-pulse duration and the number of pulses applied to the cell suspension. Significant differences in the response to pulsed fields of pulse durations of from 0.4 usec to 10 msec and field strengths of from 1 to 5 kV/cm, have been detected in cells derived from various mammalian species. The thresholds for exposure effects have also been found to be strongly dependent upon the composition of the cell suspension medium.

ENHANCED REPOPULATING CAPACITY OF A BONE MARROW CELL
SUSPENSION AFTER MICROWAVE IRRADIATION IN VITRO

D. Rotkowska and A. Vacek
Institute of Biophysics
Czechoslovak Academy of Sciences,
612 65 Brno, Czechoslovakia

In our previous papers we had shown that microwave radiation applied in vivo to mice before and after the effect of ionizing radiation enhanced the activity of hemopoietic stem cells and thus contributed to the therapy of radiation damage. The possibility of employing microwave radiation (2450 MHz, 100 mW/cm², 5 minutes) to modify the activity of mouse bone marrow cell suspension was verified using the transplantation technique, and the determination of the number of colony-forming units (CFUs) lodged in the spleen and bone marrow of lethally irradiated recipients was studied. A greater number of CFUs persisting until 30 minutes after radiation as observed following microwave irradiation. In retransplantation experiments an almost threefold elevation of the CFU's seeding factor was found in spleen and bone marrow after microwave irradiation. The mechanism of an increase of seeding after the effect of microwaves is discussed from the point of view of a possible activation of the CFU's membrane and of formation of solid bonds between CFU's and the hemopoietic microenvironment of a recipient.

CHRONIC EXPOSURE OF RATS TO 100-MHz (CW):
ASSESSMENT OF OPERANT BEHAVIOR

Michael I. Gage, Joseph D. Edwards
and Robert J. Pettinelli
U.S. Environmental Protection Agency
Health Effects Research Laboratory
Research Triangle Park, North Carolina 27711

As part of a multidisciplinary approach to assess possible biological effects of exposure to 100-MHz radiofrequency (RF) radiation, learning and performance was measured at the termination of a chronic period of daily exposure. Ten male offspring from time-bred CD rats were exposed daily for 4 hours in a transverse electromagnetic mode transmission line (Crawford Cell) at a forward power of 500 W (50 mW/cm²) from day 6 of gestation until they were 126 days old. Ten additional rats served as controls and received similar handling and sham exposure simultaneously. Behavior was evaluated by two tasks administered during the last two weeks of the exposure period. One task was a three day test of brightness discrimination and reversal learning in which rats can learn to choose either the lighted or unlighted of two panels for food pellet reinforcement in one session of 48 trials. The other task was six days of performance on a variable interval (VI) schedule of food reinforcement for head insertions into a food cup. The last daily session on each task was an extinction session, in which reinforcement was omitted. The order of task presentation was equalized across both exposed and control rats. No difference due to RF exposure was seen in acquisition or extinction on either task. Response rates on the VI schedule were similar in both exposed and control rats. The possible effects of tolerance to chronic RF exposure were evaluated by continued daily testing of all rats on the VI schedule for 16 additional days. During this time exposure to RF radiation was terminated but all other daily treatment continued as before. No changes in this schedule controlled performance were seen after cessation of RF exposure.

CHRONIC EXPOSURE OF RATS TO 2450-MHZ MICROWAVES AT 5 mW/cm²:
DEFINING FREQUENCY DEPENDENT DOSE-DETERMINANT EFFECTS

Richard H. Lovely, Sheri J.Y. Mizumori, Robert B. Johnson and
Arthur W. Guy

Bioelectromagnetics Research Laboratory
Departments of Rehabilitation Medicine and Psychology
University of Washington School of Medicine
Seattle, Washington 98195

Eight male rats were exposed for 16 weeks to 2450-MHz circularly polarized microwaves at an averaged power density of 5 mW/cm². The rats were exposed for ten hours every night for a total of approximately 1100 hours while 8 other rats were sham-exposed for the same time periods. Daily measurements of body mass, and of intake of food and of water, both in home cage and exposure apparatus, revealed statistically significant decrements in the exposed rats' daily food and water intake, although body mass failed to differentiate groups. Monthly assessments of blood chemistry parameters also failed to differentiate groups in a consistent manner as did post-exposure determinations of footpad shock threshold, open field behavior, and the acquisition of a shuttlebox conditioned avoidance response. These findings are discussed in the context of three other similar chronic exposure studies conducted in our laboratory employing 918-MHz circularly polarized guided waves incident at 10, 5 and 2.5 mW/cm². When the present findings at 2450-MHz (e.g., reduction in food intake) are compared to the 918-MHz dose-response function in terms of incident energy, the effects common to both 918-MHz and 2450-MHz chronic exposure are frequency dependent. However, when the effects are plotted as a function of SAR (W/Kg), the effects obtained here can be easily predicted from the 918-MHz dose-response curve.

EFFECTS ON BEHAVIOR OF LONG TERM EXPOSURE TO
LOW LEVEL MWR

Robert M. Lebovitz, Ph.D. and Ronald L. Seaman, Ph.D.
Department of Physiology
University of Texas Health Science
Center at Dallas

The aim of our effort is to develop a consistent set of conclusions regarding dose/response relationships between MWR exposure and detectable behavioral alterations, and to determine in what sense any such observed alterations constitute evidence for a harmful interaction. The computer controlled facility developed for these experiments provides for simultaneous irradiation and behavioral testing of 16 control and 16 irradiated rats. Pulse modulated MWR is provided via a 750 KW peak pulse power RADAR source operating at 1.3 GHz and feeding a divide-by-sixteen power divider which in turn launches circularly polarized MW energy in each of the active irradiation chambers. Dose rates are derived from a combination of chamber port measurements and whole body thermal measurements.

As to gross behavioral parameters, no differences were noted at the SAR's utilized to date (0-2.6 mW/g). In a group of rats irradiated at .96 mW/g, animal activity and position was assessed in detail. No major differences were noted between the experimental and control groups. In the long term studies of schedule controlled behavior, animals were exposed for 3 hours per day, for 9 weeks. The results to date indicate that MWR at dose rates of up to 2.6 mW/g had little effect on rewarded bar press behavior. There was only a slight indication that, at the higher dose rates, irradiated animals tended to show reduced operant behavior as satiation became a factor. There was, however, a much more apparent difference between experimental and control groups in terms of their error rates. That is, the irradiated rats had a significantly reduced error rate, especially as their rate of bar pressing for reward declined. The data support the conclusion that chronic MWR exposure differently effects rewarded versus non-rewarded instrumental behavior.

BEMS POSTER A - 40

THE EFFECT OF 9.31 GHZ PULSED MICROWAVE IRRADIATION ON THE
LEVER PRESS BEHAVIOR OF OPERANTLY RESPONDING RHESUS MONKEYS.

Robert D. McAfee^{1,2}, Richard Bishop² and S. Thomas Elder³. (1) VA Medical Center, Research Service, 1601 Perdido Street, New Orleans, LA; (2) Department of Electrical Engineering, University of New Orleans; (3) Department of Psychology, University of New Orleans, New Orleans, LA.

Twelve rhesus macaques were trained to enter an irradiation chamber and position their head directly in front of a standard gain (6.0 x 4.9 cm) microwave horn, E-field vertically polarized. By depressing a drinking tube they could obtain an apple juice reward for lever pressing on a variable schedule. The drinking tube was located 0.3 cm below a 20 cm² window in a 1 m² acrylic panel with two foot holds, one hand hold and a right hand lever. The tube was positioned so that the monkey's eyes were centered in the microwave beam 15 cm from the horn aperture. The radar was on, or not (depending on the experimental protocol) only when the drinking tube was depressed. Lever presses were counted and recorded for statistical analysis.

The microwave radiation was generated by a Model AN/CPN-6 radar that operated at 9.31 GHz. It produced a 0.5 μ s pulse at a peak power of 300 W/cm² and at an average power density of 150 mW/cm² at the locus where the monkey placed its head. Saline filled phantoms placed at this locus yielded a rate of energy coupling of at least 15 mW/g. Following 20 consecutive sessions of 15 minutes each, ten of which were irradiation sessions and ten were not, the lever press rate for 12 monkeys was analyzed by tests of significance (t) which showed that there was no significant difference in the combined means with or without irradiation although there were significant differences in individually analyzed means.

An experiment was performed on 6 monkeys to determine the trend in lever press behavior during 3 minute intervals just preceding and following a transition from microwave on to off, or vice versa. Comparisons of the monkeys' behavior on either side of the transition failed to show any effect on lever pressing, as a result of switching the radiation on or off, in the combined means of 15 sessions, although individual sessions showed considerable variability.

VIGILANCE BEHAVIOR IN RATS EXPOSED TO
1.28 GHz MICROWAVE IRRADIATION

John O. de Lorge and Clayton S. Ezell
Naval Aerospace Medical Research Laboratory
Pensacola, FL 32508, U.S.A.

ABSTRACT

Few studies of the biological effects of microwaves have investigated complex behavior in non-human organisms. One human behavior easily simulated by other animals is performance on a vigilance task. This task requires an animal to respond and produce one or more stimuli. When the stimuli change in some programmed manner the animal has to report the change to obtain a reinforcer. In the present experiment eight male hooded rats performed a vigilance task by depressing two levers, one of which produced two different tones (observing lever) and the other produced a food pellet (detection lever) when depressed in the Styrofoam boxes during daily sessions of 40 min. The boxes were located in the far zone region of a horn in an anechoic chamber. After stable response rates on the observing lever had developed the rats were exposed during their experimental sessions to 1.28 GHz microwaves pulsed at 380 pps with a pulse duration of 2 μ sec. Averaged power densities between 0 and 15 mW/cm^2 were used.

The response rate on the observing lever was consistently affected at a power density of 15 mW/cm^2 in all eight rats. The primary effect was a decreased response rate and in many animals a complete cessation of responding. Most of the rats adapted to continued presentation of the microwaves so that by the third exposure at 15 mW/cm^2 less of a decrement in observing response rate occurred. Seven animals decreased their response rates when exposed to 10 mW/cm^2 and three animals showed some behavioral disruption even at 5.5 mW/cm^2 . Other behavioral indices showed similar trends, but tended to be less sensitive than the observing response rate. These behaviorally disruptive power densities are much less intense than similarly effective power densities at 2.45 and 5.62 GHz and correspond to averaged specific absorption rates of 3 to 1 W/kg . The specific absorption rate (SAR) was measured on a rat phantom of simulated muscle tissue at 12 different points distributed throughout the model. The highest SAR was obtained in the rat phantom head and increased as the far surface of the head was approached. The SAR distribution within the head was the inverse of a distribution obtained at 5.62 GHz. It is concluded that the rat's behavior is disrupted at 1.28 GHz more easily than at higher microwave frequencies because of the deeper penetration of energy and differences in energy distribution within the animal at the lower frequency.

MICROWAVE-INDUCED CONDITIONED TASTE AVERSIONS IN RATS AT 987 MHz

G. Rufus Sessions
Department of Microwave Research
Walter Reed Army Institute of Research
Washington, D.C. 20012

After drinking a 0.1% saccharin solution, rats (N=56) were irradiated, four at a time, for thirty minutes with a horizontally polarized, 987 MHz, continuous waveform signal at power levels of either 0, 17, 25, 33, 45, or 51 mW/cm². With the exception of the 51 mW/cm² group, which received two pairings, all animals received five daily pairings of saccharin drinking followed by radiation or sham-radiation. Conditioned taste aversion learning was assessed three days after the last pairing by a 30 min. two-bottle preference test between saccharin solution and water. Rats irradiated at 42 or 51 mW/cm² showed reliable taste aversions for the saccharin solution as compared with the sham-irradiated controls. At 17 mW/cm² there was no reliable increase in deep colonic temperature during irradiation, as compared with sham-irradiated controls, but at power levels between 25 and 51 mW/cm², temperatures increased monotonically between 1.7 and 3.1 degrees Celsius. At the lowest power level sufficient to produce reliable taste aversions, 42 mW/cm², colonic temperatures increased an average of 2.6 degrees Celsius.

ALTERATION OF REPEATED ACQUISITION
IN RATS BY MICROWAVE RADIATION

Schrot, J., J.R. Thomas, and R.A. Banvard
Behavioral Sciences Department
Naval Medical Research Institute
Bethesda, MD 20014

The acute effects of microwave radiation on a repeated acquisition (learning) baseline were investigated in three rats. During each session the animals acquired a different four-member response sequence. Each of the first three correct responses advanced the sequence to the next member, and the fourth correct response produced food reinforcement. Incorrect responses produced a three-sec timeout. Responses during timeout reset the timeout period. Baseline and harness control sessions were characterized by a decrease in errors within each session. The animals were restrained in a plastic sleeve harness and exposed to a pulsed 2800 MHz field for 30 min prior to experimental sessions. Microwave power densities ranging from 0.25 to 10.0 mW/cm² were investigated. Specific absorption rates calculated from core temperature measurements yielded mean values of 0.72 and 1.73 mW/gm at the 5 and 10 mW/cm² power densities, respectively. At 0.25, 0.5, and 1.0 mW/cm² the behavioral measures were generally within the control range. At 5 mW/cm², error responding, rate of sequence completion, and the pattern of within-session acquisition were altered in two of four replications. Exposure to 10 mW/cm² increased errors, decreased the rate of sequence completion, and altered the pattern of within-session acquisition in all replications.

CHANGES IN TEMPORAL ASPECTS OF BEHAVIOR
BY LOW LEVELS OF PULSED MICROWAVES

Thomas, J.R. and R.A. Banvard. Behavioral Sciences Department, Naval Medical Research Institute, Bethesda, Maryland 20014

The effects of low levels of pulsed microwaves on timing behavior in rats were analyzed. Rats were trained to emit a particular interresponse time (IRT) that was in turn programmed on a differential-reinforcement-of-low-rate (DRL) schedule. Pulsed microwave radiation at a frequency of 2.8 GHz was found to disrupt the precise temporal discrimination generated by the reinforcement schedule. Behavioral changes were observed following 30-min exposures at average power levels of 4, 8, and 16 mW/cm² (SARs of 0.8, 1.8, and 3.4 W/kg, respectively), and the changes were power related. With the same IRT in effect, the DRL value was increased from DRL 8-sec with a 4-sec limited hold (LH) to a DRL 14-sec without the LH, and the animals were again exposed to the same radiation parameters. No microwave-induced changes in behavior were observed at the same three power levels with the larger DRL value in effect. When the animals were returned to the original DRL value with a LH and re-exposed to microwaves, decrements in behavior were again observed. Shifting back and forth between the two DRL schedules and exposing the animals to the same three power levels established that the ongoing temporal behavior was or was not affected by microwaves depending on the value of the DRL schedule.

MODULATION OF PENTOBARBITAL EFFECTS ON TIMING BEHAVIOR IN
RATS BY LOW-LEVEL MICROWAVES

Maitland, Georgia. Behavioral Sciences Department, Naval Medical
Research Institute, Bethesda, Maryland 20014

Investigations of EMR-Behavioral interactions determined that low levels of microwave radiation altered the mode of action by which the drug sodium pentobarbital (PB) modified certain key functions of behavior. Rats were trained on a temporal discrimination task to space their lever presses (responses) so that only responses which followed a preceding response by 18 to 24 sec produced food pellets (reinforcement). Analytically, two criteria were used which described the behavioral sequence: response rate was calculated from total lever presses over the total session time and the inter-response times (IRT) distribution was derived from the temporal distribution of all responses. The response distribution resembled a skewed curve with a mode around 18 sec. Without EMR exposure, behavioral effects of PB were obtained by repeated i.p. drug injections over a dose range of 1.0 to 14.0 mg/kg. Then, with the rat placed fully conscious in a plastic mesh net perpendicular to the source, the same PB dose range was administered with 30 min exposures to 1 mW/cm² or 5 mW/cm². (2.45-GHz pulsed microwave field with a pulse width of 2 μ sec and a 500-Hz repetition frequency.) Under these experimental conditions, PB and EMR irradiation acted synergistically to reduce the behavioral effective drug dose range from 8 to 13 mg/kg to 5 to 10 mg/kg.

BEMS POSTER A -46

ATTEMPTS TO CUE SUCCESSFUL ESCAPE FROM A HIGHLY INTENSE
MICROWAVE FIELD BY PHOTIC STIMULATION

Anna M. Grove and Daniel M. Levinson

Department of Psychology
University of Missouri
Kansas City, Missouri 64110

and

Don R. Justesen

Veterans Administration Medical Center
Kansas City, Missouri 64128

In a study designed to assess conditions under which a highly intense 918-MHz microwave field will motivate escape learning, different groups of hooded rats received 25 trials of training under one of four conditions (all $n_s = 4$): exposure to a highly intense field ($D = 60 \text{ mW/g}$); exposure to the field as temporally paired with a photic cue; or exposure to the photic cue alone. In all three of these conditions, crossing of a rat into a large "safe" area resulted in virtually instantaneous cessation of radiation and/or photic cueing. In the fourth condition, cessation of faradic shock to the feet of active controls served as a negative reinforcer of the escape response. Acquisition of the escape response was rapid for the shocked animals and was less rapid but reliably demonstrated by irradiated animals that were cued by light. Cessation of light did not motivate escape behavior and, although there was evidence of some learning during later trials by rats subjected only to microwave radiation, their performances failed to differ reliably from the rats in the light-only condition. These data confirm and extend those of Carroll, *et al.*, and Lovely, *et al.*, which indicate that nearly-lethal, deeply penetrating, non-pulsed microwaves in a multi-path field apparently lack the sensory qualities required to motivate aversive behavior.

BEMS POSTER A - 47

MOTOR COORDINATION OR BALANCE DIFFERENCES BETWEEN RATS
EXPOSED OR SHAM EXPOSED TO 60 Hz ELECTRICAL FIELDS

Allan H. Frey and Dale Meles
Randomline, Inc., Huntingdon Valley, PA 19006

Animals living in a 60 Hertz electrical field were tested to determine if their motor coordination or balance was influenced by such living conditions. The testing was done double blind. Two groups of rats were used. One group lived in the field and the other group lived under the same conditions in the room except that they were sham exposed. The male Sprague-Dawley rats were removed from their home cages and placed on a horizontal wooden rod. This rod was then rotated at an increasing speed until the animal lost its footing. This was continued over 14 days of testing. It was found that rats living under 60 Hz exposure stayed on the rod significantly longer than the control rats.

MODIFICATION OF TAIL PINCH CONSUMMATORY
BEHAVIOR BY MICROWAVE ENERGY EXPOSURE

Allan H. Frey and Lee S. Wesler
Randomline, Inc., Huntingdon Valley, PA 19006

The tail pinch consummatory response has been used in recent years to explore the functioning of the nigrostriatal dopamine system of the brain. We used the test to explore the possible involvement of this system in the response of a mammal to microwave energy exposure. Two groups of rats were tested while exposed to continuous wave microwave energy of $50 \mu\text{W}/\text{cm}^2$ and $125 \mu\text{W}/\text{cm}^2$, respectively. A third group was tested during sham exposure. The tests were run double blind. Each rat was run on each of eight test days with gnawing (of a wooden dowel rod), licking, and total tail pinch behavior time (gnawing time plus licking time) recorded. We found significant differences between the exposed compared to the sham exposed animals. The response patterns of the exposed groups were similar to each other and different from that of the sham exposed group.

BEMS - POSTER SESSION B
THURSDAY PM 1:30-4:50
HUB 108 WEST LOUNGE

Co-chairperson: O. P. Gandhi
University of Utah
Salt Lake City, UT

Co-chairperson: C-K. Chou
University of Washington
Seattle, WA

CELLULAR EFFECTS: RAMAN SPECTRA AND MILLIMETER WAVES (Paper Nos. 1-12)
IMMUNOLOGY (Paper Nos. 13-23)
ELF/H - FIELD EFFECTS (Paper Nos. 24-31) .
PROBE INSTRUMENTATION (Paper Nos. 32-38)
SPECIAL TOPICS (Paper Nos. 39-46)

MILLIMETER-WAVE RADIATION FAILS TO
INDUCE LAMBDA PHAGE EXPRESSION

T. Whit Athey and Barbara A. Krop
Bureau of Radiological Health
12721 Twinbrook Parkway
Rockville, MD 20857

There has been considerable current interest in the possibility that millimeter-waves can induce lysogenic or colicinogenic bacteria to express phage or synthesize colicin. Smolyanskaya and Vilenskaya reported that low levels (less than 1 mW/cm^2) of continuous-wave radiation in the frequency range 45.7 to 46.1 GHz cause the frequency-dependent induction of colicin synthesis (A. Z. Smolyanskaya and R. L. Vilenskaya, *Sov. Phys.-Usp.*, 16, 571, 1974). We have previously reported our attempts to verify this result (Swicord, et al., Workshop on Millimeter-Wave Effects, URSI Symposium, Helsinki, 1978). Preliminary data had seemed to show excess induction in exposed cells, but repeated replications of the experiments failed to show this effect.

The purpose of the present research was to determine the level of induction, if any, of lambda phage in *E. coli* strain BR-475 when irradiated by millimeter-waves in the frequency range 45.6 to 46.1 GHz. Since the same biochemical pathways which lead to colicin synthesis are also believed to be responsible for the induction of phage expression, this approach can serve to clarify the results with the colicin system.

The prophage of the lysogenic strain BR-475 (lac^-) has an extra gene, the normal *E. coli* lac gene which has been inserted (R. Elespuru and M. Yarmolinsky, *P. N. A. S.*, 1979, in press) so that when the phage genome is transcribed, the lac gene is transcribed also. A standard colorometric assay for β -galactosidase, a lac gene product, may be used to determine the levels of lambda induction, allowing improved quantification over the traditional plaque assays.

BR-475 cells were exposed in liquid media in a closed waveguide system. A slotted line was used to measure the degree of mismatch into the sample, and the mismatch was removed with a tuner. The cells were maintained in two identical sample holders, one for exposure and the other for sham-exposure, at 4°C during the 90-minute exposure period. Several levels of millimeter-wave radiation in the range $100 \mu\text{W/cm}^2$ to 10 mW/cm^2 were used. No differences in induction levels were observed between the exposed and sham-exposed cultures.

STUDIES OF MICROWAVE ABSORPTION IN LIQUIDS BY PHASE
FLUCTUATION OPTICAL HETERODYNE SPECTROSCOPY

Christopher C. Davis, Electrical Engineering Department,
University of Maryland, College Park, Maryland 20742
Mays L. Swicord, Bureau of Radiological Health, 12721 Twinbrook
Parkway, Rockville, Maryland 20857.

The operating principles of a newly developed, sensitive, technique for studying the local absorption of microwaves by liquids will be described. In this technique, which we call phase fluctuation optical heterodyne (PFLOH) spectroscopy, the liquid under study is irradiated with pulsed microwaves in an optical cell placed in one arm of a Mach-Zender interferometer. This interferometer is illuminated with a single-frequency helium-neon laser. The half of the beam from this laser which passes through the irradiated sample suffers a phase fluctuation because of the microwave-induced local thermal expansion of the sample. This phase fluctuation is coherently detected with very high sensitivity by heterodyning with the reference beam which has passed through the other arm of the interferometer. The resultant heterodyne signal is a measure of the average temperature rise of the sample along the laser beam path which results from the absorption of microwave energy. The quantitative evaluation of data obtained in this way will be discussed in terms of its dependence on the absorption coefficient of the sample and the field distribution of the irradiating antenna immersed in the liquid. Data obtained in this way for water, ethanediol and other liquids of biological significance will be evaluated for the case of an open-ended coaxial stub antenna and a more sophisticated irradiation system using a miniature dielectric-loaded X-band waveguide immersed in the sample. This latter arrangement produces a more predictable electric field distribution in the liquid and simplifies quantitative measurements.

The very high sensitivity of the optical heterodyne method for detecting small temperature rises in a transparent sample allows us to make a search for possible microwave absorption resonances in biological systems, such as aqueous solutions of DNA. Our current theoretical sensitivity can be stated in terms of a hypothetical sinusoidal induced temperature fluctuation as

$$\Delta T_{\min, H_2O} = 3.9 \times 10^{-7} \text{ } ^\circ\text{K} (\Delta f)^{1/2} (\text{Hz})^{-1/2}$$

where Δf is the bandwidth of the signal processing electronics. One of the greatest advantages of PFLOH spectroscopy in this application is that there can be no doubt about the existence, or not, of microwave absorption in the sample. If the sample does not absorb microwaves no temperature rise nor heterodyne signal results.

MILLIMETER WAVE CW CELLS IRRADIATION STUDIES
I MICROWAVE ASPECTS. COLICIN INDUCTION IN E. COLI

Shirley Motzkin, Leo Birenbaum, Saul Rosenthal, Charles Rubenstein, Scott Davidow, Renee Remily, Ronald Melnick

Departments of Life Sciences and Electrical Engineering
Microwave Research Institute
Polytechnic Institute of New York, Brooklyn, N. Y. 11201

Microwave techniques and instrumentation, used to evaluate the effects of CW mm-wave irradiation on colicin induction in E. Coli, on mitochondrial oxidative phosphorylation, and on hemoglobin and potassium leakage from red blood cells are herein described. In addition, the details of the E. Coli experiments are presented.

The exposure system, selected for its simplicity, uses 50-75 GHz (WR-15) waveguide and a Siemens RWO-60 backward wave oscillator powered by a Micro-Now 702 supply. This combination was observed to give a two-hour frequency stability near 50 GHz at least as good as one part in 2000. A similar arrangement, to be used in the 33-50 GHz (WR-22) waveguide band will permit the extension of our capabilities.

In each experiment, microwave irradiation is accomplished by positioning the rectangular aperture of a pyramidal horn about 2mm above the surface of the biological sample. The net power leaving the horn is assumed to enter the medium with a \sin^2 power distribution. Reflections from the irradiated surfaces are measured by a standing wave indicator in the waveguide system, and may be used to adjust the power density entering the surface of the biological medium to a constant value.

The effects of a single CW millimeter wave irradiation on Colicin induction in E. Coli, strains W3110 Col E₁, 1485, C600 and K125, in the 5.85-5.75mm wavelength range (51.3-52.3 GHz) at low power densities have been examined.

Col E₁ cells in log and stationary phase, concentrated on filter paper and placed in an agar filled polystyrene dish are irradiated for 60 minutes at maximum power densities (entering the medium) of 0.5 mW/cm² at 25°, 37° and 43°C in a water-jacketed temperature-controlled chamber placed beneath the horn so that the aperture plane abuts on the cover of the polystyrene dish. Colicin induction is determined by the production of clear areas or plaques following the exposure of a colicin sensitive bacterial strain, W1485, to irradiated Col E₁ bacteria (W3110 colicin producing).

Under the conditions employed, our results suggest that colicin induction is enhanced when Col E₁ are irradiated at 5.8mm. Data presented will include the effects of power density and temperature variations.

MILLIMETER WAVE CW CELLS IRRADIATION STUDIES
II MEMBRANE TRANSPORT IN MITOCHONDRIA AND ERYTHROCYTES

Ronald Melnick, Shirley Motzkin, Charles Rubenstein,
Scott Davidow, Leo Birenbaum, Saul Rosenthal

Departments of Life Sciences and Electrical Engineering
Microwave Research Institute
Polytechnic Institute of New York, Brooklyn, N. Y. 11201

Investigations of the effects of CW millimeter wave irradiation on cellular membranes were evaluated in studies of oxidative phosphorylation in mitochondria, and hemoglobin and potassium ion permeability in red blood cells.

Freshly prepared rat liver mitochondria were irradiated at 8.58mm (35 GHz) and at 40 discrete wavelengths between 5.00 and 6.00mm (60 to 50 GHz) to evaluate the effects of CW millimeter wave irradiation on oxidative phosphorylation. In initial experiments, mitochondrial suspensions (0.25ml containing 20mg. protein) were exposed for 15 minutes at 8.58mm, and subsequently evaluated for their efficiency in coupling succinate oxidation to the phosphorylation of ADP (respiratory control) by the conventional Clark-type oxygen electrode technique. Changes in respiratory control ratios were not apparent at power densities below 500mW/cm². Power density values cited in this paper are maximal values entering the medium under the irradiating horn.

As oxidative phosphorylation is a membrane dependent process and the above technique would not detect reversible membrane alterations a new biochemical assay involving a quantitative determination of ATP synthesis in actively phosphorylating mitochondria was developed. The extent of ATP synthesis coupled to succinate oxidation was virtually unaltered when mitochondria (1.5mg in 1ml) were irradiated at 25°C in a thermally regulated water jacketed cuvette for 2min. at 8.58mm (from 0.01 to 1000 mW/cm²) or for 2 min. at 5.00 to 6.00mm (in increments of 0.25mm) at 5mW/cm². The reaction had to be limited to 2 min. to eliminate oxygen depletion as a complicating factor. Our procedures have not revealed any effect of millimeter wave irradiation on mitochondrial oxidative phosphorylation.

A 250 μ l sample of packed human red blood cells, in a thermally-regulated water-jacketed polystyrene chamber, which is sealed with a glass coverslip is irradiated at 5.8mm (51.7 GHz), at 30°C for 15, 30, 60 and 120 minutes at power densities from 5-0.01mW/cm². Changes in the membrane permeability are evaluated by determining the Hb and K⁺ leakage spectrophotometrically at 576mm and with a potassium-electrode (ORION). Experimental results are compared with shams and unirradiated temperature-controlled samples. Results obtained will be discussed.

BEMS POSTER B - 5

SENSITIVITY OF C. ALBICANS CELLS TO FREQUENCY OF MODULATION IN
THE 72-74 GHz BAND

L. Dardanoni, M.V. Torregrossa, Institute of Hygiene,
University of Palermo, Italy
C. Tamburello, L. Zanforlin, Institute of Electrotechnics
and Electronics, University of Palermo, Italy

Exposure of *Candida albicans* cells to 72 GHz microwaves square modulated brings about a reduction of the number of colony forming units in comparison with continuous wave exposed cells (L. Dardanoni et. al., 3rd Symp, EMC, Wroclaw, 1976; L. Dardanoni et. al. URSI Symp. Helsinki, 1978).

Further experiments were carried out using an experimental procedure which allows the contemporaneous exposure of *C. albicans* cells suspension to continuous or to square modulated signals having the same mean power at frequency of minimal or maximal absorption in the 72-74 GHz band (C. Tamburello et. al., URSI Symp., Helsinki, 1978).

Irradiation for various period (1-3 hr) of actively growing cells in the log phase was carried out; the number of viable cells before and after irradiation was estimated by counting colony forming units on suitable culture media.

The influence of ambient temperature and of different modulation frequencies were investigated, in order to evaluate the sensitivity of the cells in different experimental conditions. The results are briefly discussed.

MILLIMETER WAVE ABSORPTION SPECTRA OF BIOLOGICAL SAMPLES

R. A. Lee, M. J. Hagmann, O. P. Gandhi, I. Tanaka,
D. W. Hill, and L. M. Partlow
Departments of Bioengineering, Electrical Engineering,
Microbiology, and Pharmacology
University of Utah, Salt Lake City, Utah 84112

ABSTRACT

We have previously described our solid-state computer-controlled system for swept frequency measurements from 26.5-90 GHz. The system allows wide-band frequency scans that would take a period of hours with hand-tuned sources, such as klystrons, to be made in a few minutes, thereby facilitating replicate runs for statistical analysis and minimizing biological and other variations of the sample during measurement. We will describe our recent results in the following areas.

1. New Sample Holders Allowing Measurement of Absolute Absorbance

We have developed a series of new sample holders which have no break in the waveguide and facilitate analysis of fields in the sample. Measurements with Ethanol/H₂O mixtures suggest that we are making proper determination of absolute absorption.

2. Low Temperature Measurements to Avoid Water-Dominated Absorbance

The strong absorbance of water (10-30 dB/mm) has caused all aqueous preparations which we have examined to date to have a water-like dependence of absorbance on frequency. We have made several measurements at dry ice and liquid nitrogen temperatures using a sample length of 20 cm at Ka band. Average insertion loss was found to be about 4 dB (approximately 0.2 dB/cm) showing the greatly reduced absorbance of water in the frozen state. Low temperature measurements will be reported for BHK cells over the entire frequency range of 26.5-90 GHz.

3. Emphasis on Cell Activity During Measurement

We have developed a system for maintaining the samples at 37°C during measurements and have emphasized other factors, such as biocompatibility of the sample holders, so that measurements may be made on active cells. We will present data regarding determination of cell viability before and after the microwave measurements.

4. Wide Range of Test Samples

We are continuing to study a wide range of test samples including red blood cells, bacteria, yeast, fungi, viral suspensions, normal and transformed mammalian cells, and relevant biological compounds, such as proteins, RNA, DNA, etc. The millimeter wave absorption spectra of these media will be presented.

A SEARCH FOR FREQUENCY-SPECIFIC BIOEFFECTS CAUSED
BY MICROWAVE IRRADIATION

L.M. Partlow, L.G. Bush, L.J. Stensaas,
D.W. Hill, A. Riazi, and O.P. Gandhi
Departments of Pharmacology, Microbiology, Physiology,
and Electrical Engineering
University of Utah
Salt Lake City, UT 84112

A method recently developed in this laboratory was used in order to directly expose cells grown in tissue culture to high levels of microwave irradiation without significant microwave-induced heating (0. 1° C). Monolayer cultures of BHK-21/C13 cells were grown on microwave-transparent polystyrene coverslips, placed directly on the open end of a waveguide which terminated in an incubator held at 36 °C, and irradiated at frequencies in the E-band (average power density = 292 mW/cm²) or in the U-band (average power density = 177 mW/cm²). Each culture was exposed for 15 minutes and four cultures were irradiated at each frequency. Frequencies corresponding to 0.1 GHz increments in the ranges from 37 to 48 GHz and from 65 to 75 GHz will be studied.

Incorporation of ³H-methionine into protein during the period of microwave irradiation was assessed by autoradiography. Incorporation by the cell monolayer was quantified by measurement of the optical density of the autoradiograms in a set of contiguous 0.1 mm wide regions which spanned the long axis of the waveguide. Since microwave power density along the major axis of the waveguide varies from its maximum at the center to zero at either edge, these data provide information on the extent of protein synthesis in BHK cells subjected to 16 or 25 different power densities in the E- or U-bands, respectively. These data sets were examined both by visual inspection and computer analysis for the presence of narrow "power windows" in which microwave bioeffects might be expressed.

Data have already been compiled on 100 frequencies ranging from 43 to 48 GHz and from 65 to 70 GHz. In agreement with earlier studies in this laboratory at the fixed frequencies of 41.80 and 73.95 GHz, amino acid incorporation by irradiated cultures did not differ significantly from that of nonirradiated "sham controls" at any frequency and no evidence of a "power window" was found. (Data on other frequencies will be presented at the meeting).

RAMAN SPECTROSCOPY OF MAMMALIAN CELLS

A. Riazi,^{*} J. R. Duffey,[†] O. P. Gandhi,^{*} and D. W. Hill^{**}

^{*}Department of Electrical Engineering

[†]Department of Physics

^{**}Department of Microbiology

University of Utah, Salt Lake City, Utah 84112

ABSTRACT

A procedure for distinguishing tumor cells from corresponding normal cells by virtue of their Raman spectra is being investigated. There are many problems associated with Raman spectroscopy of cells suspended in a liquid medium. Among these problems are fluorescence of the medium, large Rayleigh scattered light, and accompanying time dependent intensity fluctuations of the scattered light due to cell settling. These effects tend to mask the Raman scattered light from the cells. Fluorescence can be avoided by using a simple transparent medium, and cell movement can be eliminated by suspension of the cells in agarose. A relatively simple filter for reducing the Rayleigh scattered light can be made from sodium vapor when using a dye laser as the exciting source.

Results of experiments performed on various biological samples including normal and transformed mammalian cells will be presented.

A THEORETICAL BASIS FOR MICROWAVE AND RF FIELD
EFFECTS ON EXCITABLE CELLULAR MEMBRANES

Charles A. Cain
Bioacoustics Research Laboratory
Department of Electrical Engineering
University of Illinois
Urbana, Illinois 61801

A modified Hodgkin-Huxley (HH) model has been developed which provides a basis for understanding how oscillating electric fields at microwave and RF frequencies might directly affect nerve, muscle, and other electrically excitable tissue. In the HH model for the current-voltage relations in the membrane of the giant squid axon, certain rate constants are non-linear functions of the instantaneous electric field across the membrane. Due to these non-linear functions, an oscillating component of membrane potential may cause a steady (DC) change in all α and β rate constants in the HH model. These rate constant shifts result in a number of interesting predicted effects of microwave or RF exposure on nerve function.

The model predicts that an oscillating component of membrane potential will change the conductance of the membrane to all ion species which traverse voltage dependent membrane channels. Voltage sensitive channels for sodium, potassium, calcium, and other ions have been demonstrated in membrane of muscle cells (skeletal, smooth, and cardiac), in nerve cell axon and soma membrane, and even in the membrane of the extensive dendritic branches of some cells. Modified HH models of the type to be discussed may be useful in predicting the effects of CW, pulsed, or amplitude modulated RF and microwave radiation on neural and neuromuscular systems. For example, in the squid giant axon, the model predicts that an oscillating component of membrane potential would increase the membrane potassium conductance (g_K) and decrease the sodium conductance (g_{Na}) in the steady state. This increase in g_K and steady state decrease in g_{Na} results in hyperpolarization of the membrane. Hyperpolarization would have an inhibitory effect on an irradiated neuron or muscle cell. Spontaneously firing cells, e.g., pacemaker cells in neural or cardiac tissue, would be expected to decrease their action potential generating frequency in response to an oscillating electric field of sufficient magnitude. Heating produces effects which are in the opposite direction. Other predictions of the model, and possible physical interpretations, will be presented.

VIBRATIONAL SPECTRA OF IN VIVO BIOLOGICAL SYSTEMS

K.H. Illinger, Department of Chemistry, Tufts University,
Medford, MA 02155

The spectroscopic properties of in vivo biological systems are determined, in part by the (time-invariant) equilibrium system analyzable in terms of ordinary molecular fluids, and in part by non-equilibrium, steady-state (time-variant) subsystems whose analysis may require totally different constructs. One aspect of such an analysis is the contribution of the subsystem to the vibrational spectrum of biological systems in the millimeter-wave and far-infrared region. We develop the detailed spectroscopic properties of the model due to Fröhlich, and the extraction of biophysical information from such spectra. The effect of changes in the general photon distribution function $n(\omega_k)$ on the (infrared-active and Raman-active) vibrational spectra and emissivities of a system of harmonic oscillators is examined. An application is given to the Bose condensation of photons, postulated in the Fröhlich model, for in vivo biological systems, and its consequences for their millimeter-wave and far-infrared vibrational spectra and vibrational emissivities. Implications of the analysis for the interpretation of such spectra are discussed.

Of the three spectroscopic observables of the subsystem, the emissivity, $\epsilon(\omega_k j_k)$, the Raman-intensity ratio, $[I(\omega_0 + \omega_k j_k) / I(\omega_0 - \omega_k j_k)]$, and the attenuation function, $\alpha(\Delta v_k = j_k)$, the first would provide the most direct experiment for the quantitative characterization of the crucial parameters of the Fröhlich model: the frequency of the Bose-condensation mode, ω_1 , and the measure of the magnitude of the non-linear terms. The terms $\alpha(\Delta v_k = j_k)$ are invariant with $n(\omega_k)$, hence provide no information concerning the onset of the Bose condensation, and preclude facile assignment of the frequencies ω_k . The terms, $[I(\omega_0 + \omega_k j_k) / I(\omega_0 - \omega_k j_k)]$, while dependent on the form of $n(\omega_k)$, are insensitive to the value of j_k , in the (low-frequency) limit, $n(\omega_k) \gg 1$. In contrast, a single emissivity term, $\epsilon(\omega_1)$, is predicted to exhibit behavior saliently different from all the others, $\epsilon(\omega_1 j_1)$, $j \neq 1$, and $\epsilon(\omega_k j_k)$, $k \neq 1$, each of these being essentially blackbody terms, $\epsilon(\omega) \approx 1$. In spite of the experimental problems concerning the determination of $\epsilon(\omega_1)$, this experimental variable would appear to provide the most direct route to the quantification of the model. In general, direct spectroscopic determinations of millimeter-wave and far-infrared properties of in vivo biological systems possess the not inconsiderable advantage of providing biophysical information at the molecular-systems level, while global biological endpoints are intrinsically integrative effects, not currently susceptible of direct analysis.

BEMS POSTER B - 11

MOLECULAR LEVEL EFFECTS OF MICROWAVES ON NATURAL AND MODEL MEMBRANES: A RAMAN SPECTROSCOPIC INVESTIGATION

J. P. Sheridan, B. P. Gaber, F. Cavatorta and P. E. Schoen

Naval Research Laboratory
Washington, D. C. 20375

Laser Raman spectroscopy has been employed as a non-perturbing optical technique to probe changes in molecular order induced by low-moderate levels of microwave radiation in multilamellar and unilamellar bilayer preparations of a) dipalmitoyl phosphatidylcholine and b) sphingomyelin, a lipid extracted from bovine brain. These systems exhibit sharp order-disorder phase transitions within the biological temperature region involving cooperative changes in the degree of fluidity of the hydrocarbon chains which constitute the interior of the bilayers. Raman spectroscopy is a powerful method for observing and characterizing these thermally induced conformational changes.

Samples of the multibilayer membrane preparations were exposed to various power levels of CW microwave radiation in a thermostatted anechoic chamber maintained at a temperature close to their phase transitions while being monitored by the Raman technique. An increase in bilayer fluidity was observed at power levels on the order of 10mW/cm^2 at a frequency of 2.4 GHz. The increase of fluidity observed for $\sim 25\text{mW/cm}^2$ power incident upon the sample was equivalent to a rise in bilayer temperature of about 2°C while the change in bulk temperature as measured by the ruby fluorescence technique was much smaller. Thus, it was concluded that, for multibilayer membrane systems, exposure to CW microwave radiation at power levels of 10mW/cm^2 and greater results in a steady state temperature difference between the interior of the bilayers and the aqueous environment external to the liposomes.

Similar experiments conducted upon unilamellar vesicle preparations showed no differences between bilayer temperature (as measured by Raman) and bulk temperature (as measured by ruby fluorescence) over the power range $1\text{--}25\text{ mW/cm}^2$.

These results will be discussed in terms of a model involving absorption of microwave energy by bound water and two different mechanisms of thermalization.

EFFECT OF MICROWAVES ON RED BLOOD CELL COMPONENTS:
INVESTIGATIONS AT THE MOLECULAR LEVEL

B. P. Gaber and J. P. Sheridan
Naval Research Laboratory
Washington, D. C. 20375

ABSTRACT

Raman spectroscopy has been employed as a non-perturbing, specific and readily interpretable technique to probe the molecular effect of microwaves on intact erythrocytes (red blood cells) and erythrocyte ghosts (cell membranes). By excitation within the absorption band of hemoglobin, we have for the first time measured the resonance Raman spectrum of the hemoglobin bound within intact erythrocytes. Exposure to 2.4 GHz (CW) microwave radiation at power densities between 1 and 25 mW/cm² results in no discernible change in the hemoglobin spectrum. Resonance Raman spectra of heme proteins are known to be quite sensitive to changes in iron spin state, oxidation state and porphyrin ring conformation. Therefore, we conclude that none of these molecular-level factors is perturbed by microwave fields of the frequency and intensity employed here.

Conventional Raman spectra have been obtained from preparations of hemoglobin-free erythrocyte ghosts. Vibrational modes from both the protein and lipid components of the membrane have been identified. A systematic study of the temperature dependence of the relative intensities of the conformationally sensitive C-H stretching vibration shows a steep transition between ~35° and 40°C -- i.e. within the physiological temperature range. Investigation of the effect of microwave radiation on erythrocyte ghosts in this temperature regime will be reported.

MICROWAVE EFFECTS ON HUMAN COLONY FORMING MARROW CELLS

Mark J. Ottenbreit¹, James C. Lin²,
Susumu Inoue¹ and Michael Fracassa¹

Department of Pediatrics¹
Department of Electrical Engineering²

Wayne State University, Detroit, Michigan 48201

We examined the effects of 2450 MHz CW microwaves on human colony forming cells of the neutrophil lineage. Marrow cells from 3 patients with acute lymphoblastic leukemia in remission were exposed to microwaves by using a constant temperature waveguide irradiation chamber filled with 0.9% NaCl solution. All 3 specimens were exposed to 4 different power levels at 125, 250, 500 and 1000 mW/cm² for a duration of 15 minutes at 37°C, while sham exposure was conducted in the same chamber without power at 37° Celsius. The temperature of the chamber's solution during microwave irradiation showed a maximum increase less than 1°C at an incident power density of 500 mW/cm².

Both microwave and sham exposed cells were plated at an identical concentration of 4×10^4 cells/plate in methylcellulose using fetal fibroblast conditioned medium as a stimulatory source. Colonies, a group of 20 or more cells were read on days 6&12 of culture. Comparison of colony number between sham and microwave exposed cell cultures showed a significant reduction ($P < 0.01$) in cultures of cells exposed to 500 and 1000 mW/cm² power density, while cultures of cells exposed to 125 or 250 mW/cm² showed no reduction in colony number. All 3 specimens yielded similar results.

We conclude that 2450 MHz CW microwave may interact directly with human colony forming cells of the neutrophil cell lineage and that this interaction results in a CFC reduction as assayed by in vitro culture methods.

PRIMARY IMMUNE RESPONSE OF MICE EXPOSED TO CONTINUOUS
OR PULSED WAVE 425-MHz RADIOFREQUENCY RADIATION

R.J. Smialowicz, M.M. Riddle, P.L. Brugnolotti,
K.L. Compton and J.B. Kinn
Environmental Protection Agency
Health Effects Research Laboratory
Experimental Biology Division (MD-72)
Research Triangle Park, N.C. 27711

The primary immune response of mice was used to assess the effects of exposure to either continuous-(CW) or pulsed-(PW) wave modulation at 425-MHz. Female BALB/c mice were exposed in a transverse electromagnetic mode (TEM) transmission line under temperature controlled conditions for one hour on each of five consecutive days. An equal number of sham-exposed animals served as controls. Mice were exposed to 425-MHz (CW) at average forward powers of 78, 20 or 5 W equivalent to 39, 10 and 2.5 mW/cm² respectively. In other experiments mice were exposed to 425-MHz (PW) at average forward powers of 17.7, 5 or 1.25 W (9, 2.5 or 0.63 mW/cm²). For the pulsed wave exposures a 1 msec pulse with a pulse repetition rate of 250 pulses/sec was employed. The specific absorption rate for mice exposed at 70 W (CW) forward power was 7.7 mW/g as determined by twin-well calorimetry. No difference in the primary immune response to sheep erythrocytes, as determined by the direct plaque-forming cell assay, was observed between sham-exposed and exposed mice or between mice exposed to either CW or PW 425-MHz.

GROWTH OF HUMAN BONE MARROW CELLS IN AGAR CULTURE
UNDER THE INFLUENCE OF ELECTRICAL CURRENTS

J. Bojsen and B. Thing Mortensen
The Finsen Laboratory and Medical Department
The Finsen Institute
Copenhagen, Denmark

The aim with the present study was to elucidate the effects of AC- and DC-currents on growth of bone marrow cells in agar as a model.

By modification of plastic petri dishes an electrode system was constructed with two fixed platinum electrodes. Electrical contact was established to the culture by gelling of agar around each electrode and by placing a gel slab from the electrode gel to the agar culture. The agar method of culturing bone marrow cells is well characterized. Cultures were placed 7 days in a fully humidified incubator under electrical influence and the results scored as number of cell clusters (> 5 cells).

Electrical currents were supplied from 1) a biphasic square-wave generator with fixed identical amplitudes (12 volts). The current amplitudes were limited by series resistors chosen in decade steps from $1\text{ k}\Omega$ to $1\text{ M}\Omega$. In most of the experiments the impulse width were individually adjusted to $5\ \mu\text{sec}$ and $2.4\ \text{msec}$ respectively and with the repetition frequency at 8 or 80 Hz. Electrode and agar impedances were determined. 2) A mercury battery (5.4 v - 1 Ah) in series with DC-current limiting resistors ($0.2\ \text{nA}$ in decade steps to 2 mA). DC-current-voltage characteristics were measured.

Shortly, the results showed a symmetrical AC-impulse current to be without effect on cell growth, while a DC-current ($10\ \mu\text{A}$) gave severe growth reduction and protein electrophoresis in the culture. The reduction in cell growth was proportional to the logarithm of the AC-current amplitudes. However, when the frequency was changed to 8 Hz a proportional shift was seen in the growth reduction curve due to the decrease in amount of charge distributed. It could be proved that the observed growth reduction was non-related to heat production, pH changes, or protein electrophoresis. On cellular level an explanation for the found results remain obscure and need further investigation.

EFFECTS OF HYPERTHERMIA AND MICROWAVE INDUCED HYPERTHERMIC SHOCK
ON HPC CELLS.

W.A.G. Voss*, A. Kennedy**, A. Fontaine**, B. Hall** and J. Van
Netten***.

*Division of Biomedical Engineering and Applied Sciences,
Surgical Medical Research Institute, University of Alberta,
Edmonton Canada, T6G 2E1, **Department of Biology, University of
Victoria, Victoria, British Columbia and ***Royal Jubilee
Hospital, Victoria, British Columbia, Canada.

A comparison is made between slow waterbath heating ($dT/dt = 0.22^{\circ}C/s$) and rapid microwave heating ($dT/dt = 9.2^{\circ}C/s$) prior to 15 minute hyperthermic exposures for human prostate cancer cells in vitro. The effect of dT/dt is shown to be small in the exposure range $43.5 - 47.5^{\circ}C$. Data are also presented to show that microwave induced hyperthermic shock ($dT/dt = 9.2^{\circ}C/s$) followed by immediate waterbath cooling (an exposure of a few seconds above $37^{\circ}C$) has no effect on cell survival below $43^{\circ}C$. Above this temperature, the percentage cell survival (S) to hyperthermic shock decreases with increasing exposure temperature (T_E) according to the linear relationship $S = -11.6T_E + 593$, ($43 < T_E < 50^{\circ}C$) with a correlation coefficient $r = 0.95$. Effects have been assayed by cellular attachment and colony formation; they are also shown by SEM photography.

THE EFFECTS OF 9-GHz PULSED MICROWAVES ON CIRCULATING
ANTIBODY TITERS OF MICE

C.G. Liddle, J.P. Putnam, J.Y. Lewis, B. Bell,
M.W. West and O.L. Huey
Environmental Protection Agency
Health Effects Research Laboratory
Experimental Biology Division (MD-72)
Research Triangle Park, N.C. 27711

The effect of microwaves on the circulating antibody titers of mice was investigated. Female CD-1 mice were immunized against Streptococcus pneumoniae, type III, and then exposed to 9-GHz pulsed microwaves at an average incident power density of 10 mW/cm² for 2 hours daily, for 5 days. Twenty four hours following the last exposure, blood samples were taken and plasma was analyzed for antibodies to type III pneumococcal polysaccharide. The mean titer from 103 irradiated mice was compared to that of 100 sham-irradiated mice and was found to be significantly elevated (means 8.24 and 7.88 respectively, $p=0.0025$, titers expressed as $1/2^N$). Approximately half of the animals were challenged with virulent S. pneumoniae, type III, following irradiation. Mortalities in the two groups were almost identical, 47.2% among the irradiates (25/53) and 50% among the controls (27/54). It is concluded that 9-GHz pulsed microwaves at 10 mW/cm² can significantly increase the circulating antibody response of mice, but this increase did not alter the ability of the animals to withstand a challenge. This confirms the results of other investigators showing a stimulatory effect on B-lymphocytes; however, this effect does not appear to confer any additional benefit.

THE EFFECT OF RADIO FREQUENCY (148 MHz) ELECTROMAGNETIC
FIELD EXPOSURES ON HYPERSENSITIVITY RESPONSES IN MICE

Jeannine A. Majde* and James C. Lin**
*Office of Naval Research, Chicago, IL 60605
and
**Department of Electrical Engineering
Wayne State University, Detroit, MI 48202

Hypersensitivity responses in mice to red cell antigens, as expressed by paw swelling reactions at certain time intervals following antigen challenge, have proven highly sensitive to modulation by mild, intermittent environmental stress. C3H female mice maintained under low stress housing conditions were exposed to 148 MHz fields at power densities of either 0.5 mW/cm^2 (average SAR = 0.013 mW/g) or 30 mW/cm^2 (average SAR = 0.75 mW/g) in a Crawford cell. Animals were exposed for 1 hr/day for 3 successive days starting at 24 hr after subcutaneous immunization with 10^9 human type O red blood cells. Paw challenge was performed on day 14 following immunization when all 3 forms of hypersensitivity responses (anaphylactic, Arthus, delayed-type) were vigorous in controls. Paw thickness was measured with a micrometer and compared to saline injected contralateral paws. A mild but significant suppression of the anaphylactic response was seen when the mice were exposed to power densities of 30 mW/cm^2 but not at power densities of 0.5 mW/cm^2 . No consistent effect of these 148 MHz fields on the Arthus or delayed-type responses was detected. The degree of suppression of anaphylaxis was comparable to that seen in animals exposed to 1 hr in the cold on the day following immunization.

IMMUNOLOGIC AND HEMATOPOIETIC ALTERATIONS BY 2450 MHz RADIATION

Andrew T. Huang, M.D., Associate Professor and Nelda Mold, Research Assistant, Division of Hematology-Oncology, Department of Medicine, Duke University Medical Center, Durham, North Carolina 27710

Previous published work has demonstrated changes in morphology (Huang, et al., 1977) and responsiveness of lymphocytes (Wiktor-Jedrzejczak et al., 1977) attributable to the electromagnetic radiation at 2450 MHz. Data from our laboratory have also revealed an inverted U-shaped relationship between the morphologic transformation of lymphocytes and power densities ranging from 5 to 45 mW/cm² with no significant changes in rectal temperature of the test animals between 5 and 15 mW/cm² (Huang et al., 1977). These findings stimulated further investigation in search of corroborative alterations in the immunologic system of these animals.

BALB/c mice were exposed to 2450 MHz microwaves (continuous wave) under far-field conditions in a temperature and humidity controlled environment. A biphasic modulation of responsiveness of spleen lymphocytes to mitogens (phytohemagglutinin, concanavalin A for T- and lipopolysaccharide from *E. coli* for B-lymphocytes) was observed at power densities of 5 - 15 mW/cm² with exposure for 30 min/day over a period of 1 to 17 days. In comparison to sham exposed mice, a depressed response was seen in the first 2 days of exposure, followed by normalizing tendency lasting for 2-3 days. An enhanced response subsequently appeared between 7 and 9 days. Extended period of radiation beyond 10 days was associated with a lower responsiveness to mitogens. An improvement of mitogen responsiveness was observed after the removal of macrophages from spleen lymphocyte preparations. Addition of peritoneal macrophages from exposed mice suppressed unexposed spleen lymphocyte responsiveness when macrophages from sham exposed mice did not. This modulated phenomenon may be due to the interaction of two factors: 1) suppression of lymphocyte response by activated macrophages which persists throughout the entire course of radiation and 2) progressive direct stimulation of lymphocytes which culminates on the 9th day of exposure.

Using methylcellulose as a culture system, colony forming precursor B lymphocytes in the spleens of animals exposed for 9 days, 30 min/day at 15 mW/cm² of radiation were stimulated by 55% over B lymphocyte colonies from the spleens of sham exposed mice. This finding supports that of mitogen study and suggests a proliferative stimulation of lymphocytes by microwave radiation. Using the same exposure, the highly proliferative hematopoietic marrow cells from femurs of mice were also examined for their sensitivity to microwave radiation. The colony-forming units of myeloid and erythroid series from the exposed animals were consistently reduced by 50%. It is unclear whether the effect is due to marrow suppression or emigration of precursor cells from the marrow. This observation may lead to a new and more sensitive assay for studying biological effects of microwave radiation in the future.

INFLUENCE OF PULSED MICROWAVE RADIATION
ON THE LYMPHOCYTES OF RATS

Jana Pazdzerova-Vejlupkova
Department of Occupational Diseases
University Hospital
Charles University of Prague
Czechoslovakia

A group of 20 young male rats of mean initial body weight of 65.53g was irradiated for seven weeks (five days per week, four hours per day) with an electromagnetic pulsed field of the following parameters: working frequency 2736.5 MHz, pulsed rate 395 Hz, pulse width 2.6 usec, vertical polarization, mean power density 24.4 mW/cm², and accuracy of measurement + 6%. The rectal temperature of experimental animals increased during irradiation by a maximum of 0.5 °C.

Blood was taken before irradiation, at the first, third, fifth, and seventh week of exposure and at the first, second, sixth and tenth week after irradiation. There was a significant decrease in leucocyte and absolute lymphocyte count in peripheral blood during the second half of the irradiation period with the persistence of a relatively higher percentage of large lymphocytes. An attempt was made to determine whether or not an influence of pulsed microwaves at this power density upon nucleoli of lymphocytes would be present. (Compact nucleoli and nucleoli with nucleolonemas are considered to be active in the sense of synthesis RNA). No significant changes were found in the nucleolar coefficient and in the different types of nucleoli with the exception of the first week of irradiation when a significant drop of mean value of nucleolar coefficient was present.

A similar experiment was carried out in cooperation with colleagues in the Institute of Industrial Hygiene and Occupational Diseases, Academy of Medical Sciences in Moscow. Twenty-four male rats were exposed to pulsed microwave radiation of these parameters: working frequency 3000 MHz, pulse rate 300 Hz, pulse width 2.5 usec, mean power density 1 mW/cm², accuracy of measurement + 30%. No significant changes were found in either leucocyte and lymphocyte count or in the proportion between large and small lymphocytes. No significant changes were observed in the nucleolar coefficient and in different types of nucleoli in lymphocytes of irradiated animals.

KINETICS AND MECHANISMS OF THE INDUCTION OF AN INCREASE IN
COMPLEMENT RECEPTOR POSITIVE (CR⁺) MOUSE SPLEEN CELLS FOLLOWING
A SINGLE EXPOSURE TO 2450 MHZ MICROWAVES

C. Schlagel,¹ K. Sulek,² A. Ahmed,¹ H. Ho,³ and W. Leach.³ ¹Naval Medical Research Institute, Bethesda, MD; ²Military School of Medicine, Warsaw, Poland; ³Bureau of Radiological Health, FDA, Rockville, MD

We have previously shown that exposure of mice for 30 minutes to 2450 MHz microwaves induced a marked increase in the level of CR⁺ lymphoid cells in the spleen. A series of experiments were conducted to examine the kinetics of this inductive event. It was determined that a minimum of a single 15-minute exposure induced a significant increase, and a maximal increase was noted after a 45-minute exposure. The orientation of the mice in the waveguide during exposure did not alter the results.

The mechanisms for the induction of the increase of CR⁺ cells were reasoned to be: a. due to maturation of CR⁻ to CR⁺ cells; b. due to their effect on T cells, which subsequently produced factors affecting B-cell receptors; c. due to the increased permeability of the gut lining, which allowed molecules like lipopolysaccharide (LPS) from the gut flora to cause B-cell activation; and d. it could be due to a genetic susceptibility for this specific inductive event. Experiments performed with the use of athymic nu/nu mice showed data which suggested that this increase in CR⁺ cells was not due to the presence of mature T cells. Secondly, mice less than 6- to 8-weeks old, which normally possess few CR⁺ cells, failed to show an increase 3 to 6 days following microwave exposure. This suggests that if microwaves are inducing the maturation of CR⁻ to CR⁺ cells, the CR⁻ cells must first undergo a certain level in situ maturation before being converted to CR⁺ cells by microwaves. Thirdly, intraperitoneal injection of several strains of mice with LPS resembled the effect of microwaves by inducing an increase in CR⁺ cells. However, two strains of mice that showed a marked increase in CR⁺ cells following exposure to microwaves (C3H/HeJ and CBA/N) failed to show a similar increase after LPS injection, suggesting perhaps that other mechanisms were involved. Finally, using various genetically defined mice, it was determined that mice bearing the major histocompatibility (H-2^k) haplotype showed marked increases, whereas mice bearing the H-2^b and H-2^d haplotypes were refractory.

We conclude that susceptibility to the inductive events may be under H-2 control. The inductive effects of microwaves are not mediated by LPS, nor by T-cell factors that affect B-cell surface receptors. The evidence suggests that microwaves are inducing the maturation of relatively mature CR⁻ to CR⁺ B cells. We cannot exclude the possibility that microwaves are increasing the density of CR on the B-cell surface.

ALTERED IN VIVO LYMPHOCYTE MIGRATION FOLLOWING
WHOLE-BODY RFR EXPOSURE: DIFFERENTIAL
EFFECTS ON T- AND B-LYMPHOCYTES

Robert P. Liburdy
Radiation Sciences Division
USAF School of Aerospace Medicine
Brooks Air Force Base, Texas 78235

Spleen lymphocytes exhibit altered in vivo migration patterns when transplanted into recipients which are then immediately exposed to microwave radiation (2.5 GHz, 30 mW/cm², 45 W/g SAR, 30 min at 25°C) (R. Liburdy, 1978 IMPI Symposium, Ottawa, Canada; The Journal of Microwave Power, in press). These studies have demonstrated that microwave exposure results in lymphocyte trapping in the lung, impaired lymphocyte migration to the spleen, and an increased number of lymphocytes being driven into the bone marrow. The present investigation was conducted to identify which sub-population of lymphocytes, the T- or B-cell fraction, contributes to microwave-induced alterations in lymphocyte migration. A novel double-isotope labeling technique employing Cr-51 labeled T-lymphocytes and In-111-oxine labeled B-lymphocytes was used to follow both cell types simultaneously in the same mouse. In these studies T- and B-cells were purified on a Sepharose 6MB anti-mouse Ig affinity column, labeled with isotope, and i.v. transplanted into mice immediately prior to RFR exposure. Migration patterns were determined 18 hours post-exposure by quantitating CPM/organ/gm organ for the lungs, spleen, liver, and bone marrow. T-lymphocytes (>95% negative for surface immunoglobulin, Ig⁻) exhibited altered in vivo migration characterized by marked trapping in the lungs, reduced traffic to the spleen and a significant redirection of lymphocytes into the bone marrow. This pattern is identical, although more marked in degree, to the altered migration for unfractionated spleen cells. B-lymphocytes (>85% Ig⁺), however, were essentially unaffected by microwave irradiation. These results indicate that T-lymphocytes are preferentially sensitive to microwave effects on in vivo lymphocytes migration. An alteration of T-lymphocyte compartmentalization may affect cell-mediated immune function since T-lymphocytes are required for initiation and effector phases of cell-mediated immune processes. (See R.P. Liburdy, "Serum and Lymphocytes From Microwave Exposed Mice Enhance Cell-Mediated Effector Function: Increased Lymphocyte-Mediated Cytotoxicity During Allograft Rejection of EL-4 Lymphoma Cells", this symposium).

The animals involved in this study were procured, maintained, and used in accordance with the Animal Welfare Act of 1970 and the "Guide for the Care and Use of Laboratory Animals" prepared by the Institute of Laboratory Animal Resources - National Research Council.

SERUM AND LYMPHOCYTES FROM MICROWAVE EXPOSED MICE
ENHANCE CELL-MEDIATED EFFECTOR FUNCTION:
INCREASED LYMPHOCYTE-MEDIATED CYTOTOXICITY DURING
ALLOGRAFT REJECTION OF EL-4 LYMPHOMA CELLS

Robert P. Liburdy
Radiation Sciences Division
USAF School of Aerospace Medicine
Brooks Air Force Base, Texas 78235

Previous investigations have shown that whole-body microwave exposure (2.5 GHz, 30 mW/cm² (45 W/gm SAR), 30 min at 25°C) (R. Liburdy, Federation Proceedings (1978) 37(6), 1281) results in enhanced cell-mediated immunocompetence in the mouse as measured by early allograft rejection during in vivo EL-4 lymphoma tumor-cell destruction. To answer the question of whether this impact on cell-mediated immune function is the result of microwave interaction with the host immune defense system or with the transplanted EL-4 cell directly, or both, an in vitro correlate assay for in vivo EL-4 allograft rejection was used to test the effect of serum and lymphocytes from RFR exposed mice on lymphocyte-mediated cytotoxicity. Balb/c (H2-d) mice were given i.p. EL-4 (H2-b) cell transplants and irradiated for 30 minutes for ten consecutive days (2.5 GHz; 30 mW/cm² (45 W/gm SAR) or mW/cm² (15 W/gm SAR); 25°C). On day eleven serum and spleen lymphocytes were collected for use in an in vitro assay to quantitate lymphocyte-mediated cytotoxicity against Cr-51 labeled EL-4 target cells. Addition of serum or lymphocytes from microwave exposed mice to sensitized lymphocytes obtained from non-RFR treated mice significantly enhanced cytotoxicity in this assay. Similar results were obtained using target EL-4 cells from microwave treated mice. The above results indicate that a factor present in mouse serum or sensitized spleen lymphocytes from microwave treated mice can act to enhance lymphocyte-mediated cytotoxicity. The data presented here supports the notion that microwave induced enhancement of in vivo cell-mediated immune function during allograft rejection, as reported earlier, is the result of microwave impact on the lymphocyte in contrast to the EL-4 cell. The fact that serum can enhance lymphocyte-mediated cytotoxicity suggests that this enhancement is mediated by a biochemical factor that acts on the lymphocyte in vivo.

The animals involved in this study were procured, maintained, and used in accordance with the Animal Welfare Act of 1970 and the "Guide for the Care and Use of Laboratory Animals" prepared by the Institute of Laboratory Animal Resources - National Research Council.

A BEHAVIORAL PROCEDURE AND 60 HERTZ EXPOSURE
SYSTEM FOR DETERMINING FIELD DETECTION BY RATS *

S. Stern, V.G. Laties, C. Stancampiano, G.B. Inglis, E. Carstensen, S.M. Michaelson, M.W. Miller, Department of Radiation Biology and Biophysics, School of Medicine and Dentistry, University of Rochester, Rochester, New York 14642; J.O. de Lorge, Naval Aerospace Medical Research Laboratory, Pensacola, Florida 32508

A new system has been constructed to determine the threshold for detecting 60 Hertz electric fields by the rat. A variant of the Method of Constant Stimuli, which has been studied intensively by other investigators for determining the thresholds of animals to a variety of stimuli, will be used in the present study. The present report describes significant features of both the exposure system and behavioral paradigm designed to study the sensitivity of the rat to 60 Hertz electric fields.

* This report is based on work supported by a contract with the U.S. Department of Energy at the University of Rochester Department of Radiation Biology and Biophysics and has been assigned Report No. UR-3490-1557.

EFFECTS OF 60 Hz ENVIRONMENTAL ELECTRIC FIELDS ON THE
CENTRAL NERVOUS SYSTEM OF LABORATORY RATS

S.M. Bawin, I. Sabbot, B. Bystrom, P.M. Sagan, W.R. Adey
VA Medical Center, Loma Linda, CA 92357 and Depts. of
Physiology and Surgery, Loma Linda University, CA 92350

Groups of 10 male albino rats were exposed to vertical 60 Hz electric fields of 0 (ambient), 50, 500 and 1000 V/m for a period of 30d. Duplicate tests were run of 0, 500 and 1000 V/m exposures. Subjects lived in a plastic test facility for 7d prior to exposure and for 7d following the 30th of exposure.

Throughout the 44d experiment the subject's body weight, water and food consumption, urine output and general activity were measured. Urine from 6 animals was obtained by a fraction collection and all samples for selected days were tested by atomic absorption analysis for levels of K, Na and Ca. Following completion of the experiment subjects from the 500 V/m and 1000 V/m conditions were sacrificed; thyroid and adrenal tissues were removed and weighed; intracardiac blood samples were taken and fully analyzed.

Most measures in this large pilot experiment showed no statistically significant differences between experimental subjects and control subjects or between experimental subjects exposed to the various field strengths.

Two activity measurements, however, showed field correlated effects: 1) the relative size and duration of the late night activity bout was considerably reduced in the 1000 V/m condition, as compared to the 500 V/m and control conditions during the first days of field exposure; 2) relative activity during the 0900-1000 period was consistently but not significantly greater in the 1000 V/m condition than the 500 V/m and control conditions throughout the field exposure field (binomial test, 5 of 5 1000 V/m sessions greater, $p = .188$).

These effects were taken as indicating 1) a possible 'on' effect associated with the 1000 V/m field, and 2) an enhanced sensitivity to external stimuli associated with the 1000 V/m condition.

Urine analyses were closely correlated between sham and irradiated animals, including initial field exposure days associated with altered periodicity in circadian movements. These urinary electrolyte data did not suggest altered steroid excretion as a result of field exposure.

EFFECT OF CHRONIC EXPOSURE TO AN ELECTRIC FIELD
ON SUBSEQUENT DISCRIMINATION OF ELECTRIC FIELDS

Dennis L. Hjeresen
Biology Department
Pacific Northwest Laboratory
Richland, WA 99352
Operated by
Battelle Memorial Institute

An experiment was conducted to determine if pre-exposure to a 60-Hz electric field affects the subsequent ability of rats to discriminate the presence or absence of electric fields at various field strengths. Male, Sprague Dawley rats (N=120) were exposed or sham exposed to a 100 kV/m, 60-Hz electric field for 30 days (22 hours/day). Rats were subsequently tested for side of residence in a Plexiglass shuttlebox where one end was shielded from the electric field while the other end was exposed at field strengths of 0, 25, 50, 75 or 100 kV/m (N=12 pre-exposed and 12 sham pre-exposed rats per field strength). Pre-exposed rats spent significantly more time of a 45-minute session in the exposed region at 25 kV/m compared to sham pre-exposed controls. Within the pre-exposed group, there was significantly higher exposed side residence across field strengths [$F = 6.44$, $p < 0.05$, (4.55 df)], while within the sham pre-exposed group there was significantly higher unexposed side residence time among field strengths ($F = 6.84$, $p < 0.05$, (4.54 df)]. Results are discussed in terms of adaptation to an electric field stimulus.

EFFECTS OF HIGH INTENSITY 60 Hz ELECTRIC FIELDS
ON PRIMATE BEHAVIOR
EXPOSURE FACILITY, FIELD MEASUREMENT TECHNIQUES,
AND INDIVIDUAL PERFORMANCE

CHARLES S. FELDSTONE, RICHARD T. SMITH, HERMAN F. BARSUN,
EDWIN BRONAUGH, RON SPIEGEL, JIM POLONIS, EDWARD E. DEAN,
KAY ST. MARY, A. DWAIN SMITH
SOUTHWEST RESEARCH INSTITUTE
SAN ANTONIO, TEXAS

A preliminary study, sponsored by the Department of Energy (Contract No. ET-78-C-01-2875), is underway to develop and thoroughly test the experimental protocols and apparatus which are planned for a major study of the behavioral and biological effects of high intensity 60 Hz electric fields. The African baboon (Papio anubis and Papio cynocephalus) has been chosen as an animal model for the examination both of individual performance (operant conditioning) and natural (social) behavior. The behavior of baboons is being observed before, during, and after exposure to 60 Hz electric fields at a maximum intensity of 60 kV/m.

This paper is concerned with the exposure facility, the electric field measurement techniques and the individual performance tasks. There are three different tasks in this present study: a vigilance task, a matching-to-sample task, and a multiple operant schedule (fixed-ratio schedule and differential-reinforcement-for-low-response-rate schedule).

NAVIGATIONAL COMPASS IN MAGNETOTACTIC BACTERIA

R. B. Frankel, Francis Bitter National Magnet Laboratory*, MIT, Cambridge, MA 02139, R. P. Blakemore*, Department of Microbiology, University of New Hampshire, Durham, NH 03842 and Ad. J. Kalmijn and C. R. Denham, Woods Hole Oceanographic Institution†, Woods Hole, MA 02543.

Iron containing bacteria from diverse aquatic environments that orient and swim in a preferred direction in magnetic fields have been described by Blakemore [1]. Orientation of live and killed cells in the earth's magnetic field as well as orientation reversal induced by a strong (up to 600 G, 1.25 μ sec) magnetic pulse has been observed by Kalmijn and Blakemore [2], showing that the bacteria behave as magnetic dipole moments swimming in the direction of the north seeking pole. They hypothesize that these moments function as an internal compass for navigation. Frankel, Blakemore and Wolfe [3] used Mössbauer spectroscopy to show that iron-rich particles (50 nm) in a mass cultured, fresh-water, magnetotactic spirillum consist primarily of magnetite (Fe_3O_4). In this paper we will discuss the observation of Fe_3O_4 in terms of the compass hypothesis. In particular, we will show: a) magnetite particles of the observed size are in the single magnetic domain size range, larger than superparamagnetic particles and smaller than multidomain particles; b) a chain of closely spaced particles will orient with their individual moments along the chain direction and function as a single magnetic dipole; c) the total magnetic dipole moment of a single bacterium is sufficient to produce alignment in the earth's magnetic field at ambient temperature ($MH > kT$); d) the observed time required for orientation is approximated by a passive rotational mechanism; e) the applied field required for orientation reversal is consistent with the magnetocrystalline anisotropy of magnetite. These results are consistent with the hypothesis that magnetotactic bacteria are oriented by passive dipole alignment in the geomagnetic field.

* Supported by N. S. F.

† Projects supported by O. N. R. and N. S. F.

1. R. P. Blakemore, *Science* **190**, 377 (1975).
2. Ad. J. Kalmijn and R. P. Blakemore, in *Animal Migration Navigation and Homing*, K. Schmidt-Koenig and W. T. Keeton, eds., (Springer Verlag, New York 1978) p. 344.
3. R. B. Frankel, R. P. Blakemore and R. S. Wolfe, *Science* (to be published).

THRESHOLD VALUES FOR MAGNETO- AND ELECTROPHOSPHENES

- A COMPARATIVE STUDY.

P. Lövsund, P.Å. Öberg and S.E.G. Nilsson
Departments of Biomedical Engineering and Ophthalmology,
Linköping University, S-581 85 Linköping, Sweden.

It has been known for a long time that low frequency, transient magnetic fields and electric currents of moderate strengths generate visual phenomena called phosphenes. Several authors have studied the threshold values for electro- or magnetophosphenes. However, the two phenomena have never been compared under identical experimental conditions.

In this work we have compared the threshold value curves of the two different ways to induce phosphenes. The threshold values are determined at a luminance level on the eye of 3 cd/m^2 . We have used both broad spectrum light and light with the wavelength 572 nm as background illumination. At the two types of background illumination the two threshold curves are nearly identical up to a magnetic field frequency of about 20 Hz, but for higher frequencies they are diverging. The threshold curves for magnetophosphenes have a local sensitivity minimum at 30-35 Hz, which is missing in the electrophosphene curves. The preliminary results indicate that principal differences exist between an electric current and a magnetic field in the generation of phosphenes.

STUDIES OF MUTAGENIC EFFECTS OF MAGNETIC FIELDS IN BACTERIA

S. C. Causey and F. P. Hungate
Biology Department
Pacific Northwest Laboratory
Richland, WA 99352

Preliminary testing of the mutagenicity of magnetic fields, employing bacterial systems, suggests that slight increases in mutation frequency may occur following exposure. Field strengths used in these studies range from 0.1 to 1.1 Tesla (T). The most extensive data were obtained with Salmonella strain TA100 which mutates principally by base exchange. Statistical analysis shows an effect at the 95% confidence level. The data are insufficient to indicate any difference due to the level or duration of the dose. The TA98 strain, which mutates primarily by frameshift, failed to show an increase in mutation frequency.

Initial tests with E. coli have given data suggesting that increased frequencies of forward mutation to resistance to nalidixic acid and rifampicin occur following exposures in a 0.3 T field. Similar suggestive data were also obtained with B. subtilis 168 when tested for frequency of cells resistant to rifampicin and with Photobacterium fisheri, strain MAV, tested for resistance to tetracycline. In all tests, mutation frequencies of exposed cells were compared with simultaneously tested controls.

Work supported by the U. S. Department of Energy under contract EY-76-C-06-1830.

SHORT-TERM EXPOSURE OF RHESUS MONKEYS TO 20,000 GAUSS STEADY
MAGNETIC FIELD

Joseph H. Battocletti^{**}, Sergio Salles-Cunha⁺, Richard E. Halbach⁺,
Jedd Nelson⁺, Joel Mykelbust⁺, Anthony Sances, Jr.^{**}, and Fred J.
Antonich⁺

*Research Service, Veterans Administration Medical Center
Wood, Wisconsin

+Department of Neurosurgery, The Medical College of Wisconsin,
Milwaukee, Wisconsin

Tests Performed. Two adult Rhesus monkeys were exposed to a steady, relatively uniform, magnetic field of 20,000 gauss for a period of 48 hours. Blood hematology, chemistry, and gases were tested before, during, and twice after exposure. Somatosensory evoked potentials were taken from surgically implanted bilateral epidural cortical electrodes with leg or arm stimulus, both inside and outside the magnetic field. Blood pressure and heart rate were measured both inside and outside the magnetic field. It was not possible to take a meaningful ECG inside the magnetic field due to Faraday effects caused by fluid movement in the magnetic field. All measurements were made while the monkeys were sedated by ketamine hydrochloride (0.1 cc/kg).

The Magnet. The Rhesus monkeys were kept in cages made of plastic and non-ferrous metals, and placed inside the room-temperature bore of a superconducting magnet. The bore of the magnet is 63 cm I.D. and 185 cm long. The magnetic field is uniform, within 1%, over the central 69 cm length of the bore.

Results. Evoked potentials measured inside and outside the magnet were essentially the same. The latency of fast and slow waves from limb to brain was not changed by the magnetic field. The blood pressure tests show opposite results in the monkeys inside and outside the magnet. However, heart rate was lower inside the magnet. The noticeable changes in blood hematology and chemistry can be attributed to the trauma caused by the implantation of the cortical electrodes. Before exposure, white blood cell count (WBC) was high, Doehle bodies were observed in one monkey, and hypogranulation and vacuolization of PMN's (polymorpho nucleides) were noted in the other monkey. WBC decreased to normal levels during and after exposure. SGOT (transaminase) levels returned to normal 4 weeks following implantation. However, it took 10 weeks for LDH (lactic acid dehydrogenase) to return to normal. CPK (creatinine phosphokinase) levels were still elevated after 10 weeks following implantation.

Conclusion. From the tests which were performed, as described above, we conclude that there were no observable effects in the two monkeys. They are currently healthy and active, apparently unaffected by the 48-hour exposure to the 20,000 gauss magnetic field.

AN IMPROVED IMPLANTABLE ELECTRIC FIELD PROBE
FOR MICROWAVE DOSIMETRY

by H. Bassen*, K. Franke*, E. Aslan**, and S. Neuder*

*Food and Drug Administration, Bureau of Radiological
Health, Rockville, Maryland, U.S.A. 20857

**Narda Microwave Corporation, Plainview, New York 11803, USA

A miniaturized probe has been developed for microwave dosimetric measurements in phantom models and experimental animals. Its primary features are a small tip size (1 mm by 2 mm, including insulation) and optimized sensitivity, achieved through the use of a specially-selected Schottky diode whose parameters match those of the 1.5 mm-long dipole antenna. Extensive testing in free space and in muscle equivalent spheres yielded data which were compared with theoretically predicted responses. Because of the small tip size, excellent agreement with theoretically-predicted fields, was achieved in a highly repeatable manner at 915 and 2450 MHz. Three readings must be taken with this single axis device, at a point within a dielectric object or biological specimen, to obtain the total internal field strength at that site. These readings are obtained by rotating the probe in 120° increments around the axis of the handle. Rapid, continuous line scans can be made by driving the probe through phantoms, since the response time of the probe is less than 1 millisecond.

The probe's high sensitivity allows the measurement of internal field strengths of 9 to 80 V/m (SAR = 0.16 to 12.8 W/Kg) in muscle. Both CW and amplitude modulated fields can be measured. Probe sensitivity is limited by flexure noise in the high resistance lines at the low end of its range and diode non-linearity at the high end of its range (both of which could be compensated for, through additional steps). In free space, the probe's useful range is from approximately 10 microwatts per square centimeter to 5 milliwatts per square centimeter.

Present tests indicate that good accuracy should be achievable in muscle, brain, eye, and other high-water-content tissues. Preliminary in-vivo 2450 MHz measurements in mice testes were performed by Cairnie and associates of the Radiation Biology Section, Defence Research Establishment of Canada. Additional biological compatibility tests with various animals will be performed in the near future, by several groups.

A NONPERTURBING TEMPERATURE PROBE SYSTEM
DESIGNED FOR HYPERTHERMIA MONITORING

D. A. Christensen and R. J. Volz

Department of Bioengineering and Department of Electrical Engineering
University of Utah
Salt Lake City, Utah 84112

ABSTRACT

As electromagnetic energy becomes more and more utilized as the heating source for hyperthermia therapy trials, the need for accurate and convenient thermometry becomes more critical. We have developed a nonmetallic fiber-optic temperature probe with a semiconductor sensor at its tip for use in microwave and radio wave environments where metallic-bearing temperature probes may lead to large measurement errors. The sensor, fabricated from a small single crystal block of gallium arsenide, absorbs light whose narrow spectrum is near the band edge of the semiconductor. As the temperature of the sensor varies, the amount of light absorbed will vary. For the GaAs sensor, near infrared light at $\lambda = 907 \text{ nm}$ is used.

The probe consists of a bundle of 0.085-mm diameter glass fibers; some are used for transmission of the light from the LED and the remainder used for reception by a photodiode after passage through the sensor. In the tip region, the probe diameter is such that it is less than the outer diameter of a 25-gauge needle, facilitating implantation in tissue. A unique insertion set employing a Teflon sleeve has been designed to ease the implantation procedure. The range of the instrument is 15°-55°C, sufficient for practically all hyperthermia experiments.

The overall system is designed to support up to a total of six probes whose displays are integrated into a single package. An 8085 microprocessor board controls the linearization, display, and calibration of the system. Calibration of each probe is designed to be accomplished either by a built-in calibrator module under control of the microprocessor monitor, or by a single-point external temperature reference supplied by the user.

AN OPTICAL NON-PERTURBING PROBE FOR TEMPERATURE MEASUREMENTS
IN BIOLOGICAL MATERIALS EXPOSED TO MICROWAVE RADIATION

F. Cavatorta, P. E. Schoen, J. P. Sheridan
Naval Research Laboratory
Washington, D. C. 20375

In studies of the interaction of electromagnetic radiation (EM) with biological systems it is essential to monitor internal temperature by a method which neither distorts the EM field, nor is, itself, influenced by EM induced currents. Described here is a technique utilizing the temperature-dependent fluorescence of the R_1 line of ruby as a means of remotely monitoring temperature in very small biological samples. In this technique a small (<50 μm) fragment of ruby is juxtaposed to the biological sample and equilibrated in a thermostatted chamber, the temperature of which is controlled to $\pm 0.15^\circ\text{C}$. The frequency of the temperature-sensitive fluorescence maximum of R_1 line ($\sim 14402\text{ cm}^{-1}$ at room temperature) is measured at various temperatures with respect to a calibration line at 14414.06 cm^{-1} obtained from an argon lamp. For each temperature a minimum of three scans were digitally recorded at a resolution of 16 channels/ cm^{-1} . Scans were analyzed by a self-adjusting least squares fitting program in order to find the peak maximum positions. The temperature was established by taking the average of several thermocouple measurements during the course of the fluorescence scans. A plot of fluorescence frequency vs. temperature yields a straight line with a slope of $0.141\text{ cm}^{-1}/\text{deg}$ and a standard deviation of ± 0.0005 . The precision afforded by this method is $\pm 0.21^\circ$. Subsequent Raman/fluorescence runs were conducted in the presence of microwave fields of varying strength (freq = 2.4 GHz) and no perturbations were found of the fields or of the temperature calibration curve.

COMMERCIAL MICROWAVE HAZARD METERS: A LABORATORY EVALUATION

By William A. Herman and Donald M. Witters, Jr.
Bureau of Radiological Health, FDA

A test protocol has been devised to evaluate the performance of selected commercially available microwave hazard meters used in determining compliance with standards and for laboratory measurements. The protocol was designed to yield a comprehensive analysis of instrument errors associated with the more significant environmental variables and source characteristics, as well as with the instrument design and production tolerances. Among the parameters considered were calibration accuracy, response linearity, frequency response, polarization ellipticity, temperature response, near-field characteristics, RFI susceptibility, response to amplitude-modulated fields, probe receiving pattern, drift, response time, and sensitivity to changes in battery supply voltage.

Using five different laboratory test systems, procedures have been developed to evaluate the effect of each parameter. The uncertainty of each test has been analyzed.

The procedures of the test protocol have been employed in the evaluation of selected commercial hazard meters in current use. Error values for each parameter have been computed for each instrument, and a composite error has been calculated. Techniques for assessing composite uncertainties in special measurement situations have been outlined.

A HIGH-SENSITIVITY, ULTRA-BROADBAND RADIATION PROBE

S. Hopper and Z. Adler
General Microwave Corporation
Farmingdale, New York 11735

Abstract

The design, construction, and performance of an isotropic radiation probe with full-scale sensitivities ranging from $10\mu\text{W}/\text{cm}^2$ to $10\text{mW}/\text{cm}^2$ and covering the frequency range from 10 MHz to 20 GHz will be described.

DOSIMETRIC USE OF SCHOTTKY DIODES

by William A. Herman
Bureau of Radiological Health, FDA

The use of electric and magnetic field probes for dosimetric measurements has relied heavily on the use of microwave diodes. In this paper the performance of such diodes is examined at length with particular emphasis on Schottky barrier or hot-carrier diodes.

The basic characteristics of diodes in these applications are examined including physical mechanisms and equivalent microwave circuits. Analytic expressions are developed that illuminate the existence of linear, square-law, and other regions of operation. The effects of load-resistance, bias-current, and temperature are explored.

The analysis is employed in the evaluation of one E-field probe model which has been designed and used for dosimetric purposes. For this probe-type, measurement and theory are compared. Practical limitations on such probes are discussed, and means of selecting diode-parameters for maximum probe performance are presented.

POWER DENSITY FLUX MEASUREMENTS

Tadeusz M. Babij, Hubert Trzaska
Institute of Telecommunications and Acoustics
Technical University of Wrocław
Wyb. Stanisława Wyspińskiego 27
50-370 Wrocław, Poland

The measurement of E and H fields and power density flux (PDF) is important from the point of view maintaining safe labor conditions for the people working in the vicinity of the EM field sources, and environmental conditions for the general population, people's houses, hospitals, etc. Since these measurements are usually done in the vicinity of the radiation source in the zone of induction fields and multipath propagation, meters equipped with resonant size antennas, having directional radiation patterns can not be used. Thus, PDF measurements in the induction zone are based upon the use of electrically small antennas. In this work we discuss the accuracy of the determination of PDF based on E or H field strength measurements, PDF measurements with the use of a non-screened loop antenna sensitive to the E field, value of the arithmetical mean of the power densities based on electric and magnetic field measurements, and as a conclusion the authors proposal in using the geometrical mean of these power densities since this gives maximal accuracy of measurements.

The problem of interaction of an arbitrary mode field and measuring probe is discussed and it is concluded that from the point of view of accuracy the simplest antennas should be used.

CONSIDERATIONS AND CRITERIA FOR A RECOMMENDED STANDARD FOR
OCCUPATIONAL EXPOSURE TO RADIOFREQUENCY AND MICROWAVE FIELDS

Richard F. Boggs, Ph.D. and Zorach R. Glaser, Ph.D.

National Institute for Occupational Safety and Health
5600 Fishers Lane
Rockville, Maryland 20857

and

Robert F. Cleveland, Ph.D. and Joseph K. Kielman, Ph.D.

Equitable Environmental Health, Inc.
6000 Executive Boulevard
Rockville, Maryland 20852

In May 1978, NIOSH initiated the development of a criteria document and recommended standard for occupational exposure to radiofrequency (RF) and microwave fields to protect workers from these radiations. The document is scheduled for completion by August 1979. The criteria and recommendations are based upon many factors including NIOSH research and field studies prior to initiation of the formal document effort, an extensive review of world literature on the subject, communications with industry, organized labor, trade associations, professional societies and academia, and extensive internal and external review by individuals selected for their expertise in particular aspects dealt with in the document. In addition, these criteria and recommendations consider information obtained from visits to industrial, communication and military facilities where RF and microwave radiation is routinely encountered.

The recommendations are based upon a critical evaluation of the biological effects and epidemiological data (or, at times, lack thereof) and consideration of commercially available instrumentation and monitoring techniques. The recommended standard is proposed to apply to all workers exposed or potentially exposed to RF/microwave fields of frequencies between 500 kilohertz and 300 gigahertz.

While there is a lack of complete agreement in the literature on the causal relationship between exposure to RF/microwave energy and certain biological effects associated with such exposures, sufficient animal studies, human case reports, and epidemiological studies do exist to permit the recommendation of an occupational exposure limit that is expected to provide increased protection for the American worker. In addition, recommendations will be made with regard to appropriate monitoring instrumentation and procedures, medical surveillance, work practices, engineering controls, record-keeping, and procedures for informing employees of potential hazards of exposure to RF/microwave energy. The document will also outline research needed to enable the development of an improved recommended standard, and will discuss the compatibility of the recommendations with existing standards and guidelines.

DEVELOPMENT OF OCCUPATIONAL EXPOSURE RECOMMENDATIONS:
OBSERVATIONS ON THE USES OF RF/MICROWAVE ENERGY

Zorach R. Glaser, Robert F. Cleveland,
Joseph K. Kielman, and Richard F. Boggs
National Institute for Occupational Safety and Health
Rockville, Maryland
and
Equitable Environmental Health, Inc.
Rockville, Maryland

As a major part of the development of a criteria document to include a recommended occupational exposure standard for worker protection from radio frequency (RF) and microwave fields, NIOSH has attempted to gather information on the uses of RF/microwave energy. The objective was to collect facts and data on workplace practices and engineering controls involved in the production and/or use of microwave energy, and to obtain information on recognized biological effects. The scope was limited to information relevant to the production and/or use of RF/microwave energy in the frequency range from 0.5 MHz to 300 GHz; any incidental information to be collected only when and where it aids comprehension of the data; current state-of-the-art to be emphasized.

More than 300 contact letters were mailed in July 1978 to manufacturers of RF/microwave equipment, and to potential Federal and industrial users of RF/microwave energy. Letters were also sent to trade associations, professional societies, and to selected labor unions. The letters included the October 28, 1977, FR notice (42 FR 56799), and were of two types: one for manufacturers and potential users of RF/microwave energy and equipment, the other for trade associations, professional societies, and labor unions. Both types of letters announced NIOSH's plans to develop a criteria document containing a recommendation for an occupational exposure standard for RF/microwave energy, and requested from the facility or organization receiving the letter information on: bioeffects studies, engineering controls, medical/biological devices, measurement techniques and equipment for monitoring of RF/microwave fields, work practices, recordkeeping, warning devices.

A detailed description of the types of responses received, and a tabular presentation of the outcome of the responses (i.e., plant site visit, etc.) will be discussed.

Visits were made to several plants and facilities where RF/microwave energy is used. On some of these visits measurements of electromagnetic fields were made and photographs were taken. Representative slides and results of these site visits will be presented.

MEASURED MODULATION WAVEFORM OF LEAKAGE RADIATION FROM MICROWAVE OVENS

Henry S. Ho and William P. Edwards, U.S. Department of Health, Education and Welfare, Public Health Service, Food and Drug Administration, Bureau of Radiological Health, 5600 Fishers Lane, Rockville, Maryland 20857, USA.

Recent reports of biological effects indicate amplitude modulation of microwave radiation as a parameter of interest. The leakage radiation from microwave ovens is known to be low-frequency amplitude-modulated because of the effect of the mode-stirrer built into the ovens.

In the present investigation, amplitude-modulated waveforms of leakage radiation from a 2450 MHz and a 915 MHz microwave oven was measured by the use of a miniature 3-D probe which utilized microwave-diode detector chips. The frequency spectra of the resultant detected modulation envelopes were also analyzed.

The results indicated that the amplitude-modulated envelopes of both the 2450 MHz and the 915 MHz radiation had large fluctuations. These leakage radiation waveforms were essentially 100% modulated. The frequency spectrum of the detected amplitude-modulation envelope of the 915 MHz oven leakage radiation contained components which were primarily within the range of 0 to 100 Hz. The frequency components with relatively high amplitudes were concentrated within the 0 to 10 Hz range, with 1 and 3 Hz components having the highest amplitude. The detected amplitude-modulation envelope of the 2450 MHz oven leakage radiation had a frequency spectrum that contained components between 0 and 500 Hz. The frequency components of 60 Hz (and its higher harmonics) and 4 Hz (and its higher harmonics) dominated this spectrum. These two modulation spectra contained frequencies that are within the range where biological effects of modulated RF radiation have been reported (3 to 30 Hz).

MICROWAVE-INDUCED PRESSURE WAVES IN A MODEL
OF BIOLOGICAL TISSUE

Richard G. Olsen and Wayne C. Hammer
Naval Aerospace Medical Research Laboratory
Naval Air Station
Pensacola, Florida 32508

ABSTRACT

Microwave-induced pressure waves were studied in simulated muscle tissue consisting of water, salt, gelling agent, and polyethylene powder. Pulsed microwave energy at 5.62 GHz was obtained from a type AN/SPS-5D radar transmitter, and the induced elastic waves were recorded using hydrophones. Measurements were made in a 15 kg rectangular model contained in a low-density, foamed polystyrene box. The model was subjected to near-field, horn irradiation of half-microsecond pulses, each pulse having a peak incident power density calculated to be about 1 kW/cm^2 . Comparison tests of irradiated saline solutions were performed as were tests using a hydrophone ultrasonic source.

Initial results of this study showed the existence of microwave-induced pressure waves which propagated in the phantom material at a velocity of approximately 1460 meters per second, somewhat slower than similar waves observed in saline. Wave attenuation was greater in the tissue-equivalent material than in the saline; nevertheless, a single pulse that traversed the length of the model and then reflected from the back surface was still visible after a total propagation of 45 cm. These results suggest that microwave-induced elastic waves in biological tissues could exhibit the properties of focusing and of resonance under certain conditions of curvature, boundaries, propagation velocity, and pulse repetition rate.

ELECTROMAGNETIC EXPOSURE EFFECTS
ON THE VISUAL SYSTEM OF A FLYING INSECT

Sheldon S. Sandler and William Peros
Departments of Electrical Engineering and Biology
Northeastern University
Boston, Mass 02115

The pursuit responses of houseflies have been investigated by many authors (Srinivasan and Bernard J. *Comp. Physiol.* 115, 101-117 (1977), Reichardt, *Naturwissenschaften* 60, 122-138 (1973)). In the present work, houseflies were secured to a fixed tether which was connected to a device which measured the torque responses of the fly. The fly was connected to a lever arm on which a silicon strain gauge was glued. Stimulus was provided by a pendulum which moved in front of the fly. The flies tracked the pendulum and his torque response was detected by a strain gauge bridge which was connected to a paper chart recorder. The motion of the pendulum was also recorded.

A series of control tests were made to be certain of the fact that the flies do indeed track the moving target. Next, a series of tests were performed on the flies when they were exposed to 1000MHz fields in a coaxial exposure chamber. Initial results showed that the tracking behavior was being affected in the flies at exposures 150 mw/cm^2 for five minutes. These measurements were made on different flies, since metal clips were used. In the present series of measurements, plastic clips are used which allow us to use the same fly for both exposure and control tests. Limits on the minimum radiation level for affecting the visual tracking behavior of the flies is also being established.

RADIATION OF OPEN WAVEGUIDES
APPLICATION TO BIOMEDICAL PROBES

J. Audet, J.Ch. Bolomey, Ch. Pichot
Laboratoire des Signaux et Systemes
Groupe d'Electromagnetisme
C.N.R.S. - E.S.E.
91190 GIF-sur-YVETTE
France

Practical problems of radiation by open waveguides used in biological applications have been modeled by discontinuity of two rectangular waveguides and by a flanged plane waveguide.

We show that accurate results on the reflection coefficient of the principal mode and field distribution in the waveguide aperture can be deduced from the simple Fresnel reflection law.

A CORRUGATED WAVEGUIDE APPLICATOR

Q. Balzano and O. Garay, Motorola, Inc.
C. H. Sutton, U. of Miami School of Medicine

The paper describes the design and the construction of a corrugated waveguide applicator. Corrugated waveguides, propagating the HE_{11} balanced mode, are known to give E and H patterns of same beam width and very low side lobes. These features make corrugated waveguides attractive for applicator use, because they produce axially symmetric heating patterns and relatively low leakage.

The applicator presented in this paper is an alumina-loaded corrugated waveguide of 1.25 inch radiating aperture. The waveguide is constructed by alternating alumina disks of two different diameters: 1.25 inch and 2.1 inch. The disks are rimmed by metal rings of 2.3 inch OD.

The waveguide is fed by a cavity of 3 inch ID, which is partially loaded with teflon. The cavity is excited by a monopole of variable depth, which can be positioned along the axis of the cavity. The back plate of the cavity can be moved like a piston. By selecting the proper monopole length and location and by correctly positioning the back plate, it is possible to match the radiating aperture for maximum transfer of power into a biological target at any distance from the applicator.

The applicator is currently being used at the University of Miami School of Medicine for Blood Brain Barrier disruption, cerebral blood flow tests and tumor hyperthermia in mouse and rat models.

SAR measurements have shown that the applicator deposits an average of 17 mW/gr/W in rat brain tissue placed at 2 cm distance from the radiating aperture. The maximum measurement leakage at 5 cm distance in direct contact application is approximately 1 mW/cm² for 100W incident power.

MEASURED INTERNAL ELECTRIC FIELD IN PHANTOM HUMAN HEADS EXPOSED
TO LEAKAGE RADIATION FROM MICROWAVE OVENS

Henry S. Ho, William P. Edwards, and Howard Bassen, U.S.
Department of Health, Education and Welfare, Public Health
Service, Food and Drug Administration, Bureau of Radiological
Health, 5600 Fishers Lane, Rockville, Maryland 20857, USA.

Information on energy absorption induced in human bodies exposed to actual microwave sources is needed to assess health hazards through a comparison with animal biological effects data using the common denominator of local absorbed energy. The existing absorption data based on whole body exposure to plane waves cannot be readily applied to the case of exposure in the near field of sources such as microwave ovens.

In the present investigation, the internal electric field distributions of phantom human heads were measured, and the data were converted to equivalent dose rate. The sources of exposure were leaking 2450 MHz and 915 MHz microwave ovens. The phantom human heads were made of actual skulls of an adult and a child, and were filled with dielectric materials equivalent in electrical properties to that of muscle or brain. A miniature 3-D probe was used to detect the internal electric field in the phantom tissues. The ovens were made to emit 2 to 20 mW/cm^2 leakage radiation measured 5 cm from the oven surface by the use of teflon strips inserted between the door seals. The phantom heads were located as close to the oven door as possible with the maximum leakage field near the left eye which was 3 cm from the oven door. The 3-D probe was scanned along a straight path normal to the oven door surface, from the back of the phantom head to the surface of the left eye.

The results indicated that for a leakage of 5 mW/cm^2 as measured 5 cm from the surface of the 2450 MHz microwave oven, the maximum equivalent dose rate was 9.6 W/kg in the adult phantom head and 14.6 W/kg in the child phantom head. The positions of the maximum dose rates were 0.5 cm interior to the eye for the child phantom head, and at the surface of the eye for the adult phantom head. Some penetration of the microwave energy into the cavity filled with brain equivalent material in the child phantom head was evident. The peak value in the brain equivalent material was 20% of the maximum absorption in the eye. For a leakage radiation of 5 mW/cm^2 from the 915 MHz oven, the maximum equivalent dose rate was 3.0 W/kg in the adult phantom head and 5.3 W/kg in the child phantom head. The positions for these maxima were both 3 cm from the surface of the eye. Penetration of the radiation into the phantom brain region was found for both phantom heads. The peak absorption in the phantom brain region was 50% of the maximum eye absorption in both phantom heads.

AUTHOR INDEX

AARONS J.	270	BAKER K.D.	272
AARONS J.	276	BALANIS C.A.	200
ABULKASSEM A.S.	65	BALLARD K.A.	282
ACHMADIEVA A.C.	342	BALMAIN K.G.	47
ACKERMAN S.N.	394	BALMAIN K.G.	54
ADAIR E.R.	331	BALMAIN K.G.	55
ADEY W.R.	300	BALSLEY B.B.	170
ADEY W.R.	310	BALSLEY B.B.	171
ADEY W.R.	482	BALSLEY B.V.	169
ADLER Z.	493	BALTES H.P.	118
AGRAWAL A.K.	81	BALZANO Q.	502
AGRAWAL B.S.	277	BALZANO Q.	370
AHMED A.	478	BALZANO Q.	422
AHN H.	52	BANVARD R.A.	451
AKOEV I.G.	325	BANVARD R.A.	452
AKOEV I.G.	334	BARBER P.W.	129
AKOEV I.G.	342	BARBER P.W.	357
AL HAFID H.T.	430	BARBER P.W.	359
AL-HAFID H.T.	256	BARNES F.S.	299
ALBERT E.N.	335	BARNES F.S.	300
ALBERT E.N.	368	BARSUN H.F.	484
ALBERT E.N.	379	BASILI P.	171
ALBERTSEN N. CHR.	91	BASSEN H.	489
ALEKSEEV S.I.	581	BASSEN H.	501
ALEXOPOULOS N.G.	50	BATKIN S.	437
ALEXOPOULOS N.G.	113	BATTOCLETTI J.H.	488
ALI S.M.	189	BAUM C.E.	316
ALLEN S.J.	348	BAWIN S.M.	482
ALPEN E.L.	325	BAXTER R.A.	175
ALPERS W.R.	244	BEARD C.I.	208
ANDERSEN J.B.	118	BECKMANN G.M.	1
ANDRIENKO L.G.	341	BELDEN L.H.	358
ANTONICH F.J.	489	BELL B.	474
APEL J.R.	236	BELONJZHKO N.G.	386
APPEL-HANSEN J.	226	BENANE S.G.	301
ARMSTRONG J.W.	42	BENNETT C.L.	120
ARNOLD H.W.	216	BERGERON J.A.	358
ARNOLD H.W.	293	BERGMANN J.H.	214
ASLAN E.	489	BERMAN E.	397
ASSAL H.	246	BERMAN E.	406
ASSENHEIM H.M.	356	BESIERIS I.M.	67
ATHEY T.W.	375	BESIERIS I.M.	76
ATHEY T.W.	385	BESIERIS I.M.	316
ATHEY T.W.	458	BEVENSEE R.M.	97
AUDEH N.F.	88	BEYER J.B.	197
AUDET J.	501	BEZDOLNAYA I.S.	382
BABIJ T.M.	495	BIELEC M.	436
BAHAR E.	39	BIGGS A.W.	114
BAHAR E.	277	BIRENBAUM L.	466
BAIRD R.	325	BIRENBAUM L.	467

ISHOP R.	448	CARCHMAN R.	435
LACKMAN C.F.	309	CARLILE R.N.	289
LAKEMORE R.P.	485	CARLSON F.P.	157
LOCH S.C.	215	CARROLL F.B.	370
LOK T.I.S.	279	CARROLL F.B.	423
DERNER W.M.	166	CARSTENSEN E.	481
DERNER W.M.	210	CARTER D.A.	169
DERNER W.M.	266	CARTER D.A.	171
DGGS R.F.	496	CARTER H.B.	406
DGGS R.F.	497	CARVER K.R.	212
OJSEN J.	472	CASEY K.	100
OLLIG G.	118	CASEY K.F.	123
OLOMEY J. CH.	112	CASTILLO J.P.	125
OLOMEY J.CH.	501	CASTILLO J.P.	316
OOK P.S.	316	CAUSEY S.C.	487
OOKER H.G.	280	CAUTERMAN M.	192
ORGIOTTI G.V.	118	CAVALLI A.	289
OSTIAN C.W.	222	CAVATORTA F.	469
OWMAN R.R.	376	CAVATORTA F.	491
RAGG D.G.	421	CETAS T.C.	420
REMMER H.	11	CHANDLER A.S.	260
RENT R.L.	403	CHANDON J.H.	395
RISTOL T.W.	140	CHANG D.C.	65
RITTINGHAM J.N.	126	CHANG D.C.	68
RONAUGH E.	484	CHANG D.C.	83
ROWN G.J.	154	CHANG D.C.	99
ROWN G.S.	73	CHANG D.C.	103
ROWN S.	418	CHANG N.J.	108
ROWN W.D.	155	CHANG S.K.	67
ROWN W.P.	110	CHANG S.K.	87
RSSON J.C.E.	15	CHATTERJEE I.	350
RUCKNER A.P.	78	CHATTERJEE R.	109
RUEE-WOLFE V.	323	CHAUDHURI S.K.	66
RUGNOLUJTI P.L.	471	CHEN H.C.	287
UNI K.	256	CHEN H.C.H.	129
URDETTE E.C.	374	CHEN K.C.	316
URGESS B.S.	416	CHEN K.M.	352
URKE G.J.	48	CHEN K.M.	424
URKE G.J.	126	CHEN K.M.	425
URR J.G.	349	CHEN M.F.	235
URSIAN S.J.	397	CHEN T.A.	392
URTON R.W.	19	CHERNOVETZ M.E.	407
USH L.G.	464	CHEVNY V.V.	119
UTLER C.M.	107	CHEUNG A.Y.	419
UTLER C.M.	111	CHEUNG R.L.-T.	255
UTLER C.M.	118	CHO S.H.	229
UTLER C.M.	120	CHOU C.K.	352
UTLER C.M.	121	CHOU C.K.	420
YRNE H.M.	237	CHOU C.K.	433
YSTROM B.	482	CHOU C.K.	457
AHN C.R.	135	CHOW Y.L.	60
AIN C.A.	466	CHRISTENSEN D.A.	414
AIN F.L.	374	CHRISTENSEN D.A.	490
AIRNIE A.B.	440	CHRISTOPHER P.F.	113

CHU C.M.	40	DEB G.K.	10
CHU R.S.	51	DEFFENBAUGH D.M.	35
CHU T.S.	254	DEGAUQUE P.	19
CHUANG C.A.	118	DENHAM C.R.	48
CIOTTI P.	177	DEPAOLA D.	43
CLEARY S.F.	443	DESCHAMPS G.A.	13
CLEVELAND R.F.	496	DESIEYES D.	41
CLEVELAND R.F.	497	DEVASIRVATHAM D.M.J.	17
COEN S.	188	DEWOLF D.	3
COLE J.	266	DINGER R.J.	15
COLES W.A.	176	DINGER R.J.	16
COLVIN D.P.	416	DISHAL M.	11
COMPTON K.L.	471	DOE G.J.	18
CONOVER D.L.	377	DOSS J.D.	41
CONOVER D.L.	402	DOUPLE E.B.	41
CONSORTINI A.	44	DRIESSEN P.F.	3
CONSORTINI, A.	45	DRUPP J.H.	34
COOK R.B.	320	DUBROFF R.E.	26
COOPER G.R.	136	DUDLEY D.G.	1
COREY L.C.	113	DUDLEY D.G.	13
COX D.C.	213	DUDLEY, D.G.	1
COX D.C.	216	DUFFEY J.R.	46
COX D.C.	253	DUMANSKY Y.D.	34
CRAIN G.	113	DUMANSKY Y.D.	38
CRAMER P.	90	DUNDORE D.	38
CRAMER P.	92	DUNDORE D.	41
CRAMER W.L.	289	DUNHAM M.E.	28
CRANE R.K.	172	DURNEY C.H.	34
CRANE R.K.	251	DURNEY C.H.	35
CRAWFORD F.W.	283	DURNEY C.H.	35
CRAWFORD F.W.	286	DURNEY C.H.	36
CRAWFORD F.W.	290	DURNEY C.H.	36
CRAWFORD F.W.	298	DURNEY C.H.	41
CREIGHTON M.O.	441	DURNEY C.H.	42
CROISANT W.J.	321	DYBDAL R.B.	11
CROSS A.E.	185	ECKLUND W.L.	16
CUPTA S.C.	112	ECKLUND W.L.	17
DA SILVA M.T. MARTINS	25	EDWARDS J.D.	44
DANIELE V.	52	EDWARDS W.P.	49
DANIELE V.	124	EDWARDS W.P.	50
DARDANONI L.	462	EINZIGER P.	3
DAVIDOW S.	460	EKELMAN E.P. JR.	11
DAVIDOW S.	461	EKSTROM E.	40
DAVIDSON D.	215	EL HABIBY S.	11
DAVIDSON D.	221	ELDER J.A.	30
DAVIS C.C.	431	ELDER J.A.	34
DAVIS C.C.	459	ELDER S.T.	44
DAVIS F.	392	ELLIOTT R.W.	41
DAVIS J.R.	163	EMERY A.F.	38
DAVIS W.A.	104	EMERY A.F.	41
DE LORGE J.D.	449	ENANDER B.	38
DE LORGE J.D.	481	END D.	43
DE WOLF D.A.	12	ENGLISH W.J.	11
DEAN E.E.	484	EDM H.J.	20

RSDY L.	120	FURUTSU K.	74
SPOSITO P.B.	284	GABER B.P.	469
TTIENNE E.M.	442	GABER B.P.	469
VTUSHENKO G.I.	383	GABILLARD R.	192
ZELL C.S.	449	GAFFEY C.T.	343
ANTE R.L.	10	GAGE K.S.	173
ANTE R.L.	120	GAGE M.I.	445
ANTE R.L.	153	GALINDO-ISRAEL V.	63
ARNHAM W.	426	GALINDO-ISRAEL V.	90
AULK J.M.	309	GALVAD B.S.M.C.	120
AY W.J.	279	GANDHI D.P.	350
EDOR L.S.	238	GANDHI D.P.	385
EDORS J.C.	232	GANDHI D.P.	427
ELDMAN A.	417	GANDHI D.P.	453
ELDSTONE C.S.	484	GANDHI D.P.	464
ELSEN L.B.	2	GANDHI U.P.	465
ELSEN L.B.	29	GARAY O.	502
ELSEN L.B.	35	GARDIOL F.E.	15
ELSEN L.B.	228	GAVRILIUK B.K.	384
ELSEN L.G.	9	GHADEHARIAN H.	210
ERGUSON J.A.	280	GHOBRIAL S.I.	112
ISHER A.D.	234	GLASER Z.R.	393
ISHER P.	428	GLASER Z.R.	496
ITZMAURICE M.A.	433	GLASER Z.R.	497
OLEY E.D.	377	GODDARD W.R.	166
OLEY E.D.	402	GODDARD W.R.	266
OLKER M.	367	GODFREY V.W.A.	325
ONTAINE A.	473	GOLDHIRSH J.	217
OSTER K.R.	372	GOLDSTEIN J.A.	153
OSTER K.R.	373	GOLDSTEIN J.A.	163
OWLES H.M.	81	GONCHAR N.M.	380
RACASSA M.	470	GONZALEZ F.I.	245
RANCESCHETTI G.	313	GUODHART C.L.	229
RANCOSIS R.E.JR.	157	GUODWIN H.A.	316
RANKE K.	489	GOWER J.F.R.	245
RANKEL R.B.	442	GRADY J.P.	113
RANKEL R.B.	485	GRANT G.A.	355
RAZER J.W.	438	GREVING G.	112
REEMAN D.F.	150	GRINER T.A.	355
RELICH R.	176	GROVE A.M.	454
REMOUW E.J.	258	GRUENAU S.P.	367
REMOUW E.J.	269	GUPTA S.C.	256
REMOUW E.J.	273	GUPTA S.C.	430
REMOUW E.J.	275	GUY A.W.	4
REY A.H.	455	GUY A.W.	325
REY A.H.	456	GUY A.W.	362
RIEND A.W.	372	GUY A.W.	399
ROST J.K.	416	GUY A.W.	410
UKUNISHI H.	164	GUY A.W.	412
UKUZAWA K.	112	GUY A.W.	426
ULLER J.A.	16	GUY A.W.	433
UNG A.K.	184	GUY A.W.	446
UNG A.K.	204	HAGDAD H.A.	83
UNG A.K.	235	HAGEN J.B.	259

HAGMANN M.J.	350	HOOKE W.M.	291
HAGMANN M.J.	359	HOPFER S.	493
HAGMANN M.J.	463	HOUSE D.	406
HALBACH R.E.	488	HOUSE D.E.	309
HALL B.	473	HOWARD A.Q.JR.	84
HALL D.H.	266	HOWELL N.A.	120
HAMMER W.C.	499	HOWELL N.A.	120
HAMRICK P.E.	401	HRYCAK P.D.	419
HAN C.K.	351	HSU S.V.	108
HANFLING J.D.	118	HU C.J.	304
HANSEN P.M.	154	HUANG A.T.	476
HANSEN P.M.	278	HUCHITAL G.S.	192
HANSER P.L.	402	HUEY D.L.	474
HARDING R.K.	440	HUNG E.L.	361
HARGER R.O.	242	HUNGATE F.P.	487
HARRINGTON D.B.	392	HURD R.A.	60
HARRINGTON R.F.	58	ILLIGER K.H.	385
HARRINGTON R.F.	232	ILLINGER K.H.	467
HARRISON G.H.	419	INADA H.	24
HARRISON M.G.	118	INGLIS G.B.	481
HARRISON W.H.	415	INOUE S.	470
HARTSGROVE G.W.	356	IPPOLITO L.J.	223
HAYRE H.S.	257	IRWIN L.M.	365
HAYWARD R.A.	64	ISHIMARU A.	1
HELMS W.J.	260	ISHIMARU A.	12
HENDERSON L.W.	113	ISHIMARU A.	46
HERMAN W.A.	492	ISHIMARU A.	78
HERMAN W.A.	494	ISHIMARU A.	203
HESSER A.	52	ISHIMARU A.	255
HILL D.A.	17	ISKANDER J.F.	348
HILL D.A.	197	ISKANDER J.F.	414
HILL D.A.	356	ISKANDER M.F.	198
HILL D.J.	463	ISKANDER M.F.	351
HILL D.W.	464	ISKANDER M.F.	357
HILL D.W.	465	ISKANDER M.F.	421
HILLAIRE F.	112	IWASAKI H.	113
HILTON D.I.	344	JACOBSEN G.	35
HILTUN D.I.	395	JAGGARD D.L.	105
HINDERKS L.W.	18	JAGGARD D.L.	198
HJERFSEN D.L.	483	JANIAC M.	390
HO D.Y.	49	JEDLICKA R.P.	211
HO H.	478	JENSH R.P.	403
HO H.S.	498	JOHNSON J.W.	186
HO H.S.	503	JOHNSON J.W.	243
HOCKHAM G.A.	112	JOHNSON R.B.	395
HODGE D.R.	175	JOHNSON R.B.	446
HODGES G.R.	369	JOHNSON W.A.	130
HOENDEKS B.J.	118	JOHNSTON P.E.	171
HOENIG P.A.	442	JOINES W.T.	391
HOFFMAN H.H.	216	JONES R.C.	420
HOLLAND-MORITZ E.K.	138	JONES W.L.	185
HOLLINGER J.P.	231	JONES W.L.	232
HOLYAVKO E.R.	341	JONES W.L.	243
HOOGASIAN H.	279	JORDAN A.K.	183

OY E.B.	113	KUESTER E.F.	99
ULL E.V.	31	KUMAZAWA H.	113
USTESEN D.R.	326	KUZNETSOV V.I.	334
USTESEN D.R.	328	LAGO B.	239
USTESEN D.R.	369	LAMPE J.A.	309
USTESEN D.R.	407	LANDIS L.G.Z.	118
USTESEN D.R.	454	LANDSTORFER F.M.	113
ACZMAREK L.K.	302	LANDT J.A.	315
AHN W.K.	53	LANG R.I.	183
ALMIJN A.J.	301	LANG R.H.	201
ALMIJN AD.J.	485	LANG R.H.	202
ANDA M.	314	LANGENBERG K.J.	119
ANTOR G.	411	LANSINGER J.M.	275
AO H.	61	LANTAGNE R.E.	113
APLAN L.	118	LARSEN L.E.	429
APLAN R.B.	104	LARSON G.	388
ARIJULLAH K.	352	LARY J.M.	377
ASSAM S.A.	152	LARY J.M.	402
AWAKAMI H.	112	LATIES V.G.	481
ELLER W.C.	181	LE VINE D.M.	162
ELLER W.C.	185	LEACH W.	478
ELLER W.C.	240	LEBDA N.	330
ELLEY M.	272	LEBOVITZ R.M.	366
ELSD J.M.	156	LEBOVITZ R.M.	447
ENNEDY A.	473	LECK R.P.	216
HEIRALLAH H.N.	248	LECK R.P.	253
IELMAN J.K.	496	LEE C.Q.	317
IELMAN J.K.	497	LEE J.H.	425
IM C.D.	191	LEE K.S.H.	132
IM J.S.	161	LEE R.A.	463
IM Y.C.	292	LEE R.W.	174
IM Y.C.	318	LEE S.W.	92
IM Y.S.	184	LEE S.W.	112
ING H.E.	113	LEE S.W.	133
ING R.J.	191	LEE Y.M.	26
ING R.J.	224	LEHMANN J.F.	389
ING R.J.	226	LEHMANN J.F.	410
INN J.B.	397	LEHMANN J.F.	412
INN J.B.	427	LEHMANN J.F.	413
INN J.B.	471	LEHMANN J.F.	426
INEPP D.L.	272	LEISE J.A.	238
INEPP D.L.	274	LENER R.M.	231
NOTT E.F.	120	LESSELIER D.	112
OHLER W.	71	LESSELIER D.	116
OLOBUB F.A.	383	LEVIATAN Y.	119
OLOMITKIN O.V.	334	LEVINE J.S.	290
OLTUN D.M.	374	LEVINSON D.M.	454
ONG J.A.	205	LEVIS C.A.	43
ONG J.A.	206	LEWIS J.Y.	474
ORNIEWICZ H.R.	379	LIBURDY R.P.	470
OUYOUMJIAN R.G.	28	LIBURDY R.P.	480
RAMAR P.	408	LIDDLE C.G.	397
RAVTSOV Y.A.	262	LIDDLE C.G.	474
ROP B.A.	458	LIEB R.	435

LIEPA V.V.	32	MCDUGALL J.A.	426
LIN J.C.	364	MCFARLAND J.L.	113
LIN J.C.	371	MCGAHAN R.V.	153
LIN J.C.	405	MCGRATH P.W.	413
LIN J.C.	470	MCHUGH T.	403
LIN J.C.	475	MCLAUGHLIN D.W.	296
LIN M.F.	364	MCLERRAN C.	438
LIN S.H.	214	MCREE D.I.	325
LIU C.H.	271	MCREE D.I.	336
LONG S.A.	98	MCREE D.I.	401
LORDS J.L.	365	MCREE D. I.	404
LOSS A.P.	341	MEI K.	188
LOSS I.P.	382	MEI K.K.	61
LOTZ W.G.	346	MELES D.	455
LOVELY R.H.	333	MELLECKER C.	160
LOVELY R.H.	399	MELNICK R.	460
LOVELY R.H.	446	MELNICK R.	461
LOVSUND P.	339	MENDELOVICZ A.	120
LOVSUND P.	486	MENEGHINI R.	162
LU S.T.	327	MERRITT J.H.	338
LU S.T.	329	MEYERS W.D.	158
LU S.T.	330	MEYERS W.D.	163
LU S.T.	332	MICHAELSON S.M.	327
LU S.T.	345	MICHAELSON S.M.	329
LUDLOW J.	403	MICHAELSON S.M.	330
LUNEBURG E.	284	MICHAELSON S.M.	332
LYUBCHENKO S.A.	341	MICHAELSON S.M.	345
LYUBCHENKO S.A.	382	MICHAELSON S.M.	386
MAHMOUD S.F.	189	MICHAELSON S.M.	481
MAIONE A.	18	MICHALSKI K.A.	82
MAITLAND G.	453	MIERAS H.	120
MAJDE J.A.	475	MIGLIORA G.	228
MANN J.E.	353	MIKOLAJCZYK H.	439
MANNING M.R.	420	MIKUNI Y.	111
MAND K.	225	MILLER E.K.	48
MANTIPLY E.D.	360	MILLER G.E.	113
MAD Y-K.	6	MILLER M.W.	481
MARCUVITZ N.	293	MIRUTENKO V.I.	381
MARCUVITZ N.	297	MITCHELL J.C.	354
MARGOLIN L.	332	MITTRA R.	34
MAROUF E.A.	41	MITTRA R.	63
MARSH B.R.	416	MITTRA R.	93
MARSHALL R.E.	222	MITTRA R.	112
MARZEEV K.A.N.	341	MITZNER K.M.	31
MASSOUDI H.	348	MIZUMORI S.J.Y.	390
MASSOUDI H.	351	MIZUMORI S.J.Y.	440
MASSOUDI H.	357	MIZUSAWA M.	113
MASSOUDI H.	360	MOFFATT D.L.	80
MASTERS R.W.	112	MOFFATT D.L.	133
MATIC R.	418	MOHAMMADIAN A.H.	80
MCAFFEE R.D.	448	MOLD N.	470
MCCORMICK E.	422	MOLLIKA P.	390
MCCORMICK E.	434	MONAHAN J.C.	390
MCCOUGALL J.A.	412	MONGNARD N.	230

IGONTGOMERY L.D.	396	IGOLSEN R.L.	248
IGONTROSSET I.	124	IGOLSON D.F.	266
IGOODY E.	438	IGOSCAR K.J.	367
IGOORE R.K.	184	IGOTT R.H.	230
IGOORE R.K.	207	IGOTTENBREIT M.J.	470
IGORGAN M.A.	129	IGUARD B.H.	421
IGORGAN M.G.	282	IGPAINTER K.J.	46
IGORGAN M.G.	285	IGPANICALI A.R.	25
IGORITA K.	120	IGPAPPERT R.A.	229
IGORRIS J.M.	149	IGPARR W.H.	377
IGORTENSEN B.T.	472	IGPARTLOW L.M.	385
IGORTON D.L.	415	IGPARTLOW L.M.	463
IGOSIG J.R.	15	IGPARTLOW L.M.	464
IGOTLEY R.W.	291	IGPASQUALETTI F.	45
IGOTZKIN S.	385	IGPATHAK P.H.	57
IGOTZKIN S.	460	IGPATHAK P.H.	120
IGOTZKIN S.	461	IGPATRA A.L.	416
IGULLEN J.P.	270	IGPATSIQKIS S.	71
IGURRAY W.E.JR.	377	IGPAUL A.	199
IGUUS E.A.	222	IGPAZDEROVA-VEJLUPKOVA J.	477
IGYKELBUST J.	488	IGPEARSON L.W.	26
IGACKONEY D.G.	221	IGPEARSON L.W.	82
IGAGAI K.	113	IGPEDEN I.C.	1
IGAGARAJAN S.	288	IGPENG S.T.	76
IGAMAZOV S.A.	262	IGPENG S.T.	101
IGARASIMHAN J.S.	37	IGPENG S.Y.	161
IGAVAKATIKIAN M.A.	387	IGPERALA R.A.	320
IGAWROT P.	404	IGPEREIRA C.S.	120
IGEEDHAM M.A.	279	IGPEROS W.	500
IGELP W.B.	389	IGPERSINGER R.R.	249
IGELP W.B.	413	IGPERSINGER R.R.	250
IGELSON J.	488	IGPETERSON V.L.	170
IGELSON J.C.	405	IGPETTINELLI R.J.	445
IGEUDEER S.	489	IGPETTIT S.	330
IGLEVELS R.D.	107	IGPETTIT S.	345
IGLEVELS R.D.	121	IGPHAN B.C.	317
IGLEWMAN E.H.	95	IGPHILLIPS R.D.	344
IGLEWMAN E.H.	115	IGPHILLIPS R.D.	395
IGIELSEN P.	321	IGPICHOT CH.	571
IGIKITINA N.G.	341	IGPIETRASZEK A.	436
IGILSSON S.E.G.	339	IGPILETTE L.H.	417
IGILSSON S.E.G.	486	IGPILLA A.	435
IGHOWLAND W.L.	219	IGPILLA A.A.	303
IGNYQUIST D.P.	108	IGPLANT W.J.	191
IGNYQUIST D.P.	352	IGPLANT W.J.	185
IGJBERG P.A.	339	IGPLANT W.J.	240
IGJBERG P.A.	486	IGPLANT W.J.	241
IGJDOM D.B.	279	IGPOLONIS J.	484
IGJLGERST R.B.	308	IGPONTOPPIDAN K.	91
IGJLINER A.A.	101	IGPOWERS E.J.	232
IGJLSEN R.G.	56	IGPOWERS E.J.	313
IGJLSEN R.G.	187	IGPQZAK D.M.	95
IGJLSEN R.G.	355	IGPREFUNTAINE G.	363
IGJLSEN R.G.	499	IGPRESTON E.	363

PRETTYMAN G.D.	355	ROPE E.L.	64
PRICE H.J.	81	ROPE E.L.	120
PKICE R.	134	ROSENTHAL S.	460
PRICE R.	141	ROSENTHAL S.	461
PROHVATILO.Y.V.	382	ROSICH R.K.	160
PUES H.	116	ROSS D.R.	245
PURDUSKI S.M.	207	ROSS W.M.	441
PURSLEY M.B.	137	ROSZKOWSKI W.	390
PURSLEY M.V.	214	ROTKOVSKA D.	444
PUTNAM J.P.	474	ROTMAN S.R.	234
QUBOA K.	430	RUBENSTEIN C.	460
QUBOA S.H.J.	112	RUBENSTEIN C.	461
QUINCY E.A.	190	RUDNEV M.I.	380
RADCLIFF R.D.	200	RUDNEV M.I.	387
RAHMAN M.M.	190	RUFENACH C.	245
RAHMAT-SAMII Y.	27	RUFENACH C.L.	244
RAHMAT-SAMII Y.	90	RUKSPOLLMUANG S.	424
RAJAN G.G.	39	RUNSTADLER P.	415
RAJOTTE R.	428	RUSCH W.V.T.	80
RANA I.	113	RUSH C.M.	160
RANA I.E.	50	RUSH C.M.	267
RAO N.N.	261	RUSHDI A.M.	63
RAO T.C.K.	106	RUSHDI A.M.	91
RAPOPORT S.I.	367	RUSTAKO A.J.JR.	218
RAZ S.	36	SABBOT I.	482
RAZ S.	119	SACHER R.R.	114
RECH K.D.	118	SAFAVI-NAINI S.	34
REEVES D.L.	328	SAFRONOV V.P.	384
REEVES D.L.	389	SAGAN P.M.	482
REEVES D.L.	407	SAILORS D.B.	151
REGELSON W.	435	SAKAGAMI S.	120
REITER.L.W.	397	SALLES-CUNHA S.	488
REMILY R.	460	SANCES A.JR.	488
REUDINK D.O.	144	SANDERS A.P.	391
RHOADS C.M.	131	SANDHU G.S.	88
RIAZI A.	350	SANDLER S.S.	500
RIAZI A.	414	SANFORD N.A.	56
RIAZI A.	464	SANTAGO P.	222
RIAZI A.	465	SANZGIRI S.M.	111
RICARDI L.J.	145	SARKAR T.K.	85
RICHARD J.E.	112	SARKAR T.K.	118
RICHMOND J.H.	190	SARKAR T.K.	312
RIDDLE M.M.	471	SATO G.	112
RILEY V.	362	SATO R.	112
RILEY V.	433	SCHAEFER D.J.	391
RINO C.	269	SCHANDA E.	118
RISPIN L.	68	SCHEPPS J.L.	373
RISTENBATT M.P.	138	SCHEPPS J.R.	372
RITT R.K.	128	SCHLAGEL C.	479
ROBERTS D.W.	418	SCHLESACK J.J.	210
ROGERS R.R.	174	SCHOEN P.E.	468
ROMBERG K.M.	120	SCHOEN P.E.	497
RONCHI L.	44	SCHROT J.	457
RONCHI L.	45	SCHUCHMAN R.A.	241

CHULER D.L.	241	SOOFI K.	184
CHWAN H.P.	337	SOOFI K.	207
CHWAN H.P.	373	SPACKMAN D.H.	362
CHWERING F.	96	SPACKMAN D.H.	433
COTT A.C.	295	SPAULDING A.D.	159
COTT A.C.	311	SPIEGEL R.	484
COTT L.D.	81	SPIEGEL R.J.	353
EALS J.	422	STAELIN D.H.	234
EALS J.	434	STAIMAN D.	146
EAMAN R.L.	447	STAMPALIA L.J.	1
EGRETO V.A.	438	STANCAMPIANO C.	481
EIDLER W.A.	289	STARAS H.	142
EKINS K.M.	413	STAUFFER P.R.	420
EKNINS K.M.	389	STEINBERG B.D.	49
EMELSBERGER R.G.	16	STENGER F.S.	359
ENIOR T.B.A.	30	STENSAAS L.J.	464
ERAFIN J.P.	43	STERN S.	332
ESSIONS G.R.	450	STERN S.	481
ETO J.M.	394	STERZER F.	143
ETO Y.J.	394	STEWART C.V.	19
HANDALA M.G.	325	STEWART R.H.	246
HANDALA M.G.	380	STEWART-DEHAAN P.J.	441
HANDALA M.G.	382	STILES W.H.	233
HELDON R.L.	395	ST. MARY K.	484
HELTON W.W. JR.	338	STURM F.K.	415
HEMDIN O.H.	180	STREABLE C.W.	82
HEN L.C.	98	STRICKLAND J.I.	219
HEPPARD A.R.	310	STROHBEHN J.W.	418
HERIDAN J.P.	395	STUBENRAUCH C.S.	21
HERIDAN J.P.	468	STUCHLY M.A.	409
HERIDAN J.P.	469	STUCHLY S.S.	409
HERIDAN J.P.	491	STUTZMAN W.L.	222
HIBATA T.	165	STUTZMAN W.L.	249
HIMIZU K.	78	STUTZMAN W.L.	250
HIN J.G.	152	SUDHAKAR RAD K.	37
HIN R.	205	SULEK K.	478
HIN R.	206	SUTTON C.H.	370
HLANTA A.	227	SUTTON C.H.	423
HORE M.L.	400	SUTTON C.H.	502
HUBERT K.A.	86	SWENSON G.W. JR.	3
HVARTSBURG A.B.	322	SWICORD M.L.	431
HVARTSBURG A.B.	323	SWICORD M.L.	459
IKOV M.R.	396	SWIFT C.T.	178
ILVEN S.	281	SWIFT C.T.	179
LOAN S.A.	33	SWIFT C.T.	232
MIALOWICZ R.J.	397	SZMIGIELSKI S.	390
MIALOWICZ R.J.	471	SZMIGIELSKI S.	436
MIRNOVA E.N.	342	TABRAH F.L.	437
MITH A.D.	484	TAI C.T.	80
MITH L.G.	396	TAKASHIMA S.	337
MITH R.T.	484	TAMBURELLO C.	462
NIDER J.B.	252	TANAKA I.	463
OICHER H.	271	TANG D.D.	215
OLIMINI D.	177	TATEIBA M.	72

TAYLOR C.D.	94	VAN BLADEL J.	59
TAYLOR C.D.	125	VAN DE CAPEELE A.	116
TAYLOR L.S.	419	VAN LIL E.	116
TELL R.A.	347	VAN NETTEN J.	471
TELL R.A.	360	VANDENSANDE J.	116
TENFORDE T.S.	343	VANZANDT T.E.	167
TESCHE C.D.	20	VANZANDT T.E.	173
TESCHE F.M.	79	VASILENKO Y.I.	382
TESCHE F.M.	87	VAZIRI F.	98
THEILE G.A.	113	VESECKY J.F.	246
THOMAS J.R.	451	VIDMAR R.J.	286
THOMAS J.R.	452	VINIGRADOV G.I.	380
TIBERIO R.	28	VOGEL W.H.	403
TINGA W.R.	428	VOGEL W.J.	220
TOLER J.	422	VOGEL W.J.	247
TOLER J.	434	VOGES R.C.	113
TOMAR R.S.	199	VOGLER R.	434
TOMASHEWSKAYA L.A.	341	VOLZ R.J.	493
TOMASHEWSKAYA L.A.	382	VON HOERNER S.	113
TOMASIC B.	52	VOSS W.A.G.	408
TOMIYASU K.	5	VOSS W.A.G.	428
TOMIZAWA I.	165	VOSS W.A.G.	473
TONG T.C.	120	WACHTEL H.	307
TOPUZ E.	29	WACHTEL H.	336
TORREGROSSA M.V.	462	WAIT J.R.	7
TOURNEUR J.	119	WAIT J.R.	8
TOWNSEND W.F.	243	WAIT J.R.	17
TRANQUILLA J.M.	54	WAIT J.R.	197
TRANQUILLA J.M.	55	WAIT J.R.	230
TREMBLY B.S.	418	WALDMAN H.	147
TRETTER S.A.	162	WALLACE J.	410
TREVITHICK J.R.	441	WALLACE J.	412
TRICOLES G.	64	WALTON E.K.	22
TRICOLES G.	120	WALTON E.K.	23
TROY B.E.	231	WANG J.J.	374
TRZASKA H.	495	WANG J.J.H.	429
TSANG L.	205	WANG N.N.	57
TSANG L.	206	WANG S.S.	51
TULYATHAN P.	115	WARNOCK J.M.	173
TURNER R.	428	WATERMAN A.T.	174
TYASHELOV V.V.	381	WEENINK M.P.H.	288
TYAZHELOV V.V.	384	WEIFFENBACH G.	172
ULARY F.T.	233	WEIL C.M.	397
UMEDA M.	112	WEIL H.	40
USLENGHI P.L.E.	62	WEINER D.D.	312
USLENGHI P.L.E.	102	WEISS B.	332
USLENGHI P.L.E.	124	WEISS H.J.	148
USLENGHI P.L.E.	293	WEISSFELD D.M.	394
USLENGHI P.L.E.	294	WEISSMAN D.E.	186
USLENGHI P.L.E.	311	WEISSMAN D.E.	243
USLENGHI P.L.E.	317	WEST B.	435
UZUNOGLU N.K.	113	WEST M.W.	474
VACEK A.	444	WESTER L.S.	456
VALENZUELA G.R.	182	WETZEL L.B.	209

WHITNEY H.E.	270	WU T.K.	432
WILEY P.H.	222	YEH C.	110
WILLIAMS W.M.	329	YEH K.C.	261
WILLIAMSON R.C.		139	YEH K.C.	270
WINTER C.F.	112	YEH K.C.	271
WINTON L.	434	YOSHINO T.	154
WISLER M.M.	231	YOSHINO T.	165
WITTERS D.M.	411	YOUNG J.D.	23
WITTERS D.M.	492	YU W.-M.P.	227
WOLFSON R.I.	112	YUNG E.K.	112
WONG W.Y.	113	ZANFORLIN L.	462
WOOD K.	92	ZOTOV S.V.	341
WOOD R.	42	ZUG G.	118
WORLEY S.E.	369	ZUNIGA M.	205
WU F.T.	227	ZUNIGA M.	206
WU T.K.	122			

FUTURE MEETINGS

National Radio Science Meeting - Boulder, CO, 5-8 November 1979 in cooperation with various groups and societies of the IEEE (contact Professor S. W. Maley - Electrical Engineering Department, University of Colorado, Boulder, CO 80309).

Canadian/American Radio Science Meeting - Quebec City, 2-6 June 1980 to be co-sponsored by CNC/URSI and held jointly with AP-S/IEEE (contact J. A. Cummins - Université Laval, Département de Génie Électrique, Faculté des Sciences et de Génie, Cité Universitaire, Québec G1k 7P4, Canada).

International URSI - Symposium on Electromagnetic Waves - Munich, 26-29 August 1980 (contact Dr. H. Hochmuth, International URSI - Symposium Postfach 70 00 73, D-8000 München 70, Federal Republic of Germany).

The Twentieth General Assembly of the International Union of Radio Science (URSI) - Washington, DC, 10-18 August 1981 (contact R. Y. Dow, National Academy of Sciences, 2101 Constitution Avenue, N.W., Washington, DC 20418).

ROOM TIME	KANE 130	KANE 210	KANE 220	KANE 120	KANE 110	KANE WALKER AMES	HUB 106B	HUB 309A	HUB AUD	HUB 108 W-Lounge	UNIVERSITY TOWER HOTEL
MONDAY 8:30 - 12:00 a.m.	AP-1 Array Synthesis			B-1 High Frequency Scattering	F-1 Scattering by Turbulence		C-E Non-Gaussian Environment		BEMS		SUNDAY 8:00 p.m. ANSI Meeting Condon Room
1:30 - 5:00 p.m.	AP-2 (a) Reflector Antennas	AP-2 (b) Microstrip Antennas	AP-2 (c) Numerical Techniques	B-2 Waves in Random Media I	F-2 John W. Wright Memorial		C-1 High Time - Bandwidth Product	G-1 Diagnostic etc. of Ionosphere	BEMS		MONDAY 5:30 p.m. BEMS Board Meeting Presidents Room
5:00 p.m.				B-Business			6:30 p.m. Wave Prop. Standards Committee,	5:00 G-Business			
8:00 p.m.				Bremmer Lecture							
TUESDAY 8:30 - 12:00 a.m.	AP-3 Adaptive and SAR 12 a.m. Meet Ad Com			B-3 Antennas I Arrays	F-3 Propagation Earth	CCIR	C-2 New Satellite Systems	G-2 Ionospheric Irregularities	BEMS		
1:30 - 5:00 p.m.	AP-4 (a) Inverse Problems	AP-4 (b) Reflector and Fields	AP-4 (c) Guided Waves Atm. Prop.	B-4 (a) Field Penetration	F-4 Rough Surface Scattering	AP/B Poster A Antennas	E Noise	G-3 Effect of Ionosphere	B-4 (b) Waves in Random Media II	BEMS Poster	
SALMON BAKE						SALMON BAKE					

WEDNESDAY 9:00 - 11:30 a.m.	Plenary											WEDNESDAY 2:30 p.m. Antenna Standard EEB 420 UW
12:00 a.m.	Conference Luncheon, HUB Ballroom					Conference Luncheon, HUB Ballroom						
2:00 - 5:30 p.m.	AP-5 (a) Lens and Horns	AP-5 (b) Microstrips and Small Antennas	AP-5 (c) Scattering and EM	BREMMER SESSION	F-5 Earth-Space Propagation	AP/B Poster B Wave Phenomena	H-1 Plasmas		BEMS			5:00 p.m. AP-S Local Chapter Pres. Room
5:30 p.m.					F - Business		H - Business	C - Business	5 p.m. BEMS Membership Meeting			5:30 p.m. AP-S Ad-Com Condon Rm.
THURSDAY 8:30 - 12:00 a.m.	AP-6 Aspace Antenna Systems			B-5 Transients	F-6 Modes and Rays Snow and Ice		NL-1 Non-Linear EM	A-1 Measurements	BEMS			THURSDAY 12:00 a.m. EM-BIO Workshop Regents Rm.
1:30 - 5:00 p.m.	AP-7 (a) Environmental Effects	AP-7 (b) High Frequency Diffraction	AP-7 (c) Transients Dielectrics Radomes	B-6 Antennas II	F-7 Radio Oceanography	AP/B Poster C Scattering	NL-II Non-Linear EM	A-2 Measurements	BEMS Poster			5:30 p.m. A-Business Presidents Room
FRIDAY 8:30 - 12:00 a.m.	AP-8 Array Analysis Design			B-7 Guided Waves	F-8 Propagation Modeling		NL-III Non-Linear EM		BEMS			
1:30 - 5:00 p.m.									BEMS			

